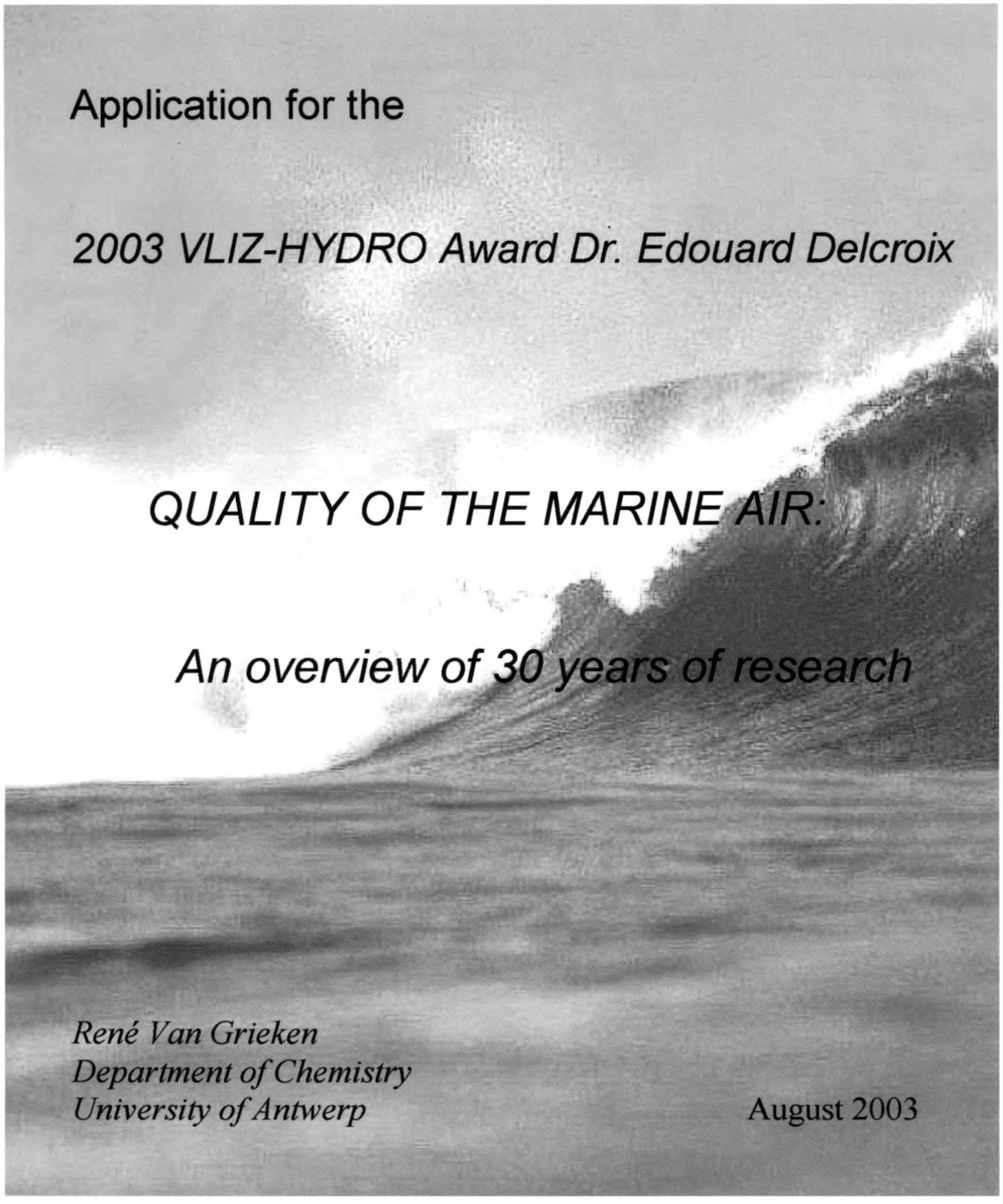

Application for the

2003 VLIZ-HYDRO Award Dr. Edouard Delcroix

QUALITY OF THE MARINE AIR:

An overview of 30 years of research

René Van Grieken
Department of Chemistry
University of Antwerp

August 2003

Application for the

2003 VLIZ-HYDRO Award Dr. Edouard Delcroix

QUALITY OF THE MARINE AIR:

An overview of 30 years of research

René Van Grieken
Department of Chemistry
University of Antwerp

August 2003

I Summary

QUALITY OF MARINE AIR: an overview of 30 years of research

Contents

Summary
QUALITY OF MARINE AIR: an overview of 30 years of research

Justification

It is clear that the marine atmosphere is a major component of the marine climate. But it is also obvious that the air that we breathe is very important from a health point of view. Heavy metals, e.g., have since long been recognised as a major health issue. Exposure to heavy metals has been linked with developmental retardation, various cancers, kidney damage, and even death in some instances of exposure to very high concentrations. Exposure to heavy metals has also been associated with the development of autoimmunity, leading to diseases of the joints and kidneys, such as rheumatoid arthritis, or diseases of the circulatory or central nervous systems. (See e.g. the website of UN Environmental Program, http://www.unep.org/unep/gpa/ich3d.htm; of World Resources Institute, http://www.wri.org/wr-98-99/metals.htm, and of the Flemish Environmental Authority, http://www.vmm.be, for much more information on heavy metal toxicity). Despite abundant evidence of these deleterious health effects, exposure to heavy metals continues in many regions of the world and may increase in the absence of concerted policy actions. Once emitted, metals can reside in the environment for hundreds of years or more, and bioaccumulation definitely occurs.

It is certain since long (but most people do not realise this) that, on average, about one third of the human heavy metal uptake is directly via the breathing of air, one third is via drinking water, and one third via food. The latter pathway does include certain edible marine organisms, but this usually forms only a minor contribution in this third food segment. In the latter context, it should also be mentioned that we found atmospheric deposition to be a major, and for some elements predominant, route for the contamination of the marine environment, hence of marine organisms. Hence, definitely, the breathing pathway is more important for human health than are the marine ecotoxicology aspects, and moreover, the latter are influenced significantly by marine air.

Solid atmospheric particles are by far the major vehicle for heavy metals in the air, and this is relevant for both the breathing uptake by humans and the atmospheric deposition to the sea and possible later uptake by marine organisms. In our work, for many years a major emphasis has thus been on marine atmospheric particles or aerosols. It has been recognised in recent years, by the way, that atmospheric aerosols are in general the most threatening component of air pollution, in many ways, and much more than any pollutant gas, like ozone or sulphur dioxide. (E.g. it has been proven recently that people living in the centre of Antwerp do have 2.5 times more asthma and other chronic obstructive pulmonary diseases than people living in the suburbs, and this is probably attributable to atmospheric particles. We are now contributing to such studies as well.) With respect to the direct human uptake of contaminants by breathing, the particle size of the particles is important. While large atmospheric particles (larger than 1 μm or so) are deposited in the upper respiratory track because, due to their momentum, they cannot follow the changing path of the air, the smaller particles can reach the deeper parts of the lungs and are deposited in the lung alveoli, from where their components can directly enter the bloodstream, within a few minutes. That is one reason why our permanent emphasis on the heavy metal and elemental concentrations of marine aerosols as a function of their particle size (and our use of suitable sampling devices and analysis techniques for size-segregated aerosols) has certainly been of importance. Finally, it is now very clear that the sea-air interaction, in both directions, of pollutants, matter and energy, forms a very important aspect of the general marine ecosystem.

Brief Outline of 30 Years of Studies and Results

(Please also refer to the enclosed publication list, and to 25 enclosed full articles; the latter are the only ones to which we'll refer in the text below)

We started research about the marine air quality about 30 years ago, in the Department of Oceanography of Florida State University (see e.g. selected article # 1). We had developed particle-induced X-ray emission analysis, which appeared to be the most suited for the heavy metal and trace analysis method for size-segregated aerosol deposits, and published the first quantitative results for this technique on aerosols in the marine environment around Florida in 1974. In these days, the ocean-atmosphere interaction had become of interest. It was suspected that air pollution could also directly affect the seawater quality, but in the foregoing decade, it had been shown that the reverse process, the impact of the seawater and sea surface composition on the coastal air quality, was also important. Indeed, it had

been shown in Eastern Florida that certain algae blooms produced toxins which were transferred into the atmospheric aerosols, which are naturally produced by the gas bubble breaking process in breaking waves, implying fast transport to the coast and leading to major human discomfort and disease in coastline dwellers. We have then studied the ocean-atmospheric transfer of heavy metals and radioisotopes, and found that the seawater surface micro layer is enriched with metals (due to their binding to hydrophobic natural compounds) and that they were highly enriched concentration in the naturally generated marine aerosols. In case of marine pollution or spills by offshore nuclear power stations (an option that was considered in Belgium in these days), the contamination could reach the land and the people via the air, much faster that one would expect at first sight (see e.g. selected article # 2).

A few years later, in the University of Antwerp, we had started a research group dealing mostly with (marine) aerosols. We focused first on the air quality and composition in very remote and pristine marine regions to define the background ("pollution is what is present minus what should be there naturally"), e.g. in the framework of National Geographic Society projects. Our measurements of heavy metal concentrations over the Atlantic and Pacific Oceans and near Antarctica still count among the ones that have been least contaminated by the ship or sampling devices (see e.g. selected article # 3, and # 6, in the journal Science).

Via contacts in Israel, we were also studying the reasons why psoriatic patients bathing in the Dead Sea were temporarily cured in most cases (see selected articles # 4 and 5). We studied the skin penetration of trace elements from the saline water and the effect on glutathion peroxidase levels, but the conclusion was unambiguous and rather surprising: it is the extremely high bromine level in the breathed Dead Sea air (due to photochemical interaction on the very bromide-rich seawater) that is taken up in the patients' blood, has a partial sedating and tranquillising effect and produces the cure. Not surprisingly the Dead Sea Works, who had sponsored this work and had hoped to find reasons for selling Dead Sea salt, discontinued their support for further detailed research after this result.

Since about 1985, we have put most emphasis on North Sea air, mostly with support of the Belgian OSTC and the Dutch Rijkswaterstaat. Firstly, we have developed different new analysis techniques for studying trace elements and heavy metals with sufficient sensitivity for marine aerosols, and we specialised additionally in multi-elemental and multi-compound micro- and single particle analysis techniques, capable of characterising large and representative numbers of individual aerosol particles (see e.g. selected publications # 7, 8 and 9). Detecting different elements and compounds together in one particle type can give much more indication than conventional bulk analysis of aerosol loaded filters about the origin and sources of the pollutants, and about their speciation, which is relevant for their toxicity. Thousands of samples have been taken for heavy metal analyses, during dozens of cruises over the whole North Sea from the R/V Belgica, during numerous aircraft flights over the Southern Bight, from the "pier" of Blankenberge and from fixed stations in Knokke and De Panne. Several millions of individual particles have been characterised by the developed microanalysis techniques, mostly by automated electron probe X-ray microanalysis. Not only airborne concentrations were measured, which could be important for direct effects on humans, but also the atmospheric deposition to the marine ecosystem was assessed. Wet atmospheric deposition was measured via rainwater analysis and dry deposition (via gravitation etc.) was calculated from the airborne concentrations via suitable models and computer programs.

This work was mostly concerned with toxic heavy metals (and other compounds of geochemical interest which could be measured simultaneously). Many questions have been addressed and answered, some of which are mentioned below.

-How high are the concentrations of heavy metals in the air over the Southern Bight of the North Sea and along the Belgian coast?

The concentrations of cadmium, lead, copper, zinc, etc., are 70-200 times higher than in really remote marine environments, but definitely of the same order of magnitude as over the Baltic and Mediterranean Seas. Reassuringly, these levels appeared not to form a direct threat to human health and are below accepted standards (See e.g. selected articles # 11, 15, 17 and 18).

-Are these concentrations lower than over land and how do they vary according to the wind direction at the coast?

The average heavy metal concentrations near the Belgian coast are generally significantly lower than the levels in the Flemish inland, as measured by the Flemish Environmental Authority VMM.

The concentrations of all heavy metals are definitely much lower when the wind is purely marine, i.e. when the air masses originate from the North or Northwest; over land, this is not be so evident. The contribution of air masses from the West/Southwest wind sectors (coming from the UK) to the atmospheric

concentration and deposition of both copper and cadmium is very predominant. Lead is rather coming from the East/Southeast, while the sources of zinc are in the East, South and West, but not in the North (See e.g. selected articles # 11, 15, 17, 18 and 22).

-What are the source processes responsible for the airborne heavy metals and what particle types are most abundant?

Single particle analyses show that cadmium is mostly included in coal fly ash particles, from thermal power plants in the UK. Lead was not mostly from leaded gasoline (even when this was still used in the 1980s), but rather from metallurgical processes (In the former instance, lead would have been present in PbClBr particles, and not as sulphides, as was the case). Also zinc is frequently present as sulphide, a chemical speciation that is indicative for the non-ferrous industry. Iron-rich particles are abundant when the wind is from the South, and their speciation is as iron oxides; both indicate the steel industry in Northern France (see e.g. selected article # 20). For eastern air mass trajectories, gypsum particles are most abundant; they can be traced to the desulphurisation processes in the German thermal power plants (see e.g. selected article # 21).

-How important is the deposition of heavy metals from the air to the marine ecosystem in comparison to the direct discharges and river inputs?

For e.g. the year 1995, well after the introduction of unleaded gasoline, the atmosphere contributed not less than 70% of the supply of lead to the Southern Bight, i.e. much more than the Scheldt and other rivers, and the direct discharges. For cadmium, this was 61 % and 40 % for copper. Clearly, the atmosphere is quantitatively a major player in the health of the marine ecosystem with respect to heavy metals (See e.g. selected articles # 10, 13, 14, 19).

We have found that the "large" atmospheric particles (see also selected article # 8), i.e. larger than 1 μm, contribute most, up to 90%, to the deposition. This was surprising since these particles are numerically relatively rare and do not travel very far (because of gravity). In most models they are not considered and most sampling strategies cannot collect them. With special sampling devices (wind tunnels), we could sample them adequately and found that their contribution to the heavy metal deposition near the coast is even predominant.

It appeared that for the marine ecology, the wet deposition over the North Sea is two times more important than the dry deposition (see e.g. selected article # 13 and 22).

The single particle composition of the seawater and surface micro layer has been compared to that of rainwater and of marine aerosols, whose changes were traced over the North Sea (see e.g. selected article # 12, 16 and 24).

-How have the concentration and deposition levels changed in recent years?

As explained, we have extensively measured the heavy metal concentrations along the North Sea over many years, but have also done complete literature surveys covering data since 1972 (see selected article #23). It appears that many metals have slightly decreased or remained more or less constant. However, for two elements, lead and zinc, the reductions have been dramatic, by a factor of ten or more. As explained above, the improvement for lead is not due to unleaded gasoline. For both elements, the spectacular reductions are obviously due to the measures taken by the metallurgical industry over the last decades.

<u>Other recent work on marine air</u>

We have recently paid attention to other problems of the North Sea and to other marine environments. At the moment, for the marine ecology, the eutrophication appears to be a major problem. We have studied the deposition of nitrogen nutrients from the air; again the atmosphere appears to be a significant contributor. The transformation of marine aerosols into nitrate by reaction with gaseous nitric acid appears to be relevant for acid rain problem (see selected article # 25). Also marine aerosols play an important role in the so-called "Whitehouse effect", i.e. the sunlight scattering and enhanced cloud formation due to atmospheric particles. Finally, the deposition of atmospheric sea salt appears to have a deteriorating effect on buildings, as far as 600 km inland. We are presently paying attention to all those problems, but these are not directly related to human health.

René Van Grieken
August 2003

PS:
During 30 years, I thus have been involved in research on the quality of the marine atmosphere in general, but with emphasis on the Southern Bight of the North Sea. In total, I have (co-)authored ca. 440 journal articles (cited once (or more times) by 3100 publications according to an Easy Search in Web-of-Science, hence probably cited around 4000 times), 180 book chapters and conference proceedings and 10 books; by the way, all the ones that appeared after 1990 can be seen at our homepage http://www.uia.ua.ac.be/u/vgrieken. Of these publications, more than 80 were dedicated explicitly to the marine and North Sea atmosphere. However, if all the publications which do not deal exclusively (or explicitly in the title) with this topic and all the publications dealing with the development and optimisation of the relevant analysis techniques are included, it would appear that about one fifth of my professional life and research has been dedicated to this issue. In addition to publications in scientific journals, we have produced numerous contributions on these issues to the IZWO newsletters, VLIZ Special Publications, Het Ingenieursblad and other more popularising publications and radio- and TV-programs.
Finally, it should be emphasised that, over the years, many have contributed to the above research, i.e. many co-workers, doctoral students and colleagues. This is clear from the authorship of all publications. Acknowledgement is made to all who contributed.

II Overall list of publications related to marine air

René VAN GRIEKEN
Department of Chemistry
University of Antwerp

OVERALL LIST OF PUBLICATIONS (total number = 82) RELATED TO MARINE AIR; those specifically on the North Sea atmosphere (total number = 42) are given in **bold.**

The publications are listed in **chronological order**.

Notes:
-Conference abstracts and reports are **not** included.
-Only these publications for which the relation to the marine or North Sea air is directly and unambiguously evident from the **title** are given here.

I) Articles in International Scientific Journals

Marine influences of aerosol composition in the coastal zone
T.B. Johansson, R.E. Van Grieken and J.W. Winchester
Journal des Recherches Atmosphériques, VIII (1974), 761-776

Trace metal fractionation effects between seawater and aerosols from bubble bursting
R.E. Van Grieken, T.B. Johansson and J.W. Winchester
Journal des Recherches Atmosphériques, VIII (1974), 611-621

Elemental abundance variation with particle size in North Florida aerosols
T.B. Johansson, R.E. Van Grieken and J.W. Winchester
Journal of Geophysical Research, 81 (1976), 1039-1046

Materiaaltransfer van de oceaan naar de atmosfeer
R. Van Grieken
Mededelingen Instituut Zeewetenschappelijk Onderzoek, 6 (juli 1976), 15-24

PIXE analysis of aerosol samples collected over the Atlantic Ocean from a sailboat
W. Maenhaut, A. Selen, P. Van Espen, R. Van Grieken and J.W. Winchester
Nuclear Instruments and Methods, 181 (1981), 399-405

Characterization of the atmospheric aerosol over the Eastern Equatorial Pacific
W. Maenhaut, H. Raemdonck, A. Selen, R. Van Grieken and J.W. Winchester
Journal of Geophysical Research, 88 (1983), 5353-5364

Characterization of individual particle types in coastal air by laser microprobe mass analysis
F. Bruynseels, H. Storms, T. Tavares and R. Van Grieken
International Journal of Environmental Analytical Chemistry, 23 (1985), 1-14

Direct detection of sulfate and nitrate layers of sampled marine aerosols by laser microprobe mass analysis
F. Bruynseels and R. Van Grieken
Atmospheric Environment, 19 (1985), 1969-1970

Chemical composition of marine atmospheric aerosols sampled worldwide
R. Van Grieken, W. Maenhaut and J.W. Winchester
National Geographic Society Research Reports, 20 (1985), 791-798

Skin penetration of minerals in psoriatics and guinea-pigs bathing in hypertonic salt solutions
J. Shani, S. Barak, D. Levi, M. Ram, E.R. Schachner, T. Schlesinger, H. Robberecht, R. Van Grieken and W.W. Avrach
Pharmacological Research Communications, 17 (1985), 501-512

Increased erythrocyte glutathione peroxidase activity in psoriatics at the Dead-Sea psoriasis treatment center
J. Shani, T. Livshitz, H. Robberecht, R. Van Grieken, N. Rubinstein and Z. Even-Paz
Pharmacological Research Communications, 17 (1985), 479-488

Internal mixture of sea salt, silicates and excess sulfate in marine aerosols
M.O. Andreae, R.J. Charlson, F. Bruynseels, H. Storms, R. Van Grieken and W. Maenhaut
Science, 232 (1986), 1620-1623

Nitric acid interaction with marine aerosols sampled by impaction
Ph. Otten, F. Bruynseels and R. Van Grieken
Bulletin des Sociétés Chimiques Belges, 95 (1986), 447-453

Study of inorganic ammonium compounds in individual marine aerosol particles by laser microprobe mass spectrometry
Ph. Otten, F. Bruynseels and R. Van Grieken
Analytica Chimica Acta, 195 (1987), 117-124

Characterization of North Sea aerosols by individual particle analyses
F. Bruynseels, H. Storms, R. Van Grieken and L. Van der Auwera
Atmospheric Environment, 22 (1988), 2593-2602

Determination of methanesulfonic acid and non sea-salt sulfate in single marine aerosol particles
L.N. Kolaitis, F.J. Bruynseels, R.E. Van Grieken and M.O. Andreae
Environmental Science and Technology, 23 (1989), 236-240

Characterization of airborne particulate matter collected over the North Sea
C.M. Rojas, Ph.M. Otten and R. Van Grieken
Journal of Aerosol Science, 20 (1989), 1257-1260

Laser microprobe mass analysis of individual Antarctic aerosol particles
L. Wouters, P. Artaxo and R. Van Grieken
International Journal of Environmental Analytical Chemistry, 38 (1990), 427-438

Chemical characterization and source apportionment of individual aerosol particles over the North Sea and the English Channel using multivariate techniques
C. Xhoffer, P. Bernard, R. Van Grieken and L. Van der Auwera
Environmental Science and Technology, 25 (1991), 1470-1478

Electron microprobe characterization of individual aerosol particles collected by aircraft above the Southern Bight of the North Sea
C.M. Rojas and R.E. Van Grieken
Atmospheric Environment, 26A (1992), 1231-1237

Characterization of individual giant aerosol particles above the North Sea
H. Van Malderen, C. Rojas and R. Van Grieken
Environmental Science and Technology, 26 (1992), 750-756

Laser microprobe mass analysis of individual North Sea aerosol particles
I. Dierck, D. Michaud, L. Wouters and R. Van Grieken
Environmental Science and Technology, 26 (1992), 802-808

Atmosferische fluxen van zware metalen naar de Noordzee
P. Otten, J. Injuk, C. Rojas en R. Van Grieken
Het Ingenieursblad, 61 (1992), 41-46
en
De Ingenieur, nr.5 (1992), 32-36

Atmospheric concentrations and size distributions of aircraft-sampled Cd, Cu, Pb and Zn over the Southern Bight of the North Sea
J. Injuk, Ph. Otten, R. Laane, W. Maenhaut and R. Van Grieken
Atmospheric Environment, 26A (1992), 2499-2508

Study of the Antarctic aerosol using X-ray fluorescence and single particle analysis
C.M. Rojas, R.E. Van Grieken and M.E. Cantillano
Scientific Series of the Chilean Antarctic Institute (Ser. Cinet. INACH), 42 (1992), 37-45

Characterization of individual particles in the North Sea surface microlayer and underlying seawater: comparison with atmospheric particles
C. Xhoffer, L. Wouters and R. Van Grieken
Environmental Science and Technology, 26 (1992), 2151-2162

Trace elements and individual particle analysis of atmospheric aerosols from the Antarctic Peninsula
P. Artaxo, M.L.C. Rabello, W. Maenhaut and R. Van Grieken
Tellus, 44B (1992), 318-334

Dry and wet deposition fluxes of Cd, Cu, Pb and Zn into the Southern Bight of the North Sea
C.M. Rojas, J. Injuk, R.E. Van Grieken and R.W. Laane
Atmospheric Environment, 27A (1993), 251-259

Comparison of three dry deposition models applied to field measurements in the Southern Bight of the North Sea
C.M. Rojas, R.E. Van Grieken and R.W. Laane
Atmospheric Environment, 27A (1993), 363-370

EDXRS study of aerosol composition variations in air masses crossing the North Sea
J. Injuk, H. Van Malderen, R. Van Grieken, E. Swietlicki, J.M. Knox and R. Schofield

X-Ray Spectrometry, 22 (1993) 220-228

An overview of wet deposition of micropollutants to the North Sea
H. Struyf and R. Van Grieken
Atmospheric Environment, 27A (1993) 2669-2687

Elemental composition of aircraft-sampled aerosols above the Southern Bight of the North Sea
C.M. Rojas, R.E. Van Grieken and W. Maenhaut
Water, Air, and Soil Pollution, 71 (1993) 391-404

Non-linear mapping of microbeam proton induced X-ray emission data for source identification of North Sea aerosols
B. Treiger, J. Injuk, I. Bondarenko, P. Van Espen, L. Breitenbach, U. Wätjen and R. Van Grieken
Spectrochimica Acta B, 49B (1994) 345-353

Performance of a nuclear microprobe to study giant marine aerosol particles
J. Injuk, L. Breitenbach, R. Van Grieken and U. Wätjen
Microchimica Acta, 114/115 (1994) 313-321

Individual aerosol particle composition variations in air masses crossing the North Sea
L.A. De Bock, H. Van Malderen and R.E. Van Grieken
Environmental Science and Technology, 28 (1994) 1513-1520

Elemental concentrations in atmospheric particulate matter sampled on the North Sea and the English Channel
P. Otten, J. Injuk and R. Van Grieken
The Science of the Total Environment, 155 (1994) 131-149

Vertical sulfur dioxide, ozone, and heavy metal concentration profiles above the Southern Bight of the North Sea
P. Otten, J. Injuk and R. Van Grieken
Israel Journal of Chemistry (Invited contribution: Special Issue on Atmospheric Chemistry), 34 (1994) 411-424

Atmospheric concentrations and deposition of heavy metals over the North Sea: a literature review
J. Injuk and R. Van Grieken
Journal of Atmospheric Chemistry, 20 (1995) 179-212

Problems in quantitatively analyzing individual salt aerosol particles using electron energy loss spectroscopy
C. Xhoffer, W. Jacob, P.R.Buseck and R. Van Grieken
Spectrochimica Acta B, 50 (1995) 1281-1292

Identification of individual aerosol particles containing Cr, Pb, and Zn above the North Sea
H. Van Malderen, S. Hoornaert and R. Van Grieken
Environmental Science and Technology, 30 (1996) 489-498

Gypsum and other calcium-rich particles above the North Sea
S. Hoornaert, H. Van Malderen and R. Van Grieken
Environmental Science and Technology, 30 (1996) 1515-1520

Characterisation of particulate matter from the Kara Sea using electron probe X-ray microanalyis
W. Jambers, A. Smekens, R. Van Grieken, V. Shevchenko and V. Gordeev
Colloids and Surfaces, 120 (1997) 61-75

Composition of individual aerosol particles above the Israelian Mediterranean coast during the summer time
E. Ganor, Z. Levin and R. Van Grieken
Atmospheric Environment, 246 (1998) 1631-1642

Deposition of atmospheric trace elements into the North Sea: coastal, ship, platform measurements, and model predictions
J. Injuk, R. Van Grieken and G. de Leeuw
Atmospheric Environment, 32 (1998) 3011-3025

Composition of aerosols in the surface boundary layer of the atmosphere over the seas of Western Russian Arctic
V.P. Shevchenko, A.P. Lisitzin, V.M. Kuptov, H. Van Malderen, J.-M. Martin, R. Van Grieken and W.W. Huang
Oceanology, 39 (1999) 128-136,
translated from Okeanologiya, 39 (1999) 142-151 (in Russian)

Composition of individual aerosol particles in the marine boundary layer over seas of the Western Russian Arctic
V.P. Shevchenko, R. Van Grieken, H. Van Malderen, A.P. Lisitzin, V.M. Kuptsov and V.V. Serova
Doklady Earth Sciences, 366 (1999) 546-551,
translated from Doklady Akademii Nauk, 366 (1999) 242-247 (in Russian)

Trend analysis of the published concentrations of heavy metals in aerosols above the North Sea and the English Channel for the period 1971-1994
S. Hoornaert, B. Treiger, R. Van Grieken and R. Laane
Environmental Reviews, 7 (1999) 191-202

Single particle and inorganic characterization of rainwater collected above the North Sea
W. Jambers, V. Dekov and R. Van Grieken

Science of the Total Environment, 256 (2000) 133-150

Single particle analysis of aerosols, observed in the marine boundary layer during the Monterey Area Ship Track Experiment (MAST), with respect to cloud droplet formation
L.A. De Bock, P.E. Joos, K.J. Noone, R.A. Pockalny and R.E. Van Grieken
Journal of Atmospheric Chemistry, 37 (2000) 299-329

A case study of ships forming and not forming tracks in moderately polluted clouds
K.J. Noone, E. Öström, R.J. Ferek, T. Garrett, P.V. Hobbs, D.W. Johnson, J.P. Taylor, L.M. Russell, R.C. Flagan, J.H. Seinfeld, C.D. O'Dowd, M.H. Smith, P.A. Durkee, K. Nielsen, J.G. Hudson, R.A. Pockalny, L. De Bock, R. Van Grieken, R.F. Gasparovic and I. Brooks
Journal of Atmospheric Sciences, 57 (2000) 2729-2747

A case study of ship track formation in a polluted marine boundary layer
K.J. Noone, D.W. Johnson, J.P. Taylor, R.J. Ferek, T. Garrett, P.V. Hobbs, P.A. Durkee, K. Nielsen, E. Öström, C. O'Dowd, M.H. Smith, L.M. Russell, R.C. Flagan, J.H. Seinfeld, L. De Bock, R.E. Van Grieken, J.G. Hudson, I. Brooks, R.F. Gasparovic and R.A. Pockalny
Journal of Atmospheric Sciences, 57 (2000) 2748-2764

Atmospheric particulate element concentrations and deposition rates in French Polynesia
C.M. Rojas, J. Injuk, R.E. Van Grieken and W. Maenhaut
Journal de Recherche Océanographique, 25 (2000) 74-86

Atmospheric deposition and its impact on ecosystems, with reference to the Mid-East region
R. Van Grieken and Y. Shevach
Eurotrac Newsletter N° 22 (2000) 39-41

Single-particle analysis of aerosols at Cheju Island, Korea, using low-Z electron probe X-ray microanalysis: a direct proof of nitrate formation from sea salts
C.-U. Ro, K.-Y. Oh, H.K. Kim, Y.P. Kim, C.B. Lee, K.-H. Kim, C.-H. Kang, J. Osan, J. de Hoog, A. Worobiec and R. Van Grieken
Environmental Science and Technology, 35 (2001) 4487-4494

II) Books and Monographies

Progress in Belgian oceanographic research
R. Van Grieken and R. Wollast
Proceedings of a Symposium, Brussels, 3-5 March 1985,
University of Antwerp, Antwerp, 1985, 479 pg.

Atmospheric particles,
R.M. Harrison and R.E. Van Grieken
IUPAC Series on Analytical and Physical Chemistry of Environmental Systems, Vol. 5, John Wiley and Sons, Chichester, 1998, 610 pg.

Atmospheric deposition and its impact on ecosystems
R. Van Grieken and Y. Shevah
University of Antwerp, Antwerp, 2002, 170 pg.

III) Chapters in Books and Proceedings of Conferences

Ocean-atmosphere interactions and oil pollution
R. Van Grieken
Proceedings of the Caracas Seminars of Ocean Resources and the Ocean Environment, Sierra Club special publication, International Series, nr. 3, Sierra Club, Washington, D.C. (1974), 9-14

Maritime influences on the atmospheric aerosol composition
R. Van Grieken
in "Studie en Beheer van het Mariene Systeem", I. Elskens, A. Sanfeld and J. Vigneron, Eds., Vol. 1, Vrije Universiteit Brussel, Brussels (1977), 139-148

Sulfur and heavy metals over the Atlantic Ocean: comparison with other marine data
W. Maenhaut, A. Selen, P. Van Espen, R. Van Grieken and J.W. Winchester
Proceedings Workshop on Long-Range Transport of Metals and Sulfur, H. Lannefors and J.W. Winchester, Eds., National Swedish Environmental Board, Stockholm, Report 1337 (1980), 37-38

Chemical characterization of individual aerosol particles from remote and polluted marine air
F. Bruynseels, H. Storms and R. Van Grieken
Proceedings of the Symposium Progress in Belgian Oceanographic Research 1985, R. Van Grieken and R. Wollast, Eds., University of Antwerp, Antwerp (1985), 178-187

Chemical characterization of airborne particulate matter above the North Sea
F. Bruynseels, H. Storms and R. Van Grieken
Proceedings of the 5th International Conference on Heavy Metals in the Environment, Vol. 1, T.D. Lekkas, Ed., ED Publishers, Edinburgh (1985), 189-191

Reaction of marine aerosols with HNO_3 vapour studied by single particle analysis
Ph. Otten, F. Bruynseels and R. Van Grieken
Proceedings of the 1985 CEE Workshop on Aerosols and Acid Deposition, CEE, Brussels (1985) 67-71

LAMMA analysis of inorganic ammonium compounds in individual marine aerosol particles
Ph. Otten, F. Bruynseels and R. Van Grieken
Proceedings of the 3rd Laser Microprobe Mass Spectrometry Workshop, University of Antwerp, Antwerp (1986), 159-163

Atmospheric deposition of heavy metals over the North Sea
R. Van Grieken, Ph. Otten and Ch. Xhoffer
in: "Environmental Quality and Ecosystem Stability", ISEEQS Publications, Jeruzalem (1989), Vol. IV, 87-88

Chemical composition, source identification and quantification of the atmospheric input into the North Sea
Ph. Otten, H. Storms, Ch. Xhoffer and R. Van Grieken
in: "Progress in Belgian Oceanographic Research - 1989", G. Pichot, Ed., Prime Minister's Services of Science Policy Office & Ministry of Public Health and Environment, Brussels (1989), 413-422

Dry aerosol deposition over the North Sea estimated from aircraft measurements
C.M. Rojas, P.M. Otten, R.E. Van Grieken and R. Laane
in: "NATO/CCMS 18th ITM on Air Pollution Modelling and its Application", University of British Columbia, Vancouver (1990), Vol.2, 409-416

Dry aerosol deposition over the North Sea estimated from aircraft measurements
C.M. Rojas, P.M. Otten, R.E. Van Grieken and R. Laane
in: "Air Pollution Modeling and Its Application - VIII", H. van Dop and D.G. Steyn, Eds., Plenum Press, New York-London (1991), 419-425

Fluxes and sources of heavy metal inputs into the Southern Bight of the North Sea
R. Van Grieken, J. Injuk, P. Otten, C. Rojas, H. Van Malderen and R. Laane
in: "Industrial Air Pollution: Assessment and Control", NATO Advanced Study Institute Series G: Ecological Sciences, Vol. 31, A. Müezzinoglu and M.L. Williams, Eds., Springer Verlag, Berlin-Heidelberg (1992), 184-193

Study of the heavy metal concentration, deposition and sources of the North Sea aerosols using X-ray emission techniques
J. Injuk, H. Van Malderen and R. Van Grieken
in: "Photo-oxidants: precursors and products", Proceedings of the EUROTRAC Symposium '92, P.M. Borrell, P. Borrell, T. Cvitas and W. Seiler, Eds., SPB Academic Publishing bv, The Hague, The Netherlands (1993), 793-795

North Sea aerosol characterization by single particle analysis techniques
H. Van Malderen, L. De Bock, J. Injuk, Ch. Xhoffer and R. Van Grieken
in: "Progress in Belgian Oceanographic Research", Royal Academy of Belgium, Brussel (1993), 119-135

Atmospheric deposition of heavy metals in the North Sea as studied by micro- and trace analysis
R. Van Grieken, L. De Bock, J. Injuk and H. Van Malderen
in: "Environmental Contamination", S.P. Varnavas, Ed., CEP Consultants Ltd., Edinburgh (1994), 284-286

Composition of aerosols over the Laptev, the Kara, the Barents, the Greenland and the Norwegian seas
V.P. Shevchenko, A.P. Lisitzin, V.M. Kuptzov, G.I. Ivanov, V.N. Lukashin, J.M. Martin, V.Yu. Rusakov, S.A. Safarova, V.V. Serova, R. Van Grieken and H. Van Malderen
in: "Russian-German Cooperation: Laptev Sea System", Berichte zur Polarforschung, Vol. 176, H.-M. Kassens, D. Piepenburg, J. Thiede, L. Timokhov, H.-W. Hebberten and S.M. Priamikov, Eds., Alfred-Wegener Institut für Polar- und Meeresforschung, Bremen (1995), 7-16

Deposition of atmospheric Ni, Cu, Zn and Pb into the North Sea, based on coastal, ship and platform measurements and on modeled predictions
J. Injuk and R. Van Grieken
in: "Preservation of Our World in the Wake of Change", Vol.VIA, Y. Steinberger, Ed., ISEEQS Publication, Jerusalem, Israel (1996) 187-189

Trend analysis of the concentration of metals in aerosols above the North Sea
S. Hoornaert, B. Treiger and R. Van Grieken
Proceedings of the 1996 Workshop on Progress in Belgian Oceanographic Research, Editions Derouaux Ordina, Liège (1996) 103-106

Atmospheric inputs of heavy metals into the North Sea
J. Injuk and R. Van Grieken
Proceedings of the 1996 Workshop on Progress in Belgian Oceanographic Research, Editions Derouaux Ordina, Liège (1996) 111-113

Chemical characterisation, source identification and quantification of the input of atmospheric particulate matter into the North Sea
H. Van Malderen, L. De Bock, S. Hoornaert, J. Injuk and R. Van Grieken
in: "Dialogue between Scientists and Users of the Sea", Federal Office for Scientific, Technical and Cultural Affairs, Brussels (1996) 103-112

The size distribution and chemical composition of cloud droplet residual particles in marine stratocumulus clouds observed during the MAST experiment
K.J. Noone, E. Öström, R.A. Pockalny, L. De Bock and R. Van Grieken
Proceedings of the 14th International Conference on Nucleation and Atmospheric Aerosols, M.K. and P.E. Wagner, Eds., Elsevier, Helsinki (1996) 868-871

Chemical and microphysical properties of cloud droplet residual particles in marine stratocumulus clouds observed during the MAST experiment
K.J. Noone, E. Öström, R.A. Pockalny, L. De Bock and R. Van Grieken
Proceedings of the 12th International Conference on Clouds and Precipitation, Page Bros., Zürich (1996) 1176-1178

Study of individual particle types and heavy metal deposition for North Sea aerosols using micro- and trace analysis techniques
J. Injuk, L. De Bock, H. Van Malderen and R. Van Grieken
Proceedings of EUROTRAC Symposium '96, P.M. Borrell, P. Borrell, T. Cvitas, K. Kelly and W. Seiler, Eds., Computational Mechanics Publications, Southampton (1996) 223

Determination of light elements in marine aerosols by grazing-emission X-ray fluorescence
M. Schmeling and R. Van Grieken
in: "Proceedings of EUROTRAC Symposium '98", Vol. 2: "Transport and Chemical Transformations in the Troposphere", P.M. Borrell and P. Borrell, Eds., WITPress, Southampton (1999) 341-343

Study of individual particle types and heavy metal deposition for North Sea aerosols using micro and trace analysis techniques
R. Van Grieken, J. Injuk, L. De Bock and H. Van Malderen
In: "Exchange and Transport of Air Pollutants over Complex Terrain and the Sea", S. Larsen, F. Fiedler and P. Borrell, Eds., Springer Verlag, Berlin-Heidelberg-New York (2000) 105-110

Characterization of aerosol particles collected at Kosan and 1100 Hill sites, Cheju Island, Korea, using ultrathin window EPMA (in Korean)
K.-Y. Oh, C.-U. Ro, HK Kim, Y.-P. Kim and R. Van Grieken
Proceedings of the 30th Meeting of the Korean Society for Atmospheric Environment, KOSAE, Seoul (2000), 325-327

Geen vuiltje aan de Noordzeelucht? Aërosolen kennen geen grenzen
R. Van Grieken and K. Eyckmans
In: "Beheer van Kust en Zee: Beleidsondersteunend Onderzoek in Vlaanderen", J. Mees and J. Seys, Eds., VLIZ Special Publication 4, Flanders Marine Institute, Ostend (2001), 22-25

Luchtkwaliteit boven de Noordzeekust. La qualité de l'air au-dessus de la zone cotière de la Mer du Nord
K. Eyckmans and R. Van Grieken
In: "Lucht zonder Grenzen. Air sans Frontières", E. Jaspers and J. Mees, Eds., VLIZ Special Publication 3, Flanders Marine Institute, Ostend (2001), 9-15

III Full versions of 25 selected articles

R. VAN GRIEKEN
Department of Chemistry
University of Antwerp

Of 25 selected journal articles, the full versions have been included. All concern marine aerosols, and the bold ones refer to the North Sea. These articles have been selected because we deemed them to be representative. The majority are in high-level journals, including Science, but mostly are in Environmental Science and Technology (impact factor = 3.12) and Journal of Geophysical Research, the top journals in this specific field, in Atmospheric Environment, etc. We included some in more popoluarising reviews as well.

Selected article # 1:

Marine influences of aerosol composition in the coastal zone
T.B. Johansson, R.E. Van Grieken and J.W. Winchester
Journal des Recherches Atmosphériques, VIII (1974), 761-776

Selected article # 2:

Trace metal fractionation effects between seawater and aerosols from bubble bursting
R.E. Van Grieken, T.B. Johansson and J.W. Winchester
Journal des Recherches Atmosphériques, VIII (1974), 611-621

Selected article # 3:

Characterization of the atmospheric aerosol over the Eastern Equatorial Pacific
W. Maenhaut, H. Raemdonck, A. Selen, R. Van Grieken and J.W. Winchester
Journal of Geophysical Research, 88 (1983), 5353-5364

Selected article # 4:

Skin penetration of minerals in psoriatics and guinea-pigs bathing in hypertonic salt solutions
J. Shani, S. Barak, D. Levi, M. Ram, E.R. Schachner, T. Schlesinger, H. Robberecht, R. Van Grieken and W.W. Avrach
Pharmacological Research Communications, 17 (1985), 501-512

Selected article # 5:

Increased erythrocyte glutathione peroxidase activity in psoriatics at the Dead-Sea psoriasis treatment center
J. Shani, T. Livshitz, H. Robberecht, R. Van Grieken, N. Rubinstein and Z. Even-Paz
Pharmacological Research Communicaitons, 17 (1985), 479-488

Selected article # 6:

Internal mixture of sea salt, silicates and excess sulfate in marine aerosols
M.O. Andreae, R.J. Charlson, F. Bruynseels, H. Storms, R. Van Grieken and W. Maenhaut
Science, 232 (1986), 1620-1623

Selected article #7:

Chemical characterization and source apportionment of individual aerosol particles over the North Sea and the English Channel using multivariate techniques
C. Xhoffer, P. Bernard, R. Van Grieken and L. Van der Auwera
Environmental Science and Technology, 25 (1991), 1470-1478

Selected article #8:

Characterization of individual giant aerosol particles above the North Sea
H. Van Malderen, C. Rojas and R. Van Grieken
Environmental Science and Technology, 26 (1992), 750-756

Selected article #9:

Laser microprobe mass analysis of individual North Sea aerosol particles
I. Dierck, D. Michaud, L. Wouters and R. Van Grieken
Environmental Science and Technology, 26 (1992), 802-808

Selected article #10:

Atmosferische fluxen van zware metalen naar de Noordzee
P. Otten, J. Injuk, C. Rojas en R. Van Grieken
Het Ingenieursblad, 61 (1992), 41-46
en
De Ingenieur, nr.5 (1992), 32-36

Selected article #11:

Atmospheric concentrations and size distributions of aircraft-sampled Cd, Cu, Pb and Zn over the Southern Bight of the North Sea
J. Injuk, Ph. Otten, R. Laane, W. Maenhaut and R. Van Grieken
Atmospheric Environment, 26A (1992), 2499-2508

Selected article #12:

Characterization of individual particles in the North Sea surface microlayer and underlying seawater: comparison with atmospheric particles
C. Xhoffer, L. Wouters and R. Van Grieken
Environmental Science and Technology, 26 (1992), 2151-2162

Selected article #13:

Dry and wet deposition fluxes of Cd, Cu, Pb and Zn into the Southern Bight of the North Sea
C.M. Rojas, J. Injuk, R.E. Van Grieken and R.W. Laane
Atmospheric Environment, 27A (1993), 251-259

Selected article #14:

An overview of wet deposition of micropollutants to the North Sea
H. Struyf and R. Van Grieken
Atmospheric Environment, 27A (1993) 2669-2687

Selected article #15:

Elemental composition of aircraft-sampled aerosols above the Southern Bight of the North Sea
C.M. Rojas, R.E. Van Grieken and W. Maenhaut
Water, Air, and Soil Pollution, 71 (1993) 391-404

Selected article #16:

Individual aerosol particle composition variations in air masses crossing the North Sea
L.A. De Bock, H. Van Malderen and R.E. Van Grieken
Environmental Science and Technology, 28 (1994) 1513-1520

Selected article #17:

Elemental concentrations in atmospheric particulate matter sampled on the North Sea and the English Channel
P. Otten, J. Injuk and R. Van Grieken
The Science of the Total Environment, 155 (1994) 131-149

Selected article #18:

Vertical sulfur dioxide, ozone, and heavy metal concentration profiles above the Southern Bight of the North Sea
P. Otten, J. Injuk and R. Van Grieken
Israel Journal of Chemistry (Invited contribution: Special Issue on Atmospheric Chemistry), 34 (1994) 411-424

Selected article #19:

Atmospheric concentrations and deposition of heavy metals over the North Sea: a literature review
J. Injuk and R. Van Grieken
Journal of Atmospheric Chemistry, 20 (1995) 179-212

Selected article #20:

Identification of individual aerosol particles containing Cr, Pb, and Zn above the North Sea
H. Van Malderen, S. Hoornaert and R. Van Grieken
Environmental Science and Technology, 30 (1996) 489-498

Selected article #21:

Gypsum and other calcium-rich particles above the North Sea
S. Hoornaert, H. Van Malderen and R. Van Grieken
Environmental Science and Technology, 30 (1996) 1515-1520

Selected article #22:

Deposition of atmospheric trace elements into the North Sea: coastal, ship, platform measurements, and model predictions
J. Injuk, R. Van Grieken and G. de Leeuw
Atmospheric Environment, 32 (1998) 3011-3025

Selected article #23:

Trend analysis of the published concentrations of heavy metals in aerosols above the North Sea and the English Channel for the period 1971-1994
S. Hoornaert, B. Treiger, R. Van Grieken and R. Laane
Environmental Reviews, 7 (1999) 191-202

Selected article #24:

Single particle and inorganic characterization of rainwater collected above the North Sea
W. Jambers, V. Dekov and R. Van Grieken
Science of the Total Environment, 256 (2000) 133-150

Selected article #25:

Single-particle analysis of aerosols at Cheju Island, Korea, using low-Z electron probe X-ray microanalysis: a direct proof of nitrate formation from sea salts
C.-U. Ro, K.-Y. Oh, HK Kim, Y.P. Kim, C.B. Lee, K.-H. Kim, C.-H. Kang, J. Osan, J. de Hoog, A. Worobiec and R. Van Grieken
Environmental Science and Technology, 35 (2001) 4487-4494

Selected article # 1:

Marine influences of aerosol composition in the coastal zone
T.B. Johansson, R.E. Van Grieken and J.W. Winchester
Journal des Recherches Atmosphériques, VIII (1974), 761-776

3508

MARINE INFLUENCES ON AEROSOL COMPOSITION IN THE COASTAL ZONE

by

T.B. JOHANSSON (*), R.E. VAN GRIEKEN (**)
and J.W. WINCHESTER

Department of Oceanography, Florida State University
Tallahassee, Florida, U.S.A.

RÉSUMÉ

Les moyennes de valeurs sélectionnées ont été utilisées pour examiner les effets de la direction des masses d'air sur les valeurs de la composition en éléments des aérosols. Les échantillons collectés en Floride du Nord, au cours du printemps et de l'été 1973, ont été influencés par des sources continentales proches et éloignées et, en outre, par des sources marines lorsque les vents venaient du Sud. Les évaluations des mouvements des masses d'air durant la collection des 32 échantillons par impactor à cascade 5 étages ont été faites par l'examen des cartes météorologiques journalières, des vents de surface pendant 3 heures à Tallahassee, et de sondages par ballons à midi jusqu'à 1 524 m. Les moyennes des abondances en éléments en fonction de la taille des particules, déterminées par émission X par induction protonique, PIXE, ont été calculées pour un groupe de 14 échantillons représentant l'air maritime et pour un groupe de 6 échantillons représentant l'air continental, à l'exclusion de 12 échantillons additionnels où les caractéristiques du flux d'air étaient variables ou lorsque des périodes de vent de très faible vitesse survenaient.

En considérant le Fe comme d'origine continentale dans tous les échantillons, les indications qualitatives de provenance suivantes ont été observées :

Elément :	S	Cl	K	Ca	Ti	V	Mn	Fe	Cu	Zn	Br	Pb
Distribution des tailles :	*S*	*L*	*(S)+L*	*L*	*L*	*S+L*	*S+L*	*L*	*S+L*	*S+L*	*S*	*S*
Petites particules :	*C*		*C*		*(M)*	*M*	*C*		*C*	*C*	*C*	*C*
Grandes particules :	*M*	*M*	*C+(M)*	*C+M*	*C*	*M*	*C*	*C*	*C*	*C*		

montrant la prédominance de petites (S) ou grandes (L) particules dans la distribution des tailles, et la prédominance de sources continentales (C) ou marines (M) dans chaque intervalle et indiquant des influences faibles quand les lettres sont données entre parenthèses.

(*) Present addresses : Dept. of Environmental Health, University of Lund, S-22002 Lund 2, Sweden.

(**) Dept. of Chemistry, Antwerp University (U.I.A.), B-2610 Wilrijk, Belgium.

ABSTRACT

Biased data set averaging has been used to examine aerosol elemental composition data for air mass directional effects. Samples collected in north Florida during spring and summer 1973 were influenced by local and remote continental sources and additionally by maritime sources when air flow was southerly. Judgements of air movements during the collection of 32 5-stage cascade impactor samples were made by examination of daily surface weather maps, 3-hourly surface winds in Tallahassee, and semi-diurnal balloon soundings to 1 524 meters. Averages of elemental abundances as a function of particle size, determined by proton-induced X-ray emission, PIXE, were computed for a 14-sample set biased toward marine air flow conditions and for a 6-sample set biased toward continental air flow, excluding 12 additional samples where air flow characteristics were variable or periods of very low wind speed were experienced. By regarding Fe to be of continental origin in all samples, the following qualitative indications of provenance were observed :

Element :	S	Cl	K	Ca	Ti	V	Mn	Fe	Cu	Zn	Br	Pb
Size Distribution :	*S*	*L*	*(S)+L*	*L*	*L*	*S+L*	*S+L*	*L*	*S+L*	*S+L*	*S*	*S*
Small Particles :	*C*		*C*		*(M)*	*M*	*C*		*C*	*C*	*C*	*C*
Large Particles :	*M*	*M*	*C+(M)*	*C+M*	*C*	*M*	*C*	*C*	*C*	*C*		

showing predominance of small, S, or large, L, particles in the size distribution (or neither, S+L), and apparent predominance of continental, C, or marine, M, sources in either size range, with minor or supplementary marine influence, (M).

INTRODUCTION.

Comparisons of atmospheric aerosol elemental composition in non-urban continental and marine environments with average earth's crust, soil dust, and sea water composition [1, 2, 3] has shown dispersed soil dust as the probable origin of some elements and dispersed sea water as the probable origin of others. Special chemical processes at or near the sea surface are suspected to cause observed anomalous atmospheric enrichments in certain cases, e.g. I [4], and are predicted to affect atmospheric concentrations in others, e.g. $PO_4^{\equiv}$ [5, 6]. However, for several « anomalous » trace elements in atmospheric particulate matter, e.g. Zn, Cu, Se, V, the relative importance of continental and marine sources has not been determined. It is of some practical interest to know if there is an average trace element flux from continental to oceanic areas or the reverse [7] in predicting the magnitude of anthropogenic impact on the large-scale atmospheric environment, and some attention has been drawn specifically to V, Pb, S and Hg in this regard [2, 8, 9, 10].

In gathering data for the study of processes which may cause « anomalous » trace element abundances in aerosols, some workers have turned to remote continental regions [1], polar regions [3] or central oceanic regions [11]. In these studies it is difficult to distinguish between nearby sources and long-range transport from others, although evaluating the extent of long-range transport from continental pollution sources over the oceans is an objective of some of the studies [12].

We have utilized a technique of biased data set averaging and applied it to a set of north Florida aerosol elemental abundance data [13] obtained using proton-induced X-ray emission, PIXE [14]. We have examined the variation of composition with particle size and air mass movement during sampling in order to determine the extent of maritime source influence in a relatively unpolluted coastal environment. With the assumption that some elements, e.g. Fe, are derived predominantly from continental soil dust, with negligible sea surface contribution in any of the samples, statistical examination of data sets biased according to marine or continental air flow regimes permits a judgement to be made of the probable importance of marine contribution to the several elements measured as a function of particle size.

Data analysis.

The results of elemental analysis of 32 aerosol samples from six sampling sites in north Florida were pooled without regard to sampling location and examined according to mean air flow. The cascade impactor samplers were operated at rooftop and near-ground locations in Tallahassee, in the Apalachicola National Forest, and along the sea coast during a total of 1 600 hours from 20 April to 28 July 1973. No major location dependent composition differences are apparent in the data [13].

For each sampling period, averaging 50 hours, daily surface weather maps were examined and a classification of the samples was made according to the probable dominant path of air flow which may affect composition. For 14 samples marine air flow appeared to dominate surface air conditions over most of the sampling time whereas for 6 samples marine air flow was minimal in comparison to continental. These two sets were selected as biased toward marine and continental conditions, respectively, and the composition averages for the two sets were computed. The remaining 12 samples, which were collected under mixed or low speed air flow, were excluded from either set (*).

The samples of each set were checked against single point records of wind speeds and directions measured every three hours at Tallahassee Municipal Airport and against balloon soundings to 1 524 meters (5 000 feet) taken every 12 hours in Tallahassee on about three-fourths of the sampling days. As an illustration, Table I presents tabulations of wind data for three samples where nearly complete sounding records were available, representing marine, continental, and mixed marine and continental flow classifications by the surface weather maps. Air flow predominantly through directions south of east-west was considered to have greater marine influence than more northerly directions. Although air flow trajectories cannot be determined precisely with this wind information, and they are undoubtedly complex and variable over the average 50-hour sampling times, these checks tend to confirm the marine and continental biasing of the two data sets.

Averages of concentrations and concentration ratios to Fe for the marine and continental air flow sets are plotted in figures 1-6 as a function of particle size. Two of the 14 marine air samples were collected very near the sea coast, so that local coastal effects may be detected, and their average is also plotted separately. In calculating the averages, only cases where the element was measured quantitatively above the detection limit have been included (Where an element was not detected, its upper limit was

---

(*) Sample identification numbers for the sets of data are [13]:
Marine: A3, A7, A17, A19, A22, B1, B3, F2, F5, F7, F8, F11, X1, X2.
Continental: A10, A11, A13, B2, X4, Y2.
Excluded: A1, A6, A16, A18, F4, F9, F10, F12, F13, F14, Z1, Z3.

TABLE I

Example of single point wind data for three samples

Sample F5. Sampling interval 6 /02-05 /73, 1845-1615 EDT.
Weather map classification « marine ».

Surface winds, direction and speed (degrees, knots = 2 xm /s)

Time (EDT)	0200	0500	0800	1100	1400	1700	2000	2300
Date :								
6 /02					070–04	100–06	090–04	100–06
6 /03	120–02	090–05	100–05	110–10	160–03	150–09	140–05	100–05
6 /04	110–06	090–05	110–06	140–10	150–06	100–03	000–00	000–00
6 /05	100–05	100–06	080–08	120–08	130–06	180–09		

Winds aloft, direction and speed (degrees, knots = 2 xm /s)

Time (EDT)	1400,6 /02	0200,6 /03	1400,6 /03	0200,6 /04	1400,6 /04	0200,6 /05	1400,6 /05
Height (m)							
1524.....	065–09	110–11	125–16	095–10	110–10	145–09	
1219.....	080–07	110–09	110–11	110–12	110–09	145–11	
914.....	085–07	130–07	115–07	130–19	130–07	130–12	120–04
610.....	085–07	160–09	140–07	135–20	150–07	120–23	135–05
305.....	070–06	160–11	150–05	120–19	145–06	115–18	135–06
Surface	055–03	150–02	140–03	105–10	10X–05	105–05	135–06

TABLE I
(continued)

Sample A10. Sampling interval 6/22-24/73, 1545-1420 EDT.
Weather map classification « continental ».

Surface winds, direction and speed (degrees, knots = 2 xm/s)

Time (EDT)	0200	0500	0800	1100	1400	1700	2000	2300
Date :								
6/22					240–05	270–05	260–04	300–04
6/23	000–00	000–00	000–00	330–06	360–10	350–11	330–04	300–04
6/24	000–00	000–00	320–03	360–11	010–12	360–08		

Winds aloft, direction and speed (degrees, knots = 2 xm/s)

Time (EDT)	1400,6/22	0200,6/23	1400,6/23	0200,6/24	1400,6/24
Height (m)					
1524		020–03		030–11	005–28
1219		010–06		010–11	005–25
914	105–02	005–08	330–16	355–10	005–25
610	135–01	360–07	345–06	355–10	010–21
305	045–01	290–07	345–04	350–11	005–14
Surface	130–04	220–04	360–10	330–04	345–10

TABLE I
(*continued*)

Sample A6. Sampling interval 6/12-14/73, 1750-1630 EDT.
Weather map classification « mixed marine + continental ».

Surface winds, direction and speed (degrees, knots = 2 xm/s)

Time (EDT)	0200	0500	0800	1100	1400	1700	2000	2300
Date :								
6/12					110–05	180–08	120–04	140–04
6/13	000–00	000–00	090–04	250–04	160–08	200–09	160–03	280–08
6/14	310–03	000–00	230–03	320–05	320–05	180–14		

Winds aloft, direction and speed (degrees, knots = 2 xm/s)

Time (EDT)	1400,6/12	0200,6/13	1400,6/13	0200,6/14	1400,6/14
Height (m)					
1524		245–08		295–05	295–06
1219		240–08		295–06	290–07
914	240–04	225–10		295–06	280–06
610	225–04	215–12	170–01	290–10	260–03
305	170–01	175–07	185–02	280–07	290–04
Surface	110–05	140–04	180–05	270–03	295–05

generally calculated to be less than measured values in the other cases, but according to our present procedures the limit value calculation is less certain than that for the measured values). The number of values used in each average is indicated in the lower part of each graph. Vertical bars represent one standard deviation calculated from the dispersion of the data set. In most cases where this is greater than 20 %, geophysical causes for variation are in excess of errors due to sampling and analysis.

Discussion.

Plots of both the concentrations and the concentration ratios of the elements to Fe should be studied for evidence of marine influence on aerosol composition. The ratio plots have been prepared on the assumption that the source of Fe is predominantly terrestrial, e.g. the dispersion of soil dust. Other elements with predominantly terrestrial sources, though not identical to the source of Fe, may be found in fixed proportion to Fe if the aerosol is well mixed. An additional source in the direction of the sea may be revealed by higher ratios to Fe during marine air flow because of dilution of land derived Fe with marine air that is low in Fe and also enriched in the element from an oceanic or coastal zone source. Of course, the directional evidence cannot distinguish sources in the open sea from those in the coastal zone, and sea surface fractionation processes are not necessarily implied by such evidence.

By inspection of figures 1-6 and noting the general differences between averages of the continental air, marine air, and two marine air samples taken at coastal stations, we note for some elements very similar concentration levels and/or ratios to Fe, but for others the marine, especially coastal marine, values differ. Except for departures of individual impactor stages for certain elements, which may or may not warrant further interpretation, we can distinguish similarity groups based on relative values of the 6 continental, 14 marine and 2 coastal marine sample averages, first for concentrations in ng/m^3 and then for ratios to Fe. The results are summarized in Table II.

The distinctly maritime element Cl, which without doubt is derived mainly from sea spray, has highest concentrations in marine air flow especially when sampled at the coast and lowest during continental air flow. Certain other elements, viz. Fe, Ti, Mn, Zn, Br and Pb, show similar concentrations during marine or continental air at the inland stations but are distinctly lower for the coastal samples, and these elements appear to be land derived. The remaining elements, viz. S, K, Ca, V and Cu, show little difference in concentration among all three data subsets, such as would result if both marine and continental sources contribute to their atmospheric concentrations.

Ratios to Fe of the elemental abundances further define these relationships. High coastal marine, intermediate average marine air, and low average continental air values are noted for S, Cl, and possibly V. High coastal marine but similar marine and continental air average values are found for K and Ca. Approximately equal ratios for all three subsets are found for Ti, Mn, Cu, Zn, Br and Pb.

The nearness of some of the ratios to Fe to those for average earth's crust material lends support to the hypothesis that dispersed soil contributes in a major way to their atmospheric concentrations, e.g. Ti, larger particle Mn, K except near the coast, and smallest particle Ca. It might also be added that the invariance of the Pb/Fe ratio with air flow direction, together with the realization that Pb is mainly derived from automobile exhaust emissions, supports the hypothesis that Fe is terrestrial in origin for all particle size ranges. On the other hand, near the coast the ratios to Fe are especially high for S, Cl, K, and Ca for all particle sizes except the smallest, implying an important supplemental marine source for these elements.

All aerosol samples are strongly enriched relative to soil composition, using Fe as a norm, for Cu, Zn and V, and for small particle K and Mn.

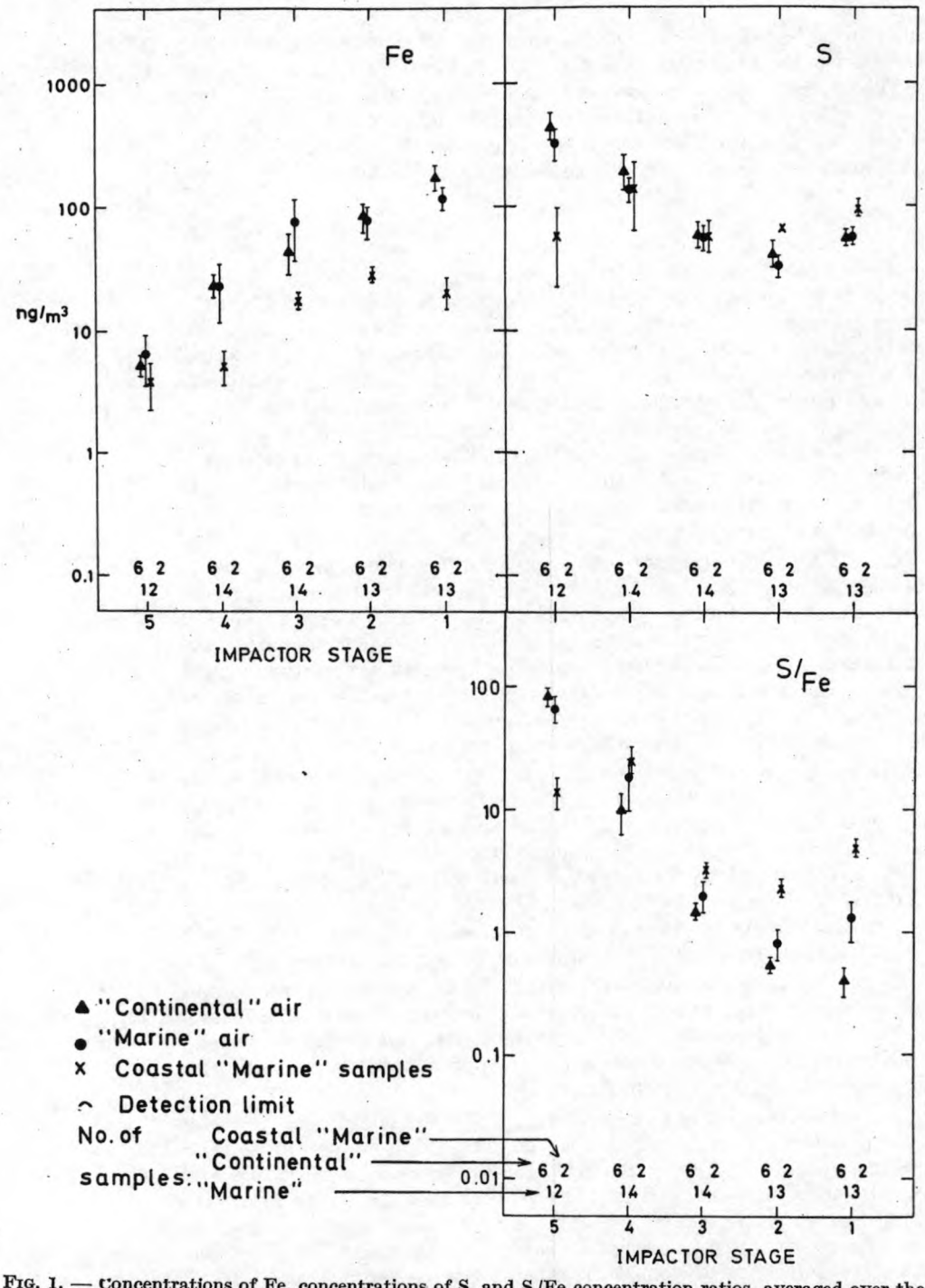

FIG. 1. — Concentrations of Fe, concentrations of S, and S/Fe concentration ratios, averaged over the number of samples indicated along the horizontal (e.g., the S/Fe stage 5 data were calculated from 6 runs with « continental » air and 12 runs with « marine » air, 2 of which were at a coastal location). Impactor stage scale is logarithmic in aerodynamic particle diameter from $> 0.25\,\mu m$ (stage 5) to $> 4\,\mu m$ (stage 1).

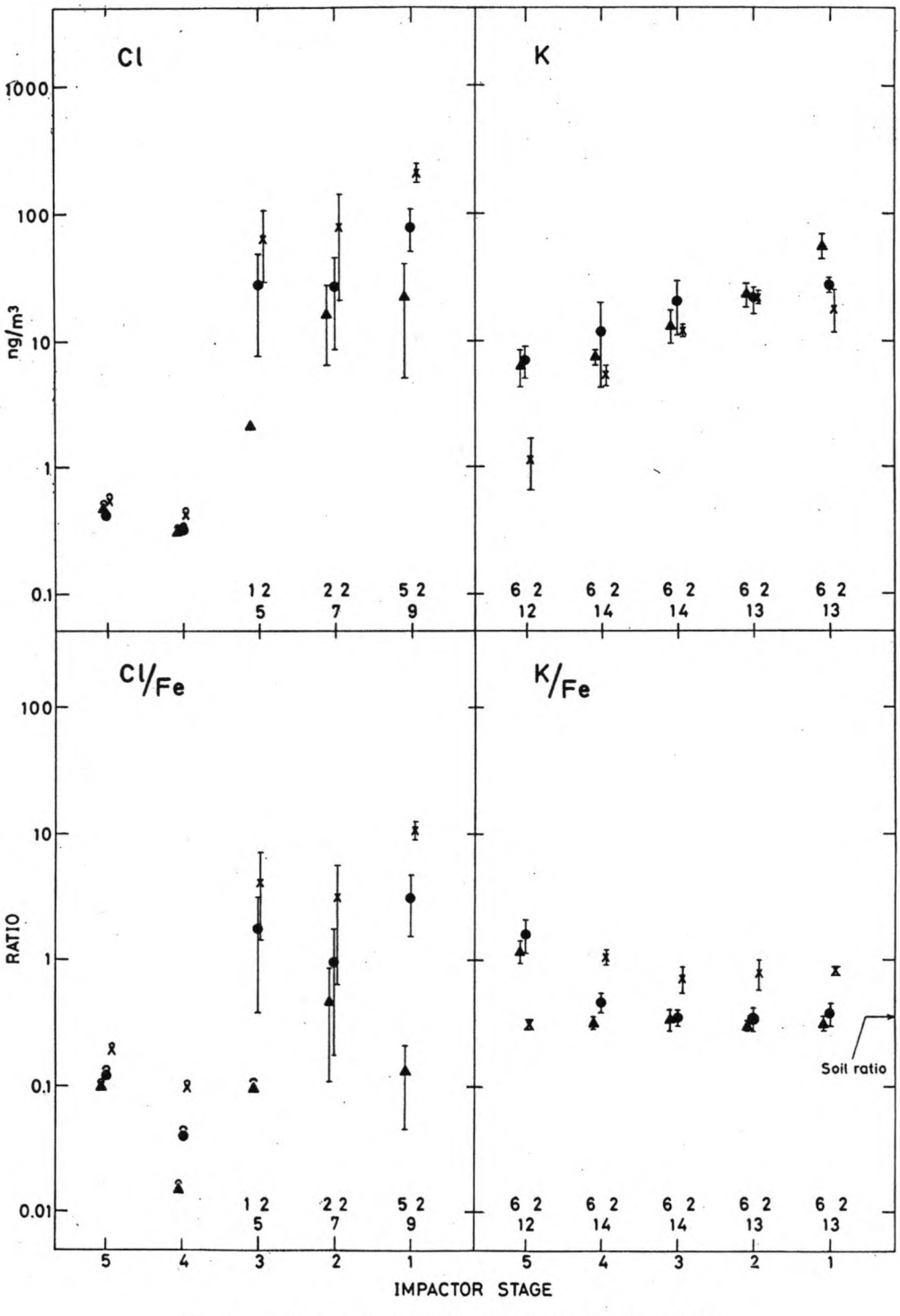

FIG. 2. — Concentrations and ratios to Fe for Cl and K.

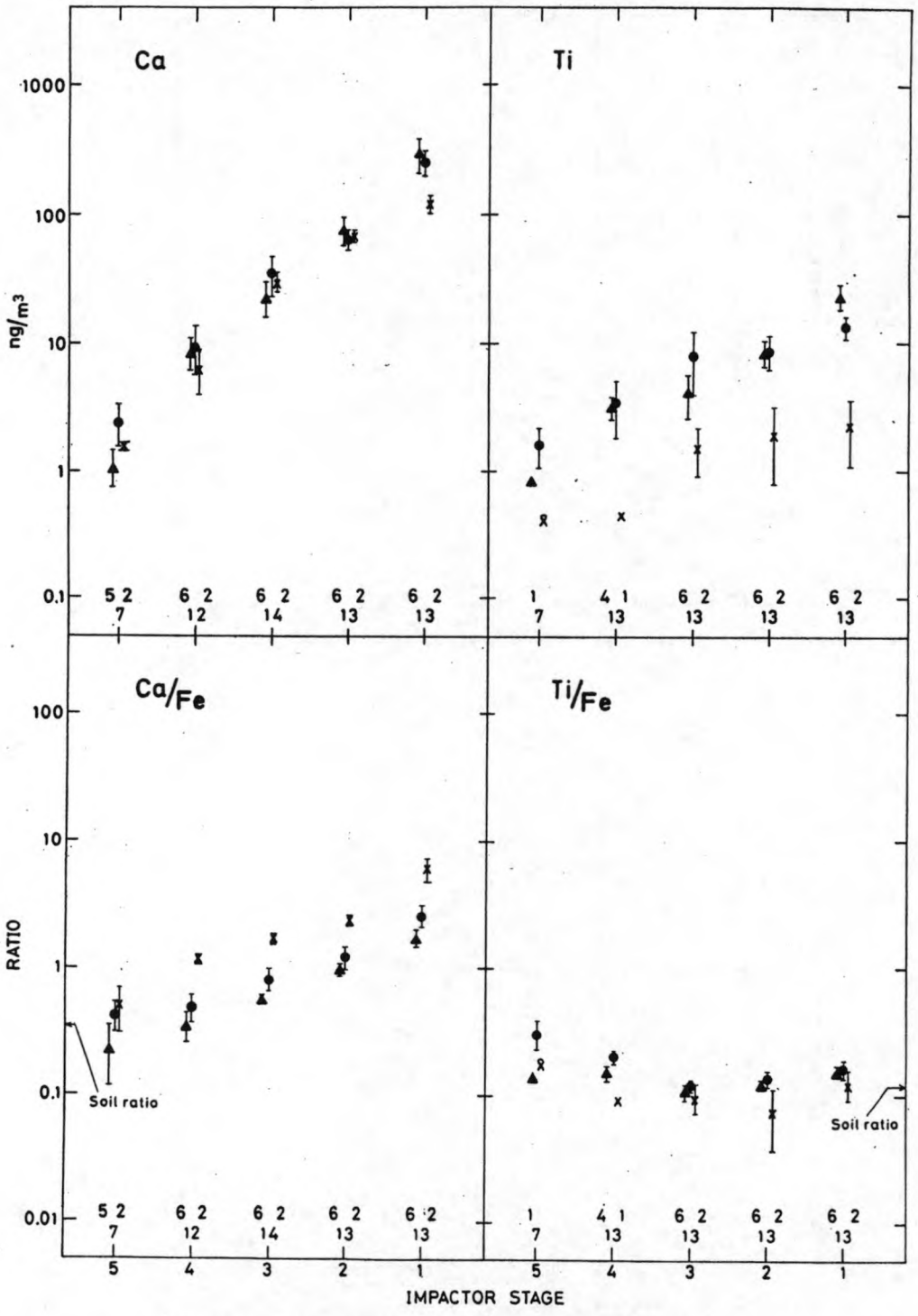

FIG. 8. — Concentrations and ratios to Fe for Ca and Ti.

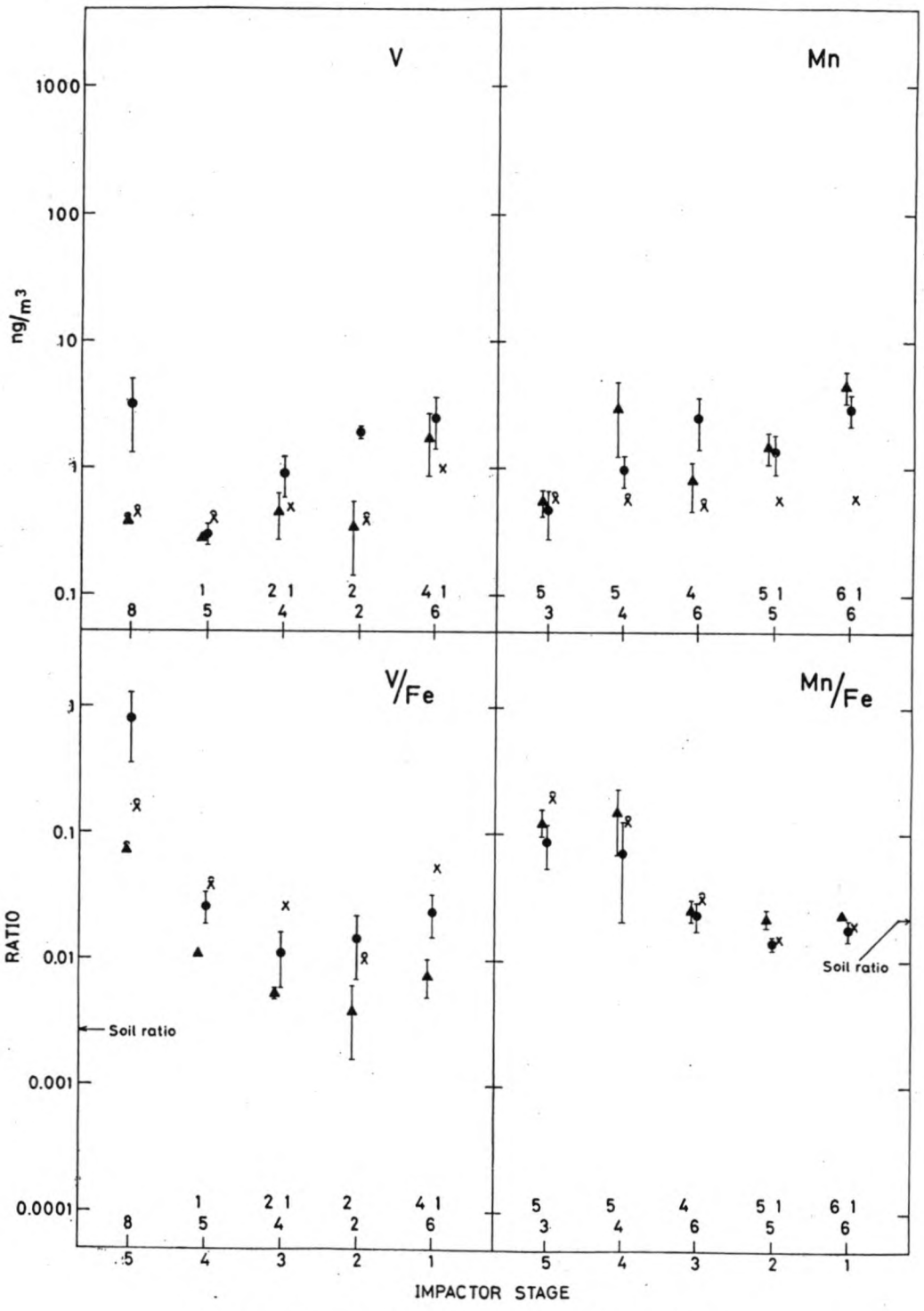

FIG. 4. — Concentrations and ratios to Fe for V and Mn.

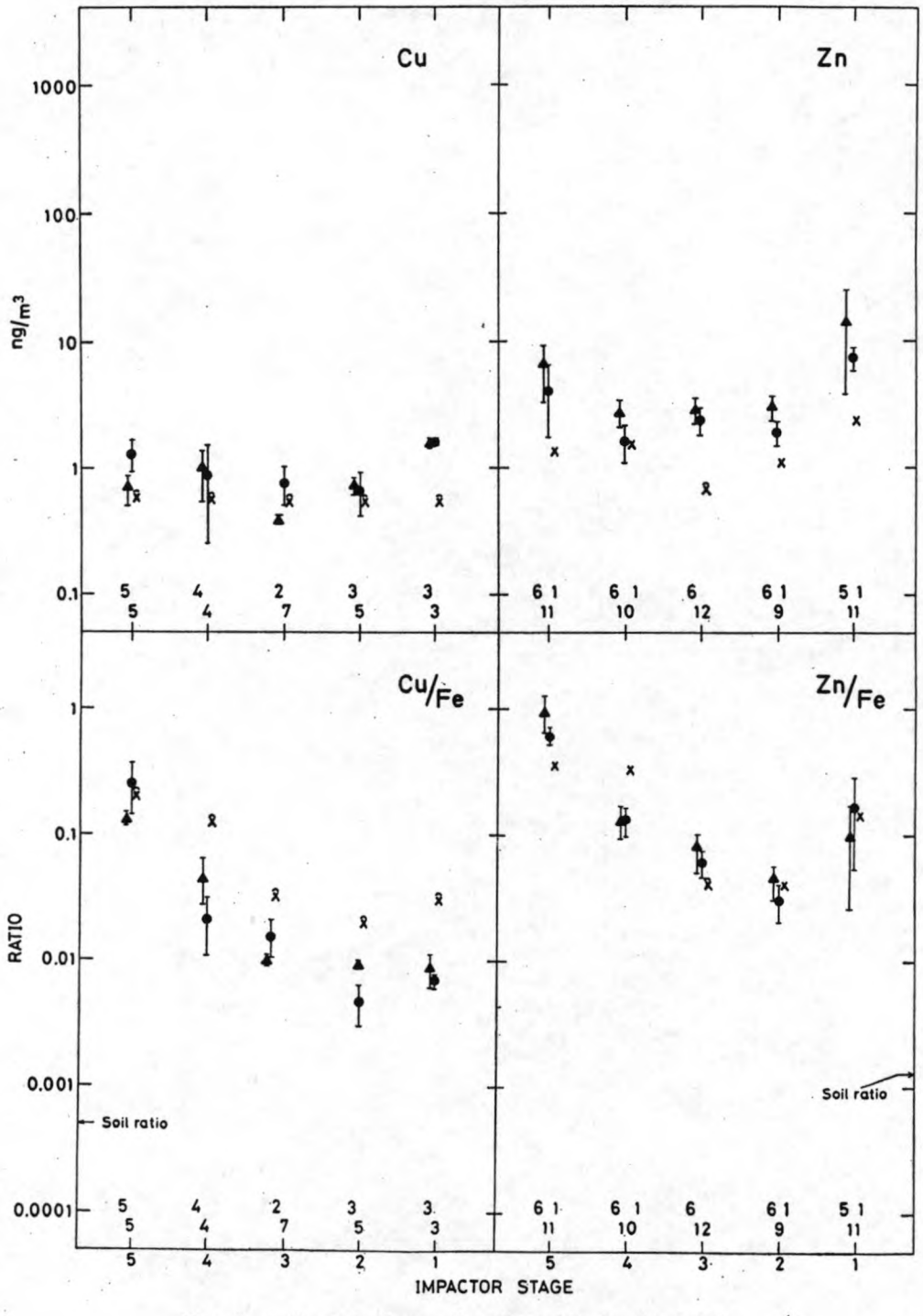

FIG. 5. — Concentrations and ratios to Fe for Cu and Zn.

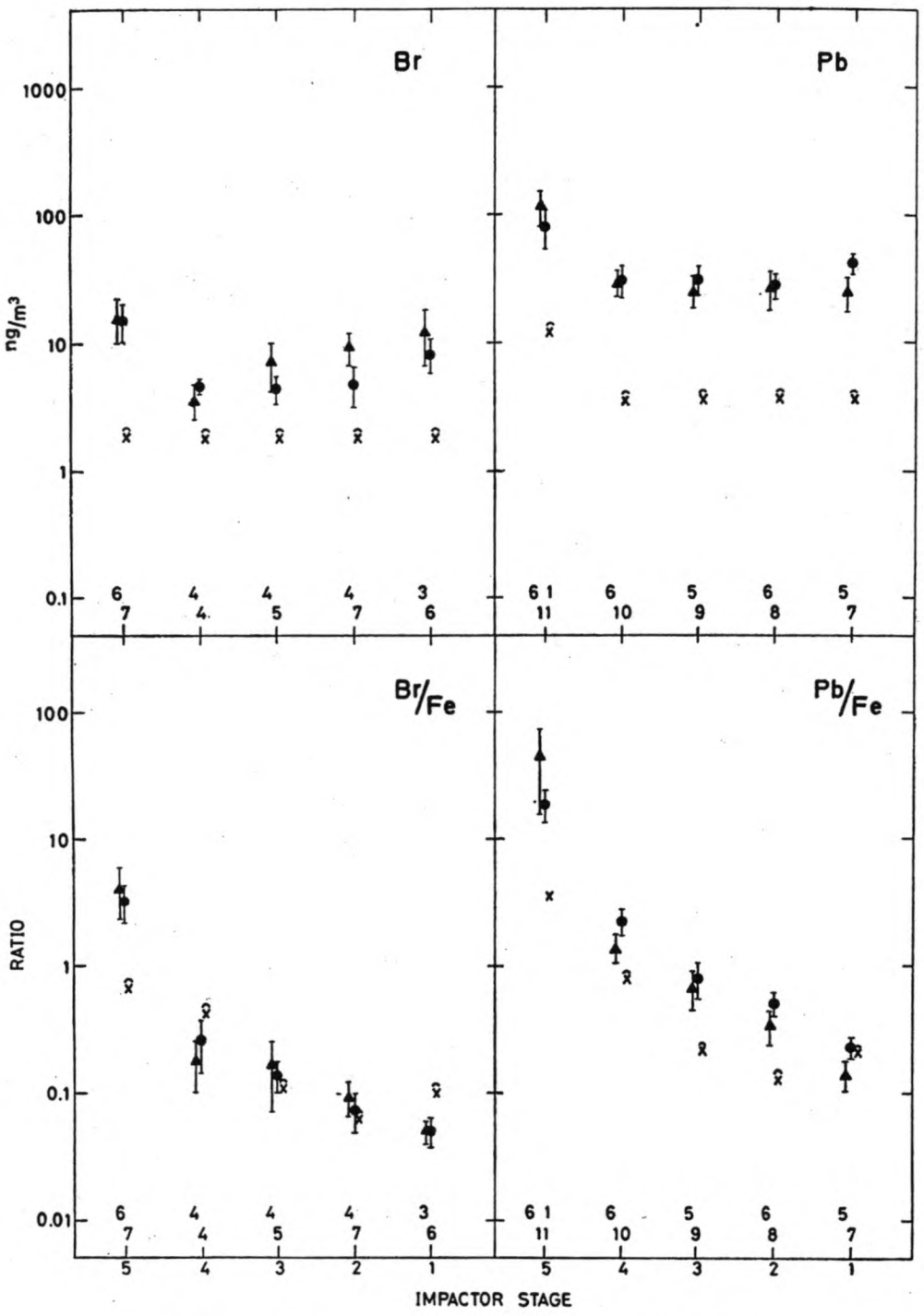

FIG. 6. — Concentrations and ratios to Fe for Br and Pb.

TABLE II

Characteristics of concentrations and ratios to Fe
for continental (Δ), *marine* (O) *and coastal marine* (X) *samples*

Concentrations			Ratios to Fe		
$X > O > \Delta$	$X \sim O \sim \Delta$	$X < O \sim \Delta$	$X > O > \Delta$	$X > O \sim \Delta$	$X \sim O \sim \Delta$
Cl	S	Fe	S	K	Ti
	K	Ti	Cl	Ca	Mn
	Ca	Mn	V		Zn
	V	Zn			Cu
	Cu	Br			
		Pb			

Furthermore, the directional evidence points to a probably terrestrial origin for Cu, Zn, and small particle K and Mn, but suggests a marine origin for V. We are ready to suggest that soil dust and sea spray serve as important sources of Fe, Ti and Mn, and of S, Cl, K, and perhaps Ca, respectively. Moreover, terrestrial pollution appears to be dominant for both Br and Pb (Br / Pb $\sim$ 0.1-0.2, both elements concentrated on small particles, and Br /Cl $\gg$ 0.0034, the sea water ratio). Particulate S may be derived for the most part from natural terrestrial or atmospheric processes supplemented by sea spray. The anomalous Zn and small particle K and Mn appear to be of terrestrial origin ; biological activity is a possible source which should be carefully examined.

The small particle Ti /Fe data indicate a directional dependence which is not seen for the large particle data. Either an additional marine source of Ti or a preferential Fe removal process could account for this observation (*).

What marine or coastal zone processes could cause the observed directional dependence of V is not apparent. It is noteworthy, however, that in two samples with the highest V concentrations of this investigation, coastal sample Z_1 and city sample B_1 [13], Ni was also detected. The Ni /V ratio was nearly the same, $\sim$ 0.3, in both samples and on all impactor stages analyzed, as appears from figure 7 where the measured Ni /V ratios and the corresponding analytical errors are shown. Ni and V are both important trace metal components of petroleum. Therefore, petroleum-derived aerosol, such as from a combustion source in the coastal zone or by petroleum dispersal at the sea surface, may contribute to the observed atmospheric V in north Florida.

The detection of statistically significant differences in aerosol composition with direction of air flow during sampling by using a technique of biased data set averaging indicates this to be a useful technique when sufficiently large sets of high precision elemental abundance data are available. Data as a function of particle size appears

(*) Although X-ray analysis is normally very specific, small peaks near 4.5 keV, the energy of Ti Kα, as seen in some impactor stage 5 analyses cannot be uniquely identified, since Ba Lα also occurs at this energy and, in the absence of weaker secondary peaks, no firm elemental identification is obtained. We have assigned these weak peaks to Ti, being the most probable element since we have never observed Ba in aerosol samples.

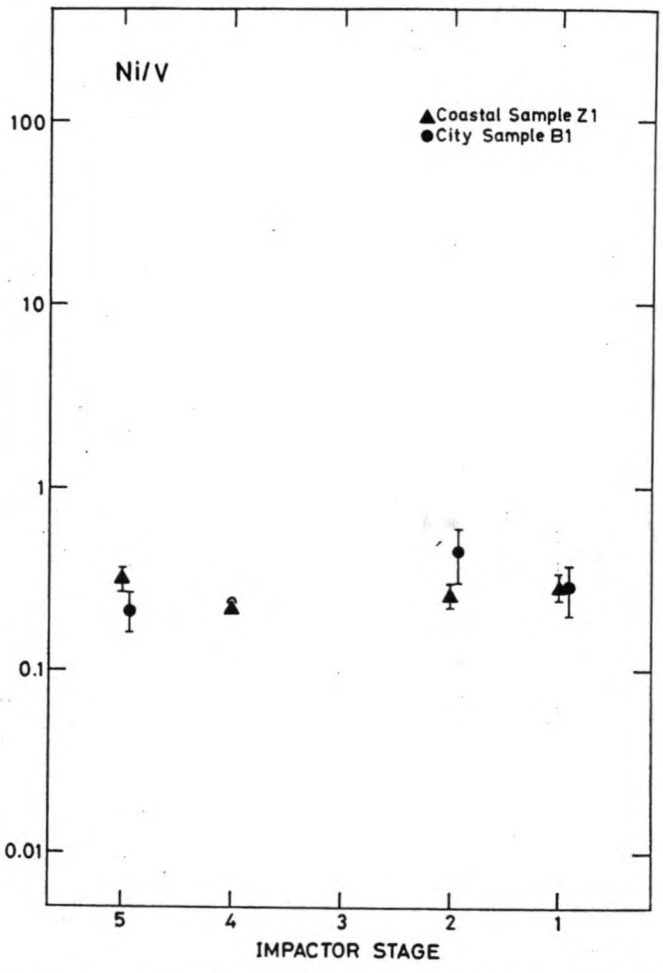

FIG. 7. — Ni /V ratios for two samples with high Ni-concentrations, simultaneously taken under marine air flow.

also to be important in making provenance inferences from the averages. We suggest that this study be extended to data acquired in offshore marine locations in order to improve the resolution of possible small marine contributions to some of the elements observed.

ACKNOWLEDGEMENTS.

We are indebted to Mr. Julian Levy and Dr. Charles Jordan for assistance with the meteorological analyses and to Dr. J.W. Nelson and Messrs Jonathan Sheline, Dennis Meinert and Martin Hudson for their ideas and assistance in sample collection and analysis. We are grateful for NATO and N.F.W.O. Fellowships (to R.E.V.G.) and travel support from the Swedish Board for Technical Development and from the Swedish Atomic Research Council (to T.B.J.). This study was supported in part by grants from the U.S. Environmental Protection Agency and National Science Foundation.

REFERENCES

[1] RAHN K.A. (1971). — Sources of trace elements in aerosols — An approach to clean air. Ph.D. Thesis, University of Michigan, Ann Arbor.

[2] MARTENS C.S., WESOLOWSKI J.J., KAIFER R., JOHN W. and HARRISS R.C. (1973). — Sources of vanadium in Puerto Rican and San Francisco Bay aerosols. *Environ. Sci. Technol.*, 7, pp. 817-20.

[3] ZOLLER W.H., GLADNEY E.S. and DUCE R.A. (1974). — Atmospheric concentrations and sources of trace metals at the South Pole. *Science*, 183, pp. 198-200.

[4] DUCE R.A., WINCHESTER J.W. and VAN NAHL T.W. (1965). — Iodine, bromine and chlorine in the Hawaiian marine atmosphere. *J. Geophys. Res.*, 70, pp. 1775-1800.

[5] BAYLOR E.R., SUTCLIFFE W.H., Jr., and HIRSCHFELD D.S. (1962). — Adsorption of phosphate onto bubbles. *Deep-Sea Res.*, 9, pp. 120-24.

[6] MACINTYRE F. and WINCHESTER J.W. (1969). — Phosphate ion enrichment in drops from breaking bubbles. *J. Phys. Chem.*, 73, pp. 2168-69.

[7] WINCHESTER J.W. (1971). — On the fluxes of atmospheric trace substances across the air-sea interface in confined bodies of water. *Bull. Amer. Meteor. Soc.*, 52, p. 1140 (abstract).

[8] MUROZUMI N., CHOW T.J. and PATTERSON C. (1969). — Chemical concentrations of pollutant lead aerosols, terrestrial dusts and sea salts in Greenland and Antarctic snow strata. *Geochim. Cosmochim. Acta*, 33, pp. 1247-94.

[9] KOIDE M. and GOLDBERG E.D. (1971). — Atmospheric sulfur and fossil fuel combustion. *J. Geophys. Res.*, 76, pp. 6589-96.

[10] WEISS H.V., KOIDE M. and GOLDBERG E.D. (1971). — Mercury in a Greenland ice sheet : evidence of recent input by man. *Science*, 174, pp. 692-94.

[11] HOFFMAN G.L., DUCE R.A. and HOFFMAN E.J. (1972). — Trace metals in the Hawaiian marine atmosphere. *J. Geophys. Res.*, 77, pp. 5322-29.

[12] DUCE R.A., PARKER P.L. and GIAM C.S. (1974). — Pollutant transfer to the marine environment. Report of IDOE workshop, Port Aransas, Texas, 11-12 January 1974, National Science Foundation.

[13] JOHANSSON T.B., VAN GRIEKEN R.E. and WINCHESTER J.W. — Elemental abundance variation with particle size in north Florida aerosols. Submitted to *J. Geophys. Res.*

[14] JOHANSSON T.B., VAN GRIEKEN R.E., NELSON J.W. and WINCHESTER J.W. — Elemental trace analysis of small samples by proton induced X-ray emission. Accepted for publication in *Anal. Chem.*

★

Selected article # 2:

Trace metal fractionation effects between seawater and aerosols from bubble bursting
R.E. Van Grieken, T.B. Johansson and J.W. Winchester
Journal des Recherches Atmosphériques, VIII (1974), 611-621

3507

TRACE METAL FRACTIONATION EFFECTS BETWEEN SEA WATER AND AEROSOLS FROM BUBBLE BURSTING

by

René E. VAN GRIEKEN (*), Thomas B. JOHANSSON (**) and John W. WINCHESTER

Department of Oceanography, Florida State University
Tallahassee, Florida, U.S.A.

RÉSUMÉ

Des expériences de laboratoire ont été poursuivies en ajoutant des traceurs radioactifs : ^{65}Zn, ^{75}Se, ^{137}Cs et ^{152}Eu à de l'eau de mer naturelle afin de déterminer les différences de composition en éléments, entre l'eau de mer et les aérosols, en fonction des classes de tailles des particules. Un flux d'air provoquait la formation de bulles qui s'élevaient et éclataient à la surface d'un récipient contenant de l'eau de mer après adjonction des traceurs radioactifs, à pH 8. Les aérosols produits étaient collectés par un impactor à cascade qui séparait les particules en classes de tailles aux fins d'analyses. Dans une expérience typique, environ 30 ml d'eau de mer, collectés dans un récipient en polyéthylène quelques heures avant le début de l'expérience, le long de la côte sablonneuse du Golfe du Mexique, étaient traversés par un courant d'air propre, qui engendrait des bulles à une profondeur de 1 à 10 cm. Deux échantillons ou plus ont été récoltés par l'impactor à cascade pendant 12 à 24 heures. Les activités présentes sur les surfaces d'impaction ont été alors mesurées par spectrométrie gamma.

Les enrichissements par rapport au sodium varient en général systématiquement avec les tailles des particules et peuvent être en excès d'un facteur 10, mais ils apparaissent très dépendants des conditions particulières de chaque expérience, comme la distance parcourue par les bulles avant l'éclatement et le temps d'équilibration entre les traceurs ajoutés et les constituants naturels de l'eau de mer. Les effets du fractionnement, souvent importants, apparaissent comme la règle plutôt que comme l'exception. En conséquence, le transfert effectif des polluants de l'eau vers l'air constitue un problème spécifique qui devrait être étudié pour chaque substance intéressante, et ceci dans des conditions variables. Pour le moins, nos résultats indiquent qu'en l'absence de données expérimentales précises, on ne peut pas poser que la composition des aérosols marins, même en première approximation, soit identique à celle de l'eau de mer.

(*) On leave from : Institute for Nuclear Sciences, Ghent University, B-9000 Ghent, Belgium.
Present address : Department of Chemistry, Antwerp University (U.I.A.), B-2610 Wilrijk, Belgium.

(**) Present address : Department of Environmental Health, University of Lund, S-22002 Lund 2, Sweden.

ABSTRACT

Laboratory experiments were performed using radioactive tracers of ^{65}Zn, ^{75}Se, ^{22}Na, ^{137}Cs and ^{152}Eu added to natural sea water to determine differences in elemental composition between sea water and aerosol droplets as a function of particle size. The experiments were conducted using a flow of air as a stream of bubbles rising and bursting at the surface of a vessel containing sea water with added radioactive tracers at pH 8. The resultant aerosol cloud was drawn through a cascade impactor which separated particle size fractions for analysis. In a typical experiment 30 ml of sea water, collected in polyethylene no more than a few hours before along a sandy Gulf of Mexico beach, and a stream of clean air, giving bubbles with a rise distance through the water of 1 to 10 cm, were used, and two or more sequential samplings, usually 12 to 24 hours in duration, were made by cascade impactor. The impaction surfaces were then counted by gamma ray spectrometer.

Enrichments relative to Na in general vary systematically with particle size and may exceed a factor of 10 but appear to depend on the particular conditions of each experiment, such as the rise distance of the bubbles and the equilibration time between the added tracers and natural constituents in sea water. Fractionation effects, often quite large, appear to be the rule rather than the exception. Consequently, efficient transfer of pollutants from water to air is a distinct possibility and should be documented for each substance of interest under varying conditions. At the very least, our results indicate that in the absence of data it is unwise to assume the composition of the marine aerosol, even as a first approximation, to be the same as sea water.

INTRODUCTION.

The announcement in September 1972 [1] in the U.S.A. of the intent to construct nuclear power plants sited in the ocean a few km from shore prompted our inquiry into the possible hazard of spilled radioactivity rendered airborne by sea spray. It has been demonstrated [2, 3] that traces of phosphate may be enriched several hundred times in droplets from bubble bursting, but similar evidence for nuclear reactor waste products is not reported in the literature. Geochemical evidence now shows anomalously high concentrations of certain trace elements in atmospheric aerosol particles, relative to simple dispersal of soil dust or sea spray [4, 5, 6], and sea surface fractionation effects remain an unexplored possibility to account for this evidence. Therefore, extensions of the present investigation may help understand such effects and their bearing on the composition of natural and pollution aerosols. Moreover, similar work might relate to the possible transfer of pollutants to the atmosphere in certain industrial processes involving aeration by bubbling or spraying. The primary objective of the present study, however, has been to document the gross features of fractionation of certain radioactive tracers added to natural near shore sea water and the effects of varying certain parameters. Since significant fractionation effects have been found, further investigations of chemical mechanisms and of the general natural and pollution aerosol problem may be warranted.

The experiments were performed using natural sea water in a special laboratory apparatus in order to vary separately several parameters which may regulate ion fractionation effects in nature. The age and organic content of the sea water, rise distance of the bubbles, and the observable characteristics of the bubbles as they break are important parameters studied in this investigation.

Because of the present focus on the properties of radioactivity added to sea water, no attempt was made to achieve isotopic exchange with natural constituents of sea water. Fractionation of natural constituents may be quantitatively different and should be studied separately.

EXPERIMENTAL.

Figure 1 represents schematically the aerosol generation chamber in which the experiments were performed. Clean air from a tank is moistened by bubbling through distilled water and led into the test solution through stainless steel or glass capillaries, providing 5-30 bubbles per second of $\sim$ 3 mm and $\sim$ 1, $\sim$ 0.3 or $\sim$ 0.1 mm diameter, respectively. Air flow drawn during aerosol collection entered the chamber through a Whatman 41 dust collection filter. The test solution of unfiltered sea water was contained in either of two polyethylene containers permitting bubble rise distances of $\sim$ 1 cm and $\sim$ 10 cm.

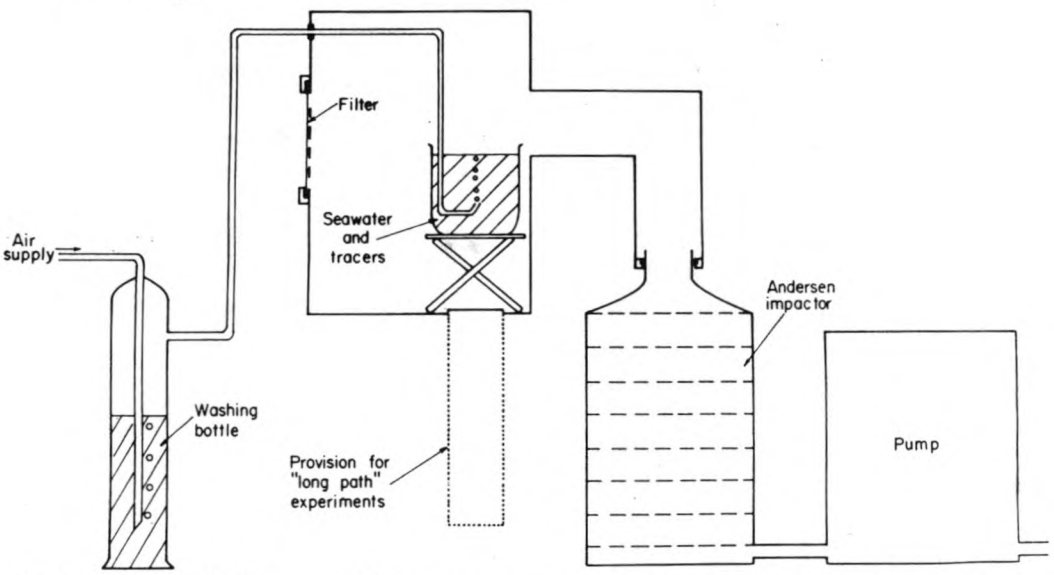

FIG. 1. — Schematic diagram of laboratory apparatus. Distance from point of bubble generation to aerosol collection by Andersen sampler was $\sim$ 35 cm horizontally and $\sim$ 10 cm vertically.

Aerosols were collected generally over a 12-24 hour period using an Andersen sampler, a six-stage cascade impactor operated at 28 liters/minute, with aerodynamic cut-off diameters for the stages varying by approximately a factor of two between 9 μm and 0.5 μm [7, 8]. Each stage of the impactor was covered with a polyethylene foil which was removed after each experiment for radioactivity counting in a Ge(Li) γ-ray spectrometer. In most experiments an after-filter was also used to collect particles $< 0.5\mu$m diameter.

Carrier-free tracers were added to natural unfiltered sea water as a neutralized mixture of high specific activity commercially obtained HCl solutions, adjusted to pH = 8 by addition of dilute NaOH. In all cases 2.58-year ^{22}Na ($E\gamma$ = 511 and 1275 keV) was included as a reference because fractionation of Na^+ relative to H_2O is believed to be insignificant during bubble rise and bursting. Either 245-day ^{65}Zn ($E\gamma$ = 511 and 1115 keV) alone or in combination with 121-day ^{75}Se ($E\gamma$ = 136, 265, 280, ...keV) was used in the major experiments, and 30-year ^{137}Cs ($E\gamma$ = 662 keV) or 13-year ^{152}Eu ($E\gamma$ = 344, 1407, 128, ...keV) in some preliminary runs. In all cases the added metal from the tracer solution was less than the amount already in the sea water. Zn and Se were chosen in the major experiments because of their biological importance, abundance in reactor wastes, contrasting aqueous chemical properties, known atmospheric chemical abundance anomalies, and availability of suitable tracers.

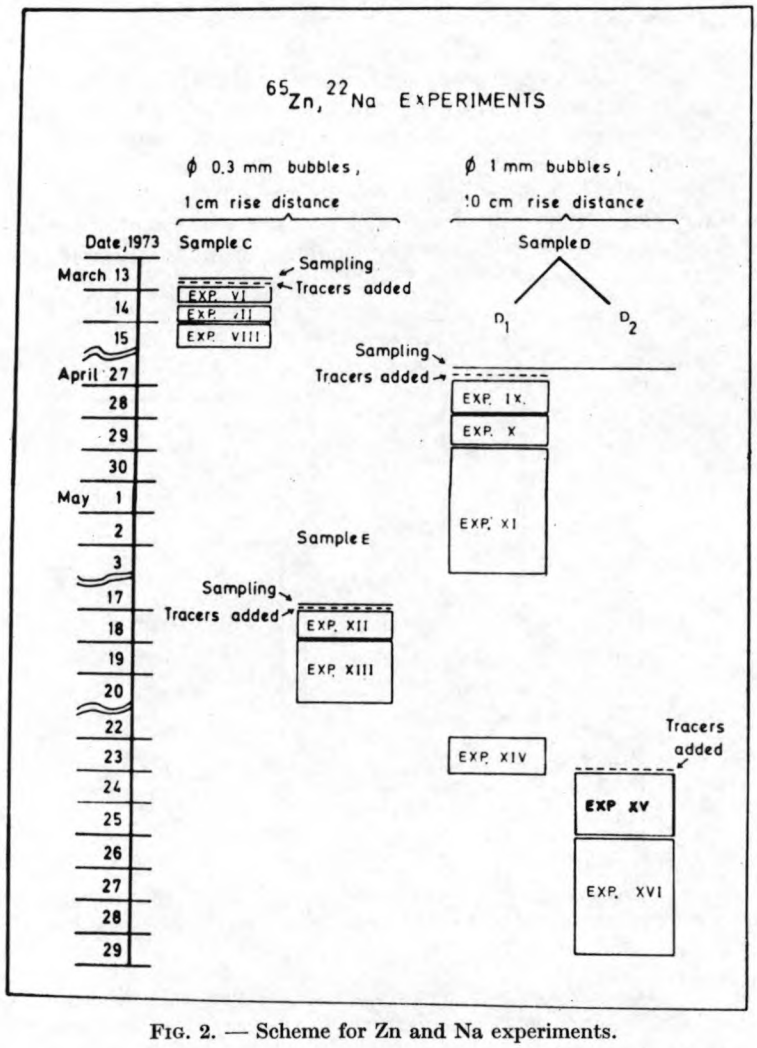

FIG. 2. — Scheme for Zn and Na experiments.

Immediately before and after each experiment, 0.1 ml of the test solution was sampled by a polypropylene pipet, and jet droplets were collected by impaction on a glass slide held over the test solution for comparison with the size fractionated aerosol generated during the experiment. The average of sea water composition before and after each experiment was used as the reference for calculating aerosol fractionation factors, F, from

$$F = \frac{(M / {}^{22}Na)_{aerosol}}{(M / {}^{22}Na)_{sea\ water}}$$

where M represents counting rates of ^{65}Zn or ^{75}Se in the major experiments and ^{152}Eu or ^{137}Cs in some preliminary experiments.

All sea water samples were collected in polyethylene bottles shortly before a sequence of experiments was undertaken. An unpolluted marsh area in the St. Marks National Wildlife Refuge on the north Florida coast of the Gulf of Mexico was selected for sampling, and careful note was made of tide variations, occurrence of rain, and other

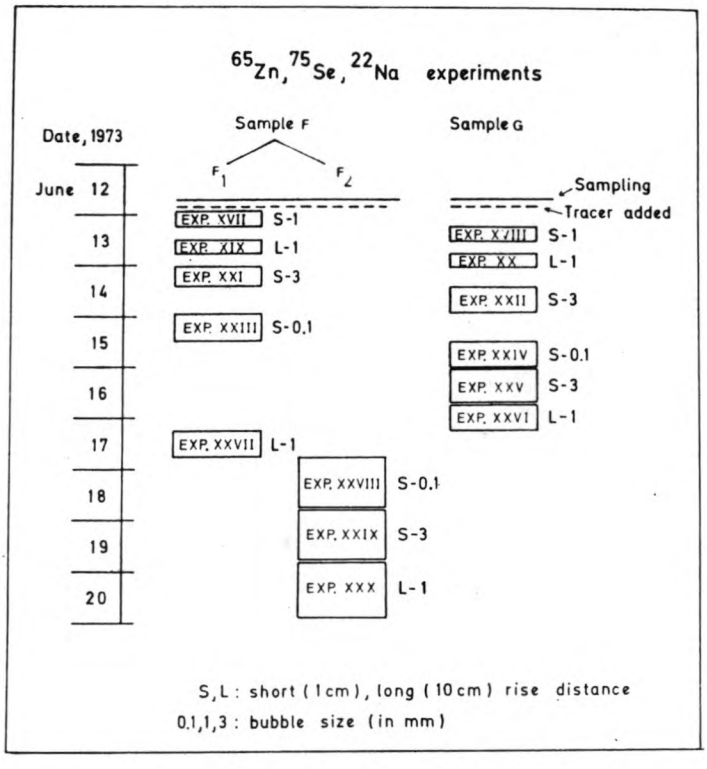

FIG. 3. — Scheme for Zn, Se and Na experiments.

factors at the time of water collection which may have affected organic content of the water or other possibly important properties.

Figures 2 and 3 present two schedules of experiments designed to test the influence of water aging, tracer equilibration time, bubble size and rise distance, and changes brought about by prolonged bubbling on aerosol composition. In any one column the sequence of experiments was performed using the same subsample of sea water. Experiments VI, VII and VIII are examples of runs done in sequence on the same sea water solution to test the effect of prolonged bubbling. Experiments XV and XVI show the effect of aging of sea water before tracer addition, in contrast with experiments XXVIII, XXIX and XXX where tracers were added before aging of sea water. Experiments were done with several combinations of bubble sizes, rise distances and length of bubbling time (indicated by vertical dimensions of the rectangles). Although the results do not show variations which are easy to interpret in terms of differences in initial sea water characteristics, it should be pointed out that samples C and E were taken at high and low tide, respectively, and D after heavy rainfall runoff into the coastal waters.

RESULTS AND DISCUSSION.

In figure 4 some typical trends are shown in the amounts of tracers found on the individual impactor stages. As expected from the literature on marine aerosol composition as it varies with particle size [9], there is a smooth trend of decreasing abundance with particle size, although the quantitative shape of the size distribution curves may depend on slight differences in the geometric arrangements for the different experiments. In

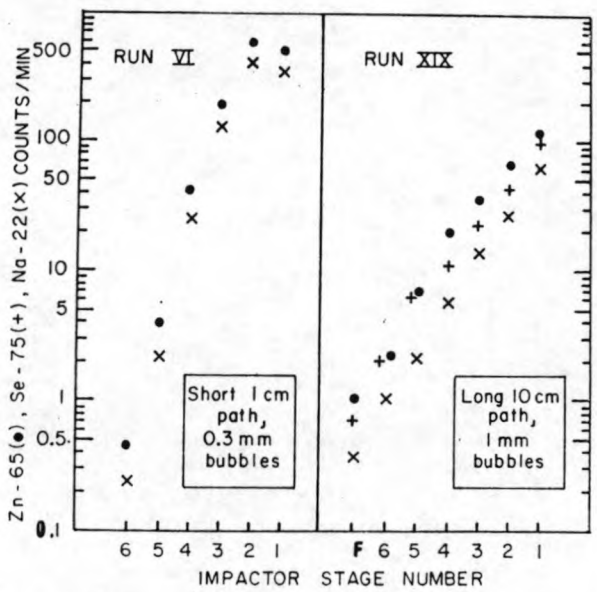

FIG. 4. — Radioactivity collected on the impactor stages as a function of particle size for two representative experiments.

the present investigation, however, emphasis has been placed on element ratios within aerosol size ranges, and the ratios should not depend on such differences.

Figures 5 and 6 show for these same experiments the variation of Zn /Na and Se /Na ratios with particle size, and between jet drop samples taken before and after the runs. The Zn /Na ratio appears to decrease appreciably in the sea water test solution during the experiments and is much less in the jet drops after compared with before the experiments. For Se /Na, where the aerosol has only slight enrichment of Se, the test solution and jet drop composition differences are less marked. In all cases, size distribution trends are smooth within the statistical errors of radioactivity measurement, shown as vertical bars of one standard deviation.

Inspection of figure 5 for a representative run with short bubble rise path shows that Zn is enriched in the aerosol size fractions, collected in experiment VI, by 4-5 times over the sea water, without strong dependence on particle size. The following experiments in the sequence, VII and VIII, which are outlined in figure 2, show Zn to be enriched by only half this amount, suggesting an effect of prolonged bubbling. The similar sequence of short bubble rise path experiments, XII and XIII, shows fractionation factors for Zn /Na not significantly different from unity for all particle sizes in both runs, an unusual result in this investigation. It suggests that the fractionation effects may depend strongly on initial water characteristics which in this case may have differed from the other experiments.

The long bubble rise experiments of the Zn and Na series are illustrated in figure 7. Experiments IX, X and XI show a consistenly high Zn /Na ratio not strongly dependent on particle size ; there is little if any decrease with prolonged bubbling. After standing three weeks without bubbling the same solution was run again, experiment XIV, and a very much lower Zn enrichment in the aerosol was found. However, experiments XV and XVI show that the same water standing in a polyethylene sampling bottle in the laboratory two months before tracer addition gave a very high Zn enrichment in the aerosol. These results suggest that aging effects which affect fractionation

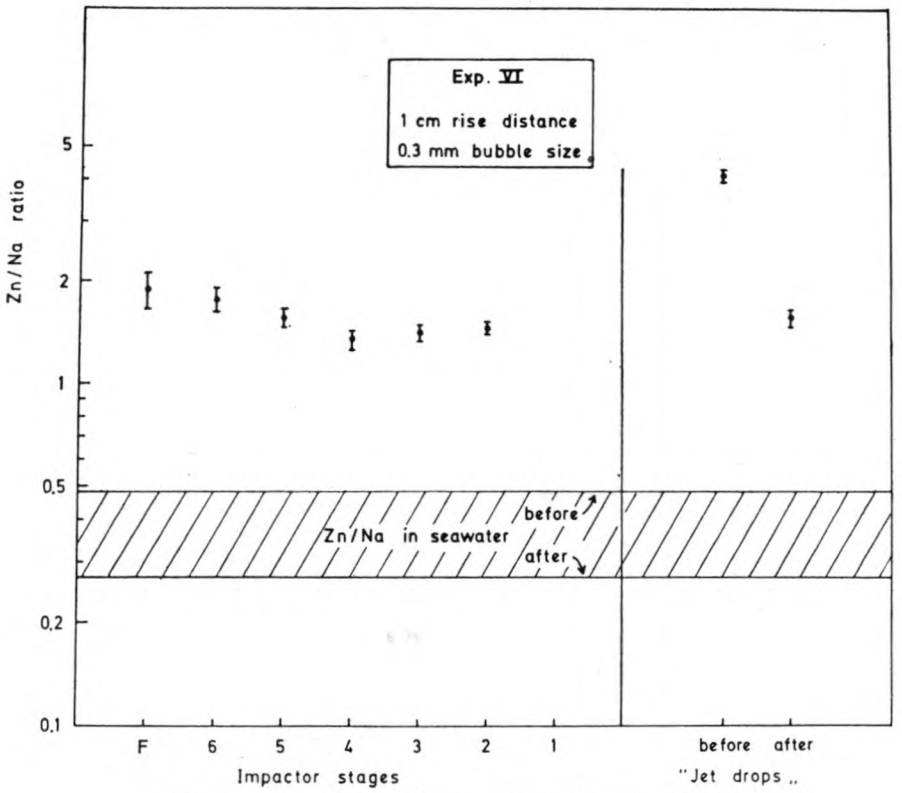

FIG. 5. — Zn/Na ratios for a representative experiment.

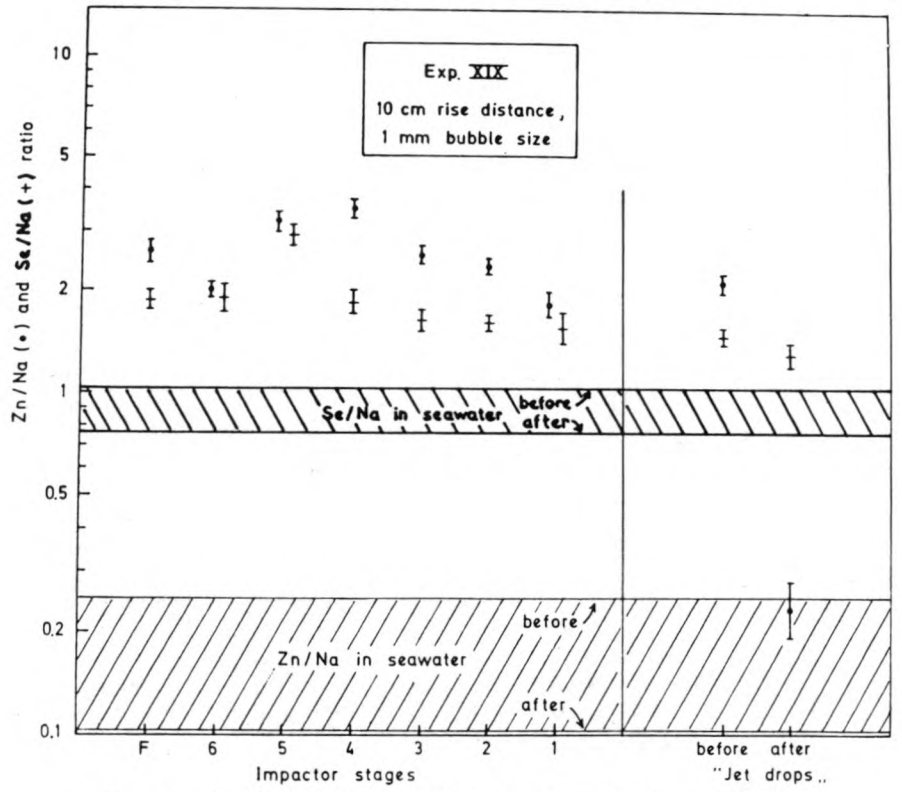

FIG. 6. — Zn/Na and Se/Na ratios for a representative experiment.

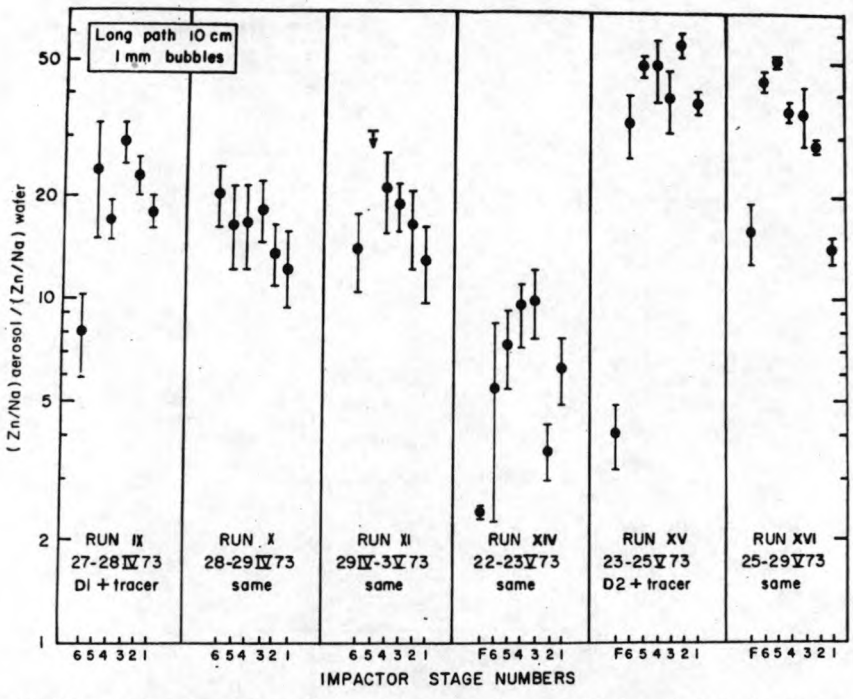

FIG. 7. — Zn/Na fractionation factors F for selected experiments with long bubble rise distances in the Zn and Na series.

of Zn and Na include tracer equilibration time and perhaps to a lesser extent prolonged bubbling action, but apparently not simple storage of water after collection.

For another series of experiments involving Zn, Se and Na tracers and outlined in figure 3, the long bubble rise path results are illustrated in figure 8. Two identical samples of sea water were collected in separate polyethylene bottles designated F and G. Splits of F were made after tracer addition, and one of these, F_2, was set aside for several days while the other, F_1, was used for short and long path runs using different bubble sizes.

Interleaved with these in time a similar series of experiments was done with water sample G. Afterwards, runs with water sample F_2 were done.

The long bubble rise path results of runs XIX and XX show strong Zn enrichments in the aerosol, consistent with the results shown in figure 7. However, for the two preceding runs XVII and XVIII done with the same bubble size, but short bubble rise, the Zn/Na fractionation factors F, averaged over all particle sizes, were 2.8 and 2.5 times lower, respectively. This result points strongly to an effect of enhanced enrichment with longer bubble rise path length, implying a mechanism of Zn enrichment by the scavenging action of rising bubbles rather than a mechanism involving only the action of the bursting bubble at the end of its rise. A similar effect for bacteria scavenging has been shown by Blanchard and Syzdek [10]. Since the longer of the two path lengths employed in these experiments is still short compared to average rise distances of small bubbles in actual ocean environments, much larger aerosol enrichments of ^{65}Zn radioactivity, freshly introduced into sea water, may be expected under natural conditions. However, as shown by runs XXVI, XXVII and XXX (figure 8) as well as in figure 7 already discussed, equilibration of the radioactivity with the sea water appears to suppress the fractionation of ^{65}Zn. This conclusion is tentative, of course, and awaits

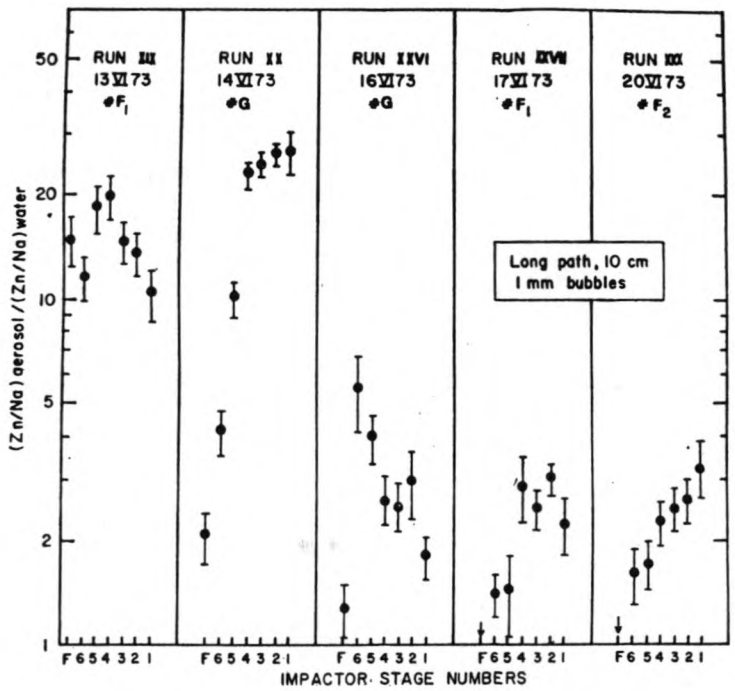

FIG. 8. — Zn /Na fractionation factors F for selected experiments with long bubble rise distances in the Zn, Se and Na series.

evaluation, among other things, of wall effects in the experimental approach which may not be present under natural conditions.

Fractionation effects for Zn and Na appeared to be enhanced to a certain extent by large bubble size. Experiments XXI and XXII showed statistically significant 30 % and 50 %, respectively, greater average Zn /Na fractionation factors F over all aerosol sizes than did experiments XVII and XVIII, in spite of the prolonged bubbling which appears in some cases to suppress Zn /Na fractionation. We see the effect of bubble size in runs XXVIII and XXIX where the average Zn /Na fractionation factors F were 1.0 and 1.9, respectively. Small fractionations for the smallest bubble sizes are also found in both of the runs XXIII and XXIV where values of F average only slightly greater than unity, except for the < 0.5 μm diameter size fractions.

Se and Na fractionation effects are consistently seen in these experiments to be much smaller than for Zn and Na. Table I presents a summary of Se /Na fractionation factors F for the runs of figure 3 as averages over all impactor size ranges, in comparison with the corresponding Zn /Na values. Although most values show an enrichment of Se in the aerosol size fractions, the effect is slight compared to that for Zn. In view of the anionic character of Se in aqueous solution at pH = 8 and the cationic character of Zn under the same conditions, this difference may be a major factor involved in the fractionation mechanism. However, in view of the almost certain involvement also of organic substances in sea water which may complex these elements to varying degrees, we cannot at this time define the reaction mechanisms further.

Preliminary experiments with ^{152}Eu and ^{137}Cs tracers showed enrichment of Eu in the aerosol, relative to Na, to be as great or greater than that for Zn. Results for Cs indicate a slightly lower Cs /Na ratio in the aerosol than in the sea water. We

TABLE I

Se/Na *and* Zn/Na *aerosol fractionation factors,* F

Experiment	Average F for all size fractions	
	Se/Na	Zn/Na
XVII	1.8	5.3
XVIII	2.0	6.6
XIX	2.3	14.7
XX	1.8	16.8
XXI	1.7	7.0
XXII	2.7	9.7
XXIII	1.9	1.7
XXIV	1.6	2.5
XXVI	1.9	2.9
XXVII	1.6	2.0
XXVIII	1.3	1.0
XXIX	2.4	1.9
XXX	1.1	2.1

believe future experiments should be directed to documenting these apparent differences and relating them to differences in chemical properties in aqueous solution.

In conclusion, enrichments in general vary in a non-random manner with particle size and may exceed a factor of 10 for any particle size, but appear to depend on the particular conditions of each experiment, such as the rise distance of the bubbles and the equilibrium time between added tracers and natural constituents in the sea water. Our general finding is that fractionation effects, often quite large, are the rule rather than the exception for these tracers studied in coastal waters. Consequently, efficient transfer of pollutants from water to air is a distinct possibility and should be documented for each substance of interest under varying conditions. At the very least, our results indicate that in the absence of data it is unwise to assume the composition of the marine aerosol, even as a first approximation, to be the same as sea water [11].

ACKNOWLEDGEMENTS.

We are grateful for NATO and N.F.W.O. Fellowship support (to R.E.V.G.), and for travel support from the Swedish Board of Technical Development and the Swedish Atomic Research Council (to T.B.J.). The study forms part of a general study of the pollution sources of trace metals in the atmosphere and was supported in part by Grant R802132 from the U.S. Environmental Protection Agency.

REFERENCES

[1] WASGHINTON POST, 1972, 24 September.

[2] MACINTYRE F. (1965). — Ion fractionation in drops from breaking bubbles. Ph. D. Thesis, Massachusetts Institute of Technology, U.S.A.

[3] MACINTYRE F. and WINCHESTER J.W. (1969). — Phosphate ion enrichment in drops from breaking bubbles. *J. Phys. Chem.*, 73, pp. 2163-69.

[4] RAHN K.A. (1971). — Sources of trace elements in aerosols — An approach to clean air. Ph. D. Thesis, University of Michigan, Ann Arbor, U.S.A.

[5] HOFFMAN G.L., DUCE R.A. and HOFFMAN E.J. (1972). — Trace metals in the Hawaiian marine atmosphere. *J. Geophys. Res.*, 77, pp. 5322-29.

[6] ZOLLER W.H., GLADNEY E.S. and DUCE R.A. (1974). — Atmospheric concentrations and sources of trace metals at the South Pole. *Science*, 183, pp. 198-200.

[7] ANDERSEN A.A. (1966). — A sampler for respiratory health hazard assessment. *J. Amer. Ind. Hyg. Assoc.*, 27, pp. 160-65.

[8] FLESCH J.P., NORRIS C.N. and NUGENT A.B., Jr. (1967). — Calibrating particulate air samples with monodispersive aerosols. *J. Amer. Ind. Hyg. Assoc.*, 28, pp. 507-16.

[9] JUNGE C. (1963). — *Air Chemistry and Radioactivity*, Academic Press, New York.

10] BLANCHARD D.C. and SYZDEK L. (1972). — Concentration of bacteria in jet drops from bursting bubbles. *J. Geophys. Res.*, 77, pp. 5087-99.

[11] A more complete presentation of experimental data on which the conclusions of this paper are based can be found in « Laboratory tracer experiments on fractionation during bubble bursting », a technical report obtainable from J.W. Winchester, Dept. of Oceanography, Florida State University, Tallahassee, FL 32306, U.S.A.

★

Selected article # 3:

Characterization of the atmospheric aerosol over the Eastern Equatorial Pacific
W. Maenhaut, H. Raemdonck, A. Selen, R. Van Grieken and J.W. Winchester
Journal of Geophysical Research, 88 (1983), 5353-5364

3398

JOURNAL OF GEOPHYSICAL RESEARCH, VOL. 88, NO. C9, PAGES 5353–5364, JUNE 20, 1983

Characterization of the Atmospheric Aerosol Over the Eastern Equatorial Pacific

WILLY MAENHAUT AND HANS RAEMDONCK

Institute for Nuclear Sciences, State University of Ghent, B-9000 Ghent, Belgium

ANDRÉ SELEN AND RENÉ VAN GRIEKEN

Department of Chemistry, University of Antwerp (U.I.A.), B-2610 Wilrijk, Belgium

JOHN W. WINCHESTER

Department of Oceanography, Florida State University, Tallahassee, Florida 32306

By using a polyester sailboat as sampling platform, a series of duplicate aerosol samples was collected by cascade impactors on a trip from Panama to Tahiti in 1979. Elemental analysis mainly by particle-induced X ray emission (PIXE) indicated, in the samples collected between Panama and the Galapagos Islands, the presence of a substantial crustal component (~0.4 $\mu g/m^3$), fine Cu (~0.4 ng/m^3) and Zn (~0.6 ng/m^3), and excess fine S and K (~100 and ~2.4 ng/m^3, respectively) in addition to the major sea salt elements. The crustal component and fine Cu and Zn are suggested to result from natural continental sources (i.e., eolian dust transport from the American continents and perhaps geothermal emissions). Samples collected west of the Galapagos Islands in the southern trades showed significantly lower concentrations for the nonseawater components. The average Si and Fe levels were as low as 4.8 and 3.3 ng/m^3, corresponding to a maximum of 0.066 $\mu g/m^3$ for an assumed mineral dust component, whereas heavy metal concentrations were all below the detection limits (typically ranging from 0.05 to 0.15 ng/m^3 for V, Cr, Mn, Ni, Cu, Zn, and Se). Excess fine S decreased to a mean of 46 ng/m^3, a level similar to those reported for other remote marine and continental locations. This all indicates that the marine atmosphere west of the Galapagos was little influenced by natural continental source processes or by anthropogenic emissions. Under these truly marine conditions, several concentration ratios of the major seawater elements were significantly different from those in bulk seawater. Ca, Sr, and S in > 1 μm diameter particles were enriched relative to K and Na, with the enrichment being substantially more pronounced (up to 50% or higher) for 1–4-μm diameter particles than for particles >4 μm. Comparison of these data with a similar data set from samples collected over the Atlantic indicates that the departures from seawater composition are significantly larger for the Pacific. Differences in sea-to-air fractionation processes, probably involving binding of divalent cations to organic matter in the oceanic surface microlayer, are suggested as being responsible for these observations.

INTRODUCTION

Reasons to study atmospheric aerosol composition over the oceans have been indicated by several authors [see *Duce et al.*, 1976; *Berg and Winchester*, 1978]. One of the reasons given is that it is necessary to assess the impact of long-range transport of anthropogenic trace substances on the composition of the marine atmosphere on a global scale to be able to estimate the possible effects on the earth's radiation balance and eventually on climate. Other reasons are related to several aspects of geochemistry, including the deposition of eolian terrestrial material and of air pollutants onto the ocean surface and their contribution to marine sediments [*Duce et al.*, 1980], as well as the transfer of particulate matter from sea to air and the possible fractionation effects involved. While it is now generally accepted that some fractionation of heavy metals may occur during sea to air transport, the presence or absence of such fractionation for the alkali and alkaline earth metals is still a controversial issue after more than 2 decades of debate [*Duce and Hoffman*, 1976; *E. Hoffman et al.*, 1980].

Over certain ocean areas, such as the North Atlantic, atmospheric aerosol composition has been investigated fairly intensively, either from large research vessels [e.g., *E. Hoffman et al.*, 1974; *Buat-Menard et al.*, 1974] or from island-based sites like Bermuda [*Duce et al.*, 1976; *Meinert and Winchester*, 1977]. Other ocean areas, including the eastern tropical Pacific, have received much less attention. *Nguyen et al.* [1974] measured SO_2 and sulfate on an expedition from France to the Antarctic, which covered a section of the eastern Pacific. *Barger and Garrett* [1976] determined organics in aerosol samples collected on a cruise from Panama to Ecuador via the Galapagos Islands. Measurements of mineral dust and sea salt over several parts of the equatorial Pacific were made by *Prospero* [1979] and *Prospero and Bonatti* [1969]. However, some of the collection techniques employed by these authors were not quantitative, no attempt was made to divide the aerosol into different size fractions, and the chemical analyses were rather limited.

It was indicated elsewhere [*Maenhaut et al.*, 1981*b*, 1983] that the high analytical sensitivity of the PIXE method allows the use of small battery-powered aerosol samplers, so that sampling at sea may be performed from small boats. This paper discusses elemental data mainly obtained by PIXE for size-fractionated aerosol samples collected on a sailboat trip between Panama and Tahiti.

Paper number 3C0417.
0148-0227/83/003C-0417$05.00

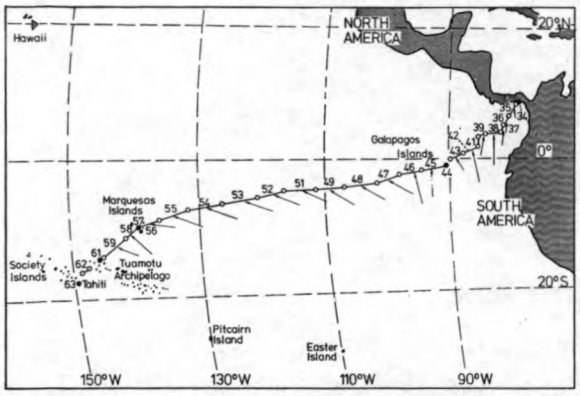

Fig. 1. Sampling track from Panama to Tahiti. Wind direction and speed are indicated by arrows. Arrow length indicates wind speed (e.g., that for sample number 35 represents 1 Beaufort, that for 39 is 2 Beaufort, and that for 45 is 3 Beaufort).

EXPERIMENTAL

Full details about the sampling procedure are given elsewhere [*Maenhaut et al.*, 1981*b*, 1983]. Basically, samples were taken by means of two 1 l/min six-stage Battelle-type cascade impactors [*Mitchell and Pilcher*, 1959], mounted side by side near the top of the mast of the 8.75 m long polyester sailboat *Simpla*, 8 m above the sea surface (6 m above deck) and 1 m upwind from the mast itself. The impactors have the following size cut-offs for stages 1–5: >4 μm, 4–2 μm, 2–1 μm, 1–0.5 μm, and 0.5–0.25 μm aerodynamic diameter (μmad). A 0.4-μm pore-size Nuclepore filter is used as the back-up filter (stage 6) for essentially quantitative collection of <0.25 μmad particles.

Samples were collected along a track between Panama and Tahiti, April–October 1979. The sampling intervals are shown in Figure 1, indicated by the numbers above line segments. In total, 27 duplicate impactor samples were collected, numbered from 34 to 63. Sample pairs 40, 50, and 60, not shown in the figure, were reserved as field blanks. To assess the effect of islands on the marine aerosol, some sample pairs were collected in harbors (i.e., numbers 34, 44, 57, 61, and 63). The arrows in Figure 1 represent the average wind direction during each sampling interval, where their length is a measure for the average wind speed (Beaufort scale). Other details about the sampling and some meteorological observations are summarized in Table 1. Most of the sample pairs (i.e., numbers 34–56) were collected in the second quarter of 1979. As a result, samples from along the first part of the track, up to about the Galapagos Islands, were collected in a region, which borders on, or partially lies within, the intertropical convergence zone (ITC). The winds experienced were rather variable and were sometimes very calm. West of sample pair 46, the wind blew consistently from the ESE direction, and it is evident that the second part of the track was sailed under the influence of the southern trade winds.

PIXE analysis of the samples was carried out by using 2.4 MeV protons, supplied by the compact isochronous cyclotron of the University of Ghent [*Maenhaut et al.*, 1981*b*]. The X ray spectra were fitted for 25 elements (i.e., Na, Mg, Al, Si, P, S, Cl, K, Ca, Ti, V, Cr, Mn, Fe, Ni, Cu, Zn, Ga, As, Se, Br, Rb, Sr, Pb, and Bi) by using the computer program AXIL [*Van Espen et al.*, 1979]. Although sodium was usually detected in the PIXE spectra, the stage 1 (>4 μmad)Na/Cl ratio could not be determined precisely owing to uncertainties in estimating the X ray attenuation corrections, which are higher for the soft Na K X rays than for those of heavier elements. (Our best estimates lead to a rather variable Na/Cl ratio which averages about half that in seawater.) For this reason, the PIXE Na results will not be further discussed. From the analysis of samples collected over the Atlantic Ocean [*Maenhaut et al.*, 1983] it was concluded also that magnesium is underestimated in our PIXE analysis when theoretical X ray absorption corrections are applied. However, the ratio between the Mg result computed from X ray data and the true concentration (based on assumed seawater ratios to higher Z sea-salt elements) was found to be constant over all samples and over the various impactor stages, and amounted to 0.70. The experimental Mg data in this work were therefore all empirically calibrated by dividing by this factor.

For certain elements (i.e., Cu, Zn, Pb and Bi) that were normally present at very low levels, inconsistent results were sometimes obtained, especially for stage 1 (>4 μmad), viz., discrepancies between the two duplicate samples of the same pair and data out of line compared to those of the other samples. The >4 μmad Pb and Bi amounts were also highly correlated and were nearly equal to each other in the different samples. These coarse particle results may be due to contamination from the aluminum alloy of the impactor itself, since analysis by spark source mass spectrometry showed that the Pb and Bi concentrations in the impactor material were both approximately 0.2% (A. Verbueken,

TABLE 1. Information About the Sampling Periods and Some Meterological Data

Sample Number*	Period, 1979	Location	Temperature,† °C	Relative Humidity,† %	Comments
34	April 25–27	Panama City	30	85	ships passing by
35–43	April 30 to May 16	Taboga-Galapagos	29	83	often rain
44	May 22–24	San Cristobal, Galapagos	27	85	sunny weather
45–56	June 2–25	Galapagos-Marquesas	28	84	little rain
57	July 25–27	Fatu Hiva, Marquesas	28	84	some rain
58–59	Sept. 2–6	Marquesas-Tuamotu	29	86	
61	Sept. 13–14	Rangiroa, Tuamotu	29	86	sunny weather
62	Sept. 14–16	Tuamotu-Tahiti	29	82	
63	Oct. 4–6	Papeete, Tahiti	29	72	close to highway

*Samples 34, 44, 57, 61, and 63 were collected in harbors, other samples at sea. Numbers 40, 50, and 60 refer to blanks. All samples were in duplicate (34A and 34B, etc.) and represent 40-hour sampling times (2 days, 20 hours/day excluding battery recharge times).

†Data listed are averages of measurements made aboard ship every 12 hours.

private communication, 1982). The fact of having two duplicate samples for each sampling period was very helpful in indicating any erratic data and allowed us to assess with a high degree of confidence when the data were trustworthy.

Selected impactor slides (i.e., stages 1, 2, and 3 of one of the two duplicate samples of pairs 46–56) were analyzed for Na, Cl, and Mg by instrumental neutron activation analysis (INAA). The INAA involved a 20-min irradiation at a thermal flux of 2×10^{12} n cm^{-2} s^{-1} followed by a 30-min count of the product nuclides ^{24}Na, ^{38}Cl, and ^{27}Mg with a large Ge(Li) detector. Concentrations were obtained by relating the activities of the samples to those of mixed standards. As the induced radioactivities in the samples were rather low (especially for ^{27}Mg), the samples were positioned as close as possible to the Ge(Li) detector. Irreproducibilities in sample positioning can therefore lead to large errors in the absolute concentrations, but the concentration ratios (e.g., Mg/Na, Cl/Na, Mg/Cl) should only marginally be affected. The average Mg/Cl ratio obtained for the 20 stage 1 and stage 2 impactor slides analyzed by INAA (Mg could not be detected in stage 3) was equal to 0.87 times the average Mg/Cl ratio obtained by PIXE (after applying the empirical correction factor of 0.7 for Mg as discussed above). This suggests that the accuracy of the PIXE Mg results is of the order of 10–15%.

Results and Discussion

The concentrations of sulfur and magnesium in the 2–4–μm aerodynamic diameter (μmad) size fraction, impactor stage 2, are plotted as a function of sample number in Figure 2*a*. Over the ocean, both elements mainly originate from the bursting of bubbles, at least for the large particle size range. Estimation of the crustal contribution to the stage 2 Mg concentrations (based upon the Fe concentration on stage 2, Fe_2, and the Mg/Fe ratio for crustal rock [*Mason*, 1966]) showed that it was less than 10% for nearly all samples. The S and Mg trends in Figure 2*a* are fairly parallel and illustrate the variability in concentration of the sea-salt component of the marine aerosol with sample location and time, as sampled by the impactors at mast height (8 m). In principle, also the S_1 and Mg_1 trends could be used to demonstrate this variability and even could be expected to be more representative, owing to the higher stage 1 than stage 2 concentrations. However, in an investigation of the marine atmosphere at Samoa [*Maenhaut et al.*, 1981*a*], a decreased stage 1 collection efficiency with increasing wind speed was observed, an effect that complicates the interpretation of the stage 1 concentration data. Concentrations on stage 2 were much less affected by wind speed. From the trends in Figure 2*a* it can be seen that S_2 and Mg_2 are on the average somewhat higher for the trade wind samples than for the ITC samples. This observation is in qualitative agreement with the generally higher wind speeds experienced in the region of the trades and with the well-established dependence of sea-salt generation on wind speed [*Woodcock*, 1953; *Lovett*, 1978].

Figure 2*b* shows the variation of silicon on stage 2, Si_2, and of the <1 μmad sulfur concentration, $S_4 + S_5 + S_6$, as a function of sample number. These two variation patterns are quite dissimilar from those for S_2 and Mg_2, with highest concentrations now being observed along the first part of the track. Up to the Galapagos Islands the fine S level remains rather constant and averages approximately 120 ng/m^3. At

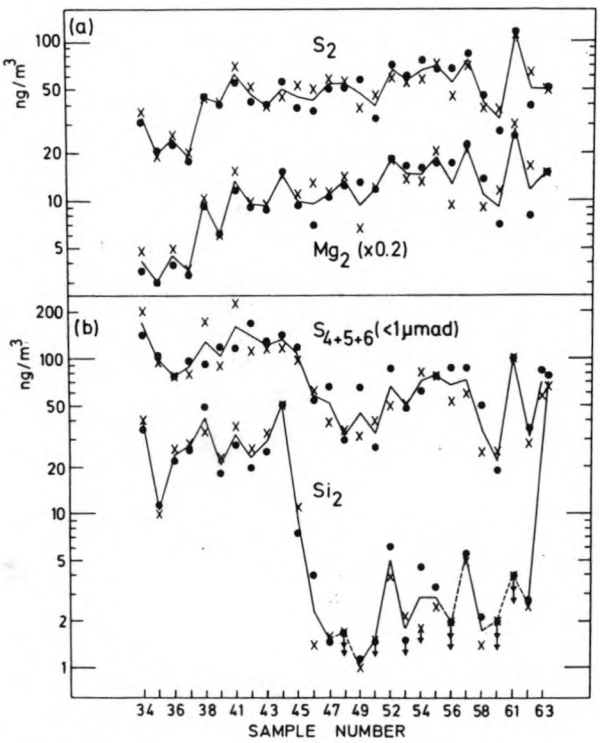

Fig. 2. Concentrations of S, Mg, and Si on stage 2(2–4 μmad) and of submicrometer S as a function of sampling location. Subscripts denote impactor stage numbers. The dots and crosses represent results obtained from duplicate impactors A and B, respectively. Upper limits are indicated by arrows.

sample 46, a sudden decrease is noticed, and the submicrometer S concentration remains around 50 ng/m^3 for the 10 subsequent sample pairs. At the end of the track, local maxima are noticed for samples collected in harbors (i.e., samples 61, 63, and, to a minor extent, also 57). The difference between the first and second part of the track is even more pronounced for Si_2, which shows average levels of 30 and 3 ng/m^3, respectively. The Fe_2 trend (not shown here) was fairly parallel to that for Si_2.

There are distinct differences between the first and the second part of the sailboat track: The first 10 sample pairs were collected relatively close to the South American continent, the other much farther away; the difference in meteorological conditions between ITC zone and trade wind region; and, finally, the trends of submicrometer S and of stage 2 Si. Because of these differences it seems appropriate to divide the samples in two separate sets. The first set was chosen to contain the sample pairs 35–45, excluding harbor sample 44, and the second set to contain pairs 46–56. Samples taken in harbors were excluded because of potential contribution from coastal or island-derived material so that both sets should only contain samples that are representative of marine air far from land, possibly influenced by long-range transport from the American continents. For each of the two sample sets average size distributions were calculated for various elements. For every sample, the elemental mass on each stage was first normalized by dividing by the total element mass summed over all stages to compensate for sample-to-sample variations in the total element concentrations. The results of the calculation are shown in Figure 3 for the elements that are present in large concentrations in

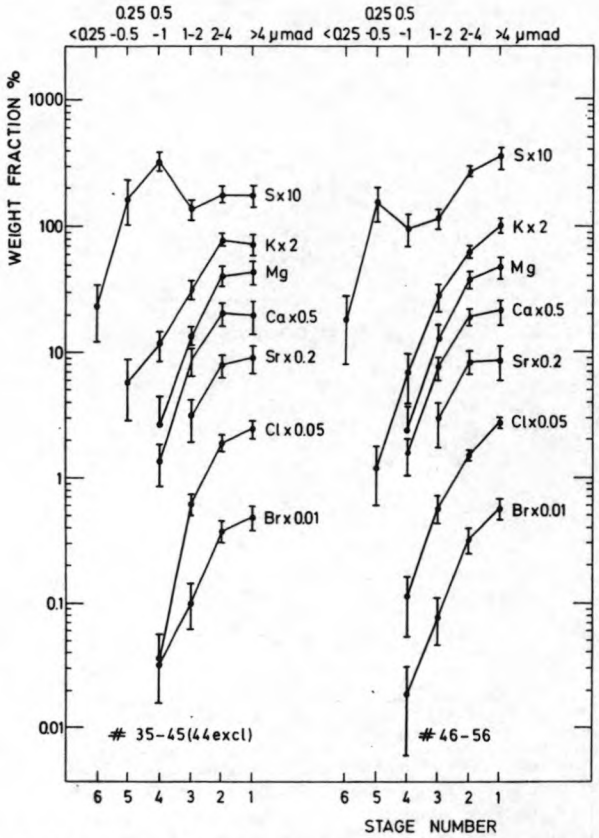

Fig. 3. Average size distributions for seawater elements.

seawater and in Figure 4 for the elements usually considered to originate from wind-blown crustal dust.

Mass median diameters (MMD's) were calculated for the various elements by plotting on logarithmic probability paper the cumulative mass percent versus aerodynamic particle size and linearly interpolating between (or extrapolating from) the two data points closest to the 50% 'cumulative mass.' The results are listed in Table 2. For the seawater cations (Mg, K, Ca, and Sr) the MMD's vary between 3 and 4 μmad. These values are significantly lower than the data for sea source elements reported by *McDonald et al.* [1981] and *Duce et al.* [1981]. Part of the discrepancy is certainly due to a lower collection efficiency for largest particles (>4 μmad) by our low volume samplers, an efficiency that also depends on wind speed. The Mg, K, Ca, and Sr size distributions for the first set of samples parallel each other fairly well in the coarse mode (>1 μmad). In the submicrometer size range (stages 4 and 5), however, the K percentages appear to be significantly higher than those for the other cations, suggesting an additional excess fine mode for K. This difference of the K size distribution is also reflected in a somewhat lower MMD. In the second set of samples, no excess fine K can be discerned. For this set, on the other hand, the K size distribution appears to be steeper than those for the other seawater cations, especially in the large particle mode. As a result, the MMD is here slightly higher for K than for Mg, Ca, and Sr.

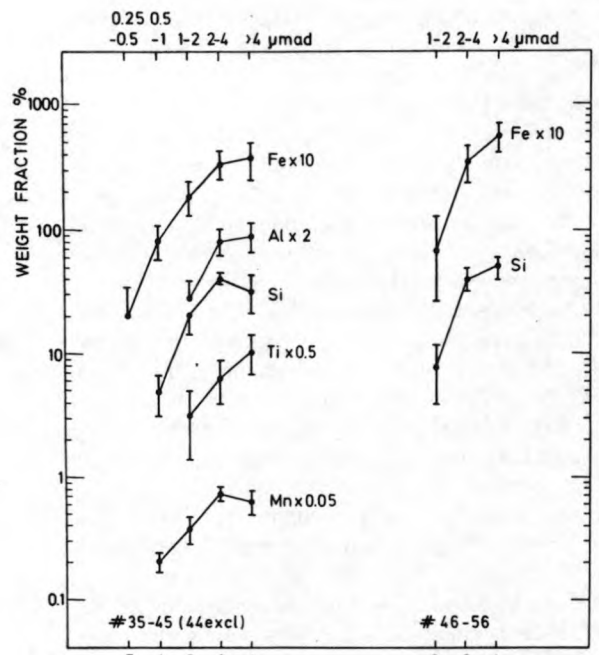

Fig. 4. Average size distributions for crustal elements.

Seawater Cations and Coarse Particle Sulfur

To investigate more closely the relationship among the different seawater cations and sulfur, interelement concentration ratios were calculated for stages 1, 2, and 3 and were normalized to the elemental ratios in seawater [*Riley and Chester*, 1971]. This procedure aids in determining whether simple dispersion of seawater is sufficient to account for aerosol composition or whether additional processes may be important (e.g., transfer of suspended particulate or surface active dissolved material from the sea surface, advection of airborne particles from terrestrial sources, or gas-particle interactions in the atmosphere). The resulting fractionation factors for K and Ca relative to Mg ($F_{Mg}(X)$, using the terminology of *Duce and Hoffman* [1976]), are plotted in Figure 5. For the first part of the track, the Mg, K, and Ca concentration data were corrected for a crustal contribution by using the Fe atmospheric concentrations and the Mg/Fe, K/Fe, and Ca/Fe concentration ratios in crustal rock [*Mason*, 1966]. The corrected net seawater fractionation factors are on the average about 0.7 times the initial values, indicat-

TABLE 2. Mass Median Diameters of Sea Salt and Crustal Elements

Element	Sample set 35–45*	46–56†
Mg	3.6	3.9
K	3.2	4.1
Ca	3.4	3.6
Sr	3.7	3.6
S	1.0	2.7
Cl	3.9	4.4
Br	3.9	4.5
Al	3.7	
Si	3.0	4.1
Ti	4.1	
Mn	2.9	
Fe	3.1	4.4

In μm aerodynamic diameter (calculated from average size distribution data plotted in Figures 3 and 4 (see text).
*Nine sample pairs, excluding 40 (blank) and 44 (harbor).
†Ten sample pairs, excluding 50 (blank).

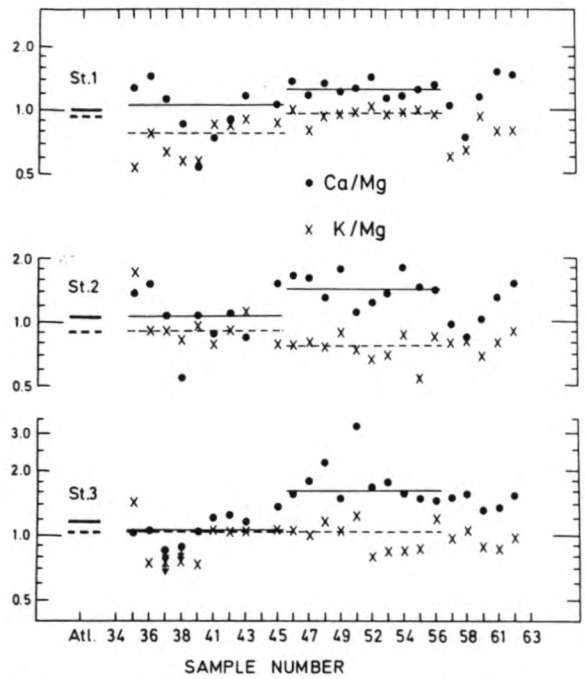

Fig. 5. Seawater fractionation factors for K and Ca relative to Mg as a function of sample number for >1-μmad particles, stages 1, 2, and 3. Data for sample numbers 35–45 were corrected for a crustal contribution (see text). Long horizontal lines represent median values for the 35–45 and 46–56 sample sets. Short horizontal lines at the left indicate average fractionation factors for a set of nine selected Atlantic sample pairs. Solid lines and dots apply to Ca, dashed lines and crosses to K.

ing a substantial crustal component for K and Ca. For the sample pairs 46–56, on the contrary, because of very low Fe concentrations the calculated crustal contribution in the K and Ca concentration data turned out to be less than 5% and was therefore neglected. Median values of the seawater fractionation factors for the first and second part of the track are indicated in the figure by horizontal lines. The data in Figure 5 are also compared with average fractionation factors, obtained for nine selected sample pairs collected over tropical and subtropical parts of the Atlantic Ocean under very clean conditions [*Maenhaut et al.*, 1983]. These nine Atlantic pairs showed low concentrations of fine S and of large particle Fe and Si, similar to the levels observed along the second part of the Pacific track.

The median seawater fractionation factors for the first set of samples are close to unity, indicating that for this section the crust-corrected levels of K, Ca, and Mg are in the same relative proportions as in unfractionated bulk seawater. These observations are in full agreement with those of *E. Hoffman et al.* [1980]. These authors found for samples collected at Bermuda that after subtracting a soil-derived component the Ca/Na, Mg/Na, and coarse particle K/Na ratios were within 10–20% of those in seawater. The situation is clearly different for the second set of samples (samples 46–56). For this section, the Ca fractionation factors appear to be systematically higher than those for K. The latter are relatively close to unity for all three impactor stages, with median values $F_{Mg}(K) = 0.97$, 0.78, and 1.04 for stages 1–3 respectively, whereas the corresponding median values for the Ca fractionation factor are $F_{Mg}(Ca) = 1.24$, 1.42, and 1.62. This suggests that the Ca enrichment in the 46–56 sample set increases with decreasing particle size.

To be more confident about this phenomenon, the fractionation factors with respect to K were also investigated (see Figure 6). Although Mg is normally considered to be a better seawater reference element than K, owing to the fact that its concentration is less influenced by crustal dust and that Mg is generally not fractionated relative to Na [*Duce and Hoffman*, 1976], PIXE Mg data should be treated cautiously because of the rather high corrections for X ray attenuation. The disadvantages of K as seawater reference element (i.e., eolian dust contribution and the presence of an excess fine K mode) do not seem to exist for the 46–56 sample set, as already was discussed earlier. For the 35–45 samples, on the other hand, the crust-derived K component was quite substantial, raising the question how to correct properly for this crustal component and what to use as reference soil or rock composition. It was therefore decided to plot uncorrected fractionation factors relative to K for all samples in Figure 6. As far as the $F_K(Ca)$ data are concerned, these uncorrected values are probably not too different from the crust-corrected data, as the Ca/K weight ratio of different soils and rocks is similar to that of bulk seawater where Ca/K = 1.01. The data in Figure 6 clearly indicate an enrichment of stage 2 and stage 3 Ca relative to K for the 45–56 sample set and confirm that the enrichment is higher for particles in the <4 μmad size range than for the larger particles. The median values of $F_K(Ca)$ in the second sample set are 1.30, 1.95, and 1.82 for stages 1, 2, and 3, respectively.

Another interesting feature of Figure 6 is that the S fractionation factors correlate well with the $F_K(Ca)$ values in the 46–56 sample set. This is especially evident for stage 2. Although the sulfur enrichments tend to be somewhat smaller than those for Ca, the $F_K(S)$ median values are also larger for stages 2 and 3 than for stage 1. The sulfur fractionation factors for the 35–45 sample set show a somewhat different

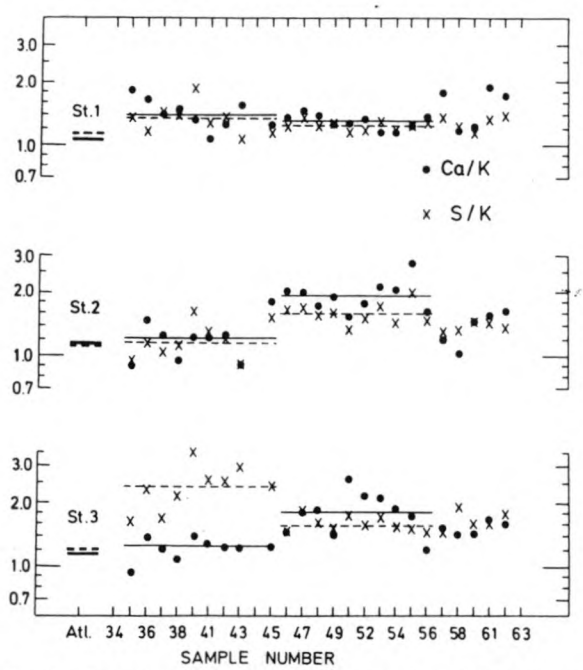

Fig. 6. Seawater fractionation factors for Ca and S relative to K as a function of sample number for >1-μmad particles, stages 1, 2, and 3. No corrections for crustal contributions were applied. See caption to Figure 5 for explanation of horizontal lines. Solid lines and dots apply to Ca, dashed lines and crosses to S.

picture and are more difficult to interpret in terms of sea spray fractionation because of the significant crustal contribution in K and because of the larger submicrometer S mode (see Figure 3), which may extend into the 1–2-μmad size range (stage 3). Except for some sample pairs collected in harbors, the Ca/Sr ratio was similar to that in bulk seawater and appeared to be fairly independent of stage number, even for the 46–56 sample set. The analytical errors associated with the individual Sr data were significantly larger than, for example, for K or Ca, owing to low Sr concentrations as well as lower PIXE sensitivity for heavier elements, but the absence of significant enrichment of Ca relative to Sr is demonstrated in Table 3, which lists average F_{Sr}(Ca) values for the 46–56 sample set as a function of stage number. Table 3 also gives average fractionation factors relative to K for the elements Mg, S, Ca, and Sr, and a comparison is made with data obtained for the 9 selected samples for the Atlantic track.

It is evident from Table 3 that there are substantial differences in fractionation factors between the Pacific and Atlantic sample sets. For the Atlantic samples the enrichment is less than 25% for all elements listed and for all impactor stages. The most significant deviations from unity are observed for sulfur. An enrichment of this element in the marine aerosol is not uncommon, and also in tracer experiments enrichments of 10–30% have been observed [*Garland*, 1981]. (Enrichments of the order of 10% in Table 3 should not be considered significant since the calibration of the PIXE set-up is only accurate to 5–10% for the elements S, Cl, K, and Ca.) For the 46–56 Pacific set, about half of the $F_K(X)$ values appear to be larger than 1.5. Since the same sampling equipment and the same PIXE set-up were used as for the Atlantic set, these deviations from unity are much greater than systematic errors in the analysis. Similarly to what we have already indicated for Ca and S, the Sr enrichments relative to K also vary with stage number in the 46–56 Pacific set, and they are significantly larger in the <4 μmad fractions than for the coarser particles. The same trend may even exist for Mg, although lower precision of the individual Mg data and the possibility of systematic errors precludes drawing firm conclusions for this element.

TABLE 3. Seawater Fractionation Factors for Sea-Salt Cations and Sulfur; Comparison of 46–56 Sample Set With Selected Atlantic Samples

Stage Number	1	2	3	4
	Pacific (46–56 Sample Set, n = 10)			
F_{Na}(K)*	1.15 ± 0.06	1.25 ± 0.12	1.31 ± 0.31	
F_K(Mg)	1.04 ± 0.08	1.38 ± 0.25	1.02 ± 0.17	
F_K(S)	1.25 ± 0.06	1.60 ± 0.19	1.61 ± 0.13	
F_K(Ca)	1.31 ± 0.09	1.97 ± 0.35	1.82 ± 0.42	1.57 ± 0.45
F_K(Sr)	1.23 ± 0.39	1.96 ± 0.29	1.47 ± 0.25	
F_{Sr}(Ca)	1.09 ± 0.30	1.11 ± 0.28	1.21 ± 0.26	
	Atlantic (9 Selected Sample Pairs, n = 9)			
F_K(Mg)	1.07 ± 0.11	1.10 ± 0.27	0.97 ± 0.18	
F_K(S)	1.13 ± 0.06	1.12 ± 0.13	1.21 ± 0.13	
F_K(Ca)	1.07 ± 0.09	1.15 ± 0.23	1.15 ± 0.15	1.05 ± 0.30
F_K(Sr)	1.07 ± 0.25	1.22 ± 0.44	0.98 ± 0.29	
F_{Sr}(Ca)	1.01 ± 0.20	1.01 ± 0.20	1.03 ± 0.10	

Values listed are averages and standard deviations, based on n sample pairs, defined, for example, by $F_K(Mg) = (Mg/K)_{sample}/(Mg/K)_{reference}$ where seawater is the reference composition.

*Obtained by combining the PIXE K/Cl ratio with the INAA Na/Cl ratio. Values listed are the averages of the 10 samples analyzed by INAA.

By combining the PIXE and INAA results for the impactor slides analyzed by both methods, fractionation factors relative to Na could be calculated. The average F_{Na}(K) values obtained are included in Table 3. The results suggest that K itself is perhaps slightly enriched relative to Na in the 46–56 Pacific set and that its enrichment increases somewhat with decreasing particle size. Consequently, the increase in enrichment with stage number observed for Ca, S, and Sr will even be accentuated if Na instead of K is selected as reference element.

Differences between the alkali-alkaline earth and large particle sulfur interelement ratios in the marine aerosol and in bulk seawater have been reported in several papers. However, in most cases these discrepancies can be attributed to the presence in the marine aerosol of a component not originating from bubble bursting, such as windblown crustal dust [*Duce and Hoffman*, 1976; *E. Hoffman et al.*, 1980; *Buat-Menard et al.*, 1974]. Such an explanation can be excluded here as the S, Ca, and Sr enrichments are observed for samples, collected far away from land and showing very low concentrations of Si and other crustal elements. Moreover, the Ca/K and also Sr/K ratios appeared to be closer to the bulk seawater values for the 35–45 sample set, which was collected closer to the continent and showed much larger Si concentrations. Also, the fact that the Ca/Sr ratios are about the same as in seawater is evidence against the presence of carbonate sands or gypsum, which have much larger Ca/Sr ratios than the seawater ratio of 50. (The sample pair 44, collected in a harbor of San Cristobal, Galapagos Islands, and having F_K(Ca) values of 13.8, 8.0, and 5.4 for stages 1, 2, and 3, respectively, showed F_{Sr}(Ca) values of 2.6, 2.4, and 2.0 for the same three stages. This is consistent with a Ca/Sr ratio of at least 100 in an excess component, which is certainly of local origin.) It should be emphasized here that the enrichments observed for the 46–56 sample set may have gone unnoticed if bulk filter samplers had been used. Indeed, as more than 40% of the K, Ca, and Sr mass sampled is contained in >4 μmad particles, and this fraction is probably less than in the atmosphere because of our sampler bias against the coarsest particles, the enrichments for the total aerosol are likely to be similar to those observed for stage 1, thus around 30% or less.

The particle-size dependent enrichment of S in the >1 μmad range and of Ca and Sr for the 46–56 sample set can virtually only be explained as originating from true sea-to-air fractionation processes. Bursting bubbles, generated as a result of wave action and believed to be the major source of sea spray [*Blanchard and Woodcock*, 1957, 1980], effectively skim the sea surface microlayer so that the sea-salt particles are produced from a thin layer, which may have a composition different from that of bulk seawater. *MacIntyre* [1974] reviewed several physical mechanisms, proposed in the literature to explain the enhancement of ionic species at the air/sea interface, but he concluded that they only affect ionic concentrations to a depth of a few molecular layers, with Gibbsian adsorption being a possible exception. He also suggested that binding to organic molecules may be a possibility and pointed out that divalent cations such as Ca^{2+} are more strongly bound than monovalent ions (e.g., Na^+). As the concentration ratio of organic material to Na tends to increase with decreasing particle size, enrichments of diva-

lent cations in the small particle size range look quite reasonable to him. This is almost exactly what we observe in the 46–56 sample set. In addition, these samples were collected over an area of the Pacific with relatively large primary productivity owing to moderate upwelling near the equator [see, e.g., *Lieth and Whittaker*, 1975], and the potential of enhanced organic concentrations in the surface microlayer is certainly present. However, as the primary productivity is of the same order or even higher in the section of the eastern equatorial Pacific between Panama and the Galapagos Islands, where no significant enrichment of Ca is observed, the picture is certainly more complicated. In any case, on the basis of the results observed here, it can be argued that sea-to-air fractionation effects exist in the alkaline earth elements (and in S in >1-μmad particles), but they apparently depend on what part of the ocean is under investigation and perhaps also upon other factors such as season and sea state.

Halogens Cl and Br

The average size distributions for the elements Cl and Br (Figure 3) are somewhat steeper than those obtained for most alkali and alkaline earth elements. This phenomenon is also reflected in the slightly larger MMD's for the halogens (see Table 2). Average Cl and Br fractionation factors relative to K are listed in Table 4 for the second part of the Pacific track together with those for the nine selected Atlantic sample pairs. Table 4 also contains Cl fractionation factors relative to Na as derived from the INAA analysis. The Cl/Na ratios could be measured very precisely with this technique, and their accuracy is estimated to be as good as 2–3%. The F_K(Cl) and F_K(Br) values for the 46–56 Pacific samples decrease significantly with decreasing particle size, but this trend is in part caused by the slight increase in K enrichment relative to Na as a function of stage number. The F_{Na}(Cl) value remains very close to unity for stages 1 and 2 but is reduced to 0.8 for stage 3. Apparent Cl fractionation factors, lower than unity and decreasing with decreasing particle size, have been reported by several authors [*Martens et al.*, 1973; *Wilkniss and Bressan*, 1972; *Meinert and Winchester*, 1977] and are normally explained as resulting from Cl loss to the gas phase after the sea-salt particles have been formed. Reactions of unfractionated NaCl with gaseous acids and/or oxidants are considered to be the major mechanisms. This may especially be true for the marine aerosol over those parts of the oceans that are strongly influenced by continental and polluted air, such as large sections of the North Atlantic. In such areas a virtual absence of Cl in the 0.25–1–μmad size range is not uncommon [*Meinert and Winchester*, 1977; M. Darzi and J. W. Winchester, unpublished results, 1980; *Maenhaut et al.*, 1983]. However, it remains somewhat controversial if an aerosol Cl deficit also exists in the 'clean' marine atmosphere. The data in Table 4 indicate that this Cl deficit is very small for the second part of the Pacific track, at least for particles >1 μmad (stages 1, 2, and 3). From the F_{Na}(Cl) data in Table 4 and the average Cl size distribution, a total Cl deficit of 5% can be calculated for the >1 μmad size fraction. As the submicrometer Na concentrations are expected to amount to less than 5% of the total Na levels the bulk Cl deficit (thus summed over all stages) is certainly less than 10%. The situation appears to be somewhat different for the clean Atlantic samples. Although Na was not measured in these samples, the F_{Na}(Cl) values are not expected to deviate much from the F_K(Cl) data as no significant alkali-alkaline earth fractionations were observed here. The Cl deficit for these samples, collected over clean tropical and subtropical parts of the North Atlantic, is in qualitative agreement with measurements made by *Kritz and Rancher* [1980]. Their Whatman filter samples, collected over the equatorial Atlantic off the West African coast, showed Cl/Na ratios varying from 0.64 to 1.60 (median: 1.27), which are lower than 1.81, the Cl/Na ratio in bulk seawater. The fact that the Cl deficit is apparently less pronounced over the clean Pacific may indicate that the concentrations of the gaseous compounds responsible for the Cl loss are lower there than over clean Atlantic regions. Any Cl loss from the aerosol may also be latitude dependent, since investigations in southern temperate latitudes indicate the absence of a Cl deficit in the marine aerosol or even a possible Cl enrichment [*Andreae*, 1982; *Lawson*, 1978].

The F_K(Br) data in Table 4 closely follow the same trend, as a function of particle size, as do the F_K(Cl) values. However, when fractionation factors relative to Cl, F_{Cl}(Br), are calculated, a moderate U-shaped behavior, displaying a minimum for the 1–2–μmad size range, becomes apparent. The F_{Cl}(Br) data, observed here for the 46–56 sample set are quite similar to those obtained by *Moyers and Duce* [1972] for samples collected at Hawaii. Although the F_{Cl}(Br) values for the clean Atlantic samples are all substantially lower, they still show the same differential behavior. Such a behavior can be explained as resulting from an exchange of Br between the particulate and gas phases. Photochemical reactions, such as discussed by *Zafiriou* [1974], may play an important role [see also *Rancher and Kritz*, 1980].

TABLE 4. Seawater Fractionation Factors for Cl and Br. Comparison of 46–56 Sample Set With Selected Atlantic Samples

Stage Number	1	2	3	4
	Pacific (46–56 Sample Set, n = 10)			
F_{Na}(Cl)*	0.96 ± 0.03	0.95 ± 0.03	0.81 ± 0.15	
F_K(Cl)	0.82 ± 0.04	0.74 ± 0.09	0.59 ± 0.19	0.49 ± 0.09
F_K(Br)	0.79 ± 0.12	0.73 ± 0.18	0.39 ± 0.12	0.36 ± 0.09
F_{Cl}(Br)	0.97 ± 0.17	0.99 ± 0.25	0.60 ± 0.14	0.78 ± 0.13
	Atlantic (9 selected sample pairs, n = 9)			
F_K(Cl)	0.91 ± 0.07	0.72 ± 0.11	0.61 ± 0.11	0.43 ± 0.15
F_K(Br)	0.57 ± 0.15	0.44 ± 0.18	0.28 ± 0.12	0.30 ± 0.09
F_{Cl}(Br)	0.62 ± 0.14	0.59 ± 0.20	0.46 ± 0.16	0.68 ± 0.30

Values listed are averages and standard deviations, based on *n* sample pairs.

*Derived from the INAA Cl/Na ratio. Values listed are the averages of the 10 samples analyzed by INAA.

Crustal Component

In the above discussions it was tacitly assumed that large particle Si and Fe are from earth crustal origin. Evidence that this supposition is at least warranted for the first part of the Pacific track is presented in Figure 7, which shows concentration ratios to Fe for the >1 μmad size range. Although Figure 4 suggests that the size distributions for the different soil elements may not be identical, the ratios to Fe were averaged over stages 1, 2, and 3 for every individual sample, and the means of these ratios are plotted in Figure 7. It is evident from this figure that the Si/Fe and Mn/Fe ratios vary but little as a function of sample number. Somewhat more scatter is observed for the Al/Fe and Ti/Fe ratios, but

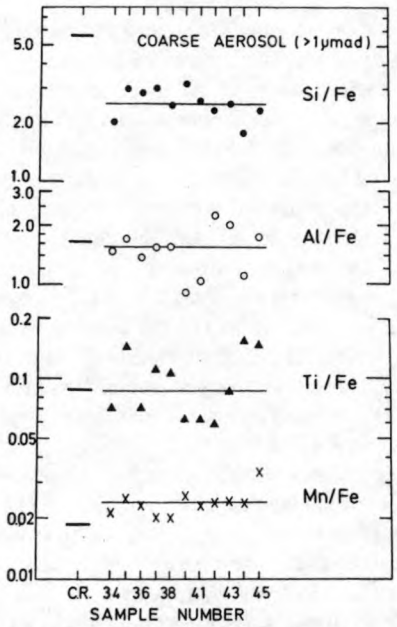

Fig. 7. Ratios of crustal elements to Fe, averaged over >1-μmad fractions, stages 1, 2, and 3, as a function of sample number. Short horizontal lines at the left indicate ratios in average crustal rock according to *Mason* [1966].

most data points still lie within ±50% of the median values. Except for the Si/Fe ratio, the median values appear to be very close to Mason's ratios for crustal rock [*Mason*, 1966]. Low Si concentrations relative to the other crustal elements are, however, not uncommon [see, e.g., *Rahn*, 1976*a*], and they were suggested by *Rahn* [1976*b*] to be due to crust-to-air fractionation.

The crustal component in the samples collected between Panama and the Galapagos Islands is almost certainly from eolian origin, due to long-range transport of wind-blown crustal dust from arid regions in the American continents. Using collection techniques, which were quite different from ours and which discriminated against the collection of particles smaller than several micrometers, *Prospero and Bonatti* [1969] found mineral dust concentrations of 0.3–0.6 $\mu g/m^3$ in the same region, and they suggested that the dust was derived from arid regions of western and southern Mexico. On the basis of a geometric mean Fe_2 concentration of 7.5 ng/m^3 (geometric standard deviation = 1.63) for the 35–45 sample set and the average Fe size distribution in Figure 4, we obtain a total Fe concentration of 22 ng/m^3, which can be converted to an estimate of 0.44 $\mu g/m^3$ for the total crustal component. This value is remarkably similar to those of *Prospero and Bonatti* [1969], although the agreement may be somewhat fortuitous, considering that not only sampling techniques but also methods of analysis were quite different.

The size distributions and mass median diameters for the crustal elements resemble those of the sea-salt elements. This observation may be surprising as long-range transport of crustal dust is expected to shift the MMD's to lower values, owing to the shorter atmospheric residence times expected for larger particles [*Junge*, 1963]. However, in samples collected over the tropical Atlantic Ocean, *Maenhaut et al.* [1983] noticed that the size distributions of the crustal elements remained relatively unchanged up to a few thousand kilometers west of the African continent, although the total dust concentration decreased by about 2 orders of magnitude. Interaction of the crustal dust with the sea surface or marine aerosol, perhaps by resuspension of floating dust during sea spray formation or by coagulation processes in the atmosphere, may be responsible for these observations.

West of the Galapagos Islands (i.e., for the 46–56 sample set), the geometric mean Si and Fe concentrations were 4.8 and 3.3 ng/m^3, respectively, 11 and 7 times lower than the corresponding values for the 35–45 sample set. On the basis of the Fe level, an average concentration of 0.066 $\mu g/m^3$ for the crustal component can be estimated, which is again rather similar to the range of 0.04–0.2 $\mu g/m^3$ observed by *Prospero and Bonatti* [1969] for the same region. These authors assumed that the dust originated from arid areas along the coast of Peru and northern Chile. However, the size distributions of Si and Fe are still heavily weighted toward the coarse particles and show a fairly good resemblance with those of Mg and K (compare also the mass median diameters). Therefore, both elements could be mainly sea surface derived (e.g., due to reinjection in the air of crustal-like material present in the sea surface microlayer). *G. Hoffman et al.* [1974] calculated that the lifetime in the oceanic surface microlayer of directly deposited atmospheric dust is at most only a few seconds. In a sample set, collected at Samoa, *Maenhaut et al.* [1981*a*] observed a nonseawater component of coarse particle size, consisting of Fe, Ti, and other elements, and they suggested it to be of sea surface origin. The size distributions for these elements were significantly steeper than those for the seawater elements, with >90% contained in >4 μm particles, and the interelement ratios were quite different from those in crustal rock. These elements may have been associated with surface active material of biological origin, not crustal dust per se, and rendered airborne by bubble bursting. Although processes qualitatively similar to those suggested for the Samoa aerosol may also have been operative on the open ocean, their quantitative aspects should depend on the possibly patchy distribution of biological material in the surface of the ocean. Their importance for the observed Fe and Si concentrations in the samples collected west of the Galapagos Islands cannot be judged with certainty.

Submicrometer S and K

A comparison between the different seawater cation size distributions in Figure 3 suggests the presence of a small excess fine mode for K in the 35–45 sample set. This excess fine mode was quite significant in certain sample pairs as is demonstrated in Figure 8*a*, which presents excess K and S concentrations in the <1 μmad range as a function of sample number. The excess concentrations were obtained by overlaying the K or S size distribution plot on that of Mg, and vertically shifting the plots until a match was obtained for the coarse particle sizes (stages 1, 2, and 3). The excess K or S concentrations were then estimated by reading on the K or S plot the concentrations that would be expected on the submicrometer stages if the same size distribution would hold as for Mg and by then subtracting these expected concentrations from the experimental data points. Similar procedures for resolving a fine aerosol component have been applied previously by *Winchester et al.* [1981*a*, *b*, *c*].

From the trends in Figure 8*a* it appears that there is some degree of correlation between the excess fine K and S

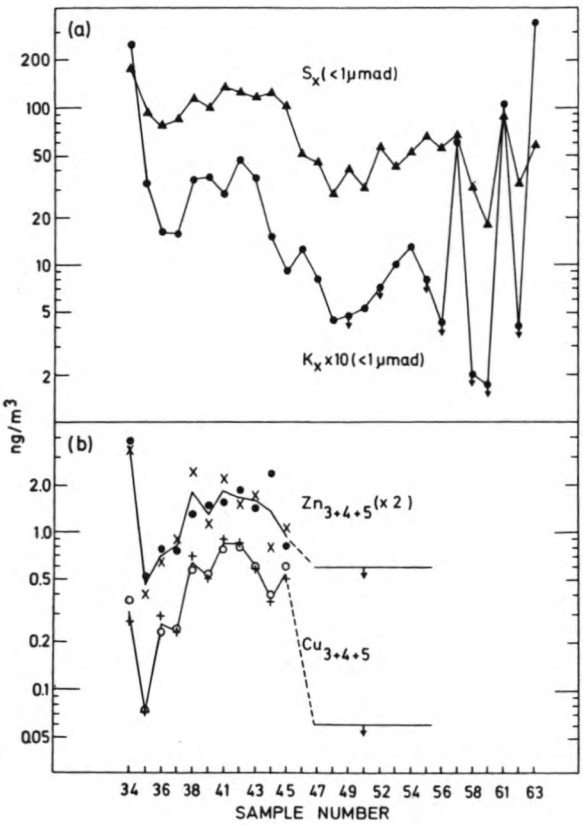

Fig. 8. Variation as a function of sample number of excess S and K concentrations in <1-μmad particles, and of Cu and Zn concentrations in the 0.25–2–μmad size range (sum of stages 3, 4, and 5). Subscript x denotes excess. Upper limits are indicated by arrows.

concentrations. However, the local maxima at harbor sample pairs 34, 57, 61, and 63 are much more pronounced for K than for S. As these sample pairs were all collected near inhabited areas, the fine K maxima may be attributed to a local source, which is likely to be biomass or fossil fuel burning. Burning of organic material in forested and agricultural areas has been shown to release fine particulate potassium [*Leslie*, 1981] and has been suggested as a major source for the excess submicrometer potassium mode observed in non-urban South American aerosol samples [*Lawson and Winchester*, 1978]. According to L. C. Boueres (personal communication, 1981), the agricultural burning of biomass releases fine particles with a S/K ratio near 0.7, and this ratio increases during airmass aging (1–3 days) to about 2. In samples collected near Brasilia and in the Goias Province, Brazil, submicrometer S/K ratios of around 1 have been observed [*Lawson and Winchester*, 1978]. The excess fine S/K ratios found in sample pairs 34, 57, 61, and 63 are, 7, 11, 8, and 1.6, respectively. This suggests that agricultural biomass burning may not be the dominant source of fine mode sulfur in these samples, except perhaps for sample pair 63. However, as the excess fine S level tends to peak at those same sample pairs, a contribution from local land-based sulfur sources seems nevertheless to be likely.

The geometric means and standard deviations of excess fine S concentrations are 104(1.21) and 46(1.33) ng/m^3 for the nine 35–45 and ten 46–56 sample pairs, respectively. These levels resemble those observed at other remote tropical and southern hemisphere sampling sites [*Lawson and Winchester*, 1979]. Oxidation of biogenic sulfur gases (e.g., dimethyl sulfide) to SO_2, followed by its conversion to sulfate, is believed to be a major source mechanism of excess aerosol sulfur in the natural marine atmosphere [*Bonsang et al.*, 1980]. Using estimates for the sea-to-air transfer rate of DMS, *Andreae* [1982] was able to explain an excess S concentration of 177 ng/m^3. If one takes into account that the samples in this work were collected over an oceanic area with substantial primary productivity, it seems justified to attribute our excess fine S levels to a similar source mechanism. The fact that the excess fine S concentration is about 2 times larger in the 35–45 sample set than in the 46–56 samples may be related to an enhanced productivity near the continent. However, the correlation between the excess fine sulfur and mineral dust (see also Figure 2*b*) suggests that at least a fraction of the submicrometer sulfur may be of continental origin in the former samples.

The excess fine K concentrations observed in the open ocean samples are somewhat difficult to explain. If they are related to biomass burning on the American continents, one could expect that the excess S to K concentration ratio, S_x/K_x, would increase with sample location east to west, in view of the fact that submicrometer sulfur is likely to be a secondary aerosol component, and potassium only primary, and also that the ocean is a potential source region of trace sulfur gases. Although there is some indication of an excess fine S to K ratio increase (the ratio ranged from 40 to over 80 in the sample pairs 46–55, versus from 30 to 50 in the samples 35–43), the difference is small and the trend is approximate. *Buat-Menard et al.* [1974] suggested that chemical fractionation processes during bubble bursting may be a source of excess fine K over productive waters, but this mechanism was considered unlikely by *E. Hoffman et al.* [1980]. It is possible that differences in air mass transport paths and in biomass burning source areas may be responsible for our observations. It also should be realized that the excess fine K mode was very low in the 46–56 sample set and is subject to uncertainties by our graphical subtraction procedure for resolving the fine component. In addition, several excess fine K data are only upper limit points.

Heavy Metals

Copper and zinc concentrations in the 0.25–2 μmad particle size range, the sum of stages 3, 4, and 5, are plotted as a function of sample number in Figure 8*b*. Both elements were also often detected on stages 1 and 2 in concentrations similar to or somewhat higher than those observed in <2 μmad particles, but the agreement between the two duplicate samples of each pair was not so good, partially as a result of larger blank corrections owing to the use of a larger proton beam area [*Maenhaut et al.*, 1981*b*]. Of the other heavy metals, arsenic and especially selenium were often detected, but only in 1–2–μm particles (stage 3) and at concentrations of about 0.2 and 0.1 ng/m^3, respectively. Although these As and Se data are of the same order as those reported for the marine atmosphere by *Walsh et al.* [1979] and *Mosher and Duce* [1981], they are only semi-quantitative as they were only slightly above the detection limits.

The Cu and Zn concentrations in the 0.25–2–μmad range, Figure 8*b*, are greater than would be expected if crustal weathering products or seawater were their source. By using geometric mean concentrations for Cu_{3+4+5}, Zn_{3+4+5}, total Fe, total Mg, and published composition data for the source

materials (*Mason* [1966] for crustal rock, *Bowen* [1979] for bulk seawater), the following average ratios of aerosol composition to reference composition (fractionation factors) are obtained for the 35–45 sample set: $F_{Fe,crust}(Cu) = 17$, $F_{Fe,crust}(Zn) = 19$, $F_{Mg,sea}(Cu) = 24000$, $F_{Mg,sea}(Zn) = 1800$. These ratios, of course, do not imply any specific process causing the observed aerosol composition, but they indicate that Cu and Zn are anomalously enriched elements (AEE), and the enrichments appear to be of the same order as those observed at other remote marine and continental locations [see, e.g., *Duce et al.*, 1975; *Adams et al.*, 1980]. Long-range transport from natural continental high-temperature sources, such as volcanoes, has been suggested to explain the atmospheric concentrations of the AEE and their occurrence in the fine particle size range [*Duce et al.*, 1975; *Maenhaut et al.*, 1979]. The AEE are also enriched in aerosols from fuel combustion [*Dams and De Jonge*, 1976; *Rahn*, 1976*a*; *Winchester et al.*, 1981*a*]. Evidence supporting a noncrustal continental source is found here in the fact that the Cu and Zn size distributions are much flatter than those for the crustal and sea-salt elements and also in the variability with sample number. Indeed, in the samples collected west of the Galapagos Islands, where the crustal component decreased significantly, Cu and Zn were below the detection limit in the 0.25–2–μmad size range. However, the ocean itself should not be completely ruled out as a possible source of Cu and Zn [*Duce et al.*, 1976; *Cattell and Scott*, 1978]. *Cattell and Scott* [1978] attributed Cu concentrations of several ng/m^3, observed in the vicinity of Tasmania, to a sea surface source. The decrease of atmospheric Cu levels farther from the continent, as noticed here, may then be related to the fact that Cu concentrations in sea water tend to be higher in near coastal areas [*Boyle et al.*, 1981].

Except for some sample pairs collected in harbors, heavy metals typical of anthropogenic liquid fuel combustion sources (i.e., Pb, V, and Ni) could not be detected. The upper limits for these and other elements in the 0.25–2–μmad size range are reported in Table 5. The Pb and V upper limits are similar to actual concentrations observed for these elements over the eastern Pacific by *Chow et al.* [1969] and *G. Hoffman et al.* [1969], and they indicate that the impact of leaded gasoline and heavy fuel oil burning on the aerosol composition in that area is quite low. Considering that only upper limits were obtained for several more elements, it may also be concluded that other industrial processes contribute little if anything to the total aerosol mass. West of the Galapagos Islands, the influence of even major natural continental source processes, such as crustal weathering, was rather minor, as could be deduced from the atmospheric Si and Fe levels.

TABLE 5. Upper Limits for Atmospheric Concentrations of Heavy Metals in the 0.25–2–μmad Size Range

Element	Upper limit, ng/m^3
V	<0.13
Cr	<0.09
Mn	<0.07
Ni	<0.04
Cu	<0.05*
Zn	<0.3*
As	<0.2†
Se	<0.15†
Pb	<0.9

*Apply only to the 46–56 sample set; see also Figure 8*b*.

†As was sometimes observed on stage 3 only, Se was often observed on that stage (see text).

SUMMARY AND CONCLUSIONS

On the basis of meteorological conditions and trends of coarse silicon and submicrometer sulfur concentration as a function of sampling sequence along a sampling track between Panama and Tahiti, April–October 1979, two regions with different aerosol composition could be discerned. Between Panama and the Galapagos Islands a substantial crustal component (geometric mean concentration = 0.44 μg/m^3), fine Cu and Zn and excess fine S and K were detected in addition to the major sea-salt elements. The crustal component is explained as resulting from long-range transport of wind-blown dust, probably originating in the vicinity of Central America. The elements Cu and Zn, present in the 0.25–2–μmad size range at geometric mean concentrations of 0.4 and 0.6 ng/m^3, respectively, were anomalously enriched with respect to either crustal rock or bulk seawater. Fuel combustion or geothermal emissions on the American continents are suggested as their principal source, but a possible sea surface origin should not be excluded. West of the Galapagos Islands, concentrations of all nonseawater components were significantly lower. In the 10 sample pairs collected between the Galapagos and the Marquesas, geometric mean Si and Fe concentrations were as low as 4.8 and 3.3 ng/m^3, respectively, corresponding to 0.066 μg/m^3 mineral dust, if both elements are assumed to be of terrestrial origin. Cu, Zn, and other heavy metals were absent in the 0.25–2–μmad size range, with upper limits between 0.05 and 0.15 ng/m^3 for the elements V, Cr, Mn, Ni, Cu, and Se. Excess sulfur in submicrometer particles averaged 46 ng/m^3, which is similar to values reported for other remote marine and continental sites. These results indicate that the marine atmosphere west of the Galapagos Islands was little influenced by natural continental source processes or by pollutant transport.

In this clean marine air, several concentration ratios among major seawater elements showed significant differences from those observed in bulk seawater. Ca, Sr, coarse S, and maybe also Mg to some extent, appeared to be enriched relative to K and Na, and the enrichment was substantially greater in <4 μmad particles than in coarser particles. True sea-to-air fractionation, perhaps involving binding of divalent cations to dissolved or particulate organic matter on the sea surface, is suggested to be likely. Comparison with a set of nine samples pairs, collected over the Atlantic Ocean under very clean conditions, indicated the absence of significant enrichment in the Atlantic samples, suggesting that the fractionation processes depend upon the area of the ocean investigated, and perhaps also upon other factors such as season and sea state. Chlorine and bromine were only slightly depleted in the marine aerosol when compared with bulk seawater, but the deficit increases somewhat with decreasing particle size. However, the total deficit, summed over all stages, was much smaller (i.e., only 5 to 10% for Cl) than has been reported in more polluted marine air. Excess fine S, but especially excess fine K, showed a tendency to exhibit highest values for sample pairs collected in harbors, suggesting local island-derived sources such as biomass and fossil fuel burning, to be responsible for the excess K and perhaps for a portion of the excess S.

Acknowledgments. We would like to thank J. Hoste for his continued interest and support throughout this work. J. Cafmeyer and L. Van 't dack provided valuable technical assistance and helped with the preparation of the manuscript. Two of us (W.M. and H.R.) are indebted to the Belgian Nationaal Fonds voor Wetenschappelijk Onderzoek for financial support. This work was supported in part by grants from the National Geographic Society and the North Atlantic Treaty Organization. Loan of sampling equipment from Florida State University and the U.S. Environmental Protection Agency greatly assisted the collection of samples.

REFERENCES

Adams, F., M. Van Craen, P. Van Espen, and D. Andreuzzi, The elemental composition of atmospheric aerosol particles at Chacaltaya, Bolivia, *Atmos. Environ., 14,* 879–893, 1980.

Andreae, M. O., Marine aerosol chemistry at Cape Grim, Tasmania and Townsville, Queensland, *J. Geophys. Res., 87,* 8875–8885, 1982.

Barger, W. R., and W. D. Garrett, Surface active organic material in air over the Mediterranean and over the eastern equatorial Pacific, *J. Geophys. Res., 81,* 3151–3157, 1976.

Berg, W. W., and J. W. Winchester, Aerosol chemistry of the marine atmosphere, in *Chemical Oceanography,* 2nd ed., vol. 7, edited by J. P. Riley and R. Chester, pp. 173–231, Academic, New York, 1978.

Blanchard, D. C., and A. H. Woodcock, Bubble formation and modification in the sea and its meteorological significance, *Tellus, 9,* 145–158, 1957.

Blanchard, D. C., and A. H. Woodcock, The production, concentration and vertical distribution of the sea-salt aerosol, *Ann. N.Y. Acad. Sci., 338,* 330–347, 1980.

Bonsang, B., B. C. Nguyen, A. Gaudry, and G. Lambert, Sulfate enrichment in marine aerosols owing to biogenic gaseous sulfur compounds, *J. Geophys. Res., 85,* 7410–7416, 1980.

Bowen, H. J. M., *Environmental Chemistry of the Elements,* Academic, New York, 1979.

Boyle, E. A., S. S. Huested, and S. P. Jones, On the distribution of copper, nickel and cadmium in the surface waters of the North Atlantic and Pacific Ocean, *J. Geophys. Res., 86,* 8048–8066, 1981.

Buat-Menard, P., J. Morelli, and R. Chesselet, Water-soluble elements in atmospheric particulate matter over the tropical and equatorial Atlantic, *J. Rech. Atmos., 5,* 661–673, 1974.

Cattell, F. C. R., and W. D. Scott, Copper in aerosol particles produced by oceans, *Science, 202,* 429–430, 1978.

Chow, T. J., J. L. Earl, and C. F. Bennett, Lead aerosols in marine atmosphere, *Environ. Sci. Technol., 3,* 737–740, 1969.

Dams, R., and J. De Jonge, Chemical composition of Swiss aerosols from the Jungfraujoch, *Atmos. Environ., 10,* 1079–1084, 1976.

Duce, R. A., and E. J. Hoffman, Chemical fractionation at the air/sea interface, *Ann. Rev. Earth Planet. Sci., 4,* 187–228, 1976.

Duce, R. A., G. L. Hoffman, and W. H. Zoller, Atmospheric trace metals at remote northern and southern hemisphere sites: Pollution or natural?, *Science, 187,* 59–61, 1975.

Duce, R. A., G. L. Hoffman, B. J. Ray, I. S. Fletcher, G. T. Wallace, J. L. Fasching, S. R. Piotrowicz, P. R. Walsh, E. J. Hoffman, J. M. Miller, and J. L. Heffter, Trace metals in the marine atmosphere: Sources and fluxes, in *Marine Pollutant Transfer,* edited by H. L. Windom and R. A. Duce, pp. 77–119, D. C. Heath, Lexington, Mass., 1976.

Duce, R. A., C. K. Unni, B. J. Ray, J. M. Prospero, and J. T. Merrill, Long-range atmospheric transport of soil dust from Asia to the tropical North Pacific: Temporal variability, *Science, 209,* 1522–1524, 1980.

Duce, R. A., C. K. Unni, B. J. Ray, P. J. Harder, A. P. Pszenny, and J. L. Fasching, The atmospheric concentration of trace metals and their deposition to the ocean at Enewetak Atoll, Marshall Islands, paper presented at the IAMAP Third Scientific Assembly, Hamburg, August 17–28, 1981.

Garland, J. A., Enrichment of sulphate in maritime aerosols, *Atmos. Environ., 15,* 787–791, 1981.

Hoffman, E. J., G. L. Hoffman, and R. A. Duce, Chemical fractionation of alkali and alkaline earth metals in atmospheric particulate matter over the North Atlantic, *J. Rech. Atmos., 8,* 675–688, 1974.

Hoffman, E. J., G. L. Hoffman, and R. A. Duce, Particle size dependence of alkali and alkaline earth metal enrichment in marine aerosols from Bermuda, *J. Geophys. Res., 85,* 5499–5502, 1980.

Hoffman, G. L., R. A. Duce, and W. H. Zoller, Vanadium, copper and aluminum in the lower atmosphere between California and Hawaii, *Environ. Sci. Technol., 3,* 1207–1210, 1969.

Hoffman, G. L., R. A. Duce, P. R. Walsh, E. J. Hoffman, B. J. Ray, and J. L. Fasching, Residence time of some particulate trace metals in the oceanic surface microlayer: Significance of atmospheric deposition, *J. Rech. Atmos., 8,* 745–759, 1974.

Junge, C. E., *Air Chemistry and Radioactivity,* Academic, New York, 1963.

Kritz, M. A., and J. Rancher, Circulation of Na, Cl and Br in the tropical marine atmosphere, *J. Geophys. Res., 85,* 1633–1639, 1980.

Lawson, D. R., Chemistry of the natural aerosol: a case study in South America, Ph. D. Dissertation, Florida State Univ., Tallahassee, Florida, 1978.

Lawson, D. R., and J. W. Winchester, Sulfur and trace element concentration relationships in aerosols from the South American continent, *Geophys. Res. Lett., 5,* 195–198, 1978.

Lawson, D. R., and J. W. Winchester, Atmospheric sulfur aerosol concentrations and characteristics from the South American continent, *Science, 205,* 1267–1269, 1979.

Leslie, A. C. D., Aerosol emissions from forest and grassland burnings in the southern Amazon Basin and central Brazil, *Nucl. Instr. Meth., 181,* 345–351, 1981.

Lieth, H., and R. H. Whittaker (eds.), *Primary Productivity of the Biosphere,* Springer-Verlag, Berlin, 1975.

Lovett, R. F., Quantitative measurement of airborne sea-salt in the North Atlantic, *Tellus, 30,* 358–364, 1978.

MacIntyre, F., Chemical fractionation and sea-surface microlayer processes, *Sea, 5,* 245–299, 1974.

Maenhaut, W., W. H. Zoller, R. A. Duce, and G. L. Hoffman, Concentration and size distribution of particulate trace elements in the South Polar atmosphere, *J. Geophys. Res., 84,* 2421–2431, 1979.

Maenhaut, W., M. Darzi, and J. W. Winchester, Seawater and nonseawater aerosol components in the marine atmosphere of Samoa, *J. Geophys. Res., 86,* 3187–3193, 1981*a*.

Maenhaut, W., A. Selen, P. Van Espen, R. Van Grieken, and J. W. Winchester, PIXE analysis of aerosol samples collected over the Atlantic Ocean from a sailboat, *Nucl. Instr. Meth., 181,* 399–405, 1981*b*.

Maenhaut, W., A. Selen, P. Van Espen, R. Van Grieken, and J. W. Winchester, Elemental concentrations in size-fractionated aerosols over the northeastern and tropical Atlantic, *J. Geophys. Res.,* in press, 1983.

Martens, C. S., J. J. Wesolowski, R. C. Harriss, and R. Kaifer, Chlorine loss from Puerto Rican and San Francisco Bay area marine aerosols, *J. Geophys. Res., 78,* 8778–8792, 1973.

Mason, B., *Principles of Geochemistry,* 3rd ed., John Wiley, New York, 1966.

McDonald, R. L., C. K. Unni, and R. A. Duce, Estimation of atmospheric sea salt dry deposition: Wind speed and particle size dependence, *J. Geophys. Res., 87,* 1246–1250, 1982.

Meinert, D. L., and J. W. Winchester, Chemical relationships in the North Atlantic marine aerosol, *J. Geophys. Res., 82,* 1778–1782, 1977.

Mitchell, R. I., and J. M. Pilcher, Improved cascade impactor for measuring aerosol particle sizes, *Ind. Eng. Chem., 51,* 1039–1042, 1959.

Mosher, B., and R. Duce, Vapor phase selenium compounds in the marine atmosphere, paper presented at the IAMAP Third Scientific Assembly, Hamburg, August 17–28, 1981.

Moyers, J. L., and R. A. Duce, Gaseous and particulate bromine in the marine atmosphere, *J. Geophys. Res., 77,* 5330–5338, 1972.

Nguyen, B. C., B. Bonsang, and G. Lambert, The atmospheric concentration of sulfur dioxide and sulfate aerosols over antarctic, subantarctic areas and oceans, *Tellus, 26,* 241–249, 1974.

Prospero, J. M., Mineral and sea salt concentrations in various ocean regions, *J. Geophys. Res., 84,* 725–731, 1979.

Prospero, J. M., and E. Bonatti, Continental dust in the atmosphere of the eastern equatorial Pacific, *J. Geophys. Res., 74,* 3362–3371, 1969.

Rahn, K. A., The chemical composition of the atmospheric aerosol, technical report, Graduate School of Oceanography, University

of Rhode Island, Kingston, 1976*a*.

Rahn, K. A., Silicon and aluminum in atmospheric aerosols: Crust-air fractionation?, *Atmos. Environ., 10,* 597–601, 1976*b*.

Rancher, J., and M. A. Kritz, Diurnal fluctuations of Br and I in the tropical marine atmosphere, *J. Geophys. Res., 85,* 5581–5587, 1980.

Riley, J. P., and R. Chester, *Introduction to Marine Chemistry,* Academic, New York, 1971.

Van Espen, P., H. Nullens, and W. Maenhaut, Computer evaluation of photon, electron, and proton-induced X-ray spectra, in *Microbeam Analysis—1979,* edited by D. E. Newbury, pp. 265–267, San Francisco Press, San Francisco, Calif., 1979.

Walsh, P. R., R. A. Duce, and J. Fasching, Tropospheric arsenic over marine and continental regions, *J. Geophys. Res., 84,* 1710–1718, 1979.

Wilkniss, P. E., and D. J. Bressan, Fractionation of the elements F, Cl, Na and K at the sea-air interface, *J. Geophys. Res., 77,* 5307–5315, 1972.

Winchester, J. W., Wang Mingxing, Ren Lixin, Lü Weixiu, H.-C. Hansson, H. Lannefors, M. Darzi, and A. C. D. Leslie, Nonurban aerosol composition near Beijing, China, *Nucl. Instr. Meth., 181,* 391–398, 1981*a*.

Winchester, J. W., Lü Weixiu, Ren Lixin, Wang Mingxing, and W. Maenhaut, Fine and coarse aerosol composition from a rural area in North China, *Atmos. Environ., 15,* 933–937, 1981*b*.

Winchester, J. W., Wang Mingxing, Ren Lixin, Lü Weixiu, M. Darzi, and A. C. D. Leslie, Aerosol composition in relation to air mass movements in north China, in *Atmospheric Aerosol: Source/Air Quality Relationships, ACS Symp. Ser. 167,* edited by E. S. Macias and P. K. Hopke, pp. 287–301, American Chemical Society, Washington, D. C., 1981*c*.

Woodcock, A. H., Salt nuclei in marine air as a function of altitude and wind force, *J. Meteorol., 10,* 362–371, 1953.

Zafiriou, O. C., Photochemistry of halogens in the marine atmosphere, *J. Geophys. Res., 79,* 2730–2732, 1974.

(Received February 16, 1982;
revised December 22, 1982;
accepted February 16, 1983.)

Selected article # 4:

Skin penetration of minerals in psoriatics and guinea-pigs bathing in hypertonic salt solutions

J. Shani, S. Barak, D. Levi, M. Ram, E.R. Schachner, T. Schlesinger, H. Robberecht, R. Van Grieken and W.W. Avrach

Pharmacological Research Communications, 17 (1985), 501-512

SKIN PENETRATION OF MINERALS IN PSORIATICS AND GUINEA-PIGS BATHING IN HYPERTONIC SALT SOLUTIONS

Shani, J.[1], Barak, S.[1], Levi, D.[1], Ram, M.[1], Schachner, E.R.[2], Schlesinger, T.[3], Robberecht, H.[3], Van Grieken, R.[3] and Avrach, W.W.[4]

[1]Dept. of Pharmacology, The Hebrew University School of Pharmacy, POB 12065, Jerusalem; [2]Asaf Harofe Hospital, Tzrifin; [3]Soreq Nuclear Research Center, Yavne; [4]Dept. Chemistry, University of Antwerp (UIA), B-2610 Wilrijk, Belgium and [4]Dept. of Dermatology, Hadassah-University Hospital, Jerusalem, Israel

Received in final form 15 February 1985

SUMMARY

Penetration of electrolytes through the human skin was measured in healthy volunteers and in psoriatic patients after bathing in the Dead-Sea or in simulated bath-salt solutions. Significant increases in the levels of serum Br, Rb, Ca and Zn were noticed only in the psoriatic patients after daily bathing in the Dead-Sea for a 4-week regimen. Guinea-pigs "bathed" in simulated Dead-Sea bath-salt solutions containing radionuclides of Ca, Mg, K and Br. Traces of each radionuclide were detected in the blood and in some internal organs after 60 minutes of bathing. The radionuclides showed a physiological pattern in their organ distribution.

Even though the whole investigation was carried out in hypertonic solutions, there is a definite penetration of salts through healthy (human and guinea-pigs) and damaged (psoriatic) epidermis. This finding suggests that improvement of the psoriatic condition after bathing in the Dead-Sea, may be partly attributed (in addition to ultraviolet irradiation) to the minerals' effect on the psoriatic skin.

0031-6989/85/060513-12/$03.00/0

INTRODUCTION

Our interest in penetration of minerals from hypertonic salt solutions into the human circulation emenates from investigating possible medical effects after bathing in the Dead-Sea. The Dead-Sea contains 300-320 g/l salts, of which KCl, $MgCl_2$, $CaCl_2$ and NaCl are the major ones (98% of the dried salt). The other two percent consist of bromide salts, heavy metals, trace elements and solids.

The balneo-therapeutic properties of the Dead-Sea have been known throughout the centuries, and have been documented since King Herod's time, but the first modern medical report on the effect of heliobalneotherapy at the hot spring of Zohar (Ein-Bokek) on psoriasis was published by Dostrovsky and Sagler only in 1959. Since then, various reports on improvement of psoriasis after bathing in the Dead-Sea have been published (Avrach, 1977a; Avrach, 1977b; Avrach & Niordsen, 1974; Montgomery, 1979), and a review on the medical properties of the Dead-Sea was published by Drugan in 1976 (6). The most recent study analyzed results in 1,631 patients who had stayed at Ein-Bokek under careful medical control for 4 weeks, 95% of them showing marked improvement (Montgomery, 1979). Because of the high rate of success in elimination of psoriatic plaques after bathing in the Dead-Sea, groups of psoriatic Danes came to the International Psoriasis Treatment Center (IPTC) in Ein-Bokek for climatotherapy, and one of those groups participated in our study.

Psoriasis is a complex proliferative skin disease, showing partially uncontrolled nonmalignant growth of the epidermis. Its etiology is unknown, but is apparently related to imbalanced cyclic nucleotides.

In such a case. a treatment for psoriasis should to a large extent be via the circulation, supplying some elemental ions for cAMP production. This aspect was studied for sodium, potassium (Hodgson, 1960), copper (Lipkin et al, 1962), selenium (Abboud, 1978) and bromine (Shani et al, 1982). Moreover, psoriasis has been treated successfully by salt combinations both externally (Justesen & Harkmark, unpublished) and internally (Troitskaia, 1965), and it was suggested that a possible mechanism of the latter treatment (NaBr administration) is partially via the known sedative effect of bromide on stress-induced psoriasis. We undertook to study whether and to what extent minerals are capable of penetrating the skin from an hypertonic solution as occurs in the Dead-Sea.

MATERIALS AND METHODS

Twenty-four healthy Israeli volunteers (12 males and 12 females, 20-48 years old) and 21 psoriatic Danes who came to Ein-Bokek for climatotherapy of their disease (10 males and 11 females, 16-60 years old), participated in this study. The healthy Israelis were divided into four groups of 6 each and bathed once only, for 30 minutes, either in the Dead-Sea or in 1.5%, 5% or 15% Dead-Sea bath-salt solutions, prepared by redissolving the dried Dead-Sea mixture and heating it to 37°C. Blood was withdrawn from their cuboidal vein before and immediately after bathing, after cleaning the area with water and then with 70° ethanol. Blood was withdrawn under similar conditions from the psoriatic Danes immediately after their arrival in Israel, again after their first 30-minute bathing, and once again after a 4-week stay in Ein-Bokek. All blood samples were left to clot at room temperature for 1 hour, the clot detached from the tube with a thin wooden applicator and the samples left refrigerated overnight for better separation. After decantation, 4-5 ml of each

untreated serum was used for bromine determination by a conventional wavelength-dispersive X-ray fluorescence (XRF) (Shani et al, 1982) and additional 250 µl aliquots were dried on a Mylar film and used for determination, in threshold, of Sr, Rb, Se, Fe, Ca, K, Zn and Cu, by an energy-dispersive XRF procedure (Roberecht et al, 1982). Sera were also analyzed for Na, Mg and Cr by Perkin-Elmer model 403 atomic absorption spectrophotometer, and Cl was titrated on a Radiometer model CMT-10 chloridometer. All participants consented to the study according to the Helsinki agreement. Significances of differences for all 5 groups (before and after bathing) were calculated by the Student's "t" test.

"Sabra" albino guinea-pigs, 250-300 g each, were used for our second experiment. Four radioisotopes of ions existing in significant quantities in the Dead-Sea were used: ^{47}Ca (Amersham), ^{28}Mg (BNL), ^{42}K and ^{82}Br (Soreq). Four groups of guinea-pigs were used for studying the penetration of each isotope: cycling, males, pregnant and lactating, 9-12 in each group. The guinea-pigs were carefully shaven, then injected IP with sodium pentobarbital 30 mg/kg and immersed, except for their heads, in a 37°C water-bath containing 15% Dead-Sea bath-salt solution with 10 µCi/l of each radionuclide. After 60 minutes of bathing, the guinea-pigs were taken out of the water-bath, rinsed under the tap, bled and decapitated. Liver, spleen, lungs, heart, brain, stomach, small intestine, skin, bone and kidneys were taken from all animals. Uteri and ovaries were taken from cycling guinea-pigs, testes from the males, placenta, amniotic fluid and fetus from the pregnant females. Milk was squeezed from the lactating mothers, from whom the pups had been removed the night before. All organs were sampled, weighed and counted. CPM/g and organ-to-blood ratios were calculated for all organs sampled.

RESULTS

Elemental analysis of human serum revealed significant penetration of four ions through the psoriatic skin, and only penetration of one ion through the healthy skin, after bathing in the Dead-Sea for one month and 30 minutes respectively (Table 1). No increase in the levels of any of the ions measured was detected in the healthy volunteers after their 30-minute bathing in the simulated bath-salt solutions (Table 1. 1.5% salt solution not shown). The ions elevated in the sera of the psoriatic patients after one month of daily bathing in the Dead-Sea were Br, Rb, Ca and Zn. Even though the serum was concentrated before its analysis, and the detection limits were low (0.06 - 4 μg/l), only 9 elements could be analyzed by XRF and 4 by atomic absorption. Further lowering of these detection limits by a factor of 10 could not have made it possible to determine more elements (Robberecht et al, 1982).

Analysis of penetration of radionuclides through the guinea-pig skin demonstrate that the same radionuclide accumulate in the same internal organs in all four groups studied - pregnant, lactating and cycling females, as well as in the mature males. Of high significance were the following elemental retentions: ^{47}Ca concentrated over 270-fold in the skin and significantly also in the bone, spleen, milk and ovaries; ^{28}Mg concentrated in the skin, ovaries, spleen, heart and bone; ^{42}K was absorbed in the skin, and found its way to the bone, ovaries, spleen and amniotic fluid, while ^{82}Br concentrated in the skin, testes and bone, but not in the spleen (Table 2-results for pregnant and lactating animals not shown). Some sporadic uptake was noticed for some of the radionuclides in other organs, i.e. ^{42}K in uteri of cycling animals and ^{82}Br in pregnant guinea-pigs' ovaries. Organ-to-blood ratios (CPM/g organ over CPM/g blood) below 3 were not considered meaningful. In some cases a certain

Table 1. Measurable serum electrolytes (mean±SEM) in healthy Israelis and psoriatic Danes, before and after bathing in the Dead-Sea or in simulated bath-salt solutions at various concentrations

Element* and its unit	Healthy Israeli Volunteers (n=6)						Psoriatic Danes (n=21)		
	5.0% Salt Solution		15% Salt Solution		Dead-Sea 30 min		After Arrival	After 1 Bath	After 4w Bathing
	Before	After	Before	After	Before	After			
Sr mg/l	0.5±0.1	0.6±0.1	0.3±0.0	0.3±0.0	0.3±0.0	0.4±0.0	0.4±0.0	0.4±0.0	0.4±0.0
Rb mg/l	0.6±0.1	0.6±0.1	0.4±0.1	0.3±0.0	0.6±0.1	0.7±0.1	0.6±0.0	0.7±0.1	1.1±0.1†
Se mg/l	0.1±0.0	0.1±0.0	0.1±0.0	0.1±0.0	0.1±0.0	0.1±0.0	0.1±0.0	0.1±0.0	0.1±0.0
Br ppm	10±0.8	10±1.1	10±1.6	12±1.8	10±2.3	8.7±1.8	3.5±0.2	4.3±0.3	9.4±0.6†
Fe ppm	4.1±0.8	3.2±0.5	2.9±0.8	3.2±0.4	1.9±0.2	2.4±0.3	3.4±0.4	2.8±0.2	3.4±0.5
Ca ppm	70±9.0	69±6.8	69±4.1	67±6.3	68±1.4	73±2.5†	71±2.3	70±2.3	75±2.6†
Zn ppm	1.3±0.2	1.3±0.1	0.8±0.0	1.0±0.1	1.0±0.1	0.8±0.0	1.0±0.0	1.0±0.0	1.4±0.1†
Cu ppm	1.0±0.2	1.0±0.1	1.0±0.1	1.0±0.1	1.0±0.1	1.0±0.0	1.2±0.0	1.1±0.1	1.1±0.0
Na meq/l	137±1.6	136±2.9	145±1.6	143±2.0	129±4.4	130±7.4	137±2.3	134±1.9	139±8.0
Mg mg/l	23±2.4	22±1.4	21±0.9	21±0.9	21±1.8	21±1.9	22±1.5	22±1.6	20±1.3
Cl meq/l	93±1.3	96±2.5	95±5.0	97±3.7	97±6.0	100±9.2	99±5.6	101±7.6	96±4.5
Cr µg/l	1.8±0.2	1.9±0.2	0.8±0.2	0.7±0.2	1.0±0.6	0.7±0.4	1.0±0.2	1.5±0.4	1.0±0.3

* K values were rejected as the sera were slightly haemolytic, which increased their potassium levels

† = $p < 0.05$

Table 2. Organ-to-blood ratios (mean±SEM) of ^{47}Ca, ^{28}Mg, ^{42}K and ^{82}Br penetrating through the skin of guinea-pigs after immersion for 60 minutes in 15% Dead-Sea bath-salt solutions at 37°C, containing 10 μCi/l of each tracer (n = 9-12).

Organ	^{47}Ca		^{28}Mg		^{24}K		^{82}Br	
	Cycling	Males	Cycling	Males	Cycling	Males	Cycling	Males
Liver	0.4±0.1	0.5±0.1	0.9±0.3	0.9±0.3	1.0±0.2	3.4±0.6	0.3±0.0	0.7±0.3
Spleen	7.4±1.1	6.1±1.6	8.6±1.6	13.0±1.8	10.0±2.4	4.2±1.2	0.3±0.1	0.8±0.1
Lungs	2.2±0.2	3.8±0.8	1.6±0.4	1.8±0.3	4.2±1.0	2.9±0.6	0.4±0.1	0.7±0.1
Heart	1.4±0.2	2.8±0.3	3.6±0.8	3.9±0.8	5.3±1.1	4.0±0.6	1.2±0.2	1.2±0.3
Brain	0.9±0.2	2.7±0.4	2.1±0.3	1.1±0.3	1.4±0.4	1.2±0.3	0.7±0.2	0.2±0.0
Stomach	1.2±0.3	0.9±0.4	1.5±0.4	1.3±0.4	2.2±0.3	3.0±0.3	1.0±0.2	1.0±0.1
Small Intestine	3.1±0.4	3.0±0.5	0.8±0.2	1.6±0.3	2.1±0.1	3.4±0.5	0.4±0.1	0.6±0.1
Skin	104.7±20	338.0±44	8.9±1.0	7.9±1.9	17.8±3.1	11.6±2.9	27.1±1.2	13.7±4.8
Bone	11.9±1.4	33.8±6.4	10.5±2.5	4.9±0.8	11.3±2.0	8.9±1.0	6.6±1.8	4.7±1.3
Kidneys	0.9±0.2	1.1±0.6	1.2±0.2	0.5±0.1	2.0±0.3	3.0±1.0	0.6±0.1	0.8±0.1
Uterus	2.3±0.4	---	3.1±0.7	---	9.6±1.0	---	0.7±0.1	---
Ovaries	6.0±1.0	---	20.7±3.5	---	35.1±8.3	---	2.0±0.4	---
Testes	---	3.2±1.2	---	3.6±0.4	---	3.4±0.4	---	5.4±1.0

radionuclide concentrated differently in the same organ excised from different animal-groups. These findings deserve further investigation.

DISCUSSION

Assuming that the therapeutic effect of the Dead-Sea is in part due to its minerals' content, clinical effectiveness studies of bathing in it were focused on the ability of its various minerals to penetrate through or into the epidermis. This is a slow process as the intact stratum corneum is limiting percutaneous absorption, and minerals are extremely insoluble in lipid membranes and their transport via the intercellular route is limited.

The questions raised in this study are whether one can expect measurable penetration of minerals through the skin after only a short (30-60 minutes) bathing in a salt solution?, and so is there any difference in penetration between psoriatic and healthy human skin?

As to the first question, there are varying views regarding the lag-time needed for ionic species to penetrate into the circulation. According to Tregear (1966a,b), ^{24}Na, ^{32}Br and ^{32}P begin to penetrate the skin within 10 minutes of their application and dynamic equilibrium is reached by 50 minutes. Our study in guinea-pigs demonstrate that after 60 minutes of bathing the whole body in the salt solution, and having a sensitive measurement system (radioisotopic counting), the concentration of the various elements in blood and body tissues could be measured with high accuracy and reliability (Robberecht et al, 1982).

This study also demonstrates that penetration of Dead-Sea minerals via psoriatic skin is more profound than through a healthy skin (Table 1). It is well established from clinical experience that absorption is increased through damaged skin, and that a skin injury comparable to eczema

is most simply induced experimentally by stripping (Tregear, 1962). We believe that in the psoriatic skin, with its abnormal capillary dilatation and damaged stratum corneum, penetration rates are higher because of the partial lack of protection of the damaged stratum corneum. An additional factor which enhances minerals' penetration into the psoriatic skin is the frequent use by the patients of a keratolytic ointment (i.e. - salicylic acid 3-5%) and vaselin. The latter base is known to increase the permeability of the stratum corneum 4 to 5 fold, as it can then take 4 times its weight of water (Blank & Scheuplein, 1969).

Permeability of the skin in different mammalian species varies remarkably (Van Dilla, Tregear, 1966a. The differences between the human and animal skin is paralleled by the differences in their electrical conductance, but the difference in permeability between the various ions in the same species is not significant (Tregear, 1966a). If any generalization is at all possible, it would seem that human skin is more impermeable then the skin of a mouse or a guinea-pig, and that guinea-pig skin may in some cases serve as useful approximation to human skin testing its permeability (Wahlberg, 1968a; Scheuplein & Blank, 1971). This is the reason why, in our studies, absorption through guinea-pig skin was measured by radionuclides, but penetration of the Dead-Sea minerals through human healthy and psoriatic skin was measured by non-radioactive methods - XRF and atomic absorption. At worse, the penetration of Dead-Sea minerals through guinea-pig skin will be an overestimation of what is occuring under similar conditions in the human.

In a series of papers Dubarry demonstrated (Dubarry et al, 1971, 1972; Tamarelle & Dubarry, 1972) that the maximum penetration of the ions through skin was observed when the solute had low salt rather than high

salt, and that the more concentrated the external solution is, the less penetrable through the skin are the ions soluble in it. Significantly less ^{131}I penetrated the skin from a 30% NaCl solution than from 3% or 1% NaCl solutions, but the amount which penetrated was still measurable in all three concentrations. Similar experiments were carried out by Giberton and Cohen (1970).

Extensive studies on this aspect were carried out by Wahlberg et al since 1962. These authors noted that the relative absorption of ^{51}Cr through the guinea-pig skin increased with increasing chromium concentration to a maximal absorption of 4%, and when the concentration was further increased, the absorption decreased to about 1%. The absolute absorption also increased with increasing chromium concentration, but at a certain concentration a plateau was obtained (Wahlberg & Skog, 1963; Wahlberg, 1968a). The same finding was confirmed later for $^{89}SrCl_2$ (Wahlberg, 1968b) : a relative absorption of about 3% and an increase in absolute absorption with increasing concentration. Wahlberg also showed that the absorption of $^{85}SrCl_2$ was of the same order of magnitude as that observed for other metal elements previously studied, and it seems that the same applies to the various elements of the Dead-Sea (Wahlberg, 1973; Wahlberg & Skog, 1963).

In conclusion, inasmuch as ions do penetrate the human skin, their absolute penetration values after bathing in the Dead-Sea brine are low. Our previous paper (Shani et al, 1982) describes higher concentration of bromine in skin of Dead-Sea workers and in psoriatic patients after a longer stay on the Dead-Sea shore. We suggest that this element also enters the body through breathing and drinking. The quantities of other elements that penetrate are apparently too low to be measured or to induce a pharmacological effect. It also seems reasonable to conclude that

psoriatic skin is more penetrable to most elements, and that some penetration may occur even if diluted Dead-Sea waters (i.e. - various conentrations of the Dead-Sea bath-salt solutions) are used. The optimal concentration of these salt solutions, and the length of time for bathing in them to insure maximal absorption and penetration through the human skin are still to be investigated.

ACKNOWLEDGMENTS

This work was supported in part by the Dead-Sea Works Ltd., Israel, by the Israeli Health Resorts Authority and by the Joint Research Fund of the Hebrew University and Hadassah. The authors acknowledge the comments of Dr. D. Albin. H. Robberecht acknowledges support from the Belgian Ministry of Health and from the Israeli-Belgian Cultural-Exchange Program.

REFERENCES

Abboud, S., Schlesinger, T., Weingarten, R. (1978). Trans. Ann. Meet. Nucl. Soc. Israel, p5C-6C.

Avrach, WW. (1977a). Proc. 2nd Intern. Symp. Psoriasis. Stanford Univ. 1976 Published by Yorke Medical Books NY pp 258-261.

Avrach, WW. (1977b). Proc. 15th Intern. Cong. Dermatology, Mexico City.

Avrach, WW., Niordsen, AM. (1974). Ugeskrift for Laeger 136, 2687-2690.

Blank, I.H., Scheuplein, R.J. (1969). Brit. J. Derm. 81, Supp. 4, 4-10.

Dostrovsky A., Sagher, F. (1959). Harefuah 57, 143-145.

Drugan, A. (1976). A medical outlook on the Dead-Sea area and its therapeutic factors. Israeli Health Resorts Authority, pp 14.

Dubarry, J.J., Blanquet, P., Tamerelle, C. (1971). Presse Therm. Climatique 108, 1-7.

Dubarry, J.J., Tamerelle, C. (1972). Presse Therm. Climatique 109, 196-200.

Giberton, A., Cohen, P. (1970). La Presse Therm. Climatique. 107, 51-52.

Hodgson, C. (1960). Brit J. Derm. 72, 409-415.

Justesen, N.P., Harkmark, W.: Artificial Dead-Sea water in the treatment of psoriasis. Arch. Derm. Submitted for publication.

Lipkin, G., Gowdey, J., Wheatley, V.R. (1962). J. Invest. Derm. 42, 205-207.

Montgomery, BJ. (1979). JAMA 241, 227-231.

Robberecht, H., Van Grieken, R., Shani, J., Barak, S. (1982). Anal. Chim. Acta 136, 285-291.

Scheuplein, R.J., Blank, I.H. (1971). Physiol. Rev. 51, 702-747.

Shani, J., Barak, S., Ram, M., Levi, D., Pfeifer, Y., Schlesinger, T., Avarach, W.W., Robberecht, H., Van Grieken, R. (1982). Pharmacology. 25, 297-307.

Tamarelle, C., Dubarry, J.J. (1972). Press Therm. Climatique 109, 37-40.

Tregear, R.T. (1966a). J. Invest. Derm. 46, 16-23.

Tregear, R.T. (1966b). in Physical Functions of Skin. Academic Press, London - NY, 1-52.

Tregear, R.T., Dirnhuber, P. (1962). J. Invest. Derm. 38, 375-382.

Troitskaia, A.D. (1965). Vestn. Derm. Vener. 39, 85-86.

Van Dilla, M.A., Richmond, C.R., Furchner, A. (1961). Los Alamos Scientific Laboratory. LAMS-2526, 164-171.

Wahlberg, J.E. (1968a). Acta Derm. Vene. 48, 549-555.

Wahlberg, J.E. (1968b). Acta Derm. 97, 336-339.

Wahlberg, J.E. (1973). Curr. Prob. Derm. 5, 1-36.

Wahlberg, J.E., Skog, E. (1963). Acta Derm. Vene. (Stockholm) 43, 102-108.

Selected article # 5:

Increased erythrocyte glutathione peroxidase activity in psoriatics at the Dead-Sea psoriasis treatment center

J. Shani, T. Livshitz, H. Robberecht, R. Van Grieken, N. Rubinstein and Z. Even-Paz

Pharmacol. Res. Comm., 17 (1985), 479-488

INCREASED ERYTHROCYTE GLUTATHIONE PEROXIDASE ACTIVITY IN PSORIATICS CONSUMING HIGH-SELENIUM DRINKING WATER AT THE DEAD-SEA PSORIASIS TREATMENT CENTER

J. Shani[a], T. Livshitz[a], H. Robberecht[b], R. Van Grieken[b], N. Rubinstein[c] and Z. Even-Paz[c]

[a]Department of Pharmacology, The Hebrew University School of Pharmacy, Jerusalem, Israel; [b]Department of Chemistry, University of Antwerp (UIA), B-2610 Wilrijk, Belgium; and [c]Department of Dermatology, Hadassah-University Hospital, Jerusalem, Israel

Received in final form 15 February 1985

SUMMARY

Erythrocyte selenium-dependent glutathione peroxidase activity was measured in psoriatic Danes, before and after their four-week balneological therapy at the Ein-Bokek International Psoriasis Treatment Center, on the Dead-Sea shore in Israel. The drinking water in Ein-Bokek was found to be rich in selenium, a trace element with anticarcinogenic properties and of great importance in human nutrition and health. The most reliable biological parameter for increase in selenium bioavailability is the erythrocytes' glutathione-peroxidase activity. As psoriasis is a proliferative skin disease, the activity of this enzyme was assayed in 35 psoriatic Danes and in 25 long-term local hotel workers, as well as in 34 volunteers drinking low-selenium water. The glutathione peroxidase activity in the psoriatic patients increased significantly during their four-week stay in Ein-Bokek. Erythrocyte glutathione peroxidase activity in the hotel workers was 50% higher than that in the healthy volunteers consuming low-selenium water. A possible role of selenium in psoriasis is suggested.

0031-6989/85/050479-10/$03.00/0

INTRODUCTION

Selenium is a trace element which is essential for human nutrition and health. It is highly homeostatically regulated in the body at a range of 100-300 ppb whole blood, with an acceptable daily requirement of 0.05-0.2 mg, deriving mostly from solid food and water intake. Apparently, waters rarely contain selenium at levels above a few μg/l (ppb), and are not generally considered a significant source of the element from either a nutritional or a toxicological viewpoint. The present American standard for drinking water set by the US Food and Nutrition Board is 10 ppb as the upper acceptable limit (Selenium, 1976). These standards are set with the understanding that the bioavailability of the element is the critical factor in its exerting a physiological effect.

The only fully documented physiological role of selenium in mammals is in the enzyme glutathione peroxidase, which plays a role in protection from lipid peroxide-initiated damage of tissues. In this enzyme selenium exists as a specific selenocysteine residue, being inserted into the enzyme residue via a post-translational mechanism. Selenium deficiency leads to decreased activity of glutathione peroxidase, which parallels its clinical deficiency symptoms, e.g. white muscle disease, cardiomyopathy, oxidative diathesis, infertility in sheep, sudden death in piglets, etc. Selenium supplementation elevates glutathione peroxidase activity and is beneficial in children with Kwashiorkor and Keshan disease and in adults with muscular complaints. It has been shown to produce a favorable response in erythrocyte glutathione peroxidase activity in neuronal lipofuscinosis (Kasperek et al, 1980), to normalize enzyme activity and erythrocyte formation in anemia (perona et al, 1973), to prevent heart diseases and to delay carcinogenesis in humans (Griffin, 1982). In American regions with high selenium water levels, lower cancer mortality was observed for both male and females, and in Canadian provinces with high selenium

levels, lower age-adjusted rates for gastrointestinal cancer have been observed (Shamberger et al, 1974).

Over a period of years many thousands of psoriatics have been treated at the IPTC balneological clinic at Ein-Bokek, on the Dead-Sea shore in Israel, for this benign proliferative disease. Due to the high outdoor temperatures they consume many liters daily of water which contains high levels of selenium. Estimation of erythrocyte glutathione peroxidase activity has been shown to be the best parameter for investigating selenium-related nutritional and health states in mammals, especially as it increases as a function of dietary selenium (Smith et al, 1974). We therefore decided to study the elevation in erythrocyte glutathione peroxidase levels in these patients and to attempt to correlate it with the improvement in their psoriatic state.

MATERIALS AND METHODS

This study includes two types of assay: (a) erythrocyte glutathione peroxidase activity in three groups of volunteers; and (b) determination of selenium concentration in thirteen Israeli hot spas and drinking waters, with special emphasis on the levels of selenium in the water at the Ein-Bokek hotels and the IPTC clinic, and in its geological sources.

Assay of erythrocyte glutathione peroxidase activity was performed in three groups of volunteers: 35 psoriatic Danes who came in June 1982 to the International Psoriasis Treatment Center (IPTC) at Ein-Bokek, for climato-therapy of their severe psoriatic condition. The group consisted of 16 male and 19 female patients, aged 24-62 years, for whom climato-therapy at the Dead-Sea was prescribed instead of hospitalization. Blood was withdrawn from each patient twice: within 24 hours of arrival at Ein-Bokek (prior to their first bath in the Dead Sea) and on the last day of their 4-week stay, upon termination of their treatment.

In addition, 28 healthy permanent workers in the Ein-Bokek hotels who had been living on the premises for at least 9 months, were studied. Blood was taken from them only once. The third group consisted of 34 healthy Jerusalemites, working in the Hadassah Medical Center for at least 9 months. The distribution of sex and age in all three groups was similar.

In accordance with the Helsinki Treaty, all volunteers were given an explanation of the experiment, and their consent obtained. Blood samples were withdrawn after cleaning the cuboidal area with water and then with 70° ethanol. The fresh heparinized venous blood samples were transferred in ice-boxes to Jerusalem, and within 2-3 hours after collection were filtered through a SE-cellulose-Sephadex G-25 mixture, deviced by Nakao et al (1973) for separation of the erythrocytes from the leukocytes and platelets, which remained in the column. The erythrocytes were lyzed by dilution with saline (0.1 ml packed cells plus 2.4 ml saline) and assayed for glutathione peroxidase activity at 37°C according to the method of Bentler (1975) using t-butyl-hydroxyperoxide (TBH) as substrate. The reaction was carried out in a spectrophotometer, the decrease in OD being followed at 340 nm for 7 minutes. Results were expressed in international units per gram of hemoglobin in erythrocytes. Hemoglobin concentration was measured in dilute ammonia solution, according to Anderson et al (1975). Statistical comparison of enzyme activity between groups of subjects was performed by the Student's "t" test.

Determinations of selenium concentrations in the spas and drinking waters along the Syrian-African rift were carried out using energy-dispersive X-ray fluorescense spectrometry, according to Robberecht and Van Grieken (1980). Suspended selenium was determined directly after filtration through a nucleopore membrane. The dissolved selenium was assessed after reduction to elemental selenium, followed by absorption on activated carbon and filtration. Thirteen water samples were collected

along the Dead-Sea and along shores of the Sea of Galilee, and one water sample was taken in Jerusalem. When it was noted that the sample taken from the water-pipe leading to the Ein-Bokek hotels, contained over 25 ppb of total selenium, assays of this water and of the Jerusalem water for selenium were repeated. The Ein-Bokek water comes from a small pool in a $CaCo_3$ rock formation, fed by eight small springs. The water output of two of these springs was too low to be sampled.

RESULTS

Table 1 presents selenium levels in both soluble and suspended forms, from 13 different spa waters in Israel, as well as from five water samples taken

Table 1. Selenium concentration in different spa waters in Israel.

Sample No.	Location	Selenium µg/l Dissolved	Se+4	Suspended Material mg/l
1	Tiberias Hot Springs (62°C)	1.20	0.05	0.49
2	Ein-Nun (Yarmuk Canyon)	1.76	0.01	1.01
3	Hammat-Gader Springs	2.20	0.07	1.66
4	Ein-Gedi Waterfall	2.80	0.09	1.44
5	Ein-Bokek (Dead-Sea)	0.65	0.60	Unfilterable
6	Hammey-Zohar (High sulfur)	0.07	0.06	1.10
7	Pipe Supplying Ein-Bokek Hotels	25.0	0.04	0.81
8	Dead-Sea (Moriah Hotel)	0.91	0.80	Unfilterable
9	Natural Mineral Spring (Katzrin)	1.67	0.04	0.98
10	Kommemiuth Drinking Water	1.48	0.04	3.38
11	Kabri Pumping Station	1.75	0.04	3.08
12	Ein-Nouit Spring	0.27	0.04	1.28
13	Neve-Zohar Spring	0.54	0.08	--
14	Jerusalem Drinking Water a	0.54	0.05	0
15	Jerusalem Drinking Water b	0.35	0.04	0
16	Jerusalem Drinking Water c	0.42	0.04	0
17	Jerusalem Drinking Water d	0.66	0.04	0
18	Jerusalem Drinking Water e	0.48	0.05	0

Table 2. Selenium concentration in the water pipe and its sources.

Sample No.	Location	Dissolved Selenium Total	µg/l Se^{+4}
7	Pipe behind the hotels	25.03	0.04
19	Pipe behind the hotels	28.43	0.06
20	Pipe behind the hotels	26.77	0.07
21	Pipe behind the hotels	26.95	0.09
22	Pipe behind the hotels	31.09	0.04
23	Pipe behind the hotels	29.02	0.04
24	Pipe behind the hotels	29.10	0.04
25	Pipe behind the hotels	29.04	0.04
26	Pipe behind the hotels	28.80	0.04
27	Source 2	25.54	0.38
28	Source 3	25.97	0.14
29	Source 5	26.68	0.32
30	Source 6	21.37	0.05
31	Source 7	24.59	0.04
32	Source 8	23.27	0.04

Table 3. Erythrocyte glutathione peroxidase activity (Mean±SEM) in psoriatic Danes before and after 4-weeks climato-therapy at the Dead-Sea, and in healthy volunteers drinking high-selenium (hotel workers) or low-selenium (Jerusalem workers) waters.

Group No.	n	Group Description	Glutathione Peroxidase Activity I.U./g Hb	P<
1	35	Psoriatic Danes before therapy	25.8±1.1	0.001
2	35	Psoriatic Danes after therapy	32.0±1.3	
3	28	Healthy Hotel Workers	40.9±2.5	0.001
4	34	Healthy Workers in Jerusalem	26.8±1.8	

in the Hadassah Medical Center in Jerusalem. In this assay, values for tetravalent selenium below 0.05 ppb are not considered statistically meaningful.

In each of the six Ein-Bokek water sources sampled, the selenium level resembled that in the pipe itself, as shown in Table 2. This table also gives selenium values in the pipe-water at various months and at various points along the facility, e.g. at the reservoir outlet (Sample 23), at the softner outlet (Sample 25) and at the softner inlet (Sample 26). All these samples had a very similar content of total selenium.

The erythrocyte glutathione peroxidase activities of the various groups are presented in Table 3. The enzyme's activity in the psoriatic Danes' erythrocytes increased 20% during their 4-week stay in Ein-Bokek, differing significantly ($p<0.001$) from their enzyme levels upon arrival in the IPTC clinic. The erythrocyte levels of glutathione peroxidase in the healthy hotel workers, who had drunk the selenium-rich water for 9 months to 10 years, were 50% higher than those of the Jerusalemites drinking low-selenium water. As the erythrocyte-enzyme levels of the psoriatic Danes on arrival were identical to those in the healthy Jerusalem volunteers, one could compare the two experimental group-pairs and conclude that the erythrocyte glutathione peroxidase activity in the hotel's workers, drinking high-selenium waters for an average of over 2 years was significantly higher than that of the Danish psoriatics, who drank the same high-selenium waters for only 4 weeks. The correlation between the psoriatic Danes' increase in enzyme-activity and the clinical improvement of their psoriatic condition as judged by disappearing of the plaques, was remarkable, having a correlation coefficient of 0.97. The two patients with the lowest individual increases in their glutathione peroxidase activity had only "partial" clinical improvement.

DISCUSSION

Dietary selenium intake correlates with selenium concentration in whole blood and erythrocytes (Smith et al, 1974). Due to differences regional selenium availability - human blood selenium values vary from 0.068 µg/ml in New Zealand, to 1.5 µg/ml in certain high-selenium regions of Venezuela. The latter value translates into a daily dietary adult uptake of about 0.5 mg. A daily diet of 45 µg selenium is sufficient to normalize the activity of erythrocyte glutathione peroxidase. When selenium supplementations of 0.45 ppm in food and additional 0.5 ppm in water were given to mice developing spontaneous adenocarcinomas, they remained tumor-free for much longer periods than the non-supplemented controls, i.e. selenium supplementation lowered the probability of cancer development and delayed its appearance (Burk et al, 1968). Moreover, different authors suggested a striking inhibitory effect of dietary selenium in animals against a variety of carcinogens, and its ability to retard the growth of certain chemically-induced transplanted or spontaneous tumors in animals (Riley, 1968). This led us to search for a possible correlation between the high water-selenium intake of psoriatics and the clinical improvement of their proliferative condition.

There are reports correlating blood selenium concentration and glutathione peroxidase activity in sheep, cows, pigs and humans (Thomson, 1977), suggesting that plasma and/or erythrocyte glutathione peroxidase activity may serve as a useful index of selenium intake (Chow and Tappel, 1974; Burk, 1976; Rudolph and Wong, 1978). Such a correlation was established for a wide range of selenium concentrations (Lane et al, 1981). In a comprehensive study in pigs, a highly significant correlation was noticed between blood selenium and glutathione peroxidase activity, suggesting that "selenium glutathione peroxidase exhibited an excellent

ings EMEP workshop on volatile organic compounds, 6–9 November 1989, Lindau, Germany.

Remoudaki E., Bergametti G. and Losno R. (1991) On the dynamic of the atmospheric input of copper and manganese into the western Mediterranean Sea. *Atmospheric Environment* **25A,** 733–744.

Romeo M. and Nicolas E. (1986) Cadmium, copper, lead and zinc in three species of planktonic crustaceans from the east coast of Corsica. *Mar. Chem.* **18,** 359–367.

Ross H. B. (1984) Methodology for the collection and analysis of trace metals in atmospheric precipitation. Report CM-67, International Meteorological Institute in Stockholm/Dept. of Met., University of Stockholm.

Ross H. B. (1987) Trace metals in precipitation in Sweden: *Water Air Soil Pollut.* **36,** 349–363.

Ross H. B. (1990) Trace metal wet deposition in Sweden: insight gained from daily wet only collection. *Atmospheric Environment* **24A,** 1929–1938.

Ruijgrok W., Visser H. and Römer F. G. (1990) Comparison of bulk and wet-only samplers for trend detection in wet deposition. Proceedings International Workshop on Cloud Chemistry and Wet Deposition, Utrecht, The Netherlands, April 1990, pp. 34–40.

Schroeder W. H., Dobson M., Kane D. M. and Johnson N. D. (1987) Toxic trace elements associated with airborne particulate matter: a review. *J. Air Pollut. Control Ass.* **37,** 1267–1284.

Schulz-Bull D. E., Petrick G. and Duinker J. C. (1991) Polychlorinated biphenyls in North Sea water. *Mar. Chem.* **36,** 365–384.

Scofield R. A. (1991) Operational estimation of precipitation from satellite data. *Palaeogeogr. Palaeoclim. Palaeoecol. (Global planet. Change Section)* **90,** 79–86.

Slinn W. G. N. (1983) Air-to-sea transfer of particles. In *Air–Sea Exchange of Gases and Particles* (edited by Liss P. S. and Slinn W. G. N.), pp. 299–405. D. Reidel, Dordrecht.

Smith F. B. (1991) Deposition processes for airborne pollutants. *Met. Mag.* **120,** 173–182.

Stoeßel R. (1987) Untersuchungen zu Naß- und Trockendeposition von Schwermetallen auf der Insel Pellworm. Ph.D. thesis, University of Hamburg, Germany.

Stone R. (1992) Swimming against the PCB tide. *Science* **255,** 798–799.

S&TWG Scientific and Technical Working Group (1987) Quality status of the North Sea. Second International Conference on the Protection of the North Sea, London, November 1987, Vol. 5, p. T8 and Vol. 6, pp. 6–10.

Subramanian A. N., Tanabe S., Tanaka H., Hidaka H. and Tatsukawa R. (1987) Gain and loss rates and biological half-life of PCBs and DDE in the bodies of Adelie Penguins. *Envir. Pollut.* **43,** 39–46.

Suess M. J. (1976) The environmental load and cycle of polycyclic aromatic hydrocarbons. *Sci. total Envir.* **6,** 239–250.

Swackhamer L. D. and Armstrong D. E. (1986) Estimation of the atmospheric and nonatmospheric contributions and losses of polychlorinated biphenyls for lake Michigan on the basis of sediment records of remote lakes. *Envir. Sci. Technol.* **20,** 879–883.

Swackhamer L. D., McVeety B. D. and Hites R. A. (1988) Deposition and evaporation of polychlorobiphenyl congeners to and from Siskiwit Lake, Isle Royale, Lake Superior. *Envir. Sci. Technol.* **22,** 664–672.

Tanabe S. (1988) PCB problems in the future: foresight from current knowledge. *Envir. Pollut.* **50,** 5–28.

Valerio F. and Pala M. (1991) Effects of temperature on the concentration of polycyclic aromatic hydrocarbons (PAHs) adsorbed onto airborne particles. *Fresenius J. analyt. Chem.* **339,** 777–779.

Van Aalst R. M., Van Ardenne R. A. M., De Kreuk J. F. and Lems Th. (1983) Pollution of the North Sea from the atmosphere. TNO report CL 82/152, Delft, The Netherlands.

Van Daalen J. (1991) Air quality and deposition of trace elements in the province of South-Holland. *Atmospheric Environment* **25A,** 691–698.

Van Jaarsveld J. A. and Onderlinden D. (1986) Modelmatige beschrijving van concentratie en depositie van kolen relevante componenten in Nederland, veroorzaakt door emissies in Europa. Nationaal Onderzoeksprogramma Kolen (NOK), deelrapport 4, April 1986, PEO, Utrecht, The Netherlands.

Van Jaarsveld J. A., Van Aalst R. M. and Onderlinden D. (1986) Deposition of metals from the atmosphere into the North Sea. RIVM Report 842015002, Bilthoven, The Netherlands.

Van Noort P. C. M. and Wondergem E. (1985) Scavenging of airborne polycyclic aromatic hydrocarbons by rain. *Envir. Sci. Technol.* **19,** 1044–1048.

Warmenhoven J. P., Duiser J. A., de Leu L. Th. and Veldt C. (1989) The contribution of the input from the atmosphere to the contamination of the North Sea and the Dutch Wadden Sea. TNO Report R89/349A, Delft, The Netherlands.

Wells E. D. and Johnstone S. J. (1978) The occurrence of organochlorine residues in rainwater. *Water Air Soil Pollut.* **9,** 271–280.

Yaaqub R. R., Davies T. D., Jickells T. D. and Miller J. M. (1991) Trace element in daily collected aerosols at a site in southeast England. *Atmospheric Environment* **25A,** 985–996.

and Slinn W. G. N.), Proceedings of the Fourth International Conference, Santa Monica, California, 29 November–3 December, 1982, pp. 395–402. Elsevier, New York.

GESAMP-IMO/FAO/UNESCO/WMO/WHO/IAEA/UN/UNEP Joint Group of Experts on the Scientific Aspects of Marine Pollution (1989) The atmospheric input of trace species to the world ocean. Reports and Studies GESAMP-WMO 38.

Graßl H., Eppel D., Pettersen G., Schneider B., Weber H., Gandrass J. G., Reinhardt K. H., Wodarg D. and Fließ J. (1989) Stofeintrag in Nord- und Ostsee über die Atmosphäre. Report GKSS-89/E/8.

Grimmer G., Brune H., Dettbarn G., Jacob J., Misfeld J., Mohr U., Naujack K.-W., Timm J. and Wenzel-Hartung R. (1991) Relevance of polycyclic aromatic hydrocarbons as environmental carcinogens. *Fresenius J. analyt. Chem.* **339,** 792–795.

Hinckley D. A. and Bidleman T. F. (1991) Atmospheric organochlorine pollutants and air–sea exchange of hexachlorocyclohexane in the Bering and Chukchi Seas. *J. geophys. Res.* **96,** 7201–7213.

Jaffrezo J. L. and Colin J. L. (1988) Rain–aerosol coupling in urban area: scavenging ratio measurement and identification of some transfer processes. *Atmospheric Environment* **5,** 929–935.

Jickells T. D., Davies T. D., Tranter M., Landsberger S. and Jarvis K. (1992) Trace elements in snow samples from the Scottish Highlands: sources and dissolved/particulate distributions. *Atmospheric Environment* **26A,** 393–401.

Kamens R. M., Guo Z., Fulcher J. N. and Bell D. A. (1988) Influence of humidity, sunlight, and temperature on the daytime decay of polyaromatic hydrocarbons on atmospheric soot particles. *Envir. Sci. Technol.* **22,** 103–108.

Kedem B., Chiu L. S. and North G. R. (1990) Estimation of mean rain rate: application to satellite observations. *J. geophys. Res.* **95,** 1965–1972.

Kersten M., Kriews M. and Förstner U. (1991) Partitioning of trace metals released from polluted marine aerosols in coastal seawater. *Mar. Chem.* **36,** 165–182.

Korfmacher W. A., Mamantov G., Wehry E. L. and Natusch D. F. S. (1980) Resistance to photochemical decomposition of polycyclic aromatic hydrocarbons vapor-absorbed on coal fly ash. *Envir. Sci. Technol.* **14,** 1094–1099.

Krell U. and Roeckner E. (1988) Model simulation of the atmosperic input of lead and cadmium into the North Sea. *Atmospheric Environment* **22,** 375–381.

Kretzschmar J. G. and Cosemans G. (1979) A five year survey of some heavy metal levels in the air at the Belgian North Sea coast. *Atmospheric Environment* **13,** 267–277.

Lane D. A., Schroeder W. H. and Johnson N. D. (1992) On the spatial and temporal variations in atmospheric concentrations of hexachlorobenzene and hexachlorocyclohexane isomers at several locations in the province of Ontario, Canada. *Atmospheric Environment* **26A,** 31–42.

Leuenberger C., Czuczwa J., Heyerdahl E. and Giger W. (1988) Aliphatic and polycyclic aromatic hydrocarbons in urban rain, snow and fog. *Atmospheric Environment* **22,** 695–705.

Levsen K., Behnert S., Priess B., Svoboda M., Winkeler H.-D. and Zietlow J. (1990) Organic compounds in precipitation. *Chemosphere* **21,** 1037–1061.

Ligocki M. P., Leuenberger C. and Pankow F. (1985) Trace organic compounds in rain—III. Particle scavenging of neutral organic compounds. *Atmospheric Environment* **19,** 1619–1626.

Lindqvist O. and Rodhe H. (1985) Atmospheric mercury—a review. *Tellus* **37B,** 136–159.

Lipiatou E. and Saliot A. (1991) Fluxes and transport of anthropogenic and natural polycyclic aromatic hydrocarbons in the western Mediterranean Sea. *Mar. Chem.* **32,** 51–71.

Losno R., Bergametti G. and Buat-Ménard P. (1988) Zinc partitioning in Mediterranean rainwater. *Geophys. Res. Lett.* **15,** 1389–1392.

Malaiyandi M. and Shah S. M. (1984) Evidence of photoisomerization of hexachlorocyclohexane. *J. envir. Sci. Health* **A19,** 887–910.

Martin J.-M., Elbaz-Poulichet F., Guieu C., Loije-Pilot M.-D. and Han G. (1989) River versus atmospheric input of material to the Mediterranean Sea: an overview. *Mar. Chem.* **28,** 159–182.

Masclet P., Pistikopoulos P., Beyne S. and Mouvier G. (1988) Long-range transport and gas/particle distribution of polycyclic aromatic hydrocarbons at a remote site in the Mediterranean Sea. *Atmospheric Environment* **22,** 639–650.

McVeety B. D. and Hites R. A. (1988) Atmospheric deposition of polycyclic aromatic hydrocarbons to water surfaces: a mass balance approach. *Atmospheric Environment* **22,** 511–536.

Migon C., Morelli J., Nicolas E. and Copin-Montegut G. (1991) Evaluation of total atmospheric deposition of Pb, Cd, Cu and Zn to the Ligurian Sea. *Sci. total Envir.* **105,** 135–148.

Murray M. W. and Andren A. W. (1992) Precipitation scavenging of polychlorinated biphenyl congeners in the Great Lakes region. *Atmospheric Environment* **26A,** 883–897.

Nakano T., Tsuji M. and Okuno T. (1990) Distribution of PCDDs, PCDFs and PCBs in the atmosphere. *Atmospheric Environment* **24A,** 1361–1368.

Oehme M. and Manø S. (1984) The long-range transport of organic pollutants to the Arctic. *Fresenius J. analyt. Chem.* **319,** 141–146.

Otten P. (1991) Transformation, concentrations and deposition of North Sea aerosols. Ph.D. thesis, University of Antwerp (UIA), Belgium.

Otten P., Rojas C., Wouters L. and Van Grieken R. (1989a) Atmospheric deposition of heavy metals (Cd, Cu, Pb and Zn) into the North Sea. Report 2, project NOMIVE*5 task No. DGW-920, Rijkswaterstaat, Dienst Getijdewateren, 's Gravenhage, The Netherlands.

Otten P., Storms H., Xhoffer C. and Van Grieken R. (1989b) Chemical composition, source identification and quantification of the atmospheric input into the North Sea. In *Progress in Belgian Oceanographic Research* (edited by Pichot G.), pp. 413–422. Prime Minister's Services of Science Policy Office & Ministry of Public Health and Environment, Brussels.

Pacyna J. M. (1984b) Estimation of the atmospheric emissions of trace elements from anthropogenic sources in Europe. *Atmospheric Environment* **18,** 41–50.

Pacyna J. M., Semb A. and Hanssen J. E. (1984a) Emission and long-range transport of trace elements in Europe. *Tellus* **36B,** 163–178.

PARCOM (1987) Current estimates of atmospheric inputs to the North Sea. 9th Annual Report on the Activities of the Paris Commission, Annex, pp. 38–42.

Peirson D. H., Cawse P. A., Salmon L. and Cambray R. S. (1973) Trace elements in the atmospheric environment. *Nature* **241,** 252–256.

Pitts J. N. Jr, Van Cauwenberghe K. A., Grosjean D., Schmid J. P., Fitz D. R., Belser W. L. Jr, Knudson G. B. and Hynds P. M. (1978) Atmospheric reactions of polycyclic aromatic hydrocarbons: facile formation of mutagenic nitro derivatives. *Science* **202,** 515–519.

Quaghebeur D., De Wulf E., Ravelingien M. C. and Janssens G. (1983) Polycyclic aromatic hydrocarbons in rainwater. *Sci. total Envir.* **32,** 35–54.

Rapaport R. A. and Eisenreich S. J. (1988) Historical atmospheric inputs of high molecular weight chlorinated hydrocarbons to eastern North America. *Envir. Sci. Technol.* **22,** 931–941.

Reinhardt K. H. and Wodarg D. (1989) On the deposition of selected organochlorine compounds into the sea. Proceed-

the data on the concentrations of the organic species in both air and precipitation and on the organic fluxes to the sea are very scarce or almost non-existent.

Therefore, it is absolutely necessary to work out a global measurement strategy for the North Sea area, if one really wants to discover any possible trends or learn about the effect of these pollutants on the marine environment. It would include precipitation and air sampling—preferably simultaneously in order to be able to calculate the scavenging rates or washout ratios—at a large number of sites (islands, cruises, platforms and coastal stations) and over a considerable period of time. Special attention should be given to the problem of sea-spray-induced errors, storage and contamination of samples, development of suitable analytical strategies for organic compounds which are present in the atmosphere at concentrations nearby or even under the detection limit, revolatilization of organics, etc. Also, the existent models should be further developed in order to achieve better agreement with the measured fluxes.

Acknowledgements—Part of this research was funded by Rijkswaterstaat, Dienst Getijdewateren, 's Gravenhage, The Netherlands, in the framework of NOMIVE task No. DWG-164. The authors wish to thank C. Xhoffer (University of Antwerp, Belgium), R. Laane (Rijkswaterstaat) and H.J. van Broekhuizen, A. van Kuijk and their colleagues at GEOSENS B.V. (Rotterdam, The Netherlands) for helpful comments and co-operation.

REFERENCES

Atlas E. and Giam C. S. (1981) Global transport of organic pollutants: ambient concentrations in the remote marine atmosphere. *Science* **211,** 163–165.

ATMOS Working group on the atmospheric input of pollutants to convention waters (1984) Heavy metal input from the atmosphere into the North Sea. ATMOS report 4/4-E.

Baeyens W. and Dedeurwaerder H. (1991) Particulate trace metals above the Southern Bight of the North Sea—I. Analytical procedures and average aerosol concentrations. *Atmospheric Environment* **25A,** 293–304.

Baeyens W., Dehairs F. and Dedeurwaerder H. (1990) Wet and dry deposition fluxes above the North Sea. *Atmospheric Environment* **24A,** 1693–1703.

Balls P. W. (1989) Trace metal and major ion composition of precipitation at a North Sea coastal site. *Atmospheric Environment* **23,** 2751–2759.

Bidleman T. F. (1988) Atmospheric processes: wet and dry deposition of organic compounds are controlled by their vapor–particle partitioning. *Envir. Sci. Technol.* **22,** 361–367.

Bidleman T. F. and Christensen E. J. (1979) Atmospheric removal processes for high molecular weight organochlorines. *J. geophys. Res.* **84,** 7857–7862.

Bidleman T. F., Wideqvist U., Jansson B. and Soderlund R. (1987) Organochlorine pesticides and polychlorinated biphenyls in the atmosphere of southern Sweden. *Atmospheric Environment* **21,** 641–654.

Björseth A., Lunde G. and Lindskog A. (1979) Long-range transport of polycyclic aromatic hydrocarbons. *Atmospheric Environment* **13,** 45–53.

Bowler S. (1990) Radar network watches where the wind blows. *New Scientist* 24 March, 30–31.

Browning K. A. (1990) Rain, rainclouds and climate. *Q.J.R. met. Soc.* **116,** 1025–1051.

Buat-Ménard P. (1984) Assessing the contribution of atmospheric transport to the total pollution load of the Mediterranean Sea: facts and models. Nato ASI on strategies and advanced techniques for marine pollution studies. Beaulieu, France, 4–14 October 1984.

Buijsman E., Jonker P. J., Asman W. A. H. and Ridder T. B. (1991) Chemical composition of precipitation collected on a weathership on the North Atlantic. *Atmospheric Environment* **25A,** 873–883.

Burton M. A. S. and Bennett B. G. (1987) Exposure of man to environmental hexachlorobenzene (HCB)—an exposure commitment assessment. *Sci. total Envir.* **66,** 137–146.

Cadle S. H., VandeKopple R., Mulawa P. A. and Muhlbaier Dasch J. (1990) Ambient concentrations, scavenging ratios, and source regions of acid related compounds and trace metals during winter in northern Michigan. *Atmospheric Environment* **24A,** 2981–2989.

Cambray R. S., Jefferies D. F. and Topping G. (1975) An estimate of the input of atmospheric trace elements into the North Sea and Clyde (1972–1973). AERE Report R7733.

Cambray R. S., Jefferies D. F. and Topping G. (1979) The atmospheric input of trace elements to the North Sea. *Mar. Sci. Comm.* **5,** 175–194.

Cautreels W. and Van Cauwenberghe K. (1978) Experiments on the distribution of organic pollutant between airborne particulate matter and the corresponding gas phase. *Atmospheric Environment* **12,** 1133–1141.

Colin J. L., Jaffrezo J. L. and Gros J. M. (1990) Solubility of major species in precipitation: factors of variation. *Atmospheric Environment* **24A,** 537–544.

Dedeurwaerder H. L. (1988) Study of the dynamic transport and the fall-out of some ecotoxicological heavy metals in the troposphere of the Southern Bight of the North Sea. Ph.D. thesis, University of Brussels (VUB), Belgium.

Dedeurwaerder H., Dehairs F., Xian Q. and Nemery B. (1985) Heavy metals transfer from the atmosphere to the sea in the Southern Bight of the North Sea. In *Proceedings "Progress in Belgian Oceanographic Research"* (edited by Van Grieken R. and Wollast R.), pp. 170–177. University of Antwerp (UIA), Belgium.

Delbeke K. and Joiris C. (1988) Accumulation mechanisms and geographical distribution of PCBs in the North Sea. *Océanis* **14,** 399–410.

Duinker J. C. and Bouchertall F. (1989) On the distribution of atmospheric polychlorinated biphenyl congeners between vapor phase, aerosols, and rain. *Envir. Sci. Technol.* **23,** 57–62.

Eisenreich S. J., Looney B. B. and Thornton D. J. (1981) Airborne organic contaminants in the Great Lakes ecosystem. *Envir. Sci. Technol.* **15,** 30–38.

Escrivá C., Morales M., La Orden A., Mañes J. and Font G. (1991) Determination of polycyclic aromatic hydrocarbons in atmospheric particulate matter of Valencia city. *Fresenius J. analyt. Chem.* **339,** 743–745.

Flament P., Noël S., Auger Y., Leman G., Puskaric E. and Wartel M. (1984) Les retombées atmosphériques sur le littoral Nord-Pas-de-Calais. *Pollution Atmosphérique* oct.–déc. 1984, 262–270.

Folkertsma F. (1989) Nationale rapportage Noordzee-Aktieprogramma deel A: inventarisatie van emissies van geselecteerde stoffen in Nederland in 1985. Dienst Binnenwateren, RIZA, Lelystad, The Netherlands.

Galloway J. N., Thornton J. D., Norton S. A., Volchok H. L. and McLean R. A. N. (1982) Trace metals in atmospheric deposition: a review and assessment. *Atmospheric Environment* **16,** 1677–1700.

Georgii H.-W. and Schmitt G. (1982) Distribution of polycyclic aromatic hydrocarbons in precipitation. In *Precipitation Scavenging, Dry Deposition, and Resuspension, Vol. 1* (coordinated by Pruppacher H. R., Semonin R. G.

Table 13. Relative contribution of atmospheric deposition to the total loading (measured and model values) of the North Sea in percent

Pollutant	Atmospheric (measured)*	Non-atmospheric†	Atmospheric (model)†	Non-atmospheric†
Cd	66	34	14	86
Cr	7–18	82–93	2	98
Cu	33	67	4	96
Pb	49	51	35	65
Hg	1–2	98–99	13	87
Zn	32	68	5	95
PAHs	—	—	48	52
PCBs	55	45	93	7
γ-HCH	85	15	92	8

Data obtained from *Otten (1991) for Cd, Cu, Pb, Zn: PARCOM (1987) for Cr, Hg; GESAMP (1989) for PCBs and Lindane; and †Warmenhoven *et al.* (1989).

Protection of the North Sea in 1987, which are based on information obtained from the countries concerned (for trace metals, PCBs and lindane). For the contaminants which are not included in the report of the Conference, the total fluxes are estimated on the basis of data on the total loading through the Rhine and the Meuse (Folkertsma, 1989). The authors point out, however, that the values calculated in this way can only serve as an indication of the order of magnitude. For instance, for the volatile substances like chlorinated hydrocarbons the estimates may well be too high, because they will partly have volatilized from the riverwater before it reaches the North Sea. Also, the contamination of the water entering the North Sea from the English Channel, the Baltic Sea and the North Atlantic is not included in the estimates. And the river catchment areas are also subject to atmospheric deposition (Warmenhoven *et al.*, 1989). In Table 12 the estimates for non-atmospheric deposition of metals and organic compounds are given.

By comparing the non-atmospheric input to the atmospheric input fluxes we discussed earlier in this paper, it is possible to get an idea of the relative importance of both pathways for the input of pollutants to the North Sea. In Table 13 we compare the non-atmospheric values to measured and model atmospheric input values, respectively. We used the values calculated by the model of Warmenhoven *et al.* (1989) and flux values measured by Otten (1991) for Cd, Cu, Pb and Zn; by PARCOM (1987) for Cr andHg and by GESAMP (1989) for the organic compounds except PAHs. Although the percentages do not agree very well (which is not surprising, as the values for the atmospheric fluxes estimated by models and measurements do not agree either, and are nevertheless compared to the same non-atmospheric input values) the most important pathway for each compound seems the same for measurements and model, except for Cd. From Table 13 we can deduce that the non-atmospheric route is significantly more important for Cr, Cu, Hg and Zn. This trend is much less clear for Pb. For the organic compounds, things are the other way around: PCBs and γ-HCH are primarily deposited by the atmosphere, while for PAHs the contribution seems to be of equal importance.

GESAMP (1989) notes that for particulate trace elements the major source is usually the rivers. However, particulate riverine material is likely to be deposited close to the source regions, while atmospheric input can easily occur to remote oceanic areas. Still, according to the GESAMP report, the global atmospheric and riverine inputs are comparable for dissolved Cu, while for Zn and Cd atmospheric inputs appear to dominate. The atmospheric input of Pb is expected to decrease over the next decade, due to the growing use of unleaded gasoline. Martin *et al.* (1989) state that the atmospheric input to the Mediterranean Sea is predominant over the river input, either dissolved or particulate. For organic contaminants as well, the riverine flux may influence only the nearshore areas, while atmospheric input is supposed to have a much wider impact over regional seas (GESAMP, 1989). HCHs are estimated to be deposited to regional seas mainly via atmospheric inputs, while for other organochlorine compounds the riverine input may well be equal to or even exceed the atmospheric flux.

However, it must be emphasized that the accuracy of the estimations of both the atmospheric and non-atmospheric input sources is still very poor (especially for organic compounds). Thus the reliability of the comparison of both pathways is very uncertain.

6. CONCLUSION

It is obvious that current knowledge about the wet deposition of micropollutants to the North Sea is insufficient. For the trace metals which were dealt with in this paper, the situation is relatively favourable, although a number of specific problems like the lack of accurate washout ratios for the North Sea area or the contribution of resuspension to the observed pollutant concentrations still have to be solved. Also,

representative for the whole of the North Sea. The authors find a strong argument in the lifetime of clouds which is not more than a few hours for a precipitating one: in this way most of the pollutant material is likely to be washed out within about 100 km from the coast. Their model simulations (and those by van Jaarsveld *et al.* (1986)) reveal a substantial decrease of the deposition across the southern and western coasts. Van Jaarsveld *et al.* (1986) state that the discrepancy might partly be due to less accurate sampling and analysis of rainwater as well. However, in Table 12 we included input values calculated from airborne concentration measurements performed during flights over the North Sea itself (Otten, 1991), and the difference between these values and those calculated by the models remains large.

Because the PAH values reported by van Aalst *et al.* (1983) have a very wide range, it is almost impossible to compare them with the model value. Model PCB and γ-HCH values appear to be higher than measured values, but this trend is not very reliable because of the large uncertainties for both input values.

4.3. *Validation of the models*

Van Jaarsveld *et al.* (1986) note that there are some assumptions inherent to their model, which do not agree with reality very well. For instance, it is not correct to assume that transport and dispersion over sea are analogous to those over land. The stability over sea is mainly determined by the temperature difference between the air and the seawater, and shows hardly any diurnal variation. Also, in the coastal zone complicated transition phenomena occur, which are not accounted for in the model. However, the authors do not think that a more realistic model would yield largely different results.

Krell and Roeckner (1988) had difficulties in validating their model because of the lack of comparison material for the North Sea. Therefore, they were obliged to simulate air and precipitation concentrations at certain sites and for certain periods (e.g. a month) for which measurements were made, and their results agreed fairly well with the measured values.

Warmenhoven *et al.* (1989) estimate that the results concerning the heavy metal deposition are the most reliable ones. For Hg, however, the deposition parameters are insufficiently founded and the contribution of the background concentration may be considerable. As far as the organic compounds go, the calculated values of the total deposition into the North Sea of PAHs, PCBs and γ-HCH are probably reasonably reliable. For chlorohydrocarbons the situation is worse: the emission data used are not up to date, nor well established, and the deposition parameters are also not well founded. Additionally, if we take into consideration that the background concentrations could be quite high, we have to conclude that these results can only be seen as rough estimates.

In general, the validity of this model is mainly governed by (i) the quality of the emission data and (ii) the choice of the emission grid (because some materials are that stable in the atmosphere, that a much larger emission area should be taken into consideration). As a result of this, the real deposition of these compounds should be higher than predicted by the model, especially for organochlorines, PAHs and Hg. Finally, the assumption that the North Sea is a well-mixed tank without any inflow or outflow except from rivers (and the atmosphere), has an influence on the deposition estimates. In this concept the contribution of atmospheric deposition would increase when the size of the North Sea used in the model is increased. Therefore, it would be more realistic to include the dynamics of the North Sea in the model.

5. RELATIVE CONTRIBUTION OF ATMOSPHERIC DEPOSITION OF MICROPOLLUTANTS TO THE TOTAL INPUT INTO THE NORTH SEA

Apart from atmospheric pollution, the North Sea is subject to a number of other sources of pollution as well (van Aalst *et al.*, 1983): e.g. input via rivers, direct discharges from industries into the estuaries, dumping of industrial wastes, dredging sludge and sewage sludge, and drainage of sewage. It is very difficult to evaluate the relative importance of the various input sources as most input estimates are subject to considerable uncertainty arising from analytical and sampling problems. Moreover, the actual quantity of pollutants entering the North Sea will vary from year to year, depending on factors like natural variations in river flows and water exchange with adjacent sea areas, economic variations (industrial expansion and reorganization, large strikes), changing legislation (emission and dumping restrictions), atmospheric conditions (wind flow patterns, rainfall intensity) and unforeseen circumstances (accidents) (Otten, 1991).

Although in a number of publications estimates of the non-atmospheric input are given (e.g. Cambray *et al.*, 1979; van Aalst *et al.*, 1983; ATMOS, 1984), we chose to use the recent data as given by Warmenhoven *et al.* (1989). They use the figures reported during the Second International Conference on the

Table 12. Total input into the North Sea by non-atmospheric sources (the input of water from the English Channel, the Baltic Sea and the North Atlantic is not included) in tons yr^{-1} (for references see text)

Pollutant	Input
Cd	95
Cr	4000
Cu	2800
Pb	3500
Hg	1200
Zn	17,000
PAHs	91
PCBs	3
γ-HCH	3

The same report also mentions the important deposition mechanisms for some pesticides. Wet deposition by the uptake of gas is of major importance for HCHs and to a lesser degree for dieldrin and DDT. For HCB, dieldrin, DDT and α-HCH dry gaseous deposition is especially important. And finally, wet deposition of DDT and DDE particles is relatively high as well.

4. WET FLUX MODELS

An alternative way of determining the deposition of micropollutants from the atmosphere to the sea involves atmospheric transport models. Basically, one uses emission data for a certain source area (e.g. Europe) in combination with a long range transport model (which requires a number of input data) to simulate the dispersion and deposition of a substance for a determined receptor area (e.g. the North Sea).

In this section the results of calculations performed using relatively recent models which have been applied to the calculation of the (total) deposition of heavy metals and/or organic compounds to the North Sea will be discussed and compared to the values obtained from field measurements.

The TREND model was developed at the Dutch National Institute of Public Health and Environmental Protection in order to calculate long term averaged concentrations and depositions (van Jaarsveld *et al.*, 1986). It is a statistical long-range version of the Gaussian plume model. The occurring meteorological situations are grouped in a limited number of classes and the calculations are carried out separately for five size classes from $<0.95\ \mu m$ to $>20\ \mu m$, each of which has its own deposition characteristics. This model has been successfully applied to a period of a month, but even shorter periods yielded reasonable results. The model of Krell and Roeckner (1988) was developed in order to estimate the dry and wet deposition of lead and cadmium into the North sea. Krell and Roeckner use a three-dimensional stochastic model to calculate the transport of trace metals in the atmosphere. The input of Pb and Cd is simulated with a long-range transport model using gridded data of the respective anthropogenic emissions in Europe and the relevant meteorological data (Krell and Roeckner, 1988), Krell and Roeckner's model is designed for episode studies particularly. The model of Graßl *et al.* (1989) is very similar to the model of Krell and Roeckner. The model of Warmenhoven *et al.* (1989) is in fact an elaborated version of the van Jaarsveld model, but instead of applying it to trace metals solely, a number of organic compounds like PAHs, PCBs, pesticides, etc. were also taken into consideration (Warmenhoven *et al.*, 1989).

4.1. *Literature data on the deposition fluxes of micropollutants based on model calculations*

The total atmospheric input of nine pollutants into the North Sea (in tons yr^{-1}) is given in Table 11. The values were calculated with the models discussed in the previous section. A comparison between the results of the different models can only be made for trace metals as only Warmenhoven *et al.* (1989) used their model to calculate the atmospheric input of organic micropollutants. The values obtained by the first three models were slightly adapted to the North Sea area considered in the study of Warmenhoven in order to be able to compare the figures. It is clear that the results agree well with each other. Taking into account that all models use more or less the same emission data, this agreement confirms the idea that the influence of the different model assumptions is not very large, at least not in the case of the total deposition into the North Sea.

4.2. *Comparison with field measurement data*

For trace elements, the model values are consistently lower than the values obtained from (extrapolations of) measurements. Krell and Roeckner (1988) claim that this discrepancy can be explained as follows: the extrapolation of coastal measurements, on which most deposition estimates up until 1988 were based, cannot be justified, because there is no reason to believe that the high rainwater concentrations measured along the southern and western coasts are

Table 11. The total atmospheric input of micropollutants into the North Sea in tons yr^{-1}

Pollutant	v. Jaarsveld *et al.* (1986)	Krell and Roeckner (1988)	Graßl *et al.* (1989)	Warmenhoven *et al.* (1989)	"Field values"*
Cd	11	11	—	15	186
Cr	58	—	—	72	300–900
Cu	100	—	—	110	1410
Pb	2000	1200	2300	1900	3390
Hg	—	—	—	7	10–30
Zn	940	—	—	930	7900
ΣPAH	—	—	—	83	50–1300
ΣPCB	—	—	—	39	3.7
γ-HCH	—	—	—	36	17.6

* References: for Cd, Cu, Pb, Zn: Otten (1991)/for Cr, Hg: PARCOM (1987)/for PAHs: van Aalst *et al.* (1983)/for PCBs, γ-HCH: GESAMP (1989).

ence is probably caused by different methodologies, which may have generated (too) high concentrations about a decade ago.

In a study by Swackhamer and Armstrong (1986) indications were found that the atmosphere is a "sink" as well as a source for PCBs. In this work estimations are made for the fluxes to and from Lake Michigan (U.S.A.), which are then compared to estimates for four remote Wisconsin lakes. In these remote lakes, volatilization back to the atmosphere was thought to account for more than 50% of the PCB losses from the lake. In a later report by Swackhamer *et al.* (1988) the deposition and evaporation to and from Siskiwit Lake (a small lake on an island in Lake Superior (U.S.A.), that only receives atmospheric inputs) for 17 PCB congeners was investigated. They observed that the removal of PCBs from the lake by volatilization made up for 65% of the total losses (so about twice as important as sedimentation). As far as the input/output scenario goes, the authors think that the input of PCBs occurs by intense and short precipitation events, while the volatilization happens slowly and gradually, over a long period, under favourable weather conditions. This is confirmed by Murray and Andren (1992). It is concluded that the atmosphere may have been a major sink for PCBs in recent years. Therefore, the residence time for PCBs in the atmosphere is likely to be much longer than expected.

Finally, Delbeke and Joiris (1988) investigated the geographical distribution of PCBs in the North Sea: high PCB levels were found in the Belgian coast zone decreasing with increasing distance from the coast (51–53°N) and close to the Dogger Bank (53–54°N) and low levels in the northern water masses (54–60°N). This gradient corresponds very well to the precipitation concentration values observed along the British coastline (Wells and Johnstone, 1978).

3.3.3. *Pesticides.* Some airborne concentrations of pesticides are displayed in Table 6, and in Table 7 the concentrations in precipitation are listed. The sites, sampling periods and other characteristics for the values reported by Eisenreich *et al.* (1981), Bidleman *et al.* (1987), the GESAMP report (1989) and Wells and Johnstone (1978) are similar to what is mentioned in our discussion on PCBs. Bidleman *et al.* (1987) came up with Swedish concentrations in air for DDT, chlordane, HCB, α-HCH and γ-HCH. For DDT it is suspected that residues in the atmosphere over northern Europe and the northern Atlantic are at least partially due to long-range transport from areas around the world, where it is still heavily used (e.g. Africa, the Middle East, India,...). Similarly to PCBs, Bidleman and Christensen (1979) concluded that the wet deposition of DDT occurs by scavenging of particles mainly. Although in Europe almost exclusively γ-HCH is used, α-HCH concentrations exceed those of γ-HCH in all samples, for which two explanations can be put forward (Bidleman *et al.*, 1987): long-range transport from countries where technical HCH is still applied and isomerization of γ-HCH to α-HCH. This latter phenomenon was observed by Oehme and Manø (1984), who compared the airborne concentrations of organic pollutants over Norway and the Arctic, and by Lane *et al.* (1992) as well. The photoisomerization of HCH isomers was studied in detail by Malaiyandi and Shah (1984): they demonstrated that both β-HCH and γ-HCH can be transformed in the presence of sunlight (and ferrous salts) to yield the α-isomer. Although α-HCH is thermodynamically not the most stable HCH-isomer, it certainly has the largest photochemical stability, which could possibly explain its persistence and observed enhanced levels in the atmosphere. α-HCH also shows a consistent temperature dependency, which suggests that temperature-dependent re-emission or volatilization processes could be a significant way to enter the atmosphere in areas far away from sources of anthropogenic emissions (Lane *et al.*, 1992). In wintertime higher γ-HCH air concentrations were observed by Oehme and Manø (1984). This can be explained by an increased photochemical transformation in the summer season and the fact that the use of lindane is mainly limited to the spring time. Van Aalst *et al.* (1983) report briefly on the possibility that some pesticides (aldrin, dieldrin and DDT) may be photolysed into similar products. HCB showed no clear temperature dependence and was consistent in concentration over the period of a year (Lane, 1992).

Washout ratios for pesticides are represented in Table 8. Reinhardt and Wodarg (1989) deduce from their values for α-HCH and γ-HCH measured at a lighthouse at Kiel Bight (Germany) that wet deposition only accounts for a proportion of total deposition. Lane *et al.* (1992) detected neither the α-HCH nor the γ-HCH in filtered particulate matter. This observation agrees very well with the fact that the vapour pressures and water solubilities of the HCHs are high enough to allow that they remain primarily as gases in the atmosphere or dissolved in water with rather small quantities sorbed onto particles (Bidleman, 1988; Hinckley and Bidleman, 1991).

According to Nakano *et al.* (1990) chlordane exists for more than 95% in the vapor phase, just like PCBs. Bidleman and Christensen (1979) state that chlordane is inefficiently removed by rainfall or dry deposition, and that it should have a longer atmospheric lifetime than PCBs or DDT in the absence of other removal processes like photodegradation.

The mean annual input of pesticides into the North Sea is estimated at 1.43 tons for DDT; 2.08 tons for total HCH and 0.27 tons for dieldrin (Wells and Johnstone, 1978). Also for the North Sea, van Aalst *et al.* (1983) estimated the total deposition of each compound to lie within the following ranges (in tons yr^{-1}): 10–100 (for total HCH) and 2–22 (for total DDT). They point out that these values are very uncertain. In the GESAMP report (1989) the following values for the total atmospheric input into the North Sea are listed (in tons yr^{-1}): 10.4 (α-HCH); 17.6 (γ-HCH); 0.9 (DDT); 1.1 (dieldrin); 0.1 (chlordane) and 0.5 (HCB).

Table 10. ΣPCB for the used references

ΣPCB	Wells and Johnstone (1978)	Bidleman and Christensen (1979)	Eisenreich *et al.* (1981)	Bidleman *et al.* (1987)	Duinker and Bouchertall (1989)	GESAMP (1989)
Aroclor 1016	(Not specified)	+	(Not specified)	(Not specified)		
Aroclor 1242						60%
Aroclor 1254		+				40%
2,2′,5					+	
2,2′,4					+	
2,3′,6					+	
2,3′,5					+	
2,2′,5,5′					+	
2,2′,4,5′					+	
2,2′,3,5′					+	
2,2′,4,5,5′					+	
2,2′,3,4′,5′,6					+	
2,3′,4,4′,5					+	
2,2′,4,4′,5,5′					+	
2,2′,3,4,4′,5′					+	
2,2′,3,3′,4′,5,6					+	
2,2′,3,4,4′,5,5′					+	

compound under consideration. When PAHs are not revolatilized but—on the contrary—are adsorbed on particles or stay in solution, they may eventually reach the bed of the various water bodies and remain there stable for very long periods, in the absence of light and under anaerobic conditions.

3.3.2. *Polychlorinated biphenyls.* In Table 6, two references are included, which give airborne concentration values for PCBs, and they seem to differ by at least a factor of 4. However, the data were generated in completely different ways: the GESAMP (1989) value in Table 6 is estimated on the basis of available literature values like the concentration to use for the calculation of the deposition fluxes above the North Sea. On the other hand, Bidleman *et al.* (1987) measured the occurrence of PCBs in the atmosphere of southern Sweden with sampling sites in Stockholm and Aspvreten (on the coast of the Baltic Sea). The vapour-to-particle ratio (V/P ratio) of PCBs was studied by Nakano *et al.* (1990). More than 95% of the PCBs were found to exist in the vapour phase. The V/P ratio is dependent on the sampling temperature and vapour pressure for each compound, for each congener and for each isomer. Van Aalst *et al.* (1983) estimated that presumably less than 15% of the PCBs occurs in the particulate form and if they do they are adsorbed on submicron aerosols particularly.

In Table 8 some washout ratios for PCBs are given. Duinker and Bouchertall (1989) determined W values in their experiments, which were considerably larger than calculated gas phase-only ratios (calculated from Henry's law constants), indicating that particles play a dominant role in determining the levels of PCBs in rain.

Wells and Johnstone (1978) performed precipitation concentration measurements at seven stations at the eastern coastline of Great Britain. Three-monthly samples were taken between June 1975 and May 1976. The results indicated a general increase in the observed PCB concentration from the most northerly station to the south. Duinker and Bouchertall (1989) analysed 14 PCB congeners in filtered air, particulates and rain, which were collected simultaneously in Kiel, Germany (western Baltic Sea). Large concentration differences for air and rain samples can be observed when the respective values for the individual samples are compared to each other (1 order of magnitude). In the filtered air the congeners with a low degree of chlorination were most abundant, while in rain and particles those with a high degree of chlorination dominated. Up to 99% of the total atmospheric concentrations of the most volatile congeners was found in the vapour phase. Nevertheless, although particulate PCBs only contributes about 1 or 2% to the total atmospheric concentration, Duinker and Bouchertall (1989) thought particle scavenging was the dominant source of PCBs in rain, which was also stated by Bidleman and Christensen (1979) and Murray and Andren (1992), who attributed this fact to their relatively high Henry's law constants.

Wells and Johnstone (1978) estimated the mean annual input for the North Sea (area of 5.75×10^5) to be 1.91 tons for PCBs. For the same area, van Aalst *et al.* (1983) found a range of 10–160 tons yr^{-1} for the total deposition of PCBs and in GESAMP (1989) a value of 3.7 tons yr^{-1} was estimated. In this last report we find that the deposition mechanisms of PCBs are divided as follows: particle/dry 0.6%—particle/wet 22.8%—gas/dry 65.3%—gas/wet 11.3%. The total annual deposition to the Great Lakes was estimated at 20–150 $\mu g\, m^{-2}$ (Eisenreich *et al.*, 1981). Assuming an annual precipitation rate of 750 mm yr^{-1}, in the Great Lakes region, Murray and Andren (1992) calculated a wet flux of 2.6 $\mu m\, m^{-2}\, yr^{-1}$, which is significantly lower than the value reported by Eisenreich *et al.* (1981). This differ-

Table 9. ΣPAH for the used references

ΣPAH	Cautreels and Van Cauwenberghe (1978)	Björseth *et al.* (1979)	Ligocki *et al.* (1985)	McVeety and Hites (1988)	Quaghebeur *et al.* (1983)	Levsen *et al.* (1990)
Naphtalene	+					
1-Methylnaphtalene	+					
2-Methylnaphtalene	+					
Ethyl- or dimethylnaphtalenes	+					
Trimethyl- or methyl, ethylnaphtalenes	+					
Tetramethyl- or diethyl- or dimethyl, ethylnaphtalenes	+					
Biphenyl	+					
Dibenzofuran			+			
Fluorene	+		+			
9-Fluorenone			+			
Phenanthrene	+	+	+	+		
Anthracene	+	+	+	+		
Methylphenanthrenes	+	+	+			
Methylanthracene	+	+				
Ethylphenanthrene	+					
Ethylanthracene	+					
9,10-Anthracenedione			+			
Fluoranthene	+	+	+	+	+	+
Pyrene	+	+	+	+		+
Benzofluorenes, methylfluoranthenes or methylpyrenes	+	+				
Benzo(*c*)phenanthrene						
Benz(*a*)anthracene	+	+	+	+		+
Chrysene	+	+	+	+		+
Triphenylene		+		+		
7-Benz(*de*)anthracenone			+			
Benzo(*b*)fluoranthene	+	+	+		+	+
Benzo(*j*)fluoranthene		+	+			
Benzo(*k*)fluoranthene	+	+	+		+	+
Benzo(*e*)pyrene	+	+	+	+		+
Benzo(*a*)pyrene	+	+	+	+	+	+
Perylene	+	+	+			
O-phenylenepyrene		+				
Benzo(*ghi*)perylene		+	+	+	+	+
Indenopyrene				+	+	+
Dibenz(*a,h*)anthracene		+			+	
Coronene			+			
Anthanthrene		+				

Table 8. Overall washout ratios for PAHs, PCBs and pesticides (n- preceding an area means northern)

Area	PAHs $\times 10^3$	PCBs	HCB $\times 10^3$	α-HCH	γ-HCH	ΣHCH	ΣDDT $\times 10^4$	Dieldrin $\times 10^3$	Chlordane	Remarks	References
South Carolina (U.S.A.)	—	5–214	—	—	—	—	<0.001–0.02 (p,p'-DDT)	—	<1–16	Measured values	Bidleman and Christensen (1979)
nPacific Ocean	—	—	—	—	34–38	—	—	—	—	Measured values	Atlas and Giam (1981)
(not specified)	—	1–9 × 10^4	1.5	—	—	5 × 10^4	2–8	2–9	—	Measured values	Eisenreich *et al.* (1981)
Portland, Oregon	1–20	—	—	—	—	—	—	—	—	Measured values	Ligocki *et al.* (1985)
Siskiwit Lake, U.S.A.	0.79–248 (rain)	—	—	—	—	—	—	—	—	Measured values	McVeety and Hites (1988)
Siskiwit Lake, U.S.A.	13.2–104 (snow)	—	—	—	—	—	—	—	—	Measured values	McVeety and Hites (1988)
Kiel Bight	—	—	—	3–5	30	—	—	—	—	Measured values	Reinhardt and Wodarg (1989)
Kiel, Germany	—	2 × 10^{-4}–138 × 10^{-2}	—	—	—	—	—	—	—	Measured values	Duinker and Bouchertall (1989)
Hannover, Germany	1–20	—	—	—	—	—	—	—	—	Source?	Levsen *et al.* (1990)

masses originating from the same source area and concluded that the PAH concentrations can be reduced by 60% by particle scavenging during precipitation events.

Precipitation concentration values for two western European sampling locations are given in Table 7. At two locations in Belgium, Melsbroek (near Brussels) and Libramont (Belgian Ardennes), precipitation samples were taken daily and the occurrence of six PAHs (see Table 9) was investigated (Quaghebeur *et al.*, 1983). Maximum concentrations were found during the winter months and they observed that in areas presumed to be almost free of pollution considerable quantities on PAHs can be determined. Georgii and Schmitt (1982) observed that the concentrations vary significantly among individual events: they are influenced by meteorological factors like type of rainfall, air temperature and the length of the dry period which precedes the rain event. Nevertheless, the concentration pattern among the individual compounds remains strictly constant: it is not affected by meteorology or type and form of precipitation, but only influenced by the relative concentration of the different compounds of the emission sources.

Van Aalst *et al.* (1983) estimated for the total deposition of PAHs to the North Sea (area of 525,000 km^2 and precipitation rate of 685 mm yr^{-1}) a value between 50 and 1300 tons yr^{-1}, which is a rather large range. They emphasize the fact that they did not take into account any sea-to-air fluxes and that their values should be considered as maximum values. For lack of other flux values for the North Sea area, it might be interesting to compare van Aalst's values to some reported fluxes for the Great Lakes area. McVeety and Hites (1988) calculated the wet flux to Siskiwit Lake for 11 compounds: it ranges from 0.061 (for benzo[*a*]anthracene) to 0.54 ng cm^{-2} yr^{-1} (for phenanthrene). It should be noted that dry deposition to the lake was found to be nine times more important for PAHs than wet deposition.

One should always be careful with the interpretation of measured or calculated fluxes of organic compounds to regional seas. They may be overestimated, because it is possible that those bodies of water only serve as a temporary sink for the pollutants. Large, deep waters have the possibility to remove the organics from the surface layers by sedimentation or mixing with undersaturated waters. For shallow seas (e.g. the North Sea) or lakes this capacity is limited and they are likely to get rid of the excess of deposited material by revolatilization (GESAMP, 1989). For Siskiwit Lake, McVeety and Hites (1988) made an estimation of the mass balance for PAHs. For the most volatile congeners (phenanthrene and anthracene), approximately 80% of the input flux is revolatilized. As the vapour pressure of the congeners decreases with increasing molecular weight, larger amounts of PAHs are removed by sedimentation. This means that—in general—for PAHs the magnitude of surface volatilization is proportional to the vapour pressure of the

Table 6. Airborne concentrations of PAHs, PCBs and pesticides over the North Sea and adjacent areas in pg m^{-3} (s- preceding an area means southern) (for more information on ΣPAH and ΣPCB see Tables 9 and 10)

Area	Period	ΣPAH $\times 10^3$	ΣPCB	HCB	α-HCH	γ-HCH	ΣDDT	Dieldrin	Chlordane	Remarks	References
Arctic	1980–1981	—	—	29–188	161–1290	12–50	—	—	—	—	Oehme and Manø (1984)
Norway	1981	—	—	55–234	347–1230	154–410	—	—	—	Rural area	Oehme and Manø (1984)
Sweden	1983–1985	—	165–173	—	118–3250	21 > 660	1–142	—	—	—	Bidleman *et al.* (1987)
North Sea	—	—	750	250	350	350	40	75	10	Value estimated	GESAMP (1989)
sNorth Sea	1986	—	—	125	70	60	—	—	—	—	Reinhardt and Wodarg (1989)
Belgium	1976	64.6	—	—	—	—	—	—	—	Aerosols–urban	Cautreels and Van Cauwenberghe (1978)
Belgium	1976	77.2	—	—	—	—	—	—	—	Gas phase–urban	Cautreels and Van Cauwenberghe (1978)
sNorway (North Sea coast)	1977	7.9	—	—	—	—	—	—	—	Aerosols	Björseth *et al.* (1979)
sSweden (Baltic coast)	1976–1977	12.4	—	—	—	—	—	—	—	Aerosols	Björseth *et al.* (1979)

Table 7. Concentrations of PAHs, PCBs and pesticides in precipitation over the North Sea and ajacent area in pg·ℓ^{-1} (for more information on ΣPAH and ΣPCB see Tables 9 and 10)

Area	Period	ΣPAH $\times 10^3$	ΣPCB	HCB	α-HCH	γ-HCH	ΣDDT	Dieldrin	Chlordane	Remarks	References
Belgium	1978–1980	140–145	—	—	—	—	—	—	—	—	Quaghebeur *et al.* (1983)
Hannover, Germany	1989–1990	50–1800	—	—	—	—	—	—	—	—	Levsen *et al.* (1990)
UK coast	1975–1976	—	1800–74,000	—	5700–17,000		300–44,000	200–1400	—	Total HCH	Wells and Johnstone (1978)

Table 5. Washout ratios for trace metals

Cd	Cr	Cu	Pb	Zn	Remarks	References
125–500	150	140–751	76–169	179–1000	Literature range	Schroeder *et al.* (1987)
—	—	—	—	1226	Value measured	Jaffrezo and Colin (1988)
200–1000	—	200–1000	200–1000	200–1000	Range used	GESAMP (1989)
150	—	150	150	150	Value used	Otten *et al.* (1989a)
—	200–1280	60–3800	20–1350	280–11,500	Value measured (snow)	Cadle *et al.* (1990)

3.3. *Data on organic compounds*

In Tables 6, 7 and 8 some literature data on airborne concentrations, precipitation concentrations and washout ratios are presented for a number of organic substances. The information published on the occurrence and deposition of these compounds in the North Sea area is scarce, especially compared to the amount of publications on the Great Lakes area (U.S.A.) for instance.

3.3.1. *Polycyclic aromatic hydrocarbons* (PAHs). Table 6 shows some literature values for PAH concentrations in air. Very high air concentrations were observed at the Scandinavian coast during winter and (early) spring (Björseth *et al.*, 1979): the higher energy generation for house heating purposes in winter leads to higher amounts of pollutants being introduced into the atmosphere. Higher atmospheric PAH levels during winter were also observed by several other authors (Leuenberger *et al.*, 1988; McVeety and Hites, 1988; Escrivá *et al.*, 1991; Valerio and Pala, 1991). Also, air masses may be transported over very long distances (e.g. from central Europe) with very little dilution because of slower vertical mixing in cold weather. And finally, the UV-light intensity is lower during winter and hence the degradation of PAHs due to photochemical processes should be lower as well (Björseth *et al.*, 1979; Valerio and Pala, 1991). In this respect it is noteworthy that Suess (1976) states that there are basically two modes of PAH degradation: physical oxidation and biological reduction after uptake by aquatic organisms. Photochemical degradation by reaction with ozone and various oxidants is often cited as an important process to remove PAHs from the atmosphere (Suess, 1976; Pitts *et al.*, 1978; Korfmacher *et al.*, 1980; Kamens *et al.*, 1988; Masclet *et al.*, 1988; Valerio and Pala, 1991). Exposure to sun light can also be the cause of the formation of directly active mutagens, when PAHs are exposed to ppm levels of gaseous components in photochemical smog (NO_2, O_3 and PAN) (Pitts *et al.*, 1978). On the other hand, most of the year—because of the climate—the conditions for this kind of decomposition of PAHs over northern Europe and the North Sea are not very suitable. However, during laboratory experiments Butler and Crossley (1981) discovered that exposure of PAHs adsorbed on soot particles to ambient air converted the PAHs into nitro derivatives, even in the absence of photolysis and ozone. Also, evidence was found that for benzo(*a*)pyrene and anthracene adsorbed on fly ash the principal degradation route is non-photochemical and that the presence of light is not really important. This implies that chemical transformation of these adsorbed PAHs in the atmosphere may be principally determined by thermal reactions (Korfmacher *et al.*, 1980).

In Table 6 a distinction is made between the gas phase and particulate concentrations of the Belgian samples. PAHs occur in both phases in the environment and their distribution depends on numerous factors. The gas/particle ratio varies with the molecular weight of the compound: the tricyclic compounds exist almost entirely in the gaseous form, while compounds with five or more rings are entirely adsorbed on the particles. Furthermore, this ratio is influenced by temperature—lower temperatures give higher amounts of adsorbed PAHs on atmospheric particulate matter (Valerio and Pala, 1991)—and precipitation events as well (see also Cautreels and Van Cauwenberghe, 1978).

As explained at the beginning of this section, it is possible to estimate the wet deposition flux of a certain compound using its atmospheric concentration and its washout ratio. In Table 8 some overall (gas + particle) PAH washout ratios are reported, though no literature values for the North Sea could be found. Generally, they are an order of magnitude larger for PAHs of MW < 202 (more volatile) than for PAHs of MW > 202 (Ligocki *et al.*, 1985). The increase in the W_p values for compounds associated with larger particles and the overall magnitude of the measured scavenging ratios both led the authors to suggest a below-cloud removal mechanism. Also, when—for each compound—the particle washout ratios are compared to the gas scavenging ratios (W_g) (ranging from 1500 to 18000), it becomes clear that gas scavenging dominates over particle scavenging for all PAHs of MW < 252 (which means most PAHs). These observations are confirmed by Van Noort and Wondergem (1985), who found out that those compounds, which are mainly present in the air on aerosols, occur in rain as a result of in-cloud scavenging; those PAHs which are mainly present in the gas phase on the other hand, enter rain as a result of below-cloud scavenging. Nevertheless, McVeety and Hites (1988) observed that the compounds which are found mainly in the gaseous phase, are not removed from the atmosphere as efficiently as those that are present as aerosols. Masclet *et al.* (1988) followed two air

Table 4. Total (dry + wet) or wet flux to the North Sea in $\mu g\,cm^{-2}.yr^{-1}$ (s- preceding an area means southern)

Area	Rain ($mm.yr^{-1}$)	Cd	Cr	Cu	Pb	Hg	Zn	Method	Remarks	References
Coastal stations	438	—	0.14	1.05	1.1	0.0013	3.1	Direct	Wet	Cambray *et al.* (1979)
Coastal stations	778–1028	0.03–0.14	—	0.61–1.62	0.56–1.35	—	2.06–5.56	Direct	Total	Flament *et al.* (1984)
Coastal stations	—	0.009–0.17	0.058	0.08–2.7	0.51–1.4	0.002	0.93–15.6	—	Total	PARCOM (1987)
Scotland (coast)	=	0.039	—	0.13	0.23	—	0.76	Direct	Wet	Balls (1989)
sNorway (coast)	1399	0.048	—	—	0.92	—	1.2	Direct	Total	S&TWG (1987)
Dutch Continental Shelf	—	0.006–0.011	0.015–0.030	0.028–0.055	0.48–0.96	0.001	0.24–0.48	—	Total	S&TWG (1987)
North Sea	680	0.01–0.05	—	0.1–0.44	0.4–2.3	—	0.5–2.3	Indirect	Total	GESAMP (1989)
North Sea	430	0.29	—	2.5	0.7	—	17	Direct	Wet (dissolved)	Baeyens *et al.* (1990)
North Sea	500	0.035	—	0.268	0.65	—	1.51	Indirect	Total	Otten (1991)
sNorth Sea	—	0.16	—	2.49	0.94	—	14.3	—	Wet	ATMOS (1984)
Southern Bight	458	0.00002	—	0.00026	0.00014	—	0.0015	Direct	Total	Dedeurwaerder *et al.* (1985)
Southern Bight	500	0.043	—	0.25	0.88	—	1.97	Indirect	Wet	Otten (1991)
Southern Bight	500	0.071	—	0.536	1.29	—	3.02	Indirect	Total	Otten (1991)

based on sampling flights and were calculated using scavenging rates.

As far as the relative importance of dry and wet deposition goes, most authors seem to agree on the fact that, for the trace metals considered in this section, the wet flux is more important than the dry flux, except perhaps for Pb, where some authors consider both fluxes to be of about the same magnitude. However, on the extent of this difference opinions vary very widely (Galloway *et al.*, 1982; ATMOS, 1984; Schroeder *et al.*, 1987; GESAMP, 1989; Martin *et al.*, 1989; Baeyens *et al.*, 1990; Otten, 1991; Remoudaki *et al.*, 1991). Martin *et al.* (1989) remark that the ratio of wet to dry deposition is controlled by many meteorological factors and also by the distance between the sampling site and the emission source (see also Migon *et al.*, 1991; Remoudaki *et al.*, 1991).

Whenever the deposition of micropollutants to a body of water is estimated, attention should be paid to the reverse fluxes (from the water to the atmosphere) as well. According to the ATMOS report (1984), for which the heavy metal content in the sea surface microlayer was determined, the maximum water-to-air fluxes are at least 30-times smaller than the total input fluxes. The authors of the GESAMP report (1989) state that, although the atmospheric concentrations of trace metals associated with large (resuspended) sea salt particles constitute only a minor fraction of the total atmospheric concentration, this fraction may well account for a significant part of the gross dry deposition flux. This complicates the assessment of the "real" deposition fluxes to the sea.

For indirect estimations of the wet flux the washout ratio used in the calculations is of considerable importance. In Table 5 some relatively recent values for trace metals are listed. They are—again—very difficult to compare. The values used in the GESAMP (1989) report and by Otten *et al.* (1989a) are "best estimates" based on published washout ratios for trace metals above the North Sea. In the ATMOS report (1984) it is stated that values for Cu, Zn and Cd above the sea are up to 5-times larger than above land. Washout ratios for Hg were calculated for the cases where both the air and precipitation concentrations had been measured: $Hg_{tot,\,rain}/Hg_{tot,\,air}$ values of 10^3–10^4 were found (Lindqvist and Rodhe, 1985). If, on the other hand, only the water-soluble fraction of the gas phase or the particulate part of the airborne Hg is considered, W is much more similar (10^5 and 10^6, respectively) to the values for the other trace metals. It is concluded that the particulate Hg and the water-soluble gaseous forms probably contribute significantly to the precipitation mercury content. In determining the flux of Hg from the atmosphere to the sea a difficulty may arise. Because mercury is such a volatile element, it is very well possible that a considerable fraction of the deposited mercury is re-emitted to the atmosphere very quickly before being actually incorporated into soil or water. This characteristic may thus give rise to a kind of "counter-flux".

deposition depends on it. For instance, dissolved metals are much more readily available to be incorporated by organisms. Flament *et al.* (1984) investigated the metal distribution over the solid and liquid phases in rain at some French coastal sites. They found the following percentages of dissolved material: Pb (21–31%), Cd (53–78%), Cu (63–94%) and Zn (68–87%). Losno *et al.* (1988) observed that Zn partitioning is governed by adsorption/desorption processes on existing particles, which are pH dependent. Nevertheless, Colin *et al.* (1990) state that the nature of the particles is also important. Jickells *et al.* (1992) conclude that the solubility of an element is the result of the complex interplay of several factors and cannot be simply assigned to one factor such as pH.

3.2.3. *Fluxes to the North Sea.* As explained at the beginning of this section the wet flux of trace metals can be estimated either directly or indirectly. Table 3 contains the amount of material (in tons) which is deposited to the North Sea each year, while in Table 4 a number of wet and total fluxes to the North Sea and its coasts are given. The total flux is the sum of the wet and the dry flux. In Table 3 the area considered to constitute the North Sea and the used value for the annual precipitation rate are included, as well as the method used (direct or indirect measurement). The first column in Table 4 is used to describe the area or sites the flux is calculated for.

It is very difficult to compare any data in Tables 3 and 4, because the authors used different rainfall rates and methods, and because both total fluxes and wet fluxes are listed. Nevertheless, it is clear that the figures obtained by an indirect estimation of the flux are generally significantly lower than those obtained in a direct way. Also, most of these direct measurements are the "oldest" values in the tables. This could mean that the fluxes calculated may have been overestimated due to sample contamination and analytical inaccuracy. In Table 3 the atmospheric flux reported in the ATMOS report (1984) is seriously higher than the other total fluxes, except for lead. The range calculated by van Aalst *et al.* (1983) is also relatively high but the other total flux values agree fairly well. The two wet deposition fluxes included in Table 3 illustrate dramatically the impossibility to compare them. They were assessed at totally different points in time, with other methods and concentration measurements to start from (coastal precipitation vs airborne concentrations, and even the area taken into consideration is different). In Table 4 the fluxes to the coast of southern Norway (S&TWG, 1987) and of Scotland (Balls, 1989) are reported to be lower than the other coastal values. And for the North Sea itself the West-Hinder values are either relatively high (except for Pb) (ATMOS, 1984; Baeyens *et al.*, 1990) or very low (Dedeurwaerder *et al.*, 1985). The former authors both report that the wet flux to the North Sea is clearly higher than that to a Belgian coastal station for the metals considered in this paper. It should be noted that the input values reported by Otten (1991) are

Table 3. Total (dry + wet) or wet atmospheric input of trace metals into the North Sea in tons yr^{-1}

Area (km^2) $\times 10^5$	Rain ($mm\,yr^{-1}$)	Cd	Cr	Cu	Pb	Hg	Zn	Method	Remarks	References
5.3	438	—	740	5600	5800	7.0	16,000	Direct	Wet	Cambray *et al.* (1979)
5.25	685	110–430	70–1400	1400–10,000	3600–13,000	<36	7200–58,000	Direct	Total	van Aalst *et al.* (1983)
5.3	—	900	—	13,542	7367	—	77,566	—	Total	ATMOS (1984)
—	—	45–240	300–900	400–1600	2600–7400	10–30	4900–11,000	—	Total	PARCOM (1987)
5.3	680	50–250	—	500–2300	2300–12,000	—	2700–12,000	Indirect	Total	GESAMP (1989)
5.25	500	113	—	910	2280	—	5190	Indirect	Wet	Otten (1991)
5.25	500	186	—	1410	3390	—	7900	Indirect	Total	Otten (1991)

Table 2. Measured precipitation concentrations over the North Sea and adjacent areas in $\mu g \cdot \ell^{-1}$ (s- preceding an area means southern)

Area	Period	Cd	Cr	Cu	Pb	Hg	Zn	Remarks	References
Holland	1982–1983	0.26–0.36	0.21–0.8	1.8–4.9	8.9–20	—	18–32	Bulk	van Jaarsveld and Onderlinden (1986)
Holland	1986–1988	0.5–0.9	1.4–1.8	6.7–8.0	13–20	—	21–31	Wet-only	van Daalen (1991)
Sweden	1984–1985	0.033–0.15	—	0.46–1.5	2–9	—	4.2–16	Bulk	Ross (1987)
Sweden	1987–1988	0.04–0.12	0.06–0.16	0.85–2.32	1.84–3.75	—	4.1–10.2	Wet-only	Ross (1990)
Scotland (Highlands)	1987	0.16	—	1.2	1.6	—	6.4	Snow (Cd, Pb dissolved only)	Jickells *et al.* (1992)
North Sea (coast)	1972–1981	0.3–1.2	0.2–4	4–30	10–35	<0.1	20–160	Literature range	van Aalst *et al.* (1983)
Norway (coast)	1978–1979	0.27	—	—	11	—	15	Weekly bulk	Pacyna *et al.* (1984a)
Norway (coast)	1980–1984	0.37	—	—	7.1	—	9.2	—	S&TWG (1987)
Scotland (coast)	1987–1988	0.68	—	2.3	4	—	13	Wet-only	Balls (1989)
sNorth Sea	1981	3	—	39.5	13	—	194	Wet-only	Dedeurwaerder *et al.* (1985)
sNorth Sea	1974–1985	0.5–9.5	—	2.5–77	10–29	—	26–490	Literature range	GESAMP (1989)
sNorth Sea	1984–1987	10	—	77	29	—	500	Wet-only	Baeyens *et al.* (1990)

hand, the values of Jickells *et al.* (1992) for Scottish snow and the wet-only values for Sweden (Ross, 1990) agree very well. The coastal values listed by van Aalst *et al.* (1983) show rather large variations, probably because they were obtained by different operators using other sampling methods at different sites and over other time intervals. However, the lowest values of these ranges agree very well with the concentrations measured at the North Sea coasts of Norway (Pacyna *et al.*, 1984a; S&TWG, 1987) and Scotland (Balls, 1989), respectively. Ross (1987) observed that the concentrations in southern Sweden were higher and that the wet deposition fluxes were higher than the Swedish anthropogenic emissions, so a long range transport of the pollutants was postulated. Clearly, the southern North Sea concentration values included in Table 2 are very high compared to the coastal values. The inconsistency of those mentioned in the GESAMP report (1989) is ascribed to sampling problems (e.g. not all measurements were wet-only) and difficult analysis associated with this kind of measurements. Also, at the West-Hinder station (and during several cruises) rainwater samples were collected (Dedeurwaerder *et al.*, 1985; Baeyens *et al.*, 1990). Although the sampling was done only when precipitation occurred and precautions were taken to avoid contamination, the concentration values reported are very high compared to the other values in Table 2. However, most of the coastal concentrations were measured in comparatively remote regions, while the West-Hinder station is located near the Belgian coast. That may be—at least in part—an explanation for the observed differences. The results of the ATMOS report (1984) point out that the heavy metal concentrations in rainwater above the sea are higher than above land (this is the "maritime effect" as reported by Cambray (1975)). Cambray (1975) thought that the maritime effect was caused by bubble bursting processes, which bring aerosols coming from an enriched sea surface layer into the atmosphere. However, Balls (1989) concluded on the basis of measurements of the enrichment factor in surface water that this process is not a significant contributor to the maritime effect. Possible alternative processes are thought to be enhanced solubility of the metals above the sea due to aging of the aerosols emitted by land based sources and/or different physico-chemical characteristics of rainwater above land and water (ATMOS, 1984).

Deposition by precipitation seems to be an important removal process for atmospheric Hg. Lindqvist and Rhode (1985) listed again a number of concentration values, determined throughout the world: they all lie in the range of 0.6 to 300 $ng \cdot \ell^{-1}$ and the mean values can be situated between 1 and 80 $ng \cdot \ell^{-1}$. In their report, van Aalst *et al.* (1983) cited one literature value of $<100\ ng \cdot \ell^{-1}$ for Hg in rainwater.

It is important to know whether a distinction can be made between the amount of a certain trace metal that reaches the surface of the earth in a dissolved or in a particulate form, because the direct impact of its

Table 1. Measured airborne concentrations over the North Sea and adjacent areas in ng m^{-3} (s- or n- preceding an area means southern or northern, respectively)

Area	Period	Cd	Cr	Cu	Pb	Hg	Zn	Remarks	References
United Kingdom	1972	<4–<18	1.0–14	<1–55	35–380	<0.05–0.24	64–415	Range for 7 sites	Peirson *et al.* (1973)
Holland	1984–1988	0.3–2	1.7–14	3.7–23	36–178	—	18–200	—	van Daalen (1991)
North Sea (coast)	1972–1981	0.5–2.5	0.5–5	<5–25	20–200	<0.1	10–100	Literature range Hg aerosol only	van Aalst *et al.* (1983)
Belgium (coast)	1972–1977	—	—	—	239	—	—	—	Kretzschmar and Cosemans (1979)
Belgium (coast)	1981–1984	3.4	—	12.8	77	—	174	—	ATMOS (1984)
Norway (coast)	1978–1979	0.3	1	7	19	—	—	—	Pacyna *et al.* (1984a)
England (coast)	1987–1988	1.1	—	—	34	—	41	—	Yaaqub *et al.* (1991)
German Bight	1986	1.9	1.9	4.7	52.6	—	46.1	Island	Kersten *et al.* (1991)
North Sea	1988	0.84	—	7.8	33	—	69	Flights	Otten *et al.* (1989a)
North Sea	1984–1988	—	—	11	39	—	54	Cruise	Otten *et al.* (1989b)
sNorth Sea	1981–1984	2.9	—	9	104	—	94	West-Hinder	ATMOS (1984)
sNorth Sea	1984–1985	0.7	—	3	39	—	41	—	Stoeßel (1987)
sNorth Sea	1980–1985	4	—	17	150	—	150	West-Hinder	Dedeurwaerder (1988)
sNorth Sea	1984–1988	—	—	17	62	—	86	Cruise	Otten *et al.* (1989b)
sNorth Sea	1980–1985	2.8	—	14.7	96	—	67.4	West-Hinder & cruises	Baeyens and Dedeurwaerder (1991)
nNorth Sea	1984–1988	—	—	2	2	—	2	Cruise	Otten *et al.* (1989b)

areas in Table 1. The oldest data, supplied by Peirson *et al.* (1973), Kretzschmar and Cosemans (1979) and van Aalst *et al.* (1983) (who give a list of concentrations measured between 1974 and 1981 at coastal stations in Great Britain, Belgium and The Netherlands), are generally higher than the other concentrations in Table 1. The use of other—less accurate—techniques in those days may be a reason, but these values are also obtained from coastal or even inland measurements, i.e. closer to the emission sources. Van Daalen (1991) measured the concentrations of trace metals over the province of South-Holland in the Netherlands and although his sampling sites were not very far removed from the North Sea coast his data show clearly higher concentrations. The rest of the coastal values in Table 1 seem to agree very well though the Belgian ones are slightly higher. And when we consider the values reported for the North Sea itself, we can very well discern a concentration gradient from the southern North Sea (high concentrations) to the northern part (low concentrations). Baeyens and Dedeurwaerder (1991) collected their samples on board of the light vessel West-Hinder and during some cruises on board of several research vessels. An ATMOS report (1984) and Dedeurwaerder (1988) also give results of West-Hinder measurements. The aircraft-measured concentrations of Otten *et al.* (1989a) agree rather well for Cu and Pb with those of the R/V Belgica cruises (Otten *et al.*, 1989b), but less for Zn. On the other hand, the Zn concentration is very comparable with the value reported by Baeyens and Dedeurwaerder (1991). The West-Hinder values are generally higher. The trace metal concentrations on the bottom line of Table 1 can be seen as background values for the area, predominantly based on measurements made in the northern part of the North Sea (during NW wind) but also on concentrations measured at the border between the English Channel and the Atlantic Ocean (during SW wind).

Data on the airborne concentrations of Hg in the North Sea area are very scarce. In addition to the literature references which were included in Table 1, Lindqvist and Rhode (1985) listed (gaseous) Hg concentrations measured between 1974 and 1985 at various places all over the world. The values range from 0.6 to 300 ng m^{-3}, while the mean values are in the range of 1.6 to 22.2 ng m^{-3}. At remote/rural European locations 2–3 ng m^{-3} was found in the summer and 4 ng m^{-3} in the winter, while in urban air the concentrations are higher. Hg on particles constitutes only a small fraction of the total airborne Hg: at remote locations the average concentrations are normally below 0.1 ng m^{-3}. This last value for particles corresponds very well to the <0.1 ng m^{-3} value reported by van Aalst *et al.* (1983).

3.2.2. *Concentrations in precipitation.* It is obvious from Table 2 that the Swedish concentrations measured by Ross (1987 and 1990) are lower than those reported for The Netherlands (van Jaarsveld and Onderlinden, 1986; van Daalen, 1991). On the other

approximation is as follows

$$\bar{F}_w = \bar{C}_p \bar{P}$$

where the annual wet flux $\bar{F}_w$ is expressed as the product of the average rainwater concentration ($\bar{C}_p$) and the yearly precipitation rate $\bar{P}$. However, when one intends to estimate the wet deposition to a sea surface directly, some major difficulties arise. Practically, collection of atmospheric material by the rain water samplers should be avoided during dry periods (Ruijgrok *et al.*, 1990), so wet-only samplers need to be used. Additional problems include sea-spray and contamination or deterioration of the samples prior to or during analysis by sampling material and handling, particularly if one deals with trace amounts (Ross, 1984; Buijsman *et al.*, 1991). Also, questions can be asked about the statistical relevance of such direct measurements. Firstly, precipitation is a discontinuous process and secondly, there is a natural variability of the concentrations of trace substances in precipitation. This means that a large number of rain events must be covered before meaningful average wet fluxes can be obtained, which is expensive and time-consuming. Also, these measurements are very much determined by the sampling location and time, which is problematic if one wants to investigate the deposition over a larger area and over a considerable period of time (Smith, 1991). For this reason, indirect approaches are often preferred. The limited amount of directly measured data is then used to check the results of these indirect approaches. For indirect measurements, the wet deposition flux of material to the ocean surface can be written as

$$\bar{F}_w = W\bar{P}\,\bar{C}_a$$

where $\bar{C}_a$ is the concentration of the substance in air, $\bar{P}$ is the yearly precipitation rate and W is the washout ratio—also called scavenging ratio—which is the ratio of the concentration of a substance in rainwater to the concentration of the same substance in air (both concentrations measured in (the same) volume units, e.g. $\mu g\ m^{-3}$).

This equation can be modified in a number of ways. Some authors for instance, add the density of air ρ as an extra factor (GESAMP, 1989):

$$\bar{F}_w = W\bar{P}\,\bar{C}_a\rho^{-1}.$$

In this case the resulting washout ratios are temperature and pressure dependent and about a factor of 1200–1300 smaller. An alternative method to calculate the wet flux is the use of scavenging rates. This subject was extensively described by Slinn (1983).

3.1. *Data on precipitation*

The existing estimates of surface precipitation (rain, snow, hail, ...) over the seas and oceans are based on a very limited data set. A serious problem with the measurement of precipitation, both on the ground and aloft, is its great variability in time and space. It cannot, for instance, be measured from a sampling vessel (Buijsman *et al.*, 1991). Moreover, the total amount of rainfall at any location can be a combination of a small number of very intense showers (of convective origin) together with comparatively extended periods of light rainfall from stratiform clouds. The overall contributions of these two kinds of precipitation are often comparable (Browning, 1990).

Even for a relatively small area as the North Sea, an accurate value for annual average rainfall is not available at present. It is, however, generally recognized that less rain falls over sea than over land (see e.g. Cambray *et al.*, 1979; Baeyens *et al.*, 1990). By measurements on a gas platform the rainfall there was observed to be about 55% of that at land-based stations at similar latitudes on either side of the North Sea (Cambray *et al.*, 1975). Taking this observation into account, a mean rainfall value of 438 mm per year was calculated for the North Sea on the basis of measurements of seventeen stations situated on adjacent land. This value was seen as a kind of "standard" value. However, Cambray himself adjusted this value to 475 mm annually on the basis of his own measurements at seven stations surrounding the North Sea (Cambray *et al.*, 1979). Van Aalst *et al.* (1983) disagree with Cambray's value, claiming that the difference between the amount of precipitation on land and at sea is lower than assumed before. Baeyens *et al.* (1990) measured the yearly precipitation volume at the West-Hinder light vessel: the mean value, based on a period of two years, amounts to 430 mm per year. They also indicated that, in general, there is less precipitation above the sea: they found an average ratio West-Hinder/De Blankaert (a Belgian coastal station) of 0.72 and a ratio of 0.60 for West-Hinder/all Belgian meteorological stations. Krell and Roeckner (1988) used a model to simulate the atmospheric input of lead and cadmium into the North Sea, and used yet another annual precipitation rate, namely 558 mm.

Balls (1989) states that the uncertainty in the amount of rainfall is the most important single error source in flux estimations. It is obvious that more reliable values are urgently needed in order to be able to calculate more accurate wet deposition fluxes. In the future, space-based techniques for measuring global rainfall will provide us with data with a good resolution and accuracy. Radars and/or radiometers, installed on satellites, will be able to measure the instantaneous intensity of the rain or hail that is falling, from which an estimation can be made of how much rain has fallen in a particular area over a certain amount of time, and all of this will happen on a routine basis (Bowler, 1990; Kedem *et al.*, 1990; Scofield, 1991).

3.2. *Data on trace metals* (Cd, Cr, Cu, Pb, Zn, Hg)

3.2.1. *Concentrations in air.* Because of the large amount of data published in this field, we only included values concerning the North Sea and adjacent

2.1. *Trace metals*

There are various sources which emit trace metals into the atmosphere, i.e. volcanic activity, vegetation, soil erosion, man-made pollution and aerosol formation from sea-spray (Dedeurwaerder *et al.*, 1985). Pacyna (e.g. 1984b) published various papers in which the atmospheric emissions of trace elements from anthropogenic sources in Europe are assessed. These compounds are emitted into the atmosphere by means of various sources, mainly combustion and industrial production processes (Warmenhoven *et al.*, 1989). Among the trace metals in this paper, mercury is somewhat of an outsider. The main reason is the fact that a dominant fraction ($\geq 80\%$) of the total Hg in the atmosphere consists of volatile gaseous mercury forms (predominantly elemental Hg, but also smaller quantities of dimethyl mercury and the very dangerous monomethyl mercury) (Lindqvist and Rhode, 1985).

Migon *et al.* (1991) state that even if present levels of heavy metals do not produce any apparent environmental harm, the threat of metal pollution probably is an underestimated problem. At high concentrations, these metals are toxic to the fauna as well as to humans who eat fish or crustaceans contaminated with these metals, and Pb and Cd in particular (Romeo and Nicolas, 1986). Therefore, a more accurate assessment of the loadings of toxic metals from the atmosphere to the sea is necessary (Migon *et al.*, 1991). Van Daalen (1991) compares the continuing increase of trace metals and especially cadmium in the environment in general to an insidious disease: once these elements are dispersed, it will be almost impossible to bring their concentrations back to acceptable levels.

2.2. *Organic compounds*

2.2.1. *Polycyclic Aromatic Hydrocarbons (PAHs).* A large number of PAHs has been identified, but mostly only about 20 of them are taken into account when measurements are being made (see Section 3). They are widespread in the environment (Björseth *et al.*, 1979), partly because PAHs are formed naturally due to endogenic synthesis by microorganisms, phytoplankton, algae and highly developed plants (Suess, 1976). Their most important anthropogenic sources include industrial production processes, combustion processes and burning of waste (Suess, 1976; Quaghebeur *et al.*, 1983; McVeety and Hites, 1988; Warmenhoven *et al.*, 1989; Lipiatou and Saliot, 1991). Many PAHs are suspected to be carcinogenic or mutagenic (Grimmer *et al.*, 1991).

2.2.2. *Polychlorinated Biphenyls (PCBs).* PCBs are biphenyl congeners in which one or more H-atoms have been substituted by Cl-atoms. Theoretically, there are 209 congeners and more than 60 of them have been identified. PCBs are highly resistant to chemical or physical attacks, are very lipophilic and have a high bio-accumulating power and toxicity, which makes them dangerous to the environment (e.g. Subramanian *et al.*, 1987; Delbeke and Joiris, 1988; Tanabe, 1988; Schulz-Bull *et al.*, 1991; Stone, 1992). However, the toxicity of PCBs is thought to be due to the action of only a few congeners, in particular the non-ortho-Cl substituted chlorobiphenyls. PCBs were made commercially available as liquid mixtures, e.g. Aroclor 1242 or Aroclor 1254. Their open use is now restricted or banned in most countries (GESAMP, 1989). Some important sources are leaks and vaporization processes (Warmenhoven *et al.*, 1989).

2.2.3. *Pesticides and volatile organochlorines.* They enter the atmosphere mainly by their agricultural use, when they are or have been applied to the crops (volatilization). Their emission depends on—for instance—the area of the region they are used in, and the applied quantities (Warmenhoven *et al.*, 1989). The pesticides dealt with in this report are DDT, chlordane, dieldrin, hexachlorobenzene and HCHs.

The DDT group includes DDT and DDE. These pesticides are very lipophilic and have a high bioaccumulating power (Subramanian *et al.*, 1987). Hexachlorocyclohexanes (HCHs) are a pesticide mixture which contains several biologically inactive isomers as well as the insecticidal lindane (γ-HCH) (technical composition: 55–70% α-HCH, 5–14% β-HCH, 10–18% γ-HCH, 6–10% δ-HCH and 3–4% ε-HCH) (Rapaport and Eisenreich, 1988; Lane *et al.*, 1992). In assessments of the deposition of these species, usually data on α- and γ-HCH are given, because their concentrations over the oceans are observed to be the highest (GESAMP, 1989). Although hexachlorobenzene (HCB) (a benzene ring with six chlorine atoms) is not known to occur as a natural product, it has become widely distributed in the environment. HCB is a very stable, non-reactive compound, which is highly lipid-soluble and thus tends to accumulate in fatty tissues (Burton and Bennett, 1987).

3. WET FLUX MEASUREMENTS

The amount of micropollutants which is deposited to the oceans over a certain period of time can be determined either directly or indirectly.

In the direct case the wet atmosphere-to-ocean material fluxes are determined as follows: rainwater is collected in rain collectors over a certain period of time and the concentrations of the substances involved are measured. For particles, the wet flux F_w can be calculated with the following formula

$$F_w = \sum_i C_{p,i} P_i$$

or the flux F_w is the sum over all individual rain events i of the product of the concentration of particles in rainwater ($C_{p,i}$) times the amount of precipitation per unit area and time (P_i). Because it is difficult to sample rainwater at each single rain event, the above equation is usually approximated. The most common

2785

Atmospheric Environment Vol. 27A, No. 16, pp. 2669–2687, 1993.
Printed in Great Britain.

0004-6981/93 $6.00+0.00

AN OVERVIEW OF WET DEPOSITION OF MICROPOLLUTANTS TO THE NORTH SEA

H. STRUYF and R. VAN GRIEKEN
University of Antwerp (U.I.A.), Department of Chemistry, Universiteitsplein 1, B-2610 Antwerpen-Wilrijk, Belgium

(*First received* 16 *July* 1992 *and in final form* 31 *March* 1993)

Abstract—An overview of the wet deposition of micropollutants (trace metals—Cd, Cr, Cu, Pb, Hg, Zn—and organic compounds—PAHs, PCBs, pesticides) to the North Sea and adjacent areas is presented. The results of (in)direct measurements of the wet flux are compared to modelling results. Attention is given to specific problems like revolatilization, sea-spray, contamination, gas-to-particle ratios in wet deposition of Hg and the organic substances. Also, the importance of wet deposition is weighted to that of dry deposition and non-atmospheric input routes to the North Sea. It is concluded that—especially for organic micropollutants—current knowledge is insufficient to yield an accurate and detailed image of the impact and importance of wet deposition to the North Sea.

Key word index: Air pollution, organic micropollutants, inorganic micropollutants, wet deposition, North Sea.

1. INTRODUCTION

The North Sea is an area of intense human activity, it is surrounded by densely populated countries and it is rich in natural resources. Especially the southern part—often called the Southern Bight—is the centre of busy commercial activity directed at the exploitation of mineral and living resources, transport, infrastructural works and recreation. The North Sea is also a shallow sea in a moderate climate, and is consequently biologically very productive and ecologically valuable: an important amount and variety of species of fish, birds, sea mammals and numerous other animals and plants live and grow in its waters and on its coasts, and form complicated and very sensitive ecosystems. However, the presence of all the industries and population centres around the North Sea exercises a constant and ever increasing pressure on the marine ecosystem, which leads to the loss of natural habitats, overexploitation and damage to its natural resources and beaches, etc. In order to take measures to reduce this conflict between commercial interests and the conservation of the marine environment to reasonable proportions, a thorough investigation of the processes which introduce pollutants into the North Sea is required.

Anthropogenic pollutants reach the seas and oceans in many different ways. The major routes include rivers, direct dumping and industrial discharges, and atmospheric transport (e.g. Buat-Ménard, 1984; Dedeurwaerder *et al.*, 1985; Martin *et al.*, 1989). For about 30 years now, one has studied the atmosphere as a (possible) pathway for the introduction of chemical species to surface waters. As the understanding of the transport and deposition mechanisms improved, it became clear that the atmospheric route gained in importance relative to the other pathways. Especially in open ocean areas, where the influence of rivers is minimal, the atmosphere appears to be the dominant contributor to marine pollution (GESAMP, 1989).

Dry deposition of metals to the North Sea has been modelled and measured recently (e.g. Otten, 1991). Wet deposition, however, has not been so well investigated (the available data lack coherence) and very little is known about the deposition of organic micropollutants. Some of the difficulties involved here are the inherent variability (in both space and time) of the wet deposition phenomenon itself, and the lack of reliable data on the precipitation rate and on the (organic) pollutant concentrations in precipitation in the North Sea area.

2. MICROPOLLUTANTS

The micropollutants which will be discussed in this paper can be divided into two categories: trace metals (Pb, Cu, Zn, Cd, Cr, Hg) and organic compounds (PCBs, PAHs, pesticides). All of these chemicals have been proven or are suspected to have a certain impact on the marine environment (GESAMP, 1989). They are present in the atmosphere as particles and/or in the gaseous form. Their atmospheric lifetime is generally long enough (>1 day) to allow them to be transported over long distances (>1000 km), but it is often too short (<1 month) to allow uniform mixing of the material in the global atmosphere (Buat-Ménard, 1984). The typical residence time for European air pollution is estimated to be 3 or 4 days (Smith, 1991).

Selected article #14:

An overview of wet deposition of micropollutants to the North Sea
H. Struyf and R. Van Grieken
Atmospheric Environment, 27A (1993) 2669-2687

PARCOM (1989) Tenth Annual Report on the Activities of the Paris Commission, London, U.K.

Peirson D. H., Cawse P. A., Salmon L. and Cambray R. S. (1973) Trace elements in the atmospheric environment. *Nature* **241,** 252–256.

Pena J. A., Norman J. M. and Thomson D. W. (1977) Isokinetic sampler for continuous airborne aerosol measurements. *J. Air Pollut. Control Ass.* **27,** 337–340.

Petersen G., Weber H. and Graßl H. (1989) Modelling the atmospheric transport of trace metals from Europe to the North Sea and the Baltic Sea. In *Control and Fate of Atmospheric Trace Metals* (edited by Pacyna J. M. and Ottar B.) Kluwer, Dordrecht.

Quality Status of the North Sea (1987) A Report by the Scientific and Technical Working group, Department of Environment, Second International Conference on the Protection of the North Sea.

Rojas C. M. (1991) Ph.D. dissertation, University of Antwerp (UIA), Antwerp, Belgium.

Rojas C. M., Otten Ph. M., Van Grieken R. E. and Laane R. W., (1991) Dry aerosol deposition over the North Sea estimated from aircraft measurements. In *Proc. 18th Int. Technical Meeting of NATO-CCMS on Air Pollution Modelling and its Application* (edited by Van Dop H. and Steyn D.), pp. 419–425. Plenum Press, New York.

Rojas C. M., Van Grieken R. E. and Laane R. W. (1993) Comparison of three dry deposition models applied to field measurements in the Southern Bight of the North Sea. *Atmospheric Environment* (in press).

Schmidt H. (1992) An estimate of the mean precipitation amount over the North Sea. *Deutsche Hydrogr. Z.* (submitted).

Slinn W. G. N. (1983) Air to sea transfer of particles. In *NATO ASI Conf. Air–Sea Exchange of Gases and Particles* (edited by Liss P. S. and Slinn W. G. N.), p. 299 D. Reidel, Dordrecht.

Slinn S. A. and Slinn W. G. N. (1980) Predictions for particle deposition on natural waters. *Atmospheric Environment* **14,** 1013–1016.

Smith S. D. (1981) Factors for adjustment of wind speed over water to a 10-m height. Report series BI-R-81-3, Bedford Institute of Oceanography, Dartmouth, Nova Scotia, Canada.

Smith S. D. (1988) Coefficients for sea surface wind stress, heat flux, and wind profiles as a function of wind speed and temperature. *J. geophys. Res.* **93,** 15467–15472.

Steiger M., Schulz M., Schwikowski M., Naumann K. and Dannecker W. (1989) Variability of aerosol size distributions above the North Sea and its implication to dry deposition estimates. *J. Aerosol Sci.* **20,** 1229–1232.

Van Aalst R. M. (1986) Dry deposition of aerosol particles. In *Aerosols* (edited by Schneider L. *et al.*). Lewis, Chelsea, MI.

Van Aalst R. M. (1988) Input from the atmosphere. In *Pollution of the North Sea: An Assessment* (edited by Salomons *et al.*), pp. 275–283 Springer, Berlin.

Van Jaarsveld J. A., Van Aalst R. M. and Onderdelinden D. (1986) Deposition of metals from the atmosphere into the North Sea: model calculations. Report RIVM 842015002, Bilthoven, Netherlands.

Warmenhoven J. P., Duiser J. A., de Leu L. Th. and Veldt C. (1989) The contribution of the input from the atmosphere to the contamination of the North Sea and the Dutch Wadden Sea. TNO report R89/349A.

Weichart G. (1973) Pollution of the North Sea. *Ambio* **2,** 99–106.

Wiman B. L., Unsworth M., Lindberg S., Bergkvist B., Jaenicke R. and Hansson H.-C. (1990) Perspectives on aerosol deposition to natural surfaces: interactions between aerosol residence times, removal processes, the biosphere and global environmental change. *J. Aerosol Sci.* **21,** 313–338.

Windom H. L. (1981) Comparison of atmospheric and riverine transport of trace elements to the continental shelf environment. In *River Inputs to Ocean Systems.* UNEP and UNESCO.

specially on their heavy metal content; (ii) the determination of solubility as a function of particle size and chemical speciation; (iii) a better knowledge on the temporal distribution of precipitation events for the North Sea area; and (iv) the determination of the functional relationship between height and precipitation intensity.

Acknowledgements—We are grateful to Rijkswaterstaat (The Hague, Netherlands) for financial support through projects NOMIVE*2: DGW-920 and DGW-217. We also acknowledge the valuable co-operation with The Royal Netherlands Meteorological Institute (De Bilt, Netherlands). We thank Dr Ph. Otten and the team of Geosens for their important participation during the sampling campaign.

REFERENCES

Arimoto R. and Duce R. A. (1986) Dry deposition models and the air sea exchange of trace elements. *J. geophys. Res.* **91**, 2787–2792.

Arimoto R., Duce R. A., Ray B. J. and Unni C. K. (1985) Atmospheric trace elements at Enewetak Atoll 2: transport to the ocean by dry and wet deposition. *J. geophys. Res.* **90**, 2391–2408.

Arnold M., Seghaier A., Martin D., Buat-Ménard P. and Chesselet R. (1982) Géochemie de l'aerosol au-dessus de la Méditterranée occidentale. Workshop on Pollution of the Mediterranean, Cannes, France.

Baeyens W., Dehairs F. and Dedeurwaerder H. (1990) Wet and dry deposition fluxes above the North Sea. *Atmospheric Environment* **24A**, 1693–1703.

Berner A., Lürzer Ch., Pohl F., Preining O. and Wagner P. (1979) The size distribution of the urban aerosol in Vienna. *Sci. Total Envir.* **13**, 245–261.

Buat-Ménard P. and Chesselet R. (1979) Variable influence of the atmospheric flux on trace metal chemistry of oceanic suspended matter. *Earth Planet. Sci. Lett.* **42**, 339–341.

Cambray R. S., Jefferies D. F. and Topping G. (1975) An estimate of the input of atmospheric trace elements into the North Sea and the Clyde Sea. [AERE-Report. 7733.] United Kingdom Atomic Energy Authority, HMSO, London.

Cambray R. S., Jefferies D. F. and Topping G. (1979) The atmospheric input of trace elements to the North Sea. *Mar. Sci. Commun.* **5**, 175–194.

Crecelius E. A. (1980) The solubility of coal fly-ash and marine aerosols in sea water. *Mar. Chem.* **8**, 245–250.

Dedeurwaerder H. L. (1988) Study of the dynamic transport and of the fall-out of some ecotoxicological heavy metals in the troposphere of the Southern Bight of the North Sea. Ph.D dissertation, Vrije Universiteit Brussel, Brussels, Belgium.

Dedeurwaerder H. L., Dehairs F. A., Decadt G. G. and Baeyens W. F. (1982) Estimates of wet and dry deposition and resuspension fluxes of several trace metals in the Southern Bight of the North Sea. In *Precipitation Scavenging, Dry Deposition and Resuspension* (edited by Pruppacher *et al.*), pp. 1219–1231. Elsevier, Amsterdam.

Dierck I., Wouters L., Michaud D. and Van Grieken R. (1992) Laser microprobe analysis of individual aircraft-sampled North Sea aerosol particles. *Envir. Sci. Technol.* **26**, 802–808.

Duce R. A., Wallace G. T. and Ray B. J. (1976a) Atmospheric trace metals over the New York Bight. NOAA technical report, ERL 361-MESA4.

Duce R. A., Hoffman G. L., Ray B. J., Fletcher I. S., Wallace G. T., Fashing G. L., Piotrowicz S. R., Walsh P. R., Hoffman E. J., Miller J. M. and Heffer J. L. (1976b) Trace metals in the marine atmosphere: sources and fluxes. In *Marine Pollutant Transfer* (edited by Windom R. and Duce R.), pp. 77–117. Heath, Lexington, MA.

Dulac F., Buat-Ménard P., Ezat U., Melki S. and Bergametti G. (1989) Atmospheric input of trace metals to the Western Mediterranean: uncertainties in modelling dry deposition from cascade impactor data. *Tellus* **41B**, 362–378.

Eliassen A. and Saltbones J. (1983) Modelling of long-range transport of sulphur over Europe: a two year model run and some model experiments. *Atmospheric Environment* **8**, 1457–1483.

Fitzgerald J. W. (1975) Approximation formulas for the equilibrium size of an aerosol particle as a function of its dry size and ambient relative humidity. *J. appl. Met.* **14**, 1044–1049.

GESAMP-IMO/FAO/UNESCO/WMO/WHO/IAEA/UN/UNEP (1985) Joint Group of Experts on the Scientific Aspects of Marine Pollution: Interchange of pollutants between the atmosphere and the oceans. Report and Studies GESAMP-WMO 23.

GESAMP-IMO/FAO/UNESCO/WMO/WHO/IAEA/UN/UNEP (1989) Joint Group of Experts on the Scientific Aspects of Marine Pollution: The atmospheric input of trace species to the world oceans. Report and Studies GESAMP-WMO 38.

Graßl H., Eppel D., Pettersen G., Schneider B., Weber H., Gandraß J. G., Reinhardt K. H., Wodarg D. and Fliess J. (1989) Stofeintrag in Nord und Ostee über die Atmosphäre. GKSS Report 89/E/8, GKSS, Geesthacht, Germany.

Hodge V., Johnson S. R. and Goldberg E. D. (1978) Influence of the atmospherically transported aerosols on surface ocean water composition. *Geochem. J.* **12**, 7–20.

Hohn R. (1971) On the climatology of the North Sea. In *North Sea Science, NATO North Sea Conference* (edited by Goldberg E. D.), pp. 183–236 Cambridge.

IDOE (1972) Baseline studies of pollutants in the marine environment and research recommendations. Workshop, Brookhaven National Laboratory, New York, p. 799.

Injuk J., Otten Ph., Rojas C., Wouters L. and Van Grieken R. (1990) Atmospheric Deposition of Heavy Metals (Cd, Cu, Pb and Zn) into the North Sea. Final report to Rijkswaterstaat (The Hague, Netherlands) on project NOMIVE*2 DGW 920, University of Antwerp (UIA), Belgium.

Jickells T. D., Knap A. H. and Church T. M. (1984) Trace metals in Bermuda rain water. *J. geophys. Res.* **73**, 8827–8836.

Kersten M., Dicke M., Kriews M., Naumann K., Schmidt D., Schulz M., Schwikowski M. and Steiger M. (1988) Distribution and fate of heavy metals in the North Sea. In *Pollution of the North Sea: An Assessment* (edited by Salomons *et al.*), pp. 300–347 Springer, Berlin.

Komy Z., Roekens E. and Van Grieken R. (1988) Analysis of rain water by differential-pulse stripping voltammetry in nitric acid medium. *Anal. Chim. Acta* **204**, 179–187.

Krell U. and Roeckner E. (1988) Model simulation of the atmospheric input of lead and cadmium into the North Sea. *Atmospheric Environment* **22**, 375–381.

Liss P. S., Jickells T. D. and Buat-Ménard P. (1988) The water–air interface. In *Pollution of the North Sea: An Assessment* (edited by Salomons *et al.*), pp. 110–117 Springer, Berlin.

Maring H. B. (1985) Impact of atmospheric aerosols on trace metal chemistry in open ocean surface seawater. Ph.D. dissertation, University of Rhode Island, Kingston, RI.

Maring H. B. and Duce R. A. (1989) Impact of atmospheric aerosols on trace metal chemistry in open ocean surface seawater. II. Copper. *J. geophys. Res.* **94**, 1039–1045.

Moore R. M., Marin J. E. and Chatt A. (1984) The potential of biological movilization of trace elements from aeolian dust in the ocean and its importance in the case of iron. *Oceanol. Acta* **7**, 221–228.

Monin A. S. and Obukhov A. M. (1954) Basic laws of turbulent mixing in the ground layer of the atmosphere. *Acad. Sci. USSR J. Geophys. Ins.* **24**, 163–187.

Table 8. Total flux (kg km^{-2} yr^{-1}) into the Southern Bight of the North Sea compared with values from other marine areas

Total flux	Cd	Cu	Pb	Zn
New York Bight (1)	0.3	—	39	14
Baltic Sea (2)	0.16	—	11	—
Baltic Sea (3)	0.14	2.9	2.4	11
W. Mediterranean (4)	0.13	0.96	10.5	11
W. Mediterranean (3)	1	4.2	29	34
S. Atlantic Bight (5)	0.09	2.2	6.6	7.5
Bermuda (6)	0.04	0.3	10	0.75
Bermuda (7)	0.09	1	12	1.76
North Atlantic (2)	0.05	—	3.1	—
Trop. N. Atlantic (8)	0.05	0.2	3.1	1.3
Trop. N. Pacific (9)	0.003	0.09	0.07	0.67
North Sea (2)	0.5	—	17	—
North Sea (3)	0.3	2.7	14	14
This work	0.59	5.1	13.8	28

References: (1) Duce *et al.* (1976a), (2) GESAMP-IMO/FAO/UNESCO/ WMO/WHO/IAEA/UN/UNEP (1985), (3) GESAMP-IMO/-FAO/UNESCO/WMO/WHO/IAEA/UN/UNEP (1989), (4) Arnold *et al.* (1982), (5) Windom (1981), (6) Duce *et al.* (1976b), (7) Jickells *et al.* (1984), (8) Buat-Ménard and Chesselet (1979), (9) Arimoto *et al.* (1985).

Table 9. Total input of Cd, Cu, Pb and Zn (in ton yr^{-1}) to the Southern Bight of the North Sea, compared with other pathways

Pathway	Cd	Cu	Pb	Zn
Rivers	39	970	768	5587
Discharges	16	243	144	1176
Dumping	23	1265	2407	8759
Atmosphere	94	806	2200	4432
Total	172	3284	5519	19,954

Table 10. Comparison of our results for the total input (ton yr^{-1}) to the North Sea with model outputs reported by other authors

Reference	Cd	Cu	Pb	Zn
Van Jaarsveld *et al.* (1986)	11	100	2000	940
Krell and Roeckner (1988)	11	—	1200	—
Graßl *et al.* (1989)	—	—	2300	—
Warmenhoven *et al.* (1989)	15	110	1900	930
This work	158	1348	3678	7409

81–84% (Hodge *et al.*, 1978); 15–86% (Hodge *et al.*, 1978; Moore *et al.*, 1984; Maring and Duce, 1989); 13–90% (Hodge *et al.*, 1978; Maring, 1985); 24–76% (Hodge *et al.*, 1978; Crecelius, 1980) for Cd, Cu, Pb and Zn, respectively. The large spreading of the solubility values appearing in the literature is evident. Moreover, the direct dumping of waste will soon decrease due to recent EC legislation, and hence the relative contribution of the atmospheric input will increase. It should also be borne in mind that the heavy metal load of rivers is, to some extent, due to leaching of atmospherically deposited pollutants from land. The very important role of atmospheric deposition to the heavy metal pollution of the North Sea is thus evident.

Comparison with modeled inputs

A comparison of our results with modeled inputs for the North Sea is shown in Table 10. In general, the four models agree very well, which can be expected since the source-emission data are similar in all of them. There are more marked differences between our results and those from the models, particularly for Cu, Cd and Zn, where the modeled outcomes represent 8, 10 and 13% of our estimates, respectively; whereas for Pb this difference is of 50%.

These discrepancies can be related to several reasons, namely, the aerosol size distribution used in these models varies significantly from ours. Indeed, in our calculations aerosols had sizes ranging from 0.09 to 23 μm (aed), with a significant heavy metal fraction (25–50%) in the range >4 μm (aed). The particle size dependence used in other models has already been discussed. On the other hand, none of these models takes into account particle growth due to high relative humidities. It has to be taken into account that our values have been estimated assuming that the aerosol concentrations for the whole North Sea are approximately 50% of those from the Southern Bight.

RECOMMENDATIONS FOR FUTURE RESEARCH

It is therefore essential that further research should be devoted toward: (i) a thorough and ample characterization of the large atmospheric particulate matter,

but consistently lower (36% on the average). This difference might be related to the fact that Baeyens *et al.* (1990) measured at a fixed location, whereas our measurements covered a distance of approximately 110 km from the Goeree platform in several directions, away from the continent.

Wet deposition

The resulting precipitation scavenging rates of 3.3×10^{-6}, 3.7×10^{-6}, 2.3×10^{-6} and $3.6 \times 10^{-6}\,s^{-1}$ for Cd, Cu, Pb and Zn, respectively are within the variation range given by Van Aalst (1988) of 2×10^{-6}–$6 \times 10^{-6}\,s^{-1}$. As for dry deposition, particles with diameters larger than 4 μm contribute enormously (more than 98%) to the total wet deposition rate. The wet deposition rates, for five different wind sectors, obtained for the Southern Bight of the North Sea are shown in Table 5. As is seen from this table, wind sectors east/northeast, south/southeast and local account for most of the wet deposition of Pb and Zn, respectively. As for dry deposition, wind sectors associated with continental air masses dominate the heavy metal deposition. As far as the wet fluxes of Cd and Cu are concerned, wind sectors west/southwest and south/southeast are predominant.

Table 6 lists the wet deposition fluxes from this work, compared with results reported by other authors. It is necessary to mention that the measurements of Peirson *et al.* (1973) were carried out at a gas platform, and those of Dedeurwaerder *et al.* (1982) and Baeyens *et al.* (1990) at the West-Hinder station, while Cambray *et al.* (1979) and Paris Commission (PARCOM, 1989) performed their sampling at coastal stations. The precipitation intensities for all these works ranged between 260 and 796 mm yr^{-1}. Last, but not least, it has to be pointed out that some of the authors base their results on the dissolved phase of the collected material. It is seen from this table that there is an enormous spread in the results of wet flux estimates. However, the good agreement between the outcomes of Cambray *et al.* (1979), Dedeurwaerder *et al.* (1982), Baeyens *et al.* (1990) and this work is striking for Pb. The lowest estimates are those reported by PARCOM (1989).

Total deposition

Table 7 shows the dry, wet and total fluxes to the Southern Bight of the North Sea. One can determine from this that, on average, 69% of the total deposition for the four elements of interest is accounted for by wet deposition. However, it is here where we lack most of the information needed to assess the real importance of wet deposition. Table 8 shows a comparison of the total atmospheric flux estimated for the Southern Bight, with that of other marine areas. The flux values for the tropical North Pacific are based on direct measurements. For all elements, the deposition fluxes show relatively high values for the Southern Bight of the North Sea, while the reported value for Pb for the New York Bight is very high. However, this value dates from 1976. Based on the figures given in Table 7, and given the total surface area for the Southern Bight of the North Sea of 160,000 km^2 (Cambray *et al.*, 1975), the total input (in ton yr^{-1}) is shown in Table 9, and compared with other pathways extracted from the report on the Quality Status of the North Sea (1987). It is seen from this table that 55, 24, 40 and 22% of the total are attributed to the atmospheric input for Cd, Cu, Pb and Zn, respectively. It is also seen that for Cu the atmospheric input is similar to that of rivers. However, these results correspond only to the soluble fraction, and the reported solubilities in sea water, which depend on the particle size and pH value, are:

Table 4. Dry deposition fluxes ($kg\,m^{-2}\,yr^{-1}$) compared with those reported by other authors

Reference	Cd	Cu	Pb	Zn
Cambray *et al.* (1975)	—	<30	24	420
Dedeurwaerder *et al.* (1982)	0.04	0.7	4.5	3.5
Baeyens *et al.* (1990)	0.19	3.5	7.5	13
This work	0.16	1.6	5.1	7.9

Table 5. Wet deposition fluxes ($kg\,km^{-2}yr^{-1}$) to the Southern Bight of the North Sea, divided in five different wind sectors

Wind sector	Cd	Cu	Pb	Zn
West/southwest	0.165	1.13	1.26	3.01
North/northwest	0.016	0.11	0.76	0.12
East/northeast	0.083	0.20	2.95	6.27
South/southeast	0.122	0.23	2.56	5.84
Local	0.044	1.79	1.14	4.52
Total	0.4	3.5	8.7	20

Table 6. Wet deposition flux estimates compared with those reported by other authors

Reference	Cd	Cu	Pb	Zn
Peirson *et al.* (1973)	4.2	21	49	53
Cambray *et al.* (1979)	—	11	11	31
Dedeurwaerder *et al.* (1982)	1.6	25	9	140
PARCOM (1989)	0.2	0.8	1.1	4.5
Baeyens *et al.* (1990)	2.9	25	7	170
This work	0.4	3.5	8.7	20

Table 7. Dry, wet and total deposition fluxes ($kg\,km^{-2}\,yr^{-1}$) to the Southern Bight of the North Sea

Type of deposition	Cd	Cu	Pb	Zn
Dry	0.16	1.6	5.1	7.9
Wet	0.43	3.5	8.7	20
Total	0.59	5.1	13.8	28

authors, only Dulac *et al.* (1989) included particle growth due to aerosol hygroscopicity. However, their size-segregated samples ranged from 0.67 to 8.9 μm in only five stages. This is the reason why their deposition velocity, e.g. for Pb, is a factor of 12 lower than the one reported here.

As is seen above, the main subject of discrepancy in the results concerning dry deposition velocities relies in the size distribution of the aerosols. Indeed, Van Aalst (1988) states that dry deposition velocities might vary in the range between 0.1 and 1 cm s^{-1}, and that most of this spread is caused by the lack of knowledge of the atmospheric particulate matter size distribution. Even though elements like Pb are more abundant in the sub-micrometer size range, these particles can coagulate with seasalt aerosols and reach super-micrometer dimensions. In order to give a quantitative idea on how important relatively large particles can be in the whole deposition process, Table 2 shows the percentage of the dry deposition flux accounted for by a given particle size class. Here only particle diameters larger than 1 μm are tabulated since the contribution of the sub-micrometer particles can be considered as negligible.

It is seen from this table that 98% of the dry deposition velocity for Cd is accounted for by particles larger than 4 μm; whereas for Cu, Pb and Zn, this percentage corresponds to 95, 96 and 97%, respectively. For the same North Sea area, Baeyens *et al.* (1990) concluded that the first two stages of their cascade impactor, i.e. particles larger than 4 μm, were responsible for 82% of the deposition of Pb. In the Mediterranean Sea, Dulac *et al.* (1989) reported that only 20% of the total deposition of Cd and Pb is accounted for by particles with sizes larger than 7 μm.

Table 2. Relative contribution (%) of the particle size classes in the determination of dry deposition fluxes

Diameter (μm)	Cd	Cu	Pb	Zn
1.4	1.1	1.5	1.1	0.4
2.8	0.4	3.1	1.4	1.7
5.6	2.2	6.3	14	11
11.3	50	5.7	39	27
23.0	46	83	43	59

The dry deposition rates as a function of the wind sector for the Southern Bight of the North Sea are shown in Table 3 for Cd, Cu, Pb and Zn, respectively. It was expected that continental air masses would contribute significantly to the dry deposition rate for all four elements. It is seen from this table that wind sector west/southwest is responsible for most of the deposition of Cd and Zn. The dry flux of Pb is mainly associated with this wind sector and with the south/southeast sector. The contribution of wind sector north/northwest is relatively low since the aerosol concentrations can be attributed to background levels for the Southern Bight of the North Sea. The contribution of the local wind sector to the dry deposition rate of Cu is also noticeable.

Table 4 shows a comparison of the dry deposition rates obtained in this work with those from the literature. It is seen from this table that an enormous difference exists between the results for dry deposition rates reported by Cambray *et al.* (1975), measured at a gas platform, with those from Dedeurwaerder *et al.* (1982), Baeyens *et al.* (1990) and this work. This spread suggests the possibility of contamination in the former results. It is also noticeable that Dedeurwaerder *et al.* (1982) and Baeyens *et al.* (1990), even though they measured at the same site (West-Hinder station, 50 km off the Belgian shoreline), report results that are almost a factor of four different for Zn. Our results, are comparable to those reported by Baeyens *et al.* (1990)

Table 3. Dry deposition to the Southern Bight of the North Sea for each wind sector. C is the elemental concentration in ng m^{-3}, V_d is the deposition velocity in cm s^{-1} and the flux is in kg km^{-2} yr^{-1}

Wind frequency:		West southwest 31.7%	North/northwest 19.8%	East/northeast 18.8%	South southeast 18.2%	Local 11.5%
Cd	C	1.47 ± 0.36	0.20 ± 0.38	2.20 ± 1.90	0.82 ± 0.44	0.43 ± 0.15
	V_d	0.69 ± 0.52	0.33 ± 0.21	0.26 ± 0.16	0.39 ± 0.25	0.29 ± 0.08
	Dry flux	0.33 ± 0.26	0.02 ± 0.04	0.19 ± 0.13	0.09 ± 0.07	0.04 ± 0.01
Cu	C	13.8 ± 5.8	1.02 ± 0.36	2.5 ± 0.4	11.7 ± 10.8	15.7 ± 6.5
	V_d	0.49 ± 0.35	0.27 ± 0.15	0.22 ± 0.13	0.19 ± 0.05	1.24 ± 0.15
	Dry flux	2.2 ± 1.8	0.09 ± 0.06	0.17 ± 0.10	0.66 ± 0.63	6.2 ± 2.7
Pb	C	68 ± 5	6.0 ± 3.4	59 ± 15	126 ± 20	72 ± 15
	V_d	0.26 ± 0.14	0.31 ± 0.15	0.29 ± 0.10	0.25 ± 0.09	0.12 ± 0.04
	Dry flux	5.7 ± 3.0	0.60 ± 0.44	5.5 ± 2.3	10.1 ± 3.9	2.7 ± 1.1
Zn	C	61 ± 7	2.0 ± 1.2	76 ± 21	160 ± 40	81 ± 16
	V_d	0.56 ± 0.27	0.21 ± 0.09	0.38 ± 0.13	0.14 ± 0.04	0.48 ± 0.09
	Dry flux	10.9 ± 5.5	0.13 ± 0.09	9.3 ± 4.0	7.1 ± 2.7	12.4 ± 3.4

	Cd	Cu	Pb	Zn
Total dry fluxes (weighted):	0.16 ± 0.11	1.58 ± 0.67	5.08 ± 1.25	7.94 ± 2.00

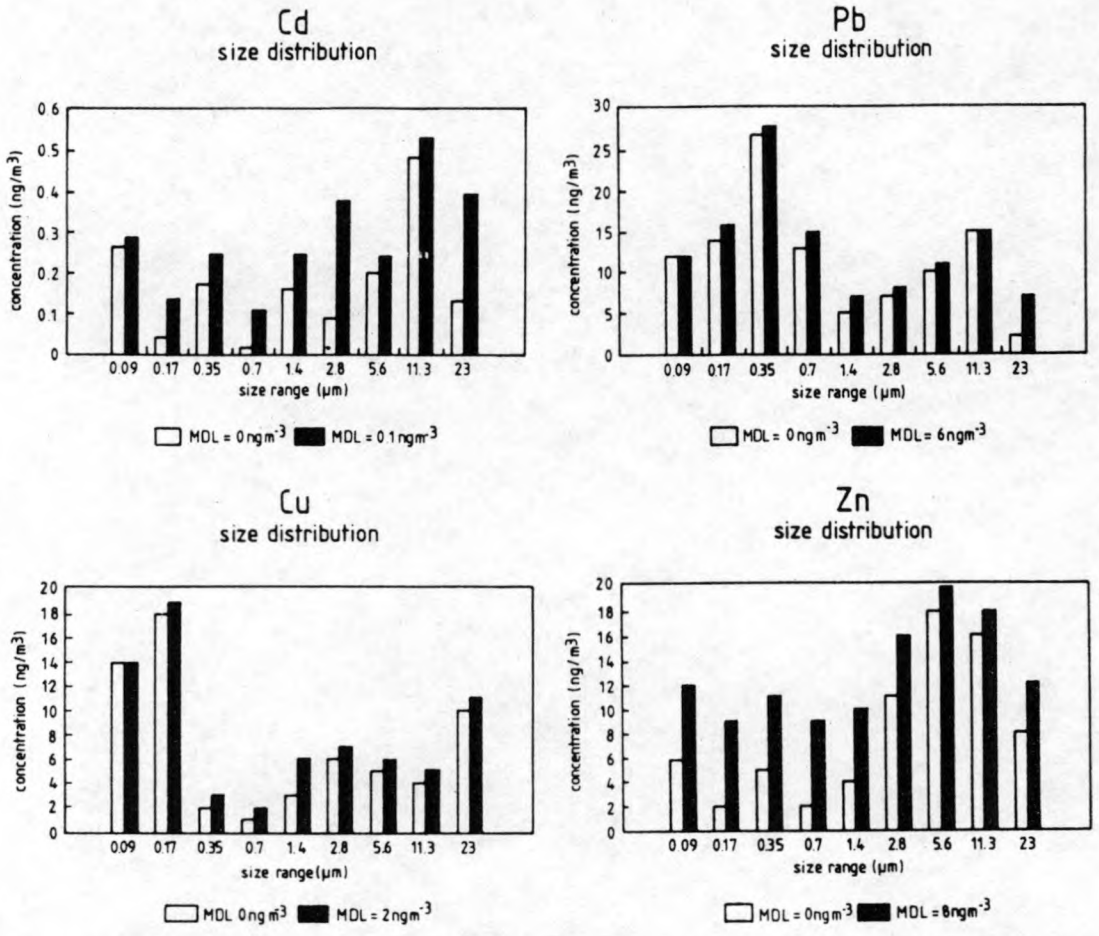

Fig. 2. Average size distribution of Cd, Cu, Pb and Zn obtained from the 9-stage Berner cascade impactor. Average obtained replacing missing values with zeros are represented by the hollow bars, whereas those obtained replacing the missing values with the detection limit correspond to the filled bars.

Table 1. Average dry deposition velocities for Cd, Cu, Pb and Zn, compared with other results reported in the literature

Reference	Cd	Cu	Pb	Zn
This work	0.39 ± 0.07	0.48 ± 0.17	0.25 ± 0.03	0.35 ± 0.07
Krell and Roeckner (1988)	0.2	—	0.20	—
Steiger *et al.* (1989)	—	—	0.14	—
Van Jaarsveld *et al.* (1986)	0.22	0.22	0.22	0.22
Dulac *et al.* (1989)	0.05	—	0.04	—

and chose, for use in our deposition calculations, the aerosol size distribution obtained when all missing values were replaced with half of the detection limit.

Dry deposition

The dry deposition velocities determined for our four elements of interest (Cd, Cu, Pb and Zn) and the respective errors are shown in Table 1. These values correspond to the average taking into account all wind sectors. Also in this table, the results reported by other researchers are listed. The standard error associated with these determinations can be considered very good, taking into account the variations related to meteorology and size-segregated elemental concentrations. These dry deposition velocities are based upon a particle size ranging from 0.09 to 23 μm aerodynamic diameter (aed), while Krell and Roeckner (1988) considered aerosols only in the size range from 0.2 to 1 μm. Steiger *et al.* (1989) used particle sizes between 0.4 and 10 μm; whereas Van Jaarsveld *et al.* (1986) used five size classes for deposition calculations, the smallest being 0.95 μm and the largest 20 μm. Of these

Dry deposition model description

Dry deposition velocities were calculated using a modified version of the two-layer deposition model of Slinn and Slinn (1980). In this model, the lower atmospheric boundary layer beneath a reference height of 10 m is divided into two layers. In the first layer, particle transport is mainly governed by gravitational settling and turbulence. In the second layer, also called the deposition layer and very close to the water interface, particle transfer is dominated by diffusion and phoretic effects. In the original version of Slinn and Slinn (1980), parameters such as drag coefficient, average wind speed and friction velocity were used for a height of 10 m. Since our aircraft measurements took place at a higher altitude and due to the wide range of values that the drag coefficient can have as a function of altitude and average wind speed (Smith, 1981, 1988), our approach consisted of using the Monin and Obukhov (1954) similarity theory to determine the drag coefficient, wind speed and friction velocity for a height of 10 m when the wind speed has been measured at a higher altitude. More details on this approach can be found elsewhere (Rojas *et al.*, 1991, 1993; Rojas, 1991). The motivation for this approach was that, according to Wiman *et al.* (1990), a turbulent layer of 10 m above the water surface encompasses most of the transfer zone. Once all these parameters were known, taking into account the height correction, they were introduced in the two-layer modeling described above. Atmospheric stability corrections were also included. Dry deposition velocities have been calculated following several steps. First, it was assumed that: (i) particles are hydrophobic, i.e. particles do not grow despite of the nearly saturated characteristics of the air in the deposition layer; or (ii) particles are hygroscopic (they do grow). This resulted in two dry deposition velocities as a function of particle size depending on the particle characteristics. The deposition velocity for hygroscopic particles was then weighted with the per cent number of sulfate-bearing particles. These particles have hygroscopic properties. This number per cent was obtained from single particle observations carried out using laser mass microprobe analysis (Dierck *et al.*, 1992). The complement of this number was used to weight the dry deposition velocity for hydrophobic particles. The final deposition velocity was the summation of the two weighted values. The variation of particle size with relative humidity for sulfate particles was taken from Fitzgerald (1975).

Authors like Arimoto and Duce (1986) have calculated the dry deposition rate, dividing the total mass of each element into intervals, each containing 1% of the total mass. Then, a deposition velocity is determined for each mass interval. This is known as the granulometric approach (Dulac *et al.*, 1989). However, Dulac *et al.* (1989) have shown that this procedure yielded similar results when the mass distribution is taken directly from the impactor data and used in the calculation of the dry deposition velocities. In this work we used the mass distribution given by the cascade impactor. Thus, the dry deposition velocity is given by:

$$V_d = \frac{\sum_{i=1}^{9} V_i C_i}{\sum_{i=1}^{9} C_i} \quad (1)$$

where V_i and C_i are the dry deposition velocity and aerosol elemental concentration for particle size i of the 9-stage impactor, respectively.

The uncertainties of dry deposition velocities and dry fluxes have been calculated taking into account the uncertainties associated with pure meteorological variations, namely of wind speed, sea and air temperature and wind seasonal variations. The errors related to the determination of the aerosol concentrations in both size-segregated samples and bulk samples were also considered. A strict error propagation routine was thus performed in order to assess the reliability of the generated data.

Wet deposition model description

Wet deposition estimates are based on the model of precipitation scavenging proposed by Slinn (1983). In this model, the estimation of the scavenging of airborne particulate matter by cloud and raindrops begins with the determination of the collection efficiency. This efficiency is associated with three main processes. The collection of aerosols by a falling drop can be due to inertial impaction, i.e. when particles cannot follow the streamlines around the drop, and to their inertia impact on it. The second process is called interception. Here, even though particles can follow the streamlines, their size is large enough so that their surface and that of the falling drop get in contact. Last, but not least, Brownian diffusion also contributes to the scavenging of aerosols. Due to their random motion, particles come into contact with the drop and they are removed from the atmosphere. The average collection efficiency and scavenging coefficient for a mean drop diameter (D_m) have been determined using Slinn's (1983) approximations, with an assumed average precipitation rate for the Southern Bight of the North Sea of 600 mm yr^{-1} (Schmidt, 1992). Finally, wet deposition values have been weighted by the per cent frequency of the wind direction prevailing in the zone using the compilation of meteorological data reported by Hohn (1971). Results are grouped in five wind sectors.

As will be seen from the results, no attempt has been made to calculate the error associated with the determination of the wet fluxes, even though the uncertainties of precipitation rates reported by Schmidt (1992) have a standard error of 10%. This is motivated by several reasons: (i) The average collection efficiency was determined for a D_m with a precipitation rate measured at ground level; what happens aloft is not yet fully understood. (ii) Perhaps the most important issue is that the temporal distribution of precipitation events for the North Sea is also unknown; it does not rain every day over the North Sea as is assumed in this work.

RESULTS AND DISCUSSION

Concentrations and size distributions

The average concentrations observed above the Southern Bight of the North Sea for some heavy metals are (in ng m^{-3}): 1.1 ± 0.4 for Cd, 9 ± 3 for Cu, 65 ± 5 for Pb and 72 ± 9 for Zn. As shown by Injuk *et al.* (1990), there is some agreement between these values and those reported in the literature covering a period of about 18 years. There is also an apparent decrease of the Pb concentrations in this airshed, which could be related to a reduction of the lead emissions, e.g. use of unleaded fuels.

During this work, it was possible to determine two different aerosol size distributions (see Fig. 2), depending upon the criterion used to handle missing values. Indeed, the size distribution represented by the hollow bars was obtained when all missing values were replaced by 0; whereas the replacement of the missing values by the full detection limit led to a different aerosol size distribution (filled bars). It is seen that this practice introduces drastic variations in the size distributions of Cd and Zn, while Cu and Pb seem less affected (except for the largest size class). Since this represents two extreme cases on how missing values could be treated, we adopted an intermediate position

and mixing height data. Their results indicated that previous estimations of deposition data, extrapolated from coastal measurements, tend to overestimate the atmospheric input of anthropogenically generated heavy metals into the entire North Sea (Kersten *et al.*, 1988). On the other hand, their dry and wet deposition calculations take only into account particulate matter in the size range between 0.2 and 1 μm, which seems unrealistic, as will be shown throughout this work.

As an alternative method, Petersen *et al.* (1989) used the EMEP model (Eliassen and Saltbones, 1983), which was originally conceived for sulfur dioxide and particulate sulfur, to calculate dry and wet fluxes into the North Sea and the Baltic Sea. Even though the agreement between their model calculations and that of Krell and Roeckner (1988) is good, they conclude that a comprehensive validation of their approach is not possible due to the lack of long-term measurements of trace metal concentrations and deposition over the North Sea. If such long-term measurements were available, then model estimates and the uncertainties associated with them would be of no need.

In this work we concentrate on four elements of interest, namely Cd, Cu, Pb and Zn, and report on the dry and wet fluxes of atmospheric particulate matter over the Southern Bight of the North Sea. These fluxes have been calculated from total and size-fractionated airborne elemental concentrations, collected with the aid of an aircraft, during a 1-year period, in combination with calculated dry and wet deposition rates, related, *inter alia*, to the particle size distribution.

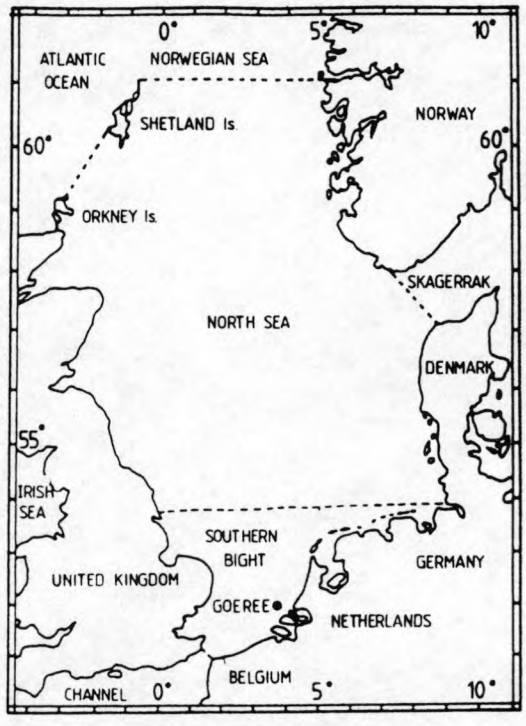

Fig. 1. Schematic representation of the Southern Bight of the North Sea. Here, the starting point of the sampling flights (Goeree platform) is also shown.

MATERIALS AND METHODS

Experimental

The sampling campaign started in September 1988, and lasted for 13 months. During this period, 23 flights were carried out using a twin-engine aircraft Piper Chieftain, PA 31-350, owned by Geosens B. V. (Rotterdam, Netherlands). All flights were performed with cloudless meteorological conditions (less than 3 oktas), and samplings did not take place during precipitation events. Each flight was planned taking into account the 36-h air mass backward trajectories provided by the Royal Netherlands Meteorological Institute (KNMI, De Bilt, Netherlands), for four different pressure levels: 1000, 925, 850 and 700 hPa, respectively. The starting point was the Goeree platform (51°55.5'N, 3°40'E), from which a spiral flight was done in order to localize the inversion layer. A map showing the area where sampling was carried out is given in Fig. 1. The aerosol sampling took place in six different tracks, each covering a distance of about 110 km towards the North Sea in the up- or downwind direction from the Goeree platform, and more or less equally spaced between the inversion height and sea level. Altitude was measured with a King Radar Altimeter model KRA 10/10a, whereas temperature and wind speed were monitored using a 102 E temperature sensor with Pt-100 element (nominal resolution 0.1°C) (Rosemount Inc., U.S.A.), and a Racall Doppler 91 radar equipped with a RSN 252 navigation compass, with a wind speed precision of 1 m s^{-1} and a position accuracy of 0.1 nautical mile. Airborne particulate matter was sampled using an isokinetic inlet designed by the Pennsylvania State University (Pena *et al.*, 1977), and collected on a set of parallel filters, namely, 0.4-μm pore size, 47-mm diameter Nuclepore membrane filter and 1-μm pore size, 47-mm diameter Millipore Teflon filter. After the air passed through the filters, it was pumped out using a Venturi system which was mounted on the wings. This had the advantage of being very light without requiring electric power. The air flow rate was 50 ℓ min^{-1}. Size-segregated aerosol samples were obtained using a multi-orifice Berner 9-stage cascade impactor (Berner *et al.*, 1979), operating at a flow rate of 30 ℓ min^{-1}. The mean particle size deposited on each stage was 11.3, 5.7, 2.8, 1.4, 0.7, 0.35, 0.17 and 0.09 μm for stages 2–9, respectively. Since the upper cut-off point for the first stage was unknown, an average size value of 23 μm was determined by least-square fitting of the mean diameter data for stages 2–9. Both Teflon filters and size-segregated samples were analysed for Cd, Cu, Zn and Pb by differential-pulse stripping voltammetry (DPSV) after extraction at a pH of 1, following the procedure used by Komy *et al.* (1988). Results of the analyses of the Nuclepore filters by energy-dispersive X-ray spectrometry (EDXRF), particle-induced X-ray emission (PIXE) and electron-probe X-ray microanalysis will be reported on in separate papers. The results reported here are based on the analysis of 108 aerosol samples. Even though the variation of the elemental concentration with height is known, the results for dry deposition are based on the elemental concentrations determined for the lowest flight level. This is not the case for wet deposition, for which all concentration values have been considered. In order to estimate the possible relationship between wind direction and airborne concentrations, all aerosol samples were classified in five different wind sectors. These were: west/southwest, north/northwest, east/northeast, south/southeast and local. The latter represents air masses with variable origin, and that in most of the cases circumscribe to the North Sea itself.

2745

Atmospheric Environment Vol. 27A, No. 2, pp. 251–259, 1993.
Printed in Great Britain.

0004–6981/93 $6.00 + 0.00

DRY AND WET DEPOSITION FLUXES OF Cd, Cu, Pb AND Zn INTO THE SOUTHERN BIGHT OF THE NORTH SEA

CARLOS M. ROJAS, JASNA INJUK and RENÉ E. VAN GRIEKEN
Department of Chemistry, University of Antwerp (UIA), Universiteitsplein 1, B-2610 Antwerp-Wilrijk, Belgium

and

REMI W. LAANE
Tidal Waters Division, Rijkswaterstaat, P.O. Box 20907, NL-2500 EX, 's Gravenhage, Netherlands

(*First received* 16 *September* 1991 *and in final form* 9 *July* 1992)

Abstract—During the period from September 1988 to October 1989, 23 sampling flights were carried out over the Southern Bight of the North Sea. In this campaign, both bulk and size-segregated airborne particulate matter samples were collected. Dry deposition velocities for Cd, Cu, Pb and Zn have been estimated using a modified version of the two-layer of Slinn and Slinn and the particle size distribution obtained from size-fractionated samples. Results pointed out that the main difference between our results and those reported in the literature lies in the aerosol size distribution. Dry deposition rates calculated using these deposition velocities as a function of wind sector showed that continental air masses, particularly those associated with the wind sector west southwest, are predominant in the deposition process. Wet flux estimates were carried out using Slinn's approach. Results were also classified taking into account different wind sectors. Here, the wet flux of Pb and Zn is mainly related to wind sectors east/northeast, south southeast and local, the latter represents air masses with variable origin; whereas those of Cd and Cu correspond to wind sectors west southwest and south southeast. Results showed that wet deposition is responsible for almost 70% of the total deposition into the Southern Bight of the North Sea. However, some topics, like heavy metal content in large aerosol particles, temporal distribution of precipitation events, variation of precipitation intensity aloft, need better knowledge before accurate assessments can be made.

Key word index: Atmospheric deposition, aerosols, North Sea, heavy metals, aircraft sampling.

INTRODUCTION

There has been growing concern regarding the pollution of coastal and shelf systems of the North Sea, especially since Weichart (1973) concluded that the southern North Sea is one of the most heavily polluted areas. Recently there have been efforts to determine the relative importance of the different pathways through which trace metals and other toxic substances reach the marine environment. These sources are mainly rivers, piped discharges, dumpings, run-off from land and, last but not least, atmospheric fallout. Here, the atmospheric input is caused by processes such as cloud or raindrop scavenging of aerosol particles, known as wet deposition, and/or by the transfer of gases and solid phases, known as dry deposition. Early studies reported by IDOE (1972) suggested that the atmospheric input of trace elements represents a significant proportion of the total input, relative to other pathways.

In order to estimate the atmospheric input of heavy metals and compare it with other pathways, Cambray *et al.* (1975, 1979), Dedeurwaerder *et al.* (1982) and Dedeurwaerder (1988) conducted direct measurements of dry and wet deposition. Despite the fact that these constitute the first attempts to assess the atmospheric fallout directly, the main drawbacks to their approach are: (i) predictions are based on coastal determinations; and (ii) the lack of reliability of the sampling technique, as has recently been discussed by Liss *et al.* (1988).

Due to a large number of constraints, direct measurements of particle pollutant fluxes over the sea are scarce (Van Aalst, 1986). In order to overcome this problem, several authors have proposed, as an alternative, the use of mathematical models to predict the atmospheric input of particulate matter to the North Sea. Indeed, Van Jaarsveld *et al.* (1986) introduced a model capable of predicting such input, and also the contribution of source areas to the total deposition. Their model is based on emission inventories and a transport-dispersion approach. The main shortcoming of this model is that most of the meteorological parameters such as wind speed, friction velocity, mixing height and rainfall statistics have been obtained from in-land measurements.

Krell and Roeckner (1988) published a new approach to modeling the deposition of Cd and Pb. They use a stochastic trajectory model, emission inventories, meteorological data and estimates of precipitation

Selected article #13:

Dry and wet deposition fluxes of Cd, Cu, Pb and Zn into the Southern Bight of the North Sea

C.M. Rojas, J. Injuk, R.E. Van Grieken and R.W. Laane

Atmospheric Environment, 27A (1993), 251-259

(39) Veldeman, E. Ph.D. Dissertation, University of Antwerp (UIA), Belgium 1991; p 249.
(40) Xhoffer, C. M.Sc. Thesis, University of Antwerp (UIA), Belgium, 1987.
(41) Mamane, Y.; Miller, J.; Dzubay, T. G. *Atmos. Environ.* **1986**, *20*, 2125–2135.
(42) Post, J. E.; Buseck, P. R. *Environ. Sci. Technol.* **1984**, *18*, 35–42.
(43) Degens, E.; Buck, B. *Cruise SO 45-B Report*; Lembar-Sumbawa Bear-Surabaya, 1986.
(44) Hood, D. W. *Environ. Sci. Technol.* **1967**, *1*, 303–305.
(45) Rona, E.; Hood, D. W.; Muse, L.; Buglio, B. *Limnol. Oceanogr.* **1962**, *7*, 201–206.
(46) Laevastu, T.; Thompson, T. G. *J. Mar. Res.* **1958**, *16*, 192.
(47) Slowey, J. F.; Jeffrey, L. M.; Hood, D. W. *Nature* **1967**, *214*, 377–378.
(48) Merlini, M. In *Impingement of Man on the Oceans*; Hood, D. W., Ed.; John Wiley & Sons, Inc.: New York, 1971; pp 461–486.
(49) Cattel, F. C. R.; Scott, W. D. *Science* **1978**, *202*, 429–430.
(50) Kremling, K. *Nature* **1983**, *303*, 225–227.
(51) Hunter, K. A. *Mar. Chem.* **1980**, *9*, 49–70.
(52) Chow, T. J.; Patterson, C. C. *Earth Planet. Sci. Lett.* **1966**, *1*, 397–400.
(53) Otten, P. Ph.D. Dissertation, University of Antwerp (UIA), Belgium, 1991.
(54) Ingri, J.; Ponter, C. *Chem. Geol.* **1986**, *56*, 105–116.
(55) Williams, J. D. H.; Jacquet, J. M.; Thomas, R. L. *J. Fish. Res. Board Can.* **1976**, *33*, 413–429.
(56) Filipek, L. H.; Owen, R. H. *Chem. Geol.* **1981**, *33*, 181–204.
(57) Johannesson, J. K. *Analyst* **1955**, *80*, 840–841.
(58) Graham, W. F.; Piotrowicz, S. R.; Duce, R. A. *Mar. Chem.* **1979**, *7*, 325.
(59) Wallace, C. T., Jr.; Duce, R. A. *Mar. Chem.* **1975**, *2*, 522.
(60) Chester, R.; Murphy, K. J. T. *Sci. Total Environ.* **1986**, *49*, 325–338.
(61) Kolaitis, L. Ph.D. Dissertation, University of Antwerp (UIA), Belgium, 1988.

Received for review December 9, 1991. Revised manuscript received May 18, 1992. Accepted June 12, 1992.

and classified into specific particle types. Assignment to one specific source (marine or continental) it is not always evident. Source apportionment is even made more difficult because there is hardly any distinction possible between some major particle types observed in either the aquatic or the atmospheric environment of the North Sea. On the contrary, chemical data from the atmospheric and riverine/estuarine environment can be used for selection criteria in the particle classification procedure.

During the collection of microlayer samples, the sea surface has to be very calm, which is not always the case in the North Sea. This might explain the low variation observed between the microlayer samples and the corresponding bulk water samples and is probably due to mixing of the water layers.

An important part of the oceanic source of particulate matter is characterized by detritus (dead organisms) like biogenic skeletons of diatoms and foraminifera, but also coccoliths, phytoplankton with minor amounts of bacteria, yeasts, and fungi are found. The organic particulate matter was more abundantly observed in the microlayer than in the underlying bulk water and showed very good correlation with the metal-rich fraction.

Aluminosilicates form the major particulate fraction (~30% of the total number concentration) classified in the North Sea water samples. We observed a relative enrichment for the bulk water compared to the microlayer. Most of these aluminosilicates are clay minerals that can partly originate from coastal sources due to marine erosion. Among the aluminosilicates, fly-ash particles were recognized in the sea surface microlayer.

Silicon-rich particles represent about 20–30% of the total particle concentration. This particle type mainly contains resuspension material and detrital quartz but also biogenic features rich in silicon. Manual search for morphological information showed the presence of diatom skeletons and fragments from sponges. There seems to be no preference for one of the analyzed water layers. Atmospheric deposition processes do not contribute to the total Si fraction in the water phase.

Si-rich and Ca-rich particulate material present in the North Sea can originate from various sources, e.g., suspended matter that contains the same minerals as the sediment, transmutation of some mineral substances such as silica and $CaCO_3$ which dissolve and are precipitated by organisms, or continental aerosol (both natural or anthropogenic) deposition processes.

The Ca-rich aluminosilicates must have an aquatic (marine or riverine) origin since no chemical analogues were observed in air masses above the North Sea.

The relative abundances for the Fe-rich, Ti-rich, and metal-rich particle types are rather too low to observe any significant difference between the microlayer and bulk water. It seems that the Fe-rich particle number concentration does not correspond well with the atmospheric number concentrations, whereas good similarity is found for the Ti-rich marine and atmospheric fraction. The metal-rich fraction showed very good correlation with the organic particulate fraction.

Registry No. S, 7704-34-9; Ti, 7440-32-6; Li, 7439-93-2; Hg, 7439-97-6; Si, 7440-21-3; Ba, 7440-39-3; Fe, 7439-89-6; Ca, 7440-70-2; K, 7440-09-7; Al, 7429-90-5; Na, 7440-23-5; Pb, 7439-92-1.

Literature Cited

(1) Södegren, A. In *Aquatic Pollutants Transformation and Biological Effects*; Hutzinger, O., Van Lelyveld, L. H., Zoeteman, B. J. C., Eds.; Pregamon Press: Oxford, England, 1977.
(2) Garrett, W. D. In *Organic Matter in Natural Waters*; Hood, D. W., Ed.; John Wiley & Sons Inc.: New York, 1970; pp 469–477.
(3) Liss, P. S. In *Chemical Oceanography*, 2nd ed.; Riley, J., Skirrow, G., Eds.; Academic Press: London, 1975; Part 2, pp 193–243.
(4) Wallace, G. T.; Duce, R. A. *Mar. Chem.* **1975**, *3*, 157–181.
(5) Blanchard, D. C. *Science* **1964**, *146*, 396–397.
(6) Barker, D. R.; Zietlin, H. *J. Geophys. Res.* **1972**, *77*, 5076–5086.
(7) Piotrowicz, S. R.; Ray, B.; Hoffman, G. L.; Duce, R. A. *J. Geophys. Res.* **1972**, *77*, 5243–5254.
(8) Duce, R. A., Quinn, J. G.; Olney, C. E.; Rotrowiez, S. R.; Ray, B. J.; Wade, T. L. *Science* **1972**, *176*, 161.
(9) Szekielda, K.-H.; Kupfermann, S. L.; Klemas, V.; Polis, D. F. *J. Geophys. Res.* **1972**, *77*, 5278–5282.
(10) Simoneit, B. R. T.; Mazurek, M. A. *CRC Crit. Rev. Environ. Control* **1985**, *11*, 219.
(11) Mopper, K.; Zika, R. G. *Nature* **1987**, *324*, 246.
(12) MacIntyre, F. In *Marine Chemistry*; Goldberg, E. D., Ed.; Wiley & Sons: New York, 1974; Vol. 5, pp 245–299.
(13) Van Espen, P. *Anal. Chim. Acta* **1984**, *165*, 31–49.
(14) Bernard, P. C.; Van Grieken, R. E.; Eisma, D. *Environ. Sci. Technol.* **1986**, *20*, 467–473.
(15) Raeymaekers, B.; Van Espen, P.; Adams, F.; Broekaert, J. A. C. *Appl. Spectrosc.* **1988**, *42*, 142–150.
(16) Xhoffer, C.; Bernard, P.; Van Grieken, R.; Van der Auwera, L. *Environ. Sci. Technol.* **1991**, *25*, 1470–1478.
(17) Verbueken, A. H.; Bruynseels, F. J.; Van Grieken, R. E. *Biomed. Mass. Spectrom.* **1985**, *12*, 438.
(18) Hillenkamp, F.; Unsold, R.; Kaufmann, R.; Nitsche, R. *Appl. Phys.* **1975**, *8*, 341.
(19) Garrett, W. D. *Limnol. Oceanogr.* **1965**, *10*, 602.
(20) Van Put, A. Ph.D Dissertation, University of Antwerp (UIA), Belgium, 1991.
(21) Koppelman, M. H.; Dillard, J. C. In *Marine Chemistry in Coastal Environment*; Church, T. M., Ed.; ACS Symposium Series 18; American Chemical Society: Washington, DC, 1975; p 186.
(22) Blackmore, A. V. *Aust. J. Soil. Res.* **1973**, *11*, 75.
(23) Fordham, A. W. *Clays Clay Miner.* **1973**, *21*, 175.
(24) Goldberg, E. D. Proceedings, Workshop in Melreux/Belgium Nov 29–Dec 3, 1976; UNESCO Press: Paris, 1978.
(25) Duedall, I. W.; Roethel, F. J.; Seligman, J. D.; O'Conners, H. B.; Parker, J. H.; Woodhead, P. M. J.; Dayal, R.; Chezar, B.; Roberts, B. K.; Mullen, H. In *Marine Science 12: Ocean Dumping of Industrial Wastes*; Ketchum, B. H., Kester, D. R., Park, P. K., Eds.; Plenum Press: New York, 1981; pp 315–346.
(26) Broecker, W. S. *Q. Res.* **1971**, *1*, 188–207.
(27) Parsons, T. R. *Prog. Oceanogr.* **1963**, *1*, 203–243.
(28) Riley, J.; Chester, R. In *Introduction to Marine Chemistry*; Riley, J., Chester, R., Eds.; Academic Press: London, 1971.
(29) Kido, K. *Mar. Chem.* **1974**, *2*, 277–285.
(30) McCrone, W. C.; Delly, J. G. *The Particle Atlas, Edition Two: An Encyclopedia of Techniques for Small Particle Identification*, Vol. III, *The Electron Microscopy Atlas*; Ann Arbor Science Publishers Inc.: Ann Arbor, MI, 1973.
(31) Wollast, R. In *In the Sea: Ideas and Observations on Progress in the Study of the Seas*; Goldberg, E. D., Ed.; J. Wiley & Sons: New York, 1974; pp 359–393.
(32) Mackenzie, F. T.; Garrels, R. M. *Science* **1965**, *150*, 57–58.
(33) Mackenzie, F. T.; Garrels, R. M.; Bricker, O. P.; Bickley, F. *Science* **1967**, *155*, 1404–1405.
(34) Vanderborght, J.-P.; Wollast, R.; Billen, R. *Mar. Chem.* **1977**, *22*, 787–793.
(35) Horne, R. A. *Marine Chemistry*; Wiley and Sons: New York, 1969; p 253.
(36) Bernard, P. Ph.D. Dissertation, University of Antwerp (UIA), Belgium, 1989.
(37) Andreae, M. O.; Charlson, R. J.; Bruynseels, F.; Storms, H.; Van Grieken, R.; Maenhaut, W. *Science* **1986**, *232*, 1620–1623.
(38) Michard, G.; Sanjuan, B.; Criaud, A.; Fouillac, C.; Pentcheva, E. N.; Petrov, P. S.; Alexieva, R. *Geochem. J.* **1986**, *20*, 159–171.

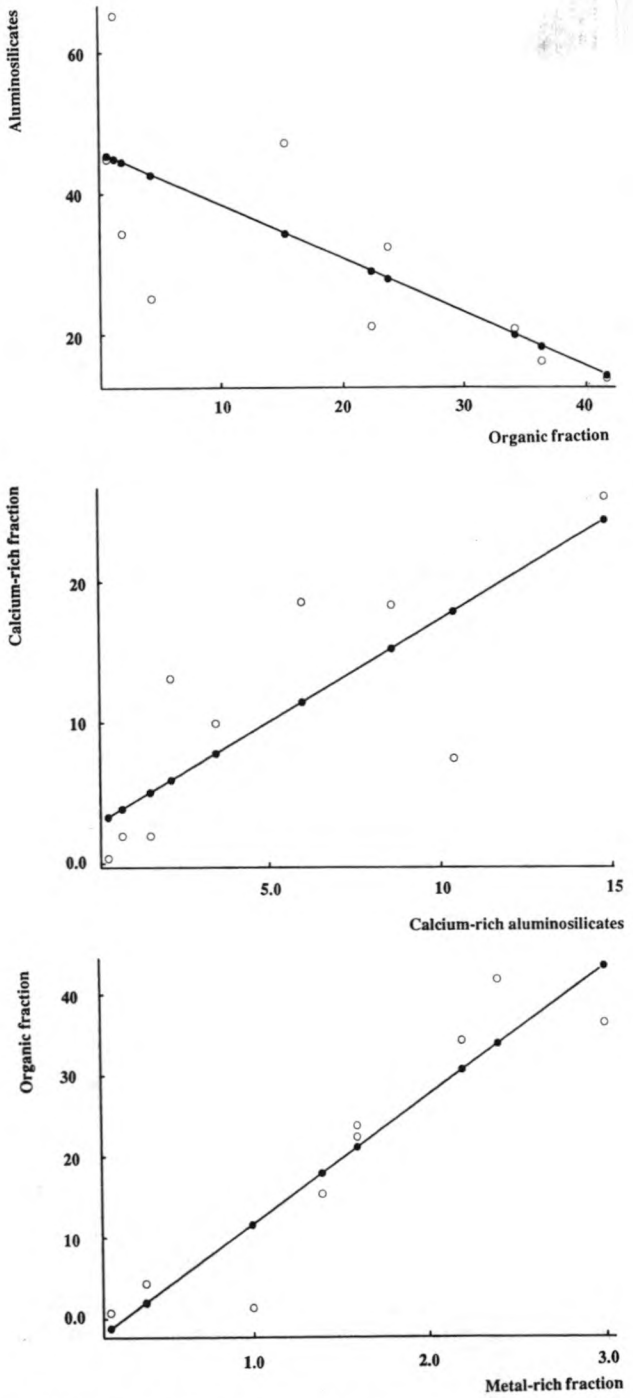

Figure 12. Two-dimensional correlation plot of (a, top) aluminosilicate fraction versus organic particulate fraction, (b, middle) organic fraction versus metal-rich fraction, (c, top) Ca-rich fraction versus the Ca-rich aluminosilicate fraction.

interpreted the low molecular weight fragment ions of nitrogen as organic-N compounds such as dissolved free amino acids and primary amines. These authors suggested that high molecular weight organic nitrogen compounds are degraded by chemical processes (in the atmosphere or in the light-intensive upper seawater layer) to low molecular weight species, e.g., primary amines and ammonium. Groups 2 and 3 classify respectively the organic and Si-rich particles. Here also, phosphates and sometimes nitrates were recognized in negative-mode spectra. The detailed composition of the organic material present in the surface microlayer is still unclear. Beside C_n^+ clusters, negative-mode fragments such as C_n^-, CNO^-, $HCNO^-$, and $HCOO^-$ could be identified. These have however little of no decisive value for compound determination. They appeared in many particles. The LAMMA spectra are most likely a superposition of many different organic compounds, and because of the fragmentation of long-chain hydrocarbons, a detailed structural interpretation of the spectra was not possible.

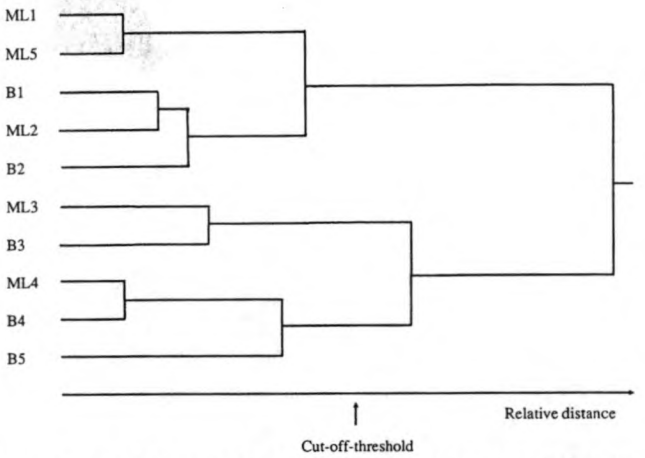

Figure 13. Dendrogram representation after hierarchical clustering performed on the microlayer and bulk water samples of the North Sea showing the cutoff threshold for a three-cluster level.

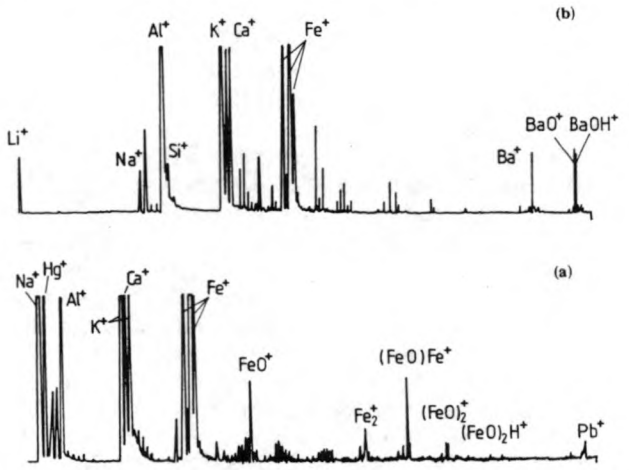

Figure 14. LAMMA spectra of (a) an Fe-rich particle present in the bulk water of the North Sea containing relative small amounts of the trace element Pb and (b) an aluminosilicate particle showing associations with Ba mass fragments.

Positive LAMMA spectra of Ca-rich particles (group 4) often reveal the presence of Sr. This result is more or less expected since calcite is known to accommodate Sr in its structure. The metal-rich cluster (group 4) is mainly characterized by Fe and Ti. The Fe-rich phase especially seemed to contain the highest relative amounts of trace elements like Pb (Figure 14a) and Ba. Barium was also found to be associated with aluminosilicates (Figure 14b). Also some very surprising particle types were observed within this group, namely, mixed particles including Cu clusters with Cl and/or CN/CNO. Indeed, Cu as well as Al, Ti, Mn, Fe, V, Zn, Ni, Pb, Cr, and Cd could be scavenged by bubbles and transported to the air/sea interface (*59*). More likely, copper can undergo fractionation in the sea surface microlayer leading to salts having enhanced concentrations relative to bulk seawater, according to Chester and Murphy (*60*). Positive-mode LAMMA spectra revealed the presence of such elements (*61*).

Conclusions

Most of the analyzed particles in the microlayer and underlying bulk water could be chemically characterized

Table IV. Cumulative Eigenvalues and Loadings for the First Two Principal Components Derived from the Covariance Matrix Performed on the North Sea Microlayer and Bulk Water Data

	principal components	
	1	2
cumulative %	69	94
aluminosilicates	0.93	−0.34
Si-rich	0.10	−0.39
Ca-rich	0.06	0.97
Ca-rich aluminosilicate	0.11	0.89
Fe-rich	−0.54	0.19
Ti-rich	0.12	−0.61
Si–S-rich	−0.15	−0.12
Al-rich	−0.37	−0.02
S-rich	−0.33	0.01
organic	−0.93	−0.34
metal-rich	−0.82	−0.47

(DPP) (*13*). The covariance matrix was used for the calculation of the principal components. The first two principal components explain more than 94% of the total variance in the data (Table IV). The loadings of the first two principal components are plotted in Figure 11a while the scores are represented in Figure 11b. The first principal component elaborates the difference between the aluminosilicates and the organic and metal-rich particles. This can be seen from the high negative correlation between these particle types. Indeed, a two-dimensional plot (Figure 12a) of the aluminosilicates versus the organic component shows a negative linear relationship ($r = -0.74$). Contrarily, Figure 12b shows the very good correlation between the organic fraction and the metal-rich particles ($r = 0.94$). The second component has high positive loadings on both the Ca-rich and Ca–Si-rich particle types (Figure 12c). The good linear correlation between these two particle types ($r = 0.80$) might indicate that these particle types can be apportioned to the same source.

When the results were studied on a three-cluster level using the results of Table III as input data, the dendrogram as seen in Figure 13 showed that one cluster is composed of the sample ML3 together with B3, one cluster of sample ML4 with B4 and B5; and one cluster of ML1, B1, ML2, B2, and ML5. Except for the ML5-B5 pair that is separated in different cluster groups, each microlayer and its corresponding bulk water sample are found in the same group. This means that the bulk and corresponding microlayer samples show more resemblance to each other than there is between the various microlayer and bulk water samples taken during the different cruises.

LAMMA Results. As mentioned previously, the LAMMA technique not only has better detection limits for most of the elements but is also able to detect elements such as C, N, and O.

About 150 particles were randomly analyzed by LAMMA. Five major particle types could be discerned from these results, as shown in Table V; the relative percent abundance of each group is based on the EPXMA data. The given particle-type abundances should be considered as a slightly biased rough estimate of the actual situation since particles were sometimes subjectively selected on the basis of their appearance. No significant differences between microlayer and bulk water samples were observed. Group 1 is the most abundant and reveals the presence of aluminosilicate ions. Negative-mode LAMMA spectra revealed that phosphates and, less frequently, nitrates are found to be present on a large fraction of the aluminosilicate particles. Graham et al. (*58*) already suggested that

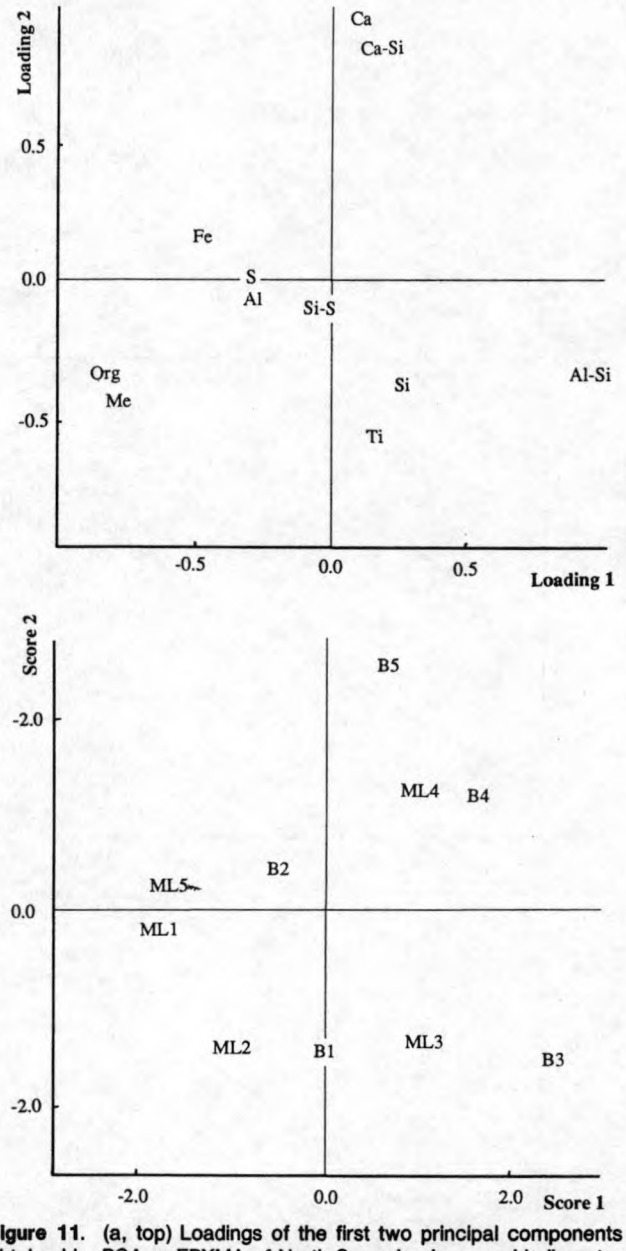

Figure 11. (a, top) Loadings of the first two principal components obtained by PCA or EPXMA of North Sea microlayer and bulk water results. (b, bottom) Component scores of the first two principal components obtained from the same data set. Particle types: Org, organic; Me, metal-rich; Fe, Fe-rich; Ti, Ti-rich; S, S-rich; Al, Al-rich; Si, Si-rich; Ca–Si, Ca-rich aluminosilicate; Al–Si, aluminosilicate.

Table V. Abundances of Particle Types Observed in the Microlayer and Bulk Seawater of the North Sea As Obtained by LAMMA Analysis

group	mass peaks observed	% abund
1	Al^+, Si^+, SiO^+ $SiAlO_4^-$, $SiAlO_5^-$, $Si_2AlO_6^-$ Cl^-, NO_2^-, NO_3^- PO_2^-, PO_3^-, $H_2PO_4^-$	46
2	C_n^+ (n = 1–10) C_n^-, CNO^-, $HCNO^-$, $HCOO^-$	19
3	Si^+, SiO^+, $HSiO^+$, Si_2O^+, $Si_2O_2^+$ SiO_2^-, SiO_3^-	26
4	$(CaO)_n^+$, $(CaO)_nH^+$	5
5	Fe^+, FeO^+, Fe_2O^+ $(CuCN)X^-$ (X = CN or Cl) $(CuCl_n)Cl^-$ Ti^+, TiO^+	4

the sea surface microlayer is a major source for organic phosphorus in the ejected drops. Mopper and Zika (*11*)

Table II. Relative X-ray Intensities Used as Criteria for the Conditioned Selection of the Particles in Different Particle Types

particle type		criteria[a]
1	aluminosilicates	Al + Si + K + Fe > 90 and 15 < Si < 85
2	Si-rich	Si > 85 and Al < 5
3	Ca-rich	Ca > 70
4	Ca-rich aluminosilicates	Ca + Si + Al + K + Fe > 90 and 15 < Ca < 70
5	Fe-rich	Fe + Mn + S + Cl + Cr + Zn + Cu > 90 and Fe > 50
6	Ti-rich	Ti + Si + Fe + Mn + Cr + Zn + Cu > 90 and Ti > 50
7	Si–S-rich	Si + S > 75
8	Al-rich	Al > 50 and Si < 15
9	S-rich	S > 75

[a] Based on relative X-ray intensities.

shows the criteria used for a particle to be selected into one particle type. The values in this table also refer to relative percent X-ray intensities that are normalized to the total net X-ray intensities of all elements collected from that particle. The same selection conditions were applied on each microlayer and bulk seawater sample. The constraints for these selection rules can be made more or less severe. However, overlap of the different groups must be avoided. The choice of the values for the selection rules can be deduced from measurement of standards or from the data obtained from reference samples. The selection criteria used were derived from the mean relative X-ray intensities of several characteristic particle types found in riverine suspensions and in air masses above the North Sea during either pure marine or continental sampling conditions. The relative intensities and therefore the chemical composition of the specific particle types such as aluminosilicate, Si-rich, Ca-rich, Fe-rich, and Ti-rich particles agree within less than 10% for these two different environments. Particle types 7 (Si–S-rich), 8 (Al-rich), and 9 (S-rich) were selected using severe conditions derived from atmospheric measurements.

The particle types, as defined by the selection rules, act as a replacement for the hierarchically obtained centroids. Since they are the same for all samples, no further classification routines are necessary.

The relative percentage abundances after such conditional selectioning for each particle type in each sample is given in Table III. The obtained data set shows good agreement with those obtained by the clustering technique (Table I). No significant differences were observed. The good comparison gives an indication that most of the particles are classified according to the proper training vectors, which implies that these training vectors are well formed and separated in space and all 10 samples show high similarity in chemical composition for the clusters; i.e., the same particle types are observed in both layers of the water column. There is also good agreement in chemical composition and elemental abundances for particles detected in the water phase of the North Sea compared to those determined in the North Sea atmosphere or in estuarine and riverine suspensions. Thus, our assumption for using these selection criteria is valid.

Closer inspection of the samples shows that, besides quartz, the Si-rich particle type is composed of different subclasses of particles with elemental composition of Si + Cl, Si + Cl + S, Si + S + Ca, and Si + Cl + Ca. Considering the presence of Cl, S, and Ca, they are probably related to or derived from a marine or biological environment.

Significant amounts of Si, P, S, Mn, and Cr can be present in the Fe-rich particles. This cluster can be subdivided into five different Fe-rich particle types, namely: iron oxide/hydroxide/carbonate and particles rich in Fe–Si, Fe–Cr, Fe–S–P, and Fe–Mn. Most of them are believed to have an authigenic character (*20*, *36*). The sometimes higher Si contents of these particles could indicate that aluminosilicates act as condensation nuclei for the precipitation of iron. Eventually, coprecipitation and/or adsorption of manganese oxides/hydroxides and of Mn(II) occurs (*54*). The association of P with Fe is due to adsorption of P onto the iron oxides or hydroxides (*55*, *56*). The iron oxides, Fe–Mn, and Fe–Cr-rich particles were also found in a continentally derived North Sea atmosphere and assigned to industrial sources. Iron oxide and Fe–Cr-rich particles are both released into the atmosphere by ferrous metallurgy processes.

Other elements detected in single particles were V, Co, Mn, and Ni. They are associated with an organic fraction as they occur in crude oils as nonvolatile porphyrins (*57*).

The "rest" group found in Table III results from the remaining particles that could not be classified in one of the other clusters and comprise particle types like aluminosilicate, Si-rich, and Ca-rich particles. However, they have element abundances that do not fulfill the proper selection rules.

Principal Component Analysis (PCA). The variations of the characteristic particle types among the various samples can be studied by applying principal component analysis (PCA). The relative percent abundances of Table III were taken as input data for a data processing program

Table III. Relative Percent Abundances for the North Sea Microlayer and Bulk Seawater Samples[a] after Conditioned Selection

	March 1986		March 1986		Nov 1987		June 1987		June 1987	
particle type	ML1	B1	ML2	B2	ML3	B3	ML4	B4	ML5	B5
Al, Si, Fe	14	32	21	21	47	65	34	45	6.2	16
Si	17	29	25	19	24	20	20	17	13	21
Ca	10	2.0	0.4	8	2.0	0.4	19	18	13	35
Ca, Si	3.5	0.8	0.4	10	1.6	0.4	6.0	8.6	2.2	15
Fe	3.5	2.4	2.0	1.6	1.0	0.4	4.4	1.6	10	1.6
Ti	1.0	1.2	2.0	0.8	1.4	1.6	1.2	1.4	1.4	0.8
Si, S	0.3	0.2		1.4	0.4	0.2				
Al	1.0	0.6	1.2	2.8	1.2		0.4			0.8
S	0.3		0.4	0.8	0.4		0.2			0.2
organic	42	24	34	22	15	1.4	2.0	0.8	36	4.4
M^{n+}[b]	2.4	1.6	2.2	1.6	1.4	1.0	0.4	0.2	3.0	0.4
rest[c]	6.0	6.2	11	11	4.4	9.0	12	7.2	15	4.4

[a] Dates indicate cruise times. [b] Percent abundance of particles that contain various metal elements (different from Fe and Ti). [c] Percent abundance of particles that was not classified in either of the above selected groups.

The mean Fe-rich particle diameter in the water phase is 1.4 μm and is almost double the observed diameter of iron oxide particles in the air. The mean shape of this particle type is 1.9, which is expressed by the shape factor (SHF) and calculated as SHF = (perimeter)$^2/4\pi$ area. It deviates strongly from sphericity (SHF = 1). However, the origin of these Fe-rich particles in the microlayer cannot be ascribed to one specific source on the basis of these data.

(7) Ti-Rich Particles. Titanium-rich particles were observed both in the microlayer and in the bulk seawater of the North Sea. Their relative number concentrations are again low (2% or less). The relative abundances correspond very well to the atmospheric North Sea concentrations of Ti-rich particles (*16*). Also, the mean particle diameter (1.1 μm) and shape factor (1.5) for this group are in accordance with the atmospheric fraction. These particles are thus more likely to be derived from continental pollution sources such as paint spray, soil dispersion, and asphalt production. However, riverine input into the North Sea may not be excluded. Both Bernard (*36*) and Van Put (*20*) found the presence of Ti-rich particles (probably rutile) in, respectively, the Scheldt and Elbe estuaries.

(8) Miscellaneous Particle Types. Occasionally, particles containing elements like Cu, Zn, Co, Cr, Ba, Pb, and Ni were detected. Among them, Cu, Zn, and Cr are the metals that were most frequently recognized. Figure 10 shows a secondary electron image of a very large chromium oxide particle with a $CaCO_3$ particle sticking to its surface. Most of the metal-rich particle types have low number concentrations, and their abundance cannot be determined with high accuracy. This is the result of the abundance variations of the more abundant particle types influencing relatively the abundance of these metal-rich particles. Nevertheless, their occurrence as individual particles can sometimes be used as indicator for source apportionment because of their specificity. Most of these metal-rich particles were clustered together with the organic fraction. Sometimes relatively low X-ray counts were observed, and the sum of the X-ray intensities did not always add to 100% because of unidentified peaks. This might indicate an association of these metals with particles of organic origin.

Hood (*44*) reported great variation of both kinds and amounts of Cu, Mn, and Zn in the water column from the Gulf of Mexico, with Cu and Zn mostly associated with the particulate fraction and Mn in solution. Much of the Zn, substantial amounts of Cu, and small amounts of Mn were nondialyzable, that is, firmly bound to organic complexes. There is also indirect evidence of an organic-bound fraction of elements such as Mn and Zn (*45*), Fe (*46*), and Cu (47). It is known that some fungicides with chlorinated hydrocarbons can have metal components such as copper (sulfate, naphthenate) and zinc (sulfite or oxide) (*48*).

Copper is a trace metal, and microlayer enrichment factors of 10^3–10^4 times are found relative to bulk seawater (*9*, *49*). The concentration of dissolved Cu in surface waters of the coastal North Sea (average ~200 ng/L) is twice as high as that in remote open oceans (average ~100 ng/L) (*50*).

Hunter (*51*) performed studies on the North Sea and found that both Fe and Mn were strongly depleted in the microlayer. He suggested that the phase bearing these two trace metals consisted of river-derived terrigenous material present on large particles. From comparing residence times of both atmospheric deposition and flotation, he deduced that bubble flotation formed the major process for the

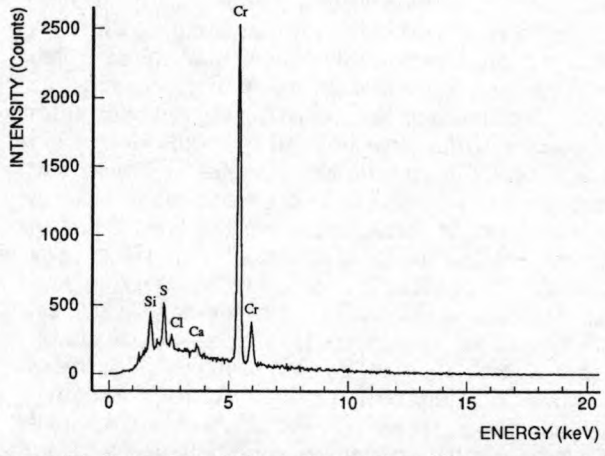

Figure 10. Secondary electron micrograph and X-ray spectrum of a chromium-rich particle with a $CaCO_3$ particle sticking to its surface.

enrichment of most trace metals in the microlayer.

Surface ocean concentrations of Pb have dramatically increased as a consequence of the "rainout" of man-introduced lead from the atmosphere. Contents of Pb in surface waters of the Northern Hemisphere today easily reach 0.07 μg of Pb/kg of seawater compared with estimated prehistoric values of 0.01–0.02 μg/kg (*52*). About 49% of the total Pb quantity (3390 ton/yr) reaches the North Sea by atmospheric input routes and the other 51% by dumping activities (2400 ton/yr), rivers (970 ton/yr), and discharges (144 ton/yr) (*53*).

Conditional Selection of Particle Types. The multivariate classification procedure, as mentioned above, can be applied when there is no previous knowledge on the chemical composition of the samples. The hierarchical classification of particles into a certain number of characteristic groups implies that indeed every particle will be added or pushed into just one group although there is only a marginal similarity. No completely satisfactory statistical test exists for determining the minimum number of significant clusters. So, more often a rather biased method, the so-called cutoff-threshold method, is applied on the connection diagram that results from the hierarchical cluster routine. In order to avoid these problems and to check the results of the final clustering, we also performed a classification procedure on objects or particles into characteristic groups based on selection rules. Table II

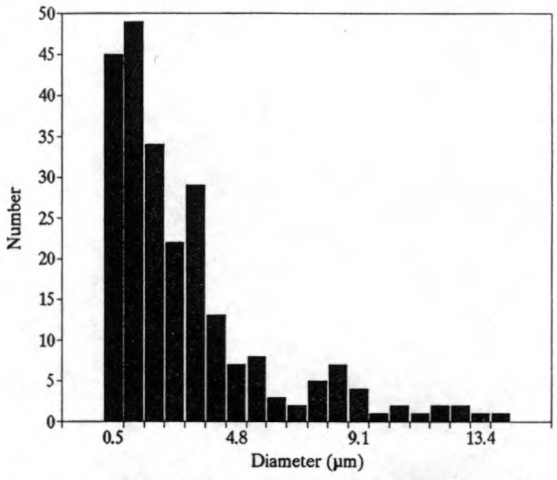

Figure 8. Particle size distribution for all calcium–aluminosilicate-rich particles present in the North Sea surface microlayer and underlying bulk water.

might indicate one major source.

Resuspension of a Ca-rich particle fraction into the marine atmosphere could occur during sea spray processes. Reactions with atmospherically S-rich species like SO_2, H_2SO_4, or dimethyl sulfoxide (DMSO) might take place with the formation of $CaSO_4$ (*37*). This transformation process can be important for the atmospheric $CaSO_4$ contribution in remote areas but will totally be suppressed by anthropogenic $CaSO_4$ emission sources in near-continental regions like the North Sea. During the March 1986, June 1987, and November 1987 sampling campaigns, sea spray production was an unimportant process, as was reflected by the absence of NaCl in the atmospheric samples. The absence of particulate $CaSO_4$ in the North Sea water samples can be explained by the sample preparation procedure applied. Indeed, during the washing procedure necessary for removing the salt fraction, other soluble particles like $CaSO_4$ will also be removed from the filter.

(4) Calcium–Aluminosilicate-Rich Particles. This particle type comprises aluminosilicates that are enriched in their Ca content. The relative abundances for this particle type are quite low. Except for the first microlayer/bulk water couple, comparable or somewhat higher concentrations are observed in the bulk water. The origin of these particles is not well-known. Several Ca-containing minerals are present in natural waters, such as anorthite ($CaAl_2Si_2O_8$), zeolites, pseudo-zeolites, clay minerals, and epidotes (*38*, *39*).

Comparable element compositions were observed in brown-coal fly-ash samples (*40*). But since this particle type was totally absent in air masses collected above the North Sea, atmospheric transport processes can be excluded, ruling out the possibility that this particle type might be fly ash derived.

A size distribution of this particle type is shown in Figure 8. The somewhat irregular shape of the distribution could suggest different sources or might be a reflection of the various minerals in the water phase.

(5) Organic Particles. Under conventional EPXMA measurements, elements lighter than Na cannot be readily detected and thus C, N, and O signals are not to be interpreted from X-ray spectrum analysis. However, one can sometimes distinguish the inorganic fraction from the organic fraction since the latter exhibits a relative noisy background in its collected spectrum (*41*, *42*). Backscattered electron signals from organic particulate matter can sometimes exceed the image threshold of the Nuclepore filter. At least some of the organic particulate residue will

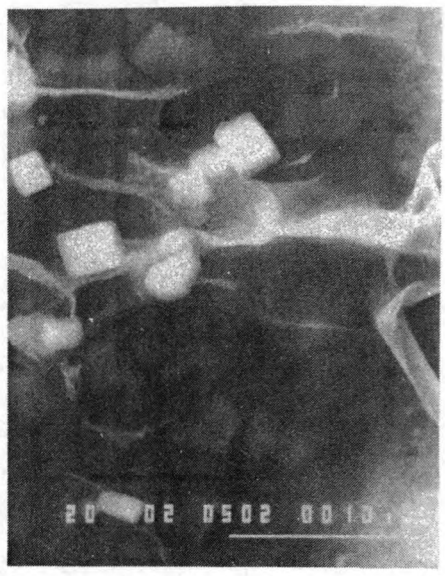

Figure 9. Secondary electron image of an organic particle enclosing various salt particles.

then be localized, sized, and analyzed, showing no interpretable X-ray peaks in the spectrum. Probably only the thicker or more dense organic particles such as biological material and microorganisms will give rise to sufficient backscattered signals.

From the EPXMA, it can be seen that organic material makes up an important part of the total particulate material in the microlayer. For four couples of samples, a clear difference in organic contribution can be observed in favor of the microlayer. In one case (ML4-B4), the relative abundances are too small to observe any significant difference. Because of the lipophilic properties of the organic material, one expects the organic contribution to be more pronounced in the microlayer, as is also seen from these data.

It was sometimes observed that organic material was incorporating other particles like sea salt, $CaCO_3$, and aluminosilicates (Figure 9). It was not possible to deduce whether these particles exist in the water phase or whether they are combined during the filter preparation process.

Note that the organic fraction observed in these samples only reflects a part of the total organic particulate material present in the water phase since an appreciable fraction will escape detection by this technique.

(6) Fe-Rich Particles. The major particles classified in this cluster have Fe as only detectable element and thus must be iron oxide, hydroxide, or carbonate. The particle abundance concentrations are too low to observe any significant differences between the microlayer and the underlying bulk sea water. Except for the June 1987 campaign, somewhat more abundant Fe-rich particles seem to be detected in favor of the microlayer. Their contribution for the June 1987 campaign is not in accordance with the sampled air masses above the North Sea since low number concentrations occurred in the corresponding air masses. In most of the marine sediments, an anoxic sulfate-rich environment can be encountered due to (a) the high initial SO_4^{2-} concentrations in the water and/or (b) organic sediments with large benthic populations. Various Fe–S-rich phases can exist, such as pyrite, marcasite (FeS_2), and organic matter. In oxic environments, as encountered in the coastal North Sea surface waters, hematite (Fe_2O_3) and goethite (FeOOH) form the major representers. Pyrite framboids can be formed through concentration of iron hydroxides and organic matter by biogenic activity by, for example, diatoms (*43*).

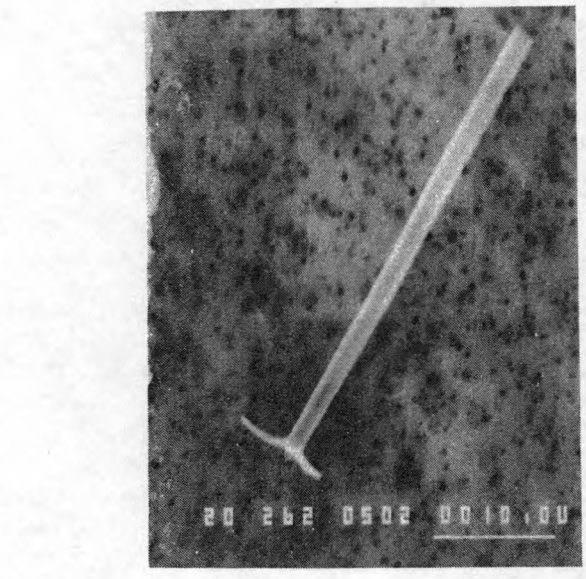

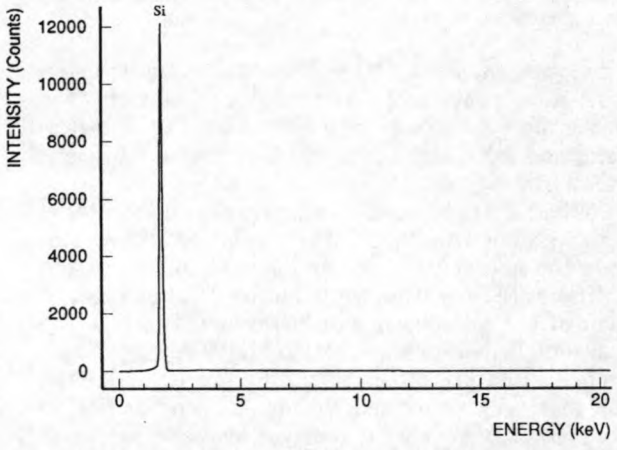

Figure 5. Secondary electron micrograph and X-ray spectrum of a skeletal fragment from a sponge present in the surface microlayer of the North Sea.

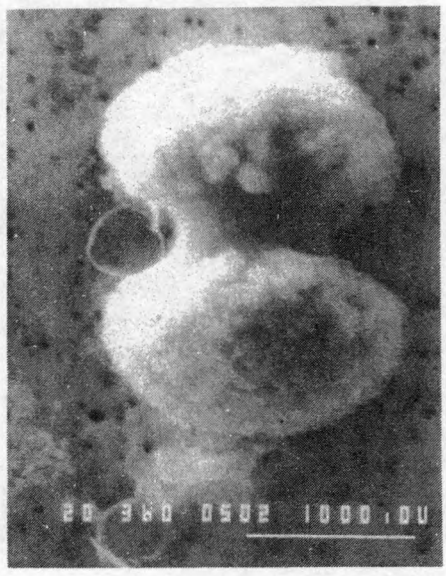

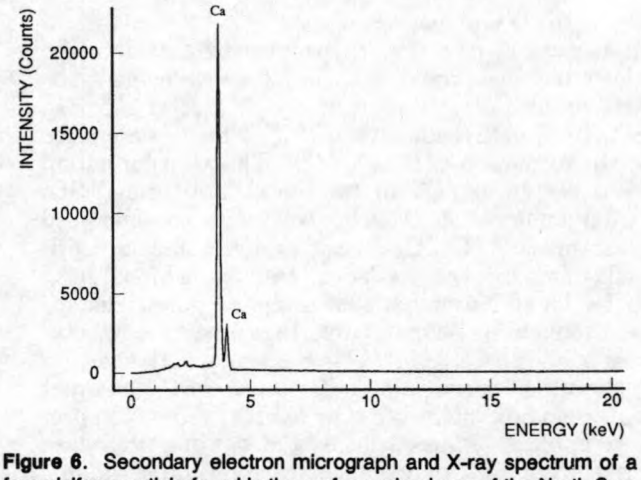

Figure 6. Secondary electron micrograph and X-ray spectrum of a foraminifora particle found in the surface microlayer of the North Sea.

cycle of uptake of dissolved silica by silica-secreting microplankton is essentially maintained by the rapid dissolution of debris of silicified skeletons during settling. The riverine input and the release of dissolved silica from interstitial waters play only a minor role in the distribution of dissolved silica in the ocean.

(3) Ca-Rich Particles. The relative abundance of this particle type varies from 0.2 to 35%. Some contradictory results are observed for the Ca-rich particle distribution between the microlayer and the underlying bulk water. For the first March 1986 sample, a higher microlayer abundance is observed, whereas for the second March 1986 and second June 1987 samples, a more pronounced enrichment is observed in the bulk water. No significant differences were noticed for ML3-B3 and ML4-B4.

Since no other elements beside Ca are detected, this particle type is identified as $CaCO_3$. The equilibrium of $CaCO_3$ in the marine environment is very complex because there exist two polymorph crystalline structures, namely, calcite and aragonite. Both substances are found in oceans, though calcite is the most important. Aragonite is sometimes formed during precipitation processes, especially from organisms. Secreted skeletal $CaCO_3$ can be either calcite or aragonite; if calcite, it can have a high or low magnesium content depending on the organism involved and/or the environmental conditions (*35*). Figure 6 shows a picture of a foraminifera particle as compared to a particle atlas (*30*). These are $CaCO_3$ skeletons, but of

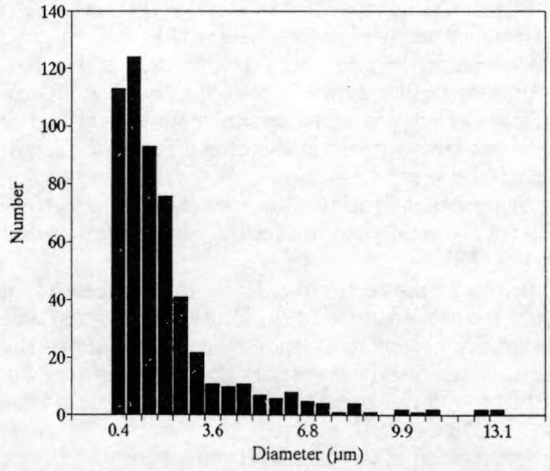

Figure 7. Particle size distribution for all calcium-rich particles present in the North Sea surface microlayer and underlying bulk water.

animals rather than plants, and calcium is by far the most intense X-ray signal in the spectrum. Many shapes and surfaces may be encountered.

Mg was detected in only very few particles (1–10% of the Ca-rich fraction). This might be the result of the high detection limit inherent to the applied fast-filter algorithm (FFA). Elements with very low atomic numbers such as Mg are not very efficiently deconvoluted by this spectrum deconvolution technique (*36*). The particle size distribution plot (Figure 7) shows a regularly decreasing shape and

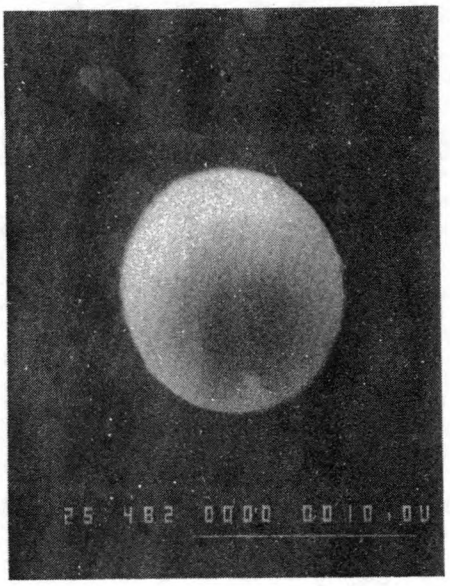

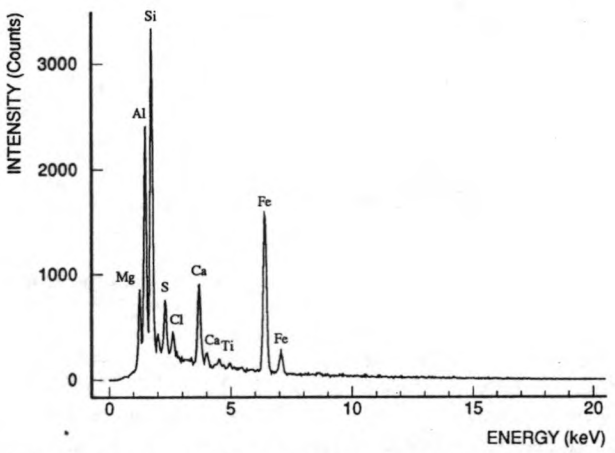

Figure 3. Secondary electron micrograph and X-ray spectrum of a fly-ash particle found in the surface microlayer of the North Sea.

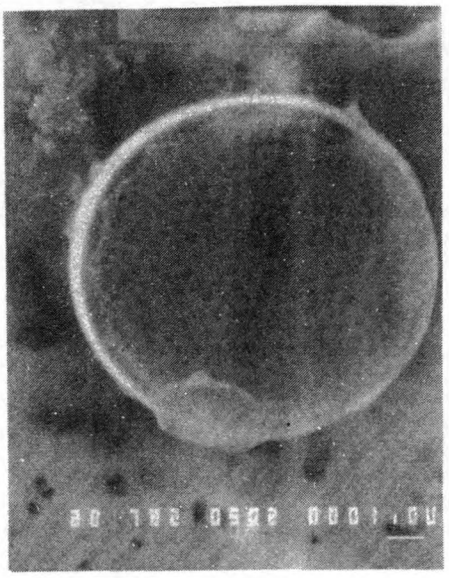

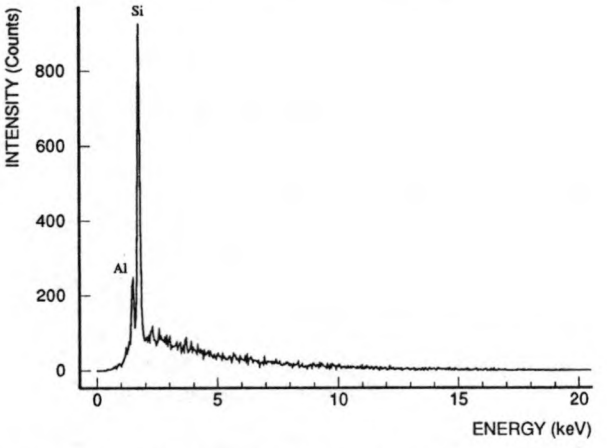

Figure 4. Secondary electron micrograph and X-ray spectrum of a diatom observed in the surface microlayer of the North Sea.

campaign show that the air masses had long residence times above Eastern European countries. Therefore, even middle-to-long distance anthropogenic emission sources can be responsible for the input of particulate material into the North Sea surface microlayer and bulk water.

(2) Silicon-Rich Particles. For this particle cluster, the mean relative Si–K X-ray intensity ranges in values from ~72% for the ML3 sample to ~99% for the B1 sample. All particles belonging to this class are denoted as Si-rich. Whereas the first March 1986 bulk sample is enriched in number concentration of Si-rich particles compared to the microlayer, the reverse is true for the second March 1986 sample. For the other samples, no significant differences were observed between microlayer and bulk samples. The Si-rich particle number concentration in bulk and microlayer water is comparable for all samples (it accounts for about 20–30% of the total particulate fraction). During the March 1986 and June 1987 sampling campaigns also, higher Si-rich particle number concentrations were detected in continentally derived air masses above the sea surface (*16*). In contrast, no Si-rich particles were observed at all in the lower North Sea atmosphere while we found high concentrations in the water phase for the November 1987 cruise. So, there cannot be a direct correlation between the presence of Si-rich particles in the atmospheric and the aquatic phase of the North Sea.

It is known that Si can be removed effectively by organisms (*26*). In fact, a great part of the phytoplankton in the sea consists of diatoms having a siliceous structure (*27–29*). Figure 4 represents a secondary electron image of a Si-rich particle observed in the microlayer. The highly symmetrical shape and the holes present in the structure suggest it to be a siliceous frustule from a diatom. They usually appear as flat structures with a regular array of holes. Figure 5 shows another Si-rich particle identified as sponge spicules (*30*). These are skeletal fragments of sponges and exist in thousands of shapes. Sometimes elements such as Ca, Cl, S, K, and even Fe are associated with them. Both the diatoms and the sponges were observed throughout the whole water column. In general, the concentration of dissolved silicate is low at the surface water due to uptake by organic activity and increases with depth where regeneration occurs because of decomposition of organisms in the deeper layer (*29*). The concentration gradient between surface water and deeper water layers becomes more marked as biological activity increases (*31*). There are also other factors controlling the Si content in the seawater such as interactions of Si with clay minerals carried into the oceans by streams (*32, 33*). The properties of the surface layer of sediments generally differ considerably from those of the deeper layers and may strongly affect the mass transport across the water/sediment interface (*34*). Mass balance estimations have shown that biological uptake of dissolved silica is 1 order of magnitude higher than that supplied by rivers and submarine activity (*31*). Biological activity in the seawater generates an extremely high chemical mobility of silica. The quasi-closed

Table I. Relative Percent Abundances for the North Sea Microlayer (ML) and Bulk (B) Seawater Samples[a] after Hierarchical and Nonhierarchical Clustering

	March 1986		March 1986		Nov 1987		June 1987		June 1987	
particle type	ML1	B1	ML2	B2	ML3	B3	ML4	B4	ML5	B5
Al, Si, K, Fe	17	34	23	29	47	66	38	50	7.0	19
Si	19	31	32	21	27	26	26	20	21	24
organic	46	27	38	24	18	2.0	2.4	1.0	43	5.2
Ca	10	2.2	0.4	9.0	2.2	0.4	19	18	13	34
Ca, Al, Si	3.3	0.6	0.2	8.8	1.6	2.2	6.4	6.8	2.4	14
Fe	4.0	4.0	0.6	2.8	2.0	2.0	6.4	3.0	10	2.0
Ti	0.8	1.2	2.0	0.8	1.8	1.6	1.4	1.4	1.6	0.8

[a] Dates indicate cruise times.

could not be performed in optimum conditions. Finally, the loaded grid was mounted in the LAMMA sample chamber where 100–150 particles were randomly selected for analysis.

Bulk seawater was collected at the same location as the microlayer samples using a Niskin bottle at 1 m below the surface. The bulk water samples were treated and analyzed in the same way as described above.

Results and Discussion

EPXMA Results. A multivariate classification procedure was applied to the elemental composition of five pairs of samples, each pair consisting of a microlayer sample and an underlying bulk seawater sample.

The elemental composition of each particle is determined by the relative percent X-ray intensity, as this expresses the ratio of the net X-ray intensity of that element to the total net X-ray intensities collected from that particle. Particles that have different chemical composition most probably originate from different sources or have been exposed to different transformation reactions during their lifetime in the environment.

As indicated by Table I, seven representative particle types could be discerned and separated on the basis of the percent abundances of more than 13 elements by applying cluster algorithms. The standard deviations of the relative abundances can be calculated by binomial statistics. For a total of 500 particles analyzed in each sample, the standard deviations range between 1 and 5% on a 2σ criterion. In addition to the automated EPXMA described in the instrumentation section, each filter was screened visually in the secondary electron mode and sometimes in the backscattered mode in order to obtain an idea about typical particle morphologies. LAMMA was applied in an attempt to obtain more information about trace element composition, organic composition, and surface characteristics. The different particle types will be discussed in more detail below.

(1) Aluminosilicates. The aluminosilicate particle type is characterized by high relative elemental X-ray intensities of Al, Si, K, and Fe and lower, though frequent contributions of Ti, Mn, and Cr. For all samples, the number concentrations of the aluminosilicate fraction is higher in the bulk seawater than in the microlayer. A size distribution for this particle type is presented in Figure 2, and it shows a maximum number of particles at a diameter of 0.8 μm. The cutoff at the lower site of the particle size distributions is mainly a consequence of two factors: (a) the magnification used during the particle analysis, higher magnifications allowing smaller particles to be detected, and (b) the setting of the cutoff for the backscattered threshold intensity criterion. No differences in size distributions were observed between the microlayer and bulk water aluminosilicates. The aluminosilicates can be subdivided into two particle fractions, namely, those enriched in Fe and those depleted or poor in Fe. Van Put (*20*) observed the same particle types in an estuarine environment and assigned them to the respective sources of Fe-smectite and/or chlorite and to an illite clay mineral. Clay minerals are known to act as an adsorbent for trace metals and as a transport medium for riverine suspensions into the estuaries and ocean systems (*21*). Various marine clay minerals like kaolinite, illite, and chlorite absorb iron and chromium species from solution (*22–24*).

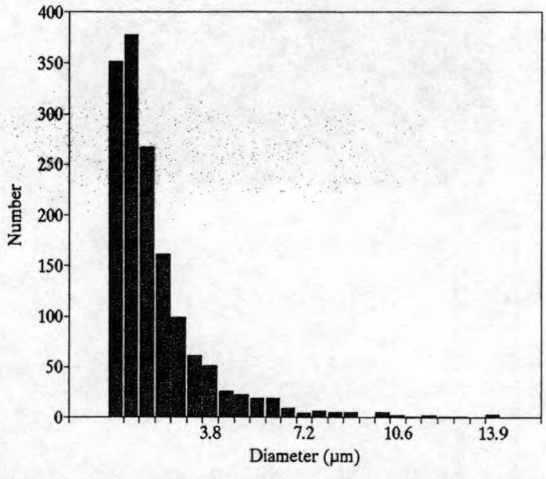

Figure 2. Particle size distribution for all aluminosilicate particles present in the North Sea surface microlayer and underlying bulk water.

In some of the microlayer and bulk seawater samples, smooth and nearly spherical aluminosilicate particles were observed (Figure 3). These typical round-shaped aerosols are often observed after high-temperature combustion processes or might be formed during gas-to-particle conversion processes. These particles could be identified as fly ash, and they maintain their structural integrity in an aquatic environment for extended periods of time (*25*). It is not possible to distinguish fly ash from, for example, soil dust on the basis of the relative X-ray intensities because their elemental compositions are very alike. Sometimes the distinction can be made by morphology studies, as was done here. Visual inspection in the secondary electron mode revealed that fly ash is more often found in the microlayer. The hollow and accordingly relatively low density structures probably have low sinking rates once they reach the water phase after atmospheric deposition. Especially during the November 1987 sampling cruise, the samples ML3 and B3 showed higher contributions of spherical aluminosilicate particles. The same observations were found for North Sea aerosols that were sampled at 11 m above the sea surface during the same cruise (*16*). Here, the number concentration of spherical aluminosilicates (fly ash) was much higher than normally observed. The 36-h air mass back-trajectories of the November 1987

Most of the previous microlayer research has been performed on chemical composition determination of the organic components or on distribution differences of heavy metal concentrations throughout the water column. The techniques are thus dealing with bulk analytical determinations.

Recently, microanalysis techniques such as automated electron microprobe X-ray analysis (EPXMA) and laser microprobe mass analysis (LAMMA) have become available and can advantageously be applied to particulate environmental samples to complement measurements made by traditional bulk analysis methods. Beside chemical composition and morphological information, such microanalytical techniques can, for example, reveal whether a specific element or compound is uniformly distributed over all the particles of a population or whether it is a major or minor component of a specific particle group.

Experimental Procedures

Instrumentation. (1) EPXMA. Electron probe X-ray microanalysis (EPXMA) has been used to gain chemical and morphological information of micrometer-sized particles. Automated EPXMA in combination with multivariate numerical techniques can analyze and classify a large population of individual particles for each sample in a fast and efficient way. Using this, particles with similar chemical composition are grouped into classes that can be related to specific sources. Although concentrations below 1000 ppm are hard to detect and elements with atomic numbers lower than sodium will not be observed, the automated EPXMA method is essentially fast and reliable.

All samples were measured with the aid of a JEOL JXCA 733 Superprobe, automated with a Tracor Northern TN 2000 system, which is controlled by an LSI 11/23 minicomputer. The microprobe is equipped with a 10-mm^2 energy-dispersive Si(Li) detector for X-ray analysis, a secondary electron and transmission electron detector for morphological studies, and a backscattered electron detector for the automated particle localization and additional composition and topographic viewing. Typical working parameters for characterization of particles in the 0.2–10-μm range are a beam current of 1 nA with an electron energy of 20 keV. Characteristic X-rays were accumulated for an acquisition time of 20 s per particle. The detection limits for the elements are typically around 1–2%. A modified particle recognition and characterization (PRC, Tracor Northern) software package was used. The analysis of one particle is performed in three sequential steps, localization, sizing, and chemical characterization, after which the electron beam searches for the next particle. For each sample, 500 particles were analyzed. The particle diameter is measured based on the projected physical diameter and might differ from the aerodynamic diameter. To reduce the total data set, hierarchical and nonhierarchical cluster analysis was performed on the samples using a data processing program (DPP) software package (*13*) so that the particles with a similar chemical composition are classified in one "particle type". Relative X-ray peak intensities were used as a measure for the elemental abundance. Principal component analysis (PCA) was used to study the variations between the different characteristic particle types. Detailed information on all these mulivariate techniques is given by Bernard et al. (*14*), Raeymaekers et al. (*15*), and Xhoffer et al. (*16*).

(2) LAMMA. Single particles were also analyzed by laser microprobe mass analysis (LAMMA). In this technique, an individual particle is vaporized and ionized by

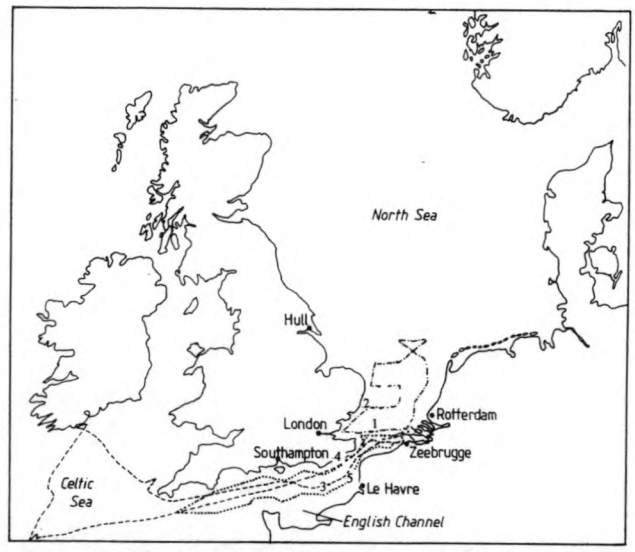

Figure 1. Location of sampling sites during different campaigns on the North Sea, English Channel, and Celtic Sea: (–·–) March 1986; (···) June 1987; (– – –) November 1987.

interaction with a 15-ns pulse of a high-power Nd/YAG laser. The formed ions are extracted and accelerated into the drift tube of a "time-of-flight" mass spectrometer. The mass spectrum obtained from the laser pulse is detected by a secondary electron multiplier. The analog signal is digitized, stored in a 100-Mhz transient recorder, and transferred to a computer for further data handling. The instrument is interfaced to a Digital MINC computer, which is part of a laboratory automation network based on a VAX-VMX computer. LAMMA is a very sensitive and multielement technique, it gives inorganic speciation and organic fingerprinting, but it is destructive. For further details concerning the LAMMA instrument, readers are referred to earlier publications (*17*, *18*).

Samples and Sample Preparation. Different sea surface microlayer and bulk seawater samples were collected during three cruises in the southern bight of the North Sea under very calm weather conditions. Figure 1 shows the followed trajectories and the respective sampling locations. The sea surface microlayer samples were collected using the Garrett screen technique (*19*). The sampler consists of a nylon window screen with openings of 400 by 400 μm and a fabric thickness of 440 μm stretched in a plexiglass frame. To avoid contamination from the research vessel (smoke stacks, corrosion products, dirt and dust particles, etc.), an uncontaminated sampling zone several hundred meters upstream was reached by a small rubber boat. Approximately 50 mL of surface water was collected, representing a water film of $\sim$100 μm. The sample was then transferred from the collecting screen to prewashed polyethylene bottles. After collection, the whole volume was immediately pressure filtered in a clean bench through 0.4-μm pore-size Nuclepore filters (diameter 2.5 mm) using a 50-mL syringe connected to a suitable filter holder. The loaded filters were flushed two times with 10 mL of deionized Milli-Q water and air-dried prior to deep-freeze storage in Petri dishes.

For LAMMA, the samples were prepared as follows: after collection, filtration, and washing over a Nuclepore filter, particulate matter was resuspended by ultrasonic agitation in a clean test tube containing Milli-Q water. Finally, a drop of suspension was deposited on a thin foil of Formvar supported by 300-mesh electron microscope (EM) grids. Prior to LAMMA, the presence of the major elements composing the particles was checked by EPXMA. However, as the grids could not be carbon coated, EPXMA

2909

Reprinted from ENVIRONMENTAL SCIENCE & TECHNOLOGY, Vol. 26, 1992

Characterization of Individual Particles in the North Sea Surface Microlayer and Underlying Seawater: Comparison with Atmospheric Particles

Chris Xhoffer,* Linda Wouters, and René Van Grieken

Department of Chemistry, University of Antwerp (UIA), B-2610 Antwerp-Wilrijk, Belgium

■ Five pairs of North Sea bulk waters and their corresponding surface microlayer samples were investigated for their particulate matter content and chemically analyzed and characterized by electron probe X-ray microanalysis and laser microprobe mass analysis. Multivariate techniques as hierarchical and nonhierarchical clustering in association with principal component analysis was performed on a data set containing more than 3000 individual particles. This classification procedure yielded eight different particle types. Differences in particle type abundances for the microlayer and bulk water were observed. They were apportioned to their most probable sources. The results were compared with atmospheric and riverine particle data. The domination of the major particle groups (aluminosilicates, Ca-rich aluminosilicates, $CaCO_3$, silicates, and organic particulate matter) suppresses the relative abundances of the metal-rich particles (Fe-rich, Ti-rich, and others). A conditioned classification was performed using selection criteria derived from riverine suspensions and atmospheric particulate North Sea data. Similar particle abundances were observed for both the multivariate and the conditional particle classification procedures.

Introduction

The sea surface microlayer is the channel of communication for material transfer between the atmosphere and the ocean. It is well-known that the surface microlayer of the ocean has unique chemical, physical, and biological properties quite different from those of the water underneath, most of which are still poorly understood (*1*). Important processes for material transport from the sea body to the microlayer comprise diffusion, convection, upwelling, and rising of bubbles (*2–4*). Dispersion of the microlayer material into the bulk water mainly occurs by sinking of particles and dissolution of water-soluble molecules. Processes like bubble bursting (*5*) and the generation of aerosols by wind action are responsible for the upward transport into the atmosphere. Additional material transfer into the microlayer results from wet and dry atmospheric deposition processes.

Many pollutants (chlorinated hydrocarbons, petroleum hydrocarbons) may be concentrated and stabilized in the microlayer. These can, just as organic acids, proteinaceous material, and other surface-active organic substances, provide complexing sites for many heavy metals (Pb, Fe, Ni, etc.) and thus be responsible for the concentration of these metals at the water surface. High concentrations of metals (*4*, *6–8*) and other trace substances are thought to be associated with particulate matter and surface-active organic material and foams (*9–11*).

Ideally, the microlayer thickness should only comprise the uppermost atomic water layer. Practically, it corresponds more or less to a thickness between 0.1 and 3 μm as defined by MacIntyre (*12*), which is near the extreme limit of nonturbulent kinetics with no wind. But much of the thickness of collection depends on the surface sampling device (*3*).

0013-936X/92/0926-2151$03.00/0

Selected article #12:

Characterization of individual particles in the North Sea surface microlayer and underlying seawater: comparison with atmospheric particles
C. Xhoffer, L. Wouters and R. Van Grieken
Environmental Science and Technology, 26 (1992), 2151-2162

Marine Pollution) (1989) The atmospheric input of trace species to the world ocean. Rep. Stud. GESAMP No. 38, World Meteorological Organization.

Guerzoni S., Lenaz R. and Quarantotto G. (1988) Field measurements at sea: atmospheric trace metals "end-members" in the Mediterranean. In *Field Measurements and Their Interpretation. Air Pollution Report* (edited by Beilke S., Morelli J. and Angeletti G.), Commission of the European Communities, 14, pp. 96–100.

Hangal S. and Willeke K. (1990) Overall efficiency of tubular inlets sampling at 0–90 degrees from horizontal aerosol flows. *Atmospheric Environment* **24**, 2379–2386.

Hohn R. (1973) On the climatology of the North Sea. In *North Sea Science* (edited by Goldberg E. D.), NATO North Sea Science Conference, Aviemore, Scotland, 15–20 November 1971.

Kretzschmar J. G. and Cosemans G. (1979) A five year study of some heavy metal levels in air at the Belgian North Sea coast. *Atmospheric Environment* **13**, 267–277.

Liu B. Y. H. and Lee K. W. (1976) Efficiency of membrane and Nuclepore filters for submicron aerosols. *Envir. Sci. Technol.* **10**, 345–350.

Maenhaut W. and Raemdonck H. (1984) Accurate calibration of a Si(Li) detector for PIXE analysis. *Nucl. Instr. Meth.* **B1**, 123–136.

Maenhaut W., Zoller W. H., Duce R. A. and Hoffman G. L. (1979) Concentration and size distribution of particulate trace elements in the South Polar atmosphere, *J. geophys. Res.* **84**, 2421–2431.

Maenhaut W., Selen A., Van Espen P., Van Grieken R. and Winchester J. W. (1981) PIXE analysis of aerosol samples collected over the Atlantic Ocean from a sailboat. *Nucl. Instr. Meth.* **181**, 399–405.

Maenhaut W., Cornille P., Pacyna J. M. and Vitols V. (1989) Trace element composition and origin of the atmospheric aerosol in the Norwegian Arctic. *Atmospheric Environment* **23**, 2551–2569.

Nriagu J. O. (1989) A global assessment of natural sources of atmospheric trace metals. *Nature* **338**, 47–48.

Nriagu J. O. and Pacyna J. M. (1988) Quantitative assessment of worldwide contamination of air, water and soils by trace metals. *Nature* **333**, 47–48.

Pacyna J. M. (1984) Estimation of the atmospheric emissions of trace elements from anthropogenic sources in Europe. *Atmospheric Environment* **18**, 41–50.

Pacyna J. M., Semb A. and Hanssen J. E. (1984) Emission and long-range transport of trace elements in Europe. *Tellus* **36B**, 163–178.

Peirson D. H., Cawse P. A. and Cambray R. S. (1974) Chemical uniformity of airborne particulate matter and a maritime effect. *Nature* **251**, 675–679.

Pena J. A. and Thomson D. W. (1977) Isokinetic sampler for continuous airborne aerosol measurements. *J. Air Pollut. Control Ass.* **27**, 337–340.

Rojas C. M. and Van Grieken R. E. (1992a) Electron microprobe characterization of individual aerosol particles collected by aircraft above the Southern Bight of the North Sea. *Atmospheric Environment* **26A**, 1231–1237.

Rojas C. M., Injuk J. and Van Grieken R. (1992b) Dry and wet deposition fluxes of Cd, Cu, Pb and Zn into the Southern Bight of the North Sea. *Atmospheric Environment* (submitted).

Schneider B. (1987) Source characterization for atmospheric trace metals over Kiel Bight. *Atmospheric Environment* **21**, 1275–1283.

Steiger M., Schulz M., Schwikowski M., Naumann K. and Dannecker W. (1989) Variability of aerosol size distributions above the North Sea and its implication to the dry deposition estimates. *J. Aerosol Sci.* **20**, 1229–1232.

Stoessel R. (1987). Untersuchugen zu Nass und Trockendeposition von Schwermetallen auf der Insel Pellworm. Ph.D. thesis, University of Hamburg, F.R.G.

Van Daalen J. (1991) Air quality and deposition of trace elements in the province of South-Holland. *Atmospheric Environment* **25A**, 691–698.

Van Jaarsveld J. A., Van Aalst R. M. and Onderdelinden D. (1986) Deposition of metals from the atmosphere into the North Sea: model calculations. Report RIVM 842015002, Bilthoven, the Netherlands.

Van Malderen H., Rojas C. and Van Grieken R. (1992) Characterization of individual giant aerosol particles above the North Sea. *Envir. Sci. Technol.* **26**, 750–756.

Wang J. (1985) *Stripping Analysis: Principles, Instrumentation and Applications*. VCH Publishers, Deerfield Beach, FL.

Wiersma G. B. and Davidson C. I. (1986) Trace metals in the atmosphere of remote areas. In *Toxic Metals in the Atmosphere* (edited by Nriagu J. O. and Davidson, C. I.), pp. 201–266. Wiley, New York.

Xhoffer C., Bernard P., Van Grieken R. and Van der Auwera L. (1991) Chemical characterization and source apportionment of individual aerosol particles over the North Sea and the English Channel using multivariate techniques. *Envir. Sci. Technol.* **25**, 1470–1478.

Yaaqub R. (1989) Ph.D. thesis, University of East Anglia, Norwich, U.K.

Table 7. Airborne concentrations (ng m^{-3}) for some marine and remote areas—literature values. Blanks mean no data reported

Reference	Location	Cd	Cu	Pb	Zn
GESAMP (1989)	western Mediterranean	1.9		39	26
	Baltic Sea	0.3		35	
	Bermuda	0.2		3	
	North Atlantic	0.13		10	
Guerzoni *et al.* (1989)	Adriatic Sea	0.02		3.8	5.9
	Ionian Sea	0.04		3.0	9.1
Maenhaut *et al.* (1979)	South Pole	<0.018	0.029	0.08	0.033
Maenhaut *et al.* (1989)	Norwegian Arctic	0.08	<0.9	3.0	3.9
Van Jaarsveld *et al.* (1986)	North Sea—model calculations	0.21	1.9	33	17
This work	southern North Sea	1.4	11	55	67

In Table 7 a comparison is made between the data from this study and results from some other marine regions and remote areas of the world. The table also includes data for the North Sea, that were calculated with the use of theoretical models. In comparison to the other sites the Southern Bight of the North Sea appears to exhibit relatively high atmospheric concentrations of the four heavy metals.

CONCLUSIONS

Using a well-equipped aircraft both total and size-fractionated atmospheric aerosol samples were collected under isokinetic conditions and with a fairly high spatial and temporal resolution. The samples were analysed for four elements, i.e. Cd, Cu, Zn and Pb, and from the results obtained the following conclusions can be inferred.

The atmospheric concentrations in the lower troposphere above the Southern Bight of the North Sea are highly variable as a function of both time and location. Rapid changes in the meteorological situation are reflected without delay in the atmospheric concentrations of the elements. Air masses with southern and southeastern origin yielded the highest concentrations for all elements. The lowest concentrations were found for the northern and northwestern wind directions. Above the temperature inversion layer, concentrations are much lower than under the temperature inversion layer. Maximum concentrations occur between 100 and 200 m. In general, the concentrations of Cd, Cu, Pb and Zn decrease with increasing altitude. However resuspension of seawater aerosols does not seem to be an important source process for the four elements above the North Sea. A good agreement between the Cu, Pb and Zn concentrations as obtained from ship-based and aircraft-based measurements indicates that ship sampling is valuable for the North Sea aerosol research.

The mass-size distributions for the four elements were bimodal with maxima in the submicrometre and in the supermicrometre size ranges. There was a clear difference between the distributions of the four elements. Pb was primary of submicrometre size whereas Zn was mostly of supermicrometre size. A significant fraction of each element was associated with particles larger than 16 μm. Such particles contribute significantly to the total deposition, in spite of their low numerical abundance and low heavy metal content (Van Malderen *et al.*, 1992).

Acknowledgements.—We are grateful to Rijkwaterstaat, the Netherlands, for financial support through projects NOMIVE*2 DGW-920 and DGW-217, and to the team of Geosens (Rotterdam) for the constructive collaboration. W. M. is indebted to the Belgian "Nationaal Fonds voor Wetenschappelijk Onderzoek" for research support.

REFERENCES

Baeyens W. and Dedeurwaerder H. (1991) Particulate trace metals above the Southern Bight of the North Sea—I. Analytical procedures and average aerosol concentrations. *Atmospheric Environment* **25A**, 293–304.

Berner A. and Lurzer C. (1980) Mass size distributions of traffic aerosols at Vienna. *J. phys. Chem.* **84**, 2079–2083.

Bouchertall F. (1989) Concentration and size distribution of atmospheric particulate matter at a coastal site on the Baltic Sea. *Atmospheric Environment* **23**, 2241–2248.

Cambray R. S., Jefferies D. F. and Topping G. (1975) An estimate of the input of atmospheric trace elements into the North Sea and the Clyde Sea (1972–1973). AERE report R7733.

Cawse P. A. (1976) A survey of atmospheric trace elements in the United Kingdom. AERE Harwell report R 7669, HMSO, London.

Dedeuwaerder H. (1988) Study of the dynamic transport and the fallout of some ecotoxicological heavy metals in the troposphere of the Southern Bight of the North Sea. Ph.D. thesis, Vrije Universiteit, Brussels, Belgium.

Diederen H. S. M. A. and Guicherit R. (1981) Bronherkenning door middel van concentratiemetingen van elementen in de buitenlucht. IMG-TNO report G 799.

Dierck I., Michaud D., Wouters L. and Van Grieken R. (1992) Laser microprobe mass analysis of individual aircraft-sampled North Sea aerosol particles. *Envir. Sci. Technol.* **26**, 802–808.

Flament P., Lepretre A., Noel S. and Auger Y. (1987) Aerosols cotiers dans le nord de la Manche. *Ocean. Acta* **10**, 49–61.

GESAMP-IMO/FAO/UNESCO/WMO/WHO/IAEA/UN/UNEP (Joint Group of Experts on the Scientific Aspects of

ten (north Holland), and an unmanned gas platform on the North Sea (position 53°5′N, 2°11′E). Between May 1972 and April 1977, Kretzschmar and Cosemans (1979) measured daily concentrations of heavy metals at a coastal location in Ostend, Belgium. They reported rather high values for all elements. Table 6 also includes measurements of Van Daalen (1991) for the Rijnmond, the largest industrial centre of the Netherlands. Although not strictly North Sea measurements, results of samples taken by Flament *et al.* (1987) at the east coast of the English Channel and the ones taken by Schneider (1987) from an artificial island in the Kiel Bight are also listed. Results from the West Hinder light-ship station located off the Belgian coast (51°23,5′N, 2°21,5′E) were reported by Baeyens and Dedeurwaerder (1991) and Dedeurwaerder (1988). Despite variations in collection procedures and the fact that the samples were taken at different sites and in different periods, the results show a fairly good consistency.

Table 4. Average percentage mass fractions for Cd, Cu, Pb and Zn in five different size ranges, and associated standard deviations, as deduced from impactor samples

Particle size (μm)	Cd	Cu	Pb	Zn
<1	39±24	40±21	63±25	31±28
1–4	21±18	29±21	10±8	21±13
4–8	12±9	8±7	9±5	22±14
8–16	19±19	6±3	11±5	15±8
>16	9±6	17±27	7±8	11±8

Table 5. Total airborne concentration C_t(ng m^{-3}) and mass median aerodynamic diameter MMD (μm) as obtained from 11 sampling campaigns with the Berner cascade impactor

Wind sector	Flight no.	Cd		Cu		Pb		Zn	
		C_t	MMD	C_t	MMD	C_t	MMD	C_t	MMD
Southwest-west	11	3.0	0.64	62	3.77	39	0.61	85	3.30
	12	2.0	0.78	41	0.69	96	0.77	100	0.83
Northwest-north	6	0.6	0.72	12	1.76	13	0.80	41	1.03
	5	1.2	0.45	19	0.12	36	1.68	66	1.17
	15	0.5	0.51	28	0.56	57	0.35	75	2.18
Northeast-east	17	0.6	0.59	17	1.18	18	0.18	60	1.62
	18	2.3	0.12	24	1.10	19	0.75	45	1.15
	19	0.5	0.70	22	1.20	58	0.17	46	0.62
Southeast-south	8	3.7	0.89	147	0.10	63	0.30	93	2.50
		0.8	0.62	84	1.44	67	0.12	48	2.63
Variable	9	0.5	1.0	23	0.16	40	0.22	51	4.29
Mean values	14	1.4	0.64	43	0.92	46	0.54	64	1.94

Table 6. Airborne concentrations (ng m^{-3}) for the North Sea—literature values. Blank means no data reported

Reference	Location	Cd	Cu	Pb	Zn
Peirson *et al.* (1974)	Leiston			160	144
	Lerwick			29	28
Cambray *et al.* (1975)	North Sea		5.8	75	62
	Leiston			100	93
	Gresham			100	81
	Collafirth			24	19
	Petten			74	58
	Lerwick			18	19
	gas platform			93	97
Cawse (1976)	Leiston	6.4	13	120	106
	Collafirth	4.0	15	20	15
Kretzschmar and Cosemans (1979)	Ostend	8	19	278	300
Van Daalen (1991)	Rijnmond	3	15	60	70
Diederen and Guicherit (1981)	Haamstede	2.5	22	180	130
	Schiermonnikoog	0.4	5	30	20
Flament *et al.* (1987)	East Channel	3	20	56	100
Schneider (1987)	Kiel Bight		40	53	57
Baeyens and Dedeurwaerder (1991)	West-Hinder	2.8	15	96	67
Yaaqub (1989)	southern North Sea	1.1		34	41
Stoessel (1987)	southern North Sea	0.7	3	39	41
Dedeurwaerder (1988)	West-Hinder	4	17	150	150
This work	southern North Sea	1.4	11	55	67

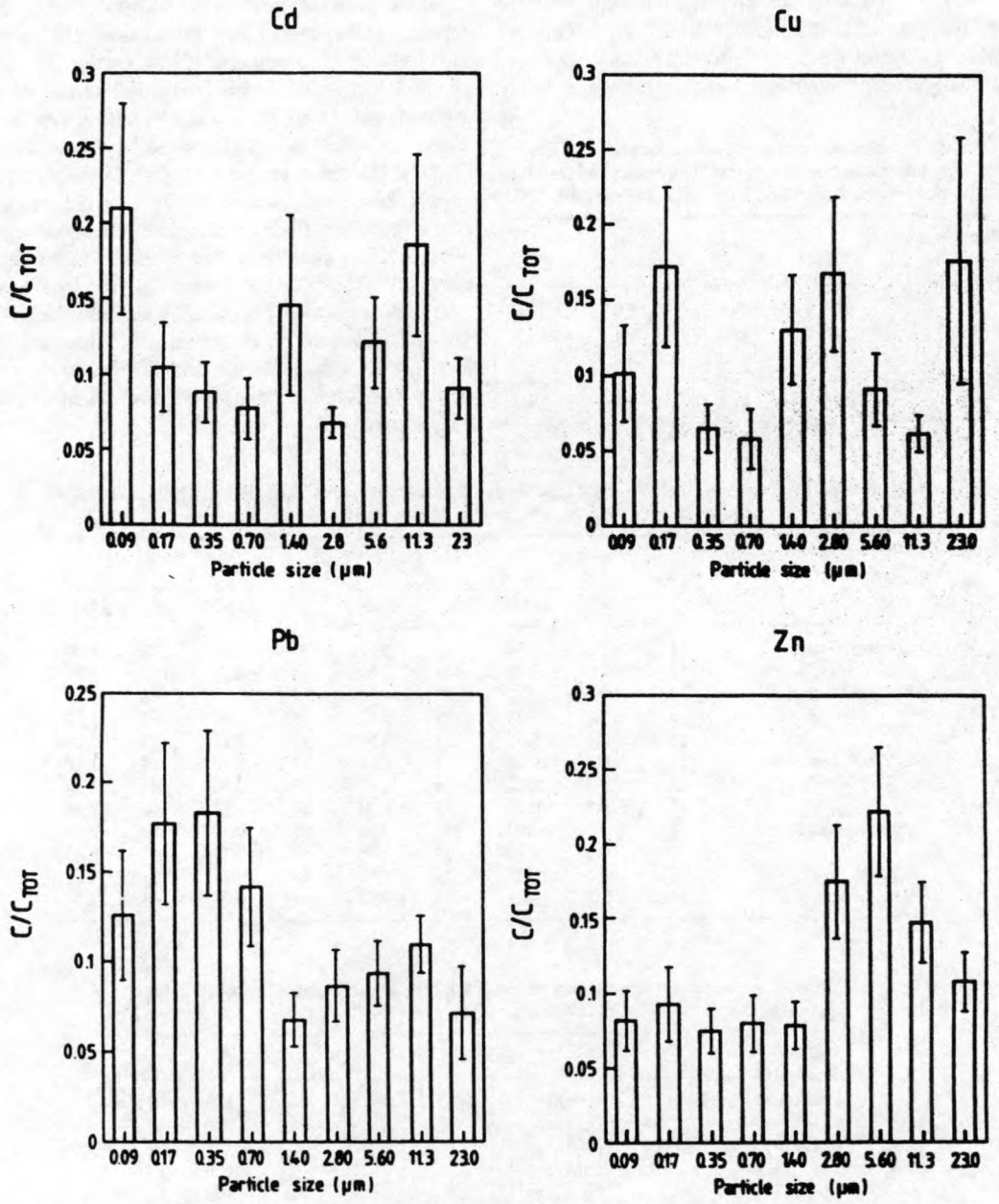

Fig. 6. Average elemental size distributions over all samples (error bars represent associated standard deviations).

in both cases. For Cu the average total concentration deduced from the impactor is 43 ng m^{-3} vs only 10 ng m^{-3} for the filter. The possibility of contamination was carefully examined. No likely explanation has been found. From the size distribution data mass median diameters (MMD values) were calculated using a computer routine (Van Espen, pers. commun.) which obtains a best-fit value of the straight line plotted on log-probability paper, as well as an interpolated or extrapolated value of the MMD of the aerosol. It appears that the MMDs for Cd, Cu, Pb and Zn are between 0.4 and 1.9 μm. This suggests that the aerosol size distribution reached a relatively stable state prior to arriving at the sampling area.

Table 6 gives an overview of literature values for the particulate Cd, Cu, Pb and Zn concentrations in the marine troposphere over the southern North Sea. The data sets cover a relatively long time period, over 16 years. Some of the reported results are from coastal measurements. Peirson *et al.* (1974), Cambray *et al.* (1975) and Cawse (1976) reported average monthly concentrations of several elements, sampled at six different locations: Leiston (Suffolk), Lerwick (Shetland), Gresham (Norfolk), Collafirth (Shetland), Pet-

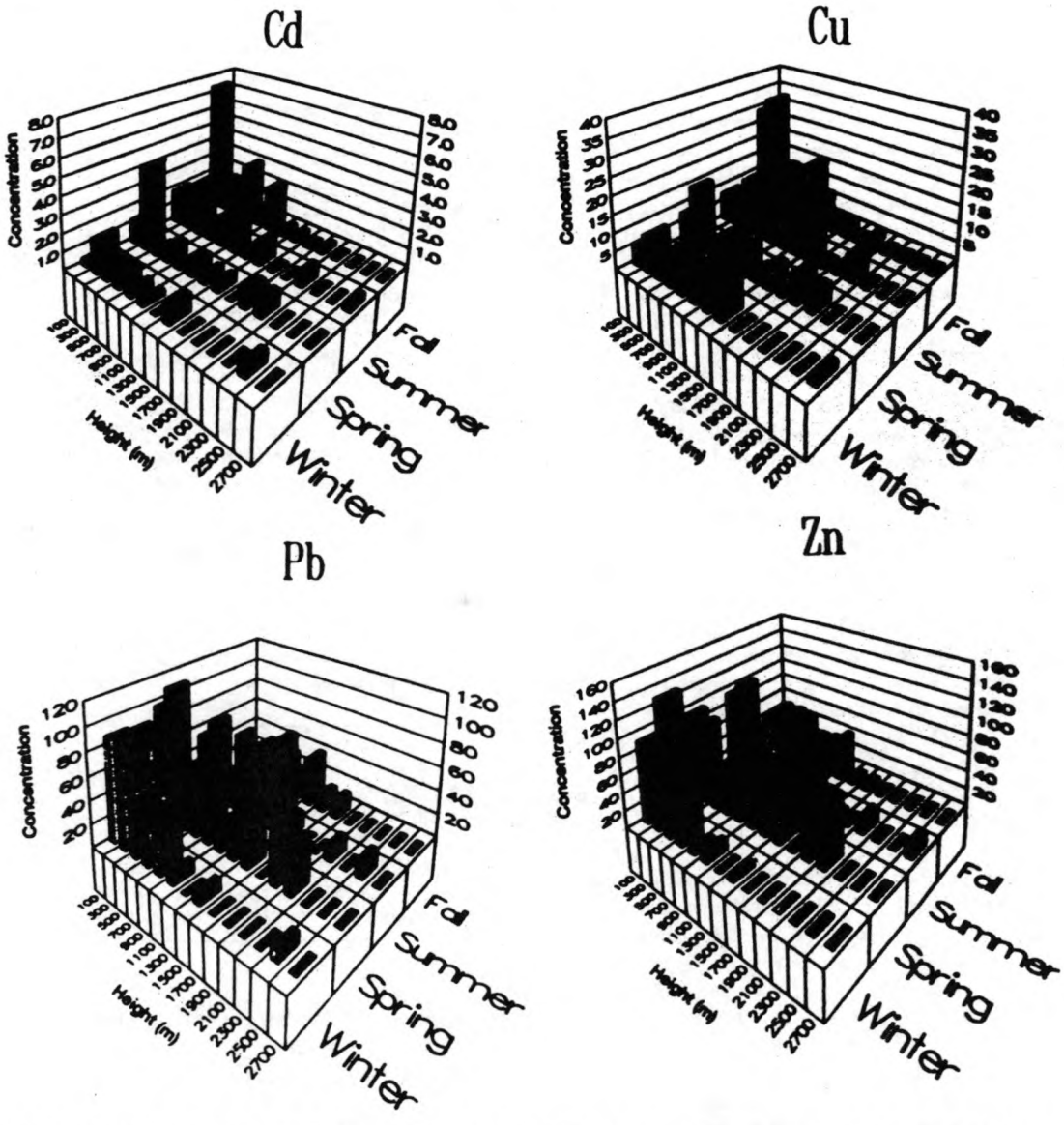

Fig. 5. Seasonal variation of Cd, Cu, Pb and Zn in aerosols collected over the Southern Bight of the North Sea during 1988–1989 (average values in ng m^{-3} over all flights).

east and southwest-west wind sector. The notable particle size fraction over 16 μm has some important implications for the calculation of deposition fluxes of trace metals to the sea surface (Steiger *et al.*, 1989). Fine particles were detected in high concentrations in all flights, except for northwest-north wind sector. The size distributions can be explained by the emission sources for the elements. Pb as a volatile element is emitted primarily from the combustion of leaded gasoline. Lesser quantities are emitted from the production of nonferrous metals, coal combustion, waste incineration and other industrial activities. The anthropogenic Pb emissions to the atmosphere are far more important than the natural sources. The Pb on the supermicrometre particles may be associated with soil dust, fly ash particle and the other coarse material. In some cases, this can reflect attachment of anthropogenically emitted submicrometre Pb to large particles, for example when Pb-containing particles deposit on soil that is subsequently resuspended. Successive deposition and resuspension processes may greatly alter the shape of the size distribution as material is transported through the environment. Cd, Cu and Zn are emitted mainly from stationary sources, including nonferrous metal production, waste incineration and fossil-fuel combustion. These processes produce a wide variety of particle sizes.

Except for Cu, the mean values for the total (summed) elemental concentrations from the impactor sampling system (Table 5) were found to agree reasonably well with concentrations from bulk filter samples (Table 1), although the sample sets were not identical

difference was quite small, presumably because of difference in height of the temperature inversion and mixing layer. The mixing layer may extend somewhat over the temperature inversion layer because of the temperature difference between emitted polluted air and the ambient air.

The vertical concentration profiles of the four metals of interest, under the temperature inversion layer, are shown in Fig. 4. A decreasing trend with increasing elevation is observed for all elements, but there are differences in the concentration profiles, which may be related to differences in sampled air masses (marine or continental). Samples collected at certain heights may have different origins and will yield different concentrations. Furthermore, the seasonal variations, winds and atmospheric stability, can also have an effect on the vertical distributions of the pollutants. Significant concentrations are less frequently observed at high altitudes in autumn and winter than during the other seasons (Fig. 5). This is because the temperature inversions occur usually at lower altitude during the cold seasons, typically between 700 and 1000 m. The Cd profile is quite uniform, but this is partially an artefact due to the significant number of samples with concentrations below the detection limit (around 0.3 ng m^{-3}). The Cd, Cu, Pb and Zn concentrations for 100–300 m (track 5) are notably higher than at higher elevations. Sampling tracks performed at very low altitudes (around 10 m) were intended to help in assessing particle resuspension and dry flux determinations. But the results indicate that the contribution of the sea to the trace metal levels at the lower altitudes should be relatively unimportant for the North Sea area under favourable atmospheric conditions.

Table 3 compares the aircraft-based measurements (PH-ECO) with ship-based measurements (R.V. *Belgica*) obtained in a previous study (Xhoffer *et al.*, 1991). Although the samples were collected in different periods (1984–1988 for the ship, and 1988–1989 for the aircraft), they were collected in the same area and with comparable sampling equipment. The good agreement between both data sets indicates that ship-based sampling is not biased by contamination from local pollution sources.

The results of the size-segregated measurements for Cd, Cu, Pb and Zn are presented in Fig. 6, where the average mass fraction and associated standard deviation are displayed as a function of the mass median diameter for every size fraction range. As indicated by the extent of the standard deviations, the size distributions of the individual samples exhibited considerable variability. However, it should be pointed out that an appreciable error is associated with the analytical data primarily because of the very small quantities of trace metals. A large fraction of the measurements, especially in the case of Cd and Cu, were below the analytical detection limit of the DPASV technique, and in such cases half of the detection limit was used. Also a possible error due to some non-isokinetic

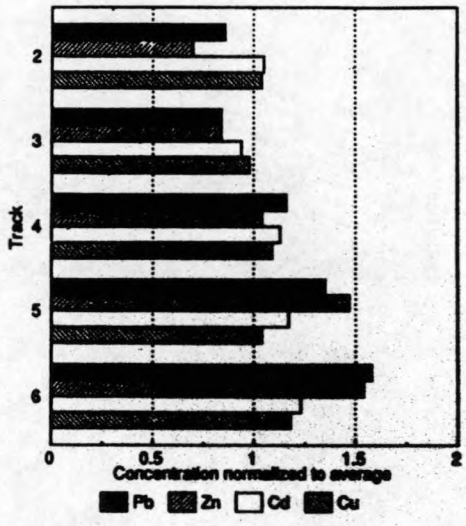

Fig. 4. Vertical concentration profiles for Cd, Cu, Pb and Zn.

Table 3. Aircraft-based vs ship-based measurements of atmospheric particulate trace elements. Concentrations in ng m^{-3}

	Cu	Pb	Zn
R.V. *Belgica*: Southern Bight of the North Sea (Xhoffer *et al.*, 1991)	9.2	77	110
PH-ECO: Southern Bight of the North Sea—sea level (this work)	9.8	73	83

collection of the large particles cannot be fully excluded. Furthermore, processes like bounce-off of particles from the front edge of the inlet, transmission loss in the inlet due to gravitational settling and direct wall impaction may change the aerosol concentration and size distribution somewhat during sampling (Hangal and Willeke, 1990). But, despite the large uncertainties, the data show reasonable patterns. All size distributions are essentially bimodal with one maximum between 0.09 and 0.7 μm and a second maximum in the coarse particle range. Similar bimodal spectra have also been reported for total mass size distribution of atmospheric particles (Steiger *et al.*, 1989; Bouchertall, 1989).

From Fig. 6 it appears that there are clearly important differences in the size distributions of the four elements. This is also demonstrated by Table 4 which presents percentage mass fractions for five size ranges. Pb is primarily of submicrometre size, found mostly in the smallest size range. Cd, Cu and particularly Zn are associated mostly with particles larger than 1 μm, although significant amounts of submicrometre Cd, Cu and Zn are also detected. The highest concentrations of coarse particles were found for the southeast-

Table 1. Concentrations of Cd, Cu, Pb and Zn, in aerosols above the southern North Sea, as a function of wind direction, collected during 18 flights in 1988–1990. Flights 1 and 10 were test flights, flight 16 engine failed, flights 20 and 23 were performed only at low altitudes (average values in ng m^{-3} ± standard deviation; n = number of data)

		Cd	Cu	Pb	Zn
Sector southwest-west					
Flight 2	$n=6$	2.8±1.1	12±4	40±10	34±10
Flight 3	$n=6$	0.8±0.7	10±4	54±30	54±31
Flight 11	$n=6$	0.5±0.3	4±5	21±17	21±21
Flight 12	$n=6$	0.4±0.2	7±8	39±34	31±25
Flight 22	$n=6$	3.7±2.6	50±59	38±25	55±39
Sector northwest-north					
Flight 6	$n=6$	0.4±0.4	3±3	7±2	3±1
Sector northeast-east					
Flight 5	$n=6$	2.6±2.0	3±0	53±25	89±55
Flight 15	$n=6$	1.4±1.8	2±1	38±23	65±45
Flight 17	$n=6$	0.9±0.6	7±5	68±33	87±36
Flight 18	$n=6$	0.4±0.1	8±6	49±25	61±20
Flight 19	$n=6$	0.3±0.2	6±8	30±17	41±28
Sector southeast-south					
Flight 7	$n=6$	0.9±0.8	10±2	113±21	157±38
Flight 8	$n=6$	0.3±0.1	6±2	98±24	132±47
Flight 13	$n=6$	7.9±5.5	21±24	148±78	143±74
Sector variable					
Flight 4	$n=6$	0.4±0.4	5±3	53±26	88±55
Flight 9	$n=6$	0.4±0.1	7±6	33±41	43±52
Flight 14	$n=6$	2.1±2.1	7±11	68±18	56±13
Flight 21	$n=6$	0.5±0.4	15±17	50±37	60±42
Averages					
Southwest-west	$n=30$	1.4±1.7	16±30	38±25	39±29
Northwest-north	$n=6$	0.4±0.4	3±3	7±2	3±1
Northeast-east	$n=30$	0.9±1.2	5±5	45±27	64±38
Southeast-south	$n=18$	3.1±4.7	12±15	120±51	144±53
Variable	$n=24$	0.9±1.2	9±11	51±32	62±44
All sectors	$n=108$	1.3±2.3	10±18	55±44	67±54
weighted for wind sector freq.		1.4±1.0	10±10	50±14	58±16
range		0.3–12	3–170	5–247	3–220

made of the wind direction distribution data, as reported by Hohn (1973), for the southern part of the North Sea. As expected, the highest concentrations for all elements are found for the southeast-south wind sector. The true trace metal concentrations for the northwest-north wind sector may be even lower than reported, because the measured levels were often close to or even less than the analytical detection limit. In the latter cases, half of the detection limit was taken as concentration value. It is obvious that even for the flights classified in the same wind sector, important differences in air-mass history may exist, so that the heavy metal concentrations may vary quite significantly within each wind sector. Small changes in the backward air-mass trajectories may indeed have a large influence on the atmospheric concentration, since some of the more important emission sources such as industrial areas are concentrated geographically. Furthermore, it should be stressed that other meteorological parameters such as the atmospheric stability and the height of the mixing layer have a large influence on the trace metal concentrations in the air.

Table 2. Average concentrations (ng m^{-3}) of different elements in aerosols above the temperature inversion layer (TIL) compared with the data for just under the inversion layer during seven flights in 1988–1990 over the southern North Sea (average value ± standard deviation)

Element	Above TIL	Under TIL
S	1960±340	4900±845
K	135±29	344±66
Ca	108±24	285±76
Fe	114±26	275±45
Cu	5±2	9±3
Zn	28±8	63±13
Cd	0.4±0.3	1.1±0.8
Pb	27±8	50±10

For the tracks that were flown just above the temperature inversion layer mean concentrations were calculated and compared with the data for just under the inversion layer (Table 2). The concentrations above the temperature inversion layer are clearly lower than those underneath; around a factor of 2.3 for Cd, Cu, Pb and Zn. For some flights, however, the

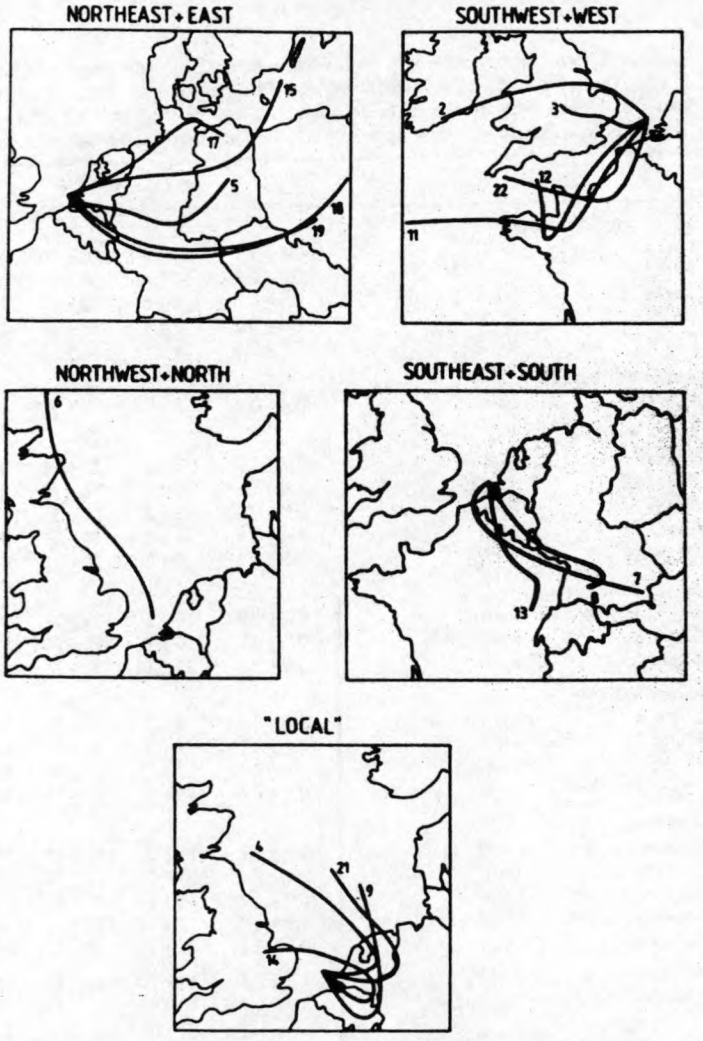

Fig. 2. The 1000 hPa air-mass trajectories for air masses arriving at the sampling site originating from five different wind sectors. "Local" refers to variable wind sector. The figures indicate flight number.

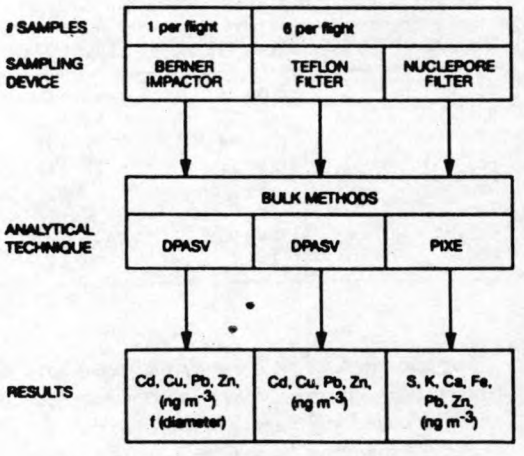

Fig. 3. Overview of the sampling and analysis.

by the north Atlantic Ocean and the English Channel. Only one flight (no. 6) was classified in the northwest-north sector, where any continental influence can be excluded. The results from this flight can be considered as representative for the North Sea atmosphere background. Results for the northeast-east sector are related to emissions in Belgium, the Netherlands, the central and northern part of Germany, eastern European countries, the Baltic Sea and Scandinavian countries. Heavy metal concentrations for air masses originating from the southeast-south sector result from emissions in Belgium, the northern part of France and the southern part of Germany. Finally, aerosols collected during flight nos 4, 9, 14 and 21 were obtained under low wind speed and variable wind direction conditions. Table 1 also gives normal average and wind-direction weighted average concentrations over all sectors. In calculating the latter use was

speed in the narrow section will be higher than the true air speed of the aircraft and thus the pressure at that section will be lower than the ambient pressure. At the narrow section the back-end of the aerosol sampling lines were placed. Because of the Venturi-effect, air is drawn from the exhaust and the Venturi operates as a pump. The use of four Venturis placed on the wings results in a slightly higher fuel consumption if the same speed is to be held, which is necessary for isokinetic sampling conditions. Since the aircraft is used for sampling at different heights and thus under different atmospheric pressures, standard flow rate devices cannot be used because their readings depend on the ambient pressure. For the flow rate measurements of the Nuclepore and the Teflon filter a Brooks model 5811N thermal mass flow-meter was used in combination with a model 5851 pressure controller. In the range between 0 and 100 ℓ min^{-1}, an accuracy of 5% can be achieved with this apparatus.

In our experimental set-up, a 47 mm diameter "aerosol-grade" Nuclepore filter with 0.4 μm pore size was used. The operational flow rate of approximately 50 ℓ min^{-1} results in a face velocity of 60–70 cm s^{-1} and a filter pressure drop of 20 cm Hg. The collection efficiency is estimated to be above 90% for particles with a diameter >0.2 μm. Besides the Nuclepore filter, a 47 mm diameter Teflon filter (Millipore, type FA) with 1 μm pore size was used. This filter has a collection efficiency above 99.99% for particles between 0.03 and 1 μm (Liu and Lee, 1976). For size-differentiated aerosol sampling, a nine-stage low-pressure Berner LPI/0.06/30 cascade impactor with equivalent aerodynamic cut-off diameters of 0.06, 0.125, 0.25, 0.5, 1, 2, 4, 8 and 16 μm was used (Berner and Lurzer, 1980). The impaction films consisted of 10 μm thick uncoated aluminium foils which are held in place by a spacer. A flow rate of 30 ℓ min^{-1} and a pressure of 150 hPa were maintained through the use of a high-volume pump, which was powered by the 24 V generator of the aircraft.

The ambient temperature was measured with a PT-100 thermocouple (Rosemount, model 102 E). Temperatures between −20 and +40°C can be measured with an accuracy of 0.25°C and a maximum resolution of 0.01°C. The dew point is measured with a Meteolabar A.G. model PT3-S device that has a measuring range from −30 to +40°C with a resolution of 0.1°C. Air velocity and height are measured with two pressure meters, PDCR 10/2L and PDCR 10/T, for measurements between 0 and 1050 hPa, and between 0 and 200 hPa, respectively. The use of a Doppler 91 sensor unit with a RNS 252 Navigation compass (RACALL) allows determination of the position with an accuracy of 0.1 nautical mile and measurement of the wind speed with an accuracy of 1 m s^{-1}.

All sampling flights were performed in the same way, in dry periods with few clouds (maximum 3/8), mainly under the temperature inversion layer (see Fig. 1). The wind speed over all sampling campaigns was between 2 and 13 m s^{-1}. Before take-off at Rotterdam and during transit to the Goeree platform (position 51°55'N, 03°40'E) all equipment was tested. One upward spiral track was performed at Goeree, during which sulphur dioxide and ozone concentrations, as well as temperature and dew point were monitored in order to localize the temperature inversion height which is taken as the boundary of the mixing layer. Then six horizontal tracks (25 min, 100 km) were flown at different heights equally spaced under the temperature inversion layer. The last track was performed at minimum altitude, 10–15 m above the sea level. Filter samples were collected on each truck while impactor samples were collected between the start of track 1 and the end of track 5 with a total sampling volume of 4.5 m^3. In some flights, 1 or 2 tracks were flown just above the inversion height, to measure concentration differences. All tracks were flown parallel to the wind direction in order to sample an air mass of which the history can be traced back as a well-defined back trajectory. For each flight, four 36-h back trajectories were calculated for four different levels (1000, 900, 850 and 700 hPa) and for two sampling times, at the beginning and at the end of sampling (Fig. 2).

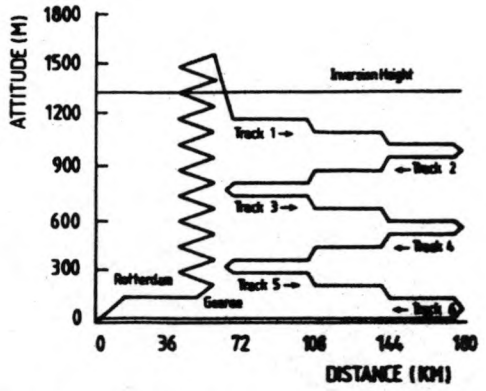

Fig. 1. Flight scheme for an assumed temperature inversion height of 1300 cm.

Analysis

The Teflon filters and cascade impactor samples were analysed with differential pulse anodic stripping voltammetry (DPASV), whereas the Nuclepore filters were analysed with proton-induced X-ray emission (PIXE). The voltammetric measurements were done by Model 264 (EG&G Princeton Applied Research, Princeton, NJ), connected to a Model 303 static mercury drop electrode unit (Wang, 1985). The aerosol samples were extracted for the analysis using a single 60 min ultrasonic extraction in 10 ml ultrapure water, prepared by a Milipore Milli-Q purification unit, and acidified to pH 1 with 70 μl of Merck Suprapure concentrated nitric acid. For the determination of Zn, the solution was neutralized to pH 4 by adding 1500 μl of 0.1 M NaAc. Quantification was done by standard addition using two spikes for each element. Calculation of the concentration was based on measurement of the peak heights. The PIXE analysis of the Nuclepore filter samples was carried out with the PIXE set-up of the University of Ghent (Maenhaut *et al.*, 1981). The calibration factors for this set-up were determined as described by Maenhaut and Raemdonck (1984). No matrix corrections were carried out in view of the light sample load. Analytical precision was typically about ±10% for DPASV, and ±5% for PIXE analysis. An overview of the sampling and analysis scheme is presented in Fig. 3.

RESULTS AND DISCUSSION

As a result of the geographical variability of the anthropogenic emission sources around the Southern Bight of the North Sea, different wind directions will result in different concentrations of air pollutants above the southern North Sea. Therefore, our results were classified into five wind sectors according to the air-mass history as inferred from the back-trajectories.

Table 1 lists the average Cd, Cu, Pb and Zn concentrations averaged over all six sampling tracks for the different wind sectors. The large standard deviations indicate that there is a significant variability in the atmospheric concentrations. Samples collected for the southwest-west sector are influenced by emissions from the United Kingdom and the northwestern part of France, but to some extent also

Atmospheric Environment Vol. 26A, No. 14, pp. 2499–2508, 1992.
Printed in Great Britain.

0004-6981/92 $5.00 + 0.00

ATMOSPHERIC CONCENTRATIONS AND SIZE DISTRIBUTIONS OF AIRCRAFT-SAMPLED Cd, Cu, Pb AND Zn OVER THE SOUTHERN BIGHT OF THE NORTH SEA

J. INJUK,* PH. OTTEN,* R. LAANE,† W. MAENHAUT‡ and R. VAN GRIEKEN*§

* Department of Chemistry, University of Antwerp (UIA), B-2610 Wilrijk-Antwerpen, Belgium, † Tidal Waters Division, Rijkswaterstaat, P.O. Box 20907, NL-2500 EX, The Hague, the Netherlands and ‡ Institute for Nuclear Sciences, Ghent State University, Proeftuinstraat 86, B-9000 Gent, Belgium

(*First received* 3 *February* 1992 *and in final form* 26 *March* 1992)

Abstract—In an effort to assess the atmospheric input of heavy metals to the Southern Bight of the North Sea, aircraft-based aerosol samplings in the lower troposphere were performed between September 1988 and October 1989. Total atmospheric particulate and size-differentiated concentrations of Cd, Cu, Pb and Zn were determined as a function of altitude, wind direction, air-mass history and season. The obtained data are compared with results of ship-based measurements carried out previously and with literature values of Cu, Pb and Zn, for the marine troposphere of the southern North Sea. The results point out the high variability of the concentrations with the meteorological conditions, as well as with time and location. The experimentally found particle size distributions are bimodal with a significant difference in fractions of small and large particles. These large aerosol particles have a direct and essential impact on the air-to-sea transfer of anthropogenic trace metals, in spite of their low numerical abundance and relatively low heavy metal content.

Key word index: Trace metals, aerosols, North Sea, concentrations, size distributions.

INTRODUCTION

For many years, research on pollution of the North Sea marine environment has focused on the most obvious inputs: those borne by rivers and direct discharges of wastes. In the work of Cambray *et al.* (1975), a first indication can be found that the atmospheric input of trace metals to the North Sea might also be a significant input route. Since then, many detailed studies were carried out in order to quantify man-made emissions (Pacyna, 1984; Pacyna *et al.*, 1984; Nriagu and Pacyna, 1988), or to estimate natural inputs into the atmosphere (Wiersma and Davidson, 1986; Nriagu, 1989).

In this work, attention is focused on atmospheric concentrations and size distributions of the toxic heavy metals Cd, Cu, Pb and Zn, sampled at different altitudes and under varying atmospheric conditions over the Southern Bight of the North Sea. The present study is part of an investigation concerning the atmospheric deposition of heavy metals into the North Sea (Rojas *et al.*, 1992b). In addition to bulk analysis, single particle analyses were carried out. About 50,000 individual aerosol particles were analysed by electron-probe X-ray microanalysis and the different aerosol sources were identified by classical cluster analysis of the data (Rojas *et al.*, 1992a) while special attention was paid to the size distribution, composition and sources of the giant aerosols (Van Malderen *et al.*, 1991). Also laser microprobe mass analysis was applied to study inorganic compounds and trace element composition at the single particle level (Dierck *et al.*, 1992).

EXPERIMENTAL

Sampling

The aircraft used is a twin-engine Piper Chieftain (PA-31-350, call-sign PH-ECO) of Geosens B. V., Rotterdam, the Netherlands. It has been modified in order to perform a large variety of atmospheric research tasks. When fully equipped and using a crew of four persons, the flight time is limited to 4½ h. Considering the transfer time between the Rotterdam airport and the North Sea, a useful sampling time of 3½ h is available during each flight.

The collection of aerosol samples was performed in a period spanning from September 1988 to October 1989. The sampling device consisted of the Pennsylvania State University (PSU) isokinetic intake (Pena and Thomson, 1977), mounted on the roof of the aircraft in such way that the intake is located outside the boundary layer of the aircraft and that no particulate or gaseous matter coming from the exhaust of the two engines can be sampled.

In the PH-ECO aircraft a quadruple Venturi-effect based pump-system is installed that requires no electric power at all and is capable of drawing approximately 50 ℓ min^{-1} of air through two parallel filters. The so-called "Venturi pump" consists of an inner and outer tube. The inner tube narrows from 26 to 16 mm diameter after 1 cm. In this way, the air

§ To whom correspondence should be addressed.

Selected article #11:

Atmospheric concentrations and size distributions of aircraft-sampled Cd, Cu, Pb and Zn over the Southern Bight of the North Sea

J. Injuk, Ph. Otten, R. Laane, W. Maenhaut and R. Van Grieken

Atmospheric Environment, 26A (1992), 2499-2508

	Cd	Cu	Pb	Zn
Rivieren	23	30	14	28
Direkte lozingen	9	7	3	6
Dumping op zee	13	39	43	44
Atmosfeer	**55**	**24**	**40**	**22**

Tabel 6 : Procentuele bijdrage van de verschillende toevoerwegen voor Cd, Cu, Pb en Zn naar de Zuidelijke Bocht van de Noordzee.

zuur. Vliegasdeeltjes (met Al, Si, S, K, Ca en Fe), afkomstig van verbrandings-processen, maken tot 70% van het totaal uit bij westelijke wind. $CaSO_4$ wordt in bijna alle monsters teruggevonden.
Natuurlijk $CaSO_4$ onstaat uit fraktionele kristallizatie van zeezoutdeeltjes.
$CaSO_4$ kan ook ontstaan uit reaktie van eolisch $CaCO_3$ en zwavelzuur. Waarschijnlijk wordt het echter hoofdzakelijk gevormd bij verbrandingsprocessen [9]. Inderdaad, alhoewel in België in geen enkele klassieke elektriciteitscentrale aan rookgasontzwaveling wordt gedaan, zijn in Nederland enkele en in Duitsland talrijke centrales uitgerust met FGD-eenheden ("flue gas desulphurization"). Ongeveer 90% daarvan genereren gips doordat de ontzwaveling met kalk of kalksteen gebeurt. In Duitsland komt dit overeen met 400.000 ton gips per jaar; men kan zich voorstellen dat een fraktie daarvan in de atmosfeer wordt verspreid.
Sferische Fe-rijke deeltjes worden in de meeste monsters teruggevonden. Deze onstaan eveneens bij verbrandingsprocessen. Sommige monsters bevatten echter ook Fe-Zn en Fe-S verbindingen. Zwavelrijke deeltjes zijn frekwent aanwezig, soms tot 70% van het totaal. Een deel van deze deeltjes wordt gekenmerkt door de aanwezigheid van een belangrijke hoeveelheid organisch materiaal. Op basis van de individuele deeltjesanalysen met EPXMA kunnen de verschillende monsters onderverdeeld worden in drie typen : monsters met weinig of geen kontinentale invloed (samenstelling : 74% zeezout, 13% getransformeerd zeezout, 13% andere deeltjes), monsters met duidelijk kontinentale invloed (samenstelling : 12% zeezout, 12% getransformeerd zeezout, 34% vliegas, 20% zwavelrijke deeltjes, 22% andere deeltjes) en monsters met uitsluitend kontinentale invloeden (samenstelling : 36% zwavelrijke deeltjes, 20% vliegas, 20% $CaSO_4$, 8% Fe-rijke deeltjes, 16% andere deeltjes).
Met behulp van LAMMA-metingen op 12.000 deeltjes werd aangetoond dat getransformeerde zeezoutdeeltjes bestaan uit een centrale NaCl kern omgeven door $NaNO_3$ en Na_2SO_4. Dit kan zowel het resultaat zijn van gefraktioneerde kristallizatie als van een heterogene reaktie tussen zeezout en zure gassen. Verder werd aangetoond dat bij oostelijke wind tot 30% van de deeltjes voor 90% bestaan uit ammoniumzouten. Roetdeeltjes met sporen Ni, V, Fe en Pb werden vooral teruggevonden in de kleinere frakties (0,25 μm).

Algemeen kan gesteld worden dat de LAMMA-techniek duidelijk naar voor bracht dat het Noordzee aerosol in veel gevallen bestaat uit een complex geheel van verschillende hoofdkomponenten gekombineerd met verscheidene sporenelementen. Deze techniek wordt hoofdzakelijk gebruikt om additionele informatie te verkrijgen over de verschillende deeltjestypen.

Konklusies

De koncentraties aan zware metalen in de atmosfeer boven de Noordzee blijken aanzienlijk verhoogd in vergelijking met minder gepollueerde mariene gebieden. Boven de Zuidelijke Bocht van de Noordzee brengt vooral de zuid-zuidoosten wind vervuilde luchtmassa's aan, o.a. uit België. Vooral worden veel vliegasdeeltjes waargenomen. Atmosferische depositie van zware metalen is een relatief belangrijke toevoerweg van polluenten naar de Noordzee, ook in vergelijking met meer evidente routes zoals rivieren en dumping op zee. Voor Cd en Pb voert de lucht niet minder dan ca. 50 % van de totale hoeveelheid aan. Zuivering van de rivieren die uitmonden in de Noordzee zal dus niet volstaan als maatregel om de belasting van de Noordzee met zware metalen aanzienlijk te verminderen.

Referenties

1. Cambray, R.S., Jefferies, D.F., Topping,G., An Estimate of the Input of Atmospheric Trace Elements into the North Sea and Clyde Sea (1972-73), AERE Report R 7733, 30pp, 1975.
2. Dedeurwaerder, H.L., Study of the Dynamic Transport and of the Fall-out of some Ecotoxicological Heavy Metals in the Troposphere of the Southern Bight of the North Sea. Ph.D. Dissertation, Free University of Brussels (VUB), Belgium 1988.
3. Stoessel, R., Untersuchungen zu Nass und Trockendeposition von Schwermetallen auf der Insel Pellworm. Ph.D. Thesis, University of Hamburg, F.R.Germany, 1987.
4. Yaaqub, R., Ph.D. Thesis, University of East Anglia, Norwich, U.K., 1989.
5. Slinn, S.A. Slinn, W.G.N., Atmos. Environ. 14, 1013, 1980.
6. Slinn, W.G.N., Air-to-sea Transfer of Particles. In : Air-Sea Exchange of Gases and Particles. Eds. Liss, P.S., and Slinn, W.G.N., D. Reidel Publishing Co. Dordrecht, The Netherlands, 299-405, 1983.
7. GESAMP-IMO/FAO/UNESCO/WMO/ WHO/IAEA/UN/UNEP Joint Group of Experts on the Scientific Aspects of Marine Pollution, Interchange of a Pollutants between the Atmosphere and the Oceans. Reports and Studies, GESAMP (23), 1985.
8. Van Aalst R.M., Van Ardenne R.A.M., De Kreuk J.F. and Lems Th., Pollution of the North Sea from the atmosphere. TNO rapport CL/82/152, 1983.
9. Storms H., Quantification of automated Electron Microprobe X-ray Analysis and application in aerosol research, Doctoraatsthesis, Universitaire Instelling Antwerpen, België, 1988.

■

Depositiefluxen van zware metalen in de zuidelijke bocht van de Noordzee

De meest evidente manier om atmosferische depositiefluxen naar het zeeoppervlak te kwantificeren zou in principe direkte depositiemetingen impliceren. Totnogtoe zijn echter zulke direkte metingen weinig suksesvol gebleken. Men kan natuurlijk ook fluxen berekenen door de koncentraties te vermenigvuldigen met een kinetische parameter, die de massatransfer weergeeft zowel bij droge als natte depositie.
Voor de berekening van de droge depositie dient men vooreerst te beschikken over deeltjesgrootte-distributie, omdat elke deeltjesgrootte-klasse natuurlijk een verschillende valsnelheid heeft. In het model van Slinn and Slinn [5] houdt men rekening met o.a. luchtstabiliteit en turbulente diffusie, en met het hydrofobe dan wel hydrofiele karakter van de deeltjes (in het laatste geval zullen de deeltjes kunnen groeien en uiteindelijk sneller uitvallen). Voor Cd, Cu, Pb en Zn waren uit vliegtuigmetingen deeltjesgrootte-distributies beschikbaar voor de verschillende windsektoren. De depositiesnelheden, die daaruit werden berekend, varieerden van 0,25 +/-0,03 cm s^{-1} voor Pb tot 0,48 +/- 0,17 cm s^{-1} voor Cu. De resulterende droge fluxen en hun onzekerheden zijn opgenomen in *Tabel 4.* Natte depositie omvat "rainout" (de opname van aerosoldeeltjes in wolkendruppels) en "washout" (het meeslepen van aerosolen door vallende regendruppels of sneeuwvlokken). Bij de berekening van natte depositie werd het model van Slinn [6] gebruikt en werd een neerslagintensiteit van 600 mm per jaar boven de Noordzee aanvaard. De resultaten voor natte en totale depositie zijn eveneens in *Tabel 4* weergegeven. Het blijkt dat de natte depositie ongeveer een faktor 2 belangrijker is, maar bvb. voor Cd blijft de onzekerheid erg groot. Ook op het eerste gezicht al lijken atmosferische depositiefluxen voor zware metalen in de buurt van één tot enkele tientallen kg km^{-2} $jaar^{-1}$ niet verwaarloosbaar.

	Cd	Cu	Pb	Zn
Droge depositie	0,16 ± 0,11	1,6 ± 0,7	5,1 ± 1,2	7,9 ± 2,0
Natte depositie	0,43	3,5	8,7	19,8
Totale depositie	0,59	5,1	13,8	27,7

Tabel 4 : Droge, natte en totale depositiefluxen (in kg. km^{-2} $jaar^{-1}$) voor Cd, Cu, Pb en Zn over de Zuidelijke Bocht van de Noordzee in 1988-90.

Totale depositie	Cd	Cu	Pb	Zn
New York Bight	0,3	-*	39	14
Baltische Zee	0,15	1,4	6,7	5,5
W. Middellandse Zee	0,55	2,1	20	22
Z. Atlantische Oceaan	0,09	2,20	6,6	7,5
Bermuda	0,06	0,65	10,9	1,25
N. Atlantische Oceaan	0,05	-	3,1	-
Trop. N. Atlantische Oceaan	0,05	0,20	3,1	1,3
Trop. N. Stille Oceaan	0,003	0,09	0,07	0,67
Noordzee	0,4	1,35	15	7
Zuidelijke Bocht van de Noordzee *(dit werk)*	0,59	5,1	13,8	27,7

* = niet gemeten

Tabel 5 : Totale depositie van zware metalen in de Noordzee (kg.km^{-2}.$jaar^{-1}$). Vergelijking met andere mariene gebieden.

De Noordzee versus andere mariene gebieden

In *Tabel 5* worden onze depositiewaarden vergeleken met de gemiddelden voor andere mariene gebieden, zoals die werden samengevat door GESAMP [7]. Voor de Noordzee zijn de resultaten een faktor 100 hoger dan deze van de meest afgelegen gebieden, zoals de tropische Stille Oceaan, en dit is uiteraard duidelijk het gevolg van kontinentale invloeden. De situatie boven de Noordzee kan het best vergeleken worden met deze boven de Middellandse Zee of de Baltische Zee.

Relatieve bijdrage van de atmosfeer tot de Noordzee-vervulling

De relatieve fraktie van zware metalen die de Zuidelijke Bocht van de Noordzee bereikt via de atmosfeer werd berekend aan de hand van de gegevens van Van Aalst et al. [8] voor rivieren, direkte lozingen en dumping, en is opgenomen in *Tabel 6.* Deze fraktie gaat van 22 tot 55 %, en is zonder meer belangrijk. Bovendien dient men er rekening mee te houden dat de hoeveelheden afkomstig van afval-dumping op zee door de recente EG-reglementering thans fors gereduceerd worden, zodat het relatieve aandeel van de atmosfeer nog aanzienlijker zal worden.

Individuele deeltjesanalyse voor bronherkenning

Met behulp van EPXMA werden bijna 50.000 deeltjes geïdentificeerd en geklasseerd in verschillende deeltjestypen, geassocieerd met verschillende natuurlijke en pollutiebronnen. Naast deeltjes waarin enkel Na en Cl voorkomt (zeezout), worden er ook deeltjes gevonden met Na, Cl en S als belangrijkste elementen. Deze zijn het resultaat van een chemische transformatie waarin HCl wordt vrijgesteld uit zeezoutdeeltjes door reaktie met zwavel-

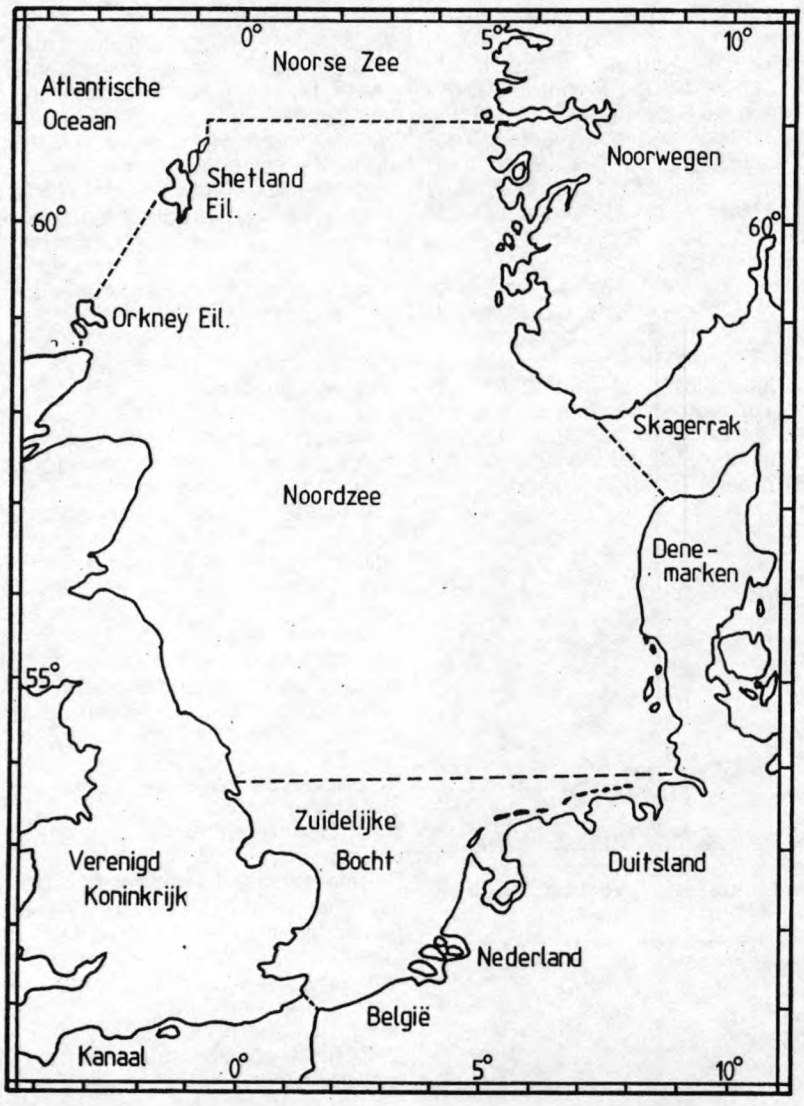

Fig. 1 : Situatieplan van de Noordzee.

de Zuidelijke Bocht van de Noordzee een faktor 5 tot 30 hoger zijn dan deze achtergrondkoncentraties.
Met behulp van faktoranalyse kan men de dataset van alle elementen (ook niet-metalen) reduceren tot 4 onafhankelijke faktoren die 90% van de totale variantie verklaren. Deze faktoren kunnen geassocieerd worden met verschillende bronnen van polluenten. Een eerste faktor bevat Cl en wordt geïdentificeerd als zeezout. De tweede faktor met Ni en V is typisch voor olieresidu (verbranding van fossiele brandstoffen). De derde faktor bevat Al, Si, S, Ca, K en Fe. Deze elementen zijn typerend voor vliegas en bodemstof. De laatste faktor bevat Al, Si, S, K, Ca, Cr, Mn, Fe, Cu, Zn, Pb, SO_4^{2-} en NH_4^+, waaronder de meeste anthropogene komponenten zijn. Elementen zoals Al, Si, S, K, Ca en Fe worden zowel teruggevonden in de derde als in de vierde faktor. Deze elementen hebben bijgevolg verschillende onafhankelijke bronnen : natuurlijke erosie van de bodem en verbrandingsprocessen.
In *Tabel 2* worden onze experimentele waarden, uitgemiddeld over alle monsters, zowel met de Belgica als het vliegtuig genomen, vergeleken met deze uit de literatuur sinds 1974. Ondanks belangrijke variaties in bemonsteringsprocedures en bemonsteringsplaatsen, is er blijkbaar toch een vrij behoorlijke overeenkomst tussen de resultaten.

Invloed van windrichting op koncentraties

Bij de vliegtuigmetingen waren telkens gedetailleerde "air mass back trajectories" beschikbaar ; deze geven informatie over de plaats waar de bemonsterde luchtmassa (voor verschillende hoogten) zich bevond tot 36 h voor de monstername, dus over de geografische gebieden waaruit de monsters verontreiniging kunnen hebben opgenomen. *Tabel 3* vat de resultaten samen naargelang de sektor waaruit de luchtmassa's werden aangevoerd. De hoogste koncentraties worden genoteerd bij zuid- en zuidoost winden, karakteristiek voor kontinentale luchtmassa's. Zoals verwacht worden de laagste koncentraties waargenomen voor de noord en noordwest windsektor, dus bij zuiver mariene luchtmassa's.

Windsektor	Cd	Cu	Pb	Zn
west + zuidwest	2,2 ± 0,7	20 ± 9	52 ± 7	53 ± 6
noord + noordwest	0,2 ± 0,1	1,1 ± 0,3	7 ± 2	2,0 ± 0,3
oost + noordoost	1,4 ± 1,0	5 ± 2	50 ± 7	73 ± 9
zuid + zuidoost	4,1 ± 2,6	17 ± 4	123 ± 13	150 ± 4
variabel	1,0 ± 0,5	14 ± 3	55 ± 15	60 ± 19

Tabel 3 : Gemiddelde koncentraties (in ng. m^{-3}), onder de inversiehoogte, voor Cd, Pb, Cu and Zn boven de Zuidelijke Bocht van de Noordzee voor verschillende windsektoren (gemiddelde koncentratie ± standaard deviatie op het gemiddelde).

DE AUTEURS

Philippe OTTEN werkte van 1985 tot 1990 als navorser in het "Micro- and Trace Analysis Centre" (MiTAC) in het Departement Scheikunde van de UIA, grotendeels aan onderzoeksprojekten over de depositie van zware metalen in de Noordzee. In april 1991 behaalde hij het Doctoraat in de Scheikunde. Thans is hij verbonden aan Degussa Antwerpen.

Jasna INJUK, afkomstig van het Rudger Boskovic Institute in Zagreb in het huidige Croatia, verricht sinds 1989 onderzoek over Noordzeepollutie in MiTAC.

Carlos ROJAS kwam in 1986 als Chileens bursaal van het International Atomic Energy Agency in MiTAC. Hij bleef er achteraf, tot begin 1992, wanneer hij er het Doctoraat in de Natuurkunde behaalde.

René VAN GRIEKEN is gewoon hoogleraar aan de UIA, en docent instrumentele analyse en milieuchemie. Zijn onderzoeksprojekten in MiTAC houden verband met metodologie van mikro- en sporenanalyse, en met de toepassingen van deze technieken in milieugericht onderzoek.

clustertechnieken, met de bedoeling de individuele deeltjes te klasseren in verschillende deeltjestypen, zoals zeezout, bodemstof, enz. LAMMA is een recente techniek voor individuele deeltjesanalyse, waarbij telkens een aerosoldeeltje wordt verdampt en geïonizeerd door een gefocusseerde laserstraal. De ionen worden vervolgens geanalyzeerd in een vluchttijd-massaspektrometer. De resulterende massaspektra bevatten een aanzienlijke hoeveelheid informatie over de elementaire en moleculaire samenstelling van de deeltjes. Detectie van sporenelementen tot op het ppm niveau, anorganische speciatie en organische fingerprinting zijn belangrijke pluspunten van deze techniek. Door een laser met sterk gereduceerde energie te gebruiken, in de zgn. "laser desorptie mode", is het mogelijk om de buitenste schil van sommige deeltjes apart te analyzeren, en zo informatie te verkrijgen over oppervlakte-aanrijkingen, en dus over eventuele heterogene chemische reakties die de deeltjes aan hun oppervlak hebben ondergaan.

Element	Zuid. Bocht	Noordzee	Achtergrond
Cu	17	11	2
Fe	350	230	16
Ni	5	7	1
Pb	62	39	2
Zn	86	54	2

Tabel 1 : Gemiddelde atmosferische koncentratie voor zware metalen boven de Noordzee (in ng.m^{-3}).

Meetresultaten

Vergeleken met de resultaten van de Belgica geven de vliegtuigmetingen vergelijkbare gemiddelden. De vertikale profielen van de koncentraties waren niet zeer uitgesproken onder de inversiehoogte ; gemiddelde koncentraties bemonsterd met het vliegtuig vlak boven het zeeniveau waren slechts ongeveer 20% hoger dan de gemiddelde koncentratie op grotere hoogten. De koncentraties die sporadisch werden gemeten boven de temperatuursinversiehoogte waren echter wel een faktor 10 tot 100 lager. Dit bevestigt dat emissie door de zee zelf geen belangrijke bron is voor zware metalen in de atmosfeer en dat de atmosfeer goed gemengd is onder de inversiehoogte. Metingen vanop schepen kunnen dus, indien lokale kontaminatie behoorlijk wordt vermeden, wel degelijk een betrouwbaar beeld geven van de atmosferische koncentraties aan zware metalen.

In *Tabel 1* vindt men de gemiddelde (over alle wind-richtingen) atmosferische koncentratie boven de Zuidelijke Bocht (zuidelijk van 54° NB, tot aan het Kanaal) en de rest van de Noordzee, voor Cu, Fe, Ni, Pb en Zn, zoals berekend uit 71 monsters gekollekteerd vanop de Belgica. De laatste kolom geeft resultaten voor monsters die werden gekollekteerd in het noordelijk deel van de Noordzee (noordelijk van 54° NB) bij noordwestenwind en in het Kanaal (tot 5° WL) bij zuidwestenwind, dus in beide gevallen voor zuiver mariene luchtmassa's ; ze worden verondersteld representatief te zijn voor de achtergrondkoncentratie van de Noordzee-atmosfeer. Uit *Tabel 1* is het duidelijk dat de koncentraties boven

Element	1972-73 [1]	1980-85 [2]	1984-85 [3]	1987-88 [4]	1984-89 [dit werk]
Al	155-240	390	*	-	-
Cd	-	4	0,7	1,1	2,1
Cu	-	17	3	-	16
Fe	290-330	560	192	216	275
Mn	14-22	28	9	10	17
Ni	5-7	-	5	3	7
Pb	96-130	150	39	34	62
V	9-11	-	7	-	-
Zn	75-120	150	41	41	79
As	4-5	-	3	-	-

* = niet gemeten

Tabel 2 : Koncentratie van verschillende elementen in aerosolen (in ng. m^{-3}) boven de Zuidelijke Bocht van de Noordzee. Vergelijking met andere gepubliceerde waarden.

LUCHTVERVUILING

Atmosferische fluxen van zware metalen naar de Noordzee

De Noordzee wordt langs verschillende wegen belast met zowel organische als anorganische polluenten. Meest evident is het transport via rivieren. Direkte lozingen langsheen de kustlijn en dumping van toxische materialen door schepen zijn twee andere oorzaken van vervuiling. Exploitatie van olie- en gasplatformen leidt eveneens tot operationele lozingen van een aantal schadelijke stoffen. "Last but not least" bereikt een deel van de polluenten de Noordzee via de atmosfeer.
Dit artikel handelt specifiek over dit laatste facet van Noordzeepollutie. Zowel gasvormig als particulair materiaal worden via verbrandings- en andere pollutieprocessen in de atmosfeer geëmitteerd. Na fysische dispersie en chemische transformatie kunnen deze polluenten in zee terecht komen via depositieprocessen. De zware metalen bevinden zich hoofdzakelijk in de particulaire faze. Bij droge weersomstandigheden worden deze deeltjes uit de atmosfeer verwijderd door gravitatie, turbulente diffusie en impactie; dit noemt men droge depositie. Bij neerslag kunnen deeltjes door regendruppels of sneeuwvlokken gevangen worden en zo in zee terecht komen: natte depositie.

P. OTTEN, J. INJUK, C. ROJAS en R. VAN GRIEKEN
Departement Scheikunde, Universiteit Antwerpen (UIA), Antwerpen-Wilrijk

In het kader van onderzoeksprojekten vanwege de Belgische Diensten voor de Programmatie van het Wetenschapsbeleid en vanwege Rijkswaterstaat Nederland werd door het Departement Scheikunde van de Universitaire Instelling Antwerpen een uitgebreid bemonsterings- en analyseprogramma opgezet om gegevens te verzamelen over de toestand van de atmosfeer boven de Noordzee en om een antwoord te geven op volgende vragen:
Wat is de chemische samenstelling van atmosferische deeltjes boven de Noordzee?
Hoe relatief belangrijk is de atmosfeer als toevoerweg van zware metalen voor de Noordzee?
Welke bronnen zijn verantwoordelijk voor de stoffen aanwezig in de Noordzee-atmosfeer?

Tussen december 1984 en oktober 1989 werden 12 bemonsterings-campagnes van gemiddeld 5 dagen op de Noordzee en het Kanaal uitgevoerd met het Belgische oceanografisch schip *Belgica*. Aerosolmonsters werden gekollekteerd met behulp van membraanfilters en cascade-impactoren. Een cascade-impactor is een bemonsteringsapparaat waarbij stofdeeltjes door hun verschil in momentum tijdens het bemonsteren worden gescheiden in funktie van hun diameter en geïmpacteerd op een oppervlak. Om kontaminatie door het schip zelf te vermijden, werden de monsterhouders op een hoogte van 10 m in de mast vooraan het schip geplaatst. Verder werd er enkel lucht bemonsterd indien de relatieve windrichting ten opzichte van het schip tussen - 45° en + 45° was. Daarenboven werden tussen juli 1988 en oktober 1989 ook 22 vluchten boven de Noordzee uitgevoerd met een twee-motorig vliegtuig van de firma Geosens, Rotterdam, om een duidelijker inzicht te krijgen in de hoogte-afhankelijkheid van de polluentkoncentraties. Het vliegtuig was speciaal uitgerust voor de kontaminatievrije bemonstering van luchtpollutie. Telkens werd opgestegen aan het Goeree-platform ter hoogte van Rotterdam tot aan de inversiehoogte, en dan werden op dalende hoogte zes trajekten van 150 km in de windrichting afgelegd. Het laagste trajekt werd steeds gevlogen tussen 10 en 30 m boven de zee. Op elk niveau werden monsters genomen voor mikro- en sporenanalyse, en voor elke vlucht werd bovendien een impactor beladen.
Figuur 1 geeft een situatieplan van de Noordzee weer.

Analytische technieken

Het gebruik van verschillende moderne analytische technieken resulteert in een ruim aanbod van ruwe gegevens die via interpretatie en modelberekeningen moeten leiden tot relevante informatie.
Energie-dispersieve XRF (X-stralen fluorescentie) werd toegepast op dunne membraanfilters. Via een spektraal deconvolutieprogramma worden kwantitatieve koncentraties voor Al, Si, P, S, Cl, K, Ca, Ti, V, Cr, Mn, Fe, Ni, Cu, Zn en Pb bekomen. Na oplossen in HNO_3 wordt op een fraktie van de filters heroplossingsvoltammetrie of anodic stripping voltammetry (ASV) toegepast, waarbij Cd, Cu, Pb en Zn zeer gevoelig kunnen worden bepaald. IC (ionenchromatografie) wordt gebruikt voor bepaling van Cl^-, NO_3^- en SO_4^{2-}, na ultrasone extraktie van de filter in een eluens.
Verder werden twee mikro-analyse technieken voor individuele deeltjes gebruikt: elektronenprobe X-stralen mikro-analyse (EPXMA) en laser mikroprobe massa analyse (LAMMA). Bij EPXMA worden in elk aerosol-monster bvb. 500 deeltjes individueel gekarakterizeerd. Van elk deeltje wordt de diameter, het oppervlak en de vormfaktor gemeten of berekend. Verder wordt er een X-stralen spektrum gekollekteerd voor ieder deeltje. De daaruit resulterende dataset wordt gereduceerd met hiërarchische en niet-hiërarchische

Selected article #10:

Atmosferische fluxen van zware metalen naar de Noordzee
P. Otten, J. Injuk, C. Rojas en R. Van Grieken
Het Ingenieursblad, 61 (1992), 41-46
en
De Ingenieur, nr.5 (1992), 32-36

sampling was performed beneath the inversion layer.

Registry No. Ba, 7440-39-3; V, 7440-62-2; Pb, 7439-92-1; Cu, 7440-50-8; Zn, 7440-66-6; Fe, 7439-89-6; Ti, 7440-32-6.

Literature Cited

(1) Rojas, C.; Van Grieken, R. *Atmos. Environ.*, in press.
(2) Wouters, L.; Michaud, D.; Van Grieken, R. *Mikrochim. Acta*, submitted.
(3) Verbueken, A.; Bruynseels, F.; Van Grieken, R. In *Inorganic Mass Spectrometry*, 1st ed.; Adams, F., Gijbels, R., Van Grieken, R., Eds.; John Wiley & Sons: New York, 1988; pp 173–256.
(4) Van Espen, P.; Van Vaeck, L.; Adams, F. *Proceedings of the 3rd International LMMS Workshop*; University of Antwerp(UIA): Antwerp, Belgium 1986; pp 195–198.
(5) Pena, J.; Norman, J.; Thomson, D. *J. Air Pollut. Control Assoc.* **1977**, *27*, 337–340.
(6) Xhoffer, C.; Bernard, P.; Van Grieken, R., Van der Auwera, L. *Environ. Sci. Technol.* **1991**, *25*, 1470–1478.
(7) Andreae, M.; Charlson, R.; Bruynseels, F.; Storms, H.; Van Grieken, R.; Maenhout, W. *Science* **1986**, *232*, 1620–1623.
(8) Otten, P.; Bruynseels, F.; Van Grieken, R. *Anal. Chim. Acta* **1987**, *195*, 117–124.
(9) Wouters, L.; Artaxo, P.; Van Grieken, R. *Int. J. Environ. Anal. Chem.* **1990**, *38*, 427–438.
(10) Blanchard, D. In *Air–Sea Exchange of Gases and Particles*, 1st ed.; Liss, P., Slinn, G., Eds.; D. Reidel Publishing Company: Dordrecht, 1983.
(11) Mallant, R.; Kos, G.; Van Wester, A. *Proceedings of the 2nd International Aerosol Conference*; Sept 1986, Berlin; pp 49–52.
(12) Savoie, D. L.; Prospero, J. M. *J. Geophys. Res. Lett.* **1982**, *9*, 1207–1211.
(13) Chessselet, R.; Morelli, J.; Buat-Ménard, P. *J. Geophys. Res.* **1972**, *77*, 5116–5131.
(14) Hoffman, E.; Hoffman, G.; Duce, R. *J. Geophys. Res.* **1980**, *85*, 5499–5502.
(15) Andreae, M. *Science* **1983**, *220*, 1148–1150.
(16) Mamane, Y. *Atmos. Environ.* **1990**, *24B*, 127–137.
(17) Crozat, G. *Tellus* **1979**, *31*, 52–57.
(18) Schneider, B. *Atmos. Environ.* **1987**, *6*, 1275–1283.
(19) Xhoffer, C. Masters Thesis, University of Antwerp, 1988.
(20) Suzuki, T.; Tsunagai, S. *J. Atmos. Chem.* **1988**, *6*, 363–374.
(21) Hopke, P. In *Receptor Modeling in Environmental Chemistry*, 1st ed.; Hopke, P., Ed.; J. Wiley & Sons: New York, 1985.
(22) Biggins, P.; Harrison, B. *Environ. Sci. Technol.* **1980**, *14*, 336–339.
(23) Finlaysson-Pitts, B.; Pitts, J. In *Atmospheric Chemistry: Fundamentals and Experimental Techniques*, 1st ed.; Finlaysson-Pitts, B., Pitts, J., Eds.; J. Wiley & Sons: New York, 1986.
(24) Pacyna, J. *Atmos. Environ.* **1984**, *18*, 41–50.
(25) Mamane, Y. *Atmos. Environ.* **1988**, *22*, 2411–2418.
(26) Injuk, J.; Otten, P.; Laane, R., Maenhaut, W., Van Grieken, R. *Atmos. Environ.*, submitted.

*Received for review November 26, 1991. Accepted December 9, 1991. This work was partially supported by the Dutch Rijkswaterstaat, Den Haag, The Netherlands, through Project NOVIME*2 Tasks No. DGW-920 and DGW-217 and by the Belgian Ministry of Science Policy through Project EUR/7/90. D.M. acknowledges a leave grant from the Ministry of Education, Québec, Canada.*

and 6. A possible explanation is the reduction in oil combustion in residential boilers as the last two flights took place in the month of May (Table I). The relative abundance of V-containing particles on the larger-size impactor stages is remarkably higher for flight 3 than for all other flights. This corresponds with the findings for NH_4^+. It appears from Table IV that V most often occurs together with Pb.

Pb-containing particles are most abundant on stage 5 (Figure 6b). The largest part of the total anthropogenic emission of Pb in Europe comes from automotive exhausts (*24*). As mentioned before, the numerous Pb- and NH_4^+-containing particles very likely originate from this source. Compared to other flights, Pb-containing particles are more abundant among the larger particles of flight 3. Similar trends are found for V and NH_4^+.

The overall Ba concentration seems to be somewhat higher for flights 3, 5, and 6 (Figure 6c). The relative amount of Ba-rich particles, associated with NH_4^+ seems remarkably low compared to all other metals (Table III). This is not surprising as hardly any Ba was detected on stage 5. Ba is more associated with Ti than with any other metal (Table IV). These two elements are used in the pigment industry, which might be a possible source. According to Hopke (*21*), combustion of kerosene, drying furnaces for Cr yellow, calcining furnaces for barite, and trucks are important Ba sources. Still, unlike the above-discussed metals, a large part of the atmospheric Ba in Western Europe seems to be associated with soil dust (e.g., ref 18).

Zn is mainly emitted from iron, steel, and ferroalloy plants and Zn–Cd smelters (*24*). Other sources are refuse incineration (*25*) and tire wear (*21*). Twenty-five percent of all detected Zn was found to be associated with KCl or K_2SO_4, which points to a refuse incinerator origin. The overall abundance per flight for this compound is somewhat higher for flight 3 (Figure 6d). According to Table IV, Zn often appears together with Pb; this is indicative of a smelter or alloy-manufacturing origin.

The main source for Ti release in the atmosphere is soil dispersion. Other possibilities are paint spray, agricultural burning, and asphalt production (*21*). Of all metals considered, Ti is mostly associated with Ba.

Cr can be regarded as an indicator of emissions from the iron and steel industry (*24*). This element seems to have a tendency to be concentrated on stages 5 and/or 4 (Figure 6f).

The main Fe sources are soil dust and ferrous metal manufacturing. Fe particles are significantly more abundant for flight 3. They predominantly appear among the smallest particles for flights 1, 2, and 5 (Figure 6g).

Bulk metal analysis (*26*) revealed that absolute Cd, Pb, and Zn concentrations were the highest for flight 3, where the wind direction during sampling was south (Table I). LAMMA for this flight shows increased relative abundances for NH_4^+, V, Pb, Zn, and Fe.

Considering the relative abundances of all investigated compounds as a function of sampling height, no distinct trends could be inferred. As an illustration, panels a–c of Figure 7 shows relative abundances of NaCl, aluminosilicate, and ammonium-rich particles. For each flight, altitudes were referred to the corresponding inversion height (Table I) in order to clarify the representation. Only relative sea salt particle abundances seem to decrease above the inversion layer, which acts as a "lid" on an air mass. Bulk analysis results, on the other hand, show a decrease in *absolute* concentration that rises to a factor of 10 for the metals Cd, Cu, Zn, and Pb.

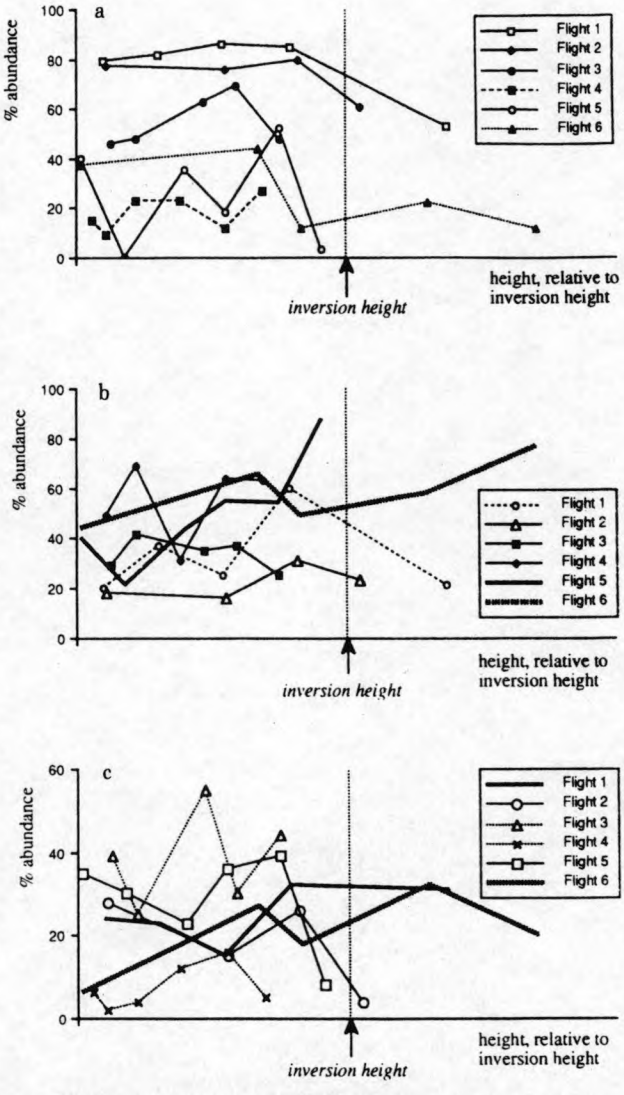

Figure 7. Relative abundances of (a) sea salt particles, (b) aluminosilicates, and (c) ammonium-containing particles as a function of sampling height (altitudes are referred to the corresponding inversion height).

Conclusion

All the individual particle types that have earlier been defined by analyzing North Sea aerosol particles with EPXMA, are detected with LAMMA. However, the particles appear very often as internal mixtures: the image of this aerosol, obtained with LAMMA, is much more complicated.

Examining relative abundances of several compounds of environmental interest as a function of particle size and wind direction during sampling allows some clear trends to be inferred. Ammonium, for example, is mainly present among the smallest particles; sea salt exhibits typical hatlike size profiles and predominates when the sampled air masses have a marine origin. Aluminosilicates and KCl particles prevail for continental air masses.

Better than bulk analysis techniques, LAMMA (and single-particle analysis techniques in general) can provide valuable information about particle origin. If not always conclusive, it does narrow the set of possible sources most of the time: e.g., in the case of the KCl particles, where some alleged sources could be definitely ruled out.

Apart from a decrease in relative sea salt particle concentration above the inversion layer, no definite trends in relative particle type abundances could be deduced as a function of sampling height. This is not surprising as most

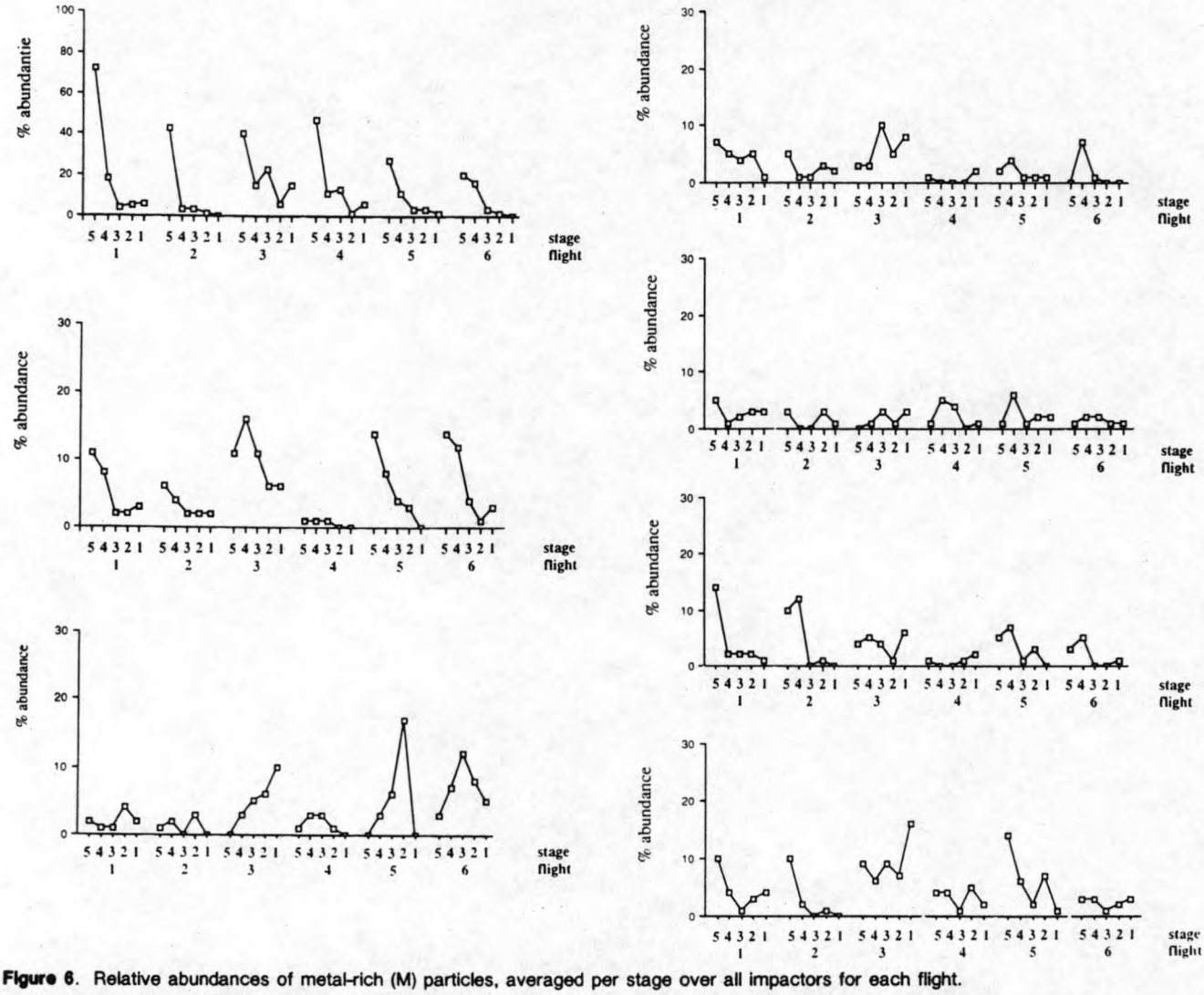

Figure 6. Relative abundances of metal-rich (M) particles, averaged per stage over all impactors for each flight.

Table II. Some Information about Detected Metals

metal	concn in North Sea aerosol, ng·m^{-3} [a]	first ionization potential, eV	detection incidence relative to V
Ba	8	5.21	0.3
V	10	6.74	1.0
Pb	53	7.42	0.4
Cr	3	6.77	0.3
Zn	57	9.89	0.3
Fe	369	7.87	0.4
Ti	27	6.82	0.2

[a] Data from the Kiel Bight (*18*).

Table III. Associations between Metal-Rich Particles, Aluminosilicates, and Ammonium

metal	% metal-rich particles, associated with aluminosilicates	ammonium
V	60	67
Pb	43	60
Ba	65	14
Cr	75	56
Zn	79	41
Fe	65	55
Ti	67	32

elements found in ambient particulate matter: the combustion of coal and oil, wood burning, waste incineration, metal mining and production, dusts, sea salt, forest fires, volcanic emissions, and emissions from vegetation. Metals detected in this case with LAMMA often occur associated with other compounds, especially with ammonium, with aluminosilicates (Table III), and with other metals (Table IV). For the latter table, metal-rich particles that also exhibit aluminosilicate peaks were not considered in order to obtain an impression about anthropogenic particles (i.e., to rule out soil dust), but in this way, fly ash particles are not considered. As noticed repeatedly above, distinguishing "pure" particles from internal mixtures is not straightforward. In the size profiles of Figure 6, a particle is considered metal-rich when the metal in question appears in the spectrum.

Table IV. Mutual Associations between Metals (%) (Not Included in Aluminosilicates)

assocd with	metal V	Pb	Ba	Cr	Zn	Fe	Ti
V		13	2.9	4.9	12	6.5	14
Pb	8.6		2.9	7.3	21	7.6	0
Ba	0.9	1.4		0	3.1	2.6	17
Cr	0.9	2.1	0		10	1.3	3.6
Zn	1.8	4.9	1.5	7.3		1.3	7.1
Fe	2.3	3.5	2.9	2.4	3.1		10
Ti	1.8	0	5.9	2.4	6.3	3.9	

V profiles (Figure 6a) largely correspond to the NH_4^+ profiles of Figure 4. As already mentioned above, V originates from fossil fuel combustion processes. The overall V abundance per flight is somewhat smaller for flights 5

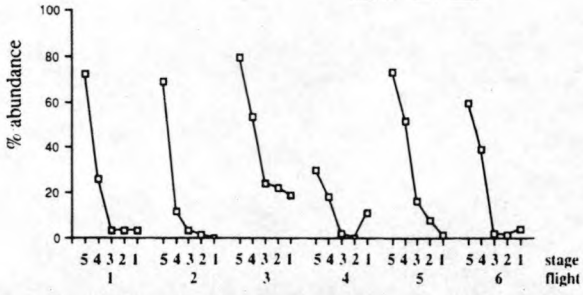

Figure 4. Relative abundances of ammonium-containing particles, averaged per stage over all impactors for each flight.

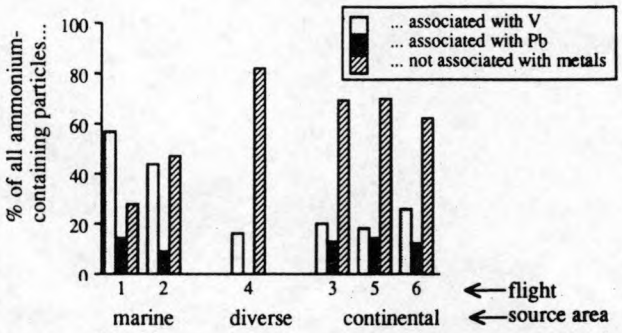

Figure 5. Relative abundances of ammonium-containing particles, associated with V and Pb and not associated with metals.

This rules out the "chemical fractionation hypothesis". As most of these particles are not associated with aluminosilicates, a soil source is also unlikely. Regarding the geographical location of the North Sea, a tropical forest origin does not seem too probable either. As mentioned before, Schneider (*18*) attributed a K excess to the combustion of lignite, also called "salt coal", which is mainly used in Eastern Europe. EPXMA of a lignite combustion aerosol, however, did not reveal the presence of individual KCl particles; K was always associated with aluminosilicates (*19*). Mammane (*16*) performed EPXMA on waste incinerator aerosol particles. Most of the particle mass consisted of soluble potassium and Zn chlorides. Since only 3% of the non–sea salt KCl, and 5% of the K_2SO_4 particles were found to be associated with Zn, incinerator products are apparently not the only source in this case. Another possibility is biomass burning. For Europe, this includes agricultural and firewood burning. Eastern Europe, especially, has a high firewood consumption.

The observed decline in sea salt content from flight 1 through flight 6 is largely compensated by an increase in aluminosilicates (Figure 3b). In this case, the size distribution pattern is very variable, which might be caused by the fact that two sources are responsible for this particle type: soil dust and fly ash. According to our experience, they are indistinguishable on the basis of their LAMMA spectra. Only those fly ash particles formed at high combustion temperatures can be identified because of their globular appearance.

For identification purposes, Ca-rich particles are defined as particles whose spectra display the typical $(CaO)_x$ and $(CaO)_xCa$ cluster ions. Analyses of Ca standards show that all Ca- and O-containing compounds provide those ions in their LAMMA spectra. According to the literature, the most plausible sources for Ca-rich particles are fractional crystallization and subsequent breaking of sea salt droplets (*7*), marine biogenic material (*7*), calcite contained in soil dust (*20*), and combustion processes (*21*). In an earlier, very extensive EPXMA investigation of North Sea aerosol particles, Ca-rich and Ca- and S-rich particles were detected (*6*). The Ca- and S-rich particles were clearly continential-derived while the Ca-rich could not be unambiguously assigned to one source type. With LAMMA, however, $CaCO_3$ and $CaSO_4$ are indistinguishable on the basis of their positive-mode spectra. $Ca_3(PO_4)_2$, on the other hand, displays some typical $CaPO_x$ peaks. Figure 3C shows the Ca-rich particle type size distributions averaged over all impactors per flight. In this case, no clear differences can be derived between marine and continental air masses.

Figure 4 shows the percent abundance of NH_4^+-containing particles, averaged per stage over all impactors for each flight. NH_4^+ seems to be mainly present in the smallest particles. Its size distribution pattern is consistent through all flights. The total relative NH_4^+ concentration for flight 4 is definitely the lowest. Compared to all other flights, NH_4^+ is very well represented in the lower impactor stages (3, 2, and 1) of flight 3. According to Otten et al. (*8*) this points to extreme pollution circumstances, enhanced by the fact that the inversion layer was situated very low (Table I), thus inhibiting the natural dispersion of pollutants. Atmospheric ammonium compounds originate from the neutralization reaction of acidic species with ammonia. The latter is generated by biological decomposition of nitrogenous matter, the use of N-rich fertilizers in agriculture, animal farming, and coal combustion. The ammonium compounds seem to be closely associated with metals, especially V (which is a typical fossil fuel combustion product) and also Pb. It is however necessary to regard this association with some caution: at least part of it might be an artifact since most of the NH_4^+ particles are detected on stage 5. The Pb-containing NH_4^+ particles are thought to be secondary reaction products of automotive exhausts: $Pb(NH_4)_2(SO_4)_2$ is formed through the reaction of lead halides with the massive amounts of $(NH_4)_2SO_4$ present in each urban atmosphere (*22*). The relative contribution of the V-containing NH_4 particles decreases when the sampled air masses have passed over Europe (Figure 5). This could be explained by an ammonia input from agricultural activities in The Netherlands and the northwestern part of Belgium. The relative amounts of Pb-containing NH_4 particles, on the other hand, do not vary significantly except for flight 4, where none are detected (Figure 5). Possible counterions for ammonium are sulfate, nitrate, and chloride. As concluded from the analysis of standard compounds, positive-mode spectra do not provide satisfactory information about the counterion's identity. However, most negative-mode spectra are dominated by the HSO_4^- ion, so SO_4^{2-} seems to be a plausible candidate. This conclusion agrees with the findings of Otten et al. (*8*). The NH_4^+ particles sampled under marine conditions (flights 1 and 2) also appear to contain Na_2SO_4 and, less frequently, NaCl. These probably are internal mixtures of $(NH4)_2SO_4$ with highly transformed sea salt.

Metals detected in these samples are Ba, V, Pb, Cr, Zn, Fe, Ti, Ge, Cd, Sr, Ni, Mn, and Cu. The last six are not included in the discussion. As stated above, Ni, Mn, and Cu suffer too much from spectral interferences to be accurately identified, whereas Ge, Sr, and Cd were detected too sporadically to obtain some conclusive information about them. Table II shows that the incidence with which a metal is detected does not always correspond to its actual concentration in the aerosol, even not when its first ionization potential, which is loosely indicative for the sensitivity, is taken into account. This points to different distributions over particles: e.g., an element might be contained in a huge amount of particles but in a concentration below the detection limit. Finlaysson-Pitts and Pitts (*23*) designate various potential sources of the trace

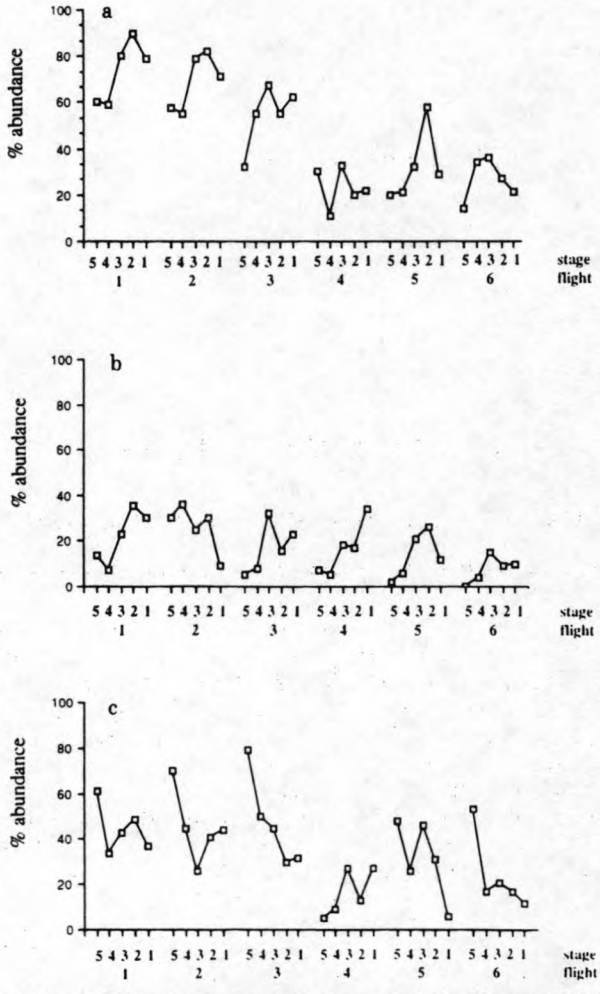

Figure 2. Relative abundances of (a) sea salt, (b) $NaNO_3$-containing, and (c) Na_2SO_4-containing particles, averaged per stage over all impactors for each flight.

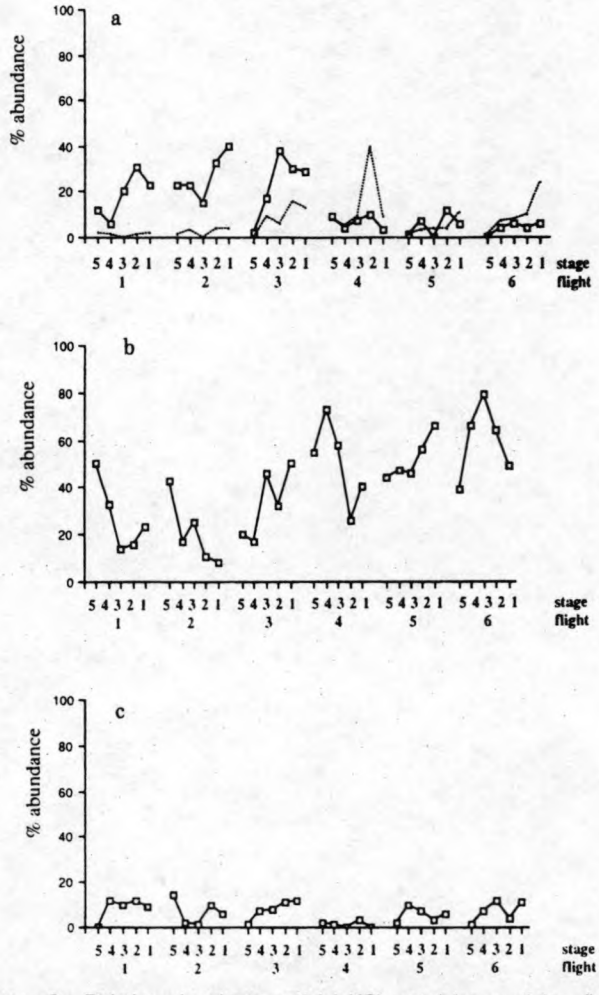

Figure 3. Relative abundances of (a) KCl-containing particles, (b) aluminosilicates, and (c) Ca-rich particles, averaged per stage over all impactors for each flight.

better than that for NH_4^+ (*8*). Differences in overall peak intensities between *different* compounds are thus by no means indicative for concentration differences.

Standard seawater spectra are largely dominated by the typical Na_xCl_y cluster ions (*9*). Therefore, a particle is considered a sea salt particle or a mixed particle containing sea salt when NaCl is detected by the search routine. Figure 2a shows the relative abundances of sea salt particles (i.e., the percentage of particles containing sea salt), averaged per stage over all impactors for each flight. The size profiles are fairly consistent over all flights. The highest abundances are reached among the particles of stage 2 or stage 3. Comparing different flights, the total sea salt content is highest for flights 1 and 2. This can be explained by two factors: longer time spent over the sea by the sampled air masses and highest wind speed during sampling for the first two flights; and an increased wind speed promoting sea salt particle production (*10*).

Sea salt can be transformed in the atmosphere by heterogeneous reactions with H_2SO_4 and/or HNO_3 vapor (*11*). These alterations are reflected in the spectra by the appearance of peaks indicative for $NaNO_3$ and Na_2SO_4 (i.e., the normal Na/O clusters and $Na_2NO_2^+$, $Na_2NO_3^+$ and $Na_3SO_3^+$, $Na_3SO_4^+$, respectively). Their size profiles are reported in Figure 2, panels b and c. Sometimes, the transformation is so complete that the Na_xCl_y clusters are not detectable any more. In this case, the particle is no longer considered a sea salt particle. Most of the $NaNO_3$ profiles match those of NaCl rather closely; this is not surprising inasmuch as 81% of all detected $NaNO_3$ was found to be associated with NaCl. The Na_2SO_4 abundance patterns, on the other hand, are very different. Except for flight 4, they are all characterized by a maximum abundance in the smallest size ranges. The NaCl to Na_2SO_4 conversion rate increases as the particle diameter decreases; as a consequence, the small particles have a high Cl^- deficiency and SO_4^{2-} enrichment, so Cl^- is very often not detectable in their spectra any more. $NaNO_3$ is not as abundant in the small-particle fraction as Na_2SO_4. This corresponds with the findings of Savoie and Prospero (*12*) and Mallant et al. (*11*), who state that the fact that HNO_3 has a much higher vapor pressure than H_2SO_4 leads to the removal of HNO_3 when condensing H_2SO_4 lowers the surface pH of the small particles.

KCl is a minor sea salt component. In standard seawater aerosols, K_xCl_y clusters appear when the Na_xCl_y clusters are in overflow. Some 35% of the KCl particles, however, do not exhibit the typical Na_xCl_y mass peaks in their spectra. These particles sometimes seem to have undergone the same transformations as sea salt: K_2SO_4 and KNO_3 peaks are regularly detected. K enrichments relative to Na have already been observed in marine aerosols. These excesses have been attributed to chemical fractionation at the air–sea interface (*13*), to soil sources (*14*), biomass combustion (*15*), waste incinerator products (*16*), long-range tropical forest aerosol transport (*17*), and the combustion of lignite (*18*). Figure 3a shows the abundance patterns of KCl particles with and without NaCl association. The relative concentrations of the latter are higher when the sampled air masses have a nonmarine origin.

Table I. General Flight Data

flight	flight date	wind sector	source area[a]	inversion height, m	wind speed at ground level, $m \cdot s^{-1}$
1	01/13/89	S + W	marine, F	1750	13.6
2	01/23/89	S + W	marine, F	950	10.8
3	03/06/89	S	NL, B, F	400	9.5
4	03/12/89	diverse	marine, UK, NL, B	800	8.8
5	05/23/89	E	NL, G, CS, PL	1500	7.8
6	05/23/89	E	G, CS, PL	1500	8.9

[a] Abbreviations are as follows: F, France; NL, The Netherlands; B, Belgium; UK, United Kingdom; G, Germany; CS, Czechoslovakia; PL, Poland.

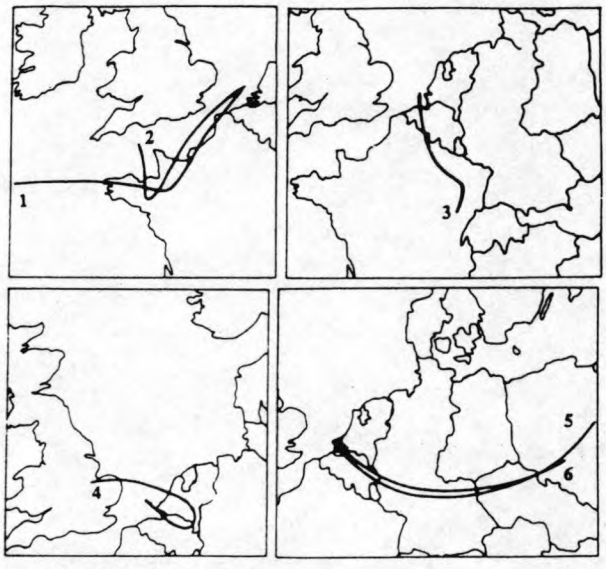

Figure 1. Back-trajectories for the flights 1–6.

equipped with Formvar (i.e., a slightly adhesive polymer) coated electron microscope grids and operated at a flow rate of 1 $L \cdot min^{-1}$. The 50% cutoff aerodynamic diameters of stages 1–5 are 4, 2, 1, 0.5, and 0.25 μm, respectively. A sampling time of ca. 25 min usually provided a satisfactory loading for LAMMA. In order to avoid distortion of the particle size distribution, sampling was performed under isokinetic conditions. In this case, the Pennsylvania State University (PSU) isokinetic sampler designed by Pena et al. (*5*) was used. The sampler was mounted on the roof of the aircraft in such a way that the intake was located outside the boundary layer of the aircraft and that no particulate or gaseous matter coming from the exhaust of the engines could be sampled. Until analysis, the samples were stored in sealed PVC Petri dishes. For each flight, four 36-h "backward in time air trajectories" (or "back-trajectories" for short) were calculated for four different levels (1000, 900, 850, and 700 mbar), providing valuable information about the source regions of the air masses. They were interpolated to yield trajectories for the six different flight levels (*1*). Figure 1 shows the back-trajectories for the different flights at 1000 mbar (sea level). General flight data (flight date, wind sector, prevailing source areas as determined from the back-trajectories, inversion height, and wind speed at ground level) are listed in Table I.

A total of some 120 samples were investigated, namely five impactor stages for four to six tracks of six flights. For each of these impactor stages, some 50 particles were randomly selected for LAMMA, resulting in approximately 6000 positive-mode spectra. With LAMMA being a destructive technique, it is impossible to record a positive-mode and a negative-mode spectrum of one particle without introducing uncertainties concerning preferential evaporation and focusing errors. The major part of this work was performed on positive-mode spectra, because they are advantageous for the identification of trace metals. Negative-mode spectra were used in an attempt to extract additional information concerning the determination of certain anions.

Results and Discussion

EPXMA of some 25 000 similar aerosol particles, sampled in a time span of 4 years from a research vessel over the North Sea, led to the definition of some well-separated particle types: sea salt, aluminosilicates, S-rich, Ca- and S-rich, Ca-rich, Si-rich, Ti-rich, and Fe-rich (*6*). Preliminary investigation of a representative sample of LAMMA spectra revealed the presence of all these particle types, but a great part of them appeared to occur as internal mixtures. For the particles of stage 5 (aerodynamic cutoff diameter of 0.25 μm) this might be an artifact, because part of them are beyond observation by the optical microscope the LAMMA is equipped with; in other words, one never knows if only one particle has been ablated by a laser shot. On the other stages, however, particles are generally well separated on the grids, so in this case, "mixed spectra" unambiguously point to internally mixed particles. These mixtures were already discussed by Andreae et al. (*7*), who attributed them to processes within clouds.

All spectra were automatically screened for the presence of compounds that characterize the different groups and their particular features. Special attention was paid to the occurrence of trace metals not detectable by EPXMA. As the limited mass resolution of the LAMMA does not allow it to distinguish different ions of the same nominal mass, the problem of possible misclassification was carefully evaluated. Generally, the possibility for misclassification diminishes when the number of peaks necessary for a positive evaluation increases. This possibility however also depends on the spectral region. A peak at $m/z = 18$ (NH_4^+) can, at least for this kind of sample, without further consideration be attributed to an ammonium compound. On the other hand, it is our experience that the identification of Cu suffers seriously from spectral interferences, even when isotopic abundances are used for peak recognition. Therefore, it was decided to omit Cu from the set of investigated metals. For the same reason, Ni and Mn were left out. As, ordinarily, metal ions always appear together with at least one metal oxide ion, these oxides were also included in the sets of peaks necessary for the identification of the elements which occur in the most crowded region of the spectrum (i.e., from $m/z = 39$ to $m/z = 165$).

In this work, the results obtained by LAMMA are discussed as a function of wind direction during sampling, of particle size and of sampling height. When the corresponding figures are being interpreted, it should be kept in mind that LAMMA has different sensitivities for different compounds; the sensitivity for Na^+ is some 150 times

2771

Reprinted from ENVIRONMENTAL SCIENCE & TECHNOLOGY, Vol. 26, 1992

Laser Microprobe Mass Analysis of Individual North Sea Aerosol Particles

I. Dierck, D. Michaud,† L. Wouters, and R. Van Grieken*

Department of Chemistry, University of Antwerp (U.I.A.), Universiteitsplein 1, B-2610 Antwerp-Wilrijk, Belgium

■ Some 6000 individual aerosol particles in the 0.5–4-μm aerodynamic diameter range, collected from an aircraft at different heights above the North Sea, were analyzed using laser microprobe mass analysis (LAMMA). In this way, various well-separated particle types could be defined. Many of these particles appeared to occur as internal mixtures. Several definite trends in particle type abundances as a function of wind direction during sampling and of particle size could be observed. This helped in identifying source processes of the aerosol. Obtaining conclusive results as a function of sampling height, on the other hand, was much less straightforward. This is not surprising, since most samples were collected under the inversion layer where extensive mixing is likely to take place.

Introduction

Considerable attention has already been paid to the determination of atmospheric particles from various regions all over the world. These observations aim to establish a global balance of man's pollutants into the air as compared to natural input.

The aerosols discussed in this paper were sampled over the Southern Bight of the North Sea, an area closely surrounded by anthropogenic pollution sources. The present work is part of a study concerning the atmospheric deposition of heavy metals into the North Sea, involving bulk as well as single-particle analyses. Individual particle analysis was performed by electron probe X-ray microanalysis (EPXMA), the results of which are presented elsewhere (*1*), and by laser microprobe mass analysis (LAMMA). EPXMA gives quantitative results about the major chemical composition of a particle, but fails to detect elements with $Z < 11$; hence, for example, ammonium compounds, which are very important from an environmental point of view, will go unnoticed. LAMMA can fill this gap. Furthermore, it can provide information about trace elements (its detection limits, although element-dependent, are generally a factor of 10 or more better than those of EPXMA) and possibly about surface coatings and organic components. Cluster ion formation in the laser plasma and different sensitivities might however obscure the compositional information to some extent. LAMMA is less automated than EPXMA, hence much more labor intensive and less appropriate to analyze huge amounts of particles.

Experimental Section

Analytical Technique. In the LAMMA-500 instrument (Leybold-Heraeus, Cologne, Germany), individual aerosol particles are vaporized by a single high-power laser pulse (τ = 15 ns) of a Q-switched frequency-quadrupled Nd:YAG laser (λ = 265 nm; power density 10^7–10^{11} W·cm^{-2}). The resulting microplasma contains atomic and molecular ions, as well as electrically neutral fragments. Depending on the spectrum polarity chosen, positive or negative ions are accelerated and collimated into the drift tube of a time-of-flight mass spectrometer, where they are separated according to their m/z ratios. The signal is then fed into a 32-KB memory transient recorder (LeCroy TR8818) and digitized. Spectra are stored on a personal computer for off-line data handling. Groups of spectra can be automatically calibrated, integrated, and compared to a library of standard spectra, which can be complemented by the user (*2*). All software applied is homemade. The instrument and part of the software package are discussed extensively by Verbueken et al. (*3*) and Van Espen et al. (*4*).

Sampling Procedure. Aerosol samples were collected under predominantly cloudless conditions during six different flights with a twin engine aircraft Piper Chieftain (PA 31-350 PH-ECO) of Geosens B.V. Company (Rotterdam, The Netherlands). At the beginning of each flight, an upward spiral was flown at the Goeree Platform (51°-55.5′N, 3°40.0′E), while SO_2 and O_3 concentrations, temperature, and dew point were continuously monitored to localize the inversion height. From there, for each flight, six tracks of 120 km were flown over the North Sea in the direction of the wind; the six tracks were about equally spaced between the sea surface and the boundary layer. For every track, a sample for LAMMA was obtained by means of five-stage single-orifice Batelle-type impactors,

† On leave from the Department of Physics, Laval University, Québec, Canada.

 0013-936X/92/0926-0802$03.00/0

Selected article #9:

Laser microprobe mass analysis of individual North Sea aerosol particles
I. Dierck, D. Michaud, L. Wouters and R. Van Grieken
Environmental Science and Technology, 26 (1992), 802-808

(36) Winchester, J. W.; Li, S. M.; Fan, S. M.; Schnell, R. C.; Bodhaine, B. A.; Naegele, P. S. *Geophys. Res. Lett.* **1984**, *11*, 995–998.
(37) Winchester, J. W.; Schnell, R. C.; Li, S. M.; Fan, S. M.; Bodhaine, B. A.; Naegele, P. S.; Hansen, A. D. A.; Rosen, H. *Atmos. Environ.* **1985**, *19*, 2167–2173.
(38) Mamane, Y. *Atmos. Environ.* **1988**, *22*, 2411–2418.
(39) Mamane, Y. *Atmos. Environ.* **1990**, *24B*, 127–135.
(40) Dierck, I.; Injuk, J.; Otten, Ph.; Rojas, C.; Van Grieken, R.; Atmospheric deposition of heavy metals into the North Sea. Report 3 to Rijkswaterstaat, Dienst Getijdewateren, 's Gravenhage, The Netherlands, in the framework of project NOMIVE*2 task No. DGW-920; University of Antwerp, 1990.
(41) Van Malderen, H., University of Antwerp, unpublished data, 1991.

*Received for review May 6, 1991. Revised manuscript received September 18, 1991. Accepted November 7, 1991. We are grateful to Rijkswaterstaat, Dienst Getijdewateren (The Netherlands) for their financial support under grants NOMIVE*2 No. DGW-920 and No. DGW-217.*

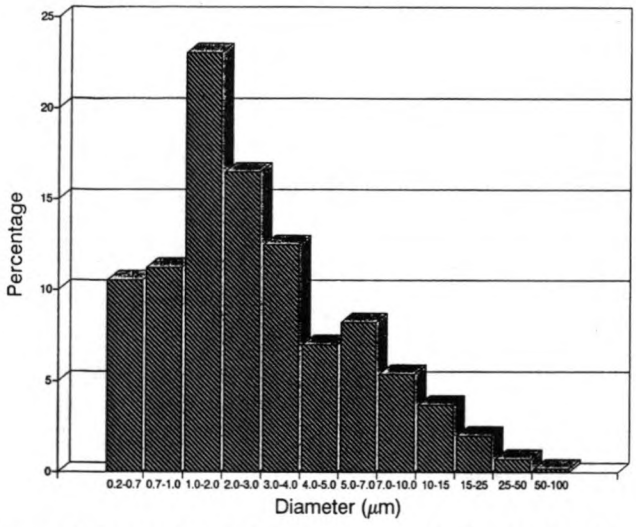

Figure 4. The number distribution (in percent) of all analyzed particles versus their diameter.

shows the size distribution of the detected particles and not the real aerosol size distribution as it can be found in the atmosphere. It can be seen that only 10% of the detected particles were smaller than 0.7 μm, which confirms the calculated cutoff point of 0.8 μm. Although particles with diameters up to 100 μm were found, only 2% had diameters larger than 15 μm. The relative low abundance of these very large particles might be a result of the splintering of big particles during the impact, especially of liquid drops (*41*).

Summary and Conclusion

In order to investigate the importance of giant airborne particles, air sampling was carried out over the southern bight of the North Sea. Analysis of the collected samples was done by EPXMA.

Four sources of giant aerosol particles were found by PFA: aluminosilicates, combustion processes, and an industrial and a marine source. Hierarchical and nonhierarchical cluster analysis enabled us to find a clear distinction between flights for which the associated air masses were marine or continental.

The most abundant particle types were fitted with a log-normal size distribution. The experimentally found distributions for sea salts, sea salts enriched with sulfur, and organic, $CaSO_4$, and Fe-rich particles were fitted well by the log-normal distribution, while aluminosilicates had a bimodal size distribution with average size maximums at 4 and 15 μm.

To confirm the importance of giant aerosol particles, further research on giant particle size distributions and collection efficiencies is needed. In the near future, more experiments with the impaction rod should lead to a method which enables us to calculate the upper size limits of the collected giant particles. The design and use of improved and new giant aerosol samplers should allow us to obtain a more precise view on the giant aerosol size distribution and composition.

Registry No. Na, 7440-23-5; Mg, 7439-95-4; Al, 7429-90-5; Si, 7440-21-3; P, 7723-14-0; S, 7704-34-9; Cl, 7782-50-5; K, 7440-09-7; Ca, 7440-70-2; Fe, 7439-89-6; Cu, 7440-50-8; Zn, 7440-66-6; Cr, 7440-47-3; O_2, 7782-44-7.

Literature Cited

(1) Injuk, J.; Otten, Ph.; Rojas, C.; Wouters, L.; Van Grieken, R. Atmospheric Deposition of Heavy Metals (Cd, Cu, Pb and Zn) into the North Sea. Final report to Rijkswaterstaat, Dienst Getijdewateren, 's Gravenhage, The Netherlands, in the framework of project NOMIVE*2 task No. DGW-920; University of Antwerp, 1990.
(2) Jaenicke, R. In *Chemistry of the Unpolluted and Polluted Troposphere*, 1st ed.; Georgii, W., Jaeschke, W., Eds.; D. Reidel Publishing Co.: Dordrecht, The Netherlands, 1982; pp 341–374.
(3) Dedeurwaerder, H. L. Ph.D. Dissertation, University of Brussels, 1988.
(4) Jaenicke, R. *Ann. N.Y. Acad. Sci.* **1980**, *338*, 317–322.
(5) Betzer, P. R.; Carder, K. L.; Duce, R. A.; Merrill, J. T.; Tindale, N. W.; Uematsu, M.; Costello, D. K.; Young, R. W.; Feely, R. A.; Breland, J. A.; Bernstein, R. E.; Greco, A. M. *Nature* **1988**, *336*, 568–571.
(6) Noll, K. E.; Pilat, M. J. *Atmos. Environ.* **1971**, *5*, 527–540.
(7) Whitby, K. T.; Husar, R. B.; Liu, Y. H. *J. Colloid Interface Sci.* **1972**, *39*, 177–204.
(8) Mészáros, Á. *Tellus* **1971**, *23*, 436–440.
(9) Yoshiaki, T. *NASA Access (TN 30)* **1965**, 37–41.
(10) De Leeuw, G. *Tellus* **1986**, *38B*, 51–61.
(11) De Leeuw, G. *J. Aerosol Sci.* **1986**, *17*, 293–296.
(12) Otten, Ph.; Rojas, C.; Wouters, L.; Van Grieken, R. Atmospheric deposition of heavy metals (Cd, Cu, Pb and Zn) into the North Sea. Report 2 to Rijkswaterstaat, Dienst Getijdewateren, 's Gravenhage, The Netherlands, in the framework of project NOMIVE*2 task No. DGW-920; University of Antwerp, 1989.
(13) Raeymaekers, B. Ph.D. Dissertation, University of Antwerp, 1986.
(14) Van Espen, P. *Anal. Chim. Acta* **1984**, *165*, 31–49.
(15) Bernard, P. C.; Van Grieken, R. E.; Eisma, D. *Environ. Sci. Technol.* **1986**, *20*, 467–473.
(16) Anderberg, M. R. *Cluster Analysis For Applications*; Academic Press: New York, 1973.
(17) Bernard, P. C. Ph.D. Dissertation, University of Antwerp, 1989.
(18) Henry, R. C.; Hidy, G. M. *Atmos. Environ.* **1979**, *13*, 1581–1596.
(19) Henry, R. C.; Hidy, G. M. *Atmos. Environ.* **1982**, *18*, 1507–1517.
(20) Rojas, C.; Artaxo, P.; Van Grieken, R. *Atmos. Environ.* **1990**, *24B*, 227–241.
(21) Schaug, J.; Rambæk, J.; Steinnes, E.; Henry, C. *Atmos. Environ.* **1990**, *24A*, 2625–2631.
(22) Wolff, G. T.; Sick, J. S.; Chan, T. L.; Korsog, P. E. *Atmos. Environ.* **1986**, *20*, 2231–2241.
(23) Rojas, C.; Van Grieken, R., submitted to *Atmos. Environ.*
(24) Slinn, W. G. N. in *Atmospheric Sciences and Power Production*; Biomedical Environmental Research, U.S. Dept. of Energy, U.S. Government Printing Office: Washington, DC, 1983.
(25) Seinfeld, J. H. *Atmospheric Chemistry and Physics of Air Pollution*, 1st ed.; John Wiley & Sons: New York, 1986; pp 621–625.
(26) Heidam, N. Z. *Atmos. Environ.* **1982**, *16*, 1923–1931.
(27) Blanchard, D. C. In *Air–Sea Exchange of Gases and Particles*, 1st ed.; Liss, P. S., Slinn, W. G. N., Eds. *NATO ASI Ser. D* **1983**, *108*, 407–444.
(28) Pacyna, J. M. *Atmos. Environ.* **1984**, *18*, 41–50.
(29) Kretzschmar, J. G.; Cosemans, G. *Atmos. Environ.* **1978**, *13*, 267–277.
(30) Eriksson, E. *Tellus* **1960**, *12*, 63–109.
(31) Hitchcock, D. R.; Spiller, L. L.; Wilson, W. E. *Atmos. Environ.* **1979**, *14*, 165–182.
(32) Clegg, S. L.; Brimblecombe, P. *Atmos. Environ.* **1984**, *19*, 465–470.
(33) Legrand, M. R.; Lorius, C.; Barkov, N. I.; Petrov, V. N. *Atmos. Environ.* **1987**, *22*, 317–331.
(34) Andreae, M. O.; Charlson, R. J.; Bruynseels, F.; Storms, H.; Van Grieken, R. E.; Maenhaut, W. *Science* **1986**, *232*, 1620–1623.
(35) Shattuck, T.; Germani, M.; Buseck, P. in *Environmental Applications of Chemometrics*, 1st ed.; Breen, J. J., Robinson, P., Eds.; ACS Symposium Series 292; American Chemical Society: Washington DC, 1985; p 119.

Table III. Average Composition, Size, and Shape for the Groups Found by the Nearest Centroid Sorting Performed on the EPXMA-Analyzed North Sea Giant Particles

group no.	group abund, %	diam, μm	relative abundance per element, wt %													
			Na	Mg	Al	Si	P	S	Cl	K	Ca	Cr	Fe	Ni	Cu	Zn	O
1	22	3.2	0.6	0.5	0.6	2.7	0.6	1.3	1.1	0.1	61	0	0.9	0	0	0	31
2	21	4.2	14	1.0	0.1	0.8	0	3.7	75	1.6	2.3	0	0.3	0	0	1.1	0
3	20	3.0	0.9	1.5	0.7	2.2	0.1	21	2.0	0.7	22	0.1	2.4	0.3	0.1	0.1	46
4	17	2.7	1.6	4.0	2.7	4.2	3.1	6.7	11	10	5.0	0.4	5.7	0.6	1.1	11	32
5	14	3.8	0.1	0.5	8.1	28	0.1	1.6	1.2	2.0	6.1	0	4.7	0	0	0.1	47
6	5	2.6	0	0.3	0.3	1.7	0.1	0.1	1.4	0.2	1.5	1.8	60	0.6	0	0.2	31
7	1	2.2	69	0	0	0	0	2.1	0.8	0.4	0	0	0	0	0.3	0	27

In flights with continental air mass history, potassium and zinc chlorides and phosphates were found. They probably result from burning organic material and municipal waste (*38*, *39*). Results point to a low content of heavy metals in the giant particle size range. Since heavy metals are commonly emitted in high-temperature combustion processes, they are mostly drained into the atmosphere as gases, which condense from the vapor phase to predominantly submicrometer particles at sudden cooling. The occurrence of submicrometer aerosols containing heavy metals above the North Sea has indeed been reported in EPXMA results (*40*).

The sea-salt particles (4%) were only found in the lowest tracks (20 m). The iron-rich and quartz particles were only found in small amounts (3–4%).

In summary, in flights with air masses with marine influence, the samples were mainly characterized by sea salts, sea salts enriched with sulfur, and $CaSO_4$ particles. Samples from flights correlated with air masses of a continental origin were high in aluminosilicates and Ca-rich, organic, and $CaSO_4$ particles.

3. Nonhierarchical Clustering. To get an overall view on the particle types collected in all samples together, a nonhierarchical clustering was performed. In order to classify the 500 measured particles into 7 particle groups in each of the 25 collected samples, a hierarchical clustering (Ward's method) was performed on each of the 25 samples separately. The average elemental abundances of 175 (7 × 25) particle groups (7 in each sample), obtained from the clustering of the 25 samples, were clustered again, which provided us again with 7 groups of average elemental abundances now for all 25 samples together. These were further used as centroids for the nonhierarchical clustering. Results of the ZAF-corrected nonhierarchical clustering are given in Table III. The oxygen in Table III has been calculated by assuming all elements were present in the form of oxides.

From Table III it appears that 22% of the detected particles consist of Ca-rich (61% Ca) particles. Nearly as much (21%) of the North Sea giant aerosols are sea salts, while 20% of the particles are found to be $CaSO_4$ particles. From Table III it can be seen that the Cl/Na ratio in group 2 is 5.4, which is greater than the seawater value. This is a result of the clustering. Since not all particles, which are brought together in the so-called "sea-salt" cluster, necessarily contain the same amount of Na and Cl, the Cl/Na weight ratio after the clustering may significantly differ from the actual Cl/Na seawater ratio. Group 4 can be identified as potassium, zinc chlorides. The abundance of this particle type (18%) is very high compared to the results obtained from the hierarchical clustering, it is likely that they have been mixed up in the nonhierarchical clustering with particles without major X-ray intensities, previously identified as organic particles. Group 5 is characterized by high contents of Al, Si, Ca, and Fe (respectively 8%, 28%, 6%, and 5%) and therefore it can be ascribed to aluminosilicates (14%). Group 6 contains Fe-rich (60% Fe) particles (5%), while the low-abundance group (1%) is identified by a high content of Na (69% Na). The size of the particles varies between 2.2 μm for the Na-rich particles and 4.2 mm for the sea salts.

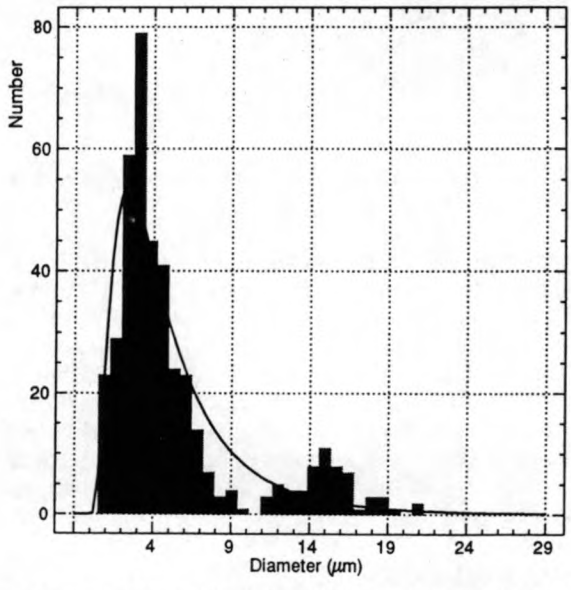

Figure 3. The log-normal fitted size distribution of the aluminosilicates.

4. Particle Size and Distribution. A description of the size distribution of several of the most abundant particle types was achieved by means of a log-normal distribution. The experimentally found size distributions of sea salts, sea salts enriched with sulfur, and $CaSO_4$, Fe-rich, and organic particles turned out to be fitted well by the log-normal distribution, and they also had average sizes between 1 and 3 μm. Aluminosilicates, on the other hand, presented a bimodal distribution; the total distribution could be split up into two separate distributions with average diameters centered at 4 and 15 μm. This suggests the presence of two completely different sources of aluminosilicates. Closer observation of the particle size and shape revealed that the smaller sizes were round in shape, while the fraction of the particles with diameters around 15 μm were often irregularly shaped. This suggests that the smaller, spherical fraction originates from high-temperature combustion processes, which lead to fly ash. Especially when the sampled air masses came from Eastern Europe, these particles were responsible for the major part of the aluminosilicates (>60%). The irregularly shaped larger aluminosilicates, on the other hand, are windblown soil dust particles. The log-normal fitted size distribution of the aluminosilicates is shown in Figure 3.

In Figure 4, a number distribution for all 12500 particles as a function of their size is shown. Attention must be drawn here to the fact the size spectrum is cut off at the lower end by the impaction rod. Therefore, Figure 4 only

Table II. Results of the Hierarchical Clustering

group no.	abund, %	av diam, μm	elements detected	identification
	(a) Flights with Little Continental Influence			
1	31	3.5	Na, Cl, S	S enriched seaspray
2	18	3.3	Na, Cl	seaspray
3	16	2.9	Ca, S	gypsum
4	10	2.0	Fe	Fe-rich
5	8	3.9	S, Cl	sulfates
6	6	3.1	Ca, S, Cl	Cl enriched gypsum
7	5	3.2	Al, Si, Cl	aluminosilicates
8	5	3.1	none	organic
9	1	1.9	Na	Na-rich
	(b) Flights with a Strong Continental Influence			
1	36	3.1	Ca (Si, P)	Ca-rich
2	17	2.1	none	organic
3	12	3.3	Ca, S	gypsum
4	11	4.3	Al, Si	aluminosilicates
5	4	2.7	K, Cl (Zn)	K, ZnCl
6	4	3.7	Cl, Na	seaspray
7	3	3.6	Fe	Fe-rich
8	2	2.6	Si	quartz

centrations of Na, Mg, S, and Cl are to be expected at lower altitudes, as observed. Factor 3 has high loadings for Cu and Zn, suggesting the existence of an industrial source for Cu and Zn. Generally, Zn is emitted evenly in Europe, whereas emissions of Cu are attributed to Central and Eastern Europe (*28*). Heavy metal concentrations in the atmosphere were reported to reach maximums with east-southeast winds (*29*) and should therefore be mainly found in flights with a continental air mass history. This was recently confirmed by Injuk et al. (*1*). Cl and K, which characterize factor 4, are probably the result of combustion processes. The burning of organic material leads to emission of K, but also the burning of municipal waste in incinerators leads to potassium and zinc chlorides. In summary, PFA on 13 variables distinguished 4 classes of giant aerosol sources: aluminosilicates (Al, Si, Ca, Fe), marine aerosols (Na, Mg, S, Cl), and aerosols from metallurgical processes (for Zn, Cu) and combustion processes (for K, Cl).

2. Hierarchical Clustering. Only 6 out of 25 samples correspond to a wind sector which is representative of marine air masses, whereas the remaining 19 samples correspond to other wind directions, which have as major sources Belgium, The Netherlands, Germany, Poland, Czechoslovakia, and Denmark. Depending on the sample, three to seven different aerosol groups were distinguished. Overall results of the hierarchical clustering for flights with, respectively, little and strong continental influences are listed in Table IIa and b. In these tables, average diameter, abundance (in percent), and the identification of each particle type are shown.

(a) Marine Air Masses. The flights with little continental influence are characterized by southwest wind directions. Then air masses come directly from the Atlantic Ocean through the English Channel, and anthropogenic influence is consequently low.

In these marine flights, mainly untransformed and transformed sea salts were found, accounting for up to 49% of the total aerosol abundance. Sea salt and transformed sea salt find their existence mostly in the mechanism of white cap formation during high-speed winds and bubble bursting. The sea-spray particles can then react with other compounds in the atmosphere. Eriksson (*30*) stated that the Cl loss in sea salt is the result of pH-lowering reactions between NaCl and acid atmospheric components such as H_2SO_4, and this was later confirmed by Hitchcock et al. (*31*). As a result, degassing of HCl takes place and Cl^- is replaced by SO_4^{2-} (*32*). The abundance of the transformed sea salt enriched with S was positively correlated with altitude. This seems in agreement with the fact that these aged aerosols had a residence time long enough to allow chemical reactions with other compounds.

Ca-rich (and especially $CaSO_4$) particles account for up to 22% of the total aerosol abundance. Ca-rich particles, which may or may not be associated with sulfur, were found in all flights. $CaSO_4$ particles were very common in marine as well as in continental flights. $CaCO_3$ could be transformed into $CaSO_4$ in the atmosphere by H_2SO_4 (*33*). Some of the $CaSO_4$ particles contain Cl^-. This might point out that $CaSO_4$ particles are partly of marine origin: interaction between marine $CaCO_3$, mainly coming from skeletons of pelagic organisms, and H_2SO_4 in the air could be a possible source. Fractionated crystallization of gypsum ($CaSO_4 \cdot 2H_2O$) out of sea spray and splitting off of the gypsum crystals could be another source (*34*). Other marine elements (such as Na, Mg, and K) were not observed in this type of particle.

In the lower tracks (under 300 m), a considerable part of the detected particles was of anthropogenic origin. The occurrence of these anthropogenic particles explains the aluminosilicates (5%) and organic (5%) and Fe-rich (10%) particles found in the hierarchical clustering. Particle resuspension could be a possible source for the anthropogenic particles, but more likely direct emission from land could explain the occurrence of these particle types. In the predominantly marine flights, air masses at lower levels came over the northwest of France. In the region of Roubaix and Le Havre (France) the iron industry is very intense, which could explain the high abundances of Fe in the lower tracks. Also the power plants in northwest France can partly explain the high abundance of $CaSO_4$.

(b) Continental Air Masses. Particle abundances during periods in which the air masses came from the continent were mostly dominated by Ca-rich, organic, and $CaSO_4$ particles and aluminosilicates. Ca-rich particles and different combinations mainly containing Ca (e.g., Ca–P, Ca–Si–S, and Ca–Fe) yield 36% of the aerosol abundance. Abundances of Ca-rich and $CaSO_4$ particles were always higher for flights with a continental air mass history than for marine flights. Ca-bearing particles can be related to high-temperature combustion processes as well: large quantities of $CaCO_3$ are used in thermal power plants, as a desulfurization agent, to enhance the oxidation of SO_2 and neutralize the SO_3; this leads to sulfates. Furthermore, some of the $CaSO_4$ particles were enriched with Si. This particle type is associated with coal combustion (*35*).

Particles with no major X-ray intensities were classified as organic (17%); they seem anticorrelated with altitude and could therefore be related to biogenic material such as pollen, spores, and bacteria. Organic particles are also emitted during combustion of fossil fuels.

Aluminosilicates are clearly less abundant in typical marine flights than in flights with continental influence, where they account for 11% of the particle abundance. The aluminosilicates can be divided into two groups: windblown soil dust and fly ash. Even though these particles have roughly the same chemical composition, they usually differ in morphology, as will be discussed later. A considerable amount of the aluminosilicates contained S, which can be related to the fact that a substantial part of these particles originates from coal combustion (fly ash). On the other hand, this might be a result of a sulfur layer formed on the soil dust particles, as reported by Winchester et al. (*36*, *37*).

Table I. Varimax Rotated Factor Loading Matrix for the 25 North Sea Giant Aerosol Samples[a]

variable	factor 1	factor 2	factor 3	factor 4	communality	standard deviation
Na	−0.42	0.69	0.36		0.814	0.09
Mg		0.75			0.627	0.13
Al	0.95				0.928	0.06
Si	0.96		−0.18		0.956	0.05
P	−0.40	−0.85			0.913	0.06
S		0.86			0.878	0.08
Cl	−0.31	0.73		0.46	0.883	0.07
K	−0.28			0.84	0.822	0.09
Ca	0.59	−0.60			0.773	0.10
Fe	0.90		−0.26		0.887	0.07
Cu	−0.30		0.83	0.25	0.867	0.08
Zn			0.85		0.813	0.09
height	0.38	−0.35	0.36	−0.52	0.672	0.11
eigenvalue	4.74	3.54	1.39	1.16		
% variance explained	36.3	27.1	10.6	8.9		
source ID	aluminosilicates	marine	industrial	combustion process		

[a] Absolute values for factor loadings smaller than 3 times their standard deviation were deleted for simplicity.

abundance. Therefore, they were excluded from the data matrix. One of the most important problems of PFA is the decision of the dimensionality of the model. The decision on how many factors should be retained is often rather subjective. But it is usually a "rule of thumb" to retain as many factors as there are eigenvalues greater than unity. More detailed information on the strategy for performing PFA on EPXMA data can be found elsewhere (*23*).

Collection Uncertainties

Collection of giant aerosols is not a straightforward matter. In aerosol sampling by filtration, suction velocities are usually too small to collect giant aerosols. Aerosol sampling by impaction as a function of particle size normally requires isokinetic conditions for representative sampling.

In order to calculate the collection efficiency E of the impaction rod on top of the aircraft, we assumed the same physics for the impactor as for the scavenging of particles by rain droplets; the impaction rod was considered as a droplet (diameter 1 cm) falling through the air with a speed equal to the speed of the airplane (75 m/s) during collection. For the calculations, the equations given by Slinn (*24*) were used. These equations treat the impaction surface as a sphere, but during the calculations this was corrected to the actual shape and dimensions of the impactor rod. Further theoretical background can be found elsewhere (*25*).

The results show (Figure 2) that an impaction rod, at aircraft speed, can be used to collect particles with a diameter above 0.8 μm. This seems to compare well with the obtained EPXMA results, where the smallest detected particles had diameters around 0.6 μm. The slight increase in collection efficiency for small particles is the result of collection by Brownian diffusion. Because Brownian diffusivity of particles increases as the particle size decreases, this effect is more distinct for small particles.

The upper size range of the collected particles is limited by bounce-off and reentrainment. When a particle strikes the surface, it can bounce off back into the gas stream or cause a previously collected particle to be knocked off the surface. In both cases, for single-stage impactors, this means that the concentration of particles collected is too small. These problems can be minimized by coating the surface of the impactor to absorb the kinetic energy of the particle. EPXMA results showed maximum diameters

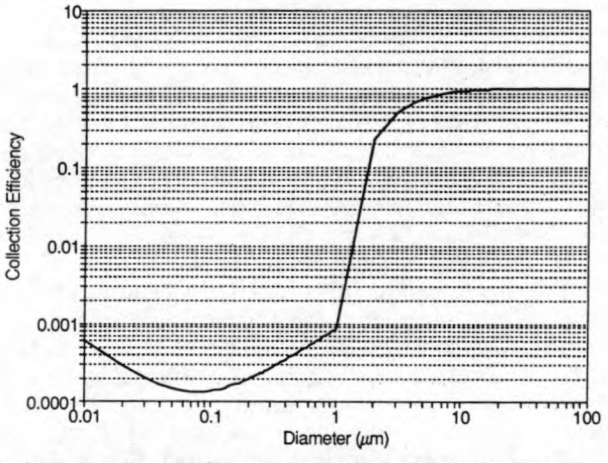

Figure 2. Calculated collection efficiency for giant North Sea particles collected with a direct impaction rod.

around 25 μm. Less than 1% of the detected particles were larger than 25 μm.

Results and Discussion

1. Principal Factor Analysis. PFA, performed on the correlation matrix of the data set, which gives the pattern of relationships between the factors, resulted in four eigenvalues greater than 1 (4.74, 3.54, 1.39, 1.16), while the fifth and sixth eigenvalues were respectively 0.71 and 0.56. Therefore, further calculations were performed with the four-factor solution.

Results of the Varimax rotated factor analysis are shown in Table I. Only factor loadings greater than 3 times their standard deviation are shown, because only these are considered as statistically significant (*26*). The four factors together explain 83% of the total variance. Communalities are high for all variables, except for Mg, Ca, and "altitude". Factor 1 has high loadings for Al, Si, Ca, and Fe. Aluminosilicates, both windblown soil dust and fly ash, which have similar chemical compositions with respect to many elements, probably correspond to this factor. Factor 1 is positively correlated with altitude, which could be explained by the presence of a long-range-transported mineral aerosol at high altitudes. Factor 2 most likely represents marine impact. Furthermore, this marine source is slightly anticorrelated with altitude. If one considers the mechanism by which matrix and trace elements are injected from the sea into the atmosphere (*27*), high con-

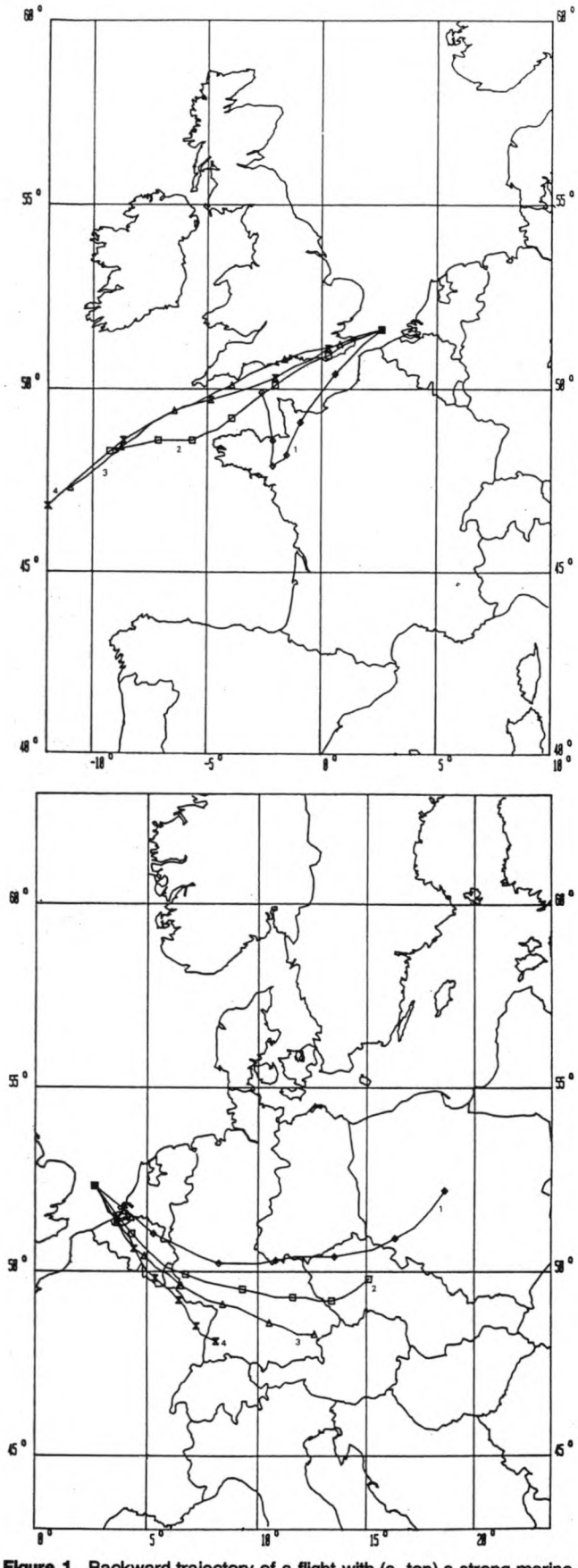

Figure 1. Backward trajectory of a flight with (a, top) a strong marine influence or (b, bottom), a strong continental influence: (1) 140 m, (2) 770 m, (3) 1450 m, (4) 3015 m.

information is stored on a disk.

3. Multivariate Methods. To allow interpretation of the obtained information, hierarchical and nonhierarchical cluster analyses were used to classify particles with similar chemical composition into "particle groups".

Hierarchical cluster analysis was used to classify the 500 particles, measured in each of the 25 samples, into groups based on their chemical composition. It was then possible to calculate the percent abundance of each group in each sample. Here, the clustering was performed on the normalized X-ray elemental intensities of each analyzed particle. We used the software package DPP (*14*). Ward's method (error sum of squares) was chosen because it yields a maximal internal homogeneity (*15*). The condition for the joining of two groups, using Ward's method, is that the decrease in homogeneity is kept as small as possible. Thus, whenever a pair of clusters is joined, the homogeneity is calculated by determining the sum of square distances of each object to the centroid of the cluster. This calculation is done for each pair of clusters and those clusters will be joined which will lead to the smallest decrease in homogeneity.

Since the hierarchical clustering cannot be used for simultaneous classification of all measured particles in all samples due to the enormous amount of computer time calculating the distances between 12 500 particles in each cycle of a hierarchical clustering would take, we used the nearest centroid sorting technique. Nearest centroid sorting is a group of nonhierarchical cluster methods, which classifies objects (particles) in clusters according to their distance from the centroids of a fixed number of previously chosen training vectors, which are obtained by a hierarchical clustering. The distances between all objects and the training vectors are calculated. All objects that were incorrectly classified in the initial clustering are relocated with the nearest centroid method. The centroids of the new clusters are calculated. This procedure is repeated until convergence appears. The result of such a clustering is that objects in a cluster are very similar to each other, while the clusters themselves are well separated. More theoretical aspects on nonhierarchical clustering can be found in publications of Anderberg (*16*) and Bernard (*17*).

After the clustering, a standardless ZAF correction was carried out in order to convert the relative peak intensities into elemental weight compositions. Performing ZAF corrections on each of the measured particles separately would, in principle, be better, but would require an enormous amount of computer calculating time. Therefore, the ZAF correction is performed after the clustering.

To identify the different sources for giant aerosols, principal factor analysis (PFA) with orthogonal Varimax rotation was performed on the data set. PFA has already been used in many other atmospheric studies, e.g., by Henry and Hidy (*18*, *19*), Rojas et al. (*20*), Schaug et al. (*21*), and Wolff et al. (*22*). The objective of PFA is to take p variables and find linear combinations of these to produce uncorrelated new variables (factors), which are ordered in decreasing order of importance so that the first one explains the largest amount of variance. It is a common practice to perform an orthogonal rotation of the original factors in order to facilitate their interpretation. In this case, the Varimax rotation was chosen. This type of orthogonal rotation consists of maximizing the variance of the squares of the factor loadings. Here the data matrix consisted of 13 variables (Na, Mg, Al, Si, P, S, Cl, K, Ca, Fe, Cu, Zn, and altitude). An element was considered to be detected if the X-ray intensity of the element was found above detection limit in one of the 500 analyzed particles for each sample. Occasionally other elements such as Pb, Ni, Cr, Br, Ti and V were detected in a particle. However, when detected, these elements were found in particles that always contributed less than 0.5% of the total aerosol

2887

Reprinted from ENVIRONMENTAL SCIENCE & TECHNOLOGY, Vol. 26, 1992

Characterization of Individual Giant Aerosol Particles above the North Sea

Hans Van Malderen,* Carlos Rojas, and René Van Grieken

Department of Chemistry, University of Antwerp (UIA), Universiteitsplein 1, B-2610 Wilrijk-Antwerp, Belgium

■ In order to investigate the importance of giant airborne particles, air sampling was carried out using an aircraft which flew at different altitudes over the southern bight of the North Sea. A set of 25 samples was collected with a steel rod on top of the airplane. Some 12500 individual particles were analyzed using electron probe X-ray microanalysis. Principal factor analysis allowed identification of four sources of giant aerosol particles: aluminosilicates, combustion processes, industrial processes, and marine sources. Hierarchical and nonhierarchical cluster analysis enabled us to classify the analyzed particles. A clear distinction was found between flights for which the associated air masses were marine or continental. The experimentally found size distributions for sea salts, sea salts enriched with sulfur, and organic, $CaSO_4$, and Fe-rich particles were fitted well by the log-normal distribution, and average sizes of these particle types were found to be ~ 3 μm. Aluminosilicates had a bimodal size distribution with average size maxima at 4 and 15 μm.

Introduction

The North Sea is surrounded by highly populated and heavily industrialized countries and consequently it is subjected to pollution of industrial, domestic, and agricultural origin through different channels. Input of contaminants, transported by rivers, and direct dumping into the North Sea have long been known as major sources of pollution. But is has been shown that atmospheric input of particulate matter or aerosols by wet and dry deposition processes contributes significantly to the North Sea pollution (*1*).

Every aerosol particle type differs in shape, size, density, and chemical composition. Each of these physical parameters has a strong influence on the behavior of the aerosol in the air.

Giant aerosol particles with a radius above 1 μm, and especially those larger than 10 μm, are of extreme importance to aerosol fluxes. Their concentration in the atmosphere is low, but is should be emphasized that a particle of, for example, 10 μm has 1000 times more mass than a 1-μm particle and its deposition velocity is ca. 100 times higher (*2*). Calculations by Dedeurwaerder (*3*) showed that deposition of giant particles explains 94% (Cd), 96% (Cu), 85% (Pb), and 88% (Zn) of the total dry deposition above the North Sea. Furthermore, if global aerosol production rates are estimated, discrepancies of 0.1–4000 tons/year occur, depending on whether particles with diameters up to 1 or 1000 μm are included in the calculations (*4*). One should expect giant particles to be of local interest only, since a typical residence time of 1 day has been reported by Jaenicke (*4*); however, the presence of giant mineral aerosols has been observed in long-range transport (*5*). All these facts point to the extreme importance of giant aerosol particles for the total deposition process.

Due to their relatively low concentrations, it was not until the early 1970s that serious interest was taken in giant aerosol particles. Noll and Pilat (*6*) and Whitby et al. (*7*) pointed to the importance of these particles in the total deposition process and cloud and precipitation processes. They stated that, of the atmospheric aerosol mass distribution, approximately 81% of the total mass was accounted for by particles larger than 1 μm (of which 45% was by particles with diameters between 10 and 50 μm). Mészáros (*8*) studied the relation between the giant particle size distribution and the relative humidity. A major part of the published articles focused on giant sea spray particles (*9–11*). But sampling difficulties and measurement errors are still the limiting factor in the study of these particles. This probably explains why the total amount of published articles on this topic is very limited until now. This article will approach the collection and analysis of the giant particles from a new and different point of view.

Experimental Section

1. **Sampling Strategy.** In order to measure at different altitudes above the North Sea, a twin engine aircraft (Geosens B.V., Rotterdam, The Netherlands) equipped with different gas and particulate matter sampling devices, was used. To collect giant aerosol particles, a special sampling device, consisting of a circular impaction surface (diameter 1 cm) covered with a particle-free sticky tape and supported by a vertical bar, was exposed outside the airplane perpendicular to the streamlines of the air around the plane and directed upwind. Only the front side of the rod was covered with a sticky tape, and therefore, particles were only collected on this side of the impaction device. Although very simple, this appeared to be an efficient way of collecting giant aerosols. More details on sampling strategy and flight plan can also be found elsewhere (*12*).

In each flight, samples were taken at different altitudes more or less equally spaced between the inversion layer and the sea level in order to obtain a vertical distribution of the giant aerosol. For every flight a set of six samples was taken for each altitude. The last track, only 10–30 m above sea level, was intended to assess particle resuspension by sea spray. All flights were carried out during relative cloudless and dry periods. Information about the origin of the collected air masses was obtained by studying the backward trajectories, which were provided by the Royal Dutch Meteorological Institute (KNMI). Two trajectories, shown in Figure 1a and b, are typical for trajectories of air masses with a marine and continental origin, respectively. The different pressure levels (1000, 925, 850, 700 hPa) correspond to the respective altitudes above sea level (140, 770, 1450, 3015 m) (SPT).

2. **Analysis.** In 5 different flights, a set of 25 samples was collected and the analysis of 12500 particles (500 in each sample) was performed by electron probe X-ray microanalysis (EPXMA) on a 733 Superprobe (JEOL, Tokyo, Japan) equipped with a TN-2000 system (Tracor Northern). For every analysis, an accelerating voltage of 20 kV and a beam current of ca. 1 nA was used. The EPXMA technique allows one to obtain morphological data such as average diameter and shape factor while the chemical composition can be derived from an energy-dispersive X-ray spectrum. The single-particle analysis program 733B (*13*) allowed us to perform automated individual particle analysis. Localization of a particle is obtained by successive horizontal scanning with the electron beam. During this process, contour pixels of a particle are stored into the memory. When all contour grid points have been stored, area, perimeter, and diameter are calculated and an X-ray spectrum is accumulated. All this

 0013-936X/92/0926-0750$03.00/0

Selected article #8:

Characterization of individual giant aerosol particles above the North Sea
H. Van Malderen, C. Rojas and R. Van Grieken
Environmental Science and Technology, 26 (1992), 750-756

dose-response relationship to dietary selenium" (Hakkarainen et al, 1978). Inasmuch as some of these studies correlate selenium dietary levels to glutathione peroxidase activity in serum or erythrocytes, the dominant contribution of the erythrocytes to the total blood enzyme activity: 85.8%, should be emphasized (Jorgensen et al, 1977). Hence, erythrocyte glutathione peroxidase is an excellent correlator for selenium intake only after 4 weeks, as it incorporates into erythrocytic glutathione peroxidase only during erythropoiesis (Hafeman et al, 1974). The erythrocyte enzyme is totally selenium-dependent, while the plasma enzyme is not. For these reasons we limited the search for a possible correlation between selenium intake and glutathione peroxidase activity in the erythrocytes, and only after 4 weeks of drinking high-selenium water.

The present U.S. Environmental Protection Agency drinking-water standard for selenium of 10 µg/l, was suggested with the unfounded rationale of selenium suspected as being a carcinogen. Lafond and Calabrese 1979 suggest that 50µg/l be determined as the upper standard for selenium in drinking water, this will providing sufficient selenium for glutathione peroxidase activity and still be below the toxic effects of this element. Such a level seems preferable in light of the now vast literature on the relevance of selenium in the human, and its possible anticarcinogenic role in high-proliferative diseases like cancer and psoriasis.

ACKNOWLEDGMENTS

The authors are indebted to Prof. S. Dikstein for his stimulation and advice, to Mrs. R. Golan and Mrs. J. Ben-Ezzer for valuable guidance in establishing the glutathione peroxidase assay, and to Dr. Rosenthal of the Hydrological Service for collecting some of the water samples. This study was supported by the Israeli Health Resorts Authority, via a grant from the Israeli Ministry of Health, and by the Belgian Ministry of Public Health, via the research project "Selenium Impact".

REFERENCES

Anderson, E.P., Kalckar, H.M., Kurahashi, K. and Isselbacher, K.J.: J. Lab. Clin. Med. 50:469-477 (1975).

Beutler, E.: Red Cell Metabolism - A manual for biochemical methods. 2nd Ed., Grune and Stratton, New York, pp 71-73 (1975).

Burk, R.F. Jr., Whitney, R., Frank, H. and Pearson, W.N.: J. Nutrition 95:420-428 (1968).

Burk, P.F.: Selenium in man. in Trace Elements in Human Health and Disease (Prasad, A.S. and Oberlas, D., Eds.), Academic Press, N.Y., 2:105-133 (1976).

Chow, C.K. and Tappel, A.L., J. Nutr. 104:444-451 (1974).

Griffin, A.C.: The chemopreventive role of selenium in carcinogenesis in Molecular Inter-relations of Nutrition and Cancer (Arnott M.S., ed.) Raven Press, 401-408 (1982).

Hafeman, D.G., Sunde, R.A. and Hoekstra, W.G., J. Nutr. 104:580-587 (1974).

Hakkarainen, J., Lindberg, P., Bengtsson, G. and Jonsson, L., Acta. Vet. Scand. 19:269-284 (1978).

Jorgensen, P.F., Hyldgaard-Jensen, J. Movstgaard, J., Acta. Vet. Scand. 18:323-334 (1977).

Kasperek, K., Lombeck, I, Feinendegen, L.E. and Bremer, H.J.: Dependence of the activity of the erythrocyte glutathione peroxidase and the selenium content of blood on different selenium intakes in dietary treated patients. in Trace Element Analytical Chemistry in Medicine and Biology. Walter de Gruyter Publ., Berlin pp 75-82 (1980).

Lane, H.W., Dudrick, S. and Warren, D.C., Proc. Soc. Expt. Biol. Med. 167:383-390 (1981).

Lafond, M.G. and Calabrese, E.J., Medical hypotheses 5:877-899 (1979).

Nakao, M. and Nakayama, T. and Tankura, T., Nature (New Biol.) 246:94 (1973).

Perona, G., Cellerino, R., Guidi, G.C., Casaril, M. and Pizzols, G.: Haematologia 62:156-166 (1977).

Riley, J.F., Experientia 24:1237-1238 (1968).

Robberecht, H.J. and Van Grieken, R.E., Anal. Chem. 52:449-453 (1980).

Rudolph, N. and Wong, S.L., Pediatr. Res. 12:789-792 (1978).

Selenium: Medical and biological effects of environmental pollutants. National Academy of Sciences, Washington, D.C., p. 22-25 (1976).

Shamberger, R.J., Tytko, S. and Willis, C., Trace Sub. Environ. Health 7:35-40 (1974).

Smith, P.J., Tappel, A.L. and Chow, C.K., Nature 247:392-393 (1974).

Thomson, C.D., Rea, H.M., Doesburg, V.M., and Robinson, M.F., Brit. J. Nutr. 37:457-460 (1977).

Selected article # 6:

Internal mixture of sea salt, silicates and excess sulfate in marine aerosols
M.O. Andreae, R.J. Charlson, F. Bruynseels, H. Storms, R. Van Grieken and W. Maenhaut
Science, 232 (1986), 1620-1623

Reprint Series
27 June 1986, Volume 232, pp. 1620–1623

SCIENCE

Internal Mixture of Sea Salt, Silicates, and Excess Sulfate in Marine Aerosols

MEINRAT O. ANDREAE,* ROBERT J. CHARLSON, FRANK BRUYNSEELS, HEDWIG STORMS, RENE VAN GRIEKEN, AND WILLY MAENHAUT

Internal Mixture of Sea Salt, Silicates, and Excess Sulfate in Marine Aerosols

MEINRAT O. ANDREAE,* ROBERT J. CHARLSON, FRANK BRUYNSEELS, HEDWIG STORMS, RENE VAN GRIEKEN, WILLY MAENHAUT

Individual aerosol particles from the remote marine atmosphere were investigated by scanning electron microscopy and electron microprobe analysis. A large fraction of the silicate mineral component of the aerosol was found to be internally mixed with sea-salt aerosol particles. This observation explains the unexpected similarity in the size distributions of silicates and sea salt that has been observed in remote marine aerosols. Reentrainment of dust particles previously deposited onto the sea surface and collision between aerosol particles can be excluded as possible source mechanisms for these internally mixed aerosols. The internal mixing could be produced by processes within clouds, including droplet coalescence. Cloud processes may also be responsible for the observed enrichment of excess (nonsea-salt) sulfate on sea-salt particles.

SILICATE DUST PARTICLES OF CONTINENTAL origin are transported in the atmosphere over long distances to remote oceanic regions (*1*) and contribute most of the nonbiogenic component of pelagic marine sediments. These particles have been characterized by bulk chemical and mineralogical analysis (*1, 2*). The particle size distribution of silicate aerosols over the remote oceans has shown two paradoxical characteristics. First, the mass median diameter of the particles does not always decrease with transport distance as much as would be expected from differential settling of the larger particles (*3, 4*). Second, over the open oceans far from continents, the apparent size distribution of the silicate component (mass median diameter, 1.5 to 4 μm) often approximates that of the sea-salt particles (mass median diameter, 4 to 8 μm) (*3–5*), a phenomenon that is unexpected in view of the different origin and atmospheric residence time of the two types of particles.

We report here the results of a microchemical investigation of individual silicate particles collected over the remote oceans. These observations are interpreted in terms of the possible modes of transport of these particles, the processes of cloud and aerosol physics that control their atmospheric behavior, and their bulk chemical composition as a function of particle size. Our results demonstrate that it is feasible to use aerosol composition as a test of the validity of hypotheses regarding chemical and physical processes in clouds (*6*).

Aerosol samples were collected from a ship in the equatorial Pacific Ocean between Ecuador and Hawaii. The cruise track and the bulk characteristics of the aerosols have been described (*5, 7*). The coarse fraction of the aerosol was collected on Nuclepore filters [50% cut-off diameter, 1.2 μm (*8*)]. Electron microscopic inspection of the filters showed that they collected only a few particles smaller than 1 μm in diameter (the median particle diameters were 2 to 3 μm). The particles present on the filters were well separated from one another, typically by about ten particle diameters; thus the likelihood that composite particles originate from the deposition of a particle onto a previously deposited one is very low.

The samples were analyzed first in an automated mode (magnification, ×300) in which several thousand particles were located, sized, and analyzed by energy-dispersive x-ray spectrometry. Particles containing silicon were then imaged by scanning electron microscopy (SEM). We analyzed individual components of composite particles by focusing the electron beam onto these components at high magnification (×10,000). We calibrated the x-ray spectra against mineral standards by using a series of fitting and correction programs.

The three particle types and their statistical distributions are shown in Fig. 1 and Table 1. This classification is based on cluster analysis of the automated scans (*9*). The first class of particles, "sea salt," includes particles that are composed predominantly of sodium, chlorine, and variable amounts of potassium, magnesium, calcium, and sulfur, and are the result of the crystallization of seawater droplets (*10*). In sample C6, collected relatively close to the coast of South America, a number of mixed-cation sulfates were commonly associated with sea-salt particles: some have the composition of evaporite deposit minerals, for example, glauberite, $Na_2Ca(SO_4)_2$, and bloedite, $Na_2Mg(SO_4)_2$. Others have compositions that cannot be explained stoichiometrically on the basis of the x-ray analyses, for example, $NaCa(SO_4)_2$, $NaMg(SO_4)_2$, $NaSO_4$, $KMg(SO_4)_3Cl$, $Na_3Mg(SO_4)_{1.5}$, and Na_3K. It is likely that the missing components in these formulas are ammonium and nitrate ions, which were observed in the ion chromatographic analysis of this sample. Although some of these crystal phases are probably an artifact of the drying process and may not represent the phase relations under atmospheric conditions, their presence gives evidence of the reaction of sea-salt particles (present in the atmosphere as a mixture of brine with evaporite minerals) with atmospheric nitrogen and sulfur species, such as NH_3, HNO_3, H_2SO_4, and SO_2? The resulting replacement of chloride by nitrate and sulfate is confirmed by the ion chromatographic analysis of this sample, which showed a loss of chloride relative to sea-salt composition.

The second class of particles consists of $CaSO_4$ particles containing little or no other sea-salt ions. These particles are especially abundant in sample C11 from the equatorial upwelling region. They could be produced by the breakup of a sea-salt particle containing a gypsum crystallite upon impact on the filter surface. A more interesting possibility, which could also explain the calcium excess often observed in remote marine aerosols (*4, 5*), is that they result from the reaction of atmospheric SO_2 with marine biogenic $CaCO_3$ particles (coccoliths), which, because of their alkalinity, would provide a suitable chemical environment for this reaction. Alternatively, $CaCO_3$ could react with H_2SO_4 as a result of aerosol interactions within clouds.

The third particle class ("silicates") contains all particles with detectable amounts of silicon. It can be further broken down into pure silicate mineral particles and particles also containing sea salt. In all three samples, the fraction of silicate particles associated with sea-salt particles (internally mixed sea-salt and silicate aerosol) is between 80 and 90%, an unexpected finding in view of predicted rates of collision between aerosol particles of this size and their atmospheric abundance. The observed internal mixing of

M. O. Andreae, Department of Oceanography, Florida State University, Tallahassee, FL 32306.
R. J. Charlson, Department of Civil Engineering, University of Washington, Seattle, WA 98195.
F. Bruynseels, H. Storms, R. Van Grieken, Department of Chemistry, University of Antwerp (Universitaire Instelling Antwerpen), B-2610 Antwerp-Wilrijk, Belgium.
W. Maenhaut, Instituut voor Nucleaire Wetenschappen, Rijksuniversiteit Gent, B-9000 Gent, Belgium.

*To whom correspondence should be addressed.

Table 1. Concentrations and characteristics of coarse aerosol particles (>1.2 μm in diameter) from the atmospheric boundary layer over the equatorial Pacific Ocean as determined by electron probe microanalysis. Air-mass back-trajectories show that the air masses sampled had in all cases come from the east and remained over the ocean in the trade wind region for at least 5 days.

Sample	Sampling period (1982)	Latitude, longitude	No. of particles analyzed	Particles per cubic meter	Particle types (%)			
					Sea salt	$CaSO_4$	Silicate–sea salt	Pure silicate
C6	7–8 July	2° to 0°S, 82° to 88°W	1492	129,000	85.6	6.0	6.8	1.6
C11	16–19 July	1°N, 118° to 125°W	2629	106,000	88.4	9.4	1.9	0.3
C15	29 July–2 August	6° to 17°N, 140°W	912	90,000	64.7	3.1	28.0	4.2

sea-salt and silicate aerosols could be responsible for the similarity in the size distribution of the silicate and sea-salt aerosols and the lack of a decrease in silicate particle size with distance from land (*3–5*).

To verify whether the observed silicate particles were representative and did not incorporate a storage or analytical artifact, we derived a bulk aerosol composition from the individual particle analyses by using the spot analyses of the silicate particles and the particle geometry as obtained from the SEM images. The results were compared with the composition of the bulk aerosol obtained by proton-induced x-ray emission (PIXE) on the same filters as used for this study, and by instrumental neutron activation analysis (INAA) of simultaneously collected high-volume samples [Table 2, PIXE and INAA data from (*5*)]. All analyses were in agreement to within a factor of 2 or better.

Two mechanisms could explain an internally mixed sea-salt/silicate aerosol: (i) the reinjection during sea-spray formation of mineral particles that have previously settled onto the sea surface, or (ii) the collision of sea-salt and silicate particles in the atmosphere. If 90% of the silicate aerosol particles are associated with sea salt, the first mechanism would imply that more than 90% of the particles deposited onto the sea surface are reinjected into the atmosphere. The feasibility of this mechanism can be tested by comparing the enrichment of aluminum (relative to sodium) in the aerosol with the aluminum enrichment in sea-spray droplets (Table 3). The observed values are higher by more than two orders of magnitude than the enrichment of aluminum observed in sea-spray material [4200 in the Atlantic, 200 in the Irish Sea (*11*)]. Furthermore, on the basis of the aluminosilicate particle density in open ocean seawater [10^5 particles per liter (*12*)] and the upper end of the estimates of sea-spray enrichment (5×10^3), we predict aluminosilicate aerosol particle densities of 50 to 100 m^{-3}, in contrast to the observed values of 2×10^3 to 3×10^4 (Table 3). Clearly, the reinjection mechanism cannot explain the observed abundance of internally mixed sea-salt/silicate aerosol particles.

Several mechanisms may bring salt and mineral particles together in the atmosphere: (i) collision due to different settling velocities, (ii) Brownian coagulation of aerosol particles, (iii) electrostatic attraction, (iv) collision of a mineral particle with a cloud droplet containing sea salt, and (v) coalescence of a cloud droplet containing a mineral particle with a droplet containing a salt particle. The first two processes are not likely to be important because of the small settling velocities of the particles involved and their small number densities. Model calculations based on the use of aerosol characteristics representative of our sample set suggest that the lifetime due to capture via differential sedimentation is greater than 10 days (*13*) and that the lifetime for a silicate particle prior to contacting a salt particle by Brownian diffusion is on the order of 100 years, both longer than the overall lifetime of a coarse aerosol particle. We shall examine possible cloud-related processes instead.

Inside clouds, there are two steps in the processing of coarse particles: activation and coalescence. If the surface of a mineral dust particle has a coating of even a small amount of water-soluble material (the residue from the last rainwater that fell on it or the product of chemical weathering), it will probably be a cloud condensation nucleus (CCN) activated at low supersaturation because of its large size. If, on the other hand, the mineral particle is hydrophobic, because of a lack of soluble material on its surface or because of a nonpolar organic coating, then it might not be a CCN. When a rising air parcel first enters a region of supersaturation, droplets grow on the existing CCN's. Subsequently, if the dust is not a CCN, the still dry dust particles can collide with and be enveloped in droplets. This initial scavenging of the mineral particles into cloud droplets is itself the result of several simultaneous processes: Brownian motion of the mineral

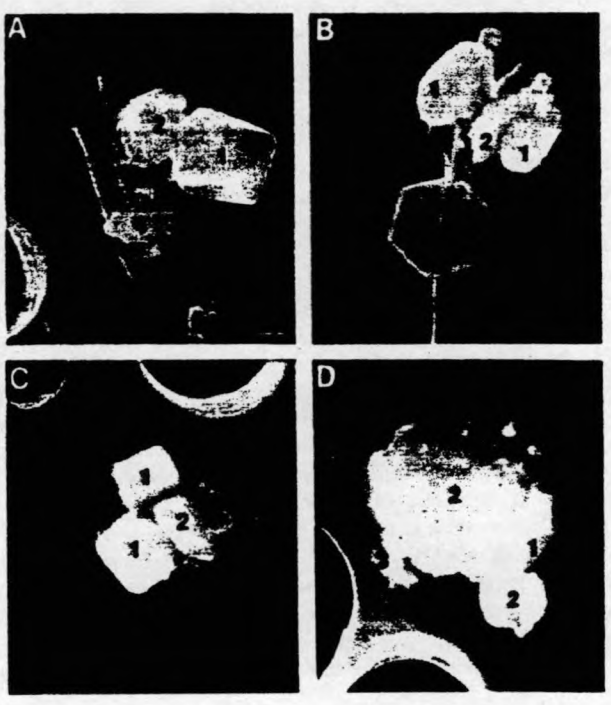

Fig. 1. Internally mixed sea-salt/silicate aerosol particles: (A and B) particles from the equatorial Pacific off Ecuador (sample C6); (C and D) particles from the intertropical convergence south of Hawaii (sample C15). Chemical composition of the component particles: 1, NaCl; 2, silicate; 3, $CaSO_4$; 4, "$NaMg(SO_4)_2$"; 5, "$Na_3Mg(SO_4)_{1.5}$"; 6, "$NaMg_2Ca(SO_4)_3$"; and 7, "Na_3K." (The formulas in quotation marks are not charge-balanced, since they include only the ions detectable by x-ray fluorescence.) Magnification, ×10,000; scale bar, 1 μm.

Table 2. Chemical composition of the coarse fraction (>1.2 μm in diameter) of aerosols from the marine boundary layer (sample origin as in Table 1) as determined by electron probe microanalysis (EPMA), ion chromatography (IC), proton-induced x-ray emission (PIXE), and instrumental neutron activation analysis (INAA).

Sample	Concentration (ng m^{-3})							Sulfur enrichment factor#	Mass % XSO_4
	Al	Si	Ti	Fe	Na	SO_4-S	XSO_4-S*		
C6	50†	93†	0.9†	25†	1760†	280‡	189‡	3.08	14.1
	<40§	41§	1.1§	19§	1080‡				
	57‖			25‖					
C11	6.6†	17†	0.4†	2.3†	1450†	207‡	53‡	1.34	2.6
	<40§	<17§	<0.8§	2.3§	1840‡				
	9.0‖			<12‖					
C15	77†	176†	3.5†	48†	1090†	153‡	81‡	2.14	8.2
	36§	131§	2.6§	27§	850‡				
	80‖			34‖					
Equatorial Pacific¶								1.46 ± 0.15	3.5 ± 1.1

*Excess (nonsea-salt) sulfate. †Determined by EPMA. ‡Determined by IC. §Determined by PIXE (*5*). ‖Determined by INAA (*5*). ¶Average of eight aerosol samples collected during the same cruise. #$(S/Na)_{aerosol}/(S/Na)_{seawater}$.

grains, turbulent diffusion in microscale eddies, convection, electrical effects, diffusiophoresis (which pushes particles in the direction of water vapor diffusion), thermophoresis (which pushes particles down temperature gradients), and differential sedimentation of droplets relative to dust grains (*14*). The time required for the wetting of an initially hydrophobic dust particle is not precisely calculable. Simple consideration of the time required for differential sedimentation to be effective in a marine cloud with 100 droplets per cubic centimeter of 40-μm radius suggests times on the order of 10^3 to 10^4 seconds. Williams (*14*) reported a similar range of lifetimes for 1-μm particles. Because droplets in marine cumuli also have lifetimes on the order of 10^3 to 10^4 seconds, the passage of dust particles through clouds even a few times would ensure that the silicate particles are wetted with cloud water.

Since most cloud droplets do not fall as rain but evaporate, the solute from the original CCN is left behind as a residue on the surface of the mineral particle. The next time such a particle enters a cloud, it will act as a CCN because of the soluble material on its surface and its large size. A similar history of events occurs for salt particles that enter a cloud, except that they are always active CCN's and therefore are solution droplets throughout their residence in the region of supersaturation. All cloud droplets undergo coalescence processes with other droplets and accumulate whatever solute was in those droplets.

Most cloud droplets in marine settings form on CCN's that are composed of sulfates; a small fraction of the droplets have sea-salt particles as their CCN's. The fraction of CCN's containing sea-salt is variable and can be estimated from the population of cloud droplets in marine clouds and from determinations of the typical number concentration of sea-salt particles. Radke (*15*) reported simultaneous measurements of both sodium-containing particles and CCN's in mid-latitude marine air. Sodium-containing particles larger than 0.2 μm that could be CCN's ranged in concentration from 0.1 to 1 cm^{-3}, which is consistent with our data (Table 1). These particles accounted for only 1% or less of the total CCN concentration (typically in the range of 50 to 100 cm^{-3}). That excess (nonsea-salt) sulfate particles dominate the remaining 99% or so of the CCN population is not directly provable in these experiments, but data on aerosol and rainwater composition in remote settings are consistent with this inference (*16*).

Any cloud coalescence process that brings sea salt together with mineral particles must also lead to interactions between sulfate-containing and sea-salt–containing droplets and therefore enrich sea-salt particles with excess sulfate. The observation of such an enrichment in coarse sea-salt particles would therefore be an independent test of our collision hypothesis. The amount of enrichment depends on the number of coalescence events that a sea-salt particle experiences during its atmospheric residence and on the concentration of excess sulfate in cloud droplets. Taking $10^{-5}M$ as a typical concentration of excess sulfate in remote marine clouds (based on rainwater composition), the expected value of 100 coalescence events needed to bring a mineral grain into contact with one of the 1% of the cloud droplets that contain sea salt, a mean droplet size of 10^{-3} cm, and a radius of 10^{-4} cm for the dry mineral and salt particles, we predict that the sea-salt particles should accumulate 10% of their mass in excess sulfate. An excess sulfate percentage of this magnitude was indeed observed in our samples (average excess sulfate content: 3.5 ± 1.1% by weight; $n = 8$) (Table 2). Such an enrichment is also consistent with our observations on sea-salt aerosol samples: we find an enrichment of sulfate on coarse (>1.5 μm in diameter) particles on the order of 2 to 5% in samples from the Southern Ocean (*17*), the tropical and temperate Atlantic (*3, 18*), and the tropical Pacific (*4*). The reaction between acid sulfates and silicate minerals brought together by in-cloud processes can also account for the presence of $CaSO_4$ particles on silicate aerosol particles (Fig. 1) and the low calcium concentrations in the silicate component of these particles (*18*), since the calcium extracted from the minerals by H_2SO_4 would crystallize as $CaSO_4$ upon evaporation of the cloud droplet.

Table 3. Comparison of the observed concentration of silicate aerosol particles with that expected from the sea-spray reentrainment of dust particles settled onto the sea surface.

Sample	Concentration (ng m^{-3})		Al/Na ratio ($\times 10^6$)	Enrichment factor‡	Silicate particles (m^{-3})	
	Na*	Al† (*11*)			Predicted	Observed
C6	1,080	50	46,000	1,000,000	54	10,800
C11	1,840	6.6	3,600	78,000	92	2,300
C15	850	77	90,000	2,000,000	43	29,000
Seawater	10.8 g kg^{-1}	0.5×10^{-6} g kg^{-1}	0.046	1		

*Determined by IC. †Determined by EPMA. ‡$(Al/Na)_{aerosol}/(Al/Na)_{seawater}$.

REFERENCES AND NOTES

1. R. A. Duce, C. K. Unni, B. J. Ray, J. M. Prospero, J. T. Merrill, *Science* **209**, 1522 (1980); J. R. Parrington, W. H. Zoller, N. K. Aras, *ibid.* **220**, 195 (1983); M. Uematsu *et al.*, *J. Geophys. Res.* **88**, 5343 (1983).
2. M. Blank, M. Leinen, J. M. Prospero, *Nature (London)* **314**, 84 (1985).
3. W. Maenhaut, A. Selen, P. Van Espen, R. Van Grieken, J. W. Winchester, *Nucl. Instrum. Methods* **181**, 399 (1981).
4. W. Maenhaut, H. Raemdonck, A. Selen, R. Van Grieken, J. W. Winchester, *J. Geophys. Res.* **88**, 5353 (1983).
5. H. Raemdonck, W. Maenhaut, M. O. Andreae, *ibid.*, in press.
6. *Global Tropospheric Chemistry: A Plan for Action* (National Academy Press, Washington, DC, 1984).
7. H. Raemdonck, W. Maenhaut, R. Ferek, M. O. Andreae, *Nucl. Instrum. Methods Phys. Res.* **B3**, 446 (1984).
8. W. John, S. Hering, G. Reischl, G. Sasaki, S. Goren, *Atmos. Environ.* **17**, 373 (1983).
9. P. Van Espen, *Anal. Chim. Acta* **165**, 31 (1984).
10. C. E. Harvie, J. H. Weare, L. A. Hardie, H. P. Eugster, *Science* **208**, 498 (1980).
11. C. P. Weisel, R. A. Duce, J. L. Fasching, R. W. Heaton, *J. Geophys. Res.* **89**, 11,607 (1984); M. I. Walker, P. S. Liss, N. J. Pattenden, W. A. McKay, *Source Newsl.* **8**, 18 (1985).
12. C. E. Lambert, C. Jehanno, N. Silverberg, J. C. Brun-Cottan, R. Chesselet, *J. Mar. Res.* **39**, 77 (1981).
13. S. K. Friedlander, *Smoke, Dust, and Haze* (Wiley, New York, 1977), p. 193.
14. A. L. Williams, in *Precipitation Scavenging*, R. G. Semonin and R. W. Beadle, Eds. (Energy Research and Development Administration, Washington, DC, 1977), p. 258.
15. L. F. Radke, thesis, University of Washington, Seattle (1968).
16. E. K. Bigg, *J. Appl. Meteorol.* **19**, 521 (1980); J. N. Galloway *et al.*, *J. Geophys. Res.* **87**, 8771 (1982).
17. M. O. Andreae, *J. Geophys. Res.* **87**, 8875 (1982).
18. ———, unpublished data.

19. The electron probe microanalysis measurements reported here were made during a sabbatical stay of M.O.A. at the Department of Chemistry, University of Antwerp (Universitaire Instelling Antwerpen); thanks are due to F. Adams for making this visit possible. We acknowledge the help of R. Nullens with the operation of the SEM and of P. Van Espen with the analysis of the data. This research was supported by the National Science Foundation (grant ATM-8407137), the Belgian Nationaal Fonds voor Wetenschappelijk Onderzoek, and the Belgian Ministry of Science Policy (grant 84-89/69).

9 December 1985; accepted 8 April 1986

Selected article #7:

Chemical characterization and source apportionment of individual aerosol particles over the North Sea and the English Channel using multivariate techniques

C. Xhoffer, P. Bernard, R. Van Grieken and L. Van der Auwera

Environmental Science and Technology, 25 (1991), 1470-1478

Reprinted from ENVIRONMENTAL SCIENCE & TECHNOLOGY, Vol. 25, 1991

Chemical Characterization and Source Apportionment of Individual Aerosol Particles over the North Sea and the English Channel Using Multivariate Techniques

Chris Xhoffer,* Paul Bernard, and René Van Grieken

Department of Chemistry, University of Antwerp (UIA), B-2610 Antwerp-Wilrijk, Belgium

Ludo Van der Auwera

Royal Meteorological Institute, Ringlaan 3, B-1180 Brussels, Belgium

■ More than 25 000 individual aerosol particles in 51 particulate matter samples, all taken from a research vessel over the North Sea and the English Channel, in a time range of 4 years, were analyzed by automated electron probe X-ray microanalysis (EPXMA). Multivariate methods were used to reduce the total data set. Single-particle analysis combined with hierarchical cluster analysis yields nine major particle types. The North Sea aerosol is predominantly composed of sea salt, sulfur-rich particles, silicates, and calcium sulfate particles. Their abundance is dependent on meteorological conditions and sample location. Differences between all samples were studied on the basis of the abundance variations by using principal component analysis. Three factors explain 91% of the total covariance between the samples. The first component represents the marine-derived aerosol fraction and is more important as wind speed increases or at more remote sampling locations. The second component differentiates anthropogenically derived $CaSO_4$-rich samples. Their relative abundance is much more pronounced as the sampled air masses spend longer residence times over the south of England. The samples of the third cluster are related to high silicate and sulfur abundances. Source apportionment of this group was obtained by a second principal component analysis. Two different clusters separate mixed marine/continental samples from pure continental-derived silicate and sulfur-rich particulate samples.

Introduction

Since the North Sea is surrounded by the western and northern parts of the European continent and by Great Britain, it undergoes strong influences from industrial, agricultural, and domestic activities. On a long term, accumulation into the North Sea could change the chemical environment. Therefore, attempts are made to estimate the impact of the surrounding anthropogenic activities on the North Sea. The man-made pollutants can reach the North Sea by several pathways including river transport, direct discharges by pipelines, dumping activities, and atmospheric transport. The North Sea aerosol is a mixture of many components, some derived from the sea itself and some having descended from aloft.

Because of internal heterogeneity of the aerosol samples (i.e., the chemical diversity of the particles as a consequence of their different production mechanisms), individual particle analysis can advantageously be applied for the source identification of various atmospheric pollution processes. The relative percentage abundance of the specific particle types can be a measure for the source strength. Besides source apportionment, microanalysis can also be useful for the investigation of the behavior of particles during transport (e.g., gas-to-particle conversion, coagulation processes, etc.). A reduced sampling time and the small amount of material needed for individual microanalysis can be advantages in the study of different dynamic processes.

Experimental Procedure

Samples and Sample Preparation. A total of 51 aerosol samples were collected over the North Sea and English Channel during various cruises in a time range of 4 years (1984–1987) aboard the R/V *Belgica*. Atmospheric aerosols were sampled on 47-mm-diameter Nuclepore filters with a pore size of 0.4 μm. The filtration units are provided with a hat-type inlet to avoid the collection of large droplets and rain. The whole is mounted in the mast on the foredeck of the ship, 6 m above deck, 11 m above the sea surface, and facing 0.5 m upwind from the mast itself. When the relative wind direction to the ship is unfavorable, or not within +45 to −45°, the power supply of the pump is cut off in order to avoid contamination by the vessel. Figure 1 shows different tracks for the various cruises. Comparison of the particle sizes for samples simultaneously collected with and without the hat-type inlet showed no differences in size range below 15 μm (*1*).

Depending on weather conditions and sampling area, the sampling time was ~8 h in order to collect 5–10 m^3 of air. For sampling sites near coastal regions, smaller sampling volumes are needed compared to "off-shore" locations. In contrast, higher sampling volumes are necessary during or after rain events because of reduced particle number concentration in the air by "rain-out" effects. To reduce chemical changes as well as compositional and morphological transformations of the atmospheric aerosol, each filter was immediately put between Petri dishes and stored in a refrigerator. A part of the Nuclepore filter was mounted on a plastic ring that fit into the electron microprobe sample holder. All samples were coated with a thin carbon layer of approximately 40 nm to improve electrical conductivity.

Instrumentation. Single-particle analysis was performed by electron probe X-ray microanalysis (EPXMA) using a JXA-733 superprobe of JEOL (Tokyo, Japan). This superprobe is equipped with energy- and wavelength-dispersive X-ray spectrometers, a secondary and transmission electron detector, and two simultaneously operating backscattered electron detectors (for topographic and compositional imaging). The probe is automated with a Tracor Northern TN 2000 system and an LSI 11/23 microcomputer controlling all EPXMA parameters. The obtained data can be stored either on magnetic tape or on double-density floppy discs. All information can, at any time, be transferred to a VAX 11/780 computer for additional off-line data processing.

Automation Methodology. During the execution of the automated particle recognition and characterization (PRC) program, the electron beam scans over a preset area of interest. When the backscattered electron intensity of

0013-936X/91/0925-1470$02.50/0

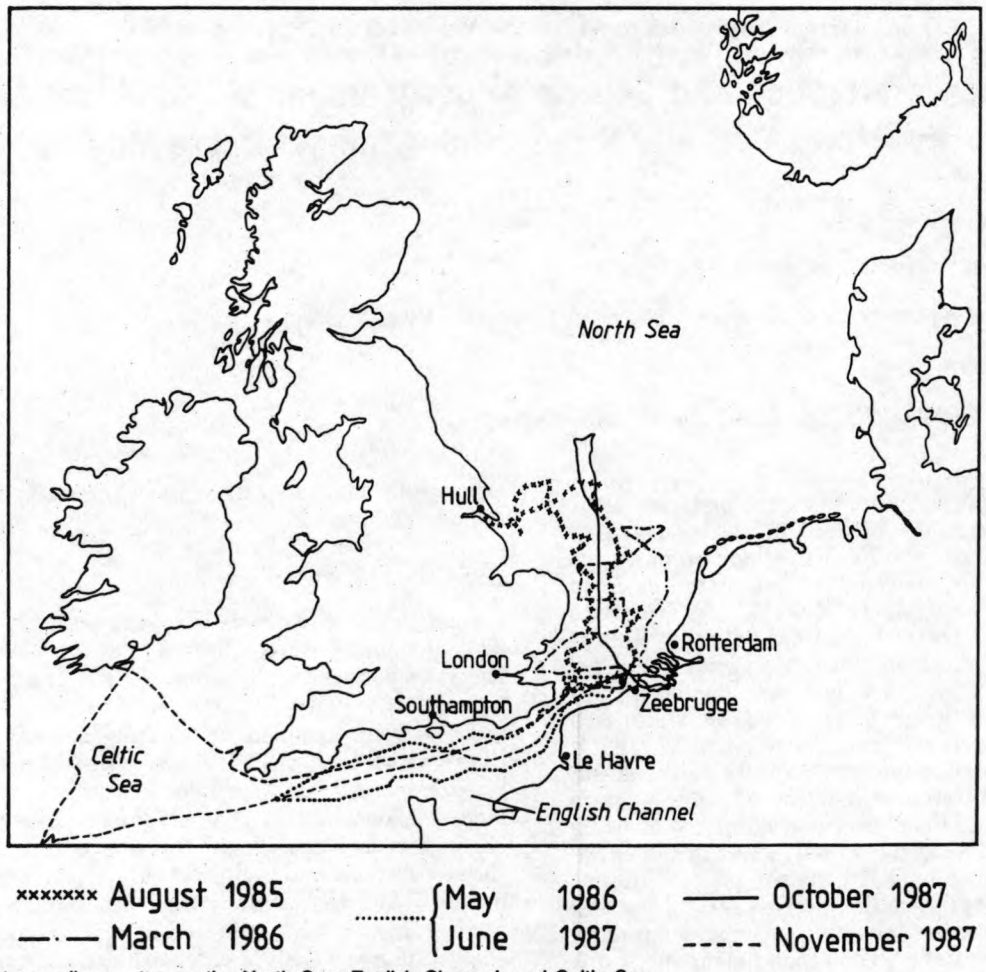

Figure 1. Different sampling routes on the North Sea, English Channel, and Celtic Sea.

the particle contour exceeds a predefined threshold value, the object is considered detected. Size parameters such as the perimeter, average diameter, and shape factor [(perimeter)^2/4π area] are calculated. The diameter measured by EPXMA is based on the projected area of the particle and might differ from the aerodynamic diameter. An X-ray spectrum can be accumulated at the center of the particle or by performing cross scans over the particle. Subsequently an X-ray spectrum is calculated and deconvoluted. Thus, the whole PRC program is set up in three sequential steps: localizing, sizing, and chemical characterization, after which the beam scans for the next particle.

For each aerosol sample, ~500 particles in a size range from 0.2 to 15 μm were automatically analyzed. X-ray spectra were accumulated for 15 s with a beam current of 1 nA and an acceleration voltage of 20 kV. This whole operation takes less than 3 h per sample and yields a huge data set. To reduce the data, two hierarchical and one nonhierarchical cluster analysis were applied for each sampling campaign (*2*). First a hierarchical cluster analysis performed on the elemental composition data of 500 particles resulted in an average composition data set. For this, every particle i is presented in a N-dimensional space as an object vector with coordinates according its N-elemental composition. Here N is the number of variables and equals the number of different elements detected in one sample. The method starts from m objects (m = 500 particles) that are to be classified, and at each step the two most similar objects (particles) or already formed clusters are merged into a single cluster. The similarity between two objects was derived from the Euclidian distance coefficient between the objects. The Ward method (error sum of squares method) was used for the calculation of the distances between newly formed clusters and the remaining objects and/or clusters. So, the more close two objects or clusters are, the more similar they are. A second hierarchical clustering was performed on the average composition data of the samples and resulted in a set of training vectors (centroids) that are representative for that sampling campaign. Finally, a nearest centroid sorting (nonhierarchical cluster analysis) is used to classify all particles from one campaign according their distance from the centroids of the clusters. The method of Forgy (*3*) minimizes the sum of squares of the distances to the centroids for a fixed number of clusters. This procedure results in an average composition data set for each North Sea sample according the centroids of the corresponding campaign.

The whole particle classification procedure involves thus a series of cluster analyses and is followed by a principal component analysis (PCA). The purpose of the PCA method is to represent the variations present in the data in such a way that, without losing significant information, the dimensionality is reduced. To achieve this, new variables (components) are constructed, according to a linear combination of the original variables, in such a way that the newly formed principal components are uncorrelated and that they are constructed with decreasing degree of importance. The principal components obtained in this way represent the linear indepenent variance present in the data of original variables. The most important sources for the variance in the data are examined by studying the first principal components. General information about the PCA technique can be found elsewhere (*4*). Several papers discuss expert systems to sort out individual particle data (*2, 5–8*).

Table I. Range for the Particle Identification Bases on the Mean Percent Abundance for Each Cluster Group

particle type	criteria: based on relative X-ray intensities		
sea salt	Cl > 75%	7% < Na < 10%	
aged sea salt	24% < S < 44%	38% < Cl < 60%	
sulfur-rich	S > 71%		
calcium sulfate	23% < Ca < 45%	46% < S < 60%	
calcium-rich	12% < Ca < 90%	5% < P < 58%	S < 16%
alumino-silicates	17% < Al < 30%	50% < Si < 62%	4% < Fe < 8%
quartz	88% < Si < 91%		
titanium-rich	72% < Ti < 82%		
iron-rich	72% < Fe < 91%		

The accuracy for the X-ray measurements is close to 1% for abundant elements. The reliability (2σ values) of the relative abundances of the particle types can be calculated from binomial statistics and is between 2 and 5% absolute when 500 particles are measured. It has been shown (*9*) that the variability on the composition of the clusters is almost entirely due to the variation in the particles' composition and is therefore a reliable measure for the heterogeneity of the clusters. The accuracy of particle sizing depends mainly on two differnt factors: (a) threshold setting of the backscattered image signal and (b) the magnification used. Accuracies within 20% are obtained (*10*). The reproducibility for particle sizing using the backscattered electron image is within 6% for the mean diameter.

Results and Discussion

Conventional X-ray microanalysis makes it possible to detect elements from $Z \geq 11$. The measured X-ray output data consist of relative peak intensities obtained by a fast filter algorithm (FFA), namely, a symmetrical convolution function by the Hardeman transformation (*11*). The relative percent X-ray intensity expresses the ratio of the net X-ray intensity of that element to the total net X-ray intensities collected from that particle. This information is important for chemical intercomparison of particles and can thus be used for the assignment of particles to various particle types. The hierarchical clustering procedure applied to the elemental composition of more than 25 000 particles collected from different parts over the North Sea, the English Channel, and the Celtic Sea resulted in the identification of nine major relevant particle types. Some low-abundance particle types were encountered; although their abundance cannot be determined with high accuracy, their occurrence in the aerosol can be important with regard to the deposition and source apportionment of some specific trace elements. The characteristics of these minor particle types will be discussed separately. Table I gives an overview of the nine major particle types with the range of the average composition of the groups for each sampling campaign. These data give an idea of the criteria by which a particle was assigned to a specific particle type by hierarchical cluster analysis. Note that the relative X-ray intensity of Na in NaCl is much lower than that of Cl. Indeed, Na has much lower sensitivity due to physical effects and because the absorption effects of the X-ray signal by the detector window are more important for Na than for Cl. Typical relative percent X-ray ratios of $1/12 \leq \mathrm{Na/Cl} \leq 1/8$ are observed.

Relative abundances or particle number concentrations (expressed in percent) of each particle type for every individual sample are given in Table II. The standard deviations of the relative abundances are given by binomial statistics. For the individual EPXMA measurements, where a total of 500 particles were analyzed, the standard deviations are between 1 and 5% on a 95% confidence interval.

The number concentration of particles present in 1 m^3 marine air can be derived from the number of particles analyzed, multiplying these with the ratio of the filter area to the analyzed area. Table III tabulates the range of number concentrations of particles between 0.2 and 15 μm above the North Sea calculated for the 51 samples analyzed. Accuracies were estimated to be ~10% as based on uncertainties in analyzed filter area and sampled air volume. The findings of these data are in good agreement with aircraft measurements performed over the North Sea at sea level (*12*). There is clearly a tendency of increasing particle number concentration as the sampled air masses originate from over the continent. Knowing the total number concentrations of aerosol particles above the North Sea, the percent abundance of each particle type, the assumed density for each particle class, and the mean equivalent spherical diameter of each particle belonging to that particle class, one can calculate the mass concentrations for each particle type. However, the accuracy for mass concentrations is worse than 60% and is highly dependent on the accuracy for the diameter determination.

The nature, source and relative abundance variations for each particle type will subsequently be discussed in more detail.

Different Particle Types. (1) Sea-Salt Particles. A particle type is defined as sea salt when the average content of Cl exceeds 75% in relative X-ray intensity. No other element, except Na, is of any significance. It is postulated that the total contribution of freshly generated NaCl present in the marine atmosphere is attributed to a marine source. The main process for the generation of fresh sea salt into the atmosphere is the breaking of waves. This process is more effective as the wind speed increases (*13*).

Very large variations in number concentrations for sea-salt aerosols are found ranging from 0 to 94% of the total number fraction. High sea-salt abundances were found in the August campaign of 1985 when samples were taken under stormy southwest winds: whitecap formation and sea spray induced by wind action are predominantly responsible for the ejection of sea salt into the atmosphere. The anthropogenic particle fraction is not necessarily low but is totally suppressed by the domination of sea salt. Contrarily, for the cruise of May 1986, the air mass trajectory went through the Channel, via the south coast of England, until the influence of the Atlantic Ocean was clearly observed. Nearing more westerly regions is reflected by an increase in sea-salt concentrations. Backtrajectories of the sampled air evolved from far over the Atlantic Ocean without continental interferences. No anthropogenically derived particulate matter was detected.

(2) Transformed or Aged Sea-Salt Particles. This particle type is rich in S and Cl. Also mixtures of $NaNO_3$, Na_2SO_4, and NaCl are possible (*14*). These S- and Cl-rich particles are identified as aged sea salt. They are formed by the conversion of NaCl into Na_2SO_4 by SO_2, implying the release of HCl in the marine atmosphere. These results are consistent with the findings of other authors (*15–18*).

The contribution of S enrichment in sea-salt aerosols is more pronounced in the samples for which an important anthropogenic influence on the marine atmosphere is expected. The mixing of air masses is always observed on passing from continental conditions toward more marine ones or vice versa. This was clearly observed for the

Table II. Relative Percent Abundances of Nine Particle Types for 51 North Sea Samples

date	sea salt	aged sea salt	S-rich	$CaSO_4$	Ca-rich	alumino-silicates	Si-rich	Ti-rich	Fe-rich
Dec 84	0	2	19	0	20	47	4	0	8
	63	10	4	0	9	3	0	0	10
	33	7	7	0	7	36	4	0	5
	0	0	35	0	15	12	2	0	36
Aug 85	77	0	2	11	0	6	4	0	1
	26	0	3	9	1	50	5	1	6
	8	0	2	8	0	71	8	0	3
	0	0	5	5	0	74	7	1	7
	0	0	33	21	0	6	9	1	30
	0	0	11	48	2	14	8	0	18
Mar 86	0	0	61	0	0	18	10	0	12
	0	0	32	4	0	42	11	0	11
	0	0	67	3	0	14	5	0	11
	0	0	61	3	0	21	8	0	7
	1	0	24	12	0	27	8	0	29
May 86	18	0	53	5	10	5	5	1	5
	20	20	35	3	10	6	3	0	3
	60	27	0	3	2	7	0	0	0
	52	40	0	2	5	1	1	0	0
	68	17	3	2	9	0	0	0	0
	84	8	4	1	3	0	0	0	0
	91	6	2	0	1	0	0	0	0
	77	4	4	5	7	2	2	0	1
	94	5	0	0	1	0	0	0	0
	91	9	0	0	1	0	0	0	0
	83	14	0	0	2	1	1	0	0
	90	4	0	2	2	2	1	0	0
	77	12	1	2	5	3	0	0	0
	56	26	7	4	8	0	0	0	1
	11	11	32	18	7	18	2	0	1
	2	0	38	9	1	32	5	5	8
June 87	0	0	13	82	0	4	1	0	0
	0	0	69	17	0	6	2	2	4
	0	0	12	5	0	59	21	1	3
	0	0	19	72	0	4	4	0	0
	0	0	2	94	0	2	0	0	1
	1	0	33	50	0	9	7	0	1
	0	0	21	68	0	3	7	0	1
	0	0	4	84	0	10	2	0	0
	0	0	85	6	0	3	6	0	0
	0	0	32	13	0	36	17	0	2
Oct 87	3	2	21	37	0	30	0	0	7
	2	36	8	8	0	46	0	0	1
	1	42	6	3	0	47	0	0	1
	1	4	41	14	0	39	0	0	0
Nov 87	0	1	43	17	0	24	0	4	10
	0	1	38	9	0	11	0	37	4
	1	0	60	19	0	8	0	9	3
	0	0	50	13	0	24	0	8	5
	0	0	56	8	0	6	0	27	2
	0	0	35	20	0	22	0	19	4
⟨diam⟩, μm	0.8	0.7	0.7	0.8	0.8	1.3	1.3	1.0	0.8

Table III. Particle Number Concentrations (m^{-3}) Observed for Three Types of Sampled Air Masses above the North Sea

air mass type	range	mean
marine	$(7.9 \pm 0.2) \times 10^3$–$(6.9 \pm 0.7) \times 10^4$	$(3.9 \pm 0.4) \times 10^4$
mixed	$(2.9 \pm 0.3) \times 10^4$–$(4.7 \pm 0.7) \times 10^5$	$(2.5 \pm 0.5) \times 10^5$
continental	$(8.7 \pm 0.9) \times 10^5$–$(2.9 \pm 0.6) \times 10^6$	$(1.9 \pm 0.7) \times 10^6$

campaign of May 1986. The corresponding back-trajectory (Figure 2) shows originally marine air traveling over the southern part of England.

(3) Sulfur-Rich Particles. In general, the S concentration is greater than 70% for this particle type, and no associations with Ca are present. Studies on particulate S present in urban sites showed that numerous secondary reactions can take place (*19*, *20*). Industrial SO_2 gas emissions are oxidized in homogeneous or heterogeneous reactions and form SO_4^{2-}. Anthropogenic emissions like combustion of fossil fuel constitute the main source for the SO_4^{2-} release into the atmosphere. Often NH_4^+ is present in continental aerosols in concentrations high enough for partial or complete neutralization of H_2SO_4 with the formation of various ammonium salts as $(NH_4)_2SO_4$, $(NH_4)HSO_4$, and $(NH_4)_3H(SO_4)_2$ (*21*). Similar particles were found in the Phoenix urban aerosol (*22*), where the only detectable element was S. Here, several of these Phoenix S-bearing particles were detected, indicating that the cores are soot. It was also observed (*23*) that biological particles (composed of light elements, such as H, C, O, and N) with their complex morphology and wet surfaces provide an attractive nucleating surface for SO_2 absorption and conversion to sulfate. In analogy to the North Sea aerosol, probably S-rich compounds have condensed onto or reacted with existing carbonaceous particles that have acted as condensation nuclei. The shape of the spectrum with its very high background is typical for organic and bio-

Figure 2. Air mass back-trajectory for aerosols collected during the May 1986 campaign. The shaded area corresponds to ca. 36-h air mass back-trajectories calculated for a height of 10 m above the North Sea. The air masses have traveled from point A toward B.

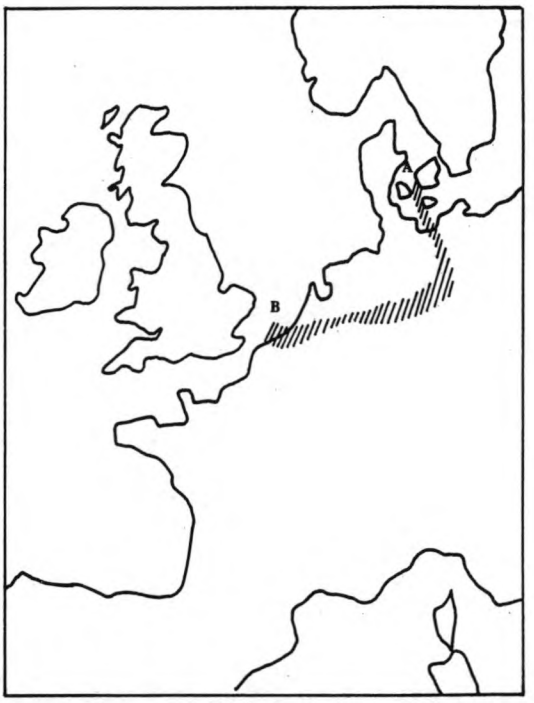

Figure 3. Air mass back-trajectory for aerosols collected during the March 1986 campaign.

logical material, although carbon X-rays cannot readily be detected with conventional EDX analysis (*23*). However, X-ray spectra can distinguish between carbonaceous particles and, e.g., crustal particles, whereas morphology studies often differentiate botanical particles from soot (*24*). Signals from organic particulate matter can exceed the backscattered electron image threshold above the Nuclepore filter necessary for the localization of particles. The image signals from the filter backing material are normally completely suppressed by this threshold setting. So, if a localized and detected particle is composed almost entirely of elements lighter than Na, the organic nature can be ascertained from the relatively noisy background in its collected X-ray spectrum (*25*, *23*). However, one must keep in mind that the total X-ray counts are still much lower than what is observed for, e.g., mineral particles.

Carbonaceous particles enriched in $(NH_4)HSO_4$ and $(NH_4)_2SO_4$ or mixtures at their surface are present over the North Sea as was also inferred from laser microprobe mass analysis (LAMMA) results (*14*). Most of these S-rich particles have a diameter in the submicrometer range. This might be an indication that they are formed by gas-to-particle conversion processes. Combustion processes are almost exclusively responsible for the high pollution gaseous sulfur compounds, although a smaller fraction can have a marine origin, as is the case for dimethyl sulfoxide (DMSO) and derived compounds. For the most westerly located sampling place of the May 1986 campaign, where only pure marine conditions were encountered, low concentrations of marine S-bearing compounds were detected.

The S-rich particulate matter was the most important particle type encountered in the sampling campaigns of March 1986 and November 1987. In March 1986, the atmosphere above the North Sea had been influenced by a long period of easterly wind and at the time of sampling the sea surface was smooth and the visibility strongly reduced due to a persistent fog. The particle concentration was very high, because of the presence of an inversion layer. The 36-h air mass back-trajectories (Figure 3) showed a steady supply of continental air traveling over West Germany, The Netherlands, and Belgium. For the November 1987 cruise, no fog and inversion conditions were observed. All filters have collected air masses originating from above Eastern European countries. Comparable S concentrations were found in the June 1987 campaign, although the air masses had long residence times above the south of England. Consequently, high S emissions must be related to industrial and automotive sources from all over Europe.

(4) Calcium Sulfate Particles. Both Ca and S are present in the same particles, with their elemental composition ranges given in Table I. These particles are very often found in both marine and continental aerosols. They are identified as $CaSO_4$. Some possible marine formation mechanisms are postulated (*27*), e.g.: (1) $CaSO_4$ can be produced by fractional crystallization of marine aerosols, a process that is especially efficient with high relative humidity. Possibly breakup of the $CaSO_4$ crystal from the sea-salt aerosol particle takes place either by impaction on the filter or during its atmospheric residence. (2) $CaSO_4$ could result from the aerosol interaction between marine or airborne $CaCO_3$ with atmospheric SO_2 or H_2SO_4, e.g., within clouds.

The abundance of $CaSO_4$ particles under purely marine conditions (May 1986) does not vary proportionally with sea salt. Furthermore, in the samples with highest $CaSO_4$ contributions, NaCl is virtually absent. Actually much higher abundances are present in the samples influenced by the continent (June 1987). The March 1986 and June 1987 campaigns were both characterized by high S-rich and Ca-rich particle number concentrations. For the reaction of particles with SO_2 and/or SO_4^{2-}, particles need to have the appropriate surface chemistry (in this aspect, calcite scores better than clay minerals and much better than silicates) and long suspension times in the air (*23*). Such sampling conditions, high humidity, persistant fog, and an inversion layer, were observed for the March 1986 sampling campaign, favoring such transformation reactions. It is, however, not evident that in the June 1987 campaign acid transformation reactions between $CaCO_3$ (may partly be derived from the cliffs of Dover) and SO_2 or SO_4^{2-} components are dominant for the formation of $CaSO_4$ particles. If such reactions would have taken place, it implies that

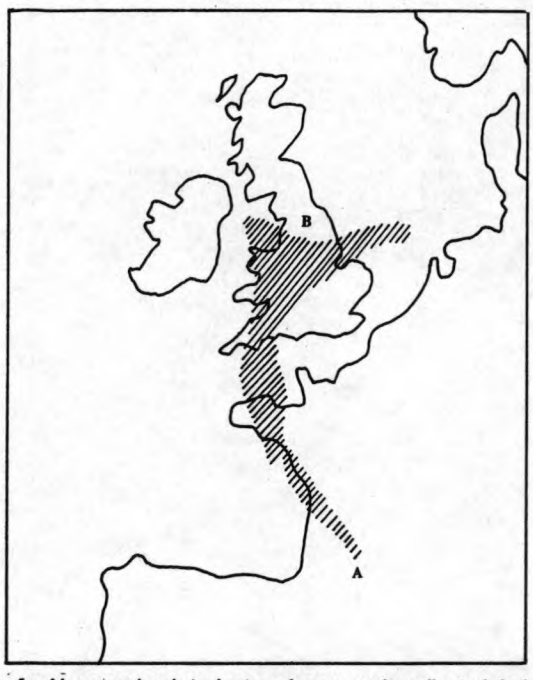

Figure 4. Air mass back-trajectory for aerosols collected during the October 1987 campaign.

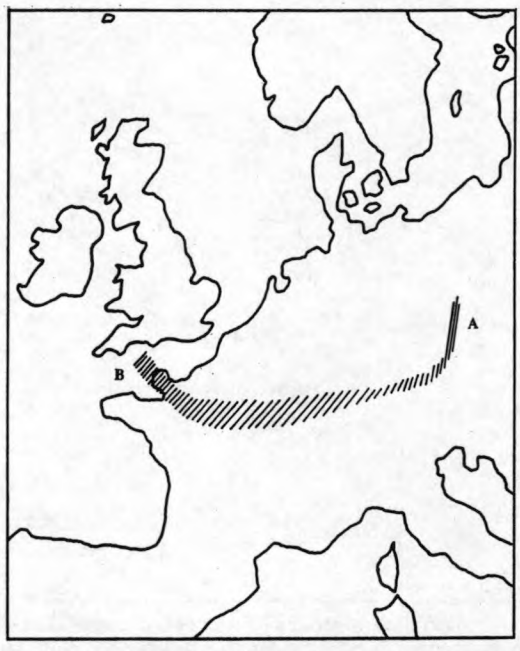

Figure 5. Air mass back-trajectory for aerosols collected during the November 1987 campaign.

all $CaCO_3$ particles had been fully transformed. Indeed, in the June samples with exceptionally high number concentrations of $CaSO_4$, the Ca-rich ($CaCO_3$) particle type, which is the obvious precursor for $CaSO_4$, was not observed at all. This means that $CaSO_4$ is predominantly emitted by anthropogenic sources such as combustion processes and by eolian transport from the continent to the North Sea. $CaSO_4$ has also been found in the fly ash particles collected from coal power plants (*28*). It is remarkable that all $CaSO_4$-rich filters were influenced by continental air masses traveling over the south of England (June 1987 and October 1987) (Figure 4). In some particular samples, the relative intensity of S is much higher than what is normally measured for $CaSO_4$. Hence, this particle type can partly be identified as $CaSO_4$ enriched with S, in the form of, e.g., $(NH_4)_2SO_4$. The formation of $CaSO_4 \cdot (NH_4)_2SO_4$ aerosols can be explained by the coagulation of $CaSO_4$ particles with submicrometer sulfate aerosols (*19*). These results were confirmed by LAMMA measurements (*14*).

(5) Calcium-Rich Particles. For the Ca-rich particle type, we can only postulate that they are mainly characterized as $CaCO_3$ although C and O cannot be detected by our method.

All Ca-rich aerosols that contain less than 16% S are classified in this group. They can originate both from the marine environment and from continental sources.

As seawater evaporates, various dissolved salts begin to crystallize out sequentially. First calcite ($CaCO_3$) and dolomite [$CaMg(CO_3)_2$] precipitate, then gypsum [$CaSO_4(aq)$], followed by halite (NaCl), and finally the Mg salts (*29*). If this crystallization effect takes place in an aerosol droplet, $CaSO_4$ as well as other salts (e.g., the remaining residues) would be detected on the filter. Only Ca-rich particles, $CaSO_4$, and NaCl were identified. Mg was detected in low abundances, never as the major cation in individual particles. Mg is mostly associated with Ca-rich or Ca–S-rich particles. Probably also the mixed salt [$CaMg(CO_3)_2$] can undergo further reaction with gaseous S-rich components. A small fraction of Ca-rich particles show up to 15% S in the relative X-ray spectrum but are not classified in the $CaSO_4$ group according to the criteria of Table I. This can be an indication of the initiation of Ca–S-rich particle formation from $CaCO_3$ and/or derived components with atmospheric SO_2 or H_2SO_4. According to the obtained data set, Ca-rich particles above the North Sea cannot unambiguously be apportioned to one source type.

(6) Aluminosilicate-Rich Particles. These particles are characterized by the presence of Al, Si, S, K, Ca, and Fe as major elements and Ti, Cr, Mn, Ni, and Zn as minor ones. This mineral type of particle finds it origin on the continent. X-ray spectra cannot distinguish whether these particles are soil dust or fly ash derived. Only morphology can sometimes differentiate their source. The soil dust particles have variable shapes and diameters ranging from submicrometer to ~5 μm. However, sometimes 40% or more of all aluminosilicates have a smooth and nearly perfect spherical shape. This is especially true for the November 1987 cruise, when the sampled air masses were influenced by Eastern European emissions (Figure 5). Hence, these particles must be fly ash derived. They are formed during high-temperature combustion processes of fossil fuel and obtain their typical shape after solidification of the molten material. Smaller fly ash contributions are also observed during air mass trajectories over England and western Europe. In ~5% of all aluminosilicates, a rather high S concentration was present in the aerosol during the March 1986 campaign. Because meteorological conditions favored high continental influences over marine ones, anthropogenic S from SO_2 emissions is very likely to be responsible for secondary reactions. H_2SO_4 derived from SO_2 emissions can have long residence times during calm weather conditions at high relative humidities. During long fog periods, high humidity, and inversion layer conditions, mineral particles that were initially hydrophobic can most probably be wetted with acidified water droplets and are left behind as possible cloud condensation nuclei (CCN) for further reactions (27). These CCN can in an initial state be composed of an aluminosilicate nucleus covered by a S-rich surface coating. But further transformation of element-specific extraction processes are also possible. Such reactions are responsible for the further breakdown of silicate mineral particles, forming silicon-rich clusters.

(7) Silicon-Rich Particles. In the Si-rich group, the Si–K X-rays constitute more than 88% of the character-

istic X-ray spectrum. These mineral quartz particles are irregularly shaped. They can be derived from soil dust and therefore are often found in the presence of aluminosilicates. Another fraction of the quartz particles are emitted during the combustion of coal in power plants (*30*, *31*). Most of the Si-rich particles are present in the size range below 1 μm. The fact that these particles, just as the Fe-rich particles, are found in the smallest size range could strengthen the hypothesis that they are formed during combustion processes.

(8) Titanium-Rich Particles. For some North Sea samples (November 1987), rather high abundances of Ti-rich particles were observed. The mean relative X-ray intensity for Ti ranges between 65 and 85%.

The mean diameter of the Ti-rich particles is 1.0 μm and the shape factor of 3 deviates far from 1 for spherical particles. The main source for Ti release into the atmosphere is pigment spray, but minor pollution processes and sources such as soil dispersion, asphalt production, and coal-fired boilers and power plants are also known (*6*). Sometimes chromium is detected in this particle group beside some contributions of Si, Zn, Pb, and Ba.

(9) Iron-Rich Particles. The samples taken near the continents show high contributions of Fe-rich particles. Within this cluster, three different Fe-rich particle types are recognized. The first subgroup consists of pure iron oxide. Most of these particles are spherical, but irregularly shaped particles are found as well. They are mainly produced by ferrous metallurgy processes. The second subgroup consists of Fe–Zn–Mn-rich particles. Within this group, the abundances for Zn and Mn are much more pronounced. They are derived from ferrous manganese furnace processes. Very often S is associated with Fe-rich particles: the Fe–S-rich particles constitute the third subgroup. These particles, probably pyrite and iron sulfate, can be formed by reaction between iron oxide and sulfuric acid, during their release in ferrous metallurgy related combustion processes.

(10) Minor Particle Type. Rare particles are also interesting because they can sometimes be apportioned unambiguously to one specific source.

Characteristic X-ray spectra showed that some S-bearing aerosols have P and Cl as detectable elements. Also, a very high X-ray background is often observed originating from an organic matrix. Organic phosphorus is primarily formed through biological activities. Bubble bursting can cause enrichments of P in the sea-salt aerosol particles by fractionation out of the sea surface microlayer (*32*). When these P-rich particles mix with anthropogenic air masses, the S components can also react with these sea-salt particles forming aged sea salt enriched in P. The major sources for particulate P in marine aerosols of New Zealand (*33*) are soil particles containing both naturally occurring and fertilizer-derived P, as well as sea-salt particles and industrial emissions. Na, Al, and V were associated with P as indicators or markers for, respectively, a marine source, a crustal weathering source, and an anthropogenic pollution source (e.g., burning of biological material). For the North Sea samples, no association between P and Al or V was detected and hence these particles probably have a marine origin.

Alternatively, the presence of P is often associated with Ca. These particles are classified into the Ca-rich group, although their percent abundance of relative X-ray intensities from Ca and P are, respectively, 13 and 55%. This particulate matter can be fertilizer derived or is a residual from biological material (e.g., pollen) and can be transported over the North Sea by wind action. Ca- and P-rich particles were also found in aerosol samples taken above the equatorial Pacific Ocean where only marine influences were expected (*31*). The relative X-ray intensities of 60% for Ca and 30% for P, compared to what we found here, suggest indeed an other, still unidentified source.

Table IV. Cumulative Eigenvalues and the Loadings for the First Three Principal Components Derived from the Covariance Matrix for Two PCA Performed on the North Sea Data

	principal components					
	for all samples (51)			for the third cluster (29)		
	1	2	3	1	2	3
cum %	54	75	91	61	80	88
variables	loadings					
sea salt	0.99	0.01	−0.09			
aged sea salt	0.42	−0.10	0.22			
marine fraction				−0.50	0.86	−0.10
sulfur	−0.66	−0.40	−0.62	0.97	−0.04	−0.21
calcium sulfate	−0.41	0.91	−0.01	0.25	−0.13	0.06
calcium-rich	0.24	−0.19	0.00	−0.08	0.29	0.39
aluminosilicates	−0.41	−0.39	0.80	−0.90	−0.37	−0.22
quartz	−0.39	−0.18	0.26	−0.21	−0.46	0.01
titanium-rich	−0.23	−0.14	−0.23	0.29	−0.06	0.02
iron-rich	−0.33	−0.21	0.00	0.11	−0.22	0.90

For some samples, higher abundances of heavier elements like Pb and Br together with Cl were detected. These Pb-rich particles originate from automobile exhaust emissions. Pb is added to the gasoline together with ethylene dihalide compounds (Br, Cl). Pb/Cl/Br compounds can be identified as $2PbBrCl{\cdot}NH_4Cl$ (*34*). The emitted lead halides can readily be converted to lead sulfates by reaction with SO_2, H_2SO_4, or $(NH_4)_2SO_4$ with the loss of HBr (*35*). However, none of the transformed lead halide particles were observed in spite of the very high S concentrations present in the sampled air masses.

Principal Component Analysis

To study variations in the abundance data set, principal component analysis (PCA) was applied using a software package, the so-called Data Processing Program (DPP) (*36*). We used the relative percent abundances of nine particle types (nine variables) for 51 North Sea samples from Table II as input data for the PCA. The covariance matrix was used for the calculation of the principal components. The first three principal components explain 91% of the total variance present in the original data set. The loadings of the first three principal components, listed in Table IV, are plotted in Figure 6a, while the scores are represented in Figure 6b. Three main clusters are recognized. The first group with a high score on the first principal component contains 14 samples with high abundances of sea salt and aged sea salt. A second cluster of eight samples is separated by the second principal component. The samples in this cluster are characterized by high $CaSO_4$ abundances. Because of the low negative score on the first principal component, the emission of $CaSO_4$ particles has to be related to continental anthropogenic sources. The third cluster of 29 samples is elongated in the direction of the first and third principal components. The third component is related to high sulfur and aluminosilicate abundance variations. To validate the robustness of these identified clusters, a hierarchical cluster analysis (Ward's method, unstandardized variables) was performed on the data. When the result was studied at a three-cluster level, exactly the same clusters were found.

Table V. Mean Relative Percent Abundances of Each Particle Type Calculated for the Four Clusters That Were Formed by Principal Component Analysis

type	no.	sea salt	aged sea salt	S-rich	$CaSO_4$	Ca-rich	alumino-silicate	Si-rich	Ti	Fe	MF[a]
marine	14	76	13	2	2	4	2	1		1	100
$CaSO_4$	8	1		16	67		9	4		4	1
mixed	7	16	17	21	7	5	30	3		3	37
S/silic	22	1		41	9	2	27	6	5	9	1
mean	51	23	6	23	16	3	18	4	2	5	33

[a] MF, marine fraction.

The third group, however, cannot be attributed unambiguously to a specific source. Therefore, further separation within this group is necessary to differentiate marine influences from continental ones.

A second PCA was applied to these 29 samples. To enhance the difference between marine and continental aerosols, a new variable, the marine fraction (%) was introduced, replacing the sea-salt and aged sea-salt variables. The marine fraction was defined as

$$\text{marine fraction (\%)} = \frac{\langle \text{ss + aged ss} \rangle}{\langle \text{ss + aged ss} \rangle_{\text{marine cluster}}} \times 100$$

ss and aged ss represent the abundance of, respectively, the sea-salt and aged sea-salt particle type for each sample, and $\langle \text{ss + aged ss} \rangle_{\text{marine cluster}}$ is the mean of the sum of the sea-salt and aged sea-salt particle-type abundances for the marine cluster. The calculated value for the latter was 89%.

The loadings of the resulting first three principal components, listed in the three columns at the right side of Table IV, are plotted in Figure 7a and the scores are represented in Figure 7b. This figure shows two distinct clusters. One of them, with high score on the second principal component, consists of seven samples, and all have a high marine fraction (mean marine fraction of 37%). This means that these analyzed particles originate from mixed marine/continental air masses. The other identified cluster contains nearly 100% continent-derived particles (22 samples), e.g., mean marine fraction of 1%. Variations in this group are mainly due to a different silicate/sulfur ratio. Principal component 1 describes this and even a negative linear relationship between the silicate and sulfur is present ($r = -0.82$). The determination of the silicate/sulfur ratio reflects the contribution ratio of their respective emission sources. The mixing ratio combined with bulk trace metal analysis can probably be used to determine the trace metal content of the distinct emission sources. Besides the relative importance of the silicate and sulfur particulate sources, iron particulate source contributions are superimposed (principal component 3). In the mixed marine/continental group, the same dependency on the silicate/sulfur ratio is found.

Table V summarizes the relative particle abundances for each of the four cluster groups as well as the mean abundance for all particles analyzed. Also the marine fraction is calculated and listed. Note that the marine fraction obtained for the mixed continental/marine sample group has a value of 37%, whereas the mean marine fraction for all samples is 33%. This suggests that the mean of all samples taken during the six campaigns is also representative for mixed sampling conditions.

Conclusions

The aerosol concentrations near sea level vary greatly depending on proximity to natural and man-made sources. From the data set resulting from 25 000 individual particle analyses of 51 North Sea aerosol samples, four different aerosol groups could be differentiated on the basis of their composition. These groups were apportioned according to distinct particle emission sources.

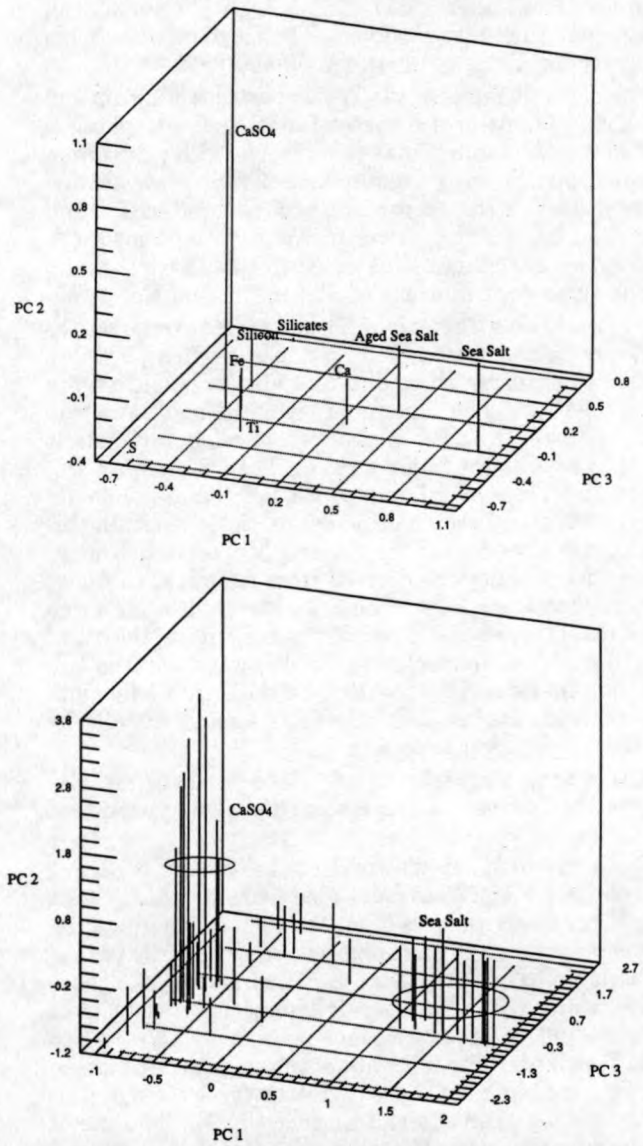

Figure 6. (a, top) Loadings of the first three principal components (51 samples), obtained by PCA of EPXMA of North Sea aerosol results. (b, bottom) Component scores of the first three principal components (51 samples), obtained by PCA of EPXMA of North Sea aerosol results.

More than 21% of all particles detected above the North Sea and surrounding waters represent sea-salt particles. Within this group, the marine contributions for S-rich, $CaSO_4$, and Ca-rich particles were estimated to be 0.5, 0.6, and 1.1%, respectively. Anthropogenic-derived S-rich particles and aluminosilicates represent 21 and 16%, respectively, of the aerosol composition, whereas industrial-derived $CaSO_4$ contributes almost 15% of all particles

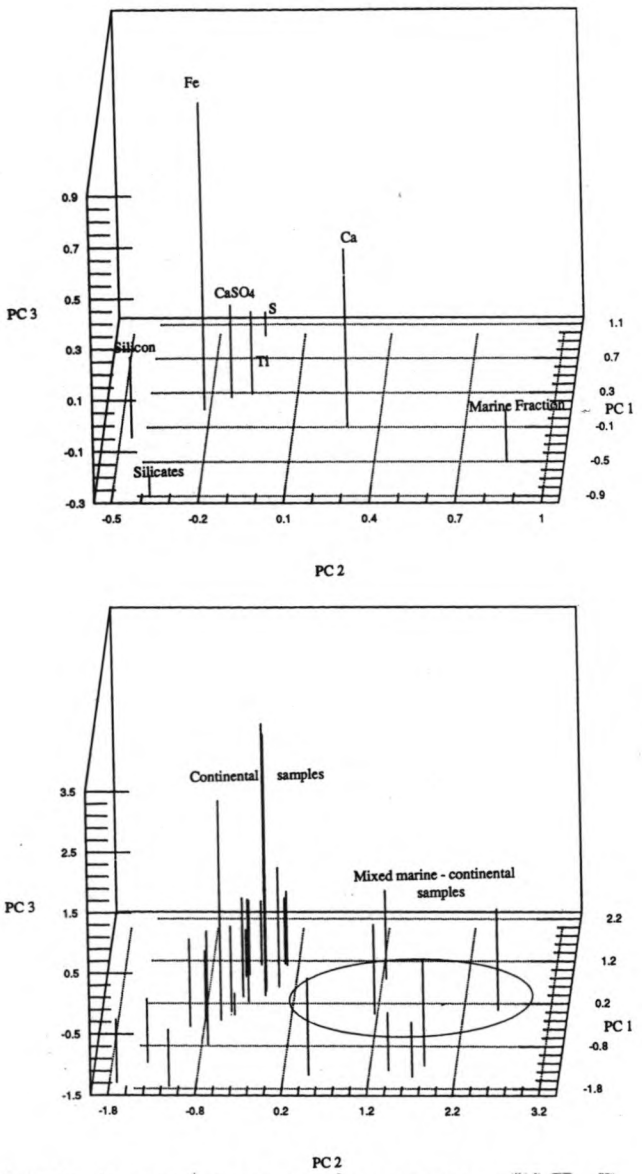

Figure 7. (a, top) Loadings of the first three principal components, obtained by a second PCA on the third cluster (29 samples) resulting from the first PCA. (b, bottom) Component scores of the first three principal components, obtained by second PCA on the third cluster (29 samples) resulting from the first PCA.

analyzed. About 13% of all North Sea particles is a mixture of particles from both marine/natural and continental/anthropogenic emission sources. For all other particle types detected, their contribution is less than 5% of the total North Sea aerosol and they are derived from various emission sources.

Registry No. S, 7704-34-9; $CaSO_4$, 7778-18-9; Ca, 7440-70-2; Si, 7440-21-3; Ti, 7440-32-6; Fe, 7439-89-6; quartz, 14808-60-7.

Literature Cited

(1) Otten, Ph., private communications, 1986.
(2) Bernard, P.; Van Grieken, R.; Eisma, D. *Environ. Sci. Technol.* **1986**, *20*, 467–473.
(3) Forgy, E. W. *Biometrics* **1965**, *21*, 768.
(4) Massart, D. L.; Kaufman, L. *The Interpretation of Analytical Data by the Use of Cluster Analysis*; Wiley: New York, 1983.
(5) Shattuck, T. W.; Germani, M. S.; Buseck, P. R. *Environmental Applications of Chemometrics*; Breen, J. J., Robinson, P. E., Eds.; ACS Symposium Series 292; American Chemical Society: Washington, DC, 1985; pp 118–129.
(6) Hopke, P. K. *Receptor Modelling in Environmental Chemistry*; John Wiley and Sons: New York, 1985.
(7) Saucy, D. A.; Anderson, J. R.; Buseck, P. R. *Atmos. Environ.* **1987**, *21*, 1649–1657.
(8) Kim, D. S.; Hopke, P. K.; Massart, D. L. *Sci. Total Environ.* **1987**, *59*, 141–155.
(9) Van Borm, W.; Adams, F. *Atmos. Environ.* **1988**, *22*, 2297–2307.
(10) Raeymaekers, B. Ph.D. Thesis, University of Antwerp, 1987.
(11) Op de Beek, J. P.; Hoste, J. *At. Energy Rev.* **1975**, *13*, 151–189.
(12) Rojas, C. M.; Otten, P.; Van Grieken, R. *J. Aerosol Sci.* **1989**, *20*, 1257.
(13) Blanchard, D. C. *Air–Sea Exchange of Gasses and Particles*; Liss, P. S., Slinn, W. G. N., Eds.; Riedel Publishing Co.: Dordrecht, The Netherlands, 1983; p 407.
(14) Bruynseels, F.; Storms, H.; Van Grieken, R.; Van der Auwera, L. *Atmos. Environ.* **1988**, *22*, 2593–2602.
(15) Martens, C. S.; Wesolowsky, J. J.; Harris, R. C.; Kaifer, R. *J. Geophys. Res.* **1973**, *78*, 8778.
(16) Erikson, E. *Tellus* **1960**, *12*, 63.
(17) Hitchcock, D. R.; Spiller, L. L.; Willson, W. E. *Atmos. Environ.* **1980**, *14*, 165–182.
(18) Clegg, S. L.; Brimblecombe, P. *Atmos. Environ.* **1985**, *19*, 465–470.
(19) Harrison, R. H.; Sturges, W. T. *Atmos. Environ.* **1984**, *18*, 1829–1833.
(20) Van Borm, W.; Adams, F.; Maenhaut, W. *Atmos. Environ.* **1989**, *32*, 1139–1151.
(21) Charlson, R. J.; Covert, D. S.; Larson, T. V.; Waggoner, A. P. *Atmos. Environ.* **1978**, *12*, 39–53.
(22) Post, J. E.; Buseck, P. R. *Environ. Sci. Technol.* **1984**, *18*, 35–42.
(23) Mamane, Y.; Noll, K. E. *Atmos. Environ.* **1985**, *19*, 611–622.
(24) Dzubay, T. G.; Mamane, Y. *Atmos. Environ.* **1989**, *23*, 467–476.
(25) Mamane, Y.; Miller, J. L.; Dzubay, T. G. *Atmos. Environ.* **1986**, *20*, 2125–2135.
(26) Reference deleted in proof.
(27) Andreae, M. O.; Charlson, R. J.; Bruynseels, F.; Storms, H.; Van Grieken, R.; Maenhaut, W. *Science* **1986**, *232*, 1620–1623.
(28) Parungo, F.; Ackerman, E.; Proulx, H.; Pueschel, R. *Electron Microscopy and X-Ray Applications to Environment and Occupational Health Analysis*; Russel, P. A., Hutchings, A. E., Eds.; Ann Arbor Science: Ann Arbor, MI, 1979.
(29) Borchert, B. In *Chemical Ocenography*; Skirrow, G., Riley, J. P., Eds.; Academic Press: London, 1965; Vol. 2.
(30) Husain, L. *Toxic Metals in the Atmosphere*; Nriagu, J. O., Davidson, C. L., Eds.; Advances in Environmental Science and Technology 17; John Wiley and Sons: New York.
(31) Xhoffer, C. M.Sc. Thesis, University of Antwerp (UIA), 1987.
(32) Graham, W.; Piotrowicz, S. R.; Duce, R. A. *Mar. Chem.* **1979**, *7*, 325–342.
(33) Chen, L.; Arimoto, R.; Duce, R. A. *Atmos. Environ.* **1985**, *19*, 779–787.
(34) Post, J. E.; Buseck, P. R. *Environ. Sci. Technol.* **1985**, *19*, 682–685.
(35) Sturges, W. T.; Harrison, R. M. *Atmos. Environ.* **1986**, *20*, 1485–1496.
(36) Van Espen, P. *Anal. Chim. Acta* **1984**, *165*, 31–49.

Received for review October 15, 1990. Accepted March 21, 1991. This work was partially supported by the Belgian Ministery for Science Policy under Contract 84-89/69 and by a NATO research grant. C.X. acknowledges a research fellowship from the Belgian Instituut ter Aanmoediging van Wetenschappelijk Onderzoek in Nijverheid en Landbouw. H. Storms carried out some of the EPXMA measurements.

Selected article #15:

Elemental composition of aircraft-sampled aerosols above the Southern Bight of the North Sea

C.M. Rojas, R.E. Van Grieken and W. Maenhaut

Water, Air, and Soil Pollution, 71 (1993) 391-404

8422

ELEMENTAL COMPOSITION OF AIRCRAFT-SAMPLED AEROSOLS ABOVE THE SOUTHERN BIGHT OF THE NORTH SEA

CARLOS M. ROJAS, RENÉ E. VAN GRIEKEN

Department of Chemistry, University of Antwerp (UIA), Universiteitsplein 1, B-2610 Antwerp-Wilrijk, Belgium

and

WILLY MAENHAUT

Institute for Nuclear Sciences, University of Ghent, Proeftuinstraat 86, B-9000 Ghent, Belgium

(Received July 2, 1988; revised September 24, 1988)

Abstract. During the period from September 1988 to October 1989, 23 flights were carried out over the Dutch Continental Shelf of the North Sea and a total of 108 aerosol filter samples were collected. The samples were analyzed for Na, Mg, Al, Si, P, S, Cl, K, Ca, Ti, V, Cr, Mn, Fe, Ni, Cu, Zn, Br and Pb using both particle-induced X-ray emission (PIXE) and energy-dispersive X-ray fluorescence (EDXRF). The results from PIXE exhibited better precision and lower detection limits than those from EDXRF. Therefore the further discussion and interpretation was based on the PIXE data only. It was observed that Si, S, V, Mn, Ni, Cu and Pb were enriched with respect to the earth's crust. It was seen that winds from the sector Southeast-South contributed most significantly to the total aerosol concentration. The vertical profiles of several elements indicated that their concentration increases with proximity to the sea. Principal factor analysis on the data matrix containing elemental concentrations, height and wind direction parameters allowed us to identify 6 possible aerosol sources, namely, a composite of $CaSO_4$ and metallurgical activities, refuse incineration, residual oil combustion, quartz, soil dust and sea-salt aerosol.

1. Introduction

There has been a growing concern regarding the pollution of coastal and shelf systems of the North Sea, especially since Weichart (1973) concluded that the North Sea is one of the most heavily polluted areas.

For several pollutants the atmospheric input to the North Sea may be of the same order or larger than the input through rivers or from coastal or other discharges. Initial efforts to assess the atmospheric input include the measurements of airborne concentrations at a gas platform, reported by Pierson *et al.* (1974), and the samplings of air pollutants carried out by Cambray *et al.* (1975, 1979) and later by Flament *et al.* (1987). Recently, Baeyens and Dedeurwaerder (1991) reported on the results from the West-Hinder light vessel, which has been used for a number of years to monitor air pollutants in the southern bight of the North Sea. In order to overcome the problems associated with aerosol sampling over natural waters, mathematical models have been developed that are capable of simulating the dispersion of air pollutants over the sea and predicting the spatial and temporal distribution of the pollutants (Van Jaarsveld *et al.*, 1986; Krell and Roeckner, 1988; Petersen *et al.*, 1989).

Water, Air, and Soil Pollution **71**: 391–404, 1993.

This paper reports on the elemental composition of tropospheric aerosols based upon a set of 108 aerosol samples that were collected with the aid of an aircraft over the Dutch continental shelf of the North Sea, during a period of 1 year, and which were analyzed using both PIXE and EDXRF. The composition of the North Sea airborne matter was studied as a function of altitude and wind direction. Furthermore, an attempt was made to identify the various aerosol sources for the southern bight of the North Sea by subjecting the multivariate data set to principal factor analysis.

Experimental

The sampling campaign started in September 1988, and lasted for 13 months. During this period, 23 flights were carried out using a twin engine aircraft Piper Chieftain, PA 31-350, owned by the company Geosens B.V. (Rotterdam, The Netherlands). All flights were performed with relatively clear skies, and avoiding precipitation. The history of the air masses was studies using the 36-h backward trajectories provided by the Royal Netherlands Meteorological Institute (KNMI, De Bilt, The Netherlands), for four different pressure levels: 1000, 925, 850 and 700 hPa, respectively. All flights started at the same reference point namely, the Goeree platform (51 °55.5′ N-3 °40′ E), from which a spiral upward flight was performed in order to locate the inversion layer. The aerosol sampling took place in six different tracks, each covering a distance of about 110 km toward the North Sea in the up or down-wind direction from the Goeree platform, and more or less equally spaced between the inversion layer and sea level. The flight alitude was measured using a King Radar Altimeter model KRA 10/10a, the ambient temperature was monitored using a 102 E temperature sensor with Pt-100 element (nominal resolution 0.1 °C) (Rosemount, Inc., USA), and the wind speed and location were determined using a Racall Doppler 91 radar equipped with a RSN 252 navigation compass, with a wind speed precision of 1 m s^{-1} and a position accuracy of 0.1 nautical mile. Airborne particulate matter was sampled using an isokinetic inlet designed by the Pennsylvania State University (Pena *et al.*, 1977), and collected on 47 mm diameter 0.4 μm poresize Nuclepore menbrane filters. No attempt was made to determine the effective cutoff diameter of the aerosol. After the air passed through the filters, it was pumped-out using a Venturi system which was mounted on the wings of the aircraft. This had the advantage of being very light without requiring electric power. The airflow was about 50 l min^{-1}. The whole sampling campaign resulted in a set of 108 aerosol samples. These samples were analyzed for Na, Mg, Al, Si, P, S, Cl, K, Ca, Ti, V, Cr, Mn, Fe, Ni, Cu, Zn, Br and Pb by PIXE. The samples were irradiated by a 2.4 MeV proton beam, supplied by the compact isochronous cyclotron of the Institute for Nuclear Sciences, University of Ghent. Full details on the PIXE setup, analytical procedures and calibration can be found elsewhere (Maenhaut *et al.*, 1981; Maenhaut and Raemdonck, 1984). For Na, the PIXE data should be considered as semi-quantitative only because of important

matrix effects. The same set of samples was analyzed for the same elements by EDXRF, using the analytical procedure described by Rojas *et al.* (1990).

Receptor Modeling

The main idea of receptor modeling is measuring concentrations of various species at a given sampling site (receptor) and using this information to identify the number of major particle sources. The receptor model used in this work was principal factor analysis. In principal factor analysis, the variability in the trace elements concentrations is used to transform the intercorrelated variables into a set of independent and uncorrelated variables. To do this, one has to determine the eigenvalues and associated eigenvectors of the correlation matrix. Those factors (eigenvectors) which satisfy a given condition (e.g. having a variance higher than unity), are retained and orthogonally rotated by a Varimax rotation (Henry and Hidy, 1979). Principal factor analysis results in both a factor-loading matrix, which represents the correlations between the retained factors and the variables and the so-called factor scores, which represent the weight of each factor for the individual cases. The identification of the various sources is based upon the principal factor solution, for this particular case, and its comparison with results reported in the literature.

Results and Discussion

Since the aerosol samples were analyzed using two separate techniques, namely PIXE and EDXRF, it was necessary to compare and assess their results. The outcomes of this comparison are summarized in Table I, while Figure 1 shows plots of the linear regression of EDXRF on PIXE for those elements (S and Pb) pre-

TABLE I

Slope and standard deviation of the linear regression of EDXRF on PIXE. The average ratio of EDXRF to PIXE, together with the detection limits for both techniques, are also tabulated

Element	EDXRF on PIXE Slope ± std dev	EDXRF/PIXE mean ± sdev	Detection limit (ng cm^{-2})	
			PIXE	EDXRF
Al	1.38 ± 0.32	2.1 ± 2.0	15	36
Si	0.32 ± 0.03	1.0 ± 0.8	10	17
S	1.08 ± 0.01	1.0 ± 0.2	8	7
K	0.68 ± 0.03	0.8 ± 0.4	5	3
Ca	1.77 ± 0.05	2.1 ± 0.5	4	9
V	1.51 ± 0.12	1.9 ± 0.7	1	4
Mn	1.41 ± 0.07	1.4 ± 0.3	0.6	2
Fe	1.48 ± 0.06	1.7 ± 0.8	0.5	2.5
Ni	1.73 ± 0.07	2.0 ± 0.3	0.4	1.4
Cu	1.86 ± 0.05	2.0 ± 0.3	0.3	1.2
Zn	1.41 ± 0.02	1.5 ± 0.3	0.3	0.9
Pb	1.03 ± 0.02	1.2 ± 0.3	0.1	1.9

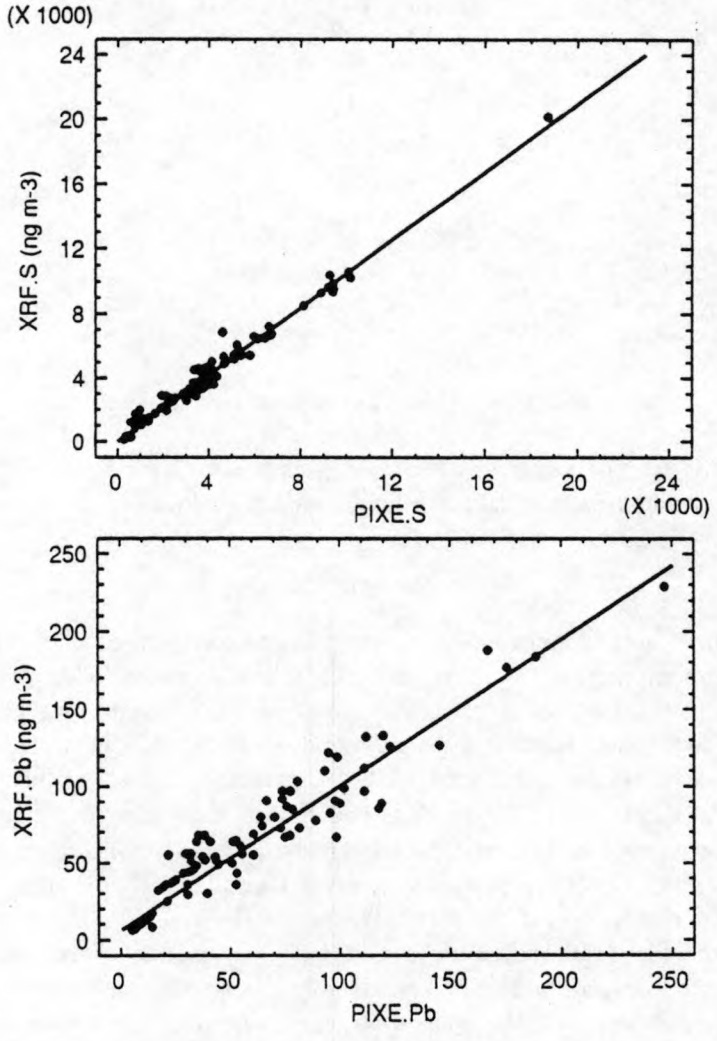

Fig. 1. Scatter plot and linear regression line of EDXRF on PIXE elemental concentrations for S and Pb, respectively.

senting the best fit. Only those elements which were detected by both techniques are tabulated. From the slope of the linear fit one can see that EDXRF presented systematically higher values than PIXE, with the exception of Si and K for which the EDXRF concentration was lower. The average difference between these two techniques reaches up to 50%. One the other hand, the detection limit for EDXRF obtained during this work appears to be on the average 4 times higher than that of PIXE (Maenhaut, 1989). It is thought that the observed differences can be attributed to several reasons, namely: heterogeneous distribution of the aerosol concentration on the filter (different sections of the filter were analyzed), the presence of spurious peaks with variable intensity, probably from coherently scattered radia-

TABLE II

Aerosol elemental concentrations for the southern bight of the North Sea. The mean values for this work were calculated replacing missing values by half of the detection limit. The figures in parentheses indicate the number of samples (out of 108) with non-missing values

Element	Mean ± Std deviation (ng m^{-3})
Na (30)	730 ± 1150
Al (30)	100 ± 190
Si (93)	1450 ± 1450
S (102)	3800 ± 3460
Cl (32)	200 ± 400
K (90)	250 ± 220
Ca (84)	130 ± 130
Ti (19)	4.8 ± 10
V (29)	8 ± 17
Mn (83)	13 ± 10
Fe (98)	180 ± 140
Ni (34)	5.2 ± 10
Cu (28)	3.1 ± 5.9
Zn (102)	60 ± 50
Pb (84)	50 ±40

tion inside the X-ray spectrometer sample chamber which introduced high variation in the blank concentrations, and last but not least, the low aerosol concentrations associated with a fairly low loading of the filters, making the determination of trace species subject to large uncertainty. Despite all of this, the agreement between PIXE and EDXRF for S and Pb is very good. There are basically two reasons for such an agreement: sulfur is an abundant element, whereas Pb was free from the above mentioned spectral interferences. Since direct tube excitation EDXRF has the disadvantage of a high background due to scattered Bremsstrahlung radiation, the detection limits are higher compared to those obtained by PIXE. Due to the lower number of samples with concentrations below detection limit, PIXE results will be used throughout this work.

Average elemental concentrations

The average elemental concentrations of Na, Al, Si, S, Cl, K, Ca, Ti, V, Mn, Fe, Ni, Cu, Zn and Pb in 108 samples, are listed in Table II. Several elements, namely Mg, P, Cr and Br, were left out because of the large number of values below the detection limit. For the other elements, when individual data were below the detection limit, they were replaced by half the detection limit.

The large standard deviation of the elemental concentrations results from two reasons: the 108 samples included those taken above the thermal inversion layer. It has been shown Injuk *et al.* (1990) that there is a difference of more than a

TABLE III

Comparison of some of the elemental concentrations reported in this work with literature data for the North Sea. Here (–) stands for not reported and the letters in parentheses indicate the cited reference

Elemental concentrations (ng m^{-3})								
Element	(a)	(b)	(c)	(d)	(e)	(f)	(g)	(h)
Na	3960	–	–	1700	–	–	2000 ± 1400	730 ± 1150
Al	190	155–240	–	550	390	–	140 ± 150	100 ± 190
V	12	9–11	7	–	–	1.1	–	8 ± 17
Mn	20	14–22	9	130	28	10	15 ± 19	13 ± 10
Fe	320	290–330	190	410	560	220	300 ± 370	180 ± 140
Ni	10	5–7	5	–	–	3	–	5 ± 10
Cu	< 20	–	3	20	17	–	15 ± 10	3 ± 6
Zn	150	75–120	40	100	150	40	67 ± 90	60 ± 50
Pb	140	96–130	40	60	150	34	100 ± 100	50 ± 40

(a) Peirson *et al.* (1974)
(b) Cambray *et al.* (1975)
(c) Stoessel (1987)
(d) Flament *et al.* (1987)
(e) Dedeurwaerder (1988)
(f) Yaaqub (1989)
(g) Beayens and Dedeurwaerder (1991)
(h) This work

factor of two between observations made above and below the inversion layer height. Secondly, the 108 samples were taken under different wind directions and different meteorological conditions.

Table III shows a comparison of some of the elemental concentrations observed in this work with those obtained in previous studies of aerosol composition above the North Sea. These include studies at a gas platform (Peirson *et al.*, 1974), coastal stations (Cambray *et al.*, 1975; Flament *et al.*, 1987), and the West-Hinder light vessel (Dedeurwarder, 1988; Baeyens and Dedeurwaerder, 1991). In general, the concentrations reported here are within the range of values given in the literature for most of the elements, although they are consistently lower than those recently reported by Baeyens and Dedeurwaerder (1991). It has to be stressed that none of the previous studies included measurements carried out aloft and that some of them (Cambray *et al.*, 1975; Dedeurwaerder, 1988) were performed at or near coastal stations. Furthermore, it is interesting to note that there are marked differences between the results reported by Dedeurwaerder (1988) and those from Baeyens and Dedeurwaerder (1991) for the same sampling site.

Natural aerosol sources

Since the aerosol at the southern bight of the North Sea is rather mixed and originates from a variety of sources including soil dust, marine and anthropogenic, it is worthwhile to resolve the average elemental composition given in Table II and

TABLE IV

Resolution of the average elemental concentrations (ng m^{-3}) observed over the southern bight of the North Sea into crustal and marine components. See text for explanation

Element	Crustal	Non-crustal	Marine	Unaccounted for
Na	35	695	695	–
Al	100	–	–	–
Si	340	1100	0.19	1100
S	0.3	3800	58	3740
Cl	0.2	200	1250	-1050
K	32	220	26	190
Ca	45	85	27	59
Ti	5.4	-0.6	–	-0.6
V	0.2	8.1	–	8.1
Mn	1.2	12	–	12
Fe	62	120	–	120
Ni	0.09	5.1	–	5.1
Cu	0.07	3.0	–	3.0
Zn	0.09	63	–	63
Pb	0.02	53	–	53

TABLE V

Contribution (in %) of crustal, marine and other aerosol sources to the atmospheric elemental concentrations over the southern bight of the North Sea

Element	Crustal	Marine	Other
Na	4.8	95.2	–
Al	100	–	–
Si	23	0.01	77
S	0.01	1.5	98.5
Cl	0.1	99.9	–
K	13	10	77
Ca	34	21	45
Ti	110	–	–
V	2.5	–	97.5
Mn	9	–	91
Fe	34	–	66
Ni	1.7	–	98.3
Cu	2.3	–	97.7
Zn	0.2	–	99.8
Pb	0.04	–	99.96

calculate the relative crustal and marine contribution to the various elements. To do this, use was made of the average crustal rock composition of Mason (1966) and the average bulk sea water composition reported by Rahn (1976). The resolution of the components of the North Sea aerosol was carried out as follows: from the average crustal rock composition, the elemental ratios to Al were calculated and

it was assumed that the Al in the aerosols was entirely from crustal origin. The results are presented in Table IV (columns 2 and 3). The non-crustal component is simply the difference between the given average concentrations and the crustal component. The fourth column in Table IV (marine) was computed using the bulk sea water composition and assuming that the non-crustal Na was totally from marine origin. The last column then represents the excess concentration and corresponds to the difference between the total for an element and the sum of its crustal and marine components. Table V summarizes the contribution of each of the these components as a percentage of the total observed concentration.

It can be seen from Tables IV and V that only 23 and 34% of the concentrations of Si and Fe could be attributed to earth's crust; while the contribution of soil and marine to the total K and Ca was 23 and 55%, respectively. The highly enriched elements are: S, V, Mn, Ni, Zn and Pb, which most likely originate from human activities.

Elemental concentrations vs wind direction

In order to determine a possible relationship between the elemental concentrations and wind direction as determined from the back trajectories, five different wind sectors were defined. These were: Southwest-West, Northwest-North, Northeast-East, Southeast-South and Local. The latter represents air masses with variable

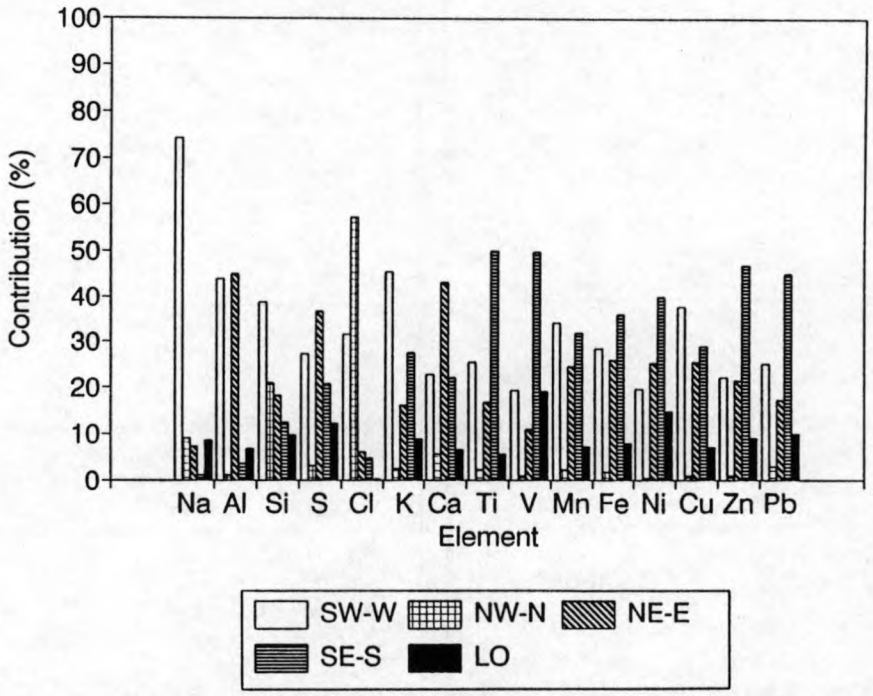

Fig. 2. Contribution (in %) from the different wind sector to the total airborne elemental concentration observed above the southern bight of the North Sea.

origin, and that in most of the cases circumscribe to the North sea itself. Since one wind sector contributed only to one sample, the apportionment from each wind sector was calculated taking into account the percent wind direction frequency, extracted from Hohn (1971).

The contribution (%) from the different wind sectors to the total airborne elemental concentration observed above the southern bight of the North Sea, is shown in Figure 2. It is seen that wind sector West-Southwest contributes significantly to the total concentration of Na, Al, Si, Cl, K, Mn and Cu. The contribution of wind sector Northwest-North is about 20% for Si and over 60% for Cl, which reflects the direct influence of the marine air masses. The elemental concentrations associated with wind sector Northeast-East were particularly high for Al, S, Ca. Winds from the Southeast-South sector were responsible for more than 40% of the total observed Ti, V, Ni, Zn and Pb. Winds from this direction also contained significant concentrations of K, Mn, Fe and Cu. Local air masses had high concentrations of V and Ni. On the basis of the data in Figure 2 it is concluded that the wind sector Southeast-South provides the largest contribution to the particulate concentration of heavy metals over the southern bight of the North Sea. This is not surprising, considering the highly industrialized character of the countries grouped in this area.

Elemental concentrations vs height

The variation of elemental concentrations with flight level (height) is shown in Figure 3. Data are presented for Na, Cl and Ti (a), Si, K, Ca and Fe (b) and S, V, Mn, Ni, Cu, Zn and Pb (c). Here, level 1 represents high altitude whereas level 6 is very close to the sea. This way of representing height has been adopted to avoid the variation of the thermal inversion height. The linear regression of the elemental concentration on level number is represented by the continuous line. For Na and Cl there is a slight increase in concentration with decreasing altitude; this is much more pronounced for Ti, with a difference of almost an order of magnitude between the two extreme levels. The Cl/Na ratio is at all levels much lower than the sea water ratio of 1.79 (Rahn, 1976). This undoubtedly results from interactions of sea-salt particles with gaseous acidic species in the atmosphere or on the filter (e.g. Martens *et al.*, 1973). The profiles of K, Ca, Fe, V, Mn, Ni, Cu, Zn and Pb (Figs, 3b and c) are rather similar and all these elements show higher concentrations at lower altitudes. This is clearly not the case for Si, for which the maximum concentration is found at level 1. This might suggest that Si originates from a distant source. This fact could explain the Si enrichment with respect to average crustal rock. As far as S is concerned, there is no real gradient with altitude, so that one may conclude that this element is homogeneously distributed between the inversion layer height and sea level.

Multivariate analysis

In an attempt to identify the various aerosol sources for the Southern North Sea airshed, the matrix containing the elemental concentrations of Na, Al, Si, S, Cl,

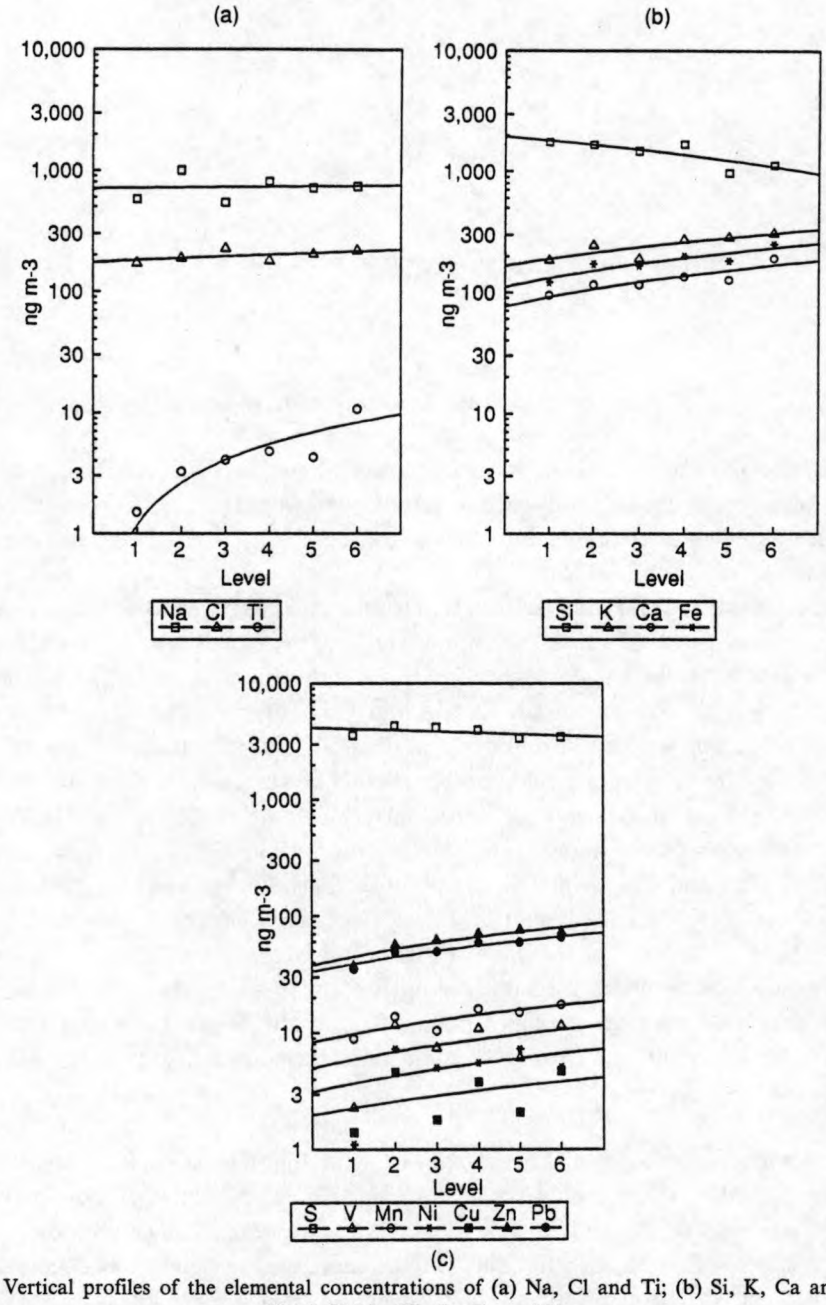

Fig. 3. Vertical profiles of the elemental concentrations of (a) Na, Cl and Ti; (b) Si, K, Ca and Fe, and (c) S, V, Mn, Ni, Cu, Zn and Pb.

K, Ca, Ti, V, Mn, Fe, Ni, Cu, Zn and Pb for the 108 aerosol samples was subjected to principal factor analysis (Henry *et al.*, 1984; Hopke, 1985). The altitude expressed as levels 1 through 6 together with the wind direction components NS and EW, calculated using the procedure described by Tuncel *et al.* (1985), were also included

TABLE VI

Varimax rotated factor loading matrix for the southern bight of the North Sea aerosol. Only loadings higher than 0.40 are tabulated

	Factor 1	Factor 2	Factor 3	Factor 4	Factor 5	Factor 6	Commun.
Na	–	–	–	0.83	–	–	0.72
Al	–	–	–	–	0.81	–	0.80
Si	–	–	–	0.71	–	–	0.75
S	0.84	–	–	–	–	–	0.77
Cl	–	–	–	–	–	0.60	0.74
K	–	0.77	–	–	–	–	0.67
Ca	0.73	–	–	–	0.40	–	0.77
Ti	–	–	–	–	0.77	–	0.80
V	–	–	0.87	–	–	–	0.80
Mn	0.73	–	–	–	–	–	0.80
Fe	0.59	–	–	–	0.50	–	0.85
Ni	–	–	0.85	–	–	–	0.74
Cu	0.60	–	–	–	–	–	0.50
Zn	0.59	0.54	0.41	–	–	–	0.90
Pb	0.49	0.55	0.55	–	–	–	0.90
Height	–	–	–	–	–	0.74	0.61
NS	–	–0.81	–	–	–	–	0.75
EW	0.45	–	–	–0.62	–	–	0.78
Eigenv.	3.5	2.5	2.4	2.0	1.9	1.3	
% Var.	19	13.8	13.3	11.1	10.5	7.2	
Possible origin	Industry	Refuse	Oil	Marine/ silicate	Soil	Marine	

in the data matrix. The principal factor solution yielded 6 eigenvalues greater than 1 and the 6 corresponding factors explained 76% of the variance in the data set. The communalities varied between 50% for Cu and 90% for Pb. The low value for Cu could be due to the large number of missing values that were replaced by half of the detection limit, by doing so, the variability of the concentration of this element was reduced. The resulting factor loadings after an orthogonal varimax rotation (Henry and Hidy, 1979) together with the communality for each variable, are given in Table VI.

Factor 1 has high loadings for S, Ca, Mn and moderate loadings for Fe, Cu, Zn, Pb and the EW variable. This factor probably represents a composite of several aerosol sources. The association of S and Ca was also observed during the microscopical characterization of the aerosol samples (Rojas and Van Grieken, 1992). The remaining elements could be related to metallurgical activities such as iron, steel and ferro-alloys manufacturing (Pacyna, 1984). The positive correlation with the EW variable indicates that the impact of these aerosol sources is associated with easterly winds. Factor 2 exhibits a high correlation for K, moderate for Zn and Pb and high but negative for the wind variable NS. These elements are often

found in refuse incineration emissions (Core *et al.*, 1984). The negative loading for NS indicates association with southern winds. Factor 3 shows high correlations for V, Ni and a moderate one for Pb. The former two elements are used as tracers for residual oil combustion (Kronborg *et al.*, 1987). There is no connection with wind direction in this factor. Factor 4 is correlated with Na, Si and anti-correlated with the EW variable. This could be the result of the coagulation of quartz particles and sea spray, associated with westerly winds. Factor 5 has high loadings for the elements that are typically associated with soil dust. Factor 6 presents a slight association of Cl with height. This factor probably represents a marine source and, as expected, Cl is more abundant at lower altitudes.

Conclusions

Two analytical techniques were used to determine the elemental concentrations in the 108 samples collected above the southern bight of the North Sea. These techniques were EDXRF and PIXE. From the comparison of these two techniques it appeared that tube excited EDXRF suffered from a verry high spectral background due to coherently scattered Bremsstrahlung. Consequently, the precision and detection limits were poorer than those in PIXE, and therefore the results from the latter technique were used throughout this work. After resolving the average elemental concentrations in contributions from the earth's crust and bulk sea water it was concluded that the anomalously enriched elements were Si, S, V, Mn, Ni, Cu, Zn and Pb. It was observed that winds associated with the sector Southeast-South contributed most to the total particulate concentration of the heavy metals above the southern bight. From the vertical profiles it appeared that for most elements the concentration increased with proximity to the sea. This was not the case for Si for which the concentration increased with high altitude. Sulfur exhibited no real vertical gradient, indicating that it is homogeneously distributed between the inversion layer height and sea level. Multivariate analysis on the data matrix containing elemental concentrations, height and wind direction parameters, resulted in 6 factors, accounting for 76% of the variance in the data set. Factor 1 was correlated with S, Ca and other elements related to metallurgical activities. Factor 2 was attributed to refuse incineration, Factor 3 to residual oil combustion, Factor 4 to a coagulation of quartz particles and sea spray, whereas factors 5 and 6 represented soil dust and marine sources.

Acknowledgements

We are grateful to Rijkswaterstaat (The Hague, the Netherlands) for financial support through project NOMIVE*2 tasks No. DGW-920 and DGW-217. One of us (W.M.) is indebted to the Belgian 'Nationaal Fonds voor Wetenschappelijk Onderzoek' for financial support.

References

Baeyens, W. and Dedeurwaerder, H.: 1990, 'Particulate Trace Metals Above the Southern Bight of the North Sea-l. Analytical Procedures and Average Aerosol Concentrations'. *Atmos. Environ.* **25A**, 293–304.

Cambray, R. S., Jefferies, D. F., and Topping, G.: 1975, 'An Estimate of the Input of Atmospheric Trace Elements into the North Sea and the Clyde Sea'. AERE Report R 7733.

Cambray, R. S., Jefferies, D. F., and Topping, G.: 1979, 'The Atmospheric Input of Trace Elements to the North Sea'. *Mar. Sci. Commun.* **5**, 175–194.

Core, J, E., Shah, J., and Cooper, J. A.: 1984, 'Receptor Model Source Composition Library'. US-EPA Report EPA-450/4-85-002 Research Triangle Park, North Carolina, N.C.

Dedeurwaerder, H. L.: 1988, 'Study of the Dynamic Transport and of the Fall-Out of some Ecoto-xicological Heavy Metals in the Troposphere of the Southern Bight of the North Sea'. Ph. D. Dissertation, Vrije Universiteit Brussel, Brussels, Belgium.

Flament, P., Lepetre, A., Noel, S., and Auger, Y.: 1987, 'Aerosols cotiers dans le nord de la Manche', *Ocean. Acta* **10**, 49–61.

Henry, R. C., Lewis, C. W., Hopke, Ph., and Williamson, H. J.: 1984, 'Review of Receptor Model Fundamentals', *Atmos. Environ.* **18**, 1507–1515.

Henry, R. C. and Hidy, G. M.: 1979, 'Multivariate Analysis of Particulate Sulfate and Other Air Quality Variables by Principal Component Analysis. l. Annual Data from Los Angeles New York', *Atmos. Environ.* **13**, 1581–1596.

Hohn, R.: 1971, 'On the Climatology of the North Sea', in: Goldberg, E.D. (ed.), *North Sea Science*, NATO North Sea Conference, Aviemore, Scotland.

Hopke, Ph.: 1985, *Receptor Modeling in Environmental Chemistry*, Wiley, New York, N.Y.

Injuk, J., Otten, Ph., Rojas, C. Wouters, L., and Van Grieken, R.: 1990, 'Atmospheric Deposition of Heavy Metals (Cd, Cu, Zn and Pb) into the North Sea', Final Report to Rijkswaterstaat, The Hague, The Netherlands.

Krell, U. and Roeckner, E.: 1988, 'Model Simulation of the Atmospheric Input of Lead and Cadmium into the North Sea. *Atmos. Environ.* **22**, 375–381.

Kronborg, D., Jensen, F. P., Keiding, K., and Heidam, N.: 1987, 'Determination of Sources of Atmospheric Aerosol in Copenhagen Based on Receptor Models', *Atmos. Environ.* **9** 1877–1889.

Maenhaut, W., Selen, A., Van Espen, P., Van Grieken, R., and Winchester, J. W.: 1981, 'PIXE Analysis of Samples Collected over the Atlantic Ocean from a Sailboat', *Nucl. Instrum. Methods* **181**, 399–405.

Maenhaut , W. and Raemdonck, H.: 1984, 'Accurate Calibration of a Si(Li) Detector for PIXE', *Nucl. Instrum. Methods* **B1**, 123–136.

Maenhaut, W.: 1989, 'Analytical Techniques for Atmospheric Trace Elements', in Pacyna, J. and Ottar, B. (eds.), *Control and Fate of Atmospheric Trace Metals*, Kluwer Academic Publisher, Dordrecht, The Netherlands.

Martens, C. S., Wesolowski, J. J., Harriss, R. C., and Kaifer, R.: 1973, 'Chlorine Loss from Puerto Rican and San Francisco Bay Area Marine Aerosols', *J, Geophys. Res.* **78**, 8778–8792.

Mason, B.: 1966, *Principles of Geochemistry*, Wiley, New York, N.Y.

Pacyna, J.: 1984, 'Estimation of the Atmospheric Emissions of Trace Elements from Anthropogenic Sources in Europe', *Atmos. Environ.* **18**, 41–50.

Pena, J. A., Norman, J. M., and Thomson, D. W.: 1977, 'Isokinetic Sampler for Continuous Airborne Measurements', *J. Air Poll. Control Ass.* **27**, 337–340.

Petersen, G., Weber, H., and Grassl, H.: 1989, 'Modelling the atmospheric transport of trace metals from Europe to the North Sea and the Baltic Sea', in Pacyna, J. and Ottar, B. (eds.), *Control and Fate of Atmospheric Trace Metals*, Kluwer Academic Publisher, Dordrecht, The Netherlands.

Rahn, K.: 1976, *The Chemical Composition of the Atmospheric Aerosol*, Technical Report Graduate School of Oceanography, University of Rhode Island, R.l.

Rojas, C. M., Artaxo, P., and Van Grieken, R. E.: 1990, 'Aerosols in Santiago de Chile: a Study Using Receptor Modeling with X-Ray Fluorescence and Single Particle Analysis', *Atmos. Environ.* **24B**, 219–241.

Rojas, C. M. and Van Grieken, R.: 1992, 'Electron Microprobe Characterization of Individual Aerosol

Particles Collected by Aircraft Above the Southern Bight of the North Sea', *Atmos. Environ.* **26A**, 1231–1237.

Stoessel, R.: 1987, 'Untersuchungen zu Nass und Trockendeposition von Schwermetallen auf der Insel Pellworm', Ph. D. Dissertation, University of Hamburg, F.R.G.

Tuncel, S. G., Olmez, l., Parrington, J. R., Gordon, G., and Stevens, R. K.: 1985, 'Composition of Fine Particle Regional Sulfate Component at Shenandoah Valley', *Environ. Sci. and Technol.* **19**, 529–537.

Van Jaarsveld, J. A., Van Aalst, R. M., and Onderdelinden, D.: 1986, *Deposition of Metals from the Atmosphere into the North Sea: Model Calculations*, Report RIVM 842015002, Bilthoven, The Netherlands.

Weichart, G.: 1973, 'Pollution of the North Sea', *Ambio* **2**, 99–106.

Yaaqub, R.: 1989, Ph. D. Dissertation, University of East Anglia, Norwich, U.K.

Selected article #16:

Individual aerosol particle composition variations in air masses crossing the North Sea

L.A. De Bock, H. Van Malderen and R.E. Van Grieken

Environmental Science and Technology, 28 (1994) 1513-1520

2570

Reprinted from ENVIRONMENTAL SCIENCE & TECHNOLOGY, Vol. 28, 1994

Individual Aerosol Particle Composition Variations in Air Masses Crossing the North Sea

Lieve A. De Bock,* Hans Van Malderen, and René E. Van Grieken

Department of Chemistry, University of Antwerp, Universiteitsplein 1, B-2610 Antwerp-Wilrijk, Belgium

Single-particle analysis on North Sea aerosol and rainwater samples was performed by electron-probe X-ray microanalysis (EPXMA). The analysis was mainly focused on the determination of the inorganic composition of giant particles with diameters above 1 μm. Multivariate techniques were used for the reduction of the data set and for source apportion. Based on the relative abundances found by hierarchical cluster analysis according to the Ward error sum method, three to eight different aerosol types were distinguished. Crossing the North Sea, the changes in air mass composition appeared as a decrease in the abundance for the aluminosilicate particles and a relative increase for NaCl and seawater crystallization products. Principal factor analysis revealed four different aerosol sources: aluminosilicates and NaCl, seawater crystallization products as a marine source, and two industrial sources. Relations between the particle composition, origin, and shape were studied by manual EPXMA, and for most of the particle types, a characterization based on their shape was obtained.

Introduction

It has been shown that atmospheric deposition represents a major input route to the North Sea for some pollutants, like heavy metals (*1*). Within the scope of the EUROTRAC Project "Air–Sea Exchange", aerosol and rainwater samples were collected above the North Sea on board two research vessels continuously positioned downwind from each other. The aim of this project was to study variations in the composition of air masses crossing the North Sea due to air–sea exchange processes in the lower troposphere. The two major exchange processes considered to be responsible for possible changes in air mass composition are dry deposition, such as sedimentation or gravitational fallout and impaction, and wet deposition, such as rainout, snowout, and washout. A decrease in particle concentration could also be the result of vertical dilution of the air masses. Obviously, chemical and physical reactions in the atmosphere as well as parameters like wind speed, relative humidity, and temperature affect these processes.

The single-particle analysis in the present study was performed by electron probe X-ray microanalysis (EPXMA), one of the most commonly used nondestructive microanalytical techniques. In spite of its unfavorable detection limits (0.1%), automated EPXMA is, in combination with multivariate techniques, a powerful method for the determination of the chemical composition and characterization of a large number of individual particles in a very short time. The determination of the chemical composition could provide assignment to specific sources while the particle group abundance characterizes the source strength. Manual EPXMA, on the other hand, offers the possibility of morphological studies and element mapping.

Bulk and alternative individual single-particle analyses have been performed on the same samples by energy-dispersive X-ray fluorescence and electron proton microprobe analyses, respectively (*2*).

The aerosol analysis in this work was mainly focused on aerosol particles with diameters above 1 μm, the so-called giant aerosols. Although the number of these giant particles in the lower troposphere is very low compared to the condensation-mode particles, their contribution to the atmospheric deposition is of extreme importance (*3–5*). Due to the slow realization of the importance of giant aerosol particles in the atmosphere together with sampling difficulties and measurement errors, many questions still remain unanswered, and further research will be necessary.

Experimental Procedures

Sampling Strategy. A sampling campaign was organized for September 15–27, 1991. During this campaign, two research vessels, F.S. *Alkor* and R.V. *Belgica*, were positioned on a circle, with a 200-km diameter, continuously downwind from each other in the central area of the North Sea (Figure 1). Sampling started on the F.S. *Alkor* (upwind ship) on the 16th at 1 a.m. and stopped on the 25th at 11 a.m. Sampling on the R.V. *Belgica* (downwind ship) was delayed according to the calculated air mass travel time, based on the actual wind speed aboard the F.S. *Alkor* and the R.V. *Belgica*. A wind speed of 10 m/s^{-1} and a distance of 200 km resulted in a transport time of ca 5.5 h by which the downwind ship had to delay its sampling interval. Every 8 h new positions were taken on the circle. When achieved, the ships were holding position within a few miles facing the wind for undisturbed sampling conditions. In this way, the same air mass was sampled with an interval of 200 km. During the travel time to reach the new position, sampling was stopped. The result of this campaign gave an idea about the changes in composition that aerosols and rainwater undergo during air mass travel.

Meteorological data were provided by radiosonde inspection aboard the F.S. *Alkor* every 8 h. The whole sampling campaign was characterized by stormy weather. Due to prevailing southwesterly winds, the United Kingdom was the main source region for anthropogenic and soil-derived components.

Aerosols were collected on the main deck using a cascade impactor and filter units, both positioned inside a wind tunnel, for single-particle and bulk analyses, respectively. In a cascade impactor, aerosols are segregated in size based on their inertial characteristics. Microscope slides covered with special coated Nuclepore filters (COSTAR Europe Ltd. Nuclepore Filtration Products) were used as the impaction surface. The special coating is necessary to reduce effects like "bounce off" and "reentrainment", which

* Address correspondence to this author; e-mail address: debockl@schs.uia.ac.be.

0013-936X/94/0928-1513$04.50/0

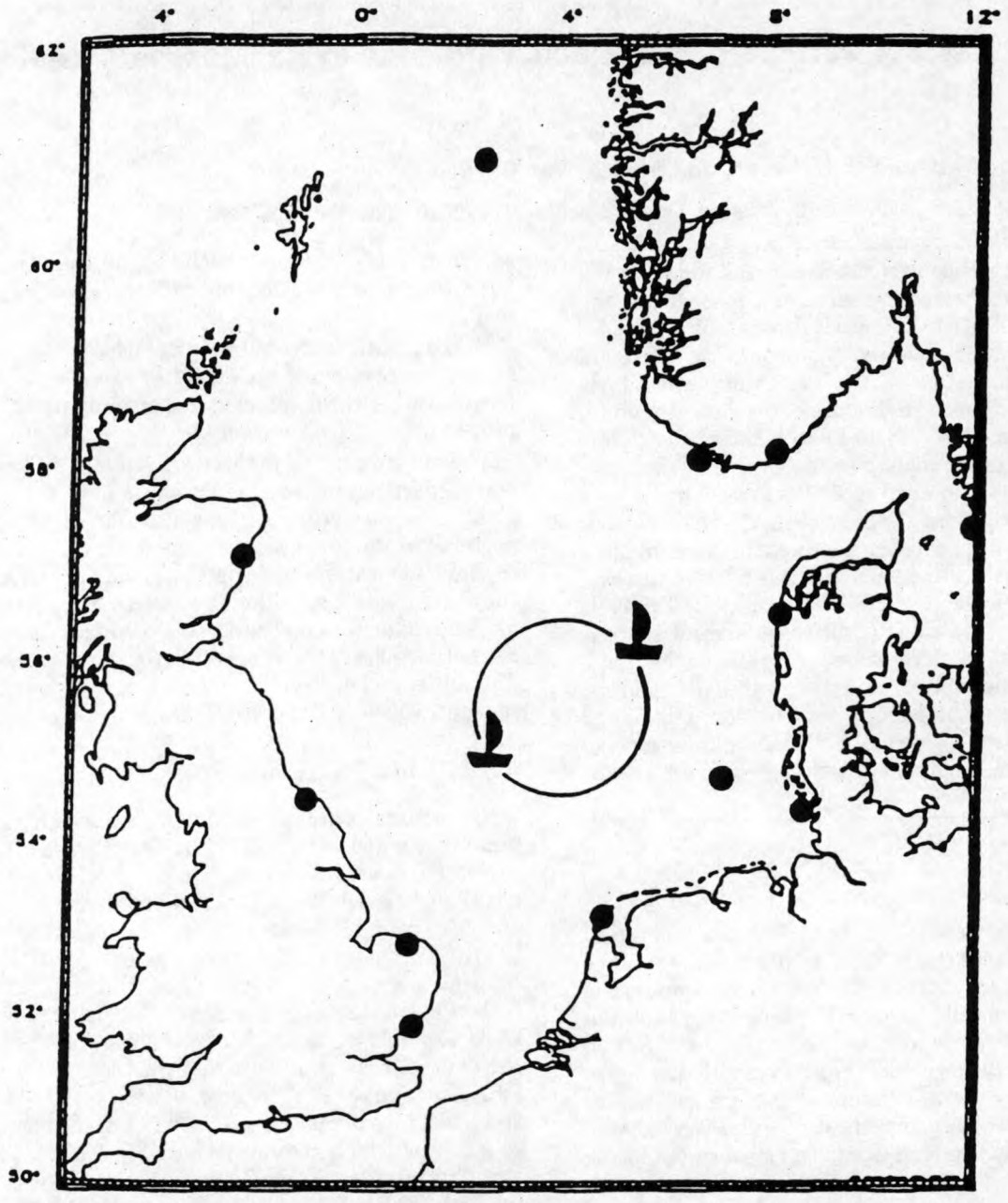

Figure 1. North Sea map with indication of the sampling sites on a circle of 200 km, around 55.0° N and 4.0° E.

influence the collection efficiency and change the apparent size distribution. The type of cascade impactor applied during this campaign was based on the design of May (*6*). It offers a very good resolution of particle size due to sharp cutoffs at different stages (20, 8, 4, 2, 1, and 0.5μm), minimal internal losses, the possibility for quantitative analyses at sampling speeds of 20 L/min, easy handling due to its compactness and fast dismantlement, and stainless steel composition to prevent corrosion. To collect the total airborne particulate matter, filter units were also applied. Because no size segregation is required, the Nuclepore filters were not coated.

A representative sampling of atmospheric aerosols is only possible when isokinetic conditions are fulfilled. This means that there cannot be any kind of disturbance of the air stream at the inlet of the impactor, resulting in a nongradual translation of the aerosol particles into the impactor nozzle. The wind tunnel used, designed at the University of Essex (*7*), consists of a 1.2-m thin-walled tube with a diameter of 0.25 m. In the middle of the tube immediately behind a honeycomb structure, which creates a laminar flow, the impactor and filter unit are positioned. At the end, a ventilator sucks air into the tunnel at the same speed as it is sucked into the sampling device by the pump, which guarantees isokinetic sampling. To keep the inlet of the tunnel in the prevailing wind direction, it is provided with a 1-m^2 wind vane. Due to the suppressing effect of a portable wind tunnel on airstream fluctuations around the impactor and the filter unit, isokinetic sampling is possible, and giant particles can quantitatively be collected also.

For the collection of rainwater, a PVC funnel was connected to a low-density polyethylene barrel on the main deck. The barrels were first treated with ultrapure nitric acid during 1 month and washed with Milli-Q water afterwards. After each rain shower, the funnel was closed, and the collected rainwater was frozen to prevent microorganism growth. In the lab, the bottles were thawed, and each time 100 mL of rainwater was filtered on a Nuclepore membrane.

Instrumentation. A set of 75 size-segregated aerosol samples and five rainwater samples was analyzed by EPXMA. The automated analyses of 27 500 particles was performed on a JEOL 733 Superprobe equipped with a Tracor Northern TN-2000 system, using the particle analysis program 733B written in Fortran (*8*). For every impactor stage, 300 particles were analyzed, and 500 particles were analyzed for each rainwater sample. The analysis was carried out at an acceleration voltage of 25 kV and a beam current of 1 nA. The energy-dispersive X-ray spectra accumulation time was fixed at 20 s to obtain satisfactory signal/noise ratios. In the 733B program, the localization of a particle is performed by successive horizontal line scans with the electron beam, followed by saving the contour pixel of the particle. After saving all the contour pixels, the area, perimeter, and diameter of the particles are calculated, and the X-ray spectrum is accumulated. All the information is stored on disks for off-line data processing on a Unix computer. Reducing the data set was performed by multivariate techniques.

To study the relations between the particle composition, origin, and shape and obtain even a possible characterization of particles based on their shape, over 200 giant aerosol particles were manually analyzed by EPXMA using the 733A program. The particles were collected for single-particle analysis on a Nuclepore filter in the wind tunnel. The only difference with 733B is that the particles are localized manually and the X-ray spectrum accumulation time was 100 s. ZAF corrections were performed on these spectra for the following elements: Na, Cl, Mg, Al, Si, P, S, K, Ca, Fe, Ti, Ni, Cu, and Zn, resulting in normalized concentrations for each element expressed in weight percentages. The sensitivity of a conventional EPXMA instrument is poor for Na; even at relatively high concentrations, Na may escape detection.

Matrix Correction and Multivariate Techniques. EPXMA is a fast method for element identification. However to obtain quantitative information about the elements present, a very complex procedure is needed, called ZAF correction. Due to electron–sample interactions, processes occur which influence the production and collection of X-rays. The ZAF procedure performs a correction for the atomic number effect (Z), the absorption effect (A), and the fluorescence effect (F). Z represents the difference in electron scattering and retardation in the sample and the standard. Loss of X-rays due to absorption in the sample is represented by A, and the artificial increase of X-ray intensity of an element due to ionization by X-rays originating from an other element is corrected by F. Without correction, errors in excess of 10% could result. After a ZAF correction, the element concentrations present are normalized and expressed in weight percentages.

Reduction of the data set was performed by hierarchical cluster analysis on each of the aerosol and rainwater samples (*9*), producing a classification into groups of particles with chemically similar composition. A hierarchical cluster analysis starts with n particles or clusters from which the most similar ones are joined successively into new clusters. Different strategies are possible to join two clusters; Ward's error sum method is the one we applied because it provides a maximum internal homogeneity into the separated groups (*10*).

Principal factor analyses (PFA) with orthogonal varimax rotation was used to discover the interrelation of 13 variables (Na, Mg, Al, Si, P, S, Cl, K, Ca, Ti, Fe, Ni, and Zn) in our aerosol data set, which led to the identification of different sources of giant aerosols. This multivariate technique splits the data set into subsets of strongly correlated variables. The rotation of these subsets or 'factors' provides a better factor loading. Elements were considered to be detected if the X-ray intensities were found above the detection limit in one of the 300 analyzed particles, for each air sample. Elements like Cu, Pb, Mn, Cr, Ba, Pt, and V were occasionally detected in particles. These elements were found in particles which contributed less than 0.5% of the total aerosol abundance, and therefore, they were further excluded from the data matrix. The major problem in PFA is the choice of the number of factors P that should be taken into account in the model or how many factors are required to estimate the communalities. The value of P was determined by the following criteria (*11*): the number of factors should be significantly less than the number of variables, a large fraction of both the total variance of the variables and the individual variable variance has to be explained by the factor variation, which means that the communalities should be close to 1 and factors that contribute with a variance less than 1 should be excluded from the model. Considering these criteria, the appropriate number of factors is established.

Table 1. Varimax Rotated Factor Loading Matrix for 75 North Sea Giant Aerosol Samples[a]

variable	factor 1	factor 2	factor 3	factor 4	communality	SD
Na	−0.34		−0.81		0.792	0.15
Mg		**0.82**			0.708	0.18
Al	**0.91**				0.851	0.15
Si	**0.87**	0.16	0.17		0.826	0.15
P	0.31			**0.87**	0.854	0.15
S		**0.85**	−0.40		0.872	0.12
Cl	−0.72		−0.23	0.31	0.678	0.21
K	0.17	**0.80**	0.30	0.25	0.824	0.15
Ca		**0.79**	−0.33		0.747	0.18
Ti	**0.83**	0.16		0.30	0.813	0.15
Fe	**0.93**		0.13		0.878	0.12
Ni	−0.18	0.12	**0.48**	**0.81**	0.933	0.09
Zn	**0.59**		**0.73**	0.18	0.912	0.12
eigenvalue	5.05	2.83	1.78	1.02		
% variance explained	38.5	21.6	13.6	7.8		

[a] Only values greater than three times their standard deviation were reported.

Results and Discussion

Automated EPXMA. *Principal Factor Analyses.* By performing PFA on the correlation matrix of the data set, four eigenvalues greater than 1 were produced (5.05, 2.83, 1.78, and 1.02); the fifth value was 0.86. Because no standard procedure exists for the selection of the number of factors, factor matrices with four and five eigenvalues were calculated. After comparing the two varimax rotated matrices, the solution with four factors was preferred, and the varimax rotated factor matrix is represented in Table 1 (the most important values are shown in bold).

To facilitate factor interpretation, factor loadings smaller than three times the standard deviation were rejected because they are considered to be not statistically significant (*11*). The four factors explain together 81.4% of the total variance of the variables, and communality values for most of the variables are high, situated between

0.74 and 0.93, except for Mg, Ca, and Cl. The first factor is determined by high loadings of Al, Si, Fe, Ti, Zn and Na and Cl. Explaining 63.7% of the total variance this factor provides the two major particle types: marine sea–salt particles and aluminosilicates such as fly ash and soil dust with a continental or anthropogenic origin. The inverse correlation between both group concentrations is expressed by the minus sign of the Na and Cl loading. The combination of the seven elements in those two element groups is confirmed by an additional factor analysis. Factor two contains mainly Mg, K, S, and Ca which indicates the presence of seawater crystallization products such as different combinations of $CaCO_3$, $CaSO_4$, K_2SO_4, $MgSO_4$, and dolomite. The NaCl crystals, which should represent the main crystallization product [70% of the total dissolved solids inside a seawater droplet (*16*)], were probably classified in the first factor due to their dominance as compared to the other crystallization salts. Recalculations of the data set by choosing three factors instead of four confirms this. The loadings of Na and Cl increase, but the communalities that describe how well the factor analysis reproduces the reality are lower. The solution with four factors is therefore more appropriate. Factors three and four can be associated mainly with industrial origins because of high loadings for Ni and Zn, inversely correlated with Na, and for Ni and P, respectively. Elements like Ni and V are released by oil combustion processes in power plants due to oil-fired furnaces. Because the low contribution of natural sources to the total emission of Ni and V, respectively 14% and 16% (*12, 13*), Ni and V are used as indicator elements of oil-fired power plants and oil combustion sources in numerous industries. Iron, steel, and ferro alloy plants are responsible for the release of Zn. The emissions are distributed evenly over Europe, but large emission areas are located in the United Kingdom, Spain, and Italy. The occurrence of P in the presence of Fe can be assigned to anthropogenic emissions because of its use in ferro alloy.

Hierarchical Clustering. Particle classification into different groups based on their chemical composition was achieved by hierarchical cluster analysis. Correct interpretation of the cluster analysis results was possible by taking into account the exact ship positions and meteorological data like wind speed, wind direction, and relative humidity during sampling periods. From September 15 to September 27, wind speed fluctuated between 3.4 and 14.5 m/s, and the prevailing wind direction was southwest, characterizing the samples by both continental and marine influences. The results of the hierarchical clustering of 300 particles for each of the five impactor stages collected on September 18 are shown in Tables 2 and 3, on the upwind and downwind ship, respectively. The stage number corresponds to the theoretical cutoff diameter of the particles collected on a certain stage. For each particle type the percent of abundance in a group of 300 particles is given as well as its average diameter (μm) and its composition. Clustering results for aerosol and rainwater samples will be discussed separately.

Aerosols. Depending on the sample, three to eight different aerosol types were distinguished. Due to stormy weather and high wind speeds, the concentration of sea-salt particles is very high in all the impactors, ranging from 10 to 90% of the total aerosol abundance. In a marine atmosphere, sea spray particles are mainly produced by the bubble-bursting mechanism. Due to breaking waves, air is captured and released as bubbles at the sea surface. Bubble breaking results in the ejection of film and jet drops into the atmosphere. This process is more effective with increasing wind speeds. Experiments performed by Deleeuw (*14*) concerning vertical profiles of giant sea spray particles deduced from their size distribution close above the sea surface confirm that particle concentration and

Table 2. Hierarchical Clustering Results of Five Aerosol Samples Taken on the F.S. *Alkor* (Upwind Ship) on September 18, 1991

stage	abundance (%)	av diameter (μm)	composition
1, $d > 20$ μm	49	6.8	NaCl
	24	5.3	organic
	6.0	4.0	Al, Si, Fe
	6.0	4.5	Cr-rich
	4.0	6.7	KCl
2, 8 μm $< d <$ 20 μm	72	3.1	NaCl
	16	4.6	NaCl, $CaSO_4$
	3.3	1.7	$CaSO_4$, Cl
	3.0	3.6	Al, Si, Fe
	2.0	3.5	Fe, Cl
3, 4 μm $< d <$ 8 μm	75	1.3	Cl-rich
	12	1.2	organic
	7.0	1.8	NaCl
	2.3	1.7	Al, Si, Fe
	1.0	1.2	Fe-rich
	1.0	2.2	Si, Cl
4, 2 μm $< d$ 4 μm	74	2.0	NaCl
	7.7	2.1	Na-rich
	6.3	2.4	$CaSO_4$, NaCl
	3.4	1.8	organic
	3.0	1.5	$CaSO_4$
	3.0	3.2	NaCl, Al, Si
5, 1 μm $< d <$ 2 μm	70	2.2	organic
	18	1.7	Cl-rich
	3.0	1.8	Si-rich

Table 3. Hierarchical Clustering Results of Five Aerosol Samples Taken on the R.V. *Belgica* (Downward Ship) on September 18, 1991, from Same Air Mass with Delay of 6 h

stage	abundance (%)	av diameter (μm)	composition
1, $d > 20$ μm	55	4.9	NaCl
	14	5.0	NaCl, $CaSO_4$
	13	5.3	Cl-rich
	11	4.0	organic
	4.3	3.6	$CaSO_4$, Cl
	2.0	5.0	Al, Si, Fe
2, 8 μm $< d <$ 20 μm	43	5.0	NaCl
	27	3.1	$CaSO_4$, Cl
	8.0	2.4	Al, Si, Fe
	7.6	4.0	Mg, S, Cl, K
	6.0	2.9	Al, Si, Fe
	5.3	2.6	Na-rich
3, 4 μm $< d <$ 8 μm	77	1.5	Cl-rich
	16	2.0	NaCl
	9.3	1.7	organic
	1.0	2.8	$CaSO_4$
	1.0	1.5	Si, Cl
4, 2 μm $< d <$ 4 μm	50	3.0	NaCl
	30	2.2	organic
	7.0	2.2	$CaSO_4$
	3.3	2.7	Al, Si, Fe
	3.3	1.7	S-rich
	2.6	2.6	Si-rich
5, 1 μm $< d <$ 2 μm	31	1.5	NaCl
	31	1.6	Cl-rich
	21	1.4	organic
	5.0	1.5	Na-rich
	4.0	1.5	Al, Si, Fe
	2.0	1.1	Fe-rich
	2.0	1.6	S, Cl

variation of sampling height are strongly influenced by wind speed. At sampling heights of 11 m, the increase in particle number concentration of 11-μm particles per particle diameter increment could be up to a factor of 10 if the wind speed increases from 2 to 16 m/s. During transport in the atmosphere, pure NaCl particles can react with sulfuric acid or SO_2 to produce transformed or aged sea-salt particles. In some of the samples, high concentrations of these sulfur-rich particles were detected, but mostly their abundance was low. This can be explained by the limited time the particles possess to react with sulfur-containing compounds, between their creation and sampling. All samples are also characterized by high abundances (3-33%) of Ca- and S-rich particles. These particles can have a marine or a continental origin and are identified as $CaSO_4$. Responsible mechanisms (*15*) could be a fractional crystallization from seawater, interaction between $CaCO_3$ aerosols and atmospheric SO_2 or H_2SO_4, release of gypsum from flue gas in desulfurization processes, and limestone building deteriorating due to air pollution. The first two mechanisms are positively influenced by high relative humidity. Seawater crystallization products such as KCl, $MgCl_2$, $MgSO_4$, and K_2SO_4 are found in 43% of the samples, and abundances are below 19%. Crystallization of successive salts appears by evaporation of seawater drops and is subdivided in four stages (*16*). The first is characterized by the crystallization of $CaCO_3$ and dolomite. $CaSO_4$ and NaCl precipitate respectively the second and third stage. Finally, sodium, potassium, and magnesium sulfates and potassium and magnesium chloride precipitate. Sometimes aluminosilicates such as fly ash and soil dust account for 30% of the total aerosol abundance. Major elements detected in these particles are Si, Al, K, Mg, Fe, and S, which are seldom accompanied by minor elements such as Ti, Cu, Zn, Cr, and Mn. Sometimes high concentrations of S and Ca were found, pointing out the existence of secondary reactions with anthropogenic emissions of SO_2 and H_2SO_4. Until now, no significant difference in composition could be found between fly ash and soil dust particles; only morphological differences appeared. Fly ash is often spherically shaped, and it is emitted by high-temperature combustion processes in power plants; on the other hand, soil dust particles are irregularly shaped and the result of soil erosion. A few times Si- and Fe-rich particles were observed. Si-rich particles originate from quartz or from the decomposition of aluminosilicates confirmed by lower concentrations of elements such as Al, Mg, S, K, and Fe. Combustion processes could also be a possible Si source, but the associated diameters should be smaller than 1 μm (*15*), which is not the case for our samples. The abundance of Fe-rich particles mainly results from metallurgical processes. Organic particles were also present in significant concentrations and probably correspond to biological materials like pollen, bacteria, bird excrements, etc. In EPXMA, the detection is limited to elements with an atomic number ≥ 11, due to the presence of a Be window in front of the Si–Li detector. The X-rays of elements like C, O, and N are too low energy to penetrate this window, and therefore during EPXMA, a particle is classified as organic if no X-rays are collected. Particle diameters were observed to be smaller, especially for large particles, than the cutoff aerodynamic diameters of the May impactor stages. In a marine environment, this can be attributed to four different effects: particle density above 1, splintering of large particles into pieces upon impaction, collection of wet particles which are reduced in volume after drying, or fractional crystallization occurring after evaporation of the water present leading to many small particles. The appearance of NaCl in low concentrations in all the hierarchical clustering tables (except for pure NaCl or transformed NaCl) can be explained as a NaCl coating. This kind of coating can be established in different ways (*17*). The two major mechanisms responsible for a possible NaCl coating at North Sea aerosols are the evaporation of seawater present in particles originating from sea spray and the collision or coalescence of particles with NaCl-containing cloud droplets. According to Andreae (*17*), if the surface of a mineral dust particle has a coating of water-soluble material (the result of a chemical reaction or the residue from a rain shower), it will probably act as a cloud condensation nucleus (CCN). Due to the adsorption of droplets at its surface, the CCN increases in size. On the other hand, if the particle is hydrophobic because lack of soluble material on its surface or because of a nonpolar organic coating, then it might not be a CCN. These particles can collide and coalescence with cloud droplets and develop possibly into CCN. If the cloud droplets disappear by evaporation instead of rainout, crystallization of the solute could appear as a coating on the particle surface.

By investigating possible changes between the samples collected during six sampling periods on board the *Alkor* and the *Belgica* (positioned at 200 km downwind from each other), the following conclusions were made: (a) No significant decrease in particle diameter was observed; the average diameter of particle "types" for each stage remains more or less constant. (b) The abundance of seawater crystallization products increases during traveling across the sea for the first two stages (particles with diameters above 20 μm and between 20 and 8 μm, respectively), with a factor 2.2 and 2.4, respectively. The discrimination between different element combinations seems to be more difficult for the *Belgica* samples. (c) In stages with particle diameters above 4 μm, a decrease in aluminosilicate abundance was noticed. (d) 48% of the analyzed samples did not contain organic particles. If present, no clear changes in relevant abundance could be discovered between samples from the two research vessels. (e) An increase in freshly produced NaCl particles was observed at the first three stages; aged sea salt almost disappears at large particle stages, and its abundance is replaced by pure NaCl. The determination of changes in diameter for each stage is very difficult because sometimes groups disappear or their composition becomes very complex. Diameters fluctuate: in some of the samples they increase, in others they decrease during air mass travel. A marine climate like the North Sea is characterized by high atmospheric concentrations of marine-derived components and a very high relative humidity, which offers particles the possibility of water absorption during their atmospheric residence. Water uptake is caused by deliquescence of soluble salt present in the particle (*18*). Each salt is associated with its critical humidity at which it is transformed from the crystal form into the liquid phase. At very high relative humidity, a mixed salt particle can even be transformed into a droplet. As mentioned above, the evaporation of water can lead to a recrystallization. Compared with the initial salt composition, different combinations can be possible after this recrystallization

process. These facts probably explain the high abundance of seawater crystallization products and their difficult compositional interpretation. The decrease and sometimes total disappearance of aluminosilicate particles in the largest particle size fractions can be interpreted as a result of the short residence time of those large and giant particles in the atmosphere due to their higher sensitiveness compared with small or Aitken particles for removal mechanisms like sedimentation, impaction, rainout, and washout. The apparent increase in pure NaCl concentration and marine crystallization products could be explained by considering the following facts. The concentration is inversely correlated with height, and the difference in concentration is very clear by comparing sampling at 0.2 and 11 m height. Concentration differences between the sampling at 11 m on board the *Alkor* and at 15 m on board the *Belgica*, however, decrease very rapidly for particle diameters smaller than 20 μm. Therefore, the main reason for the difference in sea-salt concentration and marine crystallization products on both vessels is the increasing marine influence during air mass travel over the sea; the different sampling height will be of minor importance. Due to their dominant concentrations, both particle groups suppress all other particle types. Collection close to the sea implies a shorter time between creation and sampling, which decreases the possibility for reactions with other compounds like SO_2, as mentioned before.

Wet Deposition. To study the changes in the composition of rainwater particles above the North Sea, rainwater samples were collected on board the *Alkor* and the *Belgica*. Comparing the hierarchical cluster analysis results of the rainwater suspension samples from both vessels, showed a few differences. First, a significant difference in composition was distinguished. Samples collected on board the *Alkor* contained beside aluminosilicates and Si-rich particles high abundances of S, P, Fe, and Cr in contrast with the *Belgica* samples, which contained only high abundances of aluminosilicates and Si-rich particles. These high abundances of S, P, Fe, and Cr are probably the result of the downward mixing of anthropogenic plumes of SO_2 and Fe- and Cr-rich particles from U.K. power plants. Due to the dilution of the air masses over a 200-km distance, the abundance of those elements probably decreases or even disappears. The occurrence of Cr serves as indicator for iron and steel industries (*19*), which is confirmed by the presence of Fe. In addition, a high abundance of organic material was detected in the *Alkor* samples. The exact composition of the organic material cannot be determined by EPXMA due to detection limitations. The only possible explanation for the high abundance of organic material can be either microorganism growth due to the thawing of rainwater during transport or the presence of bird excrements. Second, differences in particle diameters could be noticed. For the rain samples collected on September 16, the mean particle diameter of the *Alkor* sample was significantly larger compared with that from the *Belgica* sample. The difference between the two samples collected on September 22 was not so pronounced. A decrease in mean particle diameter could be the result of the removal of several giant and large particles from the air mass by washout and rainout during air mass travel.

Non-Automated EPXMA. North Sea aerosols are a mixture of different components, some derived from the sea itself and some supplied by the wind, sometimes from very distant places (*20*). The abundance of particle types is influenced by meteorological conditions and obviously by the sampling site. Based on their composition, seven groups of giant particles were manually analyzed: NaCl, aluminosilicates, Si-rich, S- and K-rich, Fe-rich, Ca- and S-rich particles, and particles with a high contribution of heavy metals.

Figure 2. Linearly shaped particle rich in Na and Cl at the end a Si-rich particle.

The first class of particles, sea salt, was subdivided in two groups: freshly produced sea salt and transformed or aged sea salt. In addition to the cubic shape typical for halite and the irregularly shaped NaCl particles (probably agglomerated halite crystals) described in the literature, linearly shaped particles were observed with lengths ranging from 7 to 37 μm (Figure 2). In 58% of the linearly shaped particles, higher concentrations of Cl were detected. The stoichiometry and mineral types of these NaCl-rich particles are not clear. Transformed or aged sea-salt particles were irregularly shaped with diameters varying from 4 to 9 μm. Low concentrations of Al, Si, Mg, K, and P indicate the presence of soil dust particles.

Si-rich particles and K- and S-rich particles were irregularly shaped with corresponding diameters of 3–7 and 3–9 μm, respectively. Consistent with the literature (*15*), spherical fly ash particles and irregularly shaped soil dust particles were detected. The fly ash particles, with diameters of 3–5 μm, were sometimes enriched in S, likely originating from secondary reactions with anthropogenic S compounds, and in agreement with experimental results of Kaufer (*21*), the variations in Ti and Mg concentrations were independent of particle size. Ni, Cu, and Zn were rejected from the tables because of too low concentrations. Beside the higher S concentrations, 25% of the soil dust particles contained also higher concentrations of Ca. A possible explanation could be the occurrence of reactions

between H_2SO_4 and aluminosilicate–mineral particles. Concentrations of Ni, Cu, and Zn could also be neglected. The presence of S- and K-rich particles results as described above from seawater crystallization products, and high concentrations of K may refer to a pollution or biological source.

Fe-rich particles can be spherical or irregularly shaped. The ones we examined were mainly irregularly shaped with diameters ranging from 3 to 7 μm. Beside the pure Fe-rich particles, Fe particles with enriched S concentrations were detected. S enrichment could be the result of the metallurgic processes.

Based on their shape, Ca- and S-rich particles could be divided in two groups. The irregularly shaped $CaSO_4$ particles vary in diameter from 3 to 12 μm, and lower concentrations of Si, K, Fe, Mg, and Al refer to the presence of soil dust. The second group contains apparently diamond and elongated hexagonally shaped particles with diameters from 3 to 10 μm, and no characteristic aluminosilicate elements were present. These two shapes belong to the same crystal type called gypsum. By observing the crystalline form from the top view and then from the front view, the elongated hexagonal shape (Figure 3, top) followed by the diamond shape (Figure 3, bottom) were distinguished. Particles with enriched concentrations of Ti, Zn, and Cu belong to the seventh group and are irregularly shaped with varying diameters of 3–9 μm. Compared to submicrometer particles (*22*), only low concentrations of heavy metals could be found. Due to industrial high-temperature combustion processes, gases are released which mainly convert by sudden cooling into submicrometer particles. Condensation can also occur on the surface of already existing particles. These kinds of composite particles may of course also arise from the coagulation of small particles onto large ones. Finally, we could conclude that, compared with the literature, only for NaCl and Ca- and S-rich particles were different shapes detected; the other ones matched those described in earlier published articles by different authors.

Conclusion

To study variations in composition of air masses crossing the North Sea due to air–sea exchange processes in the lower troposphere, aerosol and rainwater samples were collected on two research vessels positioned 200 km apart downwind from each other. Single-particle analysis was achieved by EPXMA.

The identification of the particle origin was possible by performing PFA on the data set resulting in four different giant aerosol sources: aluminosilicates and sea salt, seasalt crystallization processes, and two industrial sources. The classification of particles into groups of chemically similar composition was accomplished by a hierarchical cluster analyses according to Ward's error sum method. A total of eight different aerosol types could be distinguished: freshly produced and aged NaCl particles; Ca- and S-rich particles; seawater crystallization products like $NaSO_4$, K_2SO_4, KCl, and $MgCl_2$; aluminosilicates as fly ash and soil dust; Si-rich particles; Fe-rich particles; and organic particles.

By comparing aerosol clustering results of the two research vessels, three differences in composition were found after crossing a large distance above the sea: the abundance of crystallization products increases at the first two stages, leading to difficulties in the interpretations of salt compositions; the aluminosilicate abundance in the first three stages in the samples decreased; and in some of the samples, the aged sea-salt abundance decreases or sometimes disappears at higher stages in favor of pure NaCl. No significant decrease in particle diameter was observed. Compositional as well as size differences appeared in the collected rainwater samples of both research vessels.

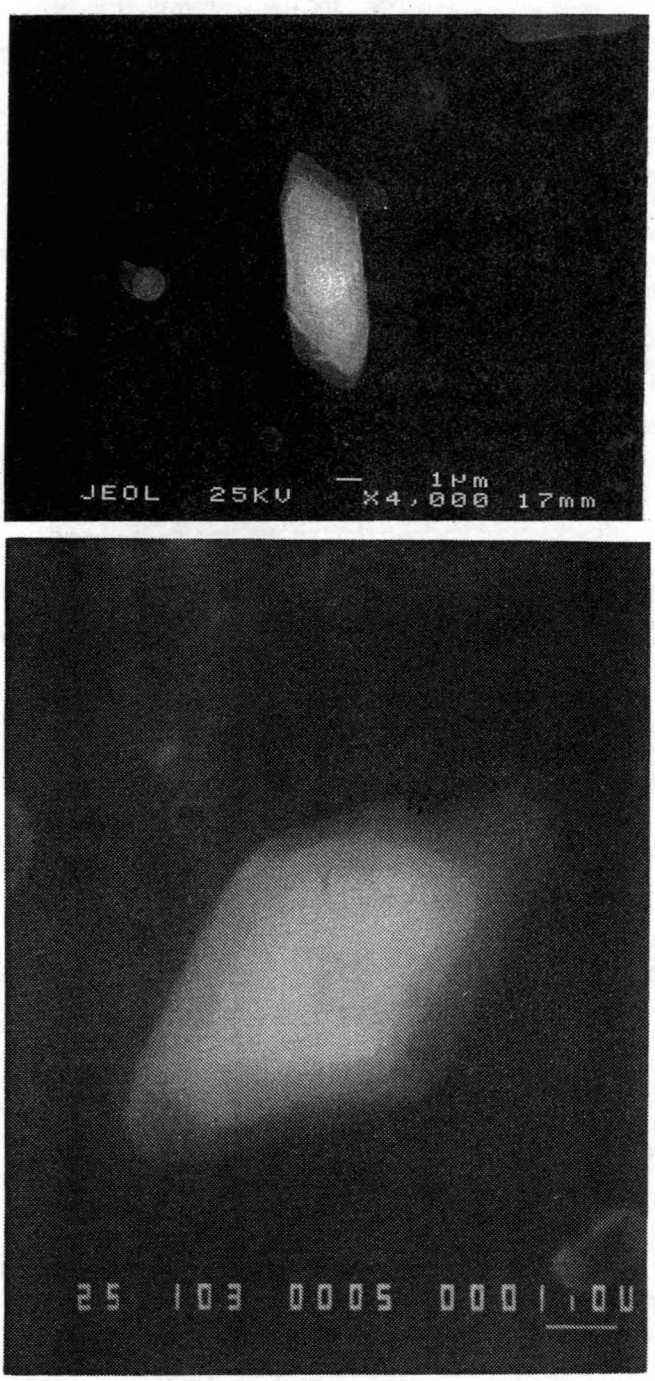

Figure 3. (Top) An elongated, hexagonally shaped $CaSO_4$ particle. (Bottom) Diamond shaped $CaSO_4$ particle.

Manual EPXMA was performed to investigate the relations between particle composition, origin, and shape. Based on their chemical composition, seven groups were determined: NaCl particles, Si-rich particles, aluminosilicates, Fe-rich particles, S- and K-rich particles, Ca- and S-rich particles, and particles with a high contribution of heavy metals. All shapes matched with those described

in literature, and only for NaCl and $CaSO_4$ were unexpected shapes detected.

Acknowledgments

This work was partially financed by the Belgian State-Prime Minister's Services-Science Policy Office, in the framework of the EUROTRAC program (under Contract EU7/08) and in the framework of the Impulse Programme on Marine Sciences (under Contract MS/06/050). We thank M. Schulz for coordinating the North Sea sampling campaign. L.D.B. acknowledges financial support by the Belgian Instituut ter bevordering van het Wetenschappelijk Onderzoek in Nijverheid en Landbouw (IWONL).

Literature Cited

(1) Rojas,C. M.; Injuk, J.; Van Grieken, R. *Atmos. Environ.* **1993**, *27A*, 251–259.
(2) Injuk, J.; Van Malderen, H.; Van Grieken, R.; Swietlicki, E.; Knox, J. M.; Schofield, R. *X-Ray Spectrom.* **1993**, *22*, 220–228.
(3) Jaenicke, R. *Ann. N.Y. Acad. Sci.* **1980**, *338*, 317–322.
(4) Jaenicke, R. In *Chemistry of the Unpolluted and Polluted Troposphere*, 1st ed.; Georgii, W., Jaeschke, W., Eds.; D. Reidel Publishing Co.: Dordrecht, The Netherlands, 1982; pp 341–374.
(5) Dedeurwaerder, H. L. Ph.D. Dissertation, Free University of Brussels, 1988.
(6) May, K. R. *J. Aerosol. Sci.* **1975**, *6*, 1–7.
(7) Vawda, Y.; Colbeck, I.; Harrison, R. M.; Nicholson, K. W. *J. Aerosol Sci.* **1989**, *20*, 1155–1158.
(8) Raeymaekers, B. Ph.D. Dissertation, University of Antwerp, 1986.
(9) Van Espen, P. *Anal. Chim. Acta* **1984**, *165*, 31–49.
(10) Bernard, P. C.; Van Grieken, R. E.; Eisma, D. *Environ. Sci. Technol.* **1986**, *20*, 467–473.
(11) Heidam, N. Z. *Atmos. Environ.* **1982**, *16*, 1923–1931.
(12) Nriagu, J. O. *Nature* **1979**, *279*, 409–411.
(13) Pacyna, J. M. Trace element emission from anthropogenic sources in Europe. Technical Report No. 10/82; The Norwegian Institute for Air Research: Lillestrom, 1982.
(14) Deleeuw, G. *Tellus* **1986**, *38B*, 51–61.
(15) Xhoffer, C.; Bernard, P.; Van Grieken, R. *Environ. Sci. Technol.* **1991**, *25*, 1470–1478.
(16) Bochert, H. *Chemical Oceanography*; Academic Press: London,1965.
(17) Andreae, M. O.; Charlson, R. J.; Bruynseels, F.; Storms H.; Van Grieken, R.; Maenhaut, W. *Science* **1986**, *232*, 1620–1632.
(18) Winkler, P. *Phys. Scr.* **1988**, *37*, 223–230.
(19) Pacyna, J. M. *Atmos. Environ.* **1984**, *18*, 41–50.
(20) Betzer, P. R. *Nature* **1988**, *336*, 569–571.
(21) Kaufer, N. *Environ. Sci. Technol.* **1984**, 18, 544–547.
(22) Van Malderen, H.; Rojas, C.; Van Grieken, R. *Environ. Sci. Technol.* **1992**, *26*, 750–756.

Received for review December 6, 1993. Revised manuscript received April 11, 1994. Accepted April 27, 1994.

• Abstract published in *Advance ACS Abstracts*, June 1, 1994.

Selected article #17:

Elemental concentrations in atmospheric particulate matter sampled on the North Sea and the English Channel

P. Otten, J. Injuk and R. Van Grieken

The Science of the Total Environment, 155 (1994) 131-149

ELSEVIER

The Science of the Total Environment 155 (1994) 131–149

the Science of the Total Environment
An International Journal for Scientific Research into the Environment and its Relationship with Man

3896

Elemental concentrations in atmospheric particulate matter sampled on the North Sea and the English Channel

Phillipe Otten, Jasna Injuk, René Van Grieken*

Department of Chemistry, University of Antwerpen (UIA), B-2610 Wilrijk-Antwerpen, Belgium

Received 8 November 1993; accepted 19 December 1993

Abstract

Air sampling on a series of 10 cruises, spanning the whole area of the North Sea, yielded detailed spatial distributions of atmospheric concentrations of Al, Si, S, Cl, P, K, Ca, Ti, V, Cr, Mn, Fe, Ni, Cu, Zn and Pb determined by EDXRF. A strong influence of the air mass history on the heavy metal concentrations was demonstrated for the whole sampling period of 5 years. Factor analysis performed on all samples collected with a stack filter unit resulted in the identification of three factors for the coarse particle fraction (sulphate particles with trace metals, sea salt particles and soil dust or metallurgic particles containing Fe) and four factors for the fine particle fraction (sea salt, sulphate with Pb and Zn), trace metal particles with Cu, Ni, Zn and fly-ash particles. The same statistics performed on all samples collected above the Southern Bight of the North Sea yielded three factors, namely: sea salt particles, particles enriched in Ni and V, originating from natural oil combustion and particles containing a variety of elements such as S, K, Ca, Fe, Pb, Cu and Zn. Compared with relevant measurements of trace elements in this area, a relatively good agreement can be found.

Keywords: Aerosols; Trace elements; North Sea; EDXRF

1. Introduction

In order to understand more about the North Sea aerosol constituents and their sources and their fate, an extensive sampling program, spanning more than 5 years, was set up with the Belgian oceanographic research vessel R/V Belgica. Aerosol samples were collected under different meteorological situations and from different regions, covering the complete North Sea and the English Channel. Particulate matter, collected on membrane-type filters, was analysed with energy-dispersive X-ray fluorescence (EDXRF) yielding atmospheric concentrations for Al, Si, P, S, Cl, K, Ca, Ti, V, Cr, Mn, Fe, Ni, Cu, Zn and Pb. The results of EDXRF measurements on 71 filter samples collected during these 10 different sampling campaigns are discussed. A multi-variate technique, factor analysis, was used for the determination of the underlying structure of the total data set.

* Corresponding author.

Elsevier Science BV.
SSDI 0048-9697(94)04146-E

2. Analytical procedure

2.1. Instrumentation

The analyses were performed by an EDXRF instrument Spectrace 5000 (Mountain View, CA, USA), which is completely controlled by and operated from an IBM-AT type microcomputer. The Spectrace 5000 uses a 17.5-watt power X-ray tube with Rh anode target. It operates within a range of 6–50 keV and with a maximum current of 0.35 mA. The exciting X-ray beam passes a 127-μm thick Be window, is collimated and finally passes through a filter system. The filter system allows the use of either no filter at all or a selection from five different filter types: a cellulose filter, a 127-μm Al filter, a 50-μm Rh filter, a 127-μm Rh filter or a 630-μm Cu filter.

At 90° relative to the incident X-ray beam, the characteristic X-rays from the sample and the scattered X-rays are detected by an energy-dispersive Si(Li) detector. Data acquisition and display is done by a PC.

2.2. Calibration

In the calibration procedure followed, a series of thin film reference standards, composed of pure elements or simple inorganic compounds evaporated on a 4-μm thick Mylar foil (Micromatter, Seattle, WA), were used. Low Z element standards were analysed with an accelerating voltage of 15 kV, using a current of 0.35 mA and an irradiation time of 1000 s. No collimator was used. Because of overlap between the Rh-L lines and the Cl-K and S-K lines, a cellulose filter was used for filtration of the incident polychromatic X-ray beam. For high Z element standards, irradiation was done during 1000 s with a 35-kV beam using a 0.35-mA current and a thin Rh-filter. For Pb, the L lines are used for calibration.

X-ray spectra were analysed with the AXIL software (Van Espen et al., 1986). The calibration procedure was evaluated by analysing two NBS reference standards consisting of a Nuclepore membrane with a deposited glass layer.

Table 1 lists the detection limits for airborne particulate matter samples, assuming 10 m^3 of air was drawn through a 47-mm diameter Nuclepore filter. Detection limits are calculated as three times the standard deviation on the peak surfaces, obtained by analysis of a blank filter. The high Cl detection limit is due to the interference of incompletely filtered Rh-L lines that coincide with the Cl-K lines.

Table 1
Detection limits assuming a sample volume of 10 m^3 and a filter diameter of 47 mm

Element	Detection limit (ng/m^3)
Al	200
Si	140
P	70
S	80
Cl	600
K	9
Ca	6
Ti	2.5
V	2.0
Cr	1.5
Mn	0.9
Fe	0.4
Ni	0.5
Cu	0.4
Zn	0.4
Pb	8

2.3. Sampling strategy

Total airborne particulate matter was collected from the R/V Belgica on 47-mm diameter, 0.4-μm pore-size polycarbonate membrane-type filters (Nuclepore, aerosol grade). In some cases, a dual filter unit was used, consisting of a 8.0-μm pore-size filter, followed by a 0.4-μm pore-size one. This double filter sampler allows separation of the coarse particle fraction (> 2 μm) from the fine particle fraction during sampling. The Plexiglass filter holder has a hat-type cover to protect the filters from contamination by seawater droplets. Table 2 shows the results of electron microscope measurements on five dual samples, with and without hat, taken on the North Sea. From the particle size distributions, the number of particles with a diameter > 2 μm was calculated. There is no systematic difference between the sampler with hat and the sampler without hat. The percentage of mass (calculated from the numerical size distribution by assuming the same

Table 2
Sampling efficiency of hat-type fitter system for 5 different dual samples

Percentage of particles > 2 μm		Percentage of mass represented by particles > 2 μm	
With hat	Without hat	With hat	Without hat
2.4	7.9	66	72
3.0	2.3	63	75
1.5	2.7	66	68
5.8	2.3	88	80
9.1	8.6	89	90

density and shape for all particles), represented by particles with a diameter larger than 2 μm, is nearly the same with the two setups used.

The filter holder was placed at the front end of the ship at a height of ~ 10 m above sea level. A 20-m plastic hose connects the filter unit to a vacuum pump (Becker type VT 6) and a dry gas meter which are placed at the upper deck near the bridge.

The pump is operated at a flow rate of ~ 35 l/min for 4–12 h for each sample in order to collect 10 m^3. Sampling was discontinued whenever the relative wind direction to the ship was $< -45°$ or $> 45°$ for reasons of possible contamination by the diesel engine exhaust of the ship itself. Therefore, although the sampling volume is nearly the same for all samples, they may be collected over a wide range of total sampling times.

Filter samples were immediately transferred to a flow hood inside the chemical laboratory on the ship and placed in a plastic box until analysis by EDXRF in the University laboratory.

3. Results

Here, an overview is given of all results concerning atmospheric concentrations of trace elements in the North Sea atmosphere. When no data are given for an element in campaign, all EDXRF results were below the detection limit during that campaign.

3.1. Campaign 1

General sampling data and meteorological information. During campaign 1, four aerosol samples were collected in the Southern Bight of the North Sea, more specifically on the Belgian Continental Shelf.

Two-dimensional, 96-h backward air mass trajectories were calculated by the Belgian weather service, KMI. Corresponding back trajectories for all four filters are shown in Fig. 1. These air mass trajectories indicate the origin and the history of the collected airborne particulate material. They often include more useful information than wind speed and wind direction data at the sampling site, since two samples collected at the same

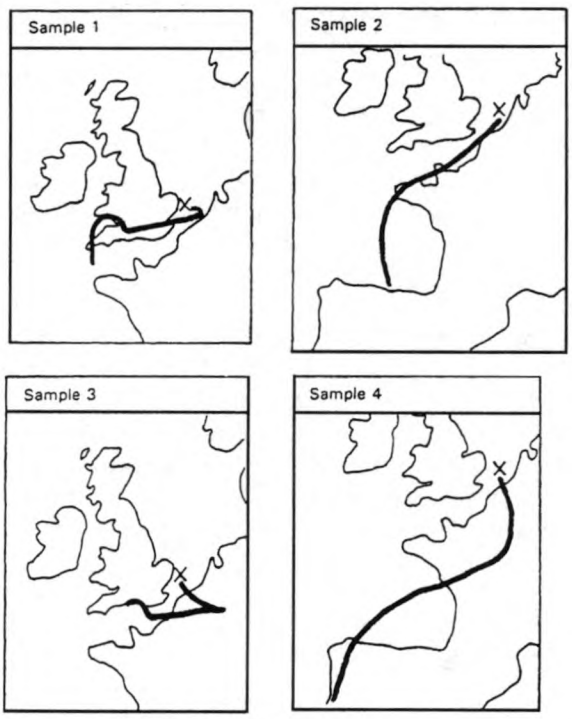

Fig. 1. The 96-h backward air mass trajectories for samples of campaign 1 (sample location indicated by an ×).

location under similar local meteorological conditions may have a completely different air mass history due to differences in the large-scale meteorological situation, i.e. the distribution of high and low pressure areas and the presence of cold and warm fronts.

EDXRF results. Table 3 lists the atmospheric concentrations obtained. In sample 1, the highest S, K, V, Ni, Cu, Zn and Pb concentrations are determined. From the air mass history (Fig. 1), the collected airborne material originated from the London area and the southern part of the UK. Sample 2 was collected under continental (French) influences (Fig. 1). Most concentrations are lower than in sample 1. The third sample was collected at higher wind speeds, up to 15 m/s. This is reflected in a higher Cl concentration, while the concentrations of all other elements are much lower than in samples 1 and 2. The fourth sample was also collected under more continental influence and at lower wind speeds, resulting in higher concentrations for anthropogenic elements and a lower Cl concentration compared with the previous sample. Although there is only an interval of 12 h between the third and the fourth sample, concentrations differ significantly; the Pb concentration goes up by a factor of 3.5 from 40 to 140 ng/m^3. Rapid changes in the meteorological situation are reflected without delay in the atmospheric concentrations of trace elements.

3.2. Campaign 2

General sampling data and meteorological information. During the first part of a 3-week campaign, between Zeebrugge (Belgium) and Bergen (Norway), 8 aerosol samples were collected on 0.4-μm pore-size Nuclepore filters. During the second part of the campaign, between Bergen and Zeebrugge, another 7 samples were collected, this time by using a stacked filter unit consisting of a 8.0-μm pore-size Nuclepore filter, followed by a 0.4-μm one.

Table 4 summarizes the available meteorological information for campaign 2: wind direction, wind speed and an indication of the air mass

Table 3
EDXRF results in ng/m^3 — Campaign 1

Element	Sample			
	1	2	3	4
S	4600	1650	600	1510
Cl	800	620	1350	< 600
K	310	310	190	270
Ca	250	450	120	140
V	70	32	18	30
Fe	470	720	300	740
Ni	15	7.0	< 0.5	< 0.5
Cu	33	8.0	< 0.4	< 0.4
Zn	180	180	32	80
Pb	210	150	40	140

Table 4
Meteorological information — Campaign 2

Sample	Wind sector	Wind speed (m/s, range)	Air mass history
1	NW–NE	1–9	North Sea
2	NE–N	2–9	North Sea
3	NE–NW	8–10	Norway, northern Atlantic, North Sea
4	NW	4–11	Northern Atlantic
5	NW	11–18	Northern Atlantic
6	W	2–9	Northern Atlantic
7	NE	15–22	Norway, north Atlantic
8	NE	4–15	Norway, northern Atlantic
9	NE–N	6–11	Norway, northern Atlantic
10	N–W	2–11	Northern Atlantic
11	Variable	4–6	Norway, North Sea
12	SE–E	10–13	North Sea, Germany, Denmark
13	Variable	4–6	North Sea, Denmark
14	N–NE	5–8	Norway, North Sea
15	NW	5–8	UK, North Sea

history. Fig. 2 shows the track followed by the R/V Belgica during campaign 2 and the 15 sampling locations.

EDXRF results. Table 5 lists the EDXRF results for samples 1–8 of campaign 2. Sample 1 shows an extremely high Cu concentration (420 ng/m^3), probably due to contamination, although the source for this contamination is not clear. Sample 5 has high concentrations for marine elements, most likely due to contamination by sea spray droplets from breaking waves at the bow of the ship. Generally speaking, concentrations are reduced rapidly after the first sample and then remain low.

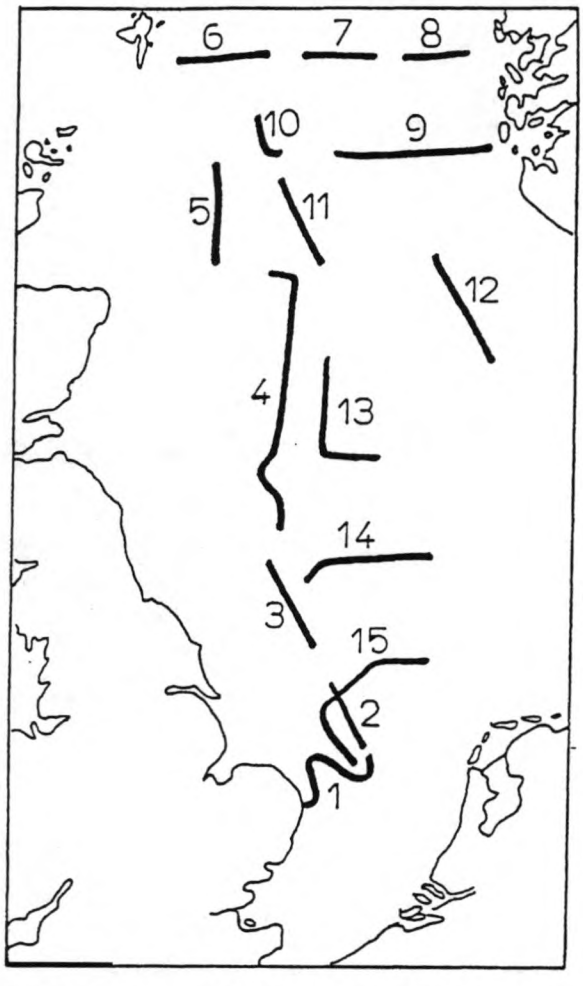

Fig. 2. Track of campaign 2 (the numbers refer to the sample numbers).

The air mass history indicates that the first sample was collected under partial influence of emissions from the UK, while samples 2–8 were collected under a predominantly northern wind with very little continental influence.

Table 6 lists the EDXRF results for the second part of campaign 2, for the coarse particle fraction. The highest wind speed, measured during collection of sample 12, is reflected in a Cl concentration of 17 200 ng/m^3. During the time samples 9–11 were being collected, the wind direction was mainly north and sampled air masses had very little continental influence, resulting in low concentrations for all elements except Cl. As the wind direction changed and the sampled air mass passed over Germany and UK, concentrations started to increase. In the fine fraction results (Table 7), this is even more clearly the case. Pb concentrations in the fine fraction increase from below the detection limit (< 8 ng/m^3) in samples 9–11 to 18–27 ng/m^3 in samples 12–15. Zn concentrations increase from 1–4 ng/m^3 to 14–19 ng/m^3 and S concentrations from 460–940 ng/m^3 to 1580–2550 ng/m^3.

3.3. Campaign 3

General sampling data and meteorological information. The track followed during campaign 3 is shown in Fig. 3. Three filter samples were collected on the way north from Zeebrugge (Belgium) to Hull (UK), while three others were collected on the way back to Zeebrugge. Wind speed and wind direction data are listed in Table 8.

EDXRF results. The relatively high wind speed during the first part of the track is reflected in high Cl concentrations for samples 1–3. Sample 3, taken at the northern part of the track, shows the lowest heavy metal (Cu, Zn and Pb) concentrations (Table 9).

During the second part of the campaign, the wind direction changed from southwest, over north to east and finally to southeast while the wind speed decreased steadily from 10–15 ms to 0–5 m/s. Similar to the results of campaign 1, we

Table 5
EDXRF results in ng/m³ — Campaign 2: first part of campaign 2, single filter used for particle collection

Element	Sample							
	1	2	3	4	5	6	7	8
P	< 70	89	< 70	120	< 70	89	< 70	< 70
S	2400	900	650	500	14 100	620	630	100
Cl	20 700	2490	5050	3140	99 600	2600	3040	910
K	560	110	140	80	4100	100	110	24
Ca	440	120	130	99	3100	82	94	31
Mn	< 0.9	2.0	1	1	< 0.9	< 0.9	< 0.9	< 0.9
Fe	30	19	12	23	17	< 0.4	10	2.0
Ni	3	< 0.5	1.0	1.0	< 0.5	< 0.5	1	< 0.5
Cu	420	1	2	1	14	1	1	0.5
Zn	12	3	5	3	35	5	< 0.4	2
Pb	14	< 8	< 8	< 8	< 8	< 8	< 8	< 8

Table 6
EDXRF results in ng/m³ — Campaign 2: second part of campaign 2, coarse particle fraction (> 2 μm)

Element	Sample						
	9	10	11	12	13	14	15
S	740	180	120	1300	365	640	860
Cl	6200	1370	665	17 200	3020	2500	4000
K	170	40	26	300	110	200	250
Ca	230	31	26	380	93	370	450
Ti	< 2.5	< 2.5	7	< 2.5	< 2.5	25	< 2.5
Fe	24	5	15	19	35	145	110
Cu	2	1	< 0.4	< 0.4	< 0.4	< 0.4	< 0.4
Zn	6	< 0.4	< 0.4	3	3	10	13
Pb	13	< 8	< 8	10	10	9	16

Table 7
EDXRF results in ng/m³ — Campaign 2: second part of campaign 2, fine particle fraction (< 2 μm)

Element	Sample						
	9	10	11	12	13	14	15
S	940	660	460	1580	2550	640	1660
Cl	< 600	< 600	< 600	< 600	< 600	2500	< 600
K	34	21	8	38	85	200	81
Ca	28	12	10	23	23	370	29
Ti	< 2.5	< 2.5	< 2.5	< 2.5	< 2.5	25	< 2.5
V	< 2.0	< 2.0	< 2.0	10	5	< 2.0	11
Mn	< 0.9	3	< 0.9	2	3	< 0.9	7
Fe	11	4	4	26	30	145	28
Ni	1	1	1	2	2	< 0.5	6
Cu	4	1	< 0.4	2	2	< 0.4	4
Zn	4	2	1	14	19	10	19
Pb	< 8	< 8	< 8	19	18	9	27

see that Mn, Zn and Pb concentrations increase relatively more than other trace metal concentrations, when the wind turns to the south.

3.4. Campaign 4

General sampling data and meteorological information. Fig. 4 shows the track during this campaign. The first 6 samples were collected with easterly wind. During samples 7 and 8, the wind direction changed slightly to the southeast. The wind speed never exceeded 7 m/s and was most of the time lower than 5 m/s.

EDXRF results. Table 10 shows the EDXRF results. Cl was not detected in a single sample. At very low wind speeds, the sea produces little sea spray droplets. In addition, high acid pollution concentrations will react with the few NaCl aerosols in the marine atmosphere, resulting in a release of HCl.

All anthropogenic elemental concentrations measured during this campaign are very high. Pb concentrations vary from 46 to 280 ng/m^3, Zn concentrations from 110 to 790 ng/m^3 and S concentrations from 6400 to 15200 ng/m^3. It is well known that, during the meteorological conditions present during this campaign, pollutant concentrations tend to rise rapidly. A combination of a low inversion height and low wind speeds limits natural dispersion of pollutants. Furthermore, the absence of any form of precipitation restricts the possibilities of concentration decrease through wet deposition processes.

At the end of campaign 4, the wind direction gradually shifted from east to southeast, resulting in the highest concentrations for all elements.

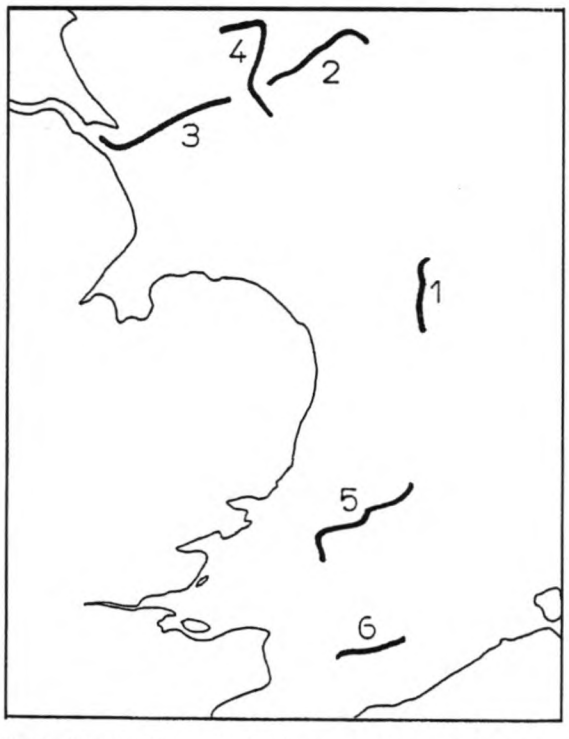

Fig. 3. Track of campaign 3 (the numbers refer to the sample numbers).

3.5. Campaign 5

General sampling data and meteorological information. Campaign 5 was performed in the English Channel, between Zeebrugge (Belgium) and the border of open Atlantic Ocean at 5°W. The track followed during this sampling campaign is shown in Fig. 5.

During the first half of the sampling campaign, a moderate wind speed of 10 m/s increased gradually to 15 m/s, while the wind direction was southwest to west. During the second half of campaign 5, the wind speed rapidly decreased to below 5 m/s and the wind direction changed to east to southeast (Table 11).

EDXRF results. As the R/V Belgica passed through the English Channel and the wind speed increased, the origin of the sampled air mass became more and more marine. This was reflected in a steady decrease in the S concentration from samples 1 to 5. While the wind direction changed from southwest to southeast and the

Table 8
Meteorological data — Campaign 3

Sample	Wind sector	Wind speed (m/s, range)
1	SW	7–10
2	SW	4–6
3	SW	7–9
4	S–SW	3–6
5	NE–E	2–4
6	E–SE	5–10

Table 9
EDXRF results in ng/m^3 — Campaign 3

Element	Sample					
	1	2	3	4	5	6
Si	< 140	260	< 140	680	190	870
P	120	< 70	< 70	< 70	< 70	< 70
S	1630	870	640	2740	4510	4960
Cl	6060	3960	5070	910	730	730
K	420	230	340	840	420	700
Ca	360	360	210	170	170	700
Ti	< 2.5	26	< 2.5	23	< 2.5	< 2.5
V	< 2.0	< 2.0	< 2.0	29	74	20
Cr	31	6.0	55	11	97	46
Mn	< 0.9	< 0.9	< 0.9	22	15	68
Fe	130	180	110	320	610	840
Ni	4.0	5.0	8.0	14	30	11
Cu	6.1	4	< 0.4	6.8	5.0	8.5
Zn	53	34	23	86	4.2	86
Pb	34	31	< 8	53	18	69

Table 10
EDXRF results in ng/m^3 — Campaign 4

Element	Sample							
	1	2	3	4	5	6	7	8
Si	840	1130	1120	940	1200	1860	2490	4820
P	290	420	370	380	380	600	690	690
S	6360	9600	8250	8790	8740	12900	14500	15200
K	300	340	330	420	400	560	740	1560
Ca	180	150	250	160	240	520	980	1970
Ti	11	20	31	15	26	69	100	180
V	14	18	13	11	17	33	42	46
Cr	2.3	4	8	21	7	8	14	27
Mn	17	17	19	23	21	33	46	180
Fe	370	360	410	400	530	980	1170	2760
Ni	8	8	6	7	7	15	21	24
Cu	11	10	15	16	14	22	21	39
Zn	140	150	110	200	150	200	220	790
Pb	120	76	46	84	73	140	170	280

Table 11
Meteorological data — Campaign 5

Sample	Wind sector	Wind speed (m/s, range)
1	SW	5–10
2	S–SW	10–15
3	S–SW	10–15
4	NW	10–15
5	W–NW	5–10
6	Variable	5–10
7	Variable	0–5

wind speed decreased at the end of the campaign, concentrations for most elements went up again (Table 12). The continental influence and the very low wind speed in sample 7 is illustrated by the low Cl concentration: < 600 ng/m^3 versus 3190 ng/m^3 in the previous sample.

3.6. Campaign 6

General sampling data and meteorological information. Campaign 6 was organized through the

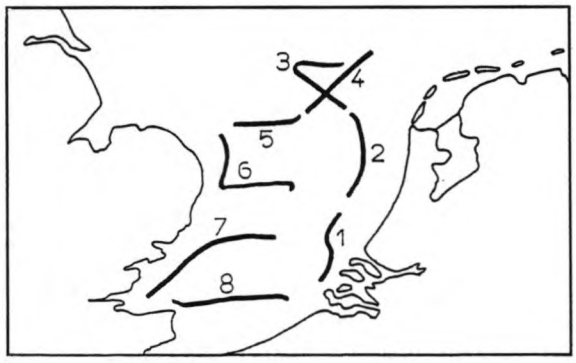

Fig. 4. Track of campaign 4 (the numbers refer to the sample numbers).

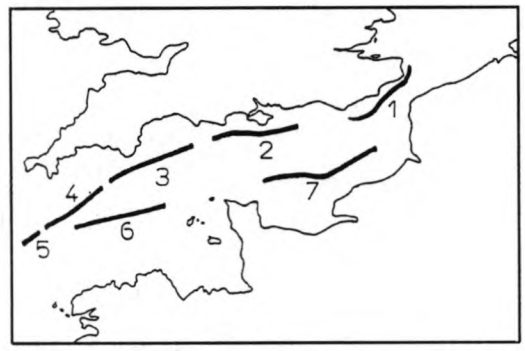

Fig. 5. Track of campaign 5 (the numbers refer to the sample numbers).

English Channel and seven filter samples were collected between Zeebrugge (Belgium) and the most westerly point of the followed track. Some 96 h backward air mass trajectories are shown in Fig. 6.

EDXRF Results. Table 13 lists the EDXRF results for sampling campaign 6. Analogous to campaign 5, the concentrations of most elements go down steadily, as the R/V Belgica passed through the English Channel and the origin of the collected air mass is mostly marine.

3.7. Campaign 7

General sampling data and meteorological information. Fig. 7 shows the track followed during campaign 7. The 96-h backward air mass trajectories for the four samples collected are shown in Fig. 8. A stacked filter unit was used for collection of the airborne particulate material.

EDXRF results. The coarse and fine particle concentrations are listed in Tables 14 and 15, respectively.

The air mass collected during samples 3 and 4

Table 12
EDXRF results in ng/m^3 — Campaign 5

Element	Sample						
	1	2	3	4	5	6	7
Al	< 200	230	< 200	230	< 200	< 200	< 200
Si	180	270	150	220	< 140	< 140	< 140
P	140	300	200	260	78	82	< 70
S	1360	1530	870	860	410	590	1200
Cl	3270	10400	7190	9990	3560	3190	< 600
K	150	280	150	180	69	95	89
Ca	180	230	150	170	80	93	160
Ti	< 2	< 2	< 2	< 2	< 2	< 2	17
V	12	9	< 2	< 2.0	2	6	18
Cr	7	7	< 1.5	< 1.5	< 1.5	< 1.5	< 1.5
Mn	2	< 0.9	< 0.9	< 0.9	< 0.9	< 0.9	3
Fe	48	5	4.1	3.7	7.3	16	105
Ni	5	5	< 0.4	< 0.4	< 0.4	< 0.4	5
Cu	< 0.4	< 0.4	< 0.4	< 0.4	< 0.4	< 0.4	2
Zn	6	2	< 0.4	< 0.4	< 0.4	2	27
Pb	10	< 8	< 8	< 8	< 8	< 8	< 8

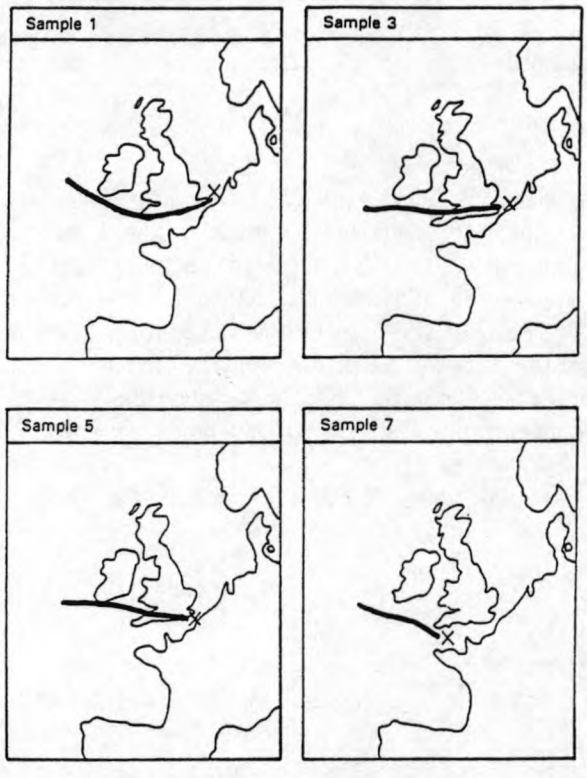

Fig. 6. Some 96-h back trajectories for campaign 6 (sampling location indicated by an ×).

has an important influence from emissions in France, while samples 1 and 2 are influenced by emissions in the UK.

3.8. Campaign 8

General sampling data and meteorological information. The track followed during campaign 8 is shown in Fig. 9. The 96-h backward trajectories are shown in Fig. 10 for samples 1–5; they indicate continental air masses. Samples 7 and 8 were collected by a stacked filter unit when the wind direction changed to the southwest and the wind speed rapidly increased up to 10–11 on the Beaufort scale.

EDXRF results. Table 16 shows the coarse particle fraction results for samples 1–8. Cl concentrations are reduced until sample 6, then a sudden increase due to a violent change in wind direction and wind speed results in a Cl concentration of 5000–6000 ng/m^3, while Fe, Zn and Pb concentrations decrease abruptly at sample 7.

Table 17 lists the fine particle fraction results for campaign 8. S, K, Fe, V, Zn and Pb all show the same profile: an abrupt decrease as the meteorological situation changes rapidly.

Table 13
EDXRF results in ng/m^3 — Campaign 6

Element	Sample						
	1	2	3	4	5	6	7
Al	250	< 200	< 200	< 200	< 200	< 200	< 200
Si	510	190	210	170	140	140	300
P	220	79	110	< 70	< 70	< 70	85
S	1890	1310	1080	1010	410	570	1040
Cl	5440	< 600	2470	< 600	< 600	< 600	1910
K	480	72	84	49	10	< 9	< 9
Ca	320	62	86	48	10	6.6	< 6
V	8	3	< 2	3	2.0	< 2.0	< 2.0
Mn	1.0	< 0.9	0.9	< 0.9	< 0.9	< 0.9	< 0.9
Fe	28	12	6	15	3	1.0	3
Ni	3.0	0.6	< 0.5	1.1	< 0.5	< 0.5	0.7
Cu	1.0	< 0.4	< 0.4	0.7	< 0.4	0.4	0.5
Zn	6.7	0.4	0.6	< 0.4	< 0.4	0.5	< 0.4
Pb	< 8	10	< 8	< 8	< 8	< 8	< 8

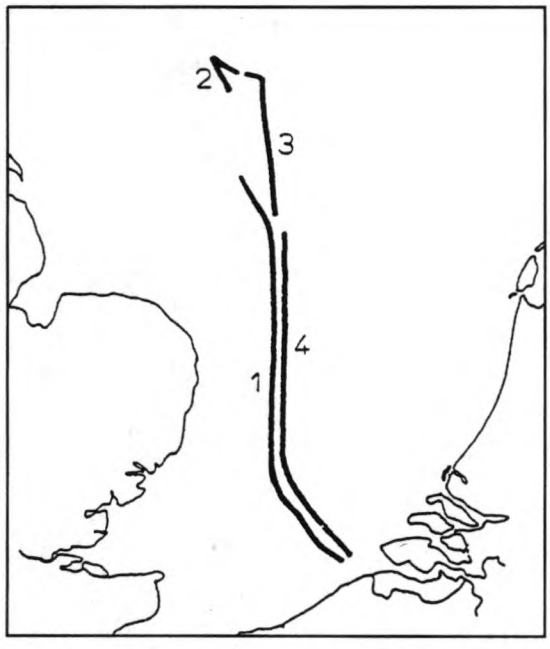

Fig. 7. Track of campaign 7 (the numbers refer to the sample numbers).

3.9. Campaign 9

General sampling data and meteorological information. Six samples were collected when crossing the Southern Bight of the North Sea, between Zeebrugge and London. The wind direction was stable during the sampling period and remained between 280 and 320. Samples 5 and 6 were collected during entrance of the Thames estuary in the direction of London.

EDXRF results. Table 18 shows the EDXRF results for campaign 9. The very high Mn concentrations in sample 1 is probably due to an unknown source of contamination. Samples 1–4 have comparable concentrations for most elements. The 10-fold increase in Fe and Zn concentrations is clearly associated with emissions from the London area and the industry in southern England. Cu and Ni concentrations go up by a factor of 5.

3.10. Campaign 10

General sampling data and meteorological information. Fig. 11 shows the track followed during campaign 10. All samples were collected under similar meteorological conditions. The wind direction stayed within the northern sector, between 320° and 30°.

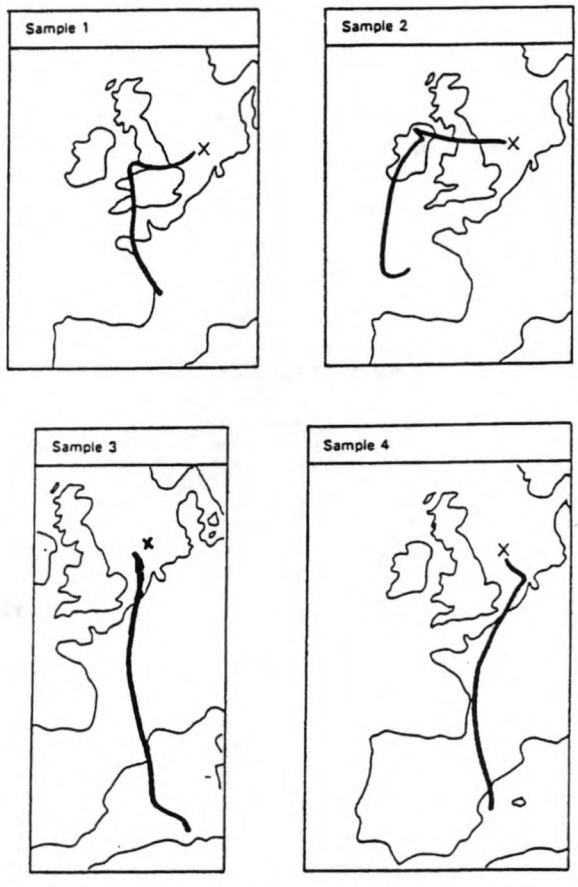

Fig. 8. The 96-h backward trajectories for campaign 7 (sampling location indicated with an ×).

EDXRF results. Table 19 lists the EDXRF results of campaign 10. All elemental concentrations in all eight samples are quite low. Not much variation is found as a function of time, which is in agreement with the constant wind direction and thus the fairly constant air mass history.

4. Average concentrations

Statistical data on the complete data set of aerosol samples are listed in Table 20: average, median, first quartile and fourth quartile concentration. These averages were calculated by leaving

Table 14
EDXRF results in ng/m^3 — Campaign 7, coarse particle fraction (> 2 μm)

Element	Sample			
	1	2	3	4
Al	300	< 200	< 200	< 200
Si	750	150	< 140	< 140
P	< 70	81	120	< 70
S	400	400	590	460
Cl	1930	4140	4890	2300
K	150	93	110	77
Ca	46	91	110	68
Ti	20	< 2.5	< 2.5	< 2.5
V	< 2.0	< 2.0	< 2.0	5
Mn	5	< 0.9	< 0.9	< 0.9
Fe	260	57	34	180
Ni	4	1.2	1.0	6
Cu	2	1.0	1.2	3
Zn	15	3	1.1	6
Pb	< 8	< 8	9	< 8

out two contaminated samples of campaign 2. These numbers can be considered as average concentrations for the total North Sea, including the English Channel.

Table 21 lists separately the average concentration for the total North Sea, the Southern Bight of the North Sea (defined as the area of the North Sea south of latitude 54°N), and the northern part of the North Sea. Altogether 35 samples were collected between 51° and 54°N. These are considered to be representative for the atmosphere above the Southern Bight of the North Sea.

It is obvious from Table 21 that concentrations in the northern part of the North Sea are much lower than in the Southern Bight. Mn, Zn, Pb and Fe all show concentrations that are more than 10 times higher in the southern part of the North

Table 15
EDXRF results in ng/m^3 — Campaign 7, fine particle fraction (< 2 μm)

Element	Sample			
	1	2	3	4
Al	240	< 200	< 200	< 200
Si	150	< 140	< 140	< 140
P	190	< 70	130	< 70
S	1150	660	740	1480
Cl	6540	1610	5300	< 600
K	150	59	24	77
Ca	35	18	14	12
V	3	< 2.0	< 2.0	< 2.0
Cr	< 1.5	5	< 15	< 1.5
Mn	3	1	< 0.9	< 0.9
Fe	40	5	7	42
Ni	2	< 0.5	1	4
Cu	< 0.4	< 0.4	1.2	1.0
Zn	11	3	3	11
Pb	13	< 8	9	9

Table 16
EDXRF results in ng/m^3 — Campaign 8, coarse particle fraction (2 μm)

Element	Sample							
	1	2	3	4	5	6	7	8
Al	310	230	< 200	< 200	< 200	< 200	< 200	< 200
Si	520	510	150	220	190	140	< 140	< 140
P	130	100	< 70	< 70	< 70	< 70	120	130
S	1720	1300	550	880	760	1060	510	670
Cl	1450	710	< 600	< 600	< 600	< 600	5080	5900
K	110	160	51	100	79	62	110	300
Ca	280	400	90	120	110	71	110	260
Ti	48	21	4	6	< 2.5	4	< 2.5	< 2.5
V	2	3	< 2.0	< 2.0	< 2.0	< 2.0	< 2.0	< 2.0
Mn	11	71	2	2	3	2	< 0.9	< 0.9
Fe	490	290	67	96	73	57	4	3
Ni	3	2	2	< 0.5	1.2	1.0	1.0	2
Cu	3	4	1.0	1.3	1.2	1.0	< 0.4	1.1
Zn	51	48	17	20	16	18	2	3
Pb	24	32	9	17	< 8	15	13	< 8

Sea compared with the northern part. Si, S, Ti and Cu concentrations are 4–6 times higher in the south. K. Ca, V and Ni have very similar 'southern part to northern part' concentration ratios: 3.6–3.9. Al, P and Cr show the least difference between the northern part concentrations and southern part. This is merely a result of the large number of observations that were below the detection limit of the analytical technique used. Average Cl concentrations are identical to within 5%.

5. Factor analysis

The main goal of applying factor analysis is to try to reduce a large number of variables (in our

Table 17
EDXRF results in ng/m^3 — Campaign 8, fine particle fraction (< 2 μm)

Element	Sample							
	1	2	3	4	5	6	7	8
Al	210	< 200	< 200	< 200	200	< 200	< 200	< 200
Si	160	180	160	< 140	< 140	< 140	< 140	< 140
P	220	200	130	190	180	170	< 70	< 70
S	3930	3470	2660	3780	3680	3200	92	< 80
Cl	610	< 600	< 600	< 600	< 600	< 600	< 600	< 600
K	200	320	190	240	140	110	10	< 9
Ca	15	33	< 6	7	< 6	7	< 6	< 6
Ti	7	3	< 2.5	3	< 2.5	4	< 2.5	5
V	20	16	10	10	8	6	2	6
Cr	6	3	2	2	< 1.5	< 1.5	4	6
Mn	13	18	10	6	5	4	< 0.9	< 0.9
Fe	197	159	25	18	9	5	< 0.4	< 0.4
Ni	3	5	2	2	1.2	1.2	< 0.5	< 0.5
Cu	3	8	3	1.3	< 0.4	< 0.4	< 0.4	< 0.4
Zn	68	107	43	32	23	20	< 0.4	< 0.4
Pb	66	135	58	52	31	31	< 8	< 8

Table 18
EDXRF results in ng/m^3 — Campaign 9

Element	Sample					
	1	2	3	4	5	6
Si	< 140	< 140	< 140	< 140	250	550
S	900	1970	1480	1070	4830	7940
Cl	4520	6200	9840	6440	< 600	970
K	280	270	640	230	330	530
Ca	330	290	1090	290	210	820
Ti	20	< 2.5	20	13	17	48
V	20	11	12	< 2.0	10	17
Cr	15	40	26	17	19	48
Mn	170	< 0.9	7.9	< 0.9	14	20
Fe	87	68	110	41	280	550
Ni	10	4.7	6.0	1.5	4.9	8.2
Cu	8	8	15	3	7	15
Zn	74	13	64	10	72	140
Pb	19	13	18	< 8	65	120

case, 16 elemental concentrations) measured in a system (in our case, the North Sea atmosphere) to a limited number of independent factors that explain the variation of the observed system.

Factor analysis was performed using STATGRAPHICS version 2.6 software that runs on an AT-type PC.

5.1. Coarse fraction versus fine fraction

Factor analysis was performed on a limited sample set of 19 aerosol samples, collected with a stacked filter unit, in order to evaluate any difference in inter-element correlations between the coarse and the fine particle fraction. The results for the coarse fraction aerosol samples are presented in Table 22. Since, in a significant number of samples, several elements are not detected, only seven variables were selected: S, Cl, K, Ca, Fe, Zn and Pb. Some 90% of the total variance can be explained by the first three independent factors. The first factor is heavily loaded with Pb (0.94), S (0.79) and Zn (0.72) and represents sulphate particles that are rich in trace metals. The second factor with K (0.96), Cl (0.83) and Ca

Table 19
EDXRF results in ng/m^3 — Campaign 10

Element	Sample							
	1	2	3	4	5	6	7	8
S	290	220	230	220	130	340	140	300
Cl	1030	670	950	< 600	< 600	2400	< 600	< 600
K	49	35	88	17	16	100	34	17
Ca	60	52	28	25	49	110	20	< 6
Ti	23	< 2	7	15	20	13	9	11
V	12	6	5	< 2.0	6	< 2.0	< 2.0	8
Cr	30	18	12	19	21	16	12	22
Fe	43	38	16	51	35	23	22	28
Ni	3	2	1.5	< 0.5	3	< 0.5	3	3
Cu	6	4	3	4	5	4	4	5
Zn	7	4	3	4	2	2	3	4

Table 20
Average, median, first and fourth quartile concentrations in ng/m^3, for all analysed samples

Element	Average	Median	First quartile–fourth quartile
Si	399	< 140	< 140–270
P	174	< 70	< 70–200
S	2750	1400	630–3900
Cl	2890	1400	< 600–4500
K	254	200	88–340
Ca	239	150	78–320
Ti	14.0	0.7	< 2.5–17
V	12.4	5.9	< 2.0–17
Cr	12.1	2.6	< 1.5–15
Mn	13.6	< 0.9	< 0.9–10
Fe	229	48	16–320
Ni	4.7	2.7	0.7–7.0
Cu	5.5	3.1	0.6–8.0
Zn	54.9	12	2.7–74
Pb	40.6	13	< 8–53

(0.77) is associated with sea salt particles. The third factor is heavily loaded with Fe (0.90) and can be associated with soil dust particles.

Factor analysis on the fine particle fraction (Table 23) yields four factors that explain 91.9% of the observed variance. Factor 1 with S (0.91), K (0.85), Pb (0.76) and Zn (0.75) is again identified with trace metal rich sulphate particles. Factor 2 is loaded with Cu (0.88), Ni (0.86) and Zn (0.62) and is also pollution related. Factor 3 with Ca (0.95) and Fe (0.67) is associated with $CaSO_4$ and fly-ash emissions. The fourth factor, with Cl (0.98), is typical for the marine aerosol.

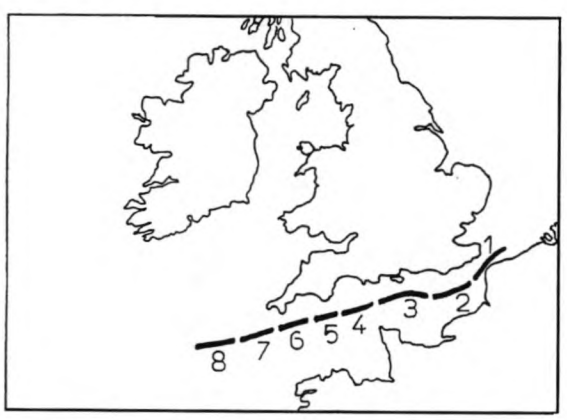

Fig. 9. Track of campaign 8 (the numbers refer to the sample numbers).

5.2. Samples collected on the Southern Bight of the North Sea

Thirty-five samples were collected when the R/V Belgica was in the Southern Bight of the North Sea, between 51° and 54°N. Factor analysis was performed on this data set using the fol-

Table 21
Average atmospheric concentrations in ng/m^3

Element	Southern Bight	Northern North Sea
Si	725	119
P	249	97
S	4780	778
Cl	2960	2830
K	401	110
Ca	382	100
Ti	24.9	4.6
V	18.8	4.9
Cr	14.2	10.1
Mn	28.5	0.8
Fe	432	31.3
Ni	7.5	2.0
Cu	9.2	1.9
Zn	107	4.7
Pb	77	5.0

lowing variables: S, Cl, K, Ca, V, Fe, Ni, Cu, Zn and Pb.

Table 24 shows that 91.5% of the observed variance can be explained by three factors. Sea salt particles are identified by the third factor with a high loading for Cl (0.92). Factor 2 is heavily loaded with V (0.92) and Ni (0.91), two elements that are typical for oil burning residue. The first factor contains all other elements: Zn (0.91), Ca (0.89), Cu (0.87), K (0.85), Fe (0.84), Pb (0.83) and S (0.69).

Factor analysis applied to our data is only able to reveal a limited number of aerosol particle sources: sea salt particles, oil burning residue and trace metal rich particles. Although there may be a larger number of particle sources and thus different particle types, the emission occurs mainly on land. After dispersion and transport, the continental aerosol will reach the marine atmosphere as a well mixed aerosol. In this way, factor analysis on bulk results can not reveal the original sources. The fact that emissions from oil burning

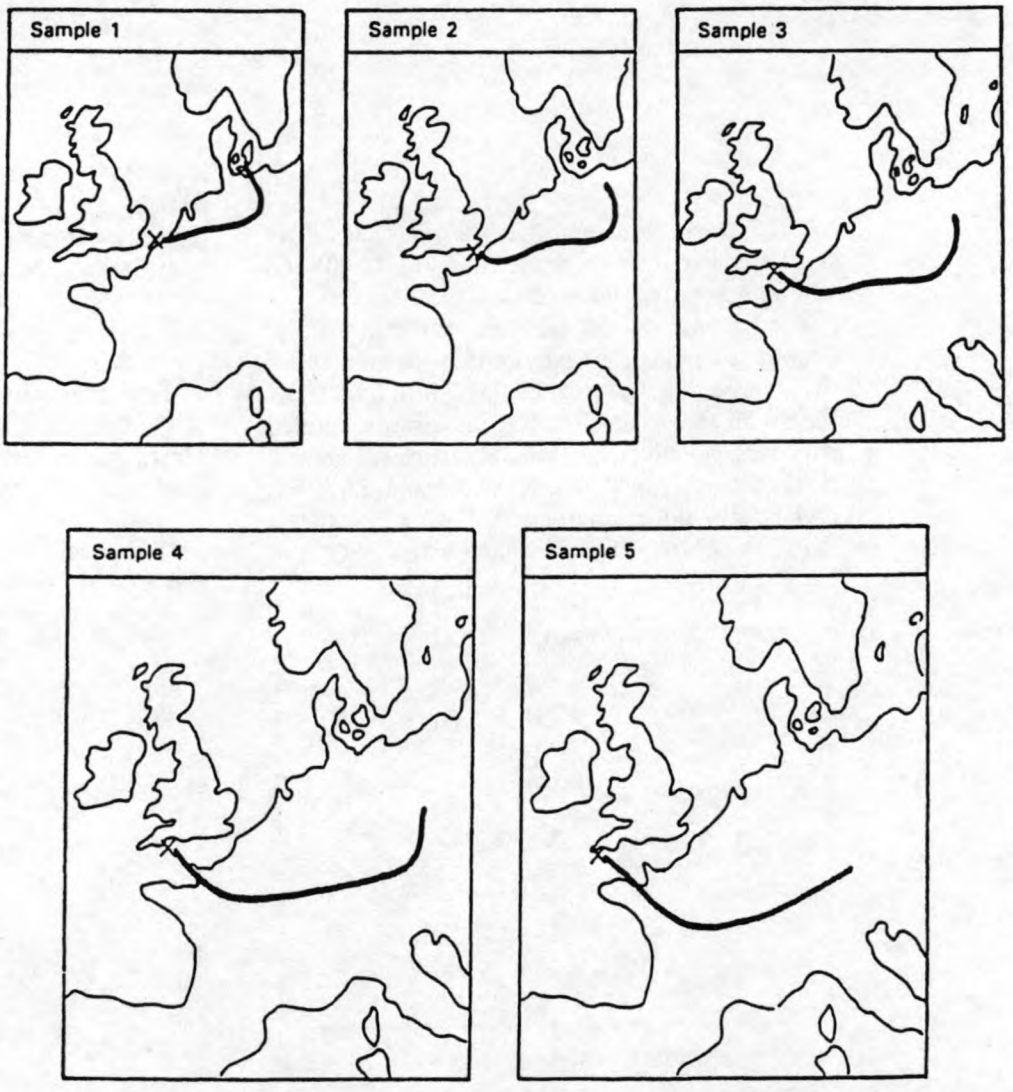

Fig. 10. Some 96-h backward air mass trajectories for campaign 8 (sampling location indicated with an ×).

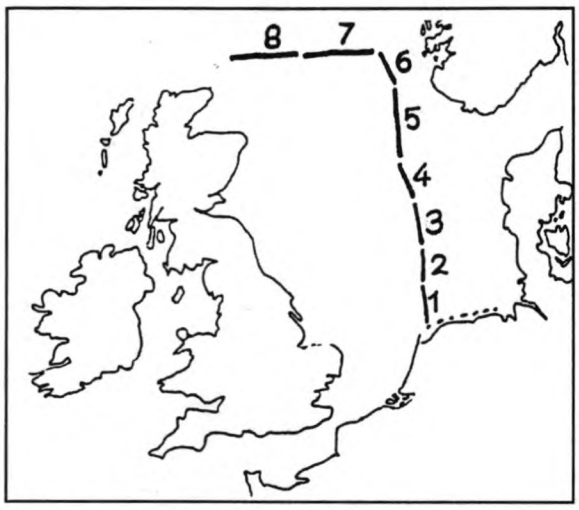

Fig. 11. Track of campaign 10 (the numbers refer to the sample numbers).

are often recognized as an independent source above the sea, suggests that this source has a somewhat different behaviour than other pollution sources. This might be explained by the emission of Ni and V through diesel engine exhaust of the numerous ships, present on the North Sea.

In order to differentiate the various continental aerosol sources, other analysis techniques should be used; single particle techniques such as electron microprobe can offer more information here (Van Grieken and Xhoffer, 1992).

6. Conclusions

Atmospheric concentrations of different elements in the lower troposphere above the North Sea are highly variable as a function of both tim and location. Rapid changes in the meteorologi cal situation are reflected without delay in th atmospheric concentrations of trace elements.

Average Cl concentration above the norther part of the North Sea are approximately the sam as above the Southern Bight of the North Sea Mn, Zn, Pb and Fe concentrations are 10–3(times lower in the northern North Sea atmo sphere than in the southern part. Si, S, Ti, Cr, K

Table 22a
Factor analysis results, coarse particle fraction

Factor	Eigenvalue %	Variance	Cumulative variance
1	3.6	51.7	51.7
2	2.3	32.9	84.5
3	0.4	6.3	90.9
4	0.4	5.6	96.4
5	0.1	1.9	98.4
6	0.1	1.2	99.6
7	0.0	0.4	100.0

Table 22b
Estimated communality

Variable	Estimated communality
S	0.871
Cl	0.826
K	0.931
Ca	0.861
Fe	0.952
Zn	0.975
Pb	0.943

Table 22c
Varimax rotated factor loading matrix

Variable	Factor		
	1	2	3
S	0.79	0.37	0.33
Cl	0.05	0.83	0.38
K	0.05	0.96	0.04
Ca	0.48	0.77	0.21
Fe	0.37	0.03	0.90
Zn	0.72	0.13	0.66
Pb	0.94	0.05	0.22

Table 23a
Factor analysis results, fine particle fraction

Factor	Eigenvalue %	Variance	Cumulative variance
1	4.97	55.2	55.2
2	1.68	18.6	73.8
3	0.85	9.4	83.3
4	0.78	8.7	91.9
5	0.38	4.2	96.1
6	0.23	2.6	98.7
7	0.87	1.0	99.7
8	0.28	0.3	100.0
9	0.02	0.0	100.0

Table 23b
Estimated communality

Variable	Estimated communality
S	0.925
Cl	0.997
K	0.933
Ca	0.949
Fe	0.863
Ni	0.790
Cu	0.899
Zn	0.972
Pb	0.946

Table 23c
Varimax rotated factor loading matrix

Variable	Factor			
	1	2	3	4
S	0.91	0.14	0.17	0.21
Cl	0.10	0.12	0.10	0.98
K	0.85	0.29	0.35	0.10
Ca	0.07	0.17	0.95	0.10
Fe	0.46	0.45	0.67	0.05
Ni	0.20	0.86	0.11	0.06
Cu	0.32	0.88	0.07	0.13
Zn	0.75	0.62	0.11	0.09
Pb	0.76	0.59	0.04	0.09

Ca, V, Ni and Cu concentrations are on the average 3–6 times lower above the northern North Sea, compared with the Southern Bight atmosphere.

Factor analysis performed on all samples distinguished several particle types, predominantly the sea-salt particles and anthropogenic particles.

Table 25 compiles some published aerosol concentration data relevant to the study area. Compared with similar results reported very recently by Ottley and Harrison (1993) ours are in relatively good agreement. However, for example, compared with the ship-based measurements performed by Dedeurwarder (1988) and Xhoffer et al. (1991), our results for the Southern Bight of the North Sea are up to 50% lower. This difference can most likely be attributed to the fact that these aerosol samples were collected in the very southern part of the North Sea, whereas our

Table 24a
Factor analysis results, Southern Bight samples

Factor	Eigenvalue	% variance	Cumulative variance
1	6.86	68.7	68.7
2	1.30	13.0	81.7
3	0.98	9.8	91.5
4	0.29	2.9	94.4
5	0.17	1.7	96.2
6	0.12	1.2	97.3
7	0.11	1.1	98.4
8	0.09	0.9	99.3
9	0.05	0.5	99.8
10	0.02	0.2	100.0

Table 24b
Estimated communality

Variable	Estimated communality
S	0.854
Cl	0.899
K	0.889
Ca	0.915
V	0.960
Fe	0.937
Ni	0.973
Cu	0.903
Zn	0.932
Pb	0.890

Table 24c
Varimax rotated factor loading matrix

Variable	Factor		
	1	2	3
S	0.69	0.26	0.56
Cl	0.08	0.21	0.92
K	0.85	0.41	0.03
Ca	0.89	0.24	0.25
V	0.25	0.92	0.24
Fe	0.84	0.43	0.21
Ni	0.36	0.91	0.15
Cu	0.87	0.26	0.27
Zn	0.91	0.20	0.25
Pb	0.83	0.16	0.41

Table 25
Comparison with some published aerosol concentration data (ng/m^3) relevant to the study area

Element	This work	Ottley and Harrison (1993)		Xhoffer et al. (1991)	Dedeurwaerder (1988)	Van Jaarsveld et al. (1986)
		North Sea	Marine*			
K	254	1239	357	—	—	—
Ca	239	467	269	—	—	—
Mn	13.6	—	—	—	58	—
Fe	229	184	156	—	560	—
Cu	5.5	6.9	1.8	9.2	17	1.9
Zn	54.9	74.6	24.1	110	150	17
Pb	40.6	29.1	3.5	77	150	33

* Marine indicates north air mass source region

samples are covering the whole area of the Southern Bight of the North Sea (south of 54°N). Model calculations by Van Jaarsveld et al. (1986) in the case of Pb show a good agreement with our observed Pb concentrations.

Acknowledgement

This work was partially prepared in the framework of the Impulse Programme in Marine Sciences, supported by the Belgian State Prime Minister's Service, Science Policy Office (contract MS/06/050).

References

Dedeurwaerder, H.L., 1988. Study of the Dynamic Transport and of the Fall-out of Some Ecotoxicological Heavy Metals in the Troposphere of the Southern Bight of the North Sea. Ph.D. Dissertation, Vrije Universiteit Brussel, Brussels, Belgium.

Ottley, C.J. and R.M. Harrison, 1993. Atmospheric dry deposition flux of metallic species to the North Sea. Atmos. Environ., 27A: 685–695.

Van Espen, P., K. Janssens, and J. Nobels, 1986. AXIL-PC, Software for the analysis of complex X-ray spectra. Chemometr. Intell. Lab. Syst., 1: 109–114.

Van Grieken, R. and C. Xhoffer, 1992. Microanalysis of individual environmental particles. J. Anal. Atom. Spectrom., 7: 81–88.

Van Jaarsveld, J.A., R.M. Van Aalst, and D. Onderlinden, 1986. Deposition of Metals from the Atmosphere into the North Sea: Model calculations, Report 842015002, RIVM, Bilthoven.

Xhoffer, C., P. Bernard, R. Van Grieken, and L. Van der Auwera, 1991. Chemical characterization and source apportionment of individual aerosol particles over the North Sea and the English Channel using multivariate techniques. Envir. Sci. Technol., 25: 1470–1478.

Selected article #18:

Vertical sulfur dioxide, ozone, and heavy metal concentration profiles above the Southern Bight of the North Sea

P. Otten, J. Injuk and R. Van Grieken

Israel Journal of Chemistry (Invited contribution: Special Issue on Atmospheric Chemistry), 34 (1994) 411-424

2648

Vertical Sulfur Dioxide, Ozone, and Heavy Metal Concentration Profiles Above the Southern Bight of the North Sea

PHILIPPE OTTEN, JASNA INJUK, AND RENÉ VAN GRIEKEN*
Department of Chemistry, University of Antwerp (UIA), B-2610 Antwerpen-Wilrijk, Belgium

(Received 1 March 1994 and in revised form 12 October 1994)

Abstract. Vertical profiles of SO_2 and O_3 concentrations were measured continuously within the lower atmosphere during 18 flights over the Southern Bight of the North Sea. The average SO_2 concentration below the temperature inversion layer ranged from 1.9 to 19.5 ppb. The highest levels were observed when the air masses came from the southeast–east and under variable wind sector conditions: 15.2 and 12.0 ppb, respectively. The highest SO_2 concentrations were found at altitudes between 100 and 200 m. The overall average O_3 concentration was 46 ppb, with values of 30–40 ppb at sea level to 60–70 ppb at altitudes above 100 m. Low O_3 concentrations reflect O_3 depletion through reaction with freshly emitted pollutants, while high O_3 concentrations are an indication of photochemical activity. O_3 concentrations are primarily dependent on seasonal influences, while SO_2 levels are dictated more by the history of the sampled air mass. The results are discussed in relation to the heavy metal concentrations, measured within the same experiment. In spite of some differences, SO_2 and trace metals showed similar trends. The individual SO_2 and O_3 profiles clearly illustrated the high variability in vertical concentration distributions.

INTRODUCTION

It is well known that the emission of SO_2 mainly results from the combustion of sulfur-containing fuels, the major share coming from the use of coal and oil in fossil fuel fired power plants, industrial combustion units, small combustion units in households, and traffic. The emissions in the traffic sector remained nearly constant despite the increase in vehicles and mileage, due to reduction of the sulfur content in diesel fuel. In the household and small business sector, the emissions decreased due to the use of lower sulfur fuels (including gas) and a decrease in energy consumption. The emissions for various types of sources in some European countries bordering the North Sea, as well as in the United States of America and Canada are strongly diminishing, as is demonstrated in Table 1. In 1990, on average about 40% of the 1980 man-made emissions of SO_2 was emitted, related to regulatory measures.

Today, there is much concern about the dramatic loss of O_3 occurring in the stratosphere, but also about the steady increase of the tropospheric O_3 concentrations in large parts of the northern hemisphere, due to emissions of hydrocarbons and nitrogen oxides. This has been confirmed in various sets of data from long-running O_3 measurements.[1] The tropospheric concentrations of O_3, which account for only 10% of the vertical O_3 column above the earth's surface, show average daily 1-h maxima of approximately 20–60 ppb.[2] In clean, dry air near sea level, pollutants such as O_3 and SO_2 are generally present in minute concentrations: 20 ppb and 0.2 ppb, respectively. Within the troposphere up to an altitude of 5 km, the SO_2 concentration decreases to values around 100 ppt. Above 5 km, a constant value up to the tropopause is observed. The SO_2 concentration of 20 to

Table 1. SO_2 emissions (ktons y^{-1}) for some countries bordering the North Sea,[6] and for the USA and Canada,[7] in 1980 and 1990

	1980	1990	Decrease (%)
Belgium	850	400	53
The Netherlands	500	200	60
West Germany	3300	1000	70
East Germany	4400	4900	–11
France	3400	1200	65
UK	4900	3900	20
USA	23100	21000	9
Canada	4500	3700	18

*Author to whom correspondence should be addressed.

100 ppt seems typical for the layer above 6 km, and can be considered a background value for the higher troposphere.[3] Above the Atlantic Ocean, nearly constant SO_2 concentrations in the troposphere were observed during aircraft flights. A background concentration of approximately 100 to 400 ppt is suggested.[3]

Table 2 shows mean SO_2 and O_3 concentration levels measured over Belgium, bordering the Southern Bight of the North Sea. Considering the North Sea area, the estimated total yearly deposition of sulfur as SO_2 is 3, 000 ktons.[4]

To our knowledge, data on SO_2 and O_3 profiles with altitude have not been published hitherto for the Southern Bight of the North Sea. Therefore, the aim of this work was to assess vertical concentration profiles of SO_2 and O_3, on the basis of the results of twenty-three flights above the Southern Bight of the Northern Sea, in relation to the particulate heavy metal content. As will be discussed below, the individual cases of vertical SO_2 distributions are strongly influenced by the vertical thermal stability of the atmosphere, while observed variations in O_3 levels through the atmosphere are primarily dependent on seasonal influences.

Table 2. Mean atmospheric SO_2 and O_3 concentrations (ppb) in Belgium[8]

		Winter (1989-90)	Summer (1989)
Cities:	O_3	4–13	13–32
	SO_2	8–45	5–46
Countryside:	O_3	8–22	15–31
	SO_2	3–20	3–11

EXPERIMENTAL

Sampling

During the period September 1988 through October 1989, twenty-three flights by a twin-engine aircraft Piper Chieftain (PA-31-350, call-sign PH-ECO) of the Geosens B.V. company (Rotterdam, The Netherlands) were flown above the Southern Bight of the North Sea (Fig. 1). The aircraft has been modified in order to perform a large variety of atmospheric research tasks. When fully equipped and using a crew of four persons, the flight time was limited to four and half hours. Considering the transfer time between the Rotterdam airport, where take-off took place, and the North Sea, a useful sampling time of three and a half hours was available during each flight. All flights were carried out during relatively cloudless periods, less than 3/8, without precipitation. On the way from Rotterdam airport to the Goeree platform, just offshore, all equipment was tested. Then, one spiral track was performed at Goeree, during which SO_2 and O_3 concentrations, as well as temperature and dew point, were monitored for the inversion height localization. In the direction of the wind, six tracks were flown over the North Sea, each for 25 min, usually at six heights mostly under the inversion layer. The last one was at minimum altitude, between 10 and 30 m above sea level. SO_2 and O_3 were measured continuously.

Analytical Equipment

In situ SO_2 measurements were performed with a pulsed fluorescence monitor (Thermao Electron, model 43A). The flow rate of the apparatus has been modified in order to increase the response time up to 12 s.

The SO_2 monitor was calibrated before take-off of each flight with a standard gas mixture of SO_2 and clean air. The detection limit was 1 ppb and the accuracy, about 1.5%.

O_3 was measured with a Bendix model 8002 (Combustion Engineering) chemiluminescence monitor. The operation of this instrument is based on the photometric detection of chemiluminescence that occurs through a gas-phase reaction of ethylene with O_3. The instrument can be used in three different modes. In the zero mode, ozone-free air is led into the reaction chamber together with ethylene. In the span mode, an O_3 generator is used for producing a known concentration of O_3. In the ambient mode, ambient air is led into the reaction chamber through a Teflon filter that removes all particles with diameter > 10 μm. The O_3 generator is made up of an ultraviolet lamp and a quartz tube. Dried O_3-free air, which was passed through a chemical filter consisting of molecular sieves, silica gel, and activated charcoal, is passed through the quartz tube where O_3 is generated by UV light. The detector cell in the O_3 analyzer consists of a photomultiplier. Inside the detector, thermo-electrical coders are used to maintain the temperature at 5 °C. This increases the lifetime of the detector and reduces the background. In the reaction chamber, the sampled atmosphere is mixed with ethylene. A window is placed between the reaction chamber and the photomultiplier for protective purposes. Calibration was performed with O_3-free air and with standard gas mixtures with known O_3 concentration. This calibration was performed before take-off of each flight. A detection limit of 0.2 ppb, an accuracy of 1%, and a response time of 4 s were achieved with this apparatus.

Data acquistion was established by use of the three recorders (BBC model SEA 430), each with three input/output channels. A modified Olivetti PC model M21 with 5 1/4" diskette was used for the collection of all parameters, with a frequency of 12 data-set collections per minute. If necessary, data transmission to a ground station was possible with an HF radio connection.

Sampling of airborne particulate matter was accomplished with a Pennsylvania State University (PSU) isokinetic sampler. Air enters the sampler through a carefully designed intake 2.03 cm in diameter, and is reduced in speed through a 7° conical expansion that terminates in a cylindrical sampling chamber. The expansion angle of 7° minimizes both dissipative losses and flow separation. The air speed is reduced by a factor of 16.6 from the aircraft speed. The sampler chamber has an inner diameter of 8.28 cm and a total length of 22.86 cm. In this chamber, a small fraction (< 10%)

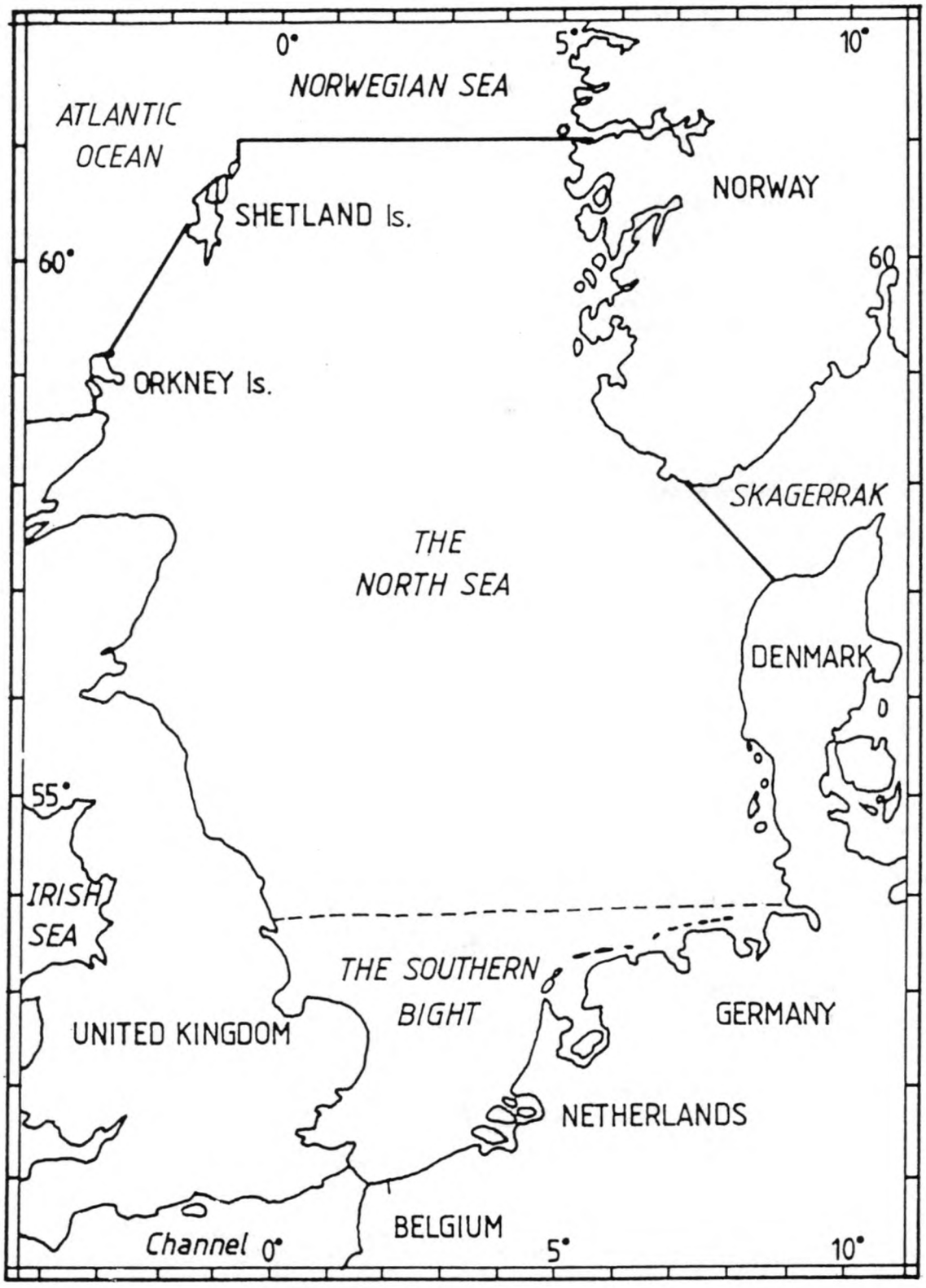

Fig. 1. The North Sea map with measurement region of the Southern Bight.

of the total air flow is removed by the aerosol instruments. The tubes leading to the individual instruments all have a gradual bend, and are adopted for isokinetic sampling by using an appropriate nozzle size to match the local air speed in the sample chamber to the instrument flow rate. The PSU sampler is mounted on the roof of the aircraft in such a way that the intake is located outside the boundary layer of the aircraft and no particulate or gaseous matter coming from the exhaust of the two engines can be sampled. In our experimental setup two filter types were used: a 0.4 μm pore size Nuclepore filter, 47 mm in diameter, and a 1.0 μm pore size Teflon filter (Millipore, type FA), 47 mm in diameter. For size-differentiated aerosol sampling, a nine-stage low-pressure Berner cascade LPI/0.06/30 (with cut-off diameters of 0.06, 0.125, 0.25, 0.5, 1, 2, 4, 8, and 16 μm) was used. The use of low pressure results in a reduction of the frictional forces of the gas on the particles; the slip correction factor increases significantly for particles of around 1 μm when the pressure is reduced. In addition, a reduction in pressure results in an increase in volume flow through the smaller jets and a correlated increase in inertial forces. Hence, at low pressures, smaller particles are deposited in the impactor. The deposits were collected on 10-μm-thick aluminum foils. A flow rate of 30 L min^{-1} was maintained through the use of a high-volume pump which was powered by the 24 V generator of the aircraft.

The airborne particulate matter samples were analyzed with a differential pulse anodic stripping voltammetry (DPASV) unit, model EG & G (Princeton Applied Research, Princeton, NJ, USA). For our samples, the extraction consisted of a single 60 min ultrasonic treatment, placing the filter in 10 ml ultrapure water (prepared by a Milipore Mili-Q purification unit), and acidifying with 70 μl of Merck Suprapure concentrated HNO_3. For the determination of Zn, the sample was neutralized to pH 4.0 by adding 1500 μl of 0.1 M NaAc. Quantification was done by standard addition using 2 spikes for each element. Calculation of the concentration was based on measurement of the peak heights. The average relative standard deviation per measurement appeared to be between 10 and 15% for the overall analytical procedure.

RESULTS AND DISCUSSION

Average SO_2 and O_3 Profiles

The average SO_2 and O_3 concentrations for each track of all 18 flights were divided into 10 altitude classes (0–100 m, 100–200 m, 400–600 m, 600–800 m, 800–1000 m, 1000–1200 m, 1200–1400 m, 1400–1800 m, and 1800–2800 m). In Fig. 2, the average SO_2 and O_3 values for the conditions of these experiments are given. The average O_3 profile shows a clear increase in concentration with increasing altitude. At sea level, an average O_3 concentration of 35 ppb was measured, while above 100 m, average values of 60 to 70 ppb were obtained.

For SO_2, a reverse trend can be observed. Generally, SO_2 concentrations at lower levels are higher than at higher altitudes. The maximum average SO_2 was measured at between 100 and 200 m (16 ppb), while at sea level, an average value of 10 ppb was measured. This is in good agreement with the average trace metal profiles measured during the same experiment,[5] as displayed in Fig. 3. All samples from all flights were divided into 10 classes of altitude (1–100, 100–200, 200–400, 400–600, 600–800, 800–1000, 1000–1200, 1200–1400, 1400–1800, and 1800–2800), and an average concentration was calculated for each altitude-class. The high value for the Cu concentration between 1200 and 1400 m is due to one outlier concentration of 189 ng m^{-3}. Discarding this one value, all four trace metal levels yield maxima between 100 and 200 m.

In the next subsection, some specific profiles of a few selected but representative flights are discussed.

Flight 6. Figure 4 shows the temperature, SO_2, and O_3 profiles measured during flight 6. This flight was performed when the sampled air masses originated from

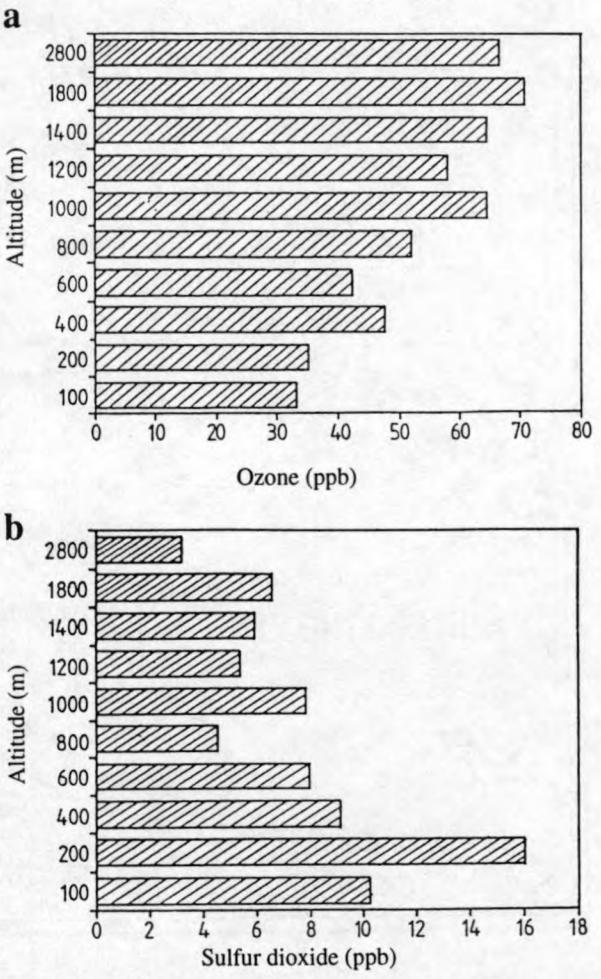

Fig. 2. Average (a) O_3 and (b) SO_2 concentrations as a function of altitude above the Southern Bight of the North Sea.

the northwest. The measured concentration profiles can therefore be regarded as background profiles for the atmosphere above the Southern Bight of the North Sea.

The temperature profile shows some layering, which can result in the trapping of plumes from power plants and some other sources. A lapse rate of –0.92 °C/100 m is measured between 15 and 1970 m. A sharp temperature inversion is located at an altitude of 1970 m. The SO_2 concentration below the temperature inversion layer was nearly constant and very low, with an average of 2.8 ppb. The O_3 profile shows a steady increase from 35 ppb at 15 m to 45 ppb at 1400 m. Between 1400 m and 2000 m, a slight decrease of the O_3 concentration can be observed.

Flight 12. The profile measurements of flight 12, carried out under a southwesterly wind, illustrate the capture of pollutants underneath a low-altitude radiative inversion layer (Fig. 5). The temperature profile shows a narrow, stable, almost isothermal layer at an altitude of around 350 m. A sharp subsidence inversion is found at 950 m.

The SO_2 profile shows a maximum concentration of 50 to 60 ppb at sea level, decreasing very rapidly to less than 5 ppb at 500 m. At 350 m, a small SO_2 peak of 40 ppb can be observed.

The O_3 profile shows opposite behavior. The sea-level O_3 concentration is less than 10 ppb, increasing rapidly to 40 ppb at 500 m. Above this altitude, the O_3 concentration remains 40 ppb.

Flight 15. The profile measurements performed during flight 15, with the air masses coming from the eastern sector, are an example of trapping of pollutants under a subsidence inversion (Fig. 6). The temperature profile shows some layering (probably due to the capture of pollutants) and a subsidence inversion layer between 1040 m and 1190 m. The SO_2 concentration below 1040 m is quite constant (15 to 17 ppb). In the inversion layer a sharp SO_2 peak of 26 ppb is observed.

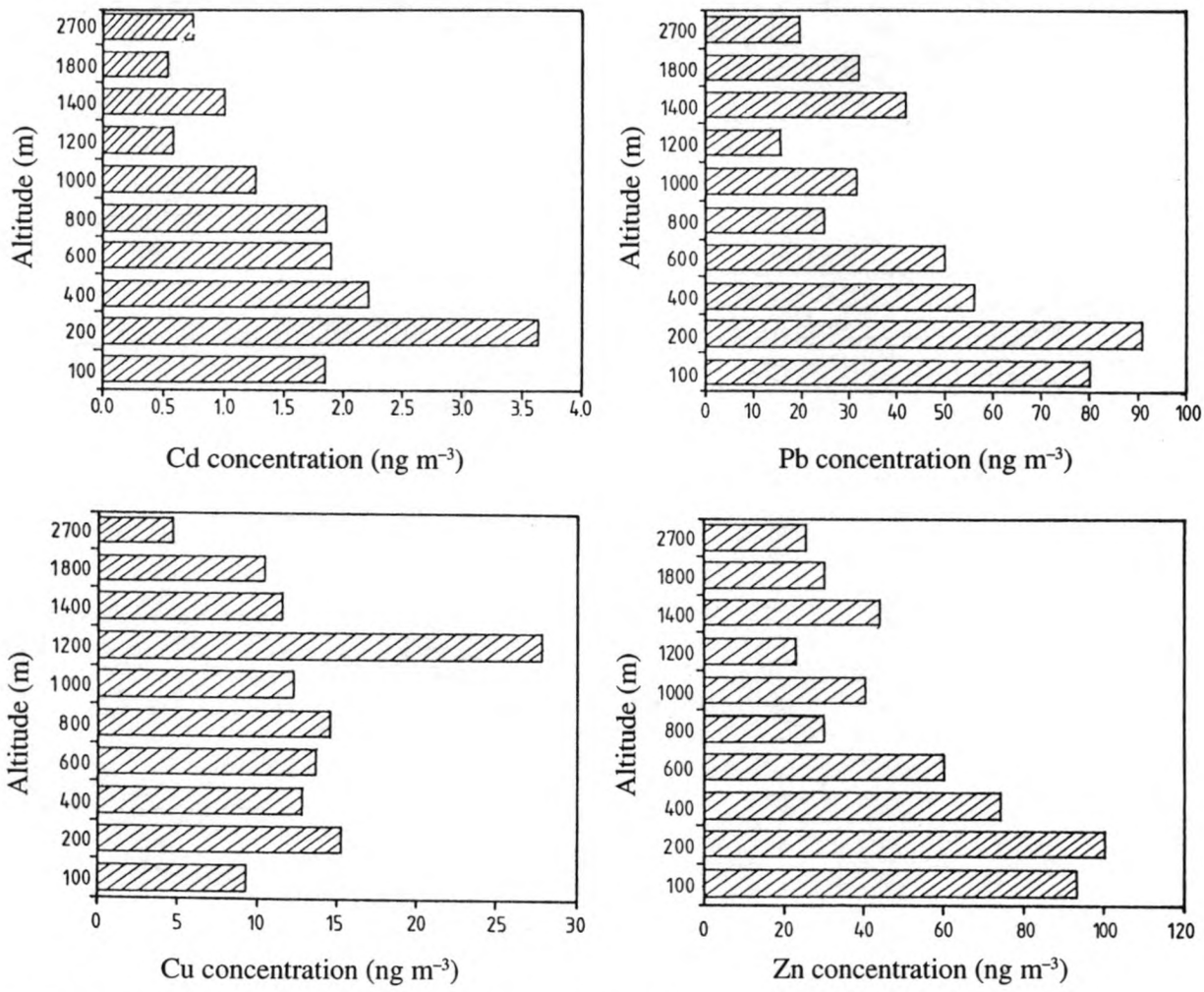

Fig. 3. Cd, Cu, Pb, and Zn concentration profiles as a function of altitude.[5]

Above 1190 m, the SO_2 concentration decreases very rapidly to 10 ppb.

The O_3 profile is also very constant below 1040 m, with concentrations from 25 to 30 ppb. At the inversion layer, a sharp increase of the O_3 concentration up to 45 to 50 ppb occurs.

Flight 16. Besides a radiative inversion layer between sea level and 450 m and a subsidence inversion layer between 2350 and 2450 m, the temperature profile of flight 16 (east wind sector) yields a lapse rate of –0.86 °C per 100 m, which results in a neutral atmosphere that does not allow good mixing of pollutants (Fig. 7). Here, the

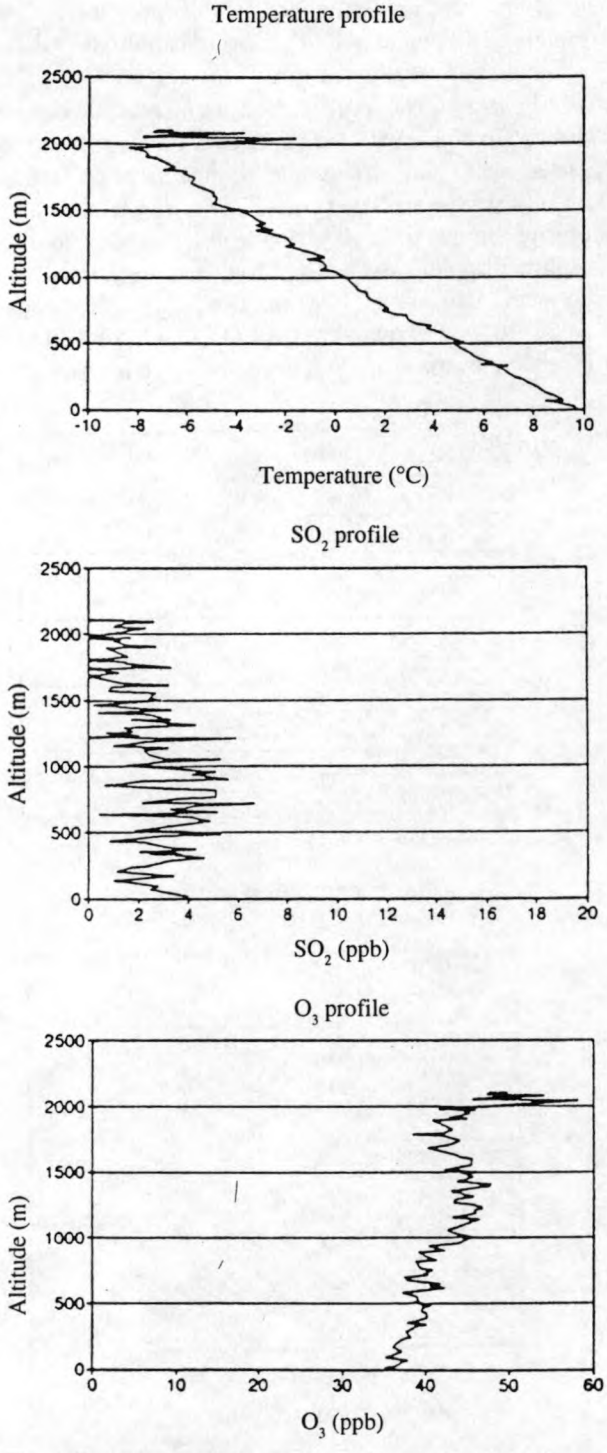

Fig. 4. Temperature, SO_2, and O_3 profiles during flight 6.

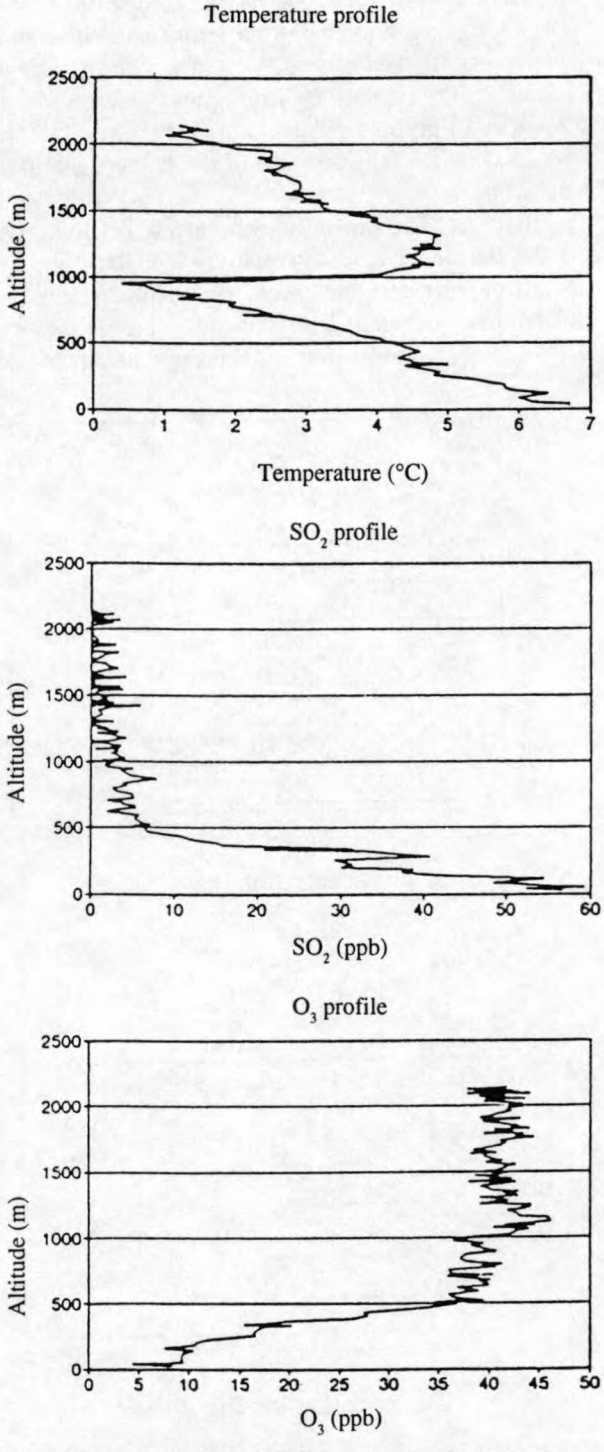

Fig. 5. Temperature, SO_2, and O_3 profiles during flight 12.

multilayer structure of the atmosphere is displayed, as was the case during flights 6 and 15.

The SO_2 profile indicates a minimum level of 20 ppb between the two inversion layers. Superimposed on this minimum concentration, several high SO_2 peaks can be located: 60 ppb at 620 m, 115 ppb at 940 m, and 95 ppb at 1140 m. The presence of several sharp SO_2 peaks and also opposite behavior of SO_2 and O_3 represent typical plume pollutant dispersion.

The fact that the SO_2 concentration above the subsidence inversion layer and underneath the radiative inversion layer goes down rapidly from 20 ppb to 5 ppb

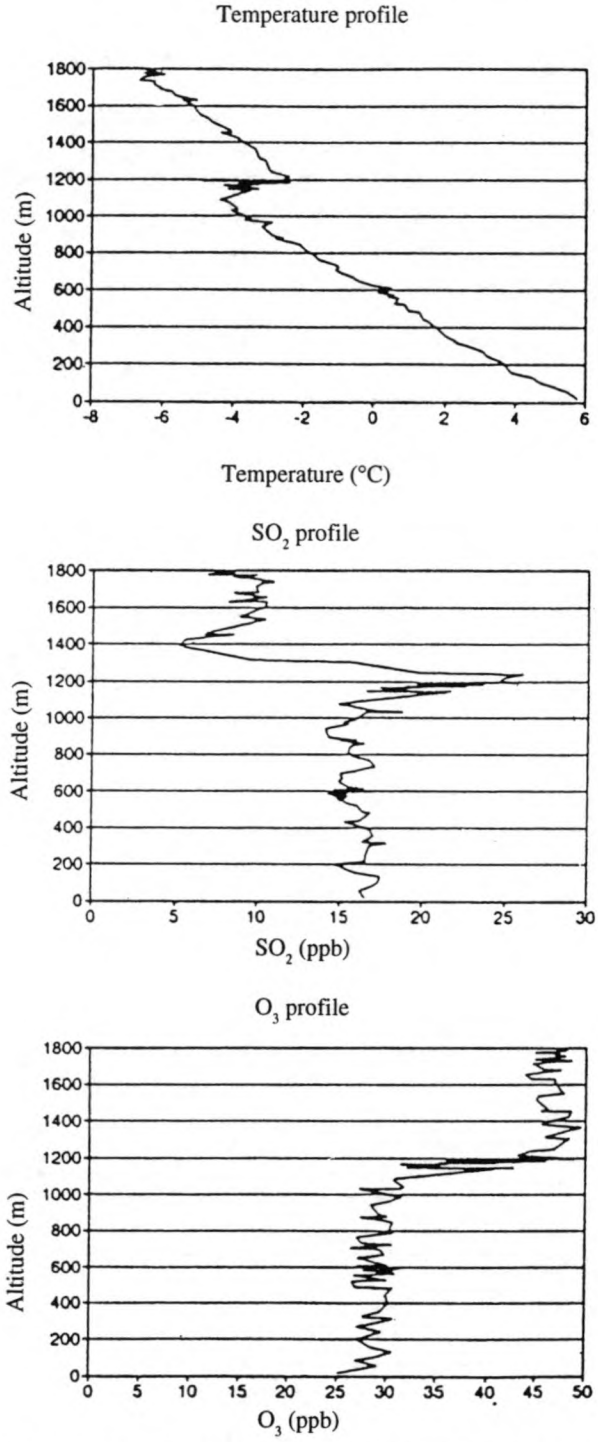

Fig. 6. Temperature, SO_2, and O_3 profiles during flight 15.

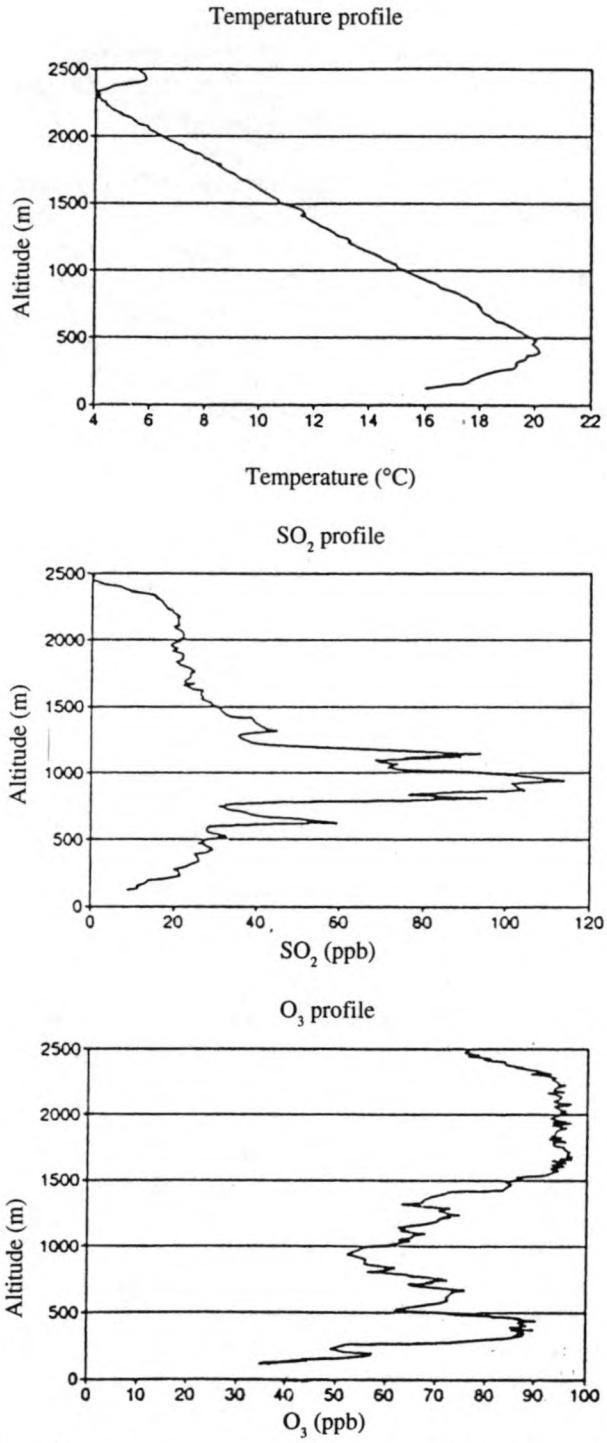

Fig. 7. Temperature, SO_2, and O_3 profiles during flight 16.

illustrates that all pollutants are trapped between the two inversion layers.

The O_3 profile of flight 16 shows a sharp increase in concentration from 35 ppb at sea level to 85–90 ppb at 450 m. Between 450 m and 1500 m, a large gap at 940 m is present, corresponding to the high SO_2 concentration at that level. Between 1500 m and 2350 m, high O_3 concentrations of 90–100 ppb are present. These high levels are probably due to photochemical reactions involving pollutants such as hydrocarbons and nitrogen oxides, since above the subsidence inversion layer, O_3 levels decrease again to about 75 ppb.

Flight 17. A low radiative inversion at 250 m and a subsidence inversion at 2200 m are illustrated in the temperature profile of flight 17, performed with easterly winds. According to Fig. 8, the measured lapse rate is –0.8°/100 m, which represents neutral atmospheric stability. The multilayer structure of the atmosphere may be affected by its instability upwind of sampling site or on a previous day. A sharp SO_2 peak of 24 ppb is present below the lower inversion, while SO_2 concentrations between the two inversion layers show a rather uniform profile.

The O_3 profile indicates an increase in O_3 levels from 40 ppb at 250 m to 115 ppb at 2200 m. Above the subsidence inversion, the O_3 levels decrease to 80 ppb, indicating that the high O_3 concentrations between the two inversion layers are due to photochemical smog formation.

Flight 21. The temperature profile of flight 21 (variable winds) illustrates a twofold inversion layer at low altitude (one at 200 m and one at 370 m), a neutral atmosphere with a lapse rate of –0.85 °C per 100 m between 430 and 1160 m, and an isothermal layer between 1160 and 1480 m (Fig. 9). The multilayer structure of atmosphere very possibly indicates the long-distance transport of pollutants.

In the SO_2 profile, two peak concentrations can be found corresponding to the twofold inversion layer at low altitude: 12 ppb at 150 to 210 m, and 8 ppb at 350 m. The stable layer traps two SO_2 peaks at 810 m (9 ppb) and at 1050 m (10 ppb).

O_3 concentrations above 1550 m are about 40 ppb. In all three layers below this altitude, higher O_3 levels indicate the presence of photochemical activity. In the isothermal layer, an O_3 peak of 56 ppb is found at 1420 m. In the stable layer, two peak levels are measured at 1030 m (95 ppb) and at 860 m (100 ppb). Two other peaks are located at the twofold low-altitude inversions: 74 ppb at 400 m, and 68 ppb at 300 m.

Flight 23. During flight 23, two spiral tracks were performed at a different location with an interval of 37 min (Fig. 10). The first track was flown at 51°95'N, 4°41'E (location A) and between 11.13 h and 11.18 h (October 17, 1989). The wind direction varied between 220° and 260°.

The second spiral flight was flown much more easterly at position 51°84'N, 2°26'E (location B) and between 11.50 h and 11.56 h, on the same day. Doppler-

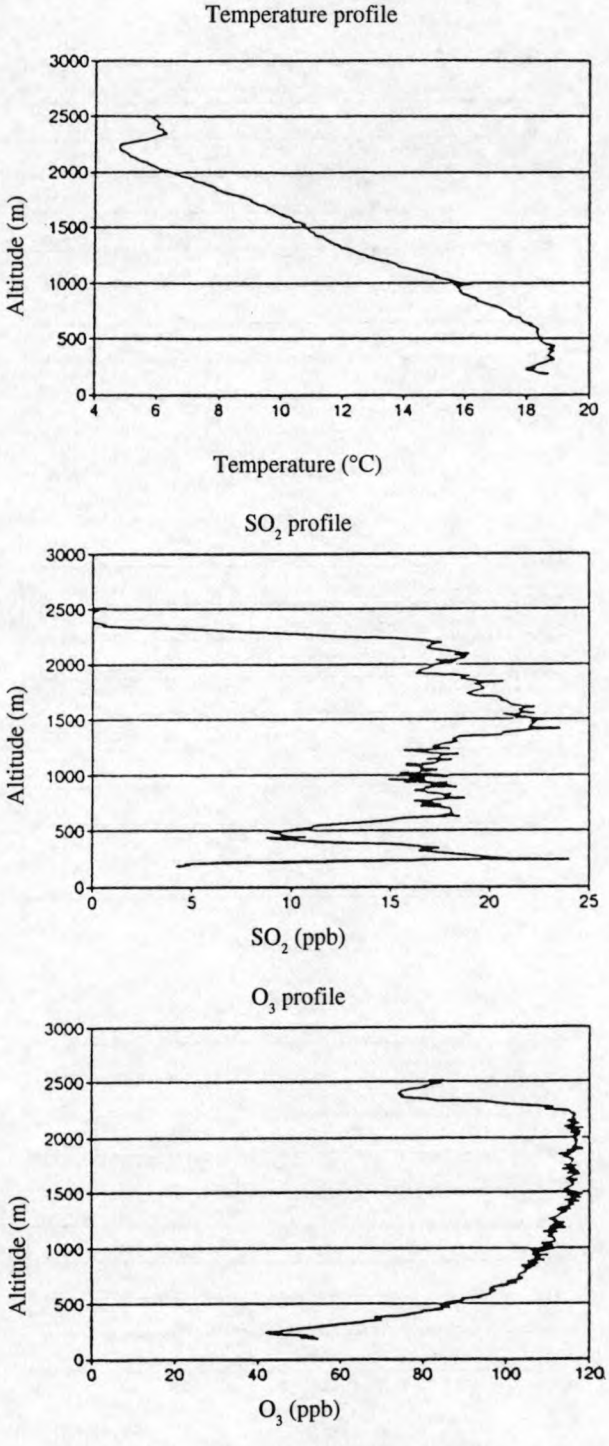

Fig. 8. Temperature, SO_2, and O_3 profiles during flight 17.

radar-measured wind directions varied between 200° and 235°.

If we compare both temperature profiles we can see that during the first track, the temperature inversion layer is located between 590 and 900 m (Fig. 11). In the second track, this inversion layer is located between 720 and 950 m, and a second inversion has been formed between 340 and 440 m (Fig. 12). This inversion layer could be a frontal inversion formed by the interaction of two air masses with different meteorological characteristics.

The SO_2 profiles are quite different. The first profile shows a sharp decrease in SO_2 concentration with altitude, while the second profile shows a very sharp SO_2 peak at 480 m (24 ppb). In the O_3 profile, less variation is obvious.

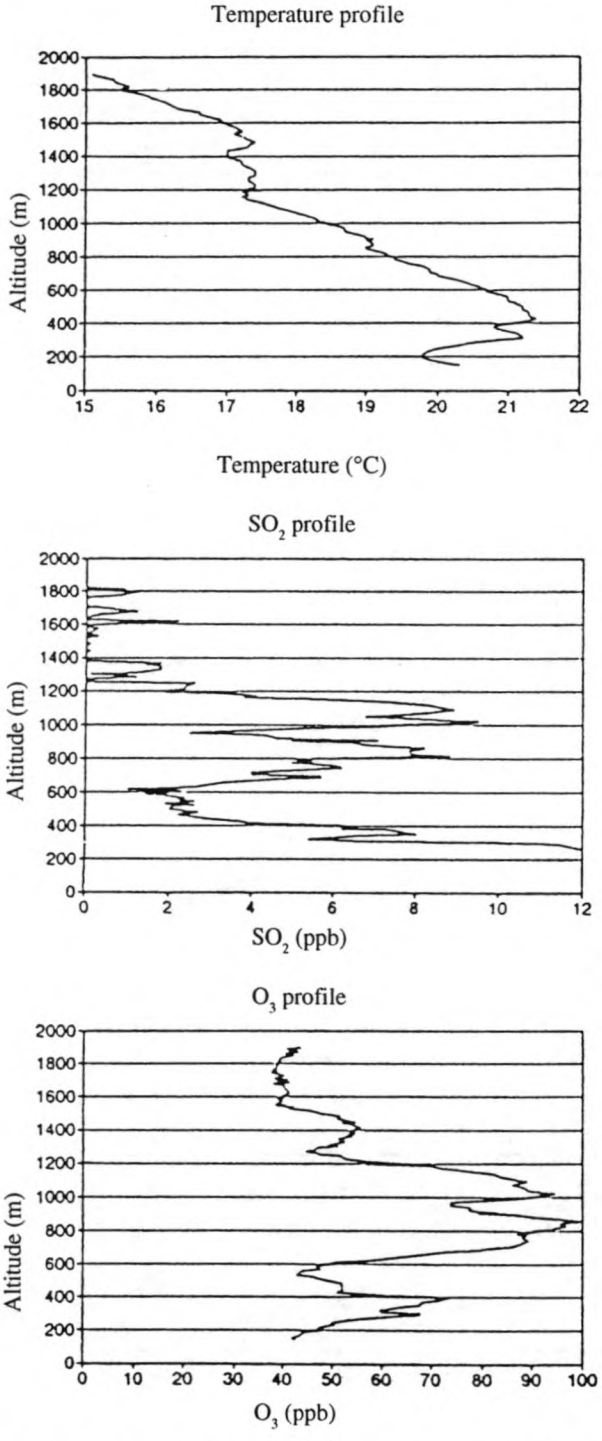

Fig. 9. Temperature, SO_2, and O_3 profiles during flight 21.

AVERAGE SO_2 AND O_3 CONCENTRATIONS UNDER THE TEMPERATURE INVERSION LAYER

SO_2 and O_3 Concentrations as a Function of Wind Direction

Table 3 lists the average SO_2 and O_3 concentration for the different wind sectors. The average SO_2 concen-tration for all flights, below the temperature inversion layer, equals 10.0 ppb. For individual flights, the average SO_2 concentration varies from 1.9 ppb for flight 18 to 19.5 ppb for flight 13. Although important variations are observed within each wind sector, the average SO_2 concentration per wind sector indicates that similar concentrations are found for the NE–E and the SW–W sectors. The NW–N sector yields much lower concentrations, while the SE–S and the variable wind sectors show higher average SO_2 concentrations (Table 3). Air masses originating from the SW–W sector are influenced by emissions from the United Kingdom and the northwestern part of France, and, to some extent, by the north Atlantic Ocean and the English Channel. The NW–N wind sector can be identified as without any continental influence, and the obtained SO_2 values can be considered as representative for the North Sea atmosphere background. Results for the NE–E sector are related to emissions in Belgium, the Netherlands, the central and northern part of Germany, Eastern European countries, the Baltic Sea, and Scandinavian countries. Finally, SO_2 concentrations measured in the air-masses originating from the SE–E sector result from emissions in Belgium, the northern part of France, and the southern part of Germany.

The average O_3 concentration below the temperature inversion layer, measured over 18 flights, equals 46 ppb. The lowest concentration (8 ppb) was measured during flight 9, while the highest concentration was observed during flight 17 (96 ppb). Three wind sectors (SW–W, NW–N, and variable) yield similar O_3 concentrations: 46, 43, and 40 ppb, respectively. For the SE–S sector, the average O_3 concentration is a factor of 2 lower (22 ppb), while for the NE–E sector, a relatively high O_3 concentration of 66 ppb is observed.

Seasonal Influence in SO_2 and O_3 Concentrations

Figure 13 plots the average SO_2 and O_3 concentrations below the temperature inversion layer as a function of the flight number. Flights 2 to 6 were performed between September and October 1988, flights 7 to 15 between November 1988 and April 1989, and flights 17 to 22 between May 1989 and August 1989. The O_3 concentration shows a clear seasonal dependence. All flights from 7 to 15 (winter period) yield O_3 concentrations below 40 ppb, while all other flights show show O_3 concentrations above 40 ppb.

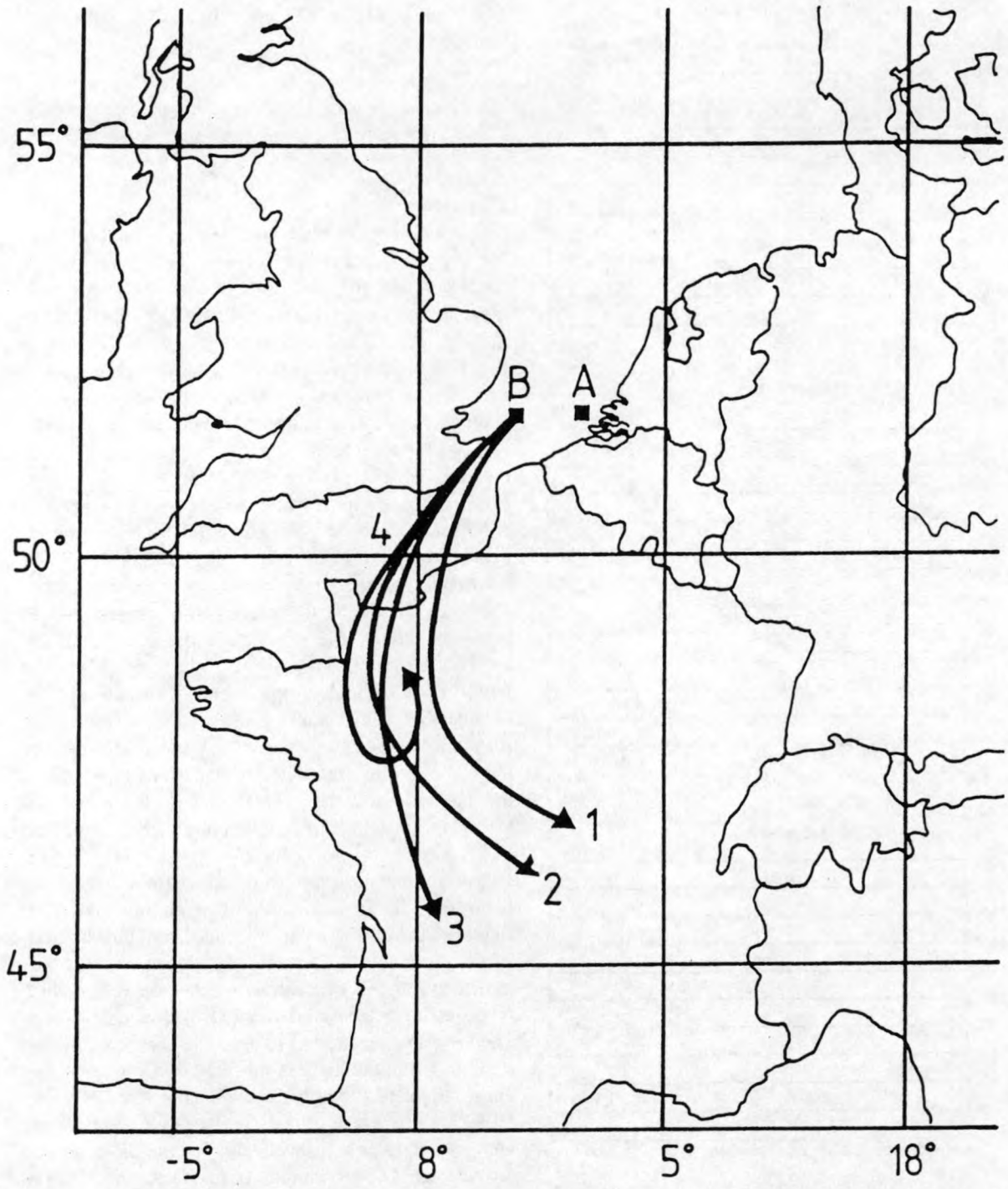

Fig. 10. Sampling points (spiral track A and B) and 36 h backward air mass trajectories (1 = 1000 mbar, 2 = 925 mbar, 3 = 850 mbar, and 4 = 700 mbar) for flight 23.

Although the SO_2 concentrations are generally anticorrelated with the O_3 concentrations, no obvious seasonal trend can be observed for SO_2. It seems that SO_2 concentrations are primarily dependent on the wind direction, and O_3 concentrations are rather dependent on the season.

RELATION BETWEEN SO_2 AND TRACE METALS

Figure 14 shows average SO_2 concentrations and trace metal concentrations below the temperature inversion layer as a function of the flight number. Generally speaking, similar trends can be found although some exceptions are obvious.

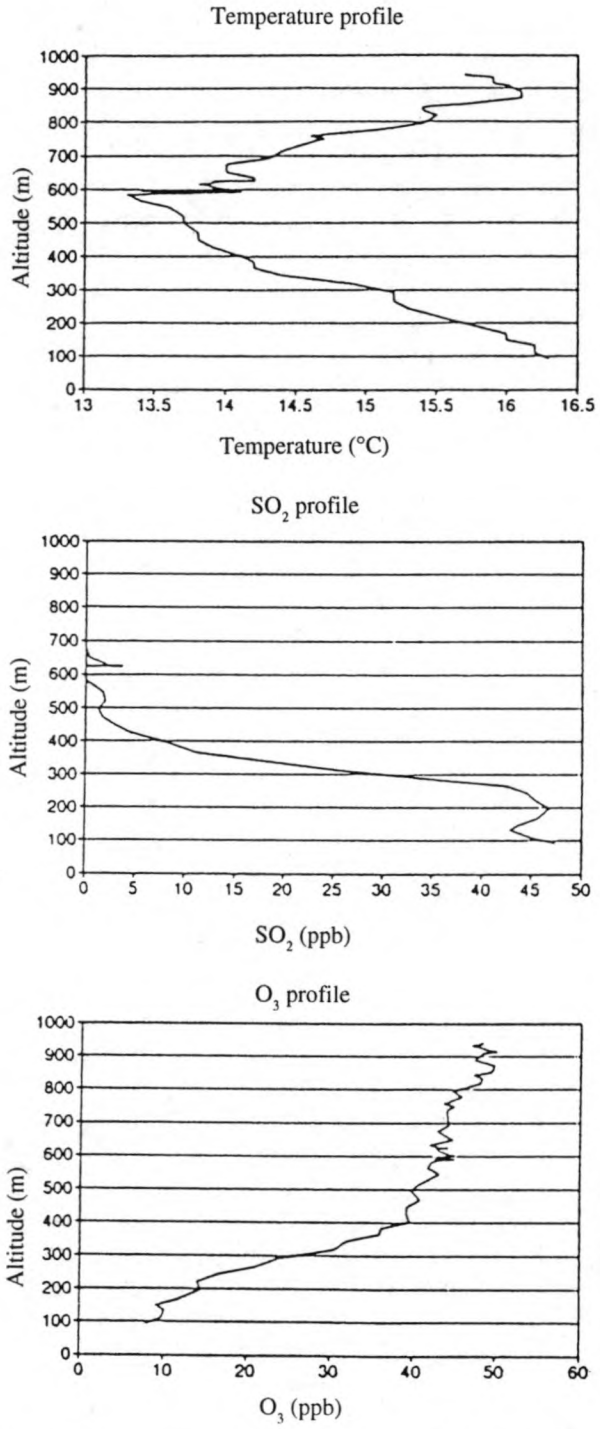

Fig. 11. Temperature, SO_2, and O_3 profiles during flight 23, track A.

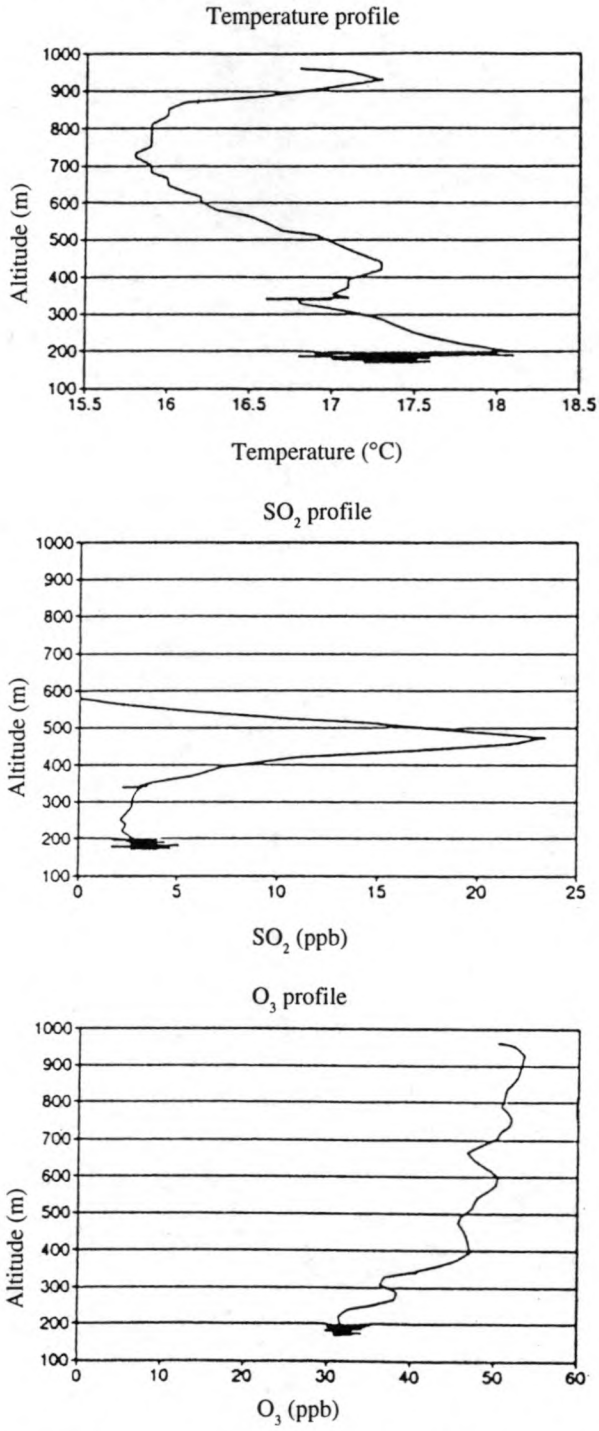

Fig. 12. Temperature, SO_2, and O_3 profiles during flight 23, track B.

Table 3. Average SO_2 and O_3 concentrations below the temperature inversion layer for different wind sectors (rel. error is around 1.5%)

	SO_2 (ppb)	O_3 (ppb)
Southwest–West		
Flight 2	9.1	75
Flight 3	10.5	45
Flight 11	9.5	22
Flight 12	7.3	26
Flight 22	4.8	62
Northwest–North		
Flight 6	2.8	43
Northeast–East		
Flight 5	7.8	50
Flight 15	11.7	38
Flight 17	12.4	96
Flight 18	2.8	70
Flight 19	7.4	76
Southeast–South		
Flight 7	14.5	20
Flight 8	11.5	13
Flight 13	19.5	34
Variable		
Flight 4	1.9	50
Flight 9	15.2	8
Flight 14	14.7	35
Flight 21	16.3	66
Averages		
Southwest–West	8.2	46
Northwest–North	2.8	43
Northeast–East	8.4	66
Southeast–South	15.2	22
Variable	12.0	40
All sectors	10.0	46

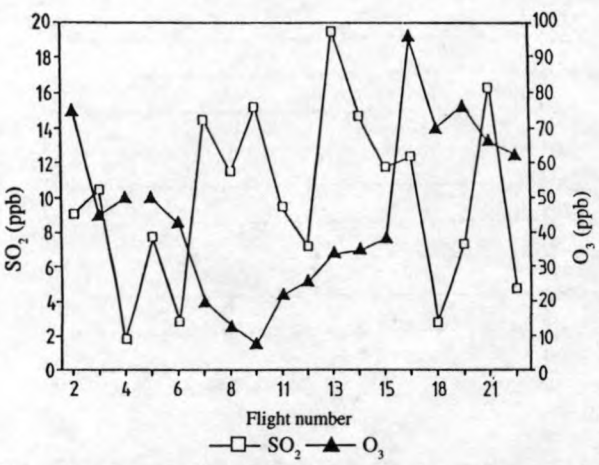

Fig. 13. Average SO_2 and O_3 concentrations below the temperature inversion layer as a function of the flight number.

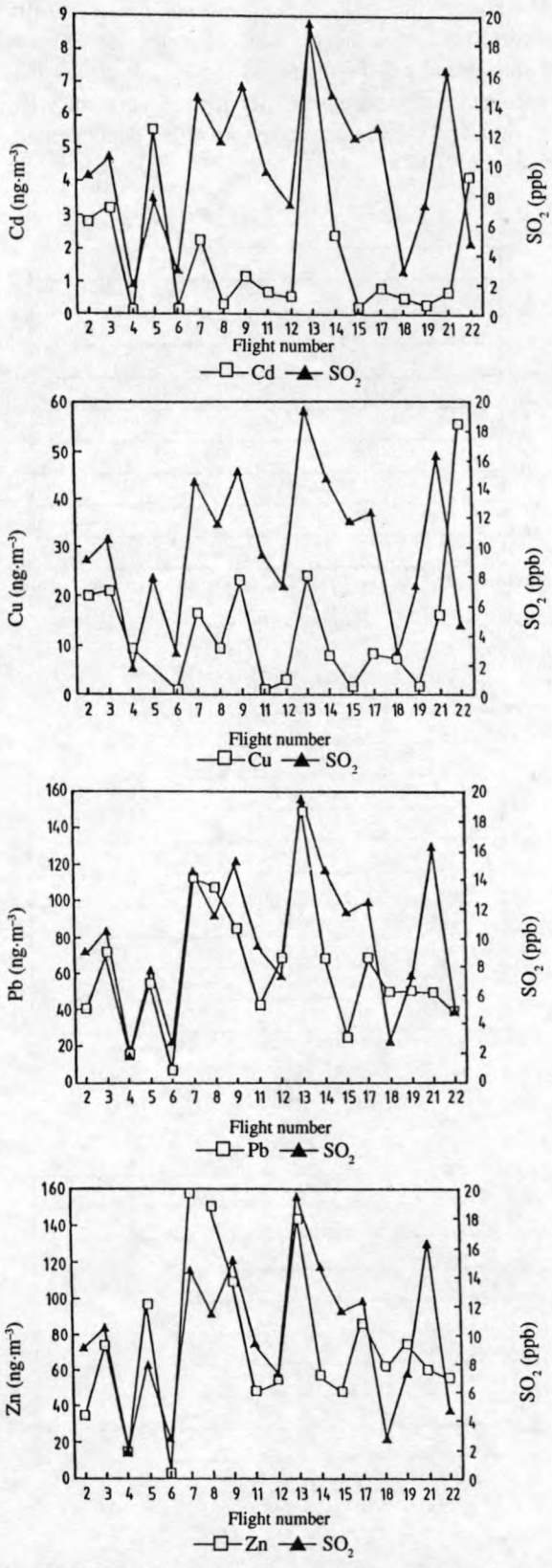

Fig. 14. (a) Cd, (b) Cu, (c) Pb, and (d) Zn concentrations vs. SO_2 concentration: average values under the temperature inversion layer as a function of the flight number.

Table 4. SO_2 and O_3 values (ppb) reported for different regions in the world — comparison with our data

Location	SO_2 (ppb)	Period	Reference
Brussels (100 km from southern North Sea)	17	1990–1991	(8)
Ostende (Belgian coast)	9	1990–1991	(8)
The Netherlands (coastal countryside)	5	1991	(6)
Western North Atlantic: US Coast			
Bermuda	1	1986	(9)
North Sea	2–4	1990	(6)
Northwest England	6	1982	(10)
North Sea–Southern Bight	10	1988–1989	This work

Location	O_3 (ppb)	Period	Reference
Southwest France (pine forest)	42	1984	(11)
North Pacific	40	1989	(12)
The Netherlands (countryside)	20	1991	(6)
Northwest England	32	1982	(10)
North Sea–Southern Bight	46	1988–1989	This work

CONCLUSION

During 18 sampling flights over the Southern Bight of the North Sea, SO_2 and O_3 concentrations were measured in the lower troposphere.

Average SO_2 concentrations below the temperature inversion layer ranged from 1.9 to 19.5 ppb. For the NE–E and the SW–W wind sectors, the average SO_2 concentrations were very similar: 8.4 and 8.2 ppb, respectively. The NW–N sector yielded a much lower average concentration of 2.8 ppb SO_2, while the SE–S and the variable sectors showed higher average SO_2 concentrations of 15.2 and 12.0 ppb, respectively.

The average O_3 concentration, measured over all flights, was 46 ppb, ranging from 8 to 96 ppb. Low O_3 concentrations illustrate O_3 depletion through reaction with freshly emitted pollutants, while high O_3 levels reflect photochemical activity due to automotive emissions. The SW–W, NW–N, and variable wind sectors showed similar average O_3 concentrations of 46, 43, and 40 ppb, respectively. For the SE–S sector, the average O_3 concentration was two times lower (22 ppb), while the NE–E sector yielded a high average of 66 ppb. In Table 4, our results are compared with some recently published values.

O_3 concentrations seem to be primarily dependent on seasonal influence, while SO_2 levels are more dictated by the history of the sampled air mass.

Although SO_2 and trace metal levels show similar trends, some differences are obvious. The highest SO_2 concentrations (just like the highest trace metal levels) are found at altitudes of between 100 and 200 m. The average O_3 profile shows an increase from 30–40 ppb at sea level to 60–70 ppb at altitudes above 1000 m. Individual SO_2 and O_3 profile measurements clearly illustrate the high variability in vertical concentration distributions.

Acknowledgments. This work was partially supported by Rijkswaterstaat, The Netherlands, through projects NOMIVE*2 DGW-920 and DGW-217.

REFERENCES

(1) Lippmann, M. *Environ. Sci. Technol.* 1991, **25**: 1954.
(2) Krupa, S.V.; Manning, W.J. *Environ. Pollut.* 1988, **50**: 101.
(3) Stauff, J.; Jaeschke, W. *Atmos. Environ.* 1975, **9**: 1038.
(4) North Sea Science, NATO North Sea Science Conference, Aviemore, Scotland, 15-20 November 1971; Goldberg, E.D., Ed.; MIT Press: Cambridge, MA.
(5) Injuk, J.; Otten, P.; Laane, R.; Maenhaut, W.; Van Grieken, R. *Atmos. Environ.* 1992, **26A**: 2499.
(6) RIVM. Milieudiagnose 1991, II Luchtkwaliteit, RIVM report 222101022, Bilthoven, The Netherlands, 1992.
(7) US EPA. National Air Pollutant Emission Estimates,

1940–1990. EPA-450/4-91-026, 1991.

(8) IHE. Studie van de fotochemische luchtverontreining in België, periode 1979–1990. Instituut voor Hygiëne en Epidemiologie, Brussels, 1992.

(9) Sievering, H.; Boatman, J.; Luria, M.; Van Valin, C.C. Tellus 1989, **41B**: 338.

(10) Colbeck, I.; Harrison, R.M. *Sci. Total Environ.* 1984, **34**: 87.

(11) Lopez, A.; Fontan, J.; Minga, A. *Atmos. Environ.* 1993, **27**: 555.

(12) Lenschow, H.D.; Pearson, R.; Stankov, B. *J. Geophys. Res.* 1982, **87**: 8833.

Selected article #19:

Atmospheric concentrations and deposition of heavy metals over the North Sea: a literature review

J. Injuk and R. Van Grieken

Journal of Atmospheric Chemistry, 20 (1995) 179-212

Journal of Atmospheric Chemistry **20:** 179–212, 1995.

Atmospheric Concentrations and Deposition of Heavy Metals over the North Sea: A Literature Review

JASNA INJUK and RENÉ VAN GRIEKEN
University of Antwerp (U.I.A.), Department of Chemistry, B-2610 Antwerpen-Wilrijk, Belgium

(Received: 4 January 1994; in final form: 24 May 1994)

Abstract. A literature review of the atmospheric concentration rates and dry and wet deposition fluxes of particulate Cd, Cr, Cu, Pb and Zn to the North Sea and adjacent areas is given. The results of direct measurements of dry and wet deposition fluxes are compared to indirect estimates and to modelling values. This work points out the large uncertainties in results of different studies on atmospheric input of trace elements into the North Sea. The current knowledge about the dependence of the deposition velocity upon the particle size and about the processes controlling wet deposition fluxes, and the quality and completeness of the emission data are still inadequate for describing the environmental cycle and impact of heavy metals in the North Sea.

Key words: Heavy metals, concentration, deposition, North Sea, troposphere.

1. Introduction

At present, there is much discussion on the sources and abatement policies of pollution to the sea. Atmospheric transport and deposition of pollutants over long distances have received much attention, particularly in connection with the acid rain problem, the formation of photochemical oxidants and ozone, and the global climatic effects. It is only relatively recently that it has become possible to estimate the amounts of material entering the oceans via the atmosphere. Though the pollution of the oceans is not a new phenomenon, the question of how important a role the atmosphere plays in this was addressed only a decade ago (NAS, 1978). As the calculations have become less crude, the atmospheric route seems to have gained in importance relative to the other paths, like those borne by rivers and direct discharges.

Still, quantitative data on heavy metal emissions, their concentration levels in air and their accumulation and transfer in the North Sea ecosystem have not been systematically gathered and intercompared hitherto. There are various sources which emit trace metals into the atmosphere, i.e. man-made pollution, aerosol formation from sea-spray, volcanic activity, vegetation and soil erosion. The concentrations of anthropogenic pollutants in the atmosphere are mainly due to the volatility of these elements at the high temperatures of fossil fuel combustion, and many other high-temperature industrial processes, particularly the extraction of non-ferrous metals

TABLE I. Comparison of the 1982 survey of trace element emission by Pacyna (1987) with national emission data (tons y^{-1}) for countries bordering the North Sea

Country	Cd	As	Pb	Zn	Reference
U.K.	31	117	8610	2230	Pacyna, 1987
	14	315	7590	–	Hutton and Symon, 1986
Belgium	12	85	2100	700	Pacyna, 1987
	22	–	2380	1090	Van Jaarsveld *et al.*, 1986
The Netherlands	5.5	34	2200	290	Pacyna, 1987
	3.8	–	–	–	Kendall *et al.*, 1985
Germany	80	350	5560	6660	Pacyna, 1987
	79*	500	7590	10000	*Schladot and Nürnberg, 1982 Braun *et al.*, 1984
Denmark	6.3	7	650	130	Pacyna, 1987
	5	–	–	–	Murkherje, 1986
Sweden	16	183	1053	426	Pacyna, 1987
	12	130	950	1200	Naturvardsverket, 1982
Norway	2.1	41	730	120	Pacyna, 1987
	1.7–2.7	–	–	–	Naturvardsverket, 1982

from sulphides. Among other industrial sources, waste incineration is becoming increasingly important, particularly in Western Europe, because of the emissions of Cd, Pb and other trace elements and a need to incinerate increasing amounts of wastes. A first preliminary review of the atmospheric emissions of various trace elements from anthropogenic sources in Europe, for 1979/1980, was provided by Pacyna (1983). The earlier surveys were concerned with either a single metal (van Enk, 1980; Hutton, 1982) or certain types of emission sources, e.g. fossil fuel combustion. As such, they were very valuable for control strategies, but less applicable for modelling of the long-range transport of air pollutants and their migration. The survey of Pacyna has more recently been updated and improved. In Table I, the estimates of Pacyna (1987) of trace element emissions from all sources in countries bordering the North Sea are compared with the countries' own estimates. The former estimates are based on emission factors, calculated separately for each of the countries, on statistics on the consumption of raw materials and on the production of various industrial goods in 1982.

2. Data on Trace Metal Concentrations in Air

There is quite a detailed data base of concentration measurements for trace metals in aerosols over the European regional seas (GESAMP, 1989). Table II gives an overview of literature values for the particulate Cd, Cr, Cu, Pb and Zn concentrations in the marine troposphere over the North Sea and adjacent areas. The data set covers a relatively long time period, of about 20 years. The oldest data, supplied by Peirson *et al.* (1973), Kretzschmar and Cosemans (1979) and Van Aalst *et al.* (1983) (who give a list of concentrations measured between 1974 and 1981 at coastal stations in Great Britain, Belgium and The Netherlands), are generally higher than the other reported values in Table II. The less accurate collection procedures and the precision of measurements in those days may be one reason, but these values were also obtained from coastal or even inland measurements, i.e. closer to the emission sources. Van Daalen (1991) measured the concentrations over the province of South-Holland in the Netherlands and although his sampling sites were not very far removed from the North Sea coast, his data show clearly high concentrations. The rest of the coastal values in Table II seem to agree very well with the exception of the Belgian ones from Ostende, due to very high concentrations measured in the continental air masses (factor 2 to 5 higher compared to the values for the eastern and western air-masses). Although not explicitly North Sea coastal measurements, the data collected by Flament *et al.* (1987) at the French coast in the Channel and those reported by Schneider (1987) in the Kiel Bight offer a good basis for intercomparison of results.

In contrast with measurements performed at coastal stations around the North Sea, much less data are available for samples taken on the North Sea itself. Results from the West Hinder light-ship station (51°23′ N, 2°21′ W) located off the Belgian coast were reported by Baeyens and Dedeurwaerder (1991), Dedeurwaerder (1988) and ATMOS (1984). The West-Hinder results are generally higher than comparable ones for the southern North Sea. One possible explanation is that ship West-Hinder is only separated from the coastline by a relatively small distance and is located at a very dense traffic channel (100 ships per day) on the North Sea. Values reported by Ottley and Harrison (1993) are broadly comparable to previously published values for metal concentrations in the North Sea atmosphere. The aircraft-measured values (Injuk *et al.*, 1992) agree well with those of cruises with the R/V Belgica (Otten *et al.*, 1989). Values reported by Otten *et al.* (1989), predominantly based on measurements done in the northern part of the North Sea, during north-westerly winds, can be considered as background values for the North Sea area. A concentration gradient from the southern North Sea (high concentrations) to the northern part (low concentrations) is observed.

Under the Paris Convention, an international commission (PARCOM-ATMOS) has been established to assess the state of the marine environment and formulate the policy to eliminate or reduce existing pollution. With regard to atmospheric pollution, a dual approach has been proposed: A monitoring programme at a num-

TABLE II. Measured airborne concentrations over the North Sea and adjacent areas in ng m^{-3} (s- or n-preceding an area means southern or northern, respectively)

Area	Period	Cd	Cr	Cu	Pb	Zn	Remarks	References
United Kingdom (coast)	'72	< 4–< 18	1.0–14	< 1–55	35–380	64–415	range for 7 sites	Peirson *et al.* (1973)
United Kingdom (coast)	'75	4–6	–	13–15	20–120	15–300	range for 2 sites	Cawse (1974)
The Netherlands (coast)	'84–'88	0.3–2	1.7–14	3.7–23	36–178	18–200	–	van Daalen (1991)
North Sea (coast)	'72–'81	0.5–2.5	0.5–5	< 5–25	20–200	10–100	–	van Aalst *et al.* (1983)
The Netherlands (coast)	'87	0.8	–	5.5	45	59	Hage	Cambray *et al.* (1975)
The Netherlands (coast)	'84–'85	0.7	1.3	3.3	39	40	Pellworm	Steiger (1991)
The Netherlands (coast)	'83	0.6	1.6	3.0	41	30	Tange	Kemp (1984)
Belgium (coast)	'72–'77	8	–	19	278	300	Ostende	Kretzschmar and Cosemans (1979)
Belgium (coast)	'81–'84	3.4	–	12.8	77	174	–	ATMOS (1984)
Norway (coast)	'78–'79	0.3	1	7	19	–	–	Pacyna *et al.* (1984)
Norway (coast)	'85–'86	0.14	1.1	1.6	18	15	Birkenes	Amundsen *et al.* (1992)
England (coast)	'87–'88	1.1	–	–	34	41	–	Yaaqub *et al.* (1991)
England (coast)	'72–'73	–	7.0	–	168	155	Leiston	Cambray *et al.* (1975)
German Bight	'86	1.9	1.9	4.7	52.6	46	island	Kersten *et al.* (1991)
Kiel Bight	'81–'83	–	–	40	53	57	lighthouse	Schneider (1987)
East Channel	'87	3	–	20	56	100	–	Flament *et al.* (1987)
North Sea	'86–'90	1.6	1.5	3.5	20.2	38	Helgoland	Kriews (1992)
North Sea	'87	0.9	–	3.9	28.5	42	FPN	Steiger (1991)
North Sea	'71–'73	–	4.8	–	155	161	Gasplatform	Cambray *et al.* (1975)
North Sea	'88–'89	1.4	–	11	55	67	flights	Injuk *et al.* (1992)
North Sea	'88–'89	1.3	–	6.9	29	75	cruise	Ottley and Harrison (1993)
North Sea	'84–'88	–	–	11	39	54	cruise	Otten *et al.* (1989)
sNorth Sea	'81–'84	2.9	–	9	104	94	West-Hinder	ATMOS (1984)
sNorth Sea	'84–'85	0.7	–	3	39	41	–	Stoeßel (1987)
sNorth Sea	'80–'85	4	–	17	150	150	West-Hinder	Dedeurwaerder (1988)
sNorth Sea	'84–'88	–	–	17	62	86	cruise	Otten *et al.* (1989)
sNorth Sea	'80–'85	2.8	–	14.7	96	67	West-Hinder & cruises	Baeyens and Dedeurwaerder (1991)
nNorth Sea	'72–'73	–	1.4	20	21	32	Collafirth	Cambray *et al.* (1975)
nNorth Sea	'84–'88	–	–	2	2	2	cruise	Otten *et al.* (1989)
North Sea	'91	0.2	2.0	1.9	4.5	30	Gullfaks 'C'	Dannecker *et al.* (1992)

ber of coastal stations and a modelling programme for which an emission database is being set up. The monitoring programme of PARCOM-ATMOS includes measuring concentrations in precipitation of Pb, Cd, Cu, Zn, Cr, Hg, Ni, NH_4^+ and NO_3^- and some of these species in air. In Tables III and IV, the basic description of the stations monitoring heavy metals in air and in precipitation and annual mean aerosol concentration values are given. From the summarized results in Table IV, it is obvious that only data from the Belgian stations (B1 and B2b) are not comparable with the others, due to high values for Cu, Ni, Pb and Zn. But these results agree well with reported ones for the same region by Kretzschmar and Cosemans (1979), indicating a high level of pollution for this region, or unrepresentative sampling. In Figure 1, the North Sea area with the stations which take part in the PARCOM-ATMOS monitoring program is given.

3. The Atmospheric Input of Trace Elements to the North Sea

For many years, research on pollution of the North Sea marine environment has focused on the most obvious inputs, those borne by rivers and direct discharges of wastes. In the work of Goldberg (1973) and Cambray *et al.* (1975), a first indication can be found that the atmospheric input might also be a significant contributor of trace elements to the North Sea. The first major studies of the deposition of heavy metals from the atmosphere started in the United Kingdom in the beginning of the 1970's (Cawse, 1974). The concentrations of some 40 elements were determined in dry and wet deposition at seven non-urban sites, while the water soluble and insoluble fractions of the total deposition were analyzed separately. At the same time, analyses of the deposition of heavy metals were made in Norway (Breekke, 1976), in the USA (Andren *et al.*, 1975; Feely *et al.*, 1976) and in the FRG (Ruppert, 1975). The routine monitoring of trace elements in precipitation began in Sweden in 1983 (Ross, 1987) with the aim to determine the atmospheric wet deposition of Cd, Cu, Fe, Mn, Pb and Zn.

Van Aalst *et al.* (1983) employed a simple model to assess the long-term average concentrations of various elements in the sea, and to determine the atmospheric input of a large group of contaminants into the North Sea. They have compared their results with information on the other inputs into the North Sea and concluded that atmospheric deposition was a relatively important source of contamination with Cu, Pb, Ni and Zn, and to a lesser extent with Cd and Cr. A first international attempt to estimate the input of various elements to the sea by atmospheric deposition and via other pathways was made by a European group of experts on behalf of the International Council for the Exploration of the Sea (ICES, 1978).

Since trace elements are removed from the atmosphere by dry deposition (sedimentation, interception and impaction) and by wet deposition (rainout, washout), the literature overview concerning both processes is given separately below.

TABLE III. Coastal measuring stations participating in Paris Commission Comprehensive Atmospheric Monitoring Programme (CAMP)

Number country	Name	Latitude longitude	Elevation	Distance from the sea	Parameters measured
B1 Belgium	Houtem	51°01′ N 2°35′ E	sea level	9 km	Pb, Zn in air
B2b Belgium	Bredene	51°14′ N 2°57′ E	≪ 10 m	2 km	Cu, Ni, Pb, Zn in air
B3a Belgium	Brugge	51°15′ N 3°11′ E	≪ 10 m	8 km	Cd, Cu, Pb, Zn in precipitation
GB1 Great Britain	East Ruston	52°48′ N 1°28′ E	5 m	8 km	Cd, Cr, Cu, Ni, Pb, Zn in air Cd, As, Cr, Cu, Ni, Pb, Zn in precipitation
GB2 Great Britain	Staxton Wold	54°11′ N 0°26′ W	170 m	10 km	Cd, Cr, Cu, Ni, Pb, Zn in air Cd, As, Cr, Cu, Ni, Pb, Zn in precipitation
GB3 Great Britain	Banchory	57°5′ N 2°32′ W	120 m	26.5 km	Cd, Cr, Cu, Ni, Pb, Zn in air Cd, As, Cr, Cu, Ni, Pb, Zn in precipitation
DK1 Denmark	Ulborg	56°17′ N 8°26′ E	40 m	20 km	Cd, As, Cr, Cu, Ni, Pb, Zn in air Cd, Cu, Pb, Zn in precipitation
D1 Germany	Westerland	54°53′ N 8°19′ E	5 m	2 km	Cd, Cu, Pb in air Cd, As, Cr, Cu, Ni, Pb, Zn in precipitation
NL3 The Netherlands	Kollumerwaard	53°20′ N 6°16′ E	0–5 m	10 km	Cd, As, Pb, Zn in air Cd, Cu, Ni, Pb, Zn in precipitation
NL2 The Netherlands	Leiduin	52°20′ N 4°35′ E	0–5 m	6.3 km	Cd, Cr, Cu, Ni, Pb, Zn in precipitation
N1 Norway	Birkenes	58°23′ N 8°15′ E	190 m	20 km	Cd; Pb, Zn in precipitation
N3 Norway	Lista	58°06′ N 6°34′ E	13 m	–	Cd, Cr, Cu, Ni, Pb, Zn in precipitation

TABLE IV. An overview of the data submitted to PARCOM-ATMOS as regards elemental concentrations (ng m^{-3}) in aerosols for 1988, 1989, 1990 and 1991, measured at 'CAMP' stations (ATMOS, 1990; ATMOS, 1991; ATMOS, 1992)

Station	Period	Cd	As	Cr	Cu	Ni	Pb	Zn
B1	'90	–	–	–	–	–	104	351
B2b	'89	–	–	–	–	–	112	150
	'91	–	–	–	23	15	86	222
DK1	'88	0.3	1.6	2.3	1.2	1.9	19.2	23.7
	'89	0.3	–	1.0	2.29	1.66	21.8	25.8
	'90	–	–	1.48	1.6	1.7	17	24
	'91	–	–	2.5	2.3	2	17	23
D1	'88	0.4	–	–	3.4	–	23.3	–
	'89	0.42	–	–	2.69	–	20.4	–
	'90	0.30	–	–	3.10	–	17.3	–
	'91	0.36	–	–	1.5	–	18	–
NL3	'90	0.33	0.78	–	–	–	27	52
	'91	0.4	1.48	–	–	–	30.2	51
GB1	'88	0.5	–	0.7	3.7	2.0	35.4	27.7
	'89	0.43	–	0.82	3.85	2.30	31.3	27.5
	'90	0.33	–	0.65	2.77	1.75	21	23
	'91	0.66	–	0.72	3.36	3.27	26.1	73.9
GB2	'88	0.5	–	1.2	4.6	3.1	22.3	111.3
	'89	0.64	–	1.33	3.62	2.5	27.2	59
	'91	1.9	–	0.79	3.06	2.36	17	50.7
GB3	'88	0.1	–	0.2	0.9	0.5	7.9	8.3
	'89	0.12	–	0.31	1.24	0.74	7.6	7.3
	'90	0.13	–	1.19	1.97	2.60	6.8	16.2
	'91	0.12	–	0.3	1.58	0.81	7.02	10.5

3.1. DRY DEPOSITION FLUXES TO THE NORTH SEA

Dry deposition of particles to the sea surface is the sum of all physical removal processes that take place when there is no form of precipitation (rain, snow or hail), such as gravitational settling, turbulent diffusion, Brownian diffusion or impaction. In general terms it can be stated that small particles (< 0.1 μm) are removed mainly by Brownian diffusion and large particles (> 10 μm) by gravitational settling. In the intermediate size range, impaction and interception are important. The loss of particles to the sea surface is frequently described in terms of a dry deposition velocity, which is the ratio between the deposition rate per unit area, and the ambient concentration. The dry deposition velocity of particles is strongly dependent on particle size, wind velocity and surface characteristics. Both theoretical considera-

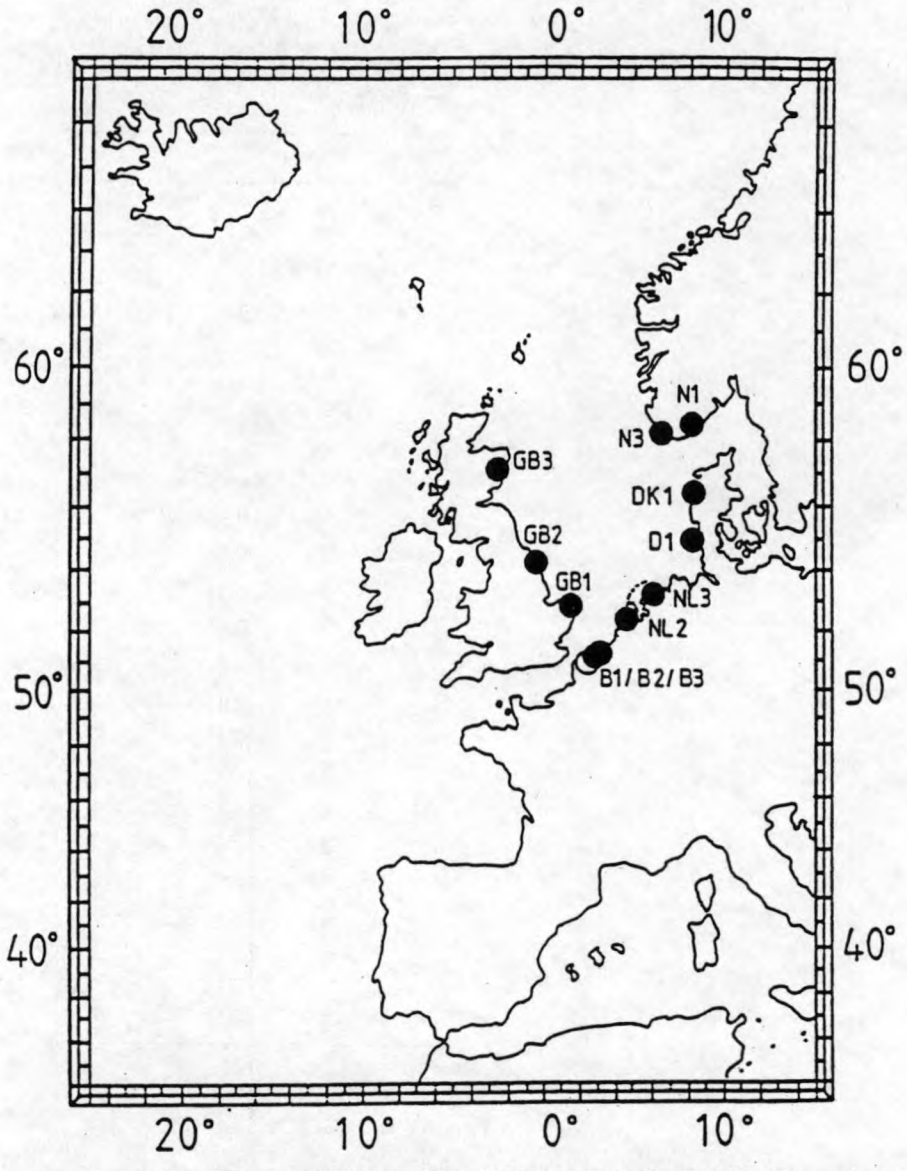

Fig. 1. The North Sea area with the stations which take part in the PARCOM Comprehensive Atmospheric Monitoring Programme (CAMP) – so called 'Central North Sea Stations'.

tions and field experiments show that the deposition velocity is small for particles with aerodynamic diameter less than 1 μm, typically of the order of 0.1 cm s^{-1}, while for the large particles it reaches a value of a few cm s^{-1}.

Transport fluxes across the air-sea interface can be determined by theoretical or semi-empirical relations (Sehmel and Hodgson, 1978; Slinn and Slinn, 1980; Williams, 1982; Friedlander *et al.*, 1986; Main and Friedlander, 1990). Dry depo-

sition velocities can also be evaluated by direct measurements of actual dry fluxes and particle concentrations in the air. Although the performance characteristics of air sampling equipment is quite well known, the properties of dry deposition collectors, as well as the structure of the laminar boundary layer above the collector and the collection efficiency still remain uncertain. It is still not clear how comparable the deposition to the surrogate surface is with the deposition to the natural sea surface. Another practical limitation, in case the deposited mass is measured, is that the results are strongly affected by the deposition of only a few large particles. Since the gravitational settling velocity is roughly proportional to the square of the particle diameter and the particle mass is proportional to the cube of the particle diameter, the deposited mass is a function of diameter to the 5th power. As a first approximation, a single 10 μm particle will therefore contribute as much to the total deposited mass as 100,000 particles of 1 μm. This makes direct measurements of the dry deposition velocity extremely difficult.

Only a few experimentalists have tried to measure directly the dry deposition of trace metals to the North Sea. Cambray *et al.* (1975) used a Whatman 541 cellulose filter, which was placed on a gas platform (53°5′ N, 2°21′ E). Samples were collected on a monthly basis. The high values found were explained by the authors as due to the possible contamination by resuspended sea water or by the platform itself.

Baeyens *et al.* (1990) measured dry deposition fluxes in a direct way with vasilinated plexiglass plates, in 14-days exposed intervals. Sampling was carried out throughout one year, at the West-Hinder lightvessel and during several cruises on the North Sea with the R/V Mechelen and the R/V Belgica. The collector plates were used horizontally and vertically. Directly measured dry deposition values were compared with the fluxes calculated by the adopted model of Slinn and Slinn (1980) and from a large set of *in situ* measured particle size distributions and their elemental concentrations. Despite the large uncertainties on the calculated dry deposition fluxes, results generally agree fairly well for both methods. The collection surfaces provide higher values, except for Mn and K, while the largest difference between both methods was observed for Pb (by a factor of 2.3).

Estimated dry deposition fluxes at the west coast of Sweden by Selin *et al.* (1992) were derived from trace element concentrations in the air in the winter of 1990 and from experimentally obtained deposition velocities.

Aircraft-based aerosol sampling in the lower troposphere was performed between September 1988 and October 1989 (Rojas *et al.*, 1993), above the Southern Bight of the North Sea. The dry deposition fluxes of Cd, Cu, Pb and Zn were calculated from size-differentiated atmospheric concentrations as a function of wind direction and dry deposition velocities obtained with the Slinn and Slinn model.

The dry deposition fluxes reported by Kriews (1992) are based on arithmetic mean values of atmospheric elemental concentrations, measured at Helgoland while for Cu, Pb and Zn, this percentage corresponds to 95, 96 and 97%, respectively.

For the same North Sea area, Baeyens *et al.* (1990) concluded that the first stages of their cascade impactor, i.e. particles larger than 4 μm, were responsible for 82% of the deposition of Pb. In the Mediterranean Sea, Dulac *et al.* (1989) reported that only 20% of the total deposition of Cd and Pb is accounted for by particles with sizes larger than 7 μm.

3.2. WET DEPOSITION FLUXES TO THE NORTH SEA

Wet deposition is the combination of rainout (in-cloud scavenging of particles) and washout (below-cloud scavenging of particles). Capture of particles by cloud droplets does not automatically lead to removal of the particles from the atmosphere, since cloud droplets may evaporate on their way to the earth's surface. This merely results in redistribution of the aerosol.

The amount of micropollutants which is deposited to the oceans over a certain period of time can be determined either directly or indirectly (Struyf and Van Grieken, 1993). In the direct way the wet atmospheric fluxes are determined by collecting rainwater in rain collectors over a certain period of time and measuring the concentrations of the substances involved. For particles, the annual wet flux F_w can be calculated with the following formula:

$$F_w = \sum_i C_i P_i,$$

or the flux F_w is the sum over all individual rain events i of the product of the concentrations in rainwater (C_i) times the amount of precipitation per unit area and time (P_i). The above equation is usually approximated as follows:

$$F_w = \overline{C} P,$$

where $\overline{C}$ is the average rainwater concentration and P the yearly precipitation rate. However, there are some major difficulties arising from determination of the wet deposition to the sea surface directly. Practically, collection of atmospheric material by rain water samplers should be avoided during dry periods (Ruijgrok *et al.*, 1990), (54°10′ N, 7°53′ E) in the period from 1986–1990, and deposition velocities following from the Slinn and Slinn model.

Atmospheric fluxes reported by ATMOS (1992) are based on mean aerosol concentration values measured at all the CAMP stations monitoring heavy metals in air during '88, '89, '90 and '91 and dry deposition velocities of 0.1 cm s^{-1} (Table V). However, the latter value is far from being generally accepted.

Estimated dry deposition fluxes by Ottley and Harrison (1993) are based upon data collected on 10 research cruises in 1988–89. A cascade impactor designed to collect efficiently size segregated aerosols, has produced detailed size distributions from which mass weighted deposition velocities were derived, followed by dry deposition flux estimates.

As seen in Table VI, published dry deposition fluxes of heavy metals to the North Sea show significant variations. In Table VII the dry deposition velocities,

TABLE V. The annual mean aerosol concentration (ng m^{-3}) and estimated dry deposition fluxes (kg km^{-2} y^{-1}) based on measurements at 'CAMP' stations (ATMOS, 1992)

Period	Param.	Cd	As	Cr	Cu	Ni	Pb	Zn
'88	conc.	0.36	1.6	1.1	2.76	1.87	21.6	42.7
	flux	0.01	0.05	0.04	0.09	0.06	0.73	1.45
'89	conc.	0.38	–	0.87	2.7	1.8	21.6	29.9
	flux	0.01	–	0.03	0.09	0.06	0.68	0.95
'90	conc.	0.27	0.78	1.1	2.4	2.0	32.2	93.2
	flux	0.01	0.03	0.03	0.07	0.06	1.0	3.0
'91	conc.	0.58	1.14	1.24	5.09	4.01	25.5	62.2
	flux	0.02	0.04	0.04	0.16	0.13	0.80	1.96

used by different authors for estimation of the dry deposition fluxes above the North Sea, are given. Considering the complex interaction of processes involved in particle deposition it is, perhaps, not surprising that inconsistencies have been evident in the reported research. Some of these inconsistencies are likely to indicate a real variability in environmental influences since an important number of factors influence the dry deposition processes. Meteorological data such as friction velocity, the aerodynamic surface roughness and the atmospheric stability are related to the deposition of particles. Humidity gradients and rainfall characteristics all affect the deposition of particles too. Furthermore, pollutant properties which vary with temperature, humidity and electrostatic gradients at the sea surface will result in a variation of the deposition characteristics of particles.

The main subject of discrepancy in the results concerning dry deposition velocities is due to the size distribution of the collected aerosols. Indeed, Van Aalst (1988) states that dry deposition velocities might vary in the range between 0.1 to 1 cm s^{-1}, and that most of this spread is caused by the lack of knowledge of the atmospheric particulate matter size distribution. Even though elements like Pb are more abundant in the sub-micrometer size range, these particles can coagulate with sea salt aerosols and reach super-micrometer dimensions. In order to give a quantitative idea on how important relatively large particles can be in the whole deposition process, Table VIII shows the percentage of the dry deposition flux accounted for by a given particle size class. Here only particle diameters larger than 1 μm are tabulated since the contribution of the sub-micrometer particles can be considered as negligible (Rojas *et al.*, 1993). It is seen from this table that 98% of the measured dry deposition velocity for Cd is accounted for by particles larger than 4 μm so wet-only samplers need to be used. Additional problems include sea-spray and contamination or deterioration of the samples prior to or during analysis by material sampling and handling, particularly if one deals with trace amounts (Ross, 1984; Buijsman *et al.*, 1991). Also, the statistical relevance

TABLE VI. Dry deposition fluxes (kg km^{-2} y^{-1}) to the North Sea – comparison of the literature data

	Cambray *et al.* (1975) Gas-platform	Stoßel (1987) Pellworm	Bayens *et al.* (1990) West-Hinder & ship		Selin *et al.* (1992) Sweden-west coast	Rojas *et al.* (1993) aircraft	ATMOS (1991) CAMP-stations	Kriews (1992) Helgo-land	Ottley and Harrison (1993) North Sea
			model	exp.					
S	–	–	–	–	275	–	–	–	–
Cr	–	–	–	–	–	–	0.04	0.34	–
Mn	6.8	–	3.5	3.0	–	–	–	1.68	–
Fe	290	155	82	180	–	–	–	76	–
Ni	–	–	–	–	0.5	–	0.13	0.23	–
Cu	30	1.1	2.8	3.5	–	1.9	0.16	0.29	0.7
Zn	420	6.8	6.2	13	1.9	10.3	1.96	3.69	4.9
As	–	–	–	–	–	–	0.04	0.11	–
Pb	24	4.3	3.3	7.5	0.4	4.23	0.80	1.06	0.7
Cd	–	0.3	–	–	–	0.28	0.02	–	0.06

TABLE VII. Dry deposition velocities (cm s^{-1}), used by different authors for estimation of dry deposition fluxes

	Van Jaarsveld and Onderlinden (1986)	Krell and Roeckner (1988)	Dulac *et al.* (1989)	Baeyens *et al.* (1990)	Selin *et al.* (1992)	Rojas *et al.* (1993)	ATMOS (1992)	Kriews (1992)	Ottley and Harrison (1993)
S	–	–	–	–	1.0	–	–	–	–
Cr	–	–	–	–	–	–	0.1	0.69	–
Mn	–	–	–	0.49	–	–	–	0.75	–
Fe	–	–	–	0.56	–	–	–	1.0	0.30
Ni	–	–	–	–	1.3	–	0.1	0.28	–
Cu	0.22	–	–	0.53	–	0.48	0.1	0.26	0.44
Zn	0.22	–	–	0.41	0.34	0.35	0.1	0.31	0.30
As	–	–	–	–	–	–	0.1	0.19	–
Pb	0.22	0.2	0.04	1.35	0.14	0.25	0.1	0.17	0.13
Cd	0.22	0.2	0.05	0.53	–	0.39	0.1	–	0.24

TABLE VIII. Relative contribution of the particle size classes in the determination of dry deposition fluxes for the Southern Bight of the North Sea (Rojas *et al.*, 1993)

Contribution to the dry deposition in %				
Diameter (μm)	Cd	Cu	Pb	Zn
1–2	1.1	1.5	1.1	0.4
2–4	0.4	3.1	1.4	1.7
4–8	2.2	6.3	14	11
8–16	50	5.7	39	27
>16	46	83	43	59

of such direct measurements is doubtful. Firstly, precipitation is a discontinuous process and secondly, there is a natural variability of the concentrations of trace substances in precipitation. This means that a large number of rain events must be covered before meaningful average wet fluxes can be obtained, which is expensive and time-consuming. Also, these measurements are very much determined by the sampling location and time, which is problematic if one wants to investigate the deposition over a larger area and over a considerable period of time (Smith, 1991). For this reason, indirect approaches are often preferred. The limited amount of directly measured data is then used to check the results of these indirect approaches. For indirect measurements, the wet deposition flux of material to the ocean surface can be written as:

$$F_w = WPC_a,$$

where C_a is the concentration of the substance in air, P is the yearly precipitation rate and W is the washout ratio – also called scavenging ratio – which is the ratio of the concentration of a substance in rainwater to the concentration of the same substance in air (both concentrations measured in the same volume units, e.g. μg m^{-3}).

This equation can be modified in a number of ways. Some authors for instance, add the density of air ρ as an extra factor (GESAMP, 1989):

$$F_w = WPC_a\rho^{-1}.$$

In this case the resulting washout ratios are temperature and pressure dependent and about a factor of 1200–1300 smaller. An alternative method to calculate the wet flux is the use of scavenging rates. This subject was extensively described by Slinn (1983).

3.2.1. *Data on Precipitation*

The existing estimates of surface precipitation (rain, snow, hail, ...) over the seas and oceans are based on a very limited data set. A serious problem with the

measurement of precipitation, both on the ground and aloft, is its great variability in time and space. Moreover, the total amount of rainfall at any location can be a combination of a small number of very intense showers (of convective origin) together with comparatively extended periods of light rainfall from stratiform clouds. The overall contributions of these two kinds of precipitation are often comparable (Browning, 1990). Even for a relatively small area such as the North Sea, an accurate value for annual average rainfall is not available at present. It is, however, generally recognized that less rain falls over sea than over land (see e.g. Cambray *et al.*, 1979; Baeyens *et al.*, 1990). By measurements on a gas platform, the rainfall there was observed to be about 55% of that at land-based stations at similar latitude on either side of the North Sea (Cambray *et al.*, 1975). Taking this observation into account, a mean rainfall value of 438 mm per year was calculated for the North Sea on the basis of measurements of seventeen stations situated on adjacent land. This value was seen as a kind of 'standard' value. However, this value was adjusted to 475 mm annually on the basis of measurements at seven stations surrounding the North Sea (Cambray *et al.*, 1979). Van Aalst *et al.* (1983) disagree with Cambray's value, claiming that the difference between the amount of precipitation on land and at sea is lower than assumed before. Baeyens *et al.* (1990) measured the yearly precipitation volume at the West-Hinder light vessel; the mean value, based on a period of two years, amounts to 430 mm per year. They also indicated that, in general, there is less precipitation above the sea. They found an average ratio West-Hinder/De Blankaert (a Belgian coastal station) of 0.72 and a ratio of 0.60 for West-Hinder/all Belgian meteorological stations. Krell and Roeckner (1988) used a model to simulate the atmospheric input of Pb and Cd into the North Sea, and used yet another annual precipitation rate, namely 558 mm.

According to Balls (1989), the uncertainty in the amount of rainfall is the most important single error source in flux estimations. It is obvious that more reliable values are urgently needed in order to be able to calculate more accurate wet deposition fluxes. In the future, space-based techniques for measuring global rainfall will provide us with data with a good resolution and accuracy. Radars and/or radiometers, installed on satellites, will be able to measure the instantaneous intensity of the rain or hail that is falling, from which an estimation can be made of how much rain has fallen in a particular area over a certain amount of time, and all of this will happen on a routine basis (Bowler, 1990; Kedem *et al.*, 1990; Scofield, 1991).

3.2.2. *Concentrations in Precipitation*

In Table IX an overview of data concerning measured precipitation concentrations over the North Sea and adjacent areas is given. It is obvious that the Swedish concentrations measured by Ross (1987 and 1990) are lower than those reported for The Netherlands (van Jaarsveld and Onderlinden, 1986; van Daalen, 1991).

The coastal values listed by van Aalst *et al.* (1983) show rather large variations, probably because they were obtained by different operators using other sampling methods at different sites and over other time intervals. However, the lowest values of these ranges agree very well with the concentrations measured at the North Sea coasts of Norway (Pacyna *et al.*, 1984; S & TWG, 1987) and in Scotland (Balls, 1989). Ross (1987) observed that the concentrations in southern Sweden were higher and that the wet deposition fluxes were higher than the Swedish anthropogenic emissions, so a long range transport of the pollutants was postulated. Clearly, the southern North Sea concentration values included in Table IX are very high compared to the other values. The inconsistency of those mentioned in the GESAMP report (1989) is ascribed to sampling problems (e.g. not all measurements were wet-only) and difficult analysis associated with this kind of measurements. The concentration values reported for the rainwater collected at the West-Hinder station and during several cruises at the Southern Bight (Dedeurwaerder *et al.*, 1985; Baeyens *et al.*, 1990) are very high compared to other values, although the sampling was done only when precipitation occurred and precautions were taken to avoid contamination. The results of the ATMOS report (1984) point out that the heavy metal concentrations in rainwater above the sea are higher than above land. Cambray (1975) thought that this so-called 'maritime effect' was caused by bubble bursting processes, which bring aerosols coming from an enriched sea surface layer into the atmosphere. However, Balls (1989) concluded on the basis of measurements of the enrichment factor in surface water that this process is not a significant contributor to the 'maritime effect'. Possible alternative processes are thought to be enhanced solubility of the metals above the sea due to ageing of the aerosols emitted by land based sources (ATMOS, 1984).

Trace metal concentrations in precipitation collected from 'CAMP' stations, around the North Sea (Table X) are quite variable from year to year, probably due to orographic effects. Also, they show much less consistency, undoubtedly because of the greater sampling and analytical problems associated with such measurements.

3.2.3. *Estimated Wet Deposition Fluxes to the North Sea*

As explained above the wet flux of trace metals can be estimated either directly or indirectly. In Table XI wet and total fluxes to the North Sea and its coasts are given. The results will depend on the area considered to constitute the North Sea and the value used for the annual precipitation rate are included, as well as on the method used (direct or indirect measurement).

It is very difficult to compare any data in the Table XI, because the authors used different rainfall rates and methods, and because both total fluxes and wet fluxes are listed. The estimated fluxes to the coast of southern Norway (S & TWG, 1987) and of Scotland (Balls, 1989) are reported to be lower than the other coastal values. And for the North Sea itself, the West-Hinder values are either relatively

TABLE IX. Measured precipitation concentrations ($\mu g\ l^{-1}$) over the North Sea and adjacent areas (s- preceding an area means southern)

Area	Period	Cd	Cr	Cu	Pb	Zn	Remarks	References
The Netherlands (coast)	'82–'83	0.26–0.36	0.21–0.8	1.8–4.9	8.9–20	18–32	bulk	van Jaarsveld and Onderdelinden (1986)
The Netherlands (coast)	'86–'88	0.5–0.9	1.4–1.8	6.7–8.0	13–20	21–31	wet-only	van Daalen (1991)
Sweden (coast)	'84–'85	0.033–0.15	–	0.46–1.5	2–9	4.2–16	bulk	Ross (1987)
Sweden (coast)	'87–'88	0.04–0.12	0.06–0.16	0.85–2.32	1.84–3.75	4.1–10.2	wet-only	Ross (1990)
North Sea (coast)	'72–'81	0.3–1.2	0.2–4	4–30	10–35	20–160	literature range	van Aalst *et al.* (1983)
Norway (coast)	'78–'79	0.27	–	–	11	15	weekly bulk	Pacyna *et al.* (1984)
Norway (coast)	'80–'84	0.37	–	–	7.1	9.2	–	S & TWG (1987)
Scotland (coast)	'87–'88	0.68	–	2.3	4	13	wet-only	Balls (1989)
sNorth Sea	'81	3	–	39.5	13	194	wet-only	Dedeurwaerder *et al.* (1985)
sNorth Sea	'74–'85	0.5–9.5	–	2.5–77	10–29	26–490	literature range	GESAMP (1989)
sNorth Sea	'84–'87	10	–	77	29	500	wet-only	Baeyens *et al.* (1990)
German Bight (platform)	'88–'91	0.26	1.88	17.8	12	275	wet-only	Schulz (1993)

TABLE X. An overview of the data submitted to ATMOS as regards elemental concentrations ($\mu g\ l^{-1}$) in precipitation for 1988, 1989, 1990 and 1991, measured at 'CAMP' stations

Station	Period	Cd	As	Cr	Cu	Ni	Pb	Zn
B3A	'91	0.1	–	–	1.26	–	2.7	8.16
DK1	'88	0.08	–	–	1.4	–	4.2	12.1
	'89	0.10	0.45	0.46	1.1	0.45	3.93	15.58
	'90	0.10	–	0.28	0.99	0.50	2.73	9.10
	'91	–	–	0.17	1.42	0.35	2.72	1350
D1	'89	0.25	0.21	0.52	2.89	3.34	4.24	11.39
	'90	0.15	0.31	0.49	1.05	0.71	2.43	11.47
NL2	'88	0.19	–	–	2.9	–	6.4	–
	'89	0.12	–	–	2.62	0.35	10.18	14.95
	'90	0.16	–	–	2.45	–	5.91	11.26
	'91	0.16	–	0.40	2.97	0.51	6.41	14.52
NL3	'90	0.16	–	–	2.53	–	2.78	12.56
	'91	0.13	–	–	3.36	0.77	6.84	13.82
GB1	'88	0.28	–	–	3	–	8.7	16.1
	'89	0.23	0.78	1.93	4.65	1.42	7.67	25.08
	'90	0.40	0.70	0.75	2.00	1.46	4.93	16.8
	'91	0.16	0.42	0.50	6.50	1.70	7.70	18.70
GB2	'88	0.58	–	–	6.5	–	22.7	46.1
	'89	0.57	1.11	1.68	7.85	3.28	22.79	61.33
	'90	0.36	1.10	1.04	3.52	2.66	10.65	33.45
	'91	0.46	1.18	0.90	7.60	5.50	19.00	49.50
GB3	'88	0.20	–	–	2.4	–	7.5	8.3
	'89	0.13	0.59	0.68	3.06	1.31	5.25	9.66
	'90	0.13	–	0.25	1.94	0.74	3.04	8.98
	'91	0.14	0.26	0.30	4.30	0.70	4.00	8.10
N1	'88	0.11	–	–	–	–	7.4	14.1
	'89	0.11	–	–	–	–	5.45	11.43
N3	'91	0.06	–	0.60	2.50	0.10	7.00	14.20

high (Baeyens *et al.* 1990) or very low (Dedeurwaerder *et al.*, 1985). Baeyens *et al.* (1990) reported that the wet flux to the North Sea is clearly higher than that at a Belgian coastal station. It should be noted that the input values reported by Rojas *et al.* (1993) are based on sampling flights and that they were calculated using scavenging rates.

As far as wet fluxes are concerned, the uncertainties are far from being known. The theoretical approach to wet deposition is rather crude in the sense that the

TABLE XI. Total (dry + wet) or wet flux to the North Sea in kg km^{-2} y^{-1} (s- preceding an area means southern)

Area	Rain [mm y^{-1}]	Cd	Cr	Cu	Pb	Zn	Method	Remarks	References
Coastal stations	438	–	1.4	10.5	11	31	direct	wet	Cambray *et al.* (1979)
Coastal stations	778–1028	0.3–1.4	–	6.1–16.2	5.6–13.5	20.6–55.6	direct	total	Flament *et al.* (1984)
Coastal stations	–	0.09–1.7	0.58	0.8–27	5.1–14	9.3–156	–	total	PARCOM (1987)
Scotland (coast)	–	0.39	–	1.3	2.3	7.6	direct	wet	Balls (1989)
sNorway (coast)	1399	0.48	–	–	9.2	12	direct	total	S & TWG (1987)
Dutch Continental Shelf	–	0.06–0.11	0.15–0.30	0.28–0.55	4.8–9.6	2.4–4.8	–	total	S & TWG (1987)
North Sea	680	0.1–0.5	–	1–4.4	4–23	5–23	indirect	total	GESAMP (1989)
North Sea	430	2.9	–	25	7	170	direct	wet (dissolved)	Bayens *et al.* (1990)
North Sea	500	0.35	–	2.68	6.5	15.1	indirect	total	Rojas *et al.* (1993)
sNorth Sea	–	1.6	–	24.9	9.4	143	–	wet	ATMOS (1984)
Southern Bight	458	0.0002	–	0.0026	0.0014	0.015	direct	total	Dedeurwaerder *et al.* (1985)
Southern Bight	500	0.43	–	2.5	8.8	19.7	indirect	wet	Rojas *et al.* (1993)
Southern Bight	500	0.71	–	5.36	12.9	30.2	indirect	total	Rojas *et al.* (1993)
German Bight	677	–	0.43	1	5.7	4.3	indirect	wet	Kriews (1992)
German Bight	–	0.34	0.95	14.4	9.2	–	direct	wet	Schulz (1993)
Sweden (west coast)	–	–	–	3	2.6	9	direct	total	Selin *et al.* (1992)

mechanisms by which atmospheric particulate matter is scavenged by rain, are not yet fully understood. For indirect estimations of the wet flux, the washout ratio used in the calculations is of considerable importance. In Table XII some relatively recent values for trace metals are listed. They are again, very difficult to compare. The values used in the GESAMP (1989) report and by Rojas *et al.* (1993) are 'best estimates' based on published washout ratios for trace metals above the North Sea. In the ATMOS report (1984), it is stated that values for Cu, Zn and Cd above the sea are up to 5 times larger than above land.

To assess the environmental effect of the atmospheric input of heavy metals into the North Sea, it is important to know whether a distinction can be made between the amount of a certain trace metal that reaches the surface of the earth in a dissolved or in a particulate form. For instance, dissolved metals are much more readily available to be incorporated by organisms. Flament *et al.* (1984) investigated the metal distribution over the solid and liquid phases in rain at some French coastal sites. They found the following percentages of dissolved material: Pb (21–31%), Cd (53–78%), Cu (63–94%) and Zn (68–87%). Losno *et al.* (1988) observed that Zn partitioning is governed by adsorption/desorption processes on existing particles, which are pH dependent. Nevertheless, Colin *et al.* (1990) state that the nature of the particles is also important. Jickells *et al.* (1992) conclude that the solubility of an element is the result of the complex interplay of several factors and cannot be simply assigned to one factor such as pH.

3.3. TOTAL DEPOSITION FLUXES TO THE NORTH SEA

The total amount of heavy metals deposited to the North Sea (5.25×10^5 km^2) as reported by several authors, is given in Table XIII. The atmospheric flux reported in the ATMOS (1984) report is significantly higher than the other values, except for Pb. The range calculated by van Aalst *et al.* (1983) is also relatively high but the other total flux values agree fairly well. They were assessed at totally different points in time, with other methods and concentration measurements to start from (coastal precipitation vs. airborne concentrations), and even the area taken into consideration was different. The annual estimation of atmospheric fluxes reported by ATMOS are based on measurements during '88, '89, '90 and '91 at the so-called 'Central North Sea stations', but taking into account concentration gradients from land to sea due to removal processes or due to dilution. For each station a bulk gradient correction factor (defined as the ratio of the average deposition at a certain station to the average deposition over the total North Sea area) was derived from model calculations developed by RIVM (van Jaarsveld *et al.*, 1986; van Jaarsveld *et al.*, 1991). It is evident that, for a number of elements, the estimated depositions reported for '91 (ATMOS, 1992) are higher than those calculated for '90 (ATMOS, 1991). The estimated increases in Pb (30%) and Cu (40%) are due to high concentrations at UK stations.

TABLE XII. Washout ratios for trace metals

Cd	Cr	Cu	Pb	Zn	Remarks	References
125–500	150	140–751	76–169	179–1000	literature range	Schroeder *et al.* (1987)
–	–	–	–	1226	value measured	Jaffrezo and Colin (1988)
200–1000	–	200–1000	200–1000	200–1000	range used	GESAMP (1989)
150	–	150	150	150	value used	Rojas *et al.* (1993)
–	200–1280	60–3800	20–1350	280–11500	value measured (snow)	Cadle *et al.* (1990)

TABLE XIII. Total (dry + wet) atmospheric input of trace metals into the North Sea, in tons y^{-1}

Rain [mm y^{-1}]	Cd	Cr	Cu	Pb	As	Zn	Method	References
–	–	740	5600	5800	460	1600	indirect	Cambray *et al.* (1979)
685	110–430	70–1400	1400–10000	3600–13000	220–720	7200–58000	direct	van Aalst *et al.* (1983)
–	–	100–530	380–1600	1800–6400	150–510	3900–12000	indirect	Stößel
–	45–240	300–900	400–1600	2600–7400	40–120	4900–11000	direct	PARCOM (1987)
–	900	–	13542	7367	–	77566	–	ATMOS (1984)
500	47	205	620	1900	95	4600	indirect	ATMOS (1990)
520	32	88	321	958	95	2740	indirect	ATMOS (1991)
650	27	94	610	1241	83	3099	indirect	ATMOS (1992)
680	50–250	–	500–2300	2300–12000	130–580	2700–12000	indirect	GESAMP (1989)
600	158	–	1348	3670	–	7409	indirect	Injuk *et al.* (1992)
677	–	–	–	3500	160	–	indirect	Dannecker *et al.* (1992)
677	–	530	5100	3200	160	–	direct	Dannecker *et al.* (1994)
677	–	400	670	3500	160	4200	indirect	Kriews (1992)

If deposition to the total North Sea area is estimated from observations at coastal stations, one has to deal with the problem of how representative those observations are for larger areas, with respect to both precipitation amounts and measured concentrations. The first problem can be solved reasonably by using a precipitation which varies from year to year, i.e. by taking a precipitation amount which is 70% of the median precipitation of all the coastal stations. The second problem can be solved only when knowledge about atmospheric residence times is included in the method. A combined method based on observations and model calculations can therefore be expected to give the most realistic results.

As far as the relative importance of dry and wet deposition goes, most authors seem to agree on the fact that, for the trace metals, the wet flux is more important than the dry flux, except perhaps for Pb, where they may be of the same magnitude. However, on the extent of this difference, opinions vary very widely (Galloway *et al.*, 1982; ATMOS, 1984; Schroeder *et al.*, 1987; GESAMP, 1989; Martin *et al.*, 1989; Baeyens *et al.*, 1990; Remoudaki *et al.*, 1991). Martin *et al.* (1989) remark that the ratio of wet to dry deposition is controlled by many meteorological factors and also by the distance between the sampling site and the emission source (see also Migon *et al.*, 1991; Remoudaki *et al.*, 1991).

Whenever the deposition of micropollutants to a water surface is estimated, attention should be paid to the reverse fluxes (from the water to the atmosphere) as well. According to the ATMOS report (1984), for which the heavy metal content in the sea surface microlayer was determined, the maximum water-to-air fluxes are at least 30 times smaller than the total input fluxes. The authors of the GESAMP (1989) report state that, although the atmospheric concentrations of trace metals associated with large (resuspended) sea salt particles constitute only a minor fraction of the total atmospheric concentration, this fraction may well account for a significant part of the gross dry deposition flux. This complicates the assessment of the 'real' deposition fluxes to the sea.

3.4. DEPOSITION FLUXES BASED ON MODEL CALCULATIONS

An alternative way of determining the deposition of micropollutants from the atmosphere to the sea involves atmospheric transport models. Basically, one uses emission data for a certain source area (e.g. Europe) in combination with a long range transport model (which requires a number of input data) to simulate the dispersion and deposition of a substance for a determined receptor area (e.g. the North Sea). Model calculations can provide independent estimates for atmospheric inputs which can be compared to input estimates from measurements. Moreover, the calculations may indicate the spatial variation of the deposition, and allow the evaluation of the representativeness of measurements at coastal stations. In this section the results of calculations performed using relatively recent models, which have been applied to the calculation of the total deposition of heavy metals to

the North Sea, will be discussed and compared to the values obtained from field measurements.

3.4.1. *Literature Data on the Deposition Fluxes Based on Model Calculations*

In the 1980's, van Aalst *et al.* (1983) employed a simple model to compare the long-term (ca. 1 year) average concentrations of various elements, and wet and dry deposition for an area of 1000 × 1000 km^2 of the North Sea. The total air concentrations at the receptor site were calculated as the sum of the contributions from the different emission areas (the 'cells' of the emission grid) weighted by the probability that the air masses would be carried down from that emission cell. Based on the mass-median diameters, a value of 0.1 to 1 cms^{-1} for the deposition velocities was used. The results showed good agreement between measurements and calculations. The data from this and other works (PARCOM, 1985) were reviewed by van Aalst and Pacyna (PARCOM, 1986) in order to assess the atmospheric inputs of trace elements to the North Sea.

A more advanced 3-dimensional trajectory model based on the Monte Carlo method has been employed to estimate the long range transport and deposition of Pb to the North Sea (Krell *et al.*, 1986). The emission data used were the numbers from Pacyna (1985). In 1988, Krell and Roeckner used a more sophisticated trajectory model to estimate the dry and wet deposition of Pb and Cd into the North Sea, via a long range transport model using gridded data of the respective anthropogenic emissions in Europe and the relevant meteorological data. The authors considered aerosols only in the size range from 0.2 to 1 μm and a deposition velocity of 0.2 cm s^{-1} was used for all heavy metals. This model is particularly designed for episode studies. The model of Graßl *et al.* (1989) is very similar to the model of Krell and Roeckner.

The total annual atmospheric input of Pb to the North Sea was determined for all the months of 1980 to be ca. 1440 tons by Petersen (1987). A relatively large contribution on the order of 50% was estimated for the UK. The Netherlands, France and Germany contributed about 12% each, Belgium 5%, Sweden 1.5%, Denmark 1% and Norway even less. However, conclusions from this work should be taken with caution. The results are based only on a one year period, which shows a significant month-to-month variability of the deposition. More recently the same author estimated the annual input of Pb to be 2300 tons (Petersen *et al.*, 1988).

The TREND model was developed at the Dutch National Institute of Public Health and Environmental Protection in order to calculate long term averaged concentrations and depositions (van Jaarsveld *et al.*, 1986). It is a statistical long-range version of the Gaussian plume model, what means that the dispersion from a source is assumed to follow the prevailing wind direction and wind speed within a sector of 30% in the horizontal plane. The vertical dispersion is limited by the earth surface and the top of a mixing layer. Due to wet and dry deposition and chemical reactions, atmospheric concentrations decrease during the transport; this

process is also taken into account. The model assumes homogeneous climatology and boundary characteristics over whole Europe. The occurring meteorological situations are grouped in a limited number of classes and the calculations are carried out separately for 5 size classes from $<0.95\ \mu$m to $>20\ \mu$m particles, each of which has its own deposition characteristics. For all heavy metals a deposition velocity of $0.22\ \text{cms}^{-1}$ was implemented. This model has been applied successfully to a period of a month, but even shorter periods yielded reasonable results.

The model of Warmenhoven *et al.* (1989) is, in fact, an elaborated version of the van Jaarsveld model, but instead of applying it to trace metals solely, a number of organic compounds like PAHs, PCBs, pesticides, etc. were also taken into consideration. The model assumes the same meteorology, surface characteristics and mass-averaged deposition velocities over the whole surface area.

The main problem concerning model based calculations is in estimating the emissions. Though, for some countries, there were explicit data on emissions of pollutants, generally the annual emissions from all countries have been estimated on the basis of industrial and agricultural activities within the countries. All the models used similar emission data as input to their model.

The total atmospheric input of some pollutants into the North Sea given by the above models is listed in Table XIV. Included is also the 'best' estimate defined as the value obtained when emissions are multiplied with the average ratio of measured/modelled air concentration. It can be seen that there is a general agreement between the results of the different models. Taking into account that all models use more or less the same emission data, this agreement confirms the idea that the influence of the different model assumptions is not very large, at least not in the case of the total deposition into the North Sea.

For the reported trace elements, the model values are consistently lower than the values obtained from field measurement data in Table XIII. Krell and Roeckner (1988) claim that this discrepancy can be explained as follows: the extrapolation of coastal measurements, on which most deposition estimates up until 1988 were based, cannot be justified, because there is no reason to believe that the high precipitation intensities/volumes measured along the southern and western coasts are representative for the whole of the North Sea. The authors find a strong argument in the life-time of clouds which is not more than a few hours for the precipitating one: in this way, most of the pollutant material is likely to be washed out within about 100 km from the coast. Their model simulations (and those by van Jaarsveld *et al.* (1986)) reveal a substantial decrease of the deposition across the southern and western coasts. Van Jaarsveld *et al.* (1986) state that the discrepancy might partly be due to less accurate sampling and analysis of rainwater as well.

3.4.2. *Validation of the Models*

Van Jaarsveld *et al.* (1986) note that there are some assumptions inherent to their model, which do not agree very well with reality. For instance, it is not correct to

TABLE XIV. Comparison of the total deposition (tons y^{-1}) to the North Sea calculated with different models

Reference	Cd	Cr	Cu	Pb	Zn	As
Earlier estimates reviewed in PARCOM (1985)	110–430	70–1400	1400–10000	3600–13000	7200–58000	220–720
PARCOM (1986)	14	70	130	2600	1200	42
Van Jaarsveld *et al.* (1986)	11	58	100	2000	940	–
Petersen (1987)	–	–	–	1440	–	–
Petersen *et al.* (1988)	–	–	–	2300	–	–
Krell and Roeckner (1988)	11	–	–	1200	–	–
Graßl *et al.* (1989)	–	–	–	2300	–	–
Warmenhoven *et al.* (1989)	15	72	110	1900	930	–
Van Jaarsveld (1991)	10	–	–	960	600	–
ATMOS (1990) – 'best' estimates (model/measurements)	13	–	–	870	1800	–

assume that transport and dispersion over sea are analogous to those over land. The stability over sea is mainly determined by the temperature difference between the air and the seawater, and shows hardly any diurnal variation. Also, in the coastal zone complicated transition phenomena occur, which are not accounted for in the model. However, the authors do not think that a more realistic model would yield largely different results.

Krell and Roeckner (1988) had difficulties in validating their model because of the lack of comparison material for the North Sea. Therefore, they were obliged to simulate air and precipitation concentrations at certain sites and for certain periods (e.g. a month) for which measurements were made, and their results agreed fairly well with the measured values.

Warmenhoven *et al.* (1989) estimate that the results concerning the heavy metal deposition are the most reliable ones. In general, the validity of this model is mainly governed by the quality of the emission data and the choice of the emission grid (because some materials are so stable in the atmosphere, that a much larger emission area should be taken into consideration). As a result of this, the real deposition of these elements should be higher than predicted by the model. Finally, the assumption that the North Sea is a well-mixed tank, without any inflow or outflow except from rivers (and the atmosphere), has an influence on the deposition estimates. In this concept it would be more realistic to include the dynamics of the North Sea in the model.

4. Relative Contribution of Atmospheric Deposition of Trace Metals to the Total Input into the North Sea

Apart from atmospheric pollution, the North Sea is subject to a number of other sources of pollution as well: e.g. input via rivers, direct discharges from industries into the estuaries, dumping of industrial wastes and drainage of sewage (van Aalst *et al.*, 1983). It is very difficult to evaluate the relative importance of the various input sources as most input estimates are subject to considerable uncertainty arising from analytical and sampling problems. Moreover, the actual quantity of pollutants entering the North Sea varies from year to year, depending on factors like natural variations in river flows and water exchange with adjacent sea areas, economic variations (industrial expansion and reorganization, large strikes), changing legislation (emission and dumping restrictions), atmospheric conditions (wind flow patterns, rainfall intensity) and unforeseen circumstances (accidents).

Although, in a number of publications, estimates of the non-atmospheric input are given (e.g. Cambray *et al.*, 1979; van Aalst *et al.*, 1983; ATMOS, 1984), we chose to use the recent data as given by Warmenhoven *et al.* (1989). They use the figures reported during the Second International Conference on the Protection of the North Sea in 1987, which are based on information obtained from the countries concerned. For the contaminants which are not included in the report of the Conference, the total fluxes are estimated on the basis of data on the total

TABLE XV. Relative contribution of atmospheric deposition to the total loading of the North Sea, in percent

Element	Atmospheric-measured ATMOS (1992)	Atmospheric-modelled Warmenhoven *et al.* (1989)
Cd	22	14
Cr	2	2
Cu	18	4
Pb	26	35
Zn	15	5

loading through the Rhine and the Meuse (Folkertsma, 1989). This author points out, however, that the values calculated in this way can only serve as in indication of the order of magnitude. Also, the contamination and natural heavy metal load of the water entering the North Sea from the English Channel, the Baltic Sea and the North Atlantic is not included in the estimates. And the river catchment areas are also subject to atmospheric deposition (Warmenhoven *et al.*, 1989). According to Warmenhoven *et al.*, 1989, the yearly estimates for non-atmospheric deposition of metals in tonnes are: 95 (Cd), 4000 (Cr), 2800 (Cu), 3500 (Pb) and 1700 (Zn). By comparing the non-atmospheric input to the atmospheric input fluxes discussed earlier, it is possible to get an idea of the relative importance of both pathways for the input of pollutants to the North Sea. In Table XV, the non-atmospheric values are compared with the measured and modeled atmospheric data. We used the values calculated by the model of Warmenhoven *et al.* (1989) and flux values reported by ATMOS (1992). The most important pathway for each compound seems the same for measurements and model. Based on this data, non-atmospheric input is more important for all the elements. GESAMP (1989) notes that, for particulate trace elements, the major source is usually the rivers. However, particulate riverine material is likely to be deposited close to the source regions, while atmospheric input can more easily occur in remote oceanic areas. Still according to the GESAMP report, the global atmospheric and riverine inputs are comparable for dissolved Cu, while for Zn and Cd atmospheric inputs appear to dominate. The atmospheric input of Pb is expected to decrease over the next decade, due to the growing use of unleaded gasoline. Martin *et al.* (1989) state that the atmospheric input to the Mediterranean Sea is predominant over the river input, either dissolved or particulate. For organic contaminants as well, the riverine flux may influence only the nearshore areas, while atmospheric input is supposed to have a much wider impact over regional seas (GESAMP, 1989).

However, it must be emphasized that the accuracy of the estimations of both the atmospheric and non-atmospheric input sources is still very poor.

5. Conclusions

From this literature review several important gaps in the knowledge of the atmospheric deposition to the North Sea have become apparent.

For aerosols, the presently available concentration data need to be improved by more accurate determinations of the size distribution of airborne particulate matter since this is directly controlling the deposition rates. The dependence of the deposition velocity upon the particle size requires further investigation and better knowledge of the kinetic parameters as deposition/transfer velocity.

It is obvious that current knowledge about the wet deposition of trace elements to the North Sea is insufficient. For the trace metals, which were dealt with in this review, a number of specific problems like the lack of accurate washout ratios for the North Sea area or the contribution of resuspension from the sea surface to the observed pollutant concentrations still have to be solved. Reported washout or scavenging ratios for a particular element vary substantially. Part of the problem is in the method by which scavenging ratios are determined; usually they are computed from rain and air concentrations measured on samples that were not collected contemporary. Therefore, it is absolutely necessary to work out a 'global' measurement strategy for the North Sea area which would include precipitation and air sampling, preferably simultaneously at a large number of sites (ship cruises, islands, platforms, coastal stations) and over a considerable period of time, in order to be able to calculate the scavenging rates from really paired rain and air samples. The considerable expansion of the geographical coverage of rain sampling programmes should eliminate the uncertainties on the temporal distributions of precipitations events for the North Sea area.

The results of different studies on the atmospheric input of trace elements into the North Sea are still indicating large uncertainties. A combined model and monitoring approach seems to be most useful for the determination of atmospheric fluxes to large surface waters. Model studies give much lower values than the studies based on measurements. The major uncertainty in model studies is the quality and completeness of the emission data and the different size distributions used in the models. Furthermore, none of the models takes into account particle growth due to high relative humidities. Emission estimates for Cd and Zn currently in use are most probably too low. Cd emissions in 1982–1989 over a whole region, should be at least 30% higher. For Zn, the general underestimating is at least a factor of 3. Therefore, research on emission processes and identification of unknown emission categories is urgently needed for heavy metals (Van Jaarsveld, 1991).

Acknowledgements

This work was partially financed by the Belgian State Prime Minister's Service – Science Policy Office, in the framework of the EUROTRAC program (contract EU

7/08) and the Impulse Programme in Marine Sciences, supported by the Belgian State – Prime Minister's Service – Science Policy Office (Contract MS/06/050).

References

Amundsen, C. E., Hanssen, J. E., Semb, A., and Steinnes, E., 1992, Long-range atmospheric transport of trace elements to Southern Norway, *Atmos. Environ.* **26A**, 1309–1324.

Andren, A. W., Lindberg, S. E., and Bate, L. C., 1975, Atmospheric input and geochemical cycling of selected trace elements in Walker Branch Watershed, Oak Ridge, TN, Oak Ridge National Laboratory, ORNL Report NSF-EATC-13.

ATMOS, 1984, Working group on the atmospheric input of pollutants to convection waters. Heavy metal input from the atmosphere into the North Sea, *ATMOS report* 4/4-E.

ATMOS, 1990, Working group on the atmospheric input of pollutants to convention waters, *ATMOS report* 8/12/1-E.

ATMOS, 1991, Working group on the atmospheric input of pollutants to convention waters, *ATMOS report* 9/18/1-E.

ATMOS, 1992, Working group on the atmospheric input of pollutants to convention waters, *ATMOS report* 10/4/2-E.

Baeyens, W., Dehairs, F., and Dedeurwaerder, H., 1990, Wet and dry deposition fluxes above the North Sea, *Atmos. Environ.* **24A**, 1693–1703.

Baeyens, W. and Dedeurwaerder, H., 1991, Particulate trace metals above the Southern Bight of the North Sea – I. Analytical procedures and average aerosol concentrations, *Atmos. Environ.* **25A**, 293–304.

Balls, P. W., 1989, Trace metal and major ion composition of precipitation at a North Sea coastal site, *Atmos. Environ.* **23**, 2751–2759.

Barrie, L. A., Lindberg, S. E., Chan, W. H., Ross, H. B., Arimoto, R., and Church, T. M., 1987, On the concentration of trace metals in precipitation, *Atmos. Environ.* **21**, 1133–1135.

Bowler, S., 1990, Radar network watches where the wind blows, *New Scientist* **24**, 30–31.

Braun, H., Vogg, H., Halbritter, G., Bräutigam, K. R., and Katzer, H., 1984, Comparison of the stack emissions from waste incineration facilities and coal fired heating power stations, *Recycling International* **1**, 1–2.

Breekke, F. H., 1976, Impact of acid precipitation forest and fresh-water ecosystems in Norway. SNSF Project Research Report, Phase 1, 1972–75. Norwegian Institute for Forest Research, Oslo.

Browning, K. A., 1990, Rain, rainclouds and climate, *Q.J.R. Meteorol. Soc.* **116**, 1025–1051.

Buijsman, E., Jonker, P. J., Asman, W. A. H., and Ridder, T. B., 1991, Chemical composition of precipitation collected on a weathership on the North Atlantic, *Atmos. Environ.* **25A**, 873–883.

Cadle, S. H., VandeKopple, R., Mulawa, P. A., and Muhlbaier Dasch, J., 1990, Ambient concentrations, scavenging ratios, and source regions of acid related compounds and trace metals during winter in northern Michigan, *Atmos. Environ.* **24A**, 2981–2989.

Cambray, R. S., Jefferies, D. F., and Topping, G., 1975, An estimate of the input of atmospheric trace elements into the North Sea at Clyde sea (1972–73), AERE Harwell, England (AERE Report R 7733).

Cambray, R. S., Jefferies, D. F., and Topping, G., 1979, The atmospheric input of trace elements to the North Sea, *Mar. Sci. Comm.* **5**, 175–194.

Cawse, P. A., 1974, A survey of atmospheric trace elements in the U.K. (1972–73), AERE, Harwell, England (AERE Report R 7669).

Colin, J. L., Jaffrezo, J. L., and Gros, J. M., 1990, Solubility of major species in precipitation: Factors of variations, *Atmos. Environ.* **24A**, 537–544.

Dannecker, W., Bredthauer, U., Kriews, M., Rebers, A., Selke, K., and Schultz, M., 1992, Preliminary Report of Atmospheric Pollutant Measurements in the Norther North Sea Region. University of Hamburg, Germany.

Dannecker, W., Hinzpeter, H., Kriews, M., Naumann, K., Schulz, M., Schwikowski, M., Steiger, M., and Terzenbach, U., 1994, Atmospheric transport of contaminants, their concentrations and input into the North Sea, in J. Sündermann (ed.), *Circulation and Contaminant Fluxes in the North Sea*, Springer Verlag Berlin, Heidelberg, New York (in press).

Dedeurwaerder, H., Dehairs, F., Xian, Q., and Nemery, B., 1985, Heavy metals transfer from the atmosphere to the sea in the Southern Bight of the North Sea, in R. Van Grieken and R. Wollast (eds.), *Proceedings 'Progress in Belgian Oceanographic Research'*, pp. 170–177, University of Antwerp (UIA), Belgium.

Dedeurwaerder, H. L., 1988, Study of the dynamic transport and the fall-out of some ecotoxicological heavy metals in the troposphere of the Southern Bight of the North Sea. Ph.D. thesis, University of Brussels (VUB), Belgium.

Dulac, F., Buat-Ménard, P., Ezat, U., Melki, S., and Bergametti, G., 1989, Atmospheric input of trace metals to the Western Mediterranean: Uncertainties in modelling dry deposition from cascade impactor data, *Tellus* **41B**, 362–378.

Flament, P., Noël, S., Auger, Y., Leman, G., Puskaric, E., and Wartel, M., 1984, Les retombées atmosphériques sur le littoral Nord-Pas-de-Calais, *Pollution atmosphérique oct.–déc. 1984*, 262–270.

Flament, P., Lepretre, A., Noël, S., and Auger, Y., 1987, Aerosols cotiers dans le nord de la Manche, *Ocean. Acta* **10**, 49–61.

Folkertsma, F., 1989, Nationale rapportage Noordzee-Aktieprogramma deel A: inventarisatie van emissies van geselecteerde stoffen in Nederland in 1985, Dienst Binnenwateren, RIZA, Lelystad, The Netherlands.

Friedlander, S. K., Turner, J. R., and Hering, S. V., 1986, A new method for estimating dry deposition velocities for atmospheric aerosols, *Atmos. Environ.* **17**, 240–244.

Galloway, J. N., Thornton, J. D., Norton, S. A., Volchok, H. L., and McLean, R. A. N., 1982, Trace metals in atmospheric deposition: A review and assessment, *Atmos. Environ.* **16**, 1677–1700.

GESAMP, 1989, IMO/FAO/UNESCO/WMO/WHO/IAEA/UN/UNEP Joint Group of Experts on the Scientific Aspects of Marine Pollution. The atmospheric input of trace species to the world ocean. Reports and Studies GESAMP-WMO 38.

Goldberg, E. D., 1973, North Sea Science, MIT Press, Cambridge, MS.

Graßl, H., Eppel, D., Pettersen, G., Schneider, B., Weber, H., Gandraß, J. G., Reinhardt, K. H., Wodarg, D., and Fließ, J., 1989, Stofeintrag in Nord- und Ostsee über die Atmosphäre. GKSS-Forschungszentrum, GKSS-89/E/8, Geesthacht, Germany.

Hutton, M. and Symon, C., 1986, The quantities of cadmium, lead, mercury and arsenic entering the U.K. environment from human activities, *Sci. Total Environ.* **57**, 129–150.

Hutton, M., 1982, Cadmium in the European Community. Monitoring and Assessment Research Centre, London (MARC Report 26).

ICES, 1978, Input of pollutants to the Oslo Commission area, Cooperative Research 77, Charlottenlund, Denmark, Int. Council for the Exploration of the Sea.

Injuk, J., Otten, Ph., Laane, R., Maenhaut, W., and Van Grieken, R., 1992, Atmospheric concentrations and size distributions of aircraft-sampled Cd, Cu, Pb and Zn over the Southern Bight of the North Sea, *Atmos. Environ.* **26A**, 2499–2508.

Jaffrezo, J. L. and Collin, J. L., 1988, Rain-aerosol coupling in urban area: Scavenging ratio measurement and identification of some transfer processes, *Atmos. Environ.* **5**, 929–935.

Jickells, T. D., Davies, T. D., Tranter, M., Landsberger, S., and Jarvis, K., 1992, Trace elements in snow samples from the Scottish Highlands: Sources and dissolved/particulate distributions, *Atmos. Environ.* **26A**, 393–401.

Kedem, B., Chiu, L. S., and North, G. R., 1990, Estimation of mean rain rate: Application to satellite observations, *J. Geophys. Res.* **95**, 1965–1972.

Kemp, K., 1984, Long term analysis of marine and nonmarine transported aerosols, *Nucl. Inst. Methods* **B3**, 470, 860–871.

Kersten, M., Kriews, M., and Förstner, U., 1991, Partitioning of trace metals released from polluted marine aerosols in coastal seawater, *Mar. Chem.* **36**, 165–182.

Kendall, P. M. H., Bevington, C. F. P., and Pearse, D. J., 1985, Atmospheric cadmium emission and deposition in the Netherlands. Metra Consulting B.V., Kockengen.

Krell, U., Lehmhaus, J., and Roeckner, E., 1986, Atmospheric input of heavy metals into the North Sea: First results of a 3-dimensional trajectory model. In: Proc. WMO Conf. on Air Pollution Modelling and Its Application, Leningrad, USSR, 18–24 May.

Krell, U. and Roeckner, E., 1988, Model simulation of the atmospheric input of lead and cadmium into the North Sea, *Atmos. Environ.* **22**, 375–381.

Kretzschmar, J. G. and Cosemans, G., 1979, A five year survey of some heavy metal levels in the air at the Belgian North Sea coast, *Atmos. Environ.* **13**, 267–277.

Kriews, M., 1992, Charakterisierung mariner Aerosole in der Deutschen Bucht sowie Prozesstudien zum Verhalten von Spurenmetallen beim Übergang Atmosphäre/Meerwasser. Ph.D. Thesis, University of Hamburg, Germany.

Losno, R., Bergametti, G., and Buat-Menard, P., 1988, Zinc partitioning in Mediterranean rainwater, *Geophys. Res. Lett.* **15**, 1389–1392.

Main, H. H. and Friedlander, S. K., 1990, Dry deposition of atmospheric aerosols by dual tracer method-I. Area source, *Atmos. Environ.* **24A**, 103–108.

Martin, J.-M., Elbaz-Poulichet, F., Guieu, C., Loije-Pilot, M.-D., and Han, G., 1989, River versus atmospheric input of material to the Mediterranean Sea: An overview, *Mar. Chem.* **28**, 159–182.

Migon, C., Morelli, J., Nicolas, E., and Copin-Montegut, G., 1991, Evaluation of total atmospheric deposition of Pb, Cd, Cu and Zn to the Ligurian Sea, *Sci. Total Environ.* **105**, 135–148.

Mukherje, A. B., 1986, The discharge of lead, cadmium and mercury into the ecosystem in relation to Finnish industry. Helsinki University of Technology (SF-02150).

Naturvardsverket, 1982, Monitor 1982. Tungmetaller och organiska miljögifter i svensk natur.

NAS, 1978, The Tropospheric Transport of Pollutants and Other Substances to the Oceans. National Academy of Sciences Press, Washington, D.C., 194 pp.

Ottley, C. J. and Harrison, R. M., 1993, Atmospheric dry deposition flux of metallic species to the North Sea, *Atmos. Environ.* **27A**, 685–685.

Otten, P., Storms, H., Xhoffer, C., and Van Grieken, R., 1989, Chemical composition, source identification and quantification of the atmospheric input into the North Sea. In Progress in Belgian Oceanographic Research (edited by G. Pichot), pp. 413–422. Prime Minister's Services of Science Policy Office & Ministry of Public Health and Environment, Brussels.

Pacyna, J. M., 1983, Trace element emission from anthropogenic sources in Europe. Report of the Norwegian Institute for Air Research. Lillestrøm (NILU TR 10/82).

Pacyna, J. M., Semb, A., and Hanssen, J. E., 1984, Emission and long-range transport of trace elements in Europe, *Tellus* **36B**, 163–178.

Pacyna, J. M., 1985, Spatial distribution of the As, Cd, Cu, Pb, V and Zn emissions in Europe within a 1.5 grid net. Norwegian Institute for Air Research. Lillestrøm (NILU OR 60/85).

Pacyna, J. M., 1987, Atmospheric emissions of arsenic, cadmium, mercury and zinc in Europe in 1982. Norwegian Institute for Air Research. Lillestrøm (EMEP/CCC-Rept. 3/86).

PARCOM, 1985, Sixth Annual Report of the Paris Commission, Annex 6, London.

PARCOM, 1986, Report from the Fourth Meeting of the Working Group on the Atmospheric Input of Pollutants to Convention Waters, Oslo 28–30 October.

PARCOM, 1987, Current estimates of atmospheric inputs to the North Sea. Ninth Annual Report on the Activities of the Paris Commission, Annex pp. 38–42.

Peirson, D. H., Cawse, P. A., Salmon, L., and Cambray, R. S., 1973, Trace elements in the atmospheric environment, *Nature* **241**, 252–256.

Petersen, G., 1987, Methodology for model calculations of the atmospheric input of trace metals into the North Sea and Baltic Sea. In: Proc. PARCOM Meeting, ATMOS-5, Berlin, 10–12 November.

Petersen, G., Weber, H., and Grassl, H., 1988, Modelling the Transport of Trace Metals from Europe to the North Sea and Baltic Sea, in J. M. Pacyna and B. Ottar (eds.), *Control and Fate of Atmospheric Trace Metals*, NATO ASI Series, Kluwer Academic Publishers, Dordrecht, The Netherlands.

Remoudaki, E., Bergametti, G., and Losno, R., 1991, On the dynamic of the atmospheric input of copper and manganese into the western Mediterranean Sea, *Atmos. Environ.* **25A**, 733–744.

Rojas, C. M., Injuk, J., Laane, R. W., and Van Grieken, R., 1993, Dry and wet deposition fluxes of Cd, Cu, Pb and Zn into the Southern Bight of the North Sea, *Atmos. Environ.* **27A**, 251–259.

Ross, H. B., 1984, Methodology for the collection and analysis of trace metals in atmospheric precipitation. Report CM-67, International Meteorological Institute in Stockholm/Dept. of Met., University of Stockholm, Sweden.

Ross, H. B., 1987, Trace metals in precipitation in Sweden, *Water, Air, and Soil Poll.* **36**, 349–363.

Ross, H. B., 1990, Trace metal wet deposition in Sweden: Insight gained from daily wet only collection, *Atmos. Environ.* **24A**, 1929–1938.

Ruijgrok, W., Visser, H., and Römer, F. G., 1990, Comparison of bulk and wet-only samplers for trend detection in wet deposition, *Proceedings International Workshop on Cloud Chemistry and Wet Deposition, Utrecht, The Netherlands*, April 1990, pp. 34–40.

Rupper, J., 1975, Geochemical investigations on atmospheric precipitation in a medium-sized city (Göttingen, FRG), *Water, Air and Soil Poll.* **4**, 447–455.

Schladot, J. D. and Nürnberg, H. W., 1982, Report Jülich, Nuclear Research Center.

Schneider, B., 1987, Source characterization for atmospheric trace metals over Kiel Bight, *Atmos. Environ.* **21**, 1275–1283.

Schroeder, W. H., Dobson, M., Kane, D. M., and Johnson, N. D., 1987, Toxic trace elements associated with airborne particulate matter: A review, *J. Air Poll. Control Ass.* **37**, 1267–1284.

Schulz, M., 1993, Räumliche und zeitliche Verteilung atmosphärischer Einträge von Spurenelementen in die Nordsee. Ph.D. thesis, University of Hamburg, Germany.

Scofield, R. A., 1991, Operational estimation of precipitation from satellite data, *Palaeogeography, Palaeoclimatology, Palaeoecology (Global and Planetary Change Section)* **90**, 79–86.

Sehmel, G. A. and Hodgson, W. J., 1978, A Model for Predicting Dry Deposition of Particles and Gases to Environmental Surfaces. Battelle, Pacific Northwest Laboratory, Richland, WA., PNL-SA-6721.

Selin, E., Mnubi, A., Isakson, J., Foltescu, V. L., and Djupström, M., 1992, Transport and Deposition of Particulate Pollution to the East Coast of Sweden. Environment, Lifestyle and Health FRN-Report 92:3, Swedish Council for Planning and Coordination of Research, 56–71.

Semb, A. and Pacyna, J. M., 1988, Toxic trace elements and chlorinated hydrocarbons: Sources, atmospheric transport and deposition. Environmental Report 1988:10. Nordic Council of Ministers, Copenhagen, ISBN Denmark.

Slinn, S. A. and Slinn, W. G. N., 1980, Predictions for particle deposition on natural waters, *Atmos. Environ.* **16**, 1785–1794.

Slinn, W. G. N., 1983, Air-to-sea transfer of particles. In Liss, P. S. and Slinn, W. G. N. (eds.): Air-sea Exchange of Gases and Particles. D. Reidel Dordrecht, pp. 299–405.

Smith, F. B., 1991, Deposition processes for airborne pollutants, *The Meteorological Magazine* **120**, 173–182.

S & TWG Scientific and Technical Working Group, 1987, Quality status of the North Sea. Second International Conference on the Protection of the North Sea, London, November 1987, Vol. 5, p. T8 and Vol. 6, pp. 6–10.

Steiger, M., Schulz, M., Schwikowski, M., Naumann, K., and Dannecker, W., 1989, Variability of aerosol size distribution above the North Sea and its implication to the dry deposition estimates, *J. Aerosol. Sci.* **20**, 1229–1232.

Steiger, M., 1991, Die anthropogenen und naturlichen Quellen urbaner und mariner Aerosole charakterisiert und quantifiziert durch Multielementanalyse und chemische Receptormodelle. Ph.D. Thesis. University of Hamburg, Germany.

Stöeßel, R., 1987, Untersuchungen zu Naß- und Trockendeposition von Schwermetallen auf der Insel Pellworm. Ph.D. Thesis, University of Hamburg, Germany.

Struyf, H. and Van Grieken, R., 1993, An overview of wet deposition of micropollutants to the North Sea, *Atmos. Environ.* **27A**, 2669–2687.

van Aalst, R. M., van Ardenne, R. A. M., de Kreuk, J. F., and Lems, Th., 1993, Pollution of the North Sea from the Atmosphere. TNO report CL 82/152, Delft, The Netherlands.

van Aalst, R. M., 1988, Input from the atmosphere. In Salomons, W., *et al.* (eds.): Pollution of the North Sea: An Assessment. Springer-Verlag, Berlin/Heidelberg, Germany.

van Daalen, J., 1991, Air quality and deposition of trace elements in the province of South-Holland, *Atmos. Environ.* **25A**, 691–698.

van Enk, R. H., 1980, The pathway of cadmium in the European Community, *European Appl. Res. Rept. Environ. and Nat. Res. Sec.*, 1:1.

Van Jaarsveld, J. A., van Aalst, R. M., and Onderdelinden, D., 1986, Deposition of metals from the atmosphere into the North Sea: Model calculations, RIVM, Bilthoven, Report 842015002.

Van Jaarsveld, J. A. and Onderdelinden, D., 1986, Modelmatige beschrijving van concentratie en depositie van kolen relevante componenten in Nederland, veroorzaakt door emissies in Europa. Nationaal Onderzoeksprogramma Kolen (NOK), deelrapport 4, April 1986, PEO, Utrecht, The Netherlands.

Van Jaarsveld, J. A., 1991, Estimating Atmospheric inputs of trace constituents to the North Sea: Methods and results. 19th NATO/CCMS-ITM on Air Pollution Modelling and its Application. 29 September–4 October 1991, Ierapetra, Greece.

Warmenhoven, J. P., Duiser, J. A., de Leu, L. Th., and Veldt, C., 1989, The contribution of the input from the atmosphere to the contamination of the North Sea and the Dutch Wadden Sea. TNO Report R 89/349A, Delft, The Netherlands.

Williams, R. M., 1982, A model for the dry deposition of particles to natural water surfaces, *Atmos. Environ.* **16**, 1933–1938.

Yaaqub, R. R., Davies, T. D., Jickells, T. D., and Miller, J. M., 1991, Trace element in daily collected aerosols at a site in southeast England, *Atmos. Environ.* **25A**, 985–996.

Selected article #20:

Identification of individual aerosol particles containing Cr, Pb, and Zn above the North Sea

H. Van Malderen, S. Hoornaert and R. Van Grieken

Environmental Science and Technology, 30 (1996) 489-498

3150

Reprinted from ENVIRONMENTAL SCIENCE & TECHNOLOGY, Vol. 30, 1996

Identification of Individual Aerosol Particles Containing Cr, Pb, and Zn above the North Sea

HANS VAN MALDEREN, STEFAAN HOORNAERT, AND RENÉ VAN GRIEKEN*

Department of Chemistry, University of Antwerp (UIA), Universiteitsplein 1, B-2610 Antwerp, Belgium

Aerosol samples have been collected over the southern bight of the North Sea from an aircraft. In this way, 96 samples were taken for single-particle analysis during 16 flights. Almost 45 000 individual particles were analyzed with electron probe X-ray microanalysis. More than 5000 of these were found to contain significant concentrations of one or more of the heavy metals Cr, Pb, and Zn. With the help of hierarchical, nonhierarchical, and fuzzy clustering techniques, various heavy metal-containing particle types could be identified. Significant differences in abundances were detected in the North Sea heavy metal aerosol, depending on the origin of the air masses. In samples with continental influence 50 times more Zn- and Pb-containing particles were found than in samples with a marine history. For Cr, on the other hand, we found abundances in the marine sector that were one-third of the values for continental sectors. This might point to a rather undefined marine source, which could be the recycling of previously deposited material by reinjection into the atmosphere by sea spray. The highest values for Cr-, Pb-, and Zn-containing particles were always detected under southeastern wind directions.

Introduction

During the past few decades, the input of heavy metals to the North Sea has increased significantly due to the growing industrial activity and car traffic in European countries. Despite the first positive signals of improvement, e.g., the reduction of atmospheric Pb levels as a result of the use of unleaded gasoline (*1*–*3*), the annual total toxicity of all heavy metals mobilized was reported to exceed the combined toxicity of all of the radioactive and organic wastes generated each year (*4*). The ever increasing dispersion of heavy metals through the atmosphere, water, and soil is a major concern due to their hazardous effect on human health, the possible changes they initiate in natural biochemical processes in all ecosystems, and their inevitable accumulation in the food chain.

* Corresponding author fax: +32-3-820-23-76; e-mail address: vgrieken@uia.ua.ac.be.

It has often been demonstrated that wet and dry deposition of pollutants from the atmosphere to the North Sea is a dominant transport system for a number of elements. For several years now, efforts have been made to assess heavy metal concentrations and size distributions over the North Sea and to quantify the deposition fluxes of these elements by using a wide variety of analytical bulk techniques (*5*). Microanalysis techniques, however, have not been widely used, despite their enormous potential to characterize the morphology and composition of micrometer-sized individual aerosol particles. Observation of particular elements allows the identification of specific particle types, characterization of their source, and investigation of their abundance as a function of physical parameters. Moreover, shorter sampling times (minutes rather than hours for bulk analysis) are needed for microanalysis, which allows one to study short time variations in atmospheric composition as a result of wind direction changes and to overcome some of the problems of airborne sampling from airplanes, where shorter sampling times evidently are needed than for ship-based measurements.

The present study is part of a large investigation regarding heavy metal deposition into the North Sea. Several articles have already been published in the framework of this study on the single-particle analysis of particulate atmospheric matter using electron probe X-ray microanalysis (EPXMA) (*6*), especially for giant aerosol particles (*7*), and using laser microprobe mass analysis (*8*). Besides single-particle analysis, bulk analysis by energy-dispersive X-ray spectrometry and proton-induced X-ray emission (*9*) and by differential pulse anodic stripping voltammetry (*10*) was performed in order to obtain atmospheric concentrations of different elements. With these data, several deposition models were tested (*11*, *12*), which in the end provided us with estimates for wet and dry deposition fluxes of heavy metals into the North Sea (*2*). The aim of the present article is the detailed identification and characterization of exactly the specific particle types that are responsible for the input of heavy metals Cr, Zn, and Pb.

Experimental Section

The samples were collected during several flights with a twin-engine aircraft, a Piper Chieftain PA 31-350 owned by Geosens B.V. (Rotterdam, The Netherlands), over a period of 13 months. All flights were performed under relatively cloudless and dry conditions. Wind speeds over the sampling campaign were between 2 and 13 m s^{-1}. After takeoff from Rotterdam airport, a spiral flight was initiated at the Goeree platform (51°55′30″ N, 3°40′ E) in order to localize the inversion layer. Once this was done, the aircraft flew tracks of ca. 110 km at six different heights more or less evenly spaced between sea level and the inversion layer. The lowest track, only 10–30 m above sea level, was intended to assess particle resuspension by sea spray. During these tracks, airborne particulate matter was collected on 0.4-μm-pore-size Nuclepore membrane filters using an isokinetic inlet (*13*). The flow rate was approximately 1 m^3 h^{-1}. All tracks were flown parallel with the wind direction to allow later calculation of backward trajectories. These 36-h isobaric back trajectories were provided by the Royal Dutch Meteorological Institute

0013-936X/96/0930-0489$12.00/0

(KNMI) and are shown in Figure 1. More detailed information about the sampling campaign can be found elsewhere (*14*).

In this way, 96 samples were collected during 16 flights. The analysis of almost 48 000 individual particles (500 in each sample) was done by EPXMA on a JXA-733 Superprobe of JEOL (Tokyo, Japan). For the analysis, an accelerating voltage of 20 kV and a beam current of 1 nA were used. The minimal detection limit for elemental concentration is around 1000 ppm, whereas the minimum detectable particle size is 0.2 μm. EPXMA permits one to obtain morphological parameters such as the diameter and shape factor of a particle, while the chemical composition is derived from an energy-dispersive (ED) X-ray spectrum. More detailed information on this method can be found elsewhere (*6*). The resulting data set contained both morphological and chemical information for almost 48 000 particles.

It is not difficult to imagine that, when working with such large data sets, some method of data reduction is needed. We chose a combined approach of several multivariate cluster techniques. A home-written Windows-based program, called IDAS, was used. More information about the program can be found elsewhere (*15*). Cluster analysis is a well-developed multivariate method, which has been used regularly in connection with single-particle analysis (*16*–*19*). Most of these publications dealt with hierarchical clustering methods. In our case, we applied a combination of hierarchical, nonhierarchical, and fuzzy clustering to our data set.

The clustering was performed on the X-ray elemental intensities emitted by each aerosol particle, and no normalization was done prior to the statistical treatment. Hierarchical cluster analysis (HCA) is the most simple of the three and therefore most frequently used. It has also the advantage of easy visual interpretation with the help of so-called dendrograms. Its main disadvantage lies in the fact that some hierarchical structure is presumed, and this is not always the case when working with atmospheric data sets. This might lead to the misclassification of some particles. Nonhierarchical clustering methods (NHCA) do not have these problems; however, they require prior knowledge about the data structure. This is solved by using the results of the hierarchical clustering as centroids for the nonhierarchical clustering. Both HCA and NHCA are so-called hard clustering methods: this means that one particle belongs to only one cluster after the clustering. In some cases, when dealing with overlapping clusters, this can lead to mistakes in the clustering. This problem is overcome by fuzzy clustering analysis (FCA). The main idea is to replace the procedure of splitting the multivariate data into a certain number of clusters by a procedure of determining the probability of belonging for each object to each cluster. Hard clustering therefore can be considered as a special case of fuzzy clustering, namely, when all membership coefficients but one are equal to 0. More detailed information can be found in a publication by Treiger et al. (*20*). The results of all three types of clustering very much depend on the correct choice of the number of clusters. Previously, this was done on the basis of the personal experience of the analyst rather than on the basis of statistical criteria. This problem was overcome by implementing Akaike's information criterion (AIC), which is based on the relation between entropy and ordering in an isolated system: if there is full ordering in the system, the entropy is minimal. Further information and examples of AIC are found elsewhere (*21*).

Results and Discussion

To investigate the aerosol composition dependence on wind direction, we divided the 16 flights into five sectors according to the air mass history obtained from 36-h backward trajectories. Chester and Bradshaw (*22*) stressed the immense importance of the air mass origin for the aerosol composition compared to the position of the sampling location. Therefore, much care was given to the division of the samples over the five sectors, which are shown in Figure 1. Only particles containing Cr, Zn, or Pb were selected. In this way we obtained all Cr-, Zn-, or Pb-containing particles divided per sector. The distribution of the flights over the different sectors and the number of particles containing one or more of these metals in each flight are shown in Table 1. Figures 2–4 show the percentage of metal-containing particles per sector.

From these figures, it is clear that the lowest occurrences of Cr-, Pb-, and Zn-rich particles were always found in sector 1. This sector is characterized by unpolluted air masses of pure marine origin and can be considered an indicator of North Sea background values. Main sources of pollution in this sector should be ships as well as gas and oil drilling platforms, which are positioned over the central area of the North Sea, but their influence seems to be rather small. Only the percentage of Cr-containing particles is significant compared with values from sectors with continental influence (ca. one-third of pure continental values), which might support the assumption of a marine source of Cr-containing particles. The reinjection by sea spray of previously deposited particles has been proposed (*23*) as a possible source for marine-derived trace metal-containing particles, but the reality and quantification of this possible recycled marine component are still controversial (*24*). Pb and Zn values are more than 50 times lower than continental values. Sector 2 has intermediate values for Cr (1.4%) and Pb (3.0%), but the amount of Zn-rich particles is rather high (7.8%). This sector accounts for emissions from the Netherlands, the northern part of Germany, eastern Europe, and all Scandinavian countries. The highest number of heavy metal-containing particles was always encountered in sector 3. This sector is identified by air masses with pure continental history, which carry emissions from Belgium, central and southern Germany, and the eastern part of France. These high numbers are not totally unexpected, since industrial sources of heavy metals alone are thought to be 10 times higher on a global scale than all natural sources combined (*25*). Sector 4 is affected by air masses from the northwestern part of France (including the industrial centers of Dunkerque, Cherbourg, and Lille) and by emissions from the United Kingdom, but also has some influence from air masses coming from the Atlantic ocean and the English Channel. Percentages in this sector are approximately half of those in sector 3. Only Cr (2.2%) abundances are on the same level as that for sector 3 (2.1%). Samples collected on flights 4, 9, and 14 were taken under low wind speeds and variable wind conditions. Therefore, they are grouped in sector 5, called "local". The values found in this sector are also quite high.

To investigate the true chemical composition of the particles containing Cr, Zn, or Pb, we needed to identify the different particle groups and determine their abundance variations over the five sectors. This was done only for

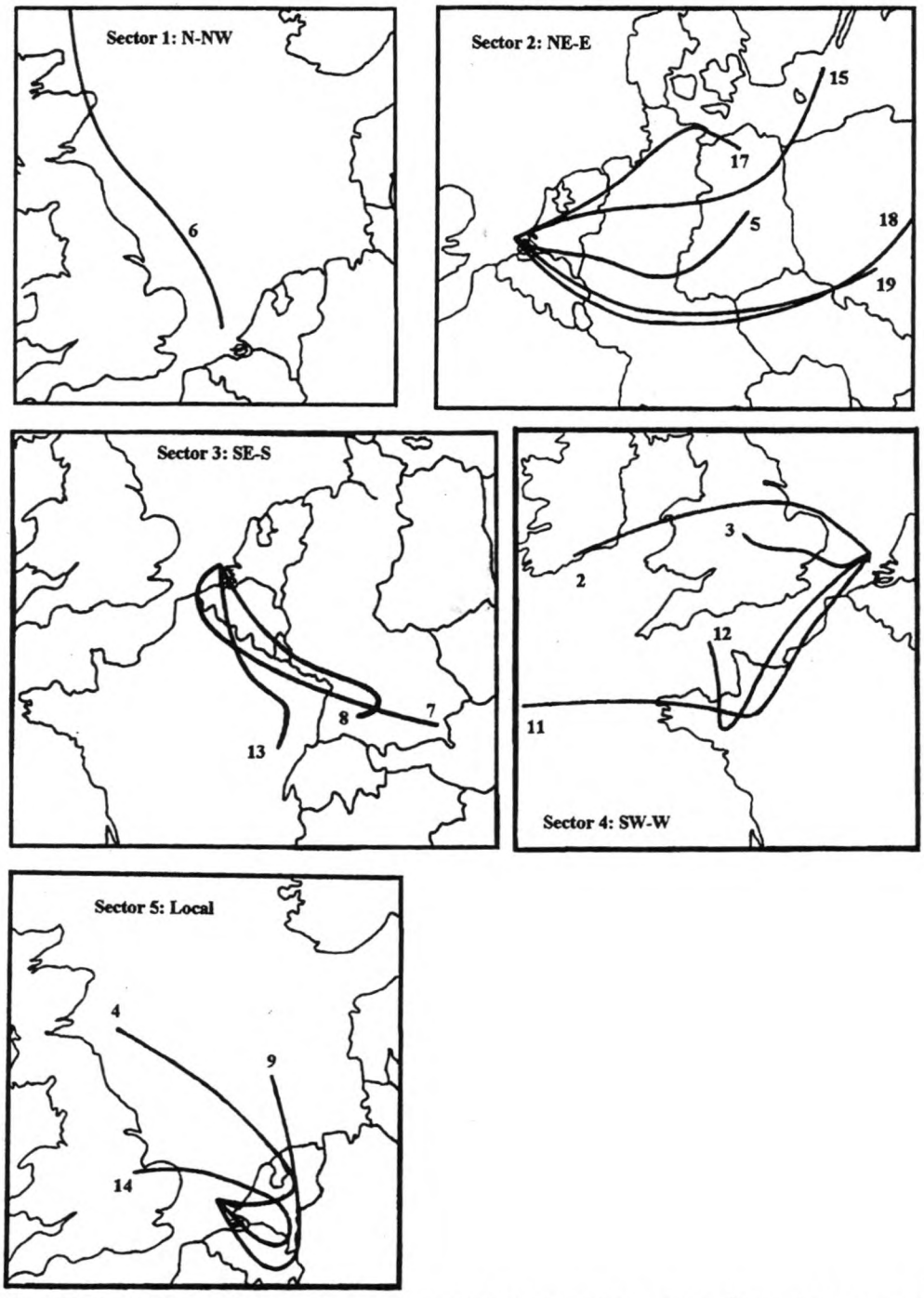

FIGURE 1. 1000-hp, 36-h air mass back trajectories at our sampling site for the five different sectors. The numbers indicate flight numbers.

particles containing one or more of the elements Cr, Zn, and Pb. Other heavy elements such as Ni, V, Sn, Cd, and Cu were not investigated, because the number of particles containing one or more of these elements was too small to obtain statistically significant information. For each of the three elements we performed hierarchical, nonhierarchical, and fuzzy clustering for each of the five sectors. The results of the hierarchical clustering were used as centroids for the nonhierarchical and fuzzy clustering. The number of groups was chosen after careful evaluation of Akaike's criterion. The fuzzy clustering was employed for studying the internal overlap between the different groups. The final interpretation was carried out on the basis of the combination of the information obtained for the three clustering techniques. The results for Cr-, Zn-, and Pb-containing particles for each of the five sectors are given in Tables 2–4.

Chromium-Containing Particles. In total, 750 particles were found containing Cr, which is 1.7% of the entire number of particles analyzed. After the clustering, several different Cr-containing particle types were detected, embodying a variety of compositions, but some frequently occurring types could be identified. The results of the clustering for the five sectors are shown in Table 2. All sectors are dominated by the appearance of Fe–Cr particles, sometimes in combination with other elements. Pure Cr particles (these are most likely Cr oxides, but since only elements with Z above 11 are detected with energy-dispersive EPXMA, O is not measured) were only encountered in sectors 2 and 4. In most sectors Cr was also detected

TABLE 1

Number of Particles Containing Cr, Pb, and Zn as a Function of the Total Number of Particles Analyzed per Flight and per Sector

flight no.	particles analyzed per flight	Cr-containing particles	Pb-containing particles	Zn-containing particles
		Sector 1: North/Northwest		
6	2922	21	4	0
total (sector 1)	2922	21 (0.7%)	4 (0.1%)	0 (0.0%)
		Sector 2: Northeast/East		
5	3401	36	88	305
15	2851	52	25	141
17	3000	39	106	234
18	1980	31	119	260
19	3000	40	87	163
total (sector 2)	14232	198 (1.4%)	425 (3.0%)	1103 (7.8%)
		Sector 3: Southeast/South		
7	3000	50	244	414
8	3000	52	176	243
13	3000	83	130	216
total (sector 3)	9000	185 (2.1%)	550 (6.1%)	873 (9.7%)
		Sector 4: Southwest/West		
2	1573	28	101	69
3	2844	41	135	164
11	2655	25	13	35
12	2880	127	38	104
total (sector 4)	9952	221 (2.2%)	287 (2.9%)	372 (3.7%)
		Sector 5: Local		
4	1764	28	156	100
9	2455	74	68	264
14	3000	50	80	103
total (sector 5)	7219	152 (2.1%)	304 (4.2%)	467 (6.5%)
total (all sectors)	43325	750 (1.7%)	1570 (3.6%)	2815 (6.5%)

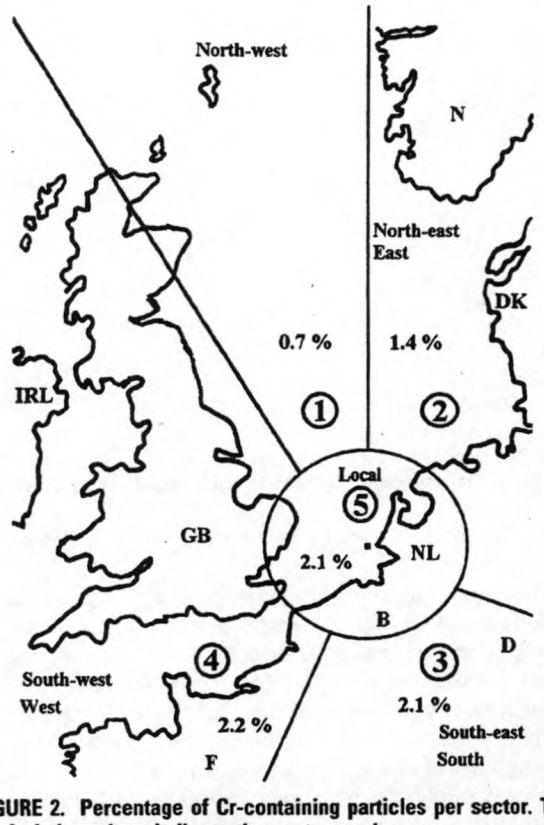

FIGURE 2. Percentage of Cr-containing particles per sector. The encircled numbers indicate the sector number.

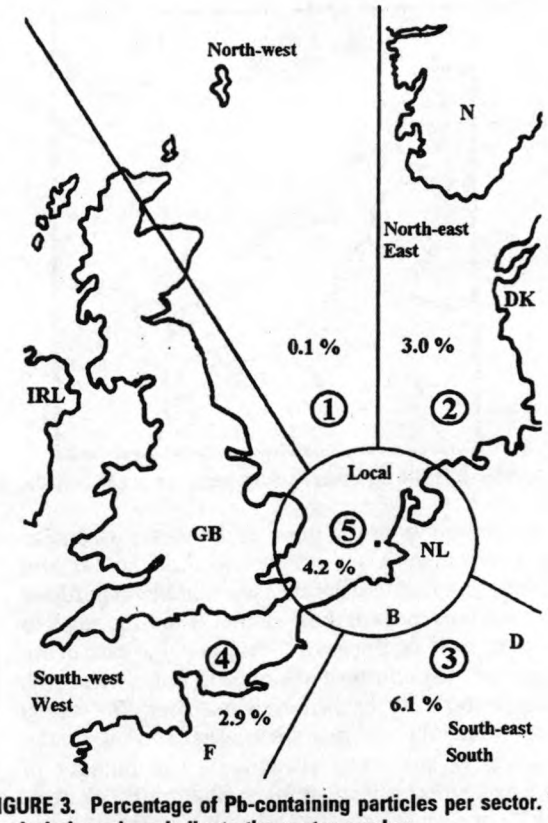

FIGURE 3. Percentage of Pb-containing particles per sector. The encircled numbers indicate the sector number.

in combination with the elements S, Ca, Cl, and K. In Table 2 they are indicated as Cr/medium-*Z*. In some sectors Cr was associated with high-*Z* elements such as Ni, Zn, Cu, and Pb. Another frequently occurring particle type is Cr associated with Si. In Table 2 these particles are noted as Si/Cr. The size of the different particle types varies between

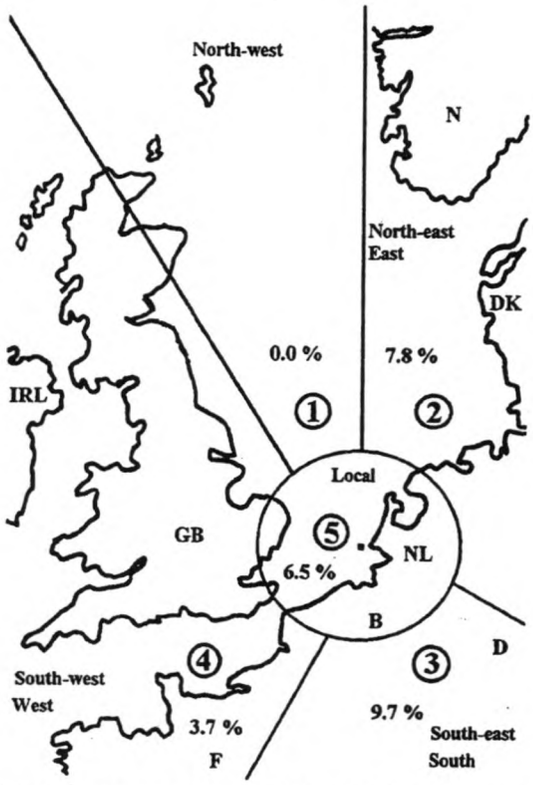

FIGURE 4. Percentage of Zn-containing particles per sector. The encircled numbers indicate the sector number.

0.3 and 2.5 μm. This variation is larger than that for Pb- and Zn-rich materials. This might point to a natural source of Cr, which is not present for Zn and Pb.

More than 10 million tons of chromite ($FeOCr_2O_3$), the only economically important Cr mineral, is used globally each year, divided over three main industries: 76% for metallurgical, 13% for refractory, and 11% for chemical applications (*26*). The different industrial applications call for different forms of Cr, such as chromite, ferrochromium, Cr metal, and several other Cr compounds. Each of these industries emits Cr in one form or another. The closest Cr-emitting industries are probably the steel factories in Boulogne, Dunkerque, Lille, and Roubaix, approximately 300 km distant from the sampling location. The industrial center of the Ruhr area, with many steel factories, lies ca. 500 km east. The source identification of all of these particles types is quite complex, considering the relatively small differences between some of the particle groups. Moreover, due to the high boiling point, Cr vapors from chromium steel production and coal combustion rapidly condense as oxides on the surface of different sorts of airborne particles (*27*). During the combustion of fuels, the volatile species in coal evaporate in the furnace and subsequently condense as submicrometer-sized particles or on ash particles. Cr was found to be significantly concentrated on the surface of combustion particles (*28*). These processes give rise to a wide variety of Cr-containing particles and complicate source identification. Several particle groups with low Cr content are probably created in this way. The influence of particle size on the occurrence of this particle type is rather unclear: sizes vary between 0.5 and 1.5 μm.

The differences in abundances between the various particle groups shown in Table 2 are not to be interpreted as final, since classification of some of the clusters was difficult and subject to personal interpretation. They do, however, give a good indication of the occurrence of the various groups.

Fe–Cr clusters are the most abundant in all of the sectors. The values vary between 39% (sector 3) and 57% (sector 1). Several publications (*4*, *27*, *29*) suggest metallurgical industries, which are the main consumers of chromite for the production of iron, steel, and stainless steel (Cr improves corrosion resistance), as the primary source of Fe–Cr-rich particles. Pacyna (*30*) also pinpoints the steel industry as the major emitter of Cr in Europe (15 000 tons $year^{-1}$). The mineralogical composition of dusts released in the different phases of iron and steel production has been identified as consisting of a significant part of Fe minerals as hematite (Fe_2O_3) and magnetite (Fe_3O_4), which sometimes contain very high concentrations (on the order of 100–1000 ppm) of heavy metals including Cr (*31*).

Cr-rich groups, which are correlated with Si and sometimes Al, were found in all sectors as well. They could be natural windblown soil dust particles. Some Saharan dusts are known to contain high levels of Cr, up to 3000 ppm. Long-range transport of such soils was expected to contribute to Cr release, even in Europe (*32*). On the other hand, they might also be the result of Cr condensation on airborne soil dust. Evidently, this Cr-containing particle type is rather large in size, often larger than 1.0 μm. This might point to a natural origin for this group. Another, and probably important, possibility is quartz (SiO_2) particles released in the steel production process, which may contain high Cr concentrations (*31*).

The main medium-*Z* elements that are found in combination with Cr are Ca, S, Cl, and K. Here again the emission from the metallurgical industry is probably the main contributor to this type of particles. Significant quantities of Ca minerals such as calcite ($CaCO_3$), dolomite ($CaMg(CO_3)_2$), and gypsum ($CaSO_4 \cdot 2H_2O$) enriched with Cr are released during the production process. Calcite is known to react with SO_2 and results in gypsum. The cement industry is another potential source of atmospheric Cr. Manufacture of cement is a high-temperature process using more than 30 raw materials, with limestone, which contains Cr concentrations in the ppm range, as a major ingredient (*32*).

Pure Cr particles were only found in the northeastern and southwestern wind directions, and not in the southeastern direction. It is possible that this is partly an artifact of the clustering, which incorporated pure Cr particles into groups with high Cr content. Metallic Cr is used primarily in nonferrous alloys, where the use of less expensive ferrochromium alloys can introduce undesirable amounts of Fe (*26*). Cr particles associated with heavy metals are also likely to originate from this source. Presumably this is also the reason why they are found in higher quantities in sectors 2 and 4. The closest important nonferrous industry in the southeastern direction is much more distant than in the other directions. The occurrence of Cl in some groups is most likely explained by the coagulation of anthropogenic Cr particles and sea salt. The size of these particles is very small (around 0.4 μm).

Lead-Containing Particles. Over the five sectors together, 1570 particles were found containing Pb. This is 3.6% of the total number of particles analyzed. Again, we tried to discover the various particle types by means of a combined clustering approach. This resulted in the identification of five major Pb-containing particle types, shown in Table 3. Approximately 50% of the particles were

TABLE 2

Abundances, Diameters, and Composition of Cr-Containing Particle Groups According to Their Different Source Sectors as Found by Statistical Clustering

particle type	total abun	abundance (%)	diameter (μm)	relative concentration (weight %) of main elements detected by EPXMA
			Sector 1: North/Northwest	
Fe/Cr	57.0	57.0	0.8	**Cr**(20), Fe(73), Ni (7)
Cr/high-*Z*	28.6	28.6	1.2	S(10), Cl(26), Ca(18), **Cr**(15), Cu(23)
Si/Cr	14.3	14.3	2.5	Si(16), **Cr**(84)
			Sector 2: Northeast/East	
Fe/Cr	45.6	14.6	0.5	**Cr**(17), Fe(80)
		14.0	0.6	Si(6), **Cr**(18), Mn (6), Fe(62)
		12.3	1.4	Si(21), S(6), Cl(6), **Cr**(14), Fe(43)
		4.7	0.4	Si(11), **Cr**(48), Fe(29)
pure Cr	31.0	31.0	0.4	**Cr**(100)
Cr/high-*Z*	11.1	6.4	0.5	S(12), Cl(10), **Cr** (10), Fe(57), Zn (7)
		4.7	0.6	S(24), K(7), Ca(11), **Cr**(20), Fe(17), Zn (10)
Cr/medium-*Z*	9.3	5.8	0.3	S(14), **Cr**(81)
		3.5	0.3	S(26), Ca(53), **Cr**(7)
Si/Cr	2.9	2.9	0.4	Mg(7), Al(6), Si(58), S(9), **Cr**(12)
			Sector 3: Southeast/South	
Fe/Cr	40.0	23.8	0.6	**Cr**(25), Fe(65)
		10.3	0.9	**Cr**(11), Fe(85)
		5.9	0.7	Si(7), S(6), **Cr**(11), Mn(32), Fe(34), Zn(7)
Cr/high-*Z*	30.2	15.1	0.4	Si(5), **Cr**(39), Fe(34), Ni(4), Zn(12)
		15.1	0.7	Si(4), **Cr**(11), Fe(60), Zn(12)
Si/Cr	16.2	9.2	0.9	Si(7), **Cr**(81), Fe(6)
		7.0	0.6	Si(47), S(6), **Cr**(25), Fe(14)
Cr/medium-*Z*	13.5	9.2	1.7	Al(6), Si(10), S(12), Cl(16), K(5), Ca(6), Ti(6), **Cr**(17), Fe(21)
		4.3	0.9	S(48), Ca(37), **Cr**(10)
			Sector 4: Southwest/West	
Fe/Cr	39.0	18.1	1.5	**Cr**(18), Fe(73), Ni (4)
		10.9	0.5	**Cr**(46), Fe(40)
		10.0	0.9	Si(14), **Cr**(14), Fe(51), S(5), Cl(3)
pure Cr	24.0	24.0	0.4	**Cr**(100)
Cr/medium-*Z*	23.9	14.9	1.4	Cl(64), **Cr**(28)
		9.0	0.4	Ca(9), **Cr**(64), Fe(8)
Cr/high-*Z*	7.7	5.0	0.9	S(20), Cl(7), Ca(19), Ti(7), V(7), **Cr**(15), Fe(9), Cu(14)
		2.7	0.4	S(52), **Cr**(43), Cu(5)
Si/Cr	5.4	5.4	1.0	Si(83), **Cr**(6)
			Sector 5: Local	
Fe/Cr	53.3	23.0	0.9	**Cr**(25), Fe(68), Ni(6)
		12.5	0.6	**Cr**(49), Fe(42)
		9.2	0.6	**Cr**(13), Fe(84)
		8.6	0.7	Cl(9), S(7), Si(5), Fe(52), **Cr**(17)
Si/Cr	20.7	11.8	1.0	Si(11), **Cr**(85)
		7.9	1.1	Si(87), **Cr**(13)
Cr/medium-*Z*	17.8	12.5	0.7	S(42), Ca(45), **Cr**(12)
		5.3	0.5	S(50), K(11), **Cr**(25)
Cr/high-*Z*	9.2	5.9	1.0	Si(7), Cl(15), **Cr**(20), Pb(4)
		3.3	1.4	Cl(4), **Cr**(17), Cu(76)

found to be "pure" Pb particles, most likely metallic Pb and Pb oxides. Other groups with high abundances were Pb chlorides, Pb associated with medium-*Z* elements such as P, Ca, and K, and Pb-containing particles with high-*Z* elements (mostly Zn, sometimes Cu and Sn). Pb correlated with Si, identified as Si/Pb in Table 3, accounted for only a few percent in most sectors.

Pb is an element that is used very extensively in a wide variety of applications. The average emission for all sources was estimated to be around 123 000 tons year^{-1} in Europe (*30*). The total deposition flux of Pb in the southern bight of the North Sea was estimated to be 13.8 kg km^{-2} year^{-1}, which is 2200 tons year^{-1} (*2*). Gasoline combustion accounts for more than 50% of the Pb emission, but the introduction of unleaded gasoline should have reduced this number dramatically. Other major emitters are coal combustion, Pb production, Cu–Ni production, Zn–Cd production, the steel industry, and cement factories (*4*). The size of Pb-containing particles varies between 0.3 and 0.8 μm and seems to be generally smaller than for Cr-containing particles.

Table 3 shows the high abundance of "pure" Pb particles (45% in sector 5, up to 54% in sector 2). The results for sector 1 are only based on four particles, so no statistical conclusions can be made. According to Fergusson (*33*), metallic Pb, $PbCO_3$, or Pb oxides (all of which could be the so-called "pure" Pb, because only elements with $Z > 11$ are detected in ED EPXMA) are created in various processes: emissions of coal-fired power stations, cement and fertilizer production, base metal smelting, and even automotive exhaust can eventually result in such species. The main components in aged vehicle aerosols are oxylead species: $PbCO_3$, $(PbO)_2{\cdot}PbCO_3$, $PbSO_4$, and PbO (*34*). Therefore, it is rather complicated to assign these "pure" Pb particles to one particular source. The size of these particles is rather small (0.4 μm).

TABLE 3

Abundances, Diameters, and Composition of Pb-Containing Particle Groups According to Their Different Source Sectors as Found by Statistical Clustering

particle type	total abun	abundance (%)	diameter (μm)	relative concentration (weight %) of main elements detected by EPXMA
		Sector 1: North/Northwest		
pure Pb	75	75	0.4	**Pb**(100)
Al/Pb	25	25	0.6	Al(60), **Pb**(40)
		Sector 2: Northeast/East		
pure Pb	53.6	53.6	0.4	**Pb**(100)
Pb/high-*Z*	24.1	8.7	0.5	K(4), Zn(64), **Pb**(27)
		5.6	0.5	Zn(46), **Pb**(52)
		4.7	0.7	Fe(56), Zn(19), **Pb**(12)
		3.5	0.5	Cu(54), Zn(5), **Pb**(38)
		1.6	0.8	Si(5), Cl(3), Sn(66), **Pb**(23)
Pb chlorides	12.3	9.9	0.7	Cl(58), **Pb**(39)
		2.4	0.6	Cl(40), K(11), Zn(22), **Pb**(27)
Pb/medium-*Z*	6.6	3.8	0.6	P(4), Ca(47), **Pb**(34)
		2.8	0.4	K(63), Zn(4), **Pb**(33)
Si/Pb	3.3	3.3	0.5	Al(5), Si(56), Fe(6), Zn(4), **Pb**(22)
		Sector 3: Southeast/South		
pure Pb	48.4	48.4	0.4	**Pb**(100)
Pb chlorides	32.7	9.6	0.4	Cl(73), **Pb**(27)
		9.5	0.7	Cl(60), **Pb**(40)
		6.5	0.8	Cl(49), **Pb**(51)
		4.2	0.6	Cl(54), **Pb**(23)
		2.9	0.7	Cl(40), **Pb**(18), P(4), Ca(5), Fe(10), Zn(25)
Pb/medium-*Z*	10.9	3.8	0.3	P(40), Cl(5), **Pb**(53)
		3.3	0.8	Ca(55), Zn(8), **Pb**(35)
		2.0	0.5	Al(27), P(13), Ti(4), Cr(8), Sn(3), **Pb**(40)
		1.8	0.4	Cl(15), K(40), Ca(6), **Pb**(38)
Pb/high-*Z*	6.9	4.2	0.7	Fe(56), Zn(13), **Pb**(19)
		2.7	0.4	Zn(55), **Pb**(43)
Si/Pb	1.1	1.1	1.0	Al(6), Si(47), K(4), Fe(7), Zn(14), **Pb**(20)
		Sector 4: Southwest/West		
pure Pb	49.8	49.8	0.5	**Pb**(100)
Pb chlorides	23.3	23.3	0.7	Cl(52), Zn(3), Br(4), **Pb**(38)
Pb/high-*Z*	18.1	10.5	0.5	Fe(3), Zn(46), **Pb**(48)
		6.6	0.5	P(13), Ca(11), Cu(16), **Pb**(47)
		1.0	0.7	Ca(11), Sn(59), **Pb**(31)
Si/Pb	6.3	6.3	0.6	Si(38), Ca(3), Fe(29), Zn(8), **Pb**(20)
Pb/medium-*Z*	2.4	2.4	0.7	Cl(4), K(62), **Pb**(35)
		Sector 5: Local		
pure Pb	44.7	44.7	0.4	**Pb**(100)
Pb chlorides	34.9	21.1	0.6	Cl(68), **Pb**(28)
		13.8	0.7	Cl(48), Zn(3), Br(3), **Pb**(38)
Si/Pb	11.2	11.2	0.5	Al (1), Si(8), P(5), Mn(2), Fe(13), Zn(24), **Pb**(36)
Pb/medium-*Z*	6.2	3.9	0.3	P(6), Ca(50), **Pb**(38)
		2.3	0.3	K(60), Zn(2), **Pb**(37)
Pb/high-*Z*	3.0	3.0	0.4	Cl(6), Cu(54), **Pb**(38)

The second most abundant particle type was Pb chlorides. These particles originate from car exhaust emissions and have been studied extensively (*35*, *36*). The primary material from the exhaust of cars is PbClBr. However, PbO, Pb(OH)Cl, Pb(OH)Br, and sometimes $PbSO_4$ and Pb may occur. PbClBr reacts in the atmosphere with many products, all resulting in the loss of halides and finally producing Pb sulfates, nitrates, and oxides (*33*). The detected percentages of traffic-related particles in the different sectors correlate quite well with the amount of car traffic in these sectors: sector 5 (35%) and sector 3 (33%) had air masses passing over densely populated areas in Belgium, The Netherlands, and Germany. Sector 4 (23%) also has a lot of traffic, but it is much more distant from the sampling area. Therefore, the particles had much more time to react with atmospheric compounds. No Pb halides were found in sector 1 (marine sector).

Another detected particle type was Pb associated with P, Ca, or K. Particles containing P and/or Ca are probably linked to emissions by cement manufacturing or fertilizer production. Zn and Cl were sometimes found in association with Pb particles holding K. They might be connected to emissions from refuse incineration, which is known to be a major source of airborne heavy metals (*37*). Pb was found together with Zn in a lot of particles classified as Pb/high-*Z*, but also with other heavy metals such as Sn and Cu. Ferroalloy production is probably the main emitter of these types of particles. Their abundances varied between 3.0% in sector 5 and 24% in sector 2. Pb particles in correlation with Si can be associated with soil. This might be partly true since windblown soil dust is known to bring 20 000 tons of Pb into the atmosphere globally every year (*30*), but they could also be fly ash particles, containing high amounts of heavy metals (*38*). These particles sometimes constitute up to 50% of the particle abundance in the North Sea atmosphere (*6*). Other possibilities for Pb silicates are base metal smelting and refining (*33*).

TABLE 4

Abundances, Diameters, and Composition of Zn-Containing Particle Groups According to Their Different Source Sectors as Found by Statistical Clustering

particle type	total abun	abundance (%)	diameter (μm)	relative concentration (weight %) of main elements detected by EPXMA
		Sector 1: North/Northwest		
no Zn-containing particles encountered				
		Sector 2: Northeast/East		
Fe/Zn	48.5	30.9	0.5	Fe(72), **Zn**(18)
		17.6	0.5	S(19), Fe(41), **Zn**(27)
Zn sulfides	25.8	13.5	0.4	S(38), **Zn**(58)
		12.3	0.5	S(60), **Zn**(26)
pure Zn	8.7	8.7	0.4	**Zn**(100)
Si/Zn	7.8	7.8	0.8	Al(6), Si(23), S(12), K(10), **Zn**(90), Sn(4)
Zn/high-*Z*	5.7	5.7	0.5	Cl(4), **Zn**(51), Pb(38)
Zn/medium-*Z*	3.4	3.4	0.5	Cl(12), Ca(59), **Zn**(11)
		Sector 3: Southeast/South		
Fe/Zn	59.6	59.6	0.5	S(4), Fe(65), **Zn**(20)
Zn chlorides	16.0	16.0	0.6	Cl(28), **Zn**(48), Pb(9)
Zn sulfides	15.6	15.6	0.5	S(48), Cl(5), Fe(7), **Zn**(26)
Si/Zn	8.8	8.8	0.5	Si(42), Mn(6), Fe(17), **Zn**(18)
		Sector 4: Southwest/West		
Fe/Zn	45.5	29.6	0.6	Fe(73), **Zn**(14)
		15.9	0.6	Si(6), S(10), Fe(45), **Zn**(22)
Zn sulfides	18.8	11.0	0.5	S(59), Ca(6), **Zn**(20)
		7.8	0.4	S(40), **Zn**(57)
Zn/high-*Z*	15.1	6.2	0.7	P(8), Cu(5), **Zn**(58), Sn(9), Pb(10)
		6.2	0.5	**Zn**(38), Pb(59)
		2.7	0.4	Cr(58), Fe(28), **Zn**(8)
Si/Zn	10.5	10.5	0.9	Al(13), Si(50), S(7), Fe(8), **Zn**(11)
Zn chlorides	10.2	10.2	0.7	Si(7), S(12), Cl(49), **Zn**(20), Pb(5)
		Sector 5: Local		
Fe/Zn	39.8	16.7	0.5	Fe(63), **Zn**(28)
		15.8	0.6	Fe(83), **Zn**(10)
		7.3	0.6	Si(2), S(9), Ca(3), Mn(26), Fe(40), **Zn**(18)
Zn sulfides	32.1	11.1	0.5	S(34), Cl(30), **Zn**(32)
		9.2	0.4	S(65), **Zn**(28), As(4)
		6.0	0.4	S(44), **Zn**(51)
		5.8	0.6	S(29), Fe(37), **Zn**(26)
Si/Zn	8.1	4.9	0.7	Al(16), Si(19), S(9), Fe(25), **Zn**(13)
		3.2	0.7	Al(8), Si(54), S(6), Fe(6), **Zn**(16)
pure Zn	7.3	7.3	0.3	**Zn**(100)
Zn chlorides	6.9	6.9	0.7	Cl(53), **Zn**(30), Pb(7)
Zn/high-*Z*	3.6	3.6	0.4	P(7), K(7), **Zn**(44), Pb(34)
Zn/medium-*Z*	2.1	2.1	0.9	P(12), S(13), Ca(55), **Zn**(16)

Zinc-Containing Particles. Except for sector 1, particles containing Zn were found in all sectors. This clearly points to the fact that a marine source for Zn is very unlikely. In the other sectors together, 2815 Zn-rich particles were detected, what is almost twice as much as Pb-containing particles. As for Cr and Pb, we performed hierarchical, nonhierarchical, and fuzzy clustering on the combined Zn-rich particles for the five different sectors. This again resulted in the identification of seven major Zn-containing particle types (Table 4). The most important group is the Fe–Zn particles, which constitute up to 60% of the particle abundance (sector 3). Dependent on the wind direction, Zn sulfides make up between 16% and 32% of the Zn particles. Zn chlorides, often in the presence of Pb, were found to account for approximately 5–16% of the detected particles. Less abundant groups were "pure" Zn particles, Zn correlated with medium-*Z* elements such as Ca and P, high-*Z* elements such as Pb and Sn, and Zn particles with significant concentrations of Si. The particle size of Zn-containing particles seems to vary between 0.3 and 1.0 μm. These rather small variations make size-related interpretation of the data difficult.

Worldwide, most Zn production originates from ZnS minerals, which are converted into metallic Zn in a series of processes. The main use of Zn is in galvanizing iron and steel products, which are coated with a layer of Zn in order to increase the corrosion resistance. Zn is also used in numerous Zn–base alloys, which are utilized in a wide variety of applications such as Ni–Zn batteries. Other applications of Zn are in plumbing materials, as a catalyst in vulcanization processes (Zn oxides), in paints (ZnS), and in cosmetic and pharmaceutical products. Natural Zn emissions (43.5×10^6 kg year^{-1}), with windblown dust as a major contributor, are estimated to be almost 10 times lower than the combined industrial emissions (314×10^6 kg year^{-1}). Here the main sources are primary Zn production, iron and steel industries, industrial applications, coal and wood combustion, and waste incineration (*4*, *39*). The yearly total deposition flux of Zn into the southern bight of the North Sea was calculated to be 28 kg km^{-2} year^{-1}, which is approximately 4432 tons per year for the total area of the southern bight (*2*).

As for Cr, the most abundant group of Zn particles is particles containing high amounts of Fe. Sometimes these

particles held small concentrations of S and Si. Rybicka (*31*) found significant concentrations of Zn (200–2500 ppm) in mineral dusts containing Fe (magnetite and hematite) emitted by the different stages of the metallurgical production processes by knowing that the iron and steel industries are the second most important source of atmospheric Zn (*4*), and considering the large amount of metallurgical complexes in a rather short distance to our sampling area (northern France, Ruhr area, Gent area, and Manchester area), this might explain the large amount of Zn-containing Fe-rich particles. Strong correlations for Fe, Zn, and Mn above the North Sea (sector 5) have been reported before by Baeyens and Dedeurwaerder (*40*). They recognized metallurgical emissions from Dunkerque, Gravelines, and Boulogne as point sources for these elements.

Zn sulfides are the second most abundant group in three out of four sectors. They might be partly related to windblown Zn ores, which are mostly stored uncovered and therefore easily taken up by the wind, and which easily react to yield a number of secondary minerals. These minerals, such as $ZnCO_3$, can be partly responsible for the detected "pure" Zn particles (again, low-*Z* elements are not detected by our method). The reaction between Zn oxides and sulfuric acid, during release in metallurgical processes, might also yield a fraction of the detected Zn–S particles.

In sectors 3–5, 7–16% of the particles were Zn chlorides. The major part is probably linked to emissions of refuse incineration. The vaporization of volatile elements, among which are heavy metals, during combustion is followed by condensation of these elements on small particles present in the exhaust. The high concentrations of Cl species in the gas stream provides an excellent opportunity to form volatile metal chlorides (*37*). In the coarse fraction of incinerator particles, Mamane (*41*) found all particles to contain at least some Zn, K, and Cl. He stated that these particles were formed through the condensation of volatile Zn, K, and Cl on existing minerals. This type of particle was the only significant heavy metal-containing giant particle type found in the North Sea aerosol (*7*).

In most sectors, approximately 10% of the Zn-rich particles contained a significant percentage of Si. They might be partially related to windblown soil dust, since the average Zn concentration in soil is 100 ppm, but some contain more than 1000 ppm (*42*). On the other hand, these Zn-rich particles are probably for a significant fraction fly ash (just as Pb/Si particles), which is known to contain important concentrations of heavy metals (*38*, *43*). Also, the small average diameter of this group (0.5 μm) points to a significant anthropogenic fraction. Although the concentrations of heavy elements such as Cr, Pb, and Zn might not be high enough in most fly ash particles to be detected with our method, this does not mean that they do not contribute to the atmospheric input of trace metals to the North Sea.

Other less frequently occurring particle types were Zn in association with Pb, Cr, and Sn. Again, ferroalloy production is presumably the main source of these particles. Abundances were as high as 15% (sector 4). Zn associated with medium-*Z* elements such as Ca and P is likely derived from the manufacture of phosphate fertilizer or from cement production (*30*).

General Overview. The combined interpretation of the three cluster techniques produced 5–7 major particle types containing Cr, Pb, or Zn. Most of the particle types were directly or indirectly connected to emissions of the metallurgical industry, which is eminently present in the northern part of France, the German Ruhr area, and the industrial centers in the middle of the United Kingdom. A major part of Pb-rich particles was found to be associated with automotive exhaust. Less important sources were cement production and refuse incineration.

On top of this, we should not forget that concentrations lower than 1000 ppm cannot be detected with ED EPXMA. Thus, we must presume that at least a fraction of the particles containing lower concentrations of Cr, Pb, and Zn were not identified as heavy metal-containing, but indeed contribute to the atmospheric heavy metal inputs. An important example of such a particle type is fly ash, which constitutes a major part of North Sea particulate matter. Only a small fraction of these fly ash particles were found with heavy metal concentrations higher than 1000 pmm. This does not mean that they do not contribute to the heavy metal inputs, when considering the high amounts of fly ash particles in some sectors.

Our results provide ample evidence for the apparent existence of a heavy metal-containing North Sea aerosol. It was mainly overlooked in previous investigations using single-particle analysis, because these particles are "drowned" in an excess of other, more abundant, particle types such as sea salt and aluminosilicates. The enormous number of particles (48 000) obtained by our automated analysis method allows us to acquire much more statistically reliable results than by manual single-particle analysis, with which only a few hundred particles can be analyzed in a reasonable time. It is exactly this huge database that allowed us to focus on special, low-abundant particle types such as heavy metal-containing particles.

Acknowledgments

We acknowledge the financial support by Rijkswaterstaat, Dienst Getijdewateren (The Netherlands) under Grants NOMIVE*2 No DGW-920 and No DGW-217 and, at a later stage, by the Belgian State—Prime Minister's Office—Services for Scientific, Technicol and Cultural Affairs (Contract MS/06/050 of the Impulse Program in Marine Sciences).

Literature Cited

(1) Katrinak, K. A.; Anderson, J. A.; Buseck, P. R. *Environ. Sci. Technol.* **1995**, *29*, 321–329.
(2) Rojas, C. M.; Injuk, J.; Van Grieken, R. E.; Laane, R. W. *Atmos. Environ.* **1993**, *27A*, 251–259.
(3) Hooper, J. F.; Ross, H. B.; Sturges, W. T.; Barrie, L. A. *Tellus* **1991**, *43B*, 45–60.
(4) Nriagu, J. O.; Pacyna, J. M. *Nature* **1988**, *333*, 134–139.
(5) Ottley, C. J.; Harrison, R. M. *Sci. Total Environ.* **1991**, *100*, 301–318.
(6) Rojas, C. M.; Van Grieken, R. E. *Atmos. Environ.* **1992**, *26A*, 1231–1237.
(7) Van Malderen, H.; Rojas, C.; Van Grieken, R. *Environ. Sci. Technol.* **1992**, *26*, 750–756.
(8) Dierck, I.; Michaud, D.; Wouters, L.; Van Grieken, R. *Environ. Sci. Technol.* **1992**, *26*, 802–808.
(9) Rojas, C. M.; Van Grieken, R. E.; Maenhaut, W. *Air Soil Pollut.* **1993**, *71*, 391–404.
(10) Injuk, J.; Otten, Ph.; Laane, R.; Maenhaut, W.; Van Grieken R. *Atmos. Environ.* **1992**, *26A*, 2499–2508.
(11) Rojas, C. M.; Otten, Ph. M.; Van Grieken, R. E.; Laane, R. W. In *Air Pollution Modelling and Its Application*; van Dop, H., Steyn, D., Eds.; Plenum Press: New York, 1991.
(12) Rojas, C. M.; Van Grieken, R. E.; Laane, R. W. *Atmos. Environ.* **1993**, *27A*, 363–370.
(13) Pena, J. A.; Norman, J. M.; Thomson, D. W. *J. Air Pollut. Control Assoc.* **1977**, *27*, 337–340.
(14) Otten, Ph.; Rojas, C.; Wouters, L.; Van Grieken, R. Atmospheric Deposition of Heavy Metals (Cd, Cu, Pb and Zn) into the North

Sea. Report 2 to Rijkswaterstaat (The Hague, The Netherlands) on Project NOMIVE*2 DGW 920, University of Antwerp (UIA), Belgium.
(15) Bondarenko, I.; Treiger, B.; Van Grieken, R.; Van Espen, P. *Spectrochim. Acta Electron.*, submitted.
(16) Crutcher, H. L.; Rhodes, R. C.; Graves, M. E.; Fairbaim, B.; Nelson, A. C. *JAPCA* **1986**, *36*, 1116–1122.
(17) Saucy, D. A.; Anderson, J. R.; Buseck, P. R. *Atmos. Environ.* **1987**, *21*, 1649–1657.
(18) Shattuck, T. W.; Germani, M. S.; Buseck, P. R. *Anal. Chem.* **1991**, *63*, 2646–2656.
(19) Bernard, P. C.; Van Grieken, R. E. *Anal. Chim. Acta* **1992**, *267*, 81–93.
(20) Treiger, B.; Bondarenko, I.; Van Malderen, H.; Van Grieken, R. *Anal. Chim. Acta*, in press.
(21) Bondarenko, I.; Van Malderen, H.; Treiger, B.; Van Espen, P.; Van Grieken, R. *Chemom. Intell. Lab. Syst.* **1994**, *22*, 87–95.
(22) Chester, R.; Bradshaw, G. F. *Mar. Pollut. Bull.* **1991**, *22*, 30–36.
(23) Duce, R. A.; Liss, P. S.; Merrill, J. T.; Atlas, E. L.; Buat-Menard, P.; Hicks, B. B.; Miller, J. M.; Prospero, J. M.; Arimoto, R.; Church, T. M.; Ellis, W.; Galloway, J. N.; Hansen, L.; Jickels, T. D.; Knap, A. H.; Reinhard, K. H.; Schneider, B.; Soudine, A.; Tokas, J. J.; Tsunogai, S.; Wollast, R.; Zhou, M. *Global Biogeochem. Cycles* **1991**, *5*, 193–259.
(24) Ottley, C. J.; Harrison, R. M. *Atmos. Environ.* **1993**, *27A*, 685–695.
(25) *Toxic Metals in the Atmosphere*; Nriagu, J. O., Davidson, C. I., Eds.; Advances in Environmental Science and Technology 17; Wiley and Sons: New York, 1986.
(26) Nriagu, J. O. In *Chromium in the Natural and Human Environments*; Nriagu, J. O., Nieboer, E., Eds.; Advances in Environmental Science and Technology 20; Wiley and Sons: New York, 1988.
(27) Moore, J. W.; Ramamoorthy, S. *Heavy Metals in Natural Waters*; Springer-Verlag: New York, 1984.
(28) Natusch, D. F.; Wallace, J. R. *Science* **1974**, *86*, 695–699.
(29) Xhoffer, C.; Bernard, P.; Van Grieken, R.; Van der Auwera, L. *Environ. Sci. Technol.* **1992**, *25*, 1470–1478.
(30) Pacyna, J. M. In *Toxic Metals in the Atmosphere*; Nriagu, J. O., Davidson, C. I., Eds.; Advances in Environmental Science and Technology 17; Wiley and Sons: New York, 1986.
(31) Rybicka, E. H. *Environ. Technol. Lett.* **1989**, *10*, 921–928.
(32) Pacyna, J. M.; Nriagu, J. O. In *Chromium in the Natural and Human Environments*; Nriagu, J. O., Nieboer, E., Eds.; Advances in Environmental Science and Technology 20; Wiley and Sons: New York, 1988.
(33) Fergusson, J. E. *The Heavy Elements*; Pergamon Press: Oxford, 1990.
(34) Harrison, R. M. In *Toxic Metals in the Atmosphere*; Nriagu, J. O., Davidson, C. I., Eds.; Advances in Environmental Science and Technology 17; Wiley and Sons: New York, 1986.
(35) Harrison, R. M.; Sturges, W. T. *Atmos. Environ.* **1983**, *17*, 311–328.
(36) Hirschler, D. A.; Gilbert, L. F.; Lamb, F. W.; Niebylski, L. M. *Ind. Eng. Chem.* **1957**, *49*, 1131–1142.
(37) Greenberg, R. R.; Zoller, W. H.; Gordon, G. E. *Environ. Sci. Technol.* **1978**, *12*, 566–573.
(38) Norton, G. A.; Malaby, K. L.; Dekalb, E. L. *Environ. Sci. Technol.* **1988**, *22*, 1279–1283.
(39) Nriagu, J. O. *Nature* **1979**, *279*, 409–411.
(40) Baeyens, W.; Dedeurwaerder, H. *Atmos. Environ.* **1991**, *25A*, 1077–1092.
(41) Mamane, Y. *Atmos. Environ.* **1988**, *22*, 2411–2418.
(42) Aubert, H.; Pinta, M. *Trace Elements in Soils*; Elsevier Scientific Publishing: Amsterdam, 1977.
(43) Ondov, J. M.; Choquette, C. E.; Zoller, W. H.; Gordon, G. E.; Biermann, A. H.; Heft, R. E. *Atmos. Environ.* **1989**, *23*, 2193–2204.

Received for review March 24, 1995. Revised manuscript received September 11, 1995. Accepted September 12, 1995.[⊗]

ES950205L

[⊗] Abstract published in *Advance ACS Abstracts,* December 1, 1995.

Selected article #21:

Gypsum and other calcium-rich particles above the North Sea
S. Hoornaert, H. Van Malderen and R. Van Grieken
Environmental Science and Technology, 30 (1996) 1515-1520

ENVIRONMENTAL
SCIENCE & TECHNOLOGY

Gypsum and Other Calcium-Rich Aerosol Particles above the North Sea

Stefaan Hoornaert, Hans Van Malderen, and René Van Grieken

Department of Chemistry, University of Antwerp (UIA), Universiteitsplein 1, B-2610 Antwerpen, Belgium

Reprinted from
ENVIRON. SCI. & TECHNOL., Volume 30, Number 5, Pages 1515–1520

Gypsum and Other Calcium-Rich Aerosol Particles above the North Sea

STEFAAN HOORNAERT, HANS VAN MALDEREN, AND RENÉ VAN GRIEKEN*

Department of Chemistry, University of Antwerp (UIA), Universiteitsplein 1, B-2610 Antwerpen, Belgium

Ca-containing particles, especially $CaSO_4$ particles, have been encountered in several atmospheric aerosol studies. An overview is given of the different sources of airborne Ca-containing particles. The North Sea atmosphere is studied to identify the different Ca-containing particle types and to find the correlation between their occurrence and the source regions of the corresponding air masses. About 50 000 individual aerosol samples were collected above the Southern Bight of the North Sea for several wind directions and analyzed for their composition using electron probe X-ray microanalysis. Nonhierarchical cluster analysis is performed on the data to reveal the different particle types, their relative abundances and their sources. $CaSO_4$ in most cases constitutes the largest fraction of the Ca-containing particles. Extremely high numbers of $CaSO_4$ particles are found for northeastern winds, coming from the central part of Germany, suggesting that a great fraction is derived from anthropogenic sources located in this region. Among the other Ca-containing particle types are the aluminosilicates, $CaCO_3$, Fe–Ca-rich particles, and $CaSO_4$ or $CaCO_3$ in combination with NaCl.

Introduction

Prior studies have pointed out that atmospheric deposition is a major source for the input of some heavy metals into the Southern Bight of the North Sea (*1*, *2*). The presence of quite considerable amounts of $CaSO_4$ particles in several studies of the North Sea atmosphere, as well as the possible interaction of hygroscopic particles in cloud formation processes (*3*), resulted in a growing interest in this type of particulates and their emission sources (*4*–*7*). In this work, we therefore want to give an overview of the sources of airborne Ca-containing, especially $CaSO_4$, particles. Neither type of particle has ever been studied in more detail. Several sources have been reported by various authors, but they have never been gathered in one paper. We discuss the results of automated electron probe X-ray microanalysis of airborne particulate matter, collected in the North Sea atmosphere with the aid of an airplane. Single-particle analysis, combined with multivariate statistical approaches, like nonhierarchical cluster analysis, has proven to be a useful tool in air pollution studies and especially in the apportionment of the different aerosol sources (*7*–*11*).

Experimental Section

Sampling Strategy. The samples used were taken over the Southern Bight of the North Sea, using a twin-engine Piper Chieftain PA 31-350 call sign PH-ECO of Geosens B.V. Co. The aircraft is equipped with an isokinetic inlet for the sampling of particulate matter (*12*). In our experimental setup, a 47 mm diameter "aerosol-grade" Nuclepore filter with 0.4 μm pore size is used. Nineteen flights were made, of which 16 yielded useful sample sets. All sampling flights were performed in the same way. At the Goeree platform (position 51°55′ N, 03°40′ E), an upward spiral track was performed, during which the temperature inversion height is localized. Once this was achieved, tracks were flown at six different heights equally spaced under the inversion layer. Filter samples were collected on each track. All tracks were flown parallel to the wind direction. Thirty-six hour back-trajectories were calculated by the KNMI (De Bilt, the Netherlands) for four different levels (1000, 900, 850, and 700 mbar). More details on the sampling campaign can be found elsewhere (*13*).

Chemical Analysis. Single-particle analysis was done by electron probe X-ray microanalysis (EPXMA) using a JEOL JXA-733 superprobe (Tokyo, Japan) equipped with a TN-2000 energy-dispersive X-ray detection system (Tracor Northern, Middleton, USA). A modified particle recognition and characterization (PRC, Tracor Northern, Middleton, WI) software package, the 733B program, allowed us to perform automated individual particle analysis. Once the particles are localized, their diameter, area, and shape factor are computed, and finally an X-ray spectrum is accumulated. For each sample (one per flight track), up to 500 particles were analyzed.

Numerical Analysis. To allow a comparison between the results for different wind directions, all flights were classified into five wind sectors according to the origin of the air masses as inferred from the back-trajectories: northeast-east (NE-E), southeast-south (SE-S), southwest-west (SW-W), northwest (NW) (Figure 1), and a "local" sector (with variable wind drections). Data reduction and interpretation, in particular classification of particles with similar chemical composition into "particle groups", was done by cluster analysis. All elements that were detected in more than 1% of the particles were considered, i.e., Na, Mg, Al, Si, P, S, Cl, K, Ca, Ti, V, Cr, Mn, Fe, Ni, Cu, Zn, and Pb. Clustering was performed on the normalized elemental X-ray intensities using the software package DPP (*14*). Because of the great number of particles, hierarchical clustering requires an enormous amount of computer time for calculating the distances between the particles in each cycle of the hierarchical clustering. Therefore, we used the nearest centroid sorting method of Forgy, a nonhierarchical clustering procedure. The number of clusters (particle groups) is determined by the so-called consistent Akaike's information criterion (CAIC), a mathematical function based on the relation between order, entropy, and information of an isolated system. Its value reaches a minimum for the optimum number of clusters. The criterion is

0013-936X/96/0930-1515$12.00/0

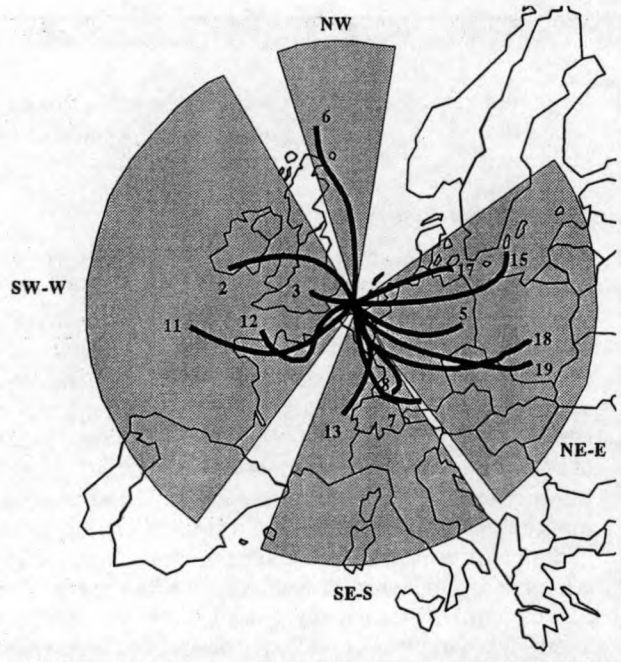

FIGURE 1. Classification of the different sampling flights into five sectors (the local sector is not shown). The indicated lines are the corresponding 1000 hPa air mass trajectories for air masses arriving at the sampling site.

discussed in more detail by Bondarenko et al. (*15*). The program for calculating the criterion forms part of the home-made integrated data analysis system (IDAS), which has recently become available (*16*). After the clustering, *ZAF* correction (a mathematical procedure to correct the observed X-ray intensities for differences in matrix composition between standards and unknown samples) was carried out in order to convert the relative peak intensities into elemental weight compositions.

Results and Discussion

Only the NW sector, which contains only flight 6, can be regarded as purely marine. The results of two sectors reflect the continental influence, natural as well as anthropogenic. These are the NE-E sector, including flights 5, 15, 17, 18, and 19, for which the air masses have passed over Belgium, the Netherlands, Germany, and some eastern European countries, and the SE-S sector, including flights 7, 8, and 13, influenced by Belgium, the southern part of Germany, and the northern and eastern parts of France. Samples collected during flights 2, 3, 11, and 12 characterize the SW-W sector and are related to the influences of the United Kingdom and the northwestern part of France, but also to some extent those of the north Atlantic Ocean and the English Channel. Finally, aerosols collected during flights 4, 9, and 14 were obtained under low wind speed and variable wind direction conditions; therefore, they are classified in the local sector.

(1) Investigation of the Ca-Containing Particles. Cluster analysis was performed on the EPXMA data in order to identify the different types of Ca-containing particles (these are particles with a Ca content >0%). Since we are mainly interested in those particles in which Ca is not just a minor element, we made a selection of all the particles having a relative Ca X-ray peak intensity >10% of that from all elements (hereafter these particles will be called "Ca-enriched" particles, not to be confused with Ca-rich particles, used in other studies, which are composed of mainly Ca). So, by using this threshold value, the clusters should be better separated, and therefore interpretation of them should be easier. Comparing the numbers of particles after selection with the original number of analyzed particles yields the "Ca > 10" fraction, which is reported for all flights and sectors in Table 1. The values shown for each flight are the averages over the six tracks.

TABLE 1

Ca > 10 Fraction for the Different Flights (Averaged over the Six Tracks) and Sectors

flight no.	Ca > 10 fraction (%)	flight no.	Ca > 10 fraction (%)
northwest		southwest-west	
6	1.6	2	16
northeast-east		3	12
5	39	11	7
15	31	12	15
17	24	average	12
18	18	local	
19	17	4	16
average	26	9	13
southeast-south		14	17
7	12	average	15
8	13		
13	16		
average	14		

(1.1) Fraction of Ca-Enriched Particles. We can see from these results that, in general, the value of the Ca > 10 fraction ranges from 7% to 18%. Four flights are exceptions to this rule: flight 6 with only 1.6%, flight 5 with 39%, flight 15 with 31%, and flight 17 with 24%. The lower fraction for flight 6 is due to the great contribution of seasalt particles in this sector as a result of the marine origin of the corresponding air masses and is probably also due to the sea being only a minor source of Ca-enriched particulates. The values of flight 17 and especially flights 5 and 15 are rather high. All three flights belong to the NE-E sector, and their respective air masses have passed over nearly the same regions, including Germany and the Netherlands, suggesting some very important sources of Ca in this region. We also found, by inspecting the Ca > 10 fractions for the different tracks separately, that Ca is distributed rather homogeneously over the six tracks for each flight (small or no decreasing or increasing trends), except again for flights 5 and 15, where higher fractions are found in the lower tracks (up to 49% and 39% for the sixth track of flights 5 and 15, respectively). These lower tracks correspond to air masses coming from even a smaller region, the central and northern parts of Germany and the Netherlands. The high values for these flights result in a high Ca fraction for the whole NE-E sector (26% in comparison to 15% for the local sector and even lower fractions in the other). The big difference between the two continental sectors (NE-E and SE-S) might suggest that mainly anthropogenic sources are responsible for the high values in the NE-E sector.

(1.2) Cluster Analysis for the Ca-Enriched Particles. The nonhierarchical cluster analysis of the Ca-enriched (Ca > 10) particles should provide us with the different particle types. The numbers of clusters, determined by the CAIC criterion, are slightly different for the five sectors. Except for the NW sector, for which four different clusters are found, the number of groups is six or seven. The results, after *ZAF* correction, are summarized in Table 2.

The results from enrichment factor (EF) and back-trajectory calculations show that the marine sources of

TABLE 2

Results of the Nonhierarchical Clustering of the Data after Selection of the Ca-Enriched Particles

cluster no.	elemental composition (wt %) (relative to all elements detectable by EPXMA)	classification	abundance (%)
	Northeast-East		
1	Ca(48) S(45)	$CaSO_4$	49
2	Si(43) Al(19) Ca(17) Fe(12)	aluminosilicates	14
3	Ca(30) Si(20) S(19) Al(12) Fe(8)		11
4	Fe(34) Ca(27) S(23)		9.1
5	Ca(58) S(10) P(5)		7.6
6	Fe(68) Ca(13)		5.6
7	Ca(96)	Ca-rich	4.3
	Southeast-South		
1	Ca(48) S(43)	$CaSO_4$	36
2	Si(43) Ca(20) Al(13) Fe(11)	aluminosilicates	17
3	Ca(26) S(26) Si(15) Fe(5)		16
4	Fe(43) Ca(19) S(13) Zn(10)		13
5	Ca(63) P(10) Pb(9)		10
6	Fe(79) Ca(10)		7.8
	Southwest-West		
1	Ca(46) S(42)	$CaSO_4$	33
2	Si(42) Al(17) Ca(17) Fe(13)	aluminosilicates	15
3	Cl(57) Na(22) Ca(15)	$NaCl-CaCO_3$	14
4	Ca(83)	Ca-rich	13
5	Ca(31) S(15) Si(14) Fe(13)		12
6	Cl(32) Ca(28) S(17) Na(11)	$NaCl-CaSO_4$	7.4
7	Fe(73) Ca(13)		6.4
	Northwest		
1	Cl(42) Na(36) Ca(12) S(8)	$NaCl-CaSO_4$	48
2	Ca(51) S(36)	$CaSO_4$	31
3	Ca(47) Fe(15) Si(14) Mg(8)		15
4	Si(47) Al(27) Ca(17) Fe(9)	aluminosilicates	6.3
	Local		
1	Ca(48) S(43)	$CaSO_4$	41
2	Si(42) Al(19) Ca(17) Fe(12)	aluminosilicates	18
3	Ca(21) S(20) Na(18) Cl(6)		14
4	Ca(51) P(11) Pb(6)		11
5	Ca(90)	Ca-rich	9.2
6	Fe(77) Ca(13)		7.7

atmospheric Ca compounds are less important than the land-based ones, natural or anthropogenic. Only about 25% of airborne Ca comes from the sea (*17*), and at least 60% of Ca is coming from nonsoil sources (*18*). So it seems that a considerable amount of the atmospheric Ca content is originating from anthropogenic sources.

With this information, we tried to relate the different particle types that resulted from our clustering with possible sources. From Table 2 it is clear that, in every case, $CaSO_4$ is the most abundant particle type, except for the NW sector. In the NE-E sector, these particles are even responsible for half of the Ca-enriched particles (49%) (expressed relative to all elements detectable by EPXMA, so excluding elements with $Z < 11$; this definition will be used systematically below), but also in the other sectors they constitute more than 30% of the total load of Ca-enriched particles (local, 41%; SE-S, 36%; SW-W, 33%; NW, 31%). The sources for these airborne particulates are discussed in part 2.2.

The aluminosilicates are the second most important Ca-enriched group for the continental sectors (NE-E and SE-S) the local and the SW-W sectors, but their abundance is much less than that of $CaSO_4$ (only 14−18%). For the marine sector, however, they constitute the least abundant group (6.3%). Considering the major elements, the composition of this cluster is nearly the same for every sector: 42−47 wt % Si, 13−27 wt % Al, 17−20 wt % Ca, and 9−12 wt % Fe. The sources for this airborne particulates are soil dust, transported into the air by the action of erosion and wind (*19*−*21*), stack emissions from coal-fired power plants and boilers (*22*), and probably also emissions from waste incinerators, which are characterized by the same elements in similar proportions (*23*).

Thus far, the results for the different sectors are very alike. Concerning the other groups, there is still a good resemblance between the main elemental compositions of most of the clusters, but there are some differences between the sectors in their relative importance. In all the air masses that have traveled over the sea to some extent, a cluster is found that is mainly composed of Cl, Na, Ca, and S. Examining the composition of the individual particles in these clusters revealed that we are dealing with mixed particles (all four elements present), so the combination of these elements is not the result of the classification of two different particle types, e.g., $CaSO_4$ and NaCl, in one and the same cluster. The high Na and Cl content can be attributed to the sea, the main source of atmospheric NaCl aerosols, which is confirmed by the absence of these particles in continental air masses. Also, the Ca component may originate from the sea under the form of $CaCO_3$ (coccoliths), as reported by Rojas and Van Grieken (*19*), which then might react with atmospheric sulfur compounds. However, one must not forget the possible coagulation between airborne $CaSO_4$ and NaCl particulates. These particles constitute nearly half of the Ca-enriched particles in the NW sector (48%), while in the local sector they are the third most abundant particle type (14%). In the SW-W sector, they are much less important (the second last group); however, here, there is a similar group that is much more important with a similar composition, except for the sulfur content, which is now much lower. This can

be interpreted as the coagulation between $CaCO_3$, which may be partly derived from the cliffs along the English Channel, situated in this sector (*7*), and NaCl or as the incomplete reaction between marine particles and atmospheric sulfur. In this sector, the role of the sea in the formation of this particle type is very clear if one considers the results for the different flights separately; the particles are much more abundant in the samples collected during flights 11 and 12, when the air was passing mainly over the English Channel, than during flights 2 and 3, when the air was coming from the UK.

The third most abundant Ca-enriched particles in both of the continental air masses (NE-E, 11%; SE-S, 16%) which are also present in the SW-W sector (12%), are composed of Ca (26−31 wt %), S (15−26 wt %), Si (14−20 wt %), and Fe (5−13 wt %) and sometimes also contain some Al. The combination of Ca, S, and Si can be thought of as being $CaSO_4$ particles with a silicate core and are most likely formed by combustion processes (*24*). This type of Ca-enriched particles is absent in the local and the marine sectors.

Except for the marine sector, Fe−Ca-rich particles are present everywhere. Two different Fe−Ca-rich particle types can be found. The first one, which is present in each of the four sectors, is composed of mainly Fe (68−79 wt %) and Ca (10−13 wt %) but is the least abundant cluster in almost every sector (5.6%−7.8%). The second type is present only in the continental air masses and is characterized by Fe (34−43 wt %), Ca (19−27 wt %), and also S (13−23 wt %) but with abundances that are somewhat higher (9.1% for the NE-E sector and 13% for the SE-S sector). According to Hopke (*23*), such Fe−Ca-rich emissions are characteristic for sewage sludge incineration and several ferrous metal-related sources. These assumptions are supported by the presence of some heavy metals like Pb and Zn (*25*).

Clusters containing only Ca are identified as $CaCO_3$ (*24*) (C and O cannot be detected by our method). In our clustering, these particles are present mainly in the SW-W sector (13%) but are also in the local (9.2%) and the NE-E sectors (4.3%). As mentioned earlier, airborne $CaCO_3$ can be of marine origin or from sources on the land. The latter include both natural and anthropogenic sources. An important natural source, which might explain the relatively higher abundance in the SW-W sector, is again the cliffs along the English Channel (*7*). Industrial sources with important Ca emissions are the production of construction materials like asphalt and concrete batch plants and limestone kilns (*20, 23*). Other important calcite-emitting industries are iron and steel plants, chemical plants, heat- and power-generating plants and cement plants (*20, 26*−*28*), agricultural liming (*20, 27, 28*), and the abrasion of streets and buildings (*28*).

The identification of the remaining particle types is less clear; however, the combination of Ca and P found mainly in the local and the SE-S sectors and also in the NE-E might suggest the cement industry (*23*).

(2) A Closer Look at the $CaSO_4$ Particles. (2.1) Fraction of CaSO4 Particles. From the above results, it is clear that the $CaSO_4$ particles are joined in a single cluster for each of the sectors, providing us with the number of $CaSO_4$ particles. In the following discussion, we use these numbers of $CaSO_4$ particles to make some comparisons. The selection of the particles with a relative Ca intensity greater than 10% should not have any influence on the number of $CaSO_4$ particles, since the latter by definition have a Ca content greater than 10%. In Table 3, a comparison is made for each flight between the $CaSO_4$ particles and the original number of particles (called the $CaSO_4$ fraction).

TABLE 3

Gypsum Fraction for the Different Flights (Averaged over the Six Tracks) and Sectors

flight no.	$CaSO_4$ fraction (%)	flight no.	$CaSO_4$ fraction (%)
northwest		southwest-west	
6	0.5	2	7
northeast-east		3	7
5	29	11	2
15	12	12	2
17	12	average	4
18	5	local	
19	4	4	5
average	13	9	6
southeast-south		14	7
7	5	average	6
8	5		
13	5		
average	5		

For the different flights, it can be said that as a general rule the value of the $CaSO_4$ fraction lies between 2% and 7%. Again, some outlying values are present for flights classified in the marine sector and the NE-E sector. Flight 6 contains only 0.5% of $CaSO_4$ particles, while flights 15, 17, and especially 5 contain much more of them (12%, 12%, and 29%, respectively). It is also clear again that, although flights 2, 3, 11, and 12 have been joined in one and the same cluster, there exists a difference between the composition of the air masses corresponding to them. The $CaSO_4$ fractions for flights 11 and 12, which are influenced mainly by the English Channel, are rather low (2%), while the fractions for flights 2 and 3, mainly influenced by the UK, are higher (7%). To get a better view on the dependence of the $CaSO_4$ fractions on the origin of the air masses for the two continental sectors, the back-trajectories for each track were compared and ordered geographically from north to south (Figure 2). Back-trajectories which were too variable and could not be assigned to a single direction were omitted. The corresponding $CaSO_4$ fractions for the ordered tracks are represented graphically in Figure 2. A remarkable trend is observed. High values (10% or more) are found for air masses passing over the northern part of Germany and the Netherlands and even much higher values (up to 40%) for the central part of Germany. For wind directions more to the south, the $CaSO_4$ fractions are much lower (less than 8%) and more uniformly distributed. Thus, it is apparent that some very important $CaSO_4$ sources are situated in Germany and its neighboring Eastern European countries.

(2.2) Sources of $CaSO_4$ Particles. *Marine Sources of $CaSO_4$.* The occurrence of pure $CaSO_4$ in the atmosphere can be the result of fractional crystallization of marine aerosols (*29, 30*). The evaporation of seawater is accompanied by sequential crystallization of several salts: as a first step, calcite ($CaCO_3$) and dolomite ($CaMg(CO_3)_2$) crystallize, next gypsum ($CaSO_4(aq)$), followed by halite (NaCl), and finally the Mg−K salts (*31*). In this way, loosely bound conglomerates of several particles are formed which are shattered during transport in the atmosphere or by impaction on the filter during sampling. This might result in the presence of one of these pure salts in the samples.

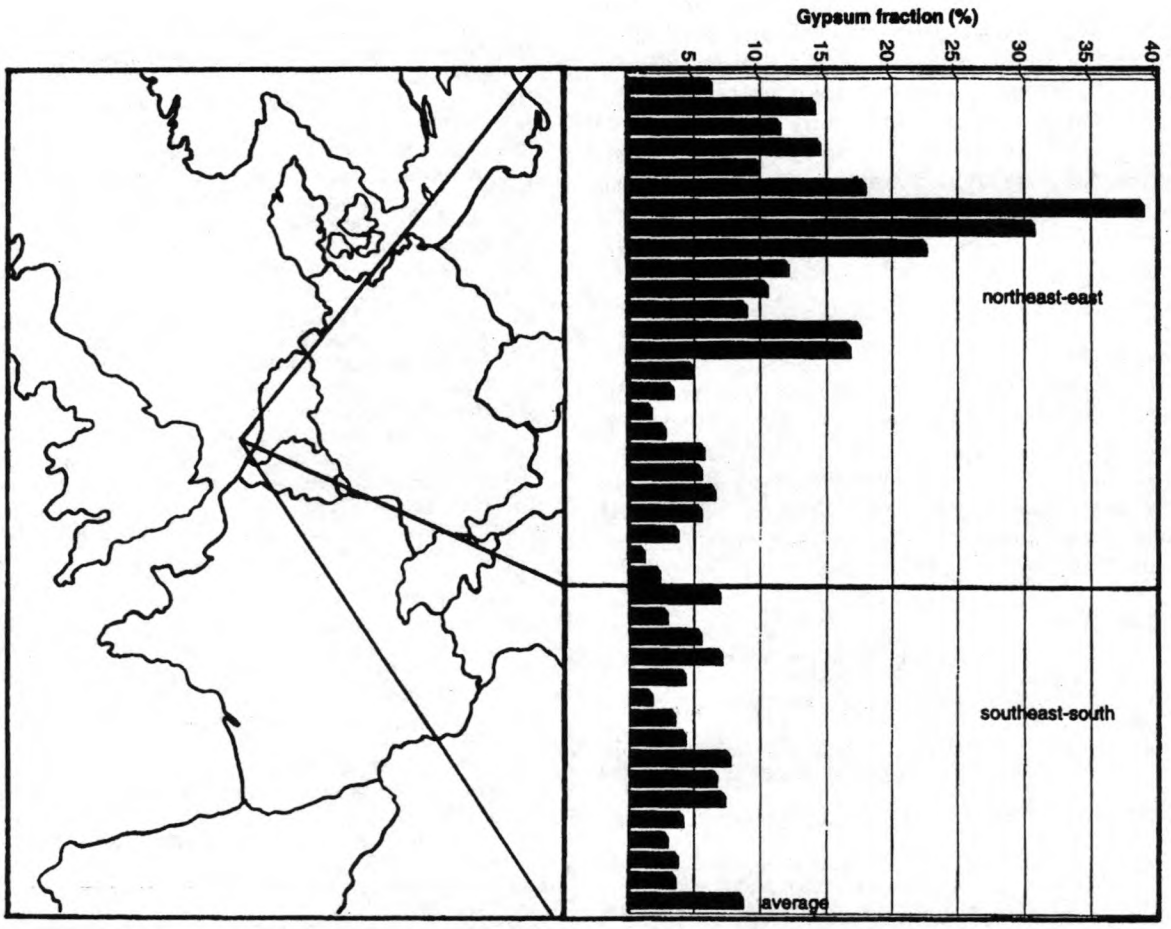

FIGURE 2. Fraction of gypsum particles of ordered geographically from north to south for both of the continental sectors.

Another marine source of $CaSO_4$, though indirect, is the reaction of marine $CaCO_3$ with atmospheric sulfur components, mainly H_2SO_4, formed by the oxidation of SO_2 (direct industrial emissions), H_2S (anaerobic decomposition), DMSO, or DMS (algae) (*4, 30, 32*). This reaction also takes place on the filters during and after sampling, resulting in a clean, fresh appearance of the crystals (*33, 34*). The marine $CaCO_3$, coming from the skeletons of pelagic organisms and coccoliths, which create a suitable chemical environment for this reaction because of their alkalinity, is introduced in the atmosphere by sea spray.

Land-Based Sources of $CaSO_4$. A variety of land-based sources of $CaSO_4$ have been suggested in the past by several authors. Van Borm et al. (*35*) indicated that primary atmospheric $CaSO_4$ particles are produced by the weathering of limestone buildings, covered by a crust of gypsum, which is formed by interaction with atmospheric sulfur compounds. Other sources of $CaSO_4$ are proposed by Biggins and Harrison (*36, 37*), like the attrition of building materials such as plaster and dusts from quarries, from which gypsum is extracted commercially. In the latter case, the particulates are derived from wind erosion, blasting, and transport of the quarried material. Still other sources are reported by Rybicka (*26*), who finds gypsum in dusts emitted by metallurgical plants, and by Bruynseels et al. (*4*), who suggested combustion processes and eolian transport from the continent as sources of $CaSO_4$. The former is also implied by Shattuck et al. (*24*), who associate this particle type with the combustion of coal. Del Monte and Sabbioni (*38*), who investigated the morphology and the mineralogy of fly ash from a coal-fueled power plant, discovered that the fly ash, when exposed to a high level of relative humidity, leads to the nucleation of gypsum crystals. The gypsum is thus confirmed not to be a crystalline phase of the fly ash emissions but to have an airborne origin on the fly ash particles. Also, carbonaceous particles emitted by oil combustion seem to behave in the same way. Similarly, Andreae et al. (*30*) find $CaSO_4$ particles on silicate aerosol particles. These are produced by the reaction between acid sulfates and silicate minerals brought together by in-cloud processes, and they are characterized by a low Ca content in the silicate component because of extraction of Ca from the minerals by H_2SO_4. Just as marine $CaCO_3$, land-derived $CaCO_3$ can react with atmospheric SO_2 or H_2SO_4 to form airborne $CaSO_4$. The $CaCO_3$ is present in dust from metallurgical plants, chemical plants, and cement plants (*26*) or is originating from soil dust and road wear (*35*). According to Ichikuni (*39*), it can also be the result of the world-wide spreading of desert dust, which contains $CaCO_3$ as a major constituent. Another source of airborne $CaSO_4$ is the desulfurization processes in thermal power plants that use limestone for SO_2 removal. Besides other sulfur emission control techniques, two limestone injection processes are applied. One is a dry process, in which limestone is injected into the high-temperature combustion zone as a mixture with the coal, where it is calcined as $CaCO_3 \rightarrow CO_2 + CaO$. Part of the produced CaO reacts in the furnace with SO_2 to produce $CaSO_4$ as $CaO + SO_2 + 0.5O_2 \rightarrow CaSO_4$. A second, more effective limestone injection process is the wet variant, which is initiated like the dry process, but, in addition, the combustion flue gas and unreacted limestone are scrubbed after the furnace with a lime slurry, which flows down through a marble bed in the scrubber

for further removal of SO_2 (*40*–*42*). The different flue gas desulfurization processes in Germany produce about 1 Mton of gypsum each year. Parungo et al. (*29*), who made a study of plume aerosols from a coal-fired power plant which uses such a lime slurry to scrub the SO_2 gases, found that about 10% of the particles in the plume consisted of crystalline or irregular $CaSO_4$ particles. Drops of the $CaSO_4$ solution, formed in the scrubber, escape along with the flue gas, are transformed in solid $CaSO_4$ particles after evaporation, and are released into the plume.

Acknowledgments

S.H. is supported by the Belgian National Fund for Scientific Research (NFWO). We acknowledge partial financial support by the Belgian Federal Office for Scientific, Technical and Cultural Affairs in the framework of the Impulse Programme in Marine Sciences (Contract MS/06/050) and, before, by Rijkswaterstaat, the Netherlands (Contracts NOMIVE*2 DGW-217 and -920).

Literature Cited

(1) Injuk, J.; Otten, Ph.; Laane, R.; Maenhaut, W.; Van Grieken R. *Atmos. Environ.* **1992**, *26A*, 2499–2508.
(2) Rojas, C. M.; Injuk, J.; Van Grieken, R.; Laane R. W. *Atmos. Environ.* **1993**, *27A*, 251–259.
(3) Charlson, R. J.; Schwartz, S. E.; Hales, J. M.; Cess, R. D.; Coakley, J. A., Jr.; Hansen, J. E.; Hofmann, D. J. *Science* **1992**, *255*, 423–430.
(4) Bruynseels, F.; Storms, H.; Van Grieken, R. *Atmos. Environ.* **1988**, *22*, 2593–2602.
(5) Injuk, J.; Van Malderen, H.; Van Grieken, R.; Swietlicki, E.; Knox, J. M.; Schofield, R. *X-Ray Spectrom.* **1993**, *22*, 220–228.
(6) Rojas, C. M.; Otten, P. M.; Van Grieken, R. *J. Aerosol Sci.* **1989**, *20*, 1257–1260.
(7) Xhoffer, C.; Bernard, P.; Van Grieken, R.; Van der Auwera, L. *Environ. Sci. Technol.* **1991**, *25*, 1470–1478.
(8) Van Malderen, H.; Rojas, C.; Van Grieken, R. *Environ. Sci. Technol.* **1992**, *26*, 750–756.
(9) Sanchez Gomez, M. L.; Ramos Martin, M. C. *Atmos. Environ.* **1987**, *21*, 1521–1527.
(10) Saucy, D. A.; Anderson, J. R.; Buseck, P. R. *J. Geophys. Res.* **1991**, *96*, 7407–7414.
(11) Casuccio, G. S.; Janocko, P. B.; Lee, R. J.; Kelly, J. F.; Dattner, S. L.; Mgebroff, J. S. *J. Air Pollut. Control Assoc.* **1983**, *33*, 937–943.
(12) Pena, J. A.; Norman, J. M.; Thomson, D. W. *J. Air Pollut. Control Assoc.* **1977**, *27*, 337–341.
(13) Otten, Ph.; Rojas, C.; Wouters, L.; Van Grieken, R. *Atmospheric Deposition of Heavy Metals (Cd, Cu, Pb and Zn) into the North Sea;* Second report to Rijkswaterstaat on Project NOMIVE* DGW-920; University of Antwerp (UIA), Belgium, 1989.
(14) Van Espen, P. *Anal. Chim. Acta* **1984**, *165*, 31–49.
(15) Bondarenko, I.; Van Malderen, H.; Treiger, B.; Van Espen, P.; Van Grieken, R. *Chemom. Intell. Lab. Syst.* **1994**, *22*, 87–95.
(16) Bondarenko, I.; Treiger, B.; Van Grieken, R.; Van Espen, P. *Spectrochim. Acta Electron.*, in press.
(17) Yaaqub, R. R.; Davies, T. D.; Jickells, T. D.; Miller, J. M. *Atmos. Environ.* **1991**, *25A*, 985–996.
(18) Losno, R.; Bergametti, G.; Carlier, P. *J. Atmos. Chem.* **1992**, *15*, 333–352.
(19) Rojas, C. M.; Van Grieken, R. *Atmos. Environ.* **1992**, *26A*, 1231–1237.
(20) Parekh, P. P.; Husain, L. *Atmos. Environ.* **1988**, *22*, 707–713.
(21) Sadasivan, S.; Negi, B. S. *Sci. Total Environ.* **1990**, *96*, 269–279.
(22) Bacci, P.; Caruso, E.; Braga Marcazzan, G. M.; Redaelli, P.; Sabbioni, C.; Ventura, A. *Nucl. Instrum. Methods Phys. Res.* **1984**, *B3*, 522–525.
(23) Hopke, P. K. *Receptor modeling in environmental chemistry;* John Wiley and Sons: New York, 1985; pp 267–314.
(24) Shattuck, T. W.; Germani, M. S.; Buseck, P. R. In *Environmental Applications of Chemometrics;* Breen, J. J., Robinson, P. E., Eds.; ACS Symposium Series 292; American Chemical Society: Washington, DC, 1985; pp 118–129.
(25) Usero, J.; Rosa, F.; Ternero, M.; Gracia, I. *Int. J. Environ. Anal. Chem.* **1988**, *33*, 233–244.
(26) Rybicka, E. H. *Environ. Technol. Lett.* **1989**, *10*, 921–928.
(27) Kowalczyk, G. S.; Choquette, C. E.; Gordon, G. E. *Atmos. Environ.* **1978**, *12*, 1143–1153.
(28) Kowalczyk, G. S.; Gordon, G. E.; Rheingrover, S. W. *Environ. Sci. Technol.* **1982**, *16*, 79–90.
(29) Parungo, F. P.; Nagamoto, C. T.; Harris, J. M. *Atmos. Res.* **1986**, *20*, 23–37.
(30) Andreae, M. O.; Charlson, R. J.; Bruynseels, F.; Storms, H.; Van Grieken, R.; Maenhaut, W. *Science* **1986**, *232*, 1620–23.
(31) Borchert, H. In *Chemical Oceanography;* Riley, J. P., Skirrow, G., Eds.; Academic: London, 1965; pp 205–276.
(32) Moharram, M. A.; Sowelim, M. A. *Atmos. Environ.* **1980**, *14*, 853–856.
(33) Savoie, D. L.; Prospero, J. M. *J. Geophys. Res.* **1980**, *85*, 385–392.
(34) Prodi, F.; Santachiara, G.; Oliosi, F. *J. Geophys. Res.* **1983**, *88*, 10957–10968.
(35) Van Borm, W. A.; Adams, F. C.; Maenhaut, W. *Atmos. Environ.* **1989**, *23*, 1139–1151.
(36) Biggins, P. D. E.; Harrison, R. M. *J. Air Pollut. Control Assoc.* **1979**, *29*, 838–840.
(37) Biggins, P. D. E.; Harrison, R. M. *Atmos. Environ.* **1979**, *13*, 1213–1216.
(38) Del Monte, M.; Sabbioni, C. *Arch. Meteorol. Geophys. Bioklimatol.* **1984**, *B35*, 93–104.
(39) Ichikuni, M. *J. Geophys. Res.* **1978**, *83*, 6249–6252.
(40) Perkins, H. C. *Air Pollution;* McGraw-Hill: New York, 1974; pp 273–283.
(41) Nishimura, H. *How to Conquer Air Pollution, a Japanese Experience;* Elsevier: Amsterdam, 1989; pp 150–153.
(42) Breihofer, D.; Mielenz, A.; Rentz, O. *Emission Control of SO_2, NO_x and VOC at Stationary Sources in the Federal Republic of Germany;* Report supported by the Bundesminister für Umwelt, Naturschutz und Reaktorsicherheit/Umweltbundesamt, Karlsruhe, 1991.

Received for review June 22, 1995. Revised manuscript received January 12, 1996. Accepted January 15, 1996.[⊗]

ES9504350

[⊗] Abstract published in *Advance ACS Abstracts,* March 15, 1996.

Selected article #22:

Deposition of atmospheric trace elements into the North Sea: coastal, ship, platform measurements, and model predictions

J. Injuk, R. Van Grieken and G. de Leeuw

Atmospheric Environment, 32 (1998) 3011-3025

Pergamon

Atmospheric Environment Vol. 32, No. 17, pp. 3011–3025, 1998

Printed in Great Britain
PII: S1352-2310(97)00497-4
1352-2310/98 $19.00 + 0.00

DEPOSITION OF ATMOSPHERIC TRACE ELEMENTS INTO THE NORTH SEA: COASTAL, SHIP, PLATFORM MEASUREMENTS AND MODEL PREDICTIONS

JASNA INJUK,*† RENÉ VAN GRIEKEN† and GERRIT DE LEEUW‡

†Department of Chemistry, University of Antwerp (UIA), B-2610 Antwerp, Belgium; and ‡TNO Physics and Electronics Laboratory, P.O. Box 96864, NL-2509 JG The Hague, The Netherlands

(First received 17 *June* 1997 *and in final form October* 1997. *Published June* 1998)

Abstract–The atmospheric input of up to 16 trace and other elements into the North Sea is further assessed from aerosol concentrations measured at a coastal station in Belgium, on ships during two cruises, and on a platform, in the years 1992–1994. The Slinn and Slinn model is used to calculate the dry deposition from the measured aerosol concentrations. The total (dry and wet) deposition into the North Sea environment is estimated to be (in tonnes per year): 560 for V, 1300 for Cr, 650 for Ni, 690 for Cu, 3500 for Zn and 1970 for Pb. The "giant" particles dominate the fluxes. The atmospheric contribution to the total input into the North Sea, including riverine inputs and direct discharges, are estimated to be 28% for Cu, 29% for Zn and 57% for Pb. The inputs estimated from the experimental data are compared with results from a model applied for the same area and period. The experimental and model results agree within 56%, which is considered as "satisfactory" in view of both the experimental and the model uncertainties. © 1998 Elsevier Science Ltd. All rights reserved

Key word index: Aerosols, heavy metals, deposition fluxes, North Sea.

INTRODUCTION

Budget calculations, based on inputs by rivers, direct discharges, incineration and industrial waste, suggest that atmospheric inputs of metals and nutrients to the world's oceans are significant (Jickells, 1995). This view is supported by measurements at sea that clearly demonstrate not only the importance of the atmospheric input in mass terms but also the nature of the atmosphere/ocean interaction.

In this paper we report on deposition fluxes based on size-segregated airborne concentrations that were obtained by applying the total-reflection X-ray fluorescence (TXRF) analysis technique to impactor samples collected in the North Sea area. Dry deposition velocities were calculated from these concentrations with the Slinn and Slinn (1980) model. Wet deposition fluxes are derived from the mean aerosol concentrations, rainfall intensity and theoretical scavenging rates. In comparison with previous work (Rojas *et al.*, 1993; Baeyens *et al.*, 1990; Ottley and Harrison, 1991; Ottley and Harrison, 1993; Otten *et al.*, 1994), here we combine measurements at a coastal station, on ships and on a platform to assess the atmospheric inputs to the North Sea, and we compare the results with model calculations for the same area and period of time.

In addition, the use of TXRF as an appropriate analytical method for atmospheric studies is confirmed; it allows a short sampling time of, e.g. half an hour, virtually no sample preparation and simultaneous determination of 17 and more elements with detection limits down to 0.2 ng m^{-3}.

EXPERIMENTAL

Sampling strategy

The dry and wet deposition fluxes, reported here for the southern and central North Sea area, are derived from airborne concentrations measured over the North Sea in the period between September 1992 and May 1994. A huge data set of more than 1000 mass-segregated samples was collected during research cruises aboard the R/V Belgica (21–27 August 1993) and Hr. Ms. Tydeman (MAPTIP experiment, 11 October–5 November 1993 (De Leeuw *et al.*, 1994), on the research platform "Nordsee" (FPN: 54°42′N, 7°10′E; NOSE Experiment'92, 2–21 September 1992) and at a station located approximately 100 m from the Belgian coastal line in Blankenberge (from October 1992 to May 1994). The samples on R/V Belgica were taken during a cruise along the east coast of England, starting in Ipswich (52°3′N, 1°9′E); the end of cruise was at 54°27′N, 0°30′E. The MAPTIP experiment was centred around the Dutch research tower Meetpost Noordwijk (MPN: 52°16′N, 4°17′E, 9 km from the Dutch coast). Hr. Ms. Tydeman was used to study lateral homogeneity in this part of the North Sea along tracks of up to 150–200 km from MPN. The sampling locations are indicated in Fig. 1.

* Author to whom correspondence should be addressed.

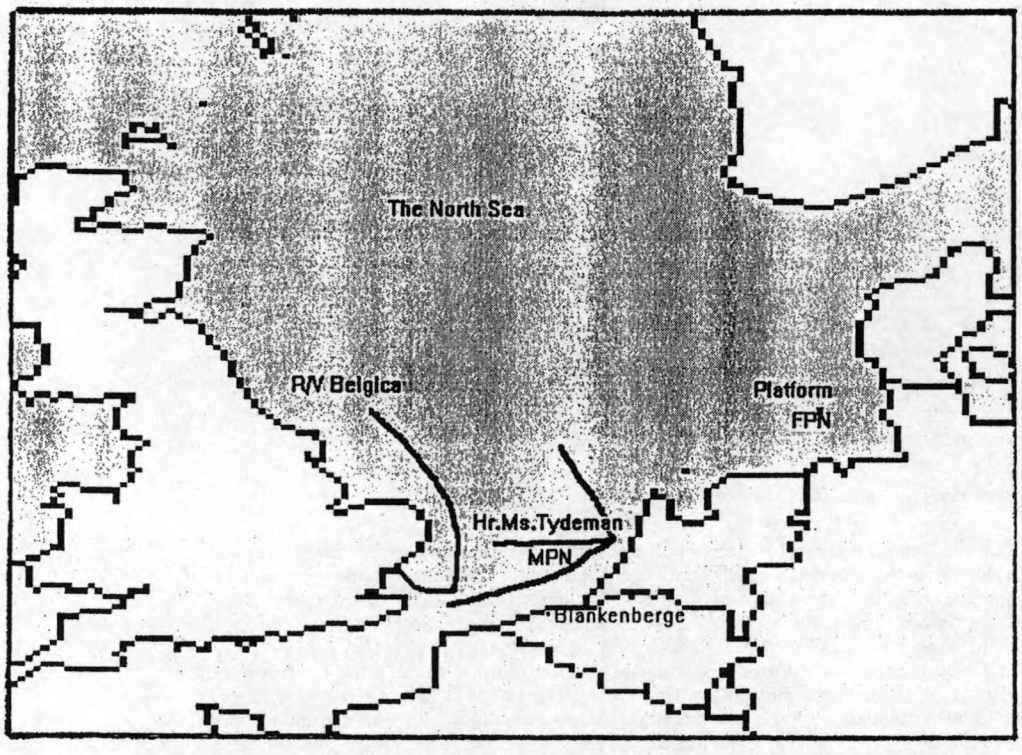

Fig. 1. The North Sea map with the sampling locations (Belgian coastal station-Blankenberge, "Nordsee" platform-FPN, MPN platform) and cruise tracks of R/V Belgica and Hr. Ms. Tydeman.

Size-segregated samples were collected utilizing a 7-stage Battelle cascade-impactor with cut-off diameters of 0.25, 0.5, 1, 2, 4, 8 and 16 μm at a flow-rate of 1.2 $1\,min^{-1}$. The impactor was mounted inside a wind tunnel (Vawda *et al.*, 1992) where a forced air flow was maintained to avoid problems associated with non-isokinetic sampling of large particles (from 4 μm in diameter) with a cut-off that varies with wind direction and wind speed. The tunnel is directed into the wind by means of a light wind vane. A ventilator produces a constant forced air stream inside the tunnel to adjust the linear velocity of the particles in the air exactly to the intake velocity in the sampling device. The aerosol was impacted on polished quartz discs (30 mm diameter, 3 mm thickness) that were also used as target in the TXRF analysis. The discs were cut in a special way to allow for appropriate mounting above the stage orifice. A steel spring presses them firmly against the three disc holders.

Sample preparation and analysis

The use of the reflector holders of TXRF as a sample support for the direct impaction of size-segregated airborne material is a rather new method that has not been widely attempted thus far (Schneider, 1989; Salvá *et al.*, 1993; Injuk and Van Grieken, 1995a). Prior to the collection, the quartz discs were coated with silicone to reduce both blow-off and bounce-off effects. This was achieved by dispersing a 5 μl drop of silicone solution (SERVA, Polylab). After sample collection, a Ga solution aliquot was added as an internal standard. Subsequently, the samples were dried in an exsiccator under reduced pressure, and analyzed.

All samples were analyzed by TXRF. The prototype TXRF module, used in this study, was developed in the Atominstitut in Vienna (Wobrauschek and Aiginger, 1975). The equipment consists of a 2 kW Mo tube (Philips), TXRF unit and a Kevex Si(Li) detector, with a resolution of 165 eV at the Mn Kα line. The detector was positioned with the Be-window looking upward, at a distance of about 4 mm from the sample on the reflector. The equipment is designed as a mechanically stable unit; once the adjustments were completed, a series of measurements could be analyzed without any instrumental problems. It generally allows for absolute detection limits down to a few 100 pg. All samples were irradiated for 500 s at 20 mA and 45 kV. X-ray spectra were evaluated with the computer programme AXIL (Van Espen *et al.*, 1986).

RESULTS AND DISCUSSION

Atmospheric inputs of trace elements into the North Sea were determined from the concentrations of the elements in each of the size-segregated aerosol fractions. Size-dependent deposition velocities were used to calculate the dry deposition fluxes. The meteorological conditions (wind speed, relative humidity) were taken into account for these calculations. For the interpretation the wind direction is also an important factor. Therefore, meteorological parameters were recorded as part of the data sets. In addition the dry deposition fluxes, also the contribution of wet deposition was calculated. Below, the procedures used are described and the resulting fluxes are discussed.

Atmospheric concentrations

The relatively large data set from the 19 month monitoring period at the coastal station in Blankenberge has made it possible to calculate the long-term average atmospheric concentrations of S, Cl, K, Ca,

Table 1. Atmospheric concentrations determined at the Belgian coastal station in Blankenberge in the period October 1992–May 1994; arithmetic mean, standard deviation and range (all in $ng\,m^{-3}$), ND = below detection limit

	Blankenberge–summer				Blankenberge–winter			
Element	Arith. mean	St. dev.	Min.	Max	Arith mean	St dev.	Min.	Max
S	1240	590	642	2392	490	270	176	949
Cl	1140	830	70	2731	1260	1070	66	2035
K	130	70	47	295	110	60	30	141
Ca	180	120	34	405	130	120	33	335
Ti	13.9	10.5	4.1	37.8	5.5	3.7	1.9	13.1
V	5.4	3.8	1.9	12.9	3.6	2.3	0.2	6.7
Cr	6.7	8.9	0.5	32.1	3.5	2.7	0.3	6.4
Mn	13.6	8.6	3.1	22.1	4.6	2.6	0.4	8.6
Fe	310	190	85	551	130	100	32	262
Ni	4.1	5.1	0.9	19.1	2.1	1.2	0.2	3.1
Cu	3.9	2.7	0.5	6.3	3.2	2.8	0.2	12.7
Zn	22.5	19.5	3.9	68	21.8	18.2	4.1	62.3
As	2.3	1.8	0.4	6.1	0.28	0.66	ND	2.24
Se	0.5	0.2	0.4	0.7	ND	ND	ND	ND
Br	17.8	13.3	2.2	38.9	16.1	14.5	2.1	20.7
Sr	6.4	4.3	0.7	15.2	4.1	4.2	ND	6.9
Pb	14.3	3.2	1.6	10.1	12.1	15.2	ND	52.7

Ti, V, Cr, Mn, Fe, Ni, Cu, Zn, As, Se, Br, Sr and Pb and to separate the data for the summer and winter seasons. The results are reported in Table 1. The average values from the research cruises with the R/V Belgica and with Hr. Ms. Tydeman are presented in Table 2. Finally, the atmospheric concentrations measured at the FPN are given in Table 3. The data in Tables 1–3 are arithmetic mean values calculated from the total concentrations in each sample, i.e. the sum of the concentrations measured in each of the seven size classes.

The results are comparable to previously published values for trace element concentrations in the North Sea atmosphere (Injuk and Van Grieken, 1995b). Some differences are observed, which can be attributed to the effect of the air mass history on the aerosol concentrations. In their analysis of aerosol particle size distributions measured at MPN, Van Eijk and De Leeuw (1992) devided their data set in eight sectors based on geographical considerations. For each sector, the concentrations of the aerosol and their wind speed dependence were different and the various source regions could clearly be identified. Obviously, for the analysis of the chemical composition, a similar partitioning of the data will be of crucial importance to explain differences observed between the various sampling sites. In Table 3 and 4, we have made a crude classification, based on wind direction, of the data measured on the FPN and aboard R/V Belgica. The differences between the concentrations in the indicated wind sectors are obvious. During the whole sampling campaign with the R/V Belgica (Table 4), the wind direction was from the north, except on the first day when the wind was west. As a result, the anthropogenic elements (Ti, Ni, Cu, Zn) have higher concentrations when the wind is from land, i.e. from the source regions (west on R/V Belgica; southeast on MPN) and when the wind is from the open ocean the concentrations are low. Since the concentrations decrease with travel time over the sea (fetch!) a N–S gradient is expected when the wind is from land, and with no source to the North. Such results are consistent with other more limited studies in the southern North Sea done by Chester *et al.*, (1993) and Yaaqub *et al.* (1991).

This analysis clearly indicates that for the assessment of the total atmospheric input into the North Sea, the climatology is a very important factor with which the emissions in the various source regions must be weighted. Furthermore, thorough consideration should be given to the influence of factors such as the travel time from the source region, precipitation scavenging during advection, and other meteorological conditions that affect the concentration levels. During the MAPTIP experiment, part of the ship time of Hr. Ms. Tydeman was designated to address lateral homogeneity (De Leeuw *et al.*, 1994). The aim was to measure aerosol particle size distributions and meteorological parameters simultaneously at the MPN and on Hr. Ms. Tydeman, during long tracks of the ship up- or downwind from MPN. The preliminary results from the comparison of the data collected simultaneously aboard the ship and on MPN clearly shows the effect of meteorological parameters such as wind speed and air temperature on the transport of the air mass over a large water mass and on the

Table 2. Atmospheric concentrations determined during research cruises aboard R/V Belgica and Hr. Ms. Tydeman in 1993; arithmetic mean, standard deviation and range (all in ng m^{-3}), ND = below detection limit

	North Sea cruises Hr. Ms. Tydeman				North Sea cruises R/V Belgica			
Element	Arith. mean	St. dev.	Min.	Max.	Arith. mean	Std. dev.	Min.	Max
S	1650	1110	179	2886	320	190	103	380
Cl	430	580	24	1515	620	450	107	1459
K	67	10	58	79	62	18	48	93
Ca	89	59	31	151	68	20	43	92
Ti	5.2	0.5	ND	5.7	4.6	2.9	1.8	9.7
V	2.3	1.5	0.6	5.1	0.7	0.3	ND	0.9
Cr	2.9	2.6	0.3	7.2	1.5	0.4	0.4	7.2
Mn	3.3	1.2	1.2	5.3	3.1	1.5	2.6	3.4
Fe	100	30	51	122	80	70	31	217
Ni	4.4	4.6	1.4	13.5	1.7	1.2	0.5	3.3
Cu	4.2	3.3	0.7	9.4	1.9	1.0	1.5	2.3
Zn	20.5	14.7	3.1	42.2	6.2	4.2	1.1	13.2
As	ND	ND	ND	ND	ND	ND	ND	ND
Se	1.4	0.8	0.07	1.9	ND	ND	ND	ND
Br	3.9	2.9	1.9	9.7	3.6	3.9	1.6	10.7
Sr	0.9	0.6	0.2	1.9	1.1	0.6	0.4	1.6
Pb	17.4	13.1	1.6	37.4	ND	ND	ND	ND

Table 3. Average airborne concentrations and associated standard deviations (ng m^{-3}) as a function of wind direction, measured on the "Nordsee" platform in 92

Element	Northwest–north	Southwest–west	Southeast–east	All sectors (weighted)
S	180 ± 40	250 ± 50	400 ± 180	270 ± 50
Cl	700 ± 50	440 ± 40	210 ± 100	260 ± 30
Cr	0.4 ± 0.5	0.5 ± 0.24	7.9 ± 6.3	1.7 ± 0.5
Mn	1.2 ± 0.2	18.4 ± 0.4	22.7 ± 1.9	14.4 ± 0.5
Fe	29 ± 1	76 ± 1	400 ± 7	140 ± 2
Ni	0.8 ± 0.5	2.2 ± 0.3	3.5 ± 0.7	1.4 ± 0.3
Cu	1.1 ± 0.2	3.4 ± 0.2	6.7 ± 0.7	3.5 ± 0.2
Se	0.5 ± 0.2	1.1 ± 0.2	1.2 ± 0.7	0.9 ± 0.2
Br	10.7 ± 0.3	10.8 ± 0.4	7.9 ± 0.8	10.1 ± 0.3
Sr	4.5 ± 0.2	6.3 ± 0.3	7.4 ± 0.8	6.0 ± 0.2
Pb	10.8 ± 0.8	12.6 ± 0.5	24.9 ± 2.1	15.1 ± 1.1

aerosol size distributions (De Leeuw *et al.*, to be published). As regards the chemical composition, a similar analysis cannot be made because only one impactor/wind tunnel combination was available. Since this sampler was mounted on the ship, only a comparison can be made between samples near the MPN and at a large distance from the tower (the end points of the trajectories shown in Fig. 1), which were consecutively collected. An initial analysis of the impactor samples was presented in (Van Eijk *et al.*, 1995). This analysis was limited to only four elements that are representative for aerosols from anthropogenic sources (Cu, Zn, Pb and Se) and three elements that are characteristic for marine aerosols (Ca, Sr and Cl). In the easterly winds encountered during the larger part of the MAPTIP experiment, the end points of all tracks were downwind from MPN. Hence, the concentrations of the anthropogenic contributions

Table 4. Elemental concentrations in aerosols (ng m^{-3}) measured aboard R/V Belgica in October 1993 as a function of wind direction

	Sample I (east)	Samples II + III + IV + V- mean value (north)
Cl	107	660
Ti	9.7	3.3
Ni	3.3	1.3
Cu	2.3	1.2
Zn	13.6	4.5

Table 5. Elemental aerosol concentrations (ng m^{-3}) during MAPTIP '93

	A + B	C + D + E
Cl	1020	32
Ca	113	74
Sr	1.34	0.61
Cu	1.0	6.3
Zn	4.0	31
Pb	4.7	26
Se	0.08	1.52

were expected to decrease along the track, whereas the concentrations of the marine elements were expected to increase as a consequence of the larger fetch, and thus generation over a larger surface. As discussed by Van Eijk *et al.* (1995), for the marine elements Ca, Sr and Cl, indeed the concentrations were observed to increase with longer fetch, but for the anthropogenic elements the expected decrease was observed in only 50% of the cases. At present we have no sound explanation for those cases where the concentrations of the anthropogenic elements did not decrease. The MAPTIP data set on chemical composition is too small for a more detailed analysis.

A further complication is the drastic change in meteorological conditions during the MAPTIP experiments, which further limits the use of the data for a more systematic analysis. This change in meteorological conditions resulted in the occurrence of heavy fog, whereas prior to this event the visibility was generally good. Obviously, the aerosol properties had changed, both in a physical sense, as evidenced by the formation of fog, and chemically as shown in Table 5. In Table 5 the concentrations of the selected elements before (samples A and B) and after (samples C–E) the change in the meteorological conditions are compared. The general decrease in the concentrations of the marine elements and the increase of the concentrations in the anthropogenic contribution can only qualitatively be understood. The wind speed is the driving factor for most of the exchange processes of aerosols between air and sea. The wind speed during the earlier part of the MAPTIP experiment varied between 5 and 20 m s^{-1} with wave heights of 0.5–1.5 m, whereas later the wind speed did not exceed 10 m s^{-1} and wave heights were typically 0.4 m. Most likely the decrease in wind speed resulted in less surface generation and thus smaller concentrations of the marine components. The anthropogenic contribution, for which there are no sources over sea, can only become smaller due to dispersion, deposition at the surface and entrainment at the top of the mixed layer. The wind speed is a governing factor because both the dispersion and the deposition velocity are wind speed dependent. By Van Eijk and De Leeuw (1992), the wind speed dependence of the smaller particles was explained by this effect.

The data obtained with the Battelle cascade impactor consist of the elemental masses on each impaction stage, i.e the mass distribution for a large number of elements. For the assessment of the deposition velocities, which vary strongly with particle mass, it is essential to accurately analyze cascade impactor data. In Figs 2 and 3 the mass distributions for S, Cl, K, Ca, Ti, V, Cr, Mn, Fe, Ni, Cu, Zn, Se, Br, Sr, Zr, Mo and Pb are given. The masses are obviously not log-normally distributed as is they would be for an aerosol from a single source. Obviously, the North Sea aerosol originates from multiple sources. Therefore, their size distributions are multi-modal and a description in terms of a single log-normal distribution is not appropriate. Elements like K, S, V, Mn, Pb, Ni, Cu, Zn, Se are mostly associated with the small particle range below 1 μm diameter, while elements like Cl, Ca, Sr are found mostly in the larger size range, above 4 μm diameter. Figs 2 and 3 clearly confirm that the smaller aerosol is predominantly of anthropogenic origin, whereas the larger aerosol is of marine origin. This observation justifies our approach to treat the aerosol over the North Sea as a mixture of smaller aerosol of continental origin and a larger aerosol of marine origin (Injuk *et al.*, 1994). Similar approaches have been followed since over a decade to describe the physical properties of the marine aerosol, e.g. by Gathman (1983, 1989).

Dry deposition fluxes

The dry deposition flux, F_d (ng m^{-2} s^{-1}) of material to the water surface was calculated from the product of atmospheric concentrations, C_a (ng m^{-3}), and the dry deposition velocity, V_d (m s^{-1}). The dry deposition velocity of aerosols is strongly dependent on particle size and meteorological factors, primarily wind speed and humidity. The dry deposition model of Slinn and Slinn (1980) allows for taking into account the response of the size of small particles to changes in relative humidity, as well as for impaction and interception mechanisms of deposition. We have used the assumption that the relative humidity at the air–sea interface is 98.3%, and that hygroscopic particles (all elements except Fe-rich particles) instantly reach their equilibrium size [cf. response times calculated by Andreas (1990)]. During our sampling campaign in Blankenberge, the average wind speed was 4.6 m s^{-1}, while during the R/V Belgica cruise and on the "Nordsee" platform, the average wind speed varied from 5 to 10 m s^{-1}. During the MAPTIP experiment the wind speed was from 5 to 15 m s^{-1}. The current wind speeds were used to calculate the deposition velocities.

To take into account the mass dependence of the dry deposition velocities, it is necessary to normalize aerosol mass and particle size for the calculation of the total flux. The mass-weighted dry deposition velocities were derived using the following expression:

$$\text{Mass-weighted } v_{di} = \sum \frac{v_{di} C_i}{C_i}$$

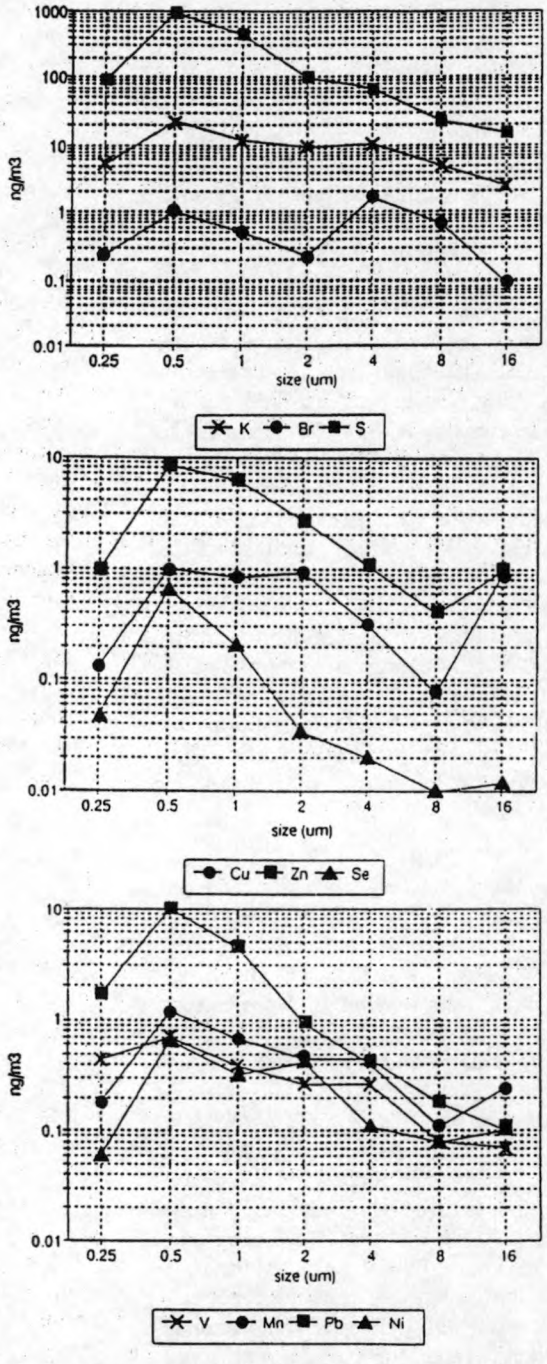

Fig. 2. Average mass distributions for K, Br, S, Cu, Zn, Se, V, Mn, Pb and Ni in aerosol samples collected over the North Sea.

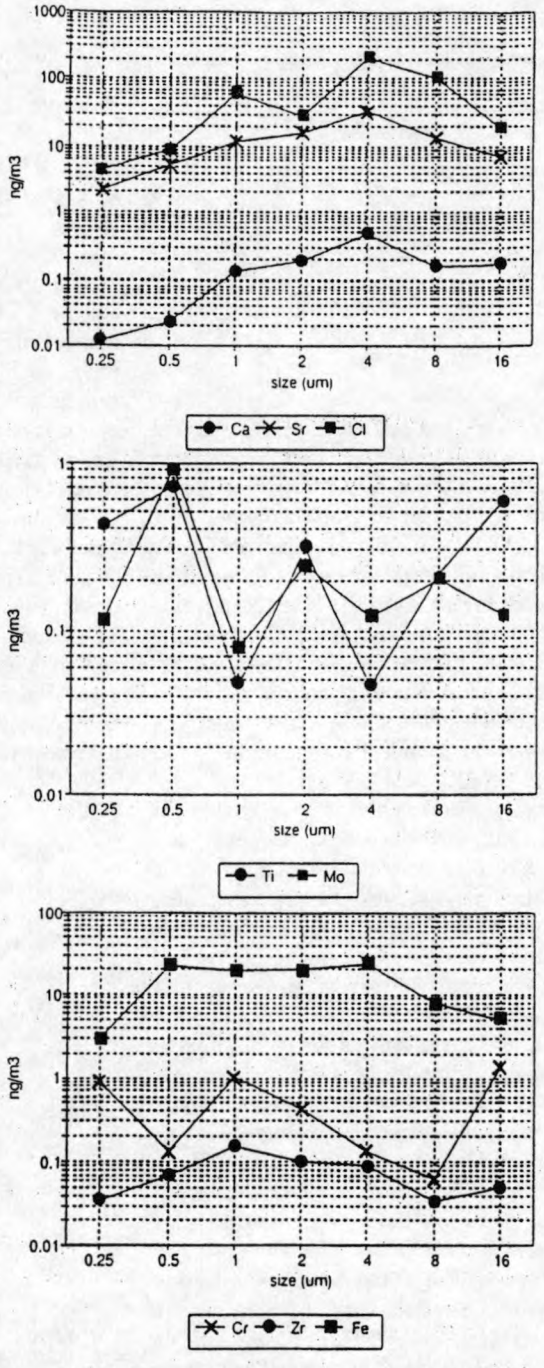

Fig. 3. Average mass distributions for Ca, Sr, Cl, Ti, Mo, Cr, Zr and Fe in aerosol samples collected over the North Sea.

where v_{di} is the deposition velocity of size fraction i and C_i the mass of a certain element in size fraction i. The mass-weighted dry deposition velocities was calculated for each element in the individual each cascade impactor samples. The arithmetic mean values for the mass-weighted deposition velocities together-with the standard deviations are given in Table 6.

For the calculation of the dry fluxes to the sea, the total concentration of an element in each cascade impactor sample was multiplied by the corresponding mass-weighted deposition velocity. The average dry deposition rates and the standard deviations, based on calculations from the different sampling campaigns in 1992–1994 are given in Table 7.

The values for the dry deposition fluxes determined in this work are generally smaller than previously published data (Injuk and Van Grieken, 1995b). These lower values may be the result of using a spatial distribution of measurements, whereas earlier estimates were obtained from extrapolation of point

Table 6. Mass–weighted deposition velocities V_d ($cm\,s^{-1}$), together with st. dev., for different aerosol size distributions as outlined in the text. The average wind speed during each sampling campaign is indicated

	Blankenberge-summer 5.0 $m\,s^{-1}$	Blankenberge-winter 5.0 $m\,s^{-1}$	"Nordsee"-platform 7.8 $m\,s^{-1}$	R/V Belgica 8.2 $m\,s^{-1}$	Hr. Ms. Tydeman 5.0 $m\,s^{-1}$	Hr. Ms. Tydeman 15.0 $m\,s^{-1}$
S	0.33 (0.14)	0.18 (0.09)	—	0.50 (0.18)	0.08 (0.01)	0.90 (0.25)
K	0.43 (0.13)	0.45 (0.15)	—	0.61 (0.20)	0.22 (0.04)	1.16 (0.25)
Ca	0.50 (0.12)	0.58 (0.17)	—	0.62 (0.19)	0.55 (0.03)	1.70 (0.17)
Ti	0.42 (0.16)	0.42 (0.12)	—	0.27 (0.16)	0.57 (0.07)	1.27 (0.90)
V	0.24 (0.16)	0.14 (0.08)	—	0.24 (0.18)	0.27 (0.07)	0.64 (0.15)
Cr	0.46 (0.26)	0.71 (0.34)	0.42 (0.21)	0.80 (0.21)	0.42 (0.08)	1.41 (0.38)
Mn	0.42 (0.21)	0.53 (0.19)	0.36 (0.18)	0.26 (0.09)	0.21 (0.09)	1.10 (0.27)
Fe	0.44 (0.14)	0.55 (0.18)	0.34 (0.10)	0.49 (0.10)	0.32 (0.06)	1.34 (0.05)
Ni	0.19 (0.08)	0.61 (0.31)	0.23 (0.09)	0.15 (0.08)	0.27 (0.03)	0.78 (0.25)
Cu	0.32 (0.07)	0.50 (0.13)	0.26 (0.10)	0.21 (0.07)	0.45 (0.34)	1.26 (0.37)
Zn	0.32 (0.17)	0.29 (0.14)	—	0.40 (0.12)	0.20 (0.08)	0.90 (0.14)
As	0.35 (0.24)	0.30 (0.19)	—	—	—	—
Se	0.63 (0.29)	—	—	—	0.07 (0.02)	0.69 (0.05)
Br	0.51 (0.24)	0.39 (0.23)	—	0.43 (0.12)	0.20 (0.02)	1.89 (0.08)
Sr	0.62 (0.15)	0.49 (0.18)	—	0.48 (0.24)	0.71 (0.33)	1.86 (0.05)
Pb	0.07 (0.06)	0.11 (0.09)	0.15 (0.11)	—	0.08 (0.004)	0.79 (0.71)

Table 7. Dry deposition fluxes into the North Sea ($kg\,km^{-2}\,yr^{-1}$) together with the standard deviations

	Blankenberge-winter	Blankenberge-summer	"Nordsee"-platform	R/V Belgica	Hr. Ms. Tydeman
S	108 (77)	28 (15)	—	570 (560)	75 (23)
K	18 (13)	16 (9)	—	13 (12)	13 (12)
Ca	29 (22)	25 (23)	—	13 (10)	33 (30)
Ti	1.54 (1.39)	0.74 (0.49)	—	0.36 (0.18)	0.96 (1.56)
V	0.31 (0.29)	0.17 (0.07)	—	0.05 (0.03)	0.21 (0.06)
Cr	1.34 (2.11)	0.26 (0.18)	0.64 (0.17)	1.39 (0.92)	1.64 (2.09)
Mn	1.53 (1.35)	0.78 (0.44)	1.47 (0.13)	0.25 (0.14)	0.40 (0.17)
Fe	36 (29)	24 (18)	18 (3)	13 (10)	22 (16)
Ni	0.16 (0.14)	0.42 (0.23)	0.51 (0.09)	0.08 (0.09)	0.48 (0.51)
Cu	0.34 (0.25)	0.49 (0.62)	0.29 (0.04)	0.13 (0.09)	0.83 (0.97)
Zn	1.55 (1.49)	1.99 (1.66)	—	0.79 (0.87)	1.57 (0.58)
As	0.25 (0.22)	0.003 (0.006)	—	—	—
Se	0.09 (0.07)	—	—	—	0.03 (0.004)
Br	4.52 (5.36)	1.67 (1.49)	—	4.87 (0.74)	1.76 (2.54)
Sr	1.58 (1.35)	0.53 (0.54)	—	1.58 (0.74)	0.52 (0.46)
Pb	0.20 (0.25)	0.44 (0.56)	0.71 (0.13)	ND	0.59 (0.29)

measurements over the whole North Sea. Furthermore, the lower levels, especially for the heavy metals, may also reflect the effect of the many voluntary and enforced emission controls implemented in recent years.

The uncertainty in the dry deposition flux strongly depends on the accuracy of the aerosol size distribution, especially the large size fraction. Numerous workers, (e.g. Dulac *et al.*, 1989; Slinn, 1983; Steiger *et al.*, 1989; Ottley and Harrison, 1993) have shown the dominant contribution of the large particle fraction to the overall dry deposition flux, even if this would contribute only a small fraction to the total mass. This is due to the large deposition velocities associated with the greater particles. The same pattern was also observed in this work. In Fig. 4, the dry deposition flux and atmospheric mass are given for each size fraction as a percentage of the total atmospheric mass and dry deposition flux for Cr, Ni, Cu and Zn. The results compare favorably with those presented in earlier publications where the dominance of the largest particle on the overall dry deposition flux was demonstrated.

Based on the average dry deposition rates given in Table 7, the total dry deposition fluxes, in tonnes yr^1, for the whole area of the North Sea have been calculated. The results are presented in Table 8.

Wet deposition fluxes

Wet deposition fluxes (Table 9) were calculated using the scavenging factors recommended by GESAMP (1989): 1500 (S, K, Ca, Br), 1000 (Ti, Fe, Sr), 500 (V, Cr, Mn, Ni, Cu, Zn, Pb) and 200 (As, Se). Despite the many legitimate concerns over the use of scavenging ratios (e.g. empirical values that are not really linked to the processes) values do appear to be relatively consistent, less than a factor of 5, for the

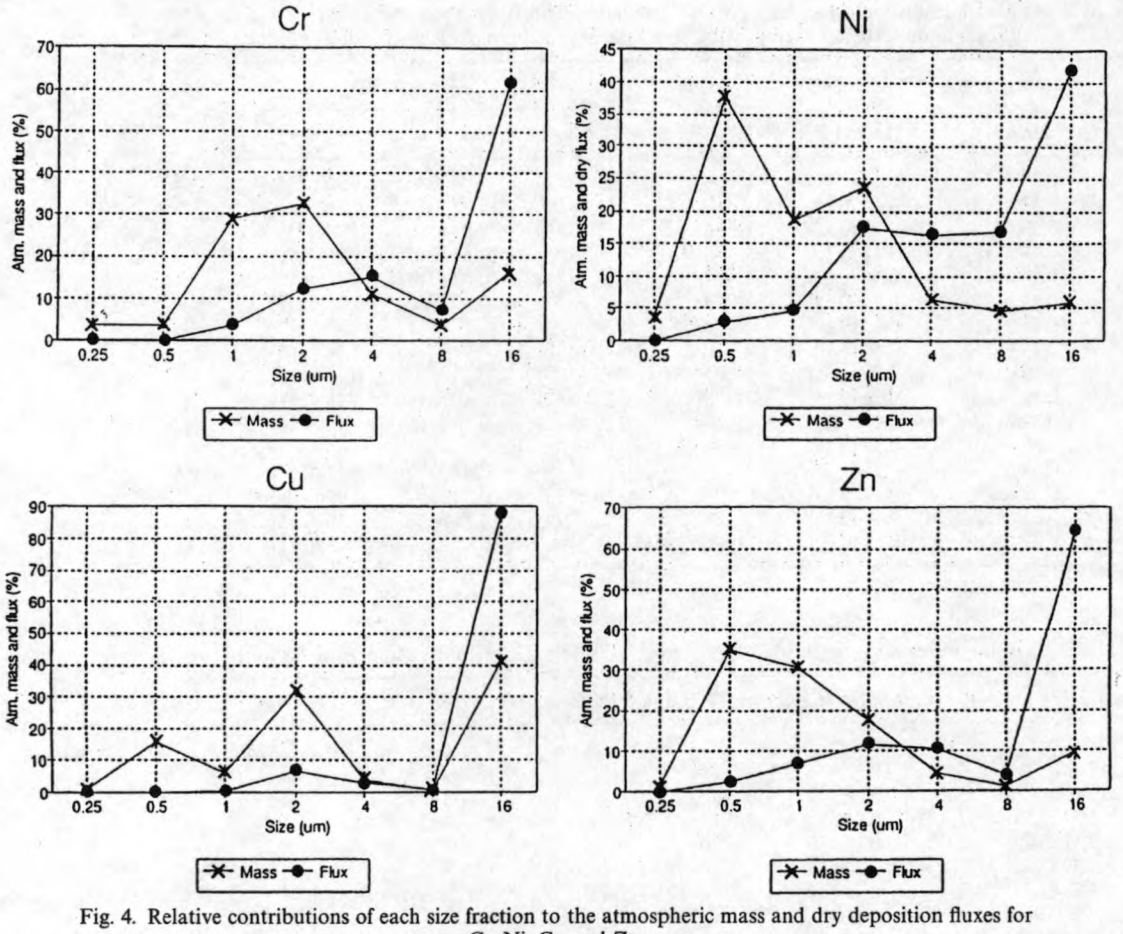

Fig. 4. Relative contributions of each size fraction to the atmospheric mass and dry deposition fluxes for Cr, Ni, Cu and Zn.

same chemical species in different environments (Kane *et al.*, 1994; Galloway *et al.*, 1993; Jaffrezo and Colin, 1988; Arimoto *et al.*, 1987; Barrie, 1992). An annual rainfall above the North Sea of 677 mm yr^{-1} and the average elemental atmospheric concentrations of the whole data set were used in the calculations. In Table 10 average wet deposition fluxes, calculated from the values given in Table 9, are given together with the total amount of wet deposited material in tonnes yr^{-1}. The data presented in Table 10 suggest that on average wet deposition fluxes are approximately a factor of 3 larger than the dry deposition fluxes, for all elements of interest.

Total deposition fluxes

In Table 11, the estimates for the total (dry and wet) atmospheric inputs to the North Sea are presented together with the recently published values given by OSPARCOM (1993). Unfortunately, from OSPARCOM compiled data are available for only few elements. For Ni, Cu, Zn, As and Pb, the total deposition fluxes obtained in this study are of similar order of magnitude as those reported by OSPARCOM. In contrast to Chester *et al.* (1993), the atmospheric Cu and Zn wet fluxes, estimated from the present study, dominate over dry. This dominance of wet deposition is also in agreement with earlier flux data for the North Sea reported by several other workers (Injuk and Van Grieken, 1995b).

Table 8. Calculated dry deposition fluxes to the North Sea

Element	Average dry flux and st. dev. (kg $km^{-2} yr^{-1}$)	Total dry flux to the North Sea (tonnes yr^{-1})
S	196 (220)	103,600
K	15 (2)	8000
Ca	25 (7)	13,300
Ti	0.91 (0.42)	490
V	0.17 (0.10)	90
Cr	1.10 (0.52)	560
Mn	0.89 (0.53)	470
Fe	22 (8)	11,900
Ni	0.33 (0.17)	180
Cu	0.42 (0.23)	220
Zn	1.47 (0.43)	790
As	0.13 (0.13)	70
Se	0.06 (0.03)	30
Br	3 (1)	1,700
Sr	1.05 (0.53)	560
Pb	0.49 (0.20)	60

Table 9. Wet deposition fluxes (kg km^{-2} yr^{-1}) into the North Sea and standard deviations, calculated for different sampling campaigns

	Blankenberge-summer	Blankenberge-winter	"Nordsee"-platform	R/V Belgica	Hr.Ms. Tydeman
S	1050 (500)	410 (230)	—	270 (160)	1390 (940)
K	110 (62)	60 (51)	—	55 (15)	57 (8)
Ca	150 (100)	120 (110)	—	58 (17)	75 (50)
Ti	7.8 (5.9)	3.1 (2.1)	—	2.6 (1.6)	2.9 (0.3)
V	1.5 (1.1)	1.1 (0.65)	—	0.2 (0.1)	0.7 (0.4)
Cr	1.9 (2.5)	1.0 (0.8)	1.2 (0.2)	1.6 (0.3)	0.8 (0.7)
Mn	3.8 (2.4)	1.3 (0.7)	4.1 (0.8)	0.9 (0.4)	0.9 (0.3)
Fe	180 (110)	76 (58)	79 (2)	45 (39)	57 (15)
Ni	1.2 (1.4)	0.6 (0.3)	1.7 (0.5)	0.5 (0.4)	1.2 (1.3)
Cu	1.1 (0.8)	0.6 (0.8)	1.0 (0.2)	0.6 (0.3)	1.2 (0.9)
Zn	6.4 (5.5)	6.2 (5.1)	—	1.7 (1.2)	5.8 (4.2)
As	0.2 (0.2)	0.03 (0.07)	—	—	—
Se	0.06 (0.02)	—	—	—	0.2 (0.1)
Br	15.1 (11.2)	13.6 (3.8)	—	3.0 (2.8)	3.3 (2.5)
Sr	3.6 (2.4)	2.3 (2.4)	—	0.6 (0.4)	0.5 (0.3)
Pb	1.3 (0.9)	3.4 (4.3)	4.3 (0.4)	—	4.9 (6.7)

Table 10. Wet deposition fluxes to the North Sea

Element	Average wet flux and st.dev. (kg km^{-2} yr^{-1})	Total wet flux to the North Sea (tonnes yr^{-1})
S	780 (459)	417,600
K	71 (23)	37,700
Ca	103 (38)	54,800
Ti	4.1 (2.2)	2200
V	0.88 (0.48)	470
Cr	1.33 (0.44)	710
Mn	1.73 (1.21)	920
Fe	89 (52)	47,400
Ni	0.88 (0.33)	470
Cu	0.88 (0.28)	470
Zn	5.03 (1.93)	2700
As	0.12 (0.09)	62
Se	0.13 (0.07)	70
Br	8.75 (5.63)	4700
Sr	2.03 (1.48)	1100
Pb	3.20 (1.47)	1700

Table 12. Estimates of inputs (tonnes yr^{-1}) to the North Sea via various pathways (OSPARCOM, 1993)

Pathway	Cu	Zn	Pb
Riverine inputs[a]	1200	6400	1000
Direct inputs[b]	290	1300	160
Atmosphere (this work)	690	3500	2000
Incineration	4.6	5.7	4.9
Industrial waste[c]	180	440	220
Sewage sludge	76	160	77

[a] Here it must be recognized that for some rivers, such as those in northeast and southeast England, inputs of metals such as Cu, Zn, Pb are largely derived from natural ores

[b] sewage effluents, sewage sludge, industrial effluents, polder effluents

[c] Chemical waste, slurries, fly-ash, minestones and colliery tailings

Table 11. Total (dry + wet) deposition fluxes to the North Sea and comparison with the literature values

Element	Total flux—this work (tonnes yr^{-1})	Total flux—OSPARCOM, 1993 (21) (tonnes yr^{-1})
S	521,000	—
K	45,700	—
Ca	68,100	—
Ti	2700	—
V	560	—
Cr	1300	—
Mn	1400	—
Fe	59,300	—
Ni	650	180—400
Cu	690	320—740
Zn	3500	2,700—5,500
As	130	95—220
Se	100	—
Br	6400	—
Sr	1600	—
Pb	1970	1,960–1,700

Table 13. Comparison of measured and calculated concentrations of Ni, Cu, Zn and Pb for the North Sea area (ng m^{-3})

	The North Sea		Belgian coast	
	Model	Measurements	Model	Measurements
Ni	< 3	2.5	3–5	3.1
Cu	3–5	3.2	5–7	3.6
Zn	< 30	13	30–60	22
Pb	< 30	11	30–60	13

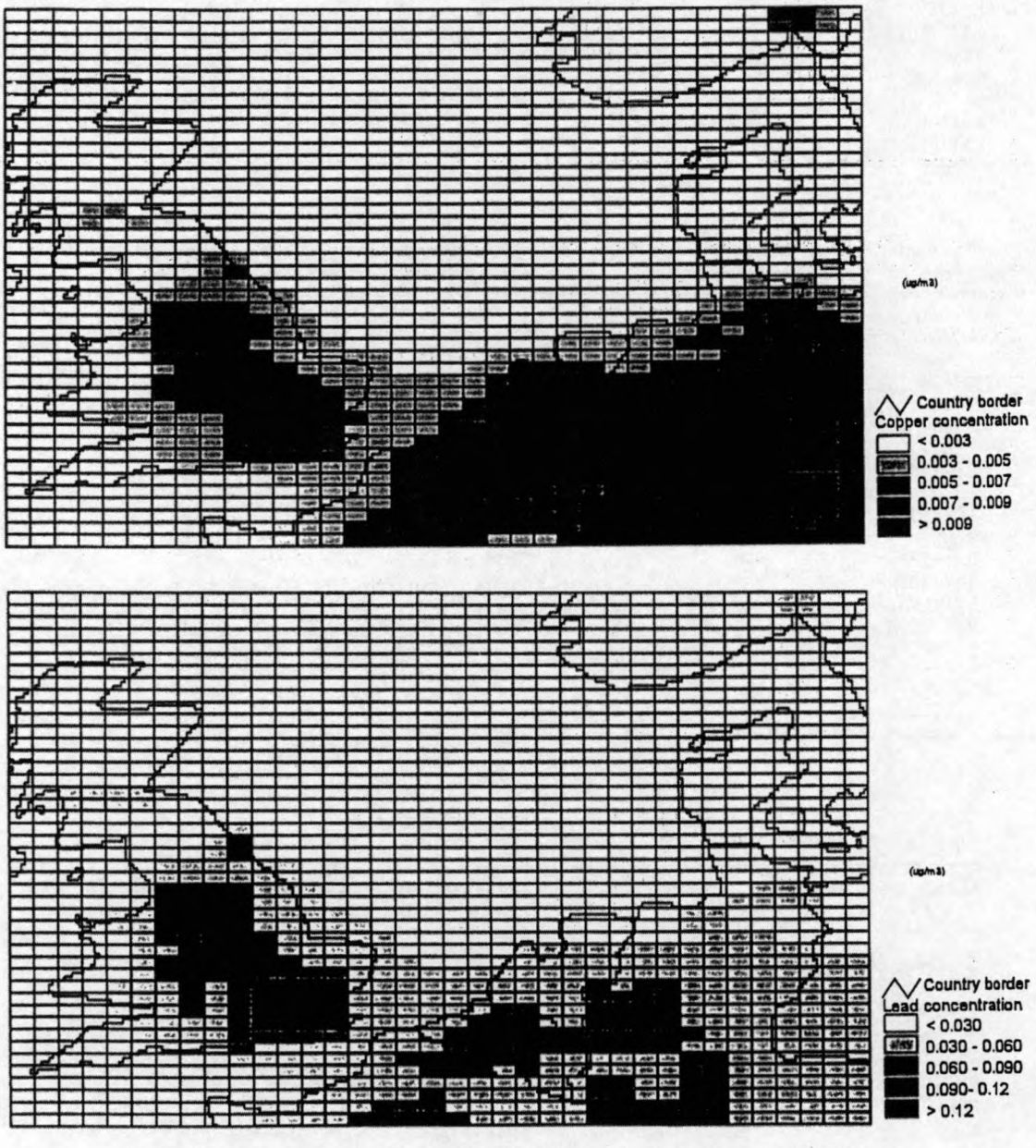

Fig. 5. Concentration maps of Ni, Cu, Zn and Pb in the North Sea area—modelled values.

Table 12 summarizes information on riverine, direct and atmospheric inputs to the North Sea together with the disposal at sea for some heavy metals. It is clear that substantial amounts of metals are introduced into the marine environment through the rivers and the atmosphere. The atmospheric deposition

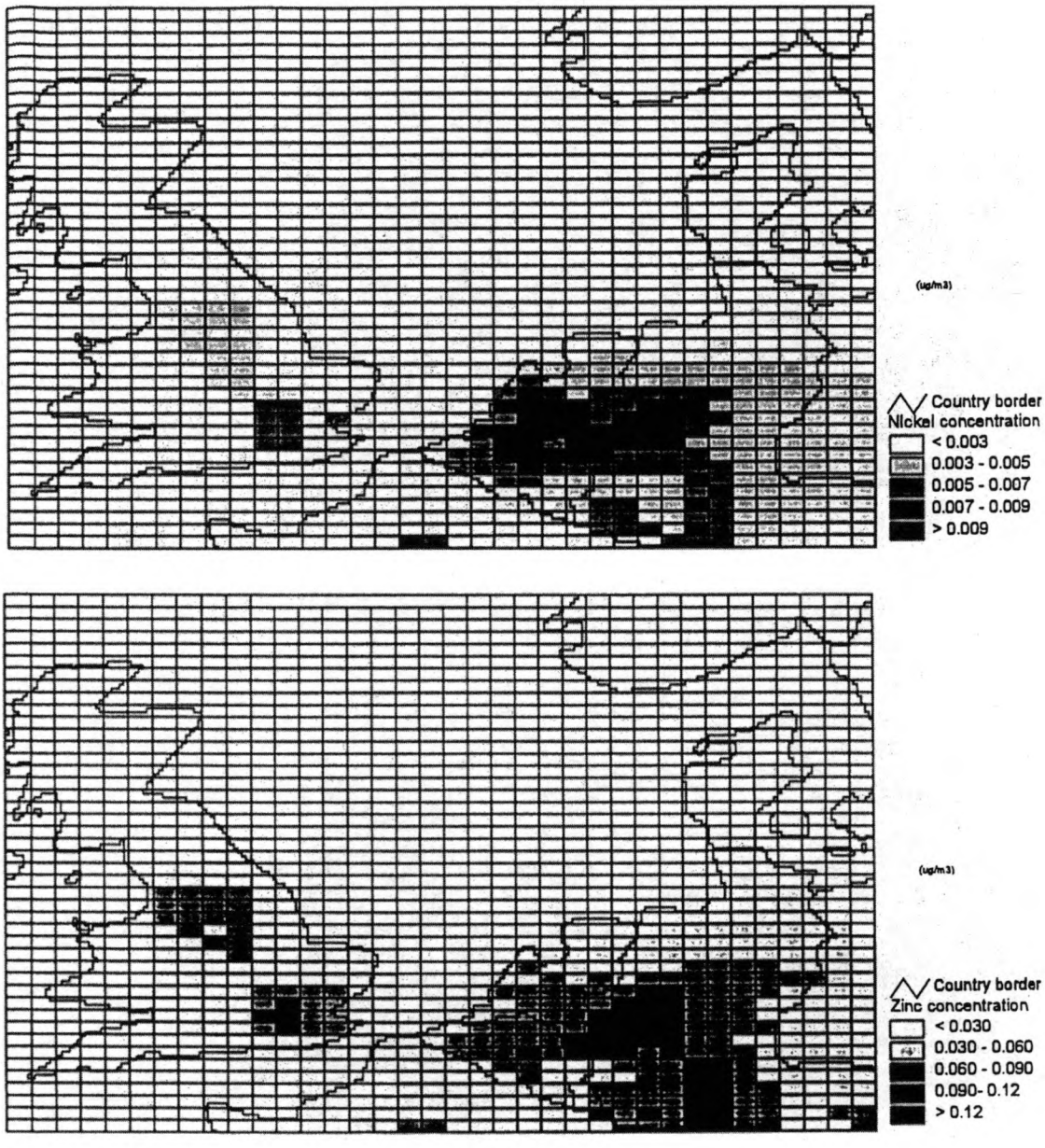

Fig. 5. Continued

Table 14. Comparison of total depositio fluxes to the North Sea determined indirectly (measurements and Slinn and Slinn model) with modelled values ($kg\,km^{-2}\,yr^{-1}$)

	Ni	Cu	Zn	Pb
Measurements and Slinn and Slinn model	1.21	1.30	6.5	3.7
Model	0.25–0.5	0.25–0.5	2.5–5	2.5–5

contributes 28% (Cu), 29% (Zn) and 57% (Pb). The impact of smaller point sources can, however, be highly significant and should not be ignored. In order to reduce inputs via the atmosphere, reduction of emissions at the source will usually prove to be the most effective or only method.

The atmospheric input data, presented here, must be used with great care: the method of extrapolating

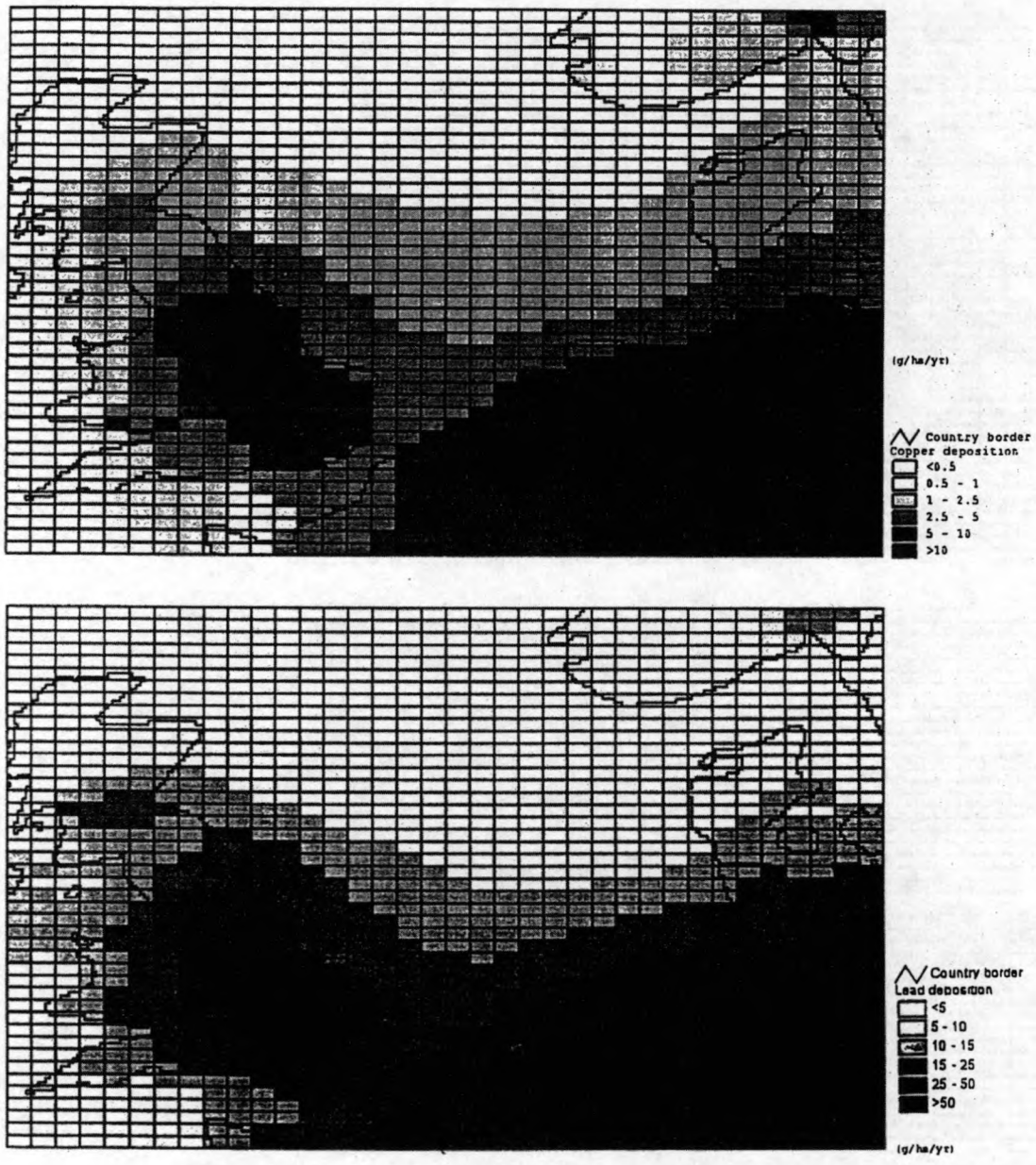

Fig. 6. Deposition maps of Ni, Cu, Zn and Pb in the North Sea area—modelled values.

measurements at a coastal station (although in this study we used also data from two ships, platform and from an off-shore tower) is crude and can result in an overestimate of inputs to the open sea. Furthermore, the accuracy is dependent on the accuracy of our concentration measurements (20%) and deposition calculations (50%) and also on the accuracy of the estimate of the other input routes (30%).

Comparison with model calculations

The indirect deposition calculations were compared with the results obtained from a model, calculated for the same area and period. The model used was the so-called EUTREND model developed at the Dutch National Institute of Public Health and Environmental Protection (Van Jaarsveld *et al.*, 1986). It is a statistical long-range version of the Gaussian plume model, i.e. the dispersion from a source is assumed to follow the prevailing wind direction and wind speed within a sector of 30% in the horizontal plane. Atmospheric processes included in the model are: emission, dispersion, advection, chemical conversion and wet and dry deposition. The model describes the behaviour of pollutants attached to particles as a function of particle size. The emission is considered to be distributed over five size classes: < 0.95, 0.95–4, 4–10, 10–20, > 20 μm. The model calculations are performed for each of the size classes separately, with specific

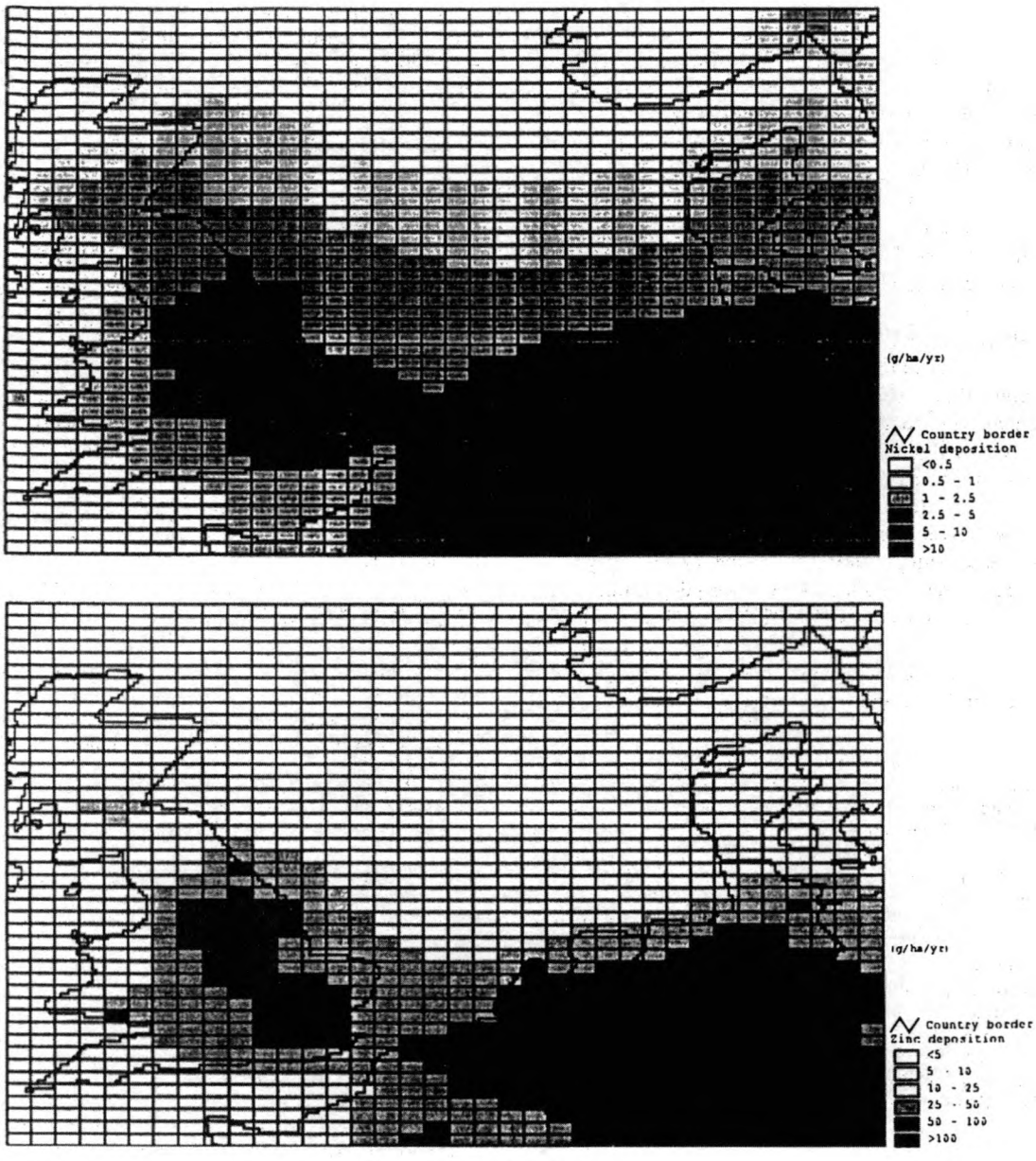

Fig. 6. Continued

deposition properties for each class. Chemical reaction rates used in the model are independent of concentration levels. The model is applied here using a fixed receptor grid over the North Sea area with a 0.5° long. × 0.25° lat. resolution. Emission factors for heavy metals were taken from the PARCOM-ATMOS emission factor manual (Van der Most and Veldt, 1992).

In Table 13 the calculated annually averaged concentrations of Ni, Cu, Zn and Pb (Fig. 5) are compared with "experimental" values, for the North Sea and for the Belgium coast. On average the measured and calculated values agree within a variation of 44–100%. The average discrepancy between the indirectly calculated deposition rates and the modelled ones (Fig. 6) is within a factor of ca. 2 (Table 14). We note here that the total uncertainty of the results is a consequence of uncertainties introduced by the model concept, in compound specific parameters and in the emission estimates. The range of uncertainty in the emissions is wide and ranges from a factor of 2–3.5. This range must be considered as a maximum margin (Baart *et al.*, 1995). Also, there is a large uncertainty in the experimental values. Taking into account all these uncertainties, we can conclude that the agreement between the atmospheric inputs estimated from our measurements and those calculated with the model is quite satisfactory.

CONCLUSIONS

In the period from 1992 to 1994, an extensive research program has been carried out for the North Sea environment, aiming to assess more quantitatively the total (dry and wet) atmospheric deposition fluxes. The fluxes were calculated from a large set of *in situ* measured particle size distributions and their elemental concentrations, using the model of Slinn and Slinn for dry deposition and, for wet deposition, the scavenging factors and the mean annual rainfall above the North Sea. The accuracy in deposition calculations is within 50%. Comparison of the results with those from a model for the same area and period shows that they reasonably agree and the observed differences are acceptable.

A rather new approach was used for the determination by TXRF of trace element concentrations in size-segregated aerosol deposits. The aerosol particles were deposited directly on the quartz discs which also served as sample supports for the TXRF analysis.

The determined total (dry + wet) deposition fluxes for 16 elements (S, K, Ca, Ti, V, Cr, Mn, Fe, Ni, Cu, Zn, As, Se, Br, Sr and Rb) have pointed out the importance of the atmosphere as a pathway for deposition of pollutants into the North Sea.

Acknowledgements—This work was supported by the Belgian State-Prime Minister's Service-office for Scientific, Technical and Cultural Affairs, in the framework of the Impulse Programme in Marine Sciences (Contract MS/06/050) the Programme in Sustainable Management of the North Sea (Contract MN/DD/10) and the EUROTRAC Programme (Contract EU 7/08). The MAPTIP experiments were supported by the Netherlands Ministry of Defence (A91-KM-615), the US Office of Naval Research (Grant N00014-91-J-1948) and NATO (Grants 6056 and 6092). The measurements aboard Hr. Ms. Tydeman were made by Dr F. P. Neele. Computational support and detailed model calculations presented in this paper were made by Arthur Baart from the TNO Institute of Environmental Sciences, Energy Research and Process Innovation, in the framework of EC DG XII project EV5V-CT93-0313.

REFERENCES

Arimoto, R., Duce, R. A., Ray, B. J., Hewitt, A. D. and Williams, J. (1987) Trace elements in the atmosphere of American Samoa: concentrations and deposition to the tropical South Pacific. *Journal of Geophysical Research* **92**, 8465–8479.

Andreas, E. L. (1990) Time constants for the evolution of sea spray droplets. *Tellus* **B42**, 481–497.

Baart, A. C., Berdowski, J. J. M. and Van Jaarsveld, J. A. (1995) Calculation of atmospheric deposition of contaminants on the North Sea. Report No. TNO-MW-R95/138, TNO Institute of Environmental Sciences, Delft, The Netherlands.

Baeyens, W., Dehairs, F. and Dedeurwaerder, H. (1990) Wet and dry deposition fluxes above the North Sea. *Atmospheric Environment* **24A**, 1693–1703.

Barrie, L. A. (1992) Scavenging ratios: black magic or a useful scientific tool. In *Precipitation Scavenging and Atmosphere-Surface Exchange*, eds S. E. Schwartz, and W. G. N. Slinn, pp. 403–420. Hemisphere, New York.

Chester, R., Bradshaw, G. F., Ottley, C. J., Harrison, R. M., Merrett J. L., Preston, M. R., Rendell, A. R., Kane, M. M. and Jickells, T. D. (1993) The atmospheric distribution of trace metals, trace organics and nitrogen species over the North Sea. *Philos. Trans. Roy. Soc.* **A343**, 543–556.

De Leeuw, G., Van Eijk, A. M. J. and Jensen, D. R. (1994) MAPTIP experiment, marine aerosol properties and thermal imager performance: an overview. Report FEL-94-A140, TNO Physics and Electronics Laboratory.

De Leeuw, G., Moerman, M. and Van Eijk, A. M. J. (to be published).

Dulac, F., Buat-Menard, P., Ezat, U., Melki, S. and Bergametti, G. (1989) Atmospheric input of trace metals to the western mediterranean: uncertainties in modelling dry deposition from cascade impactor data. *Tellus* **41B**, 362–378.

Galloway, J. N., Savoie, D. L., Keene, W. C. and Prospero, J. M. (1993) The temporal and spatial variability of scavenging ratios for NNS sulphate, nitrate, methonesulphonate and sodium in the atmosphere over the North Atlantic Ocean. *Atmospheric Environment* **27A**, 235–250.

Gathman, S. G. (1983) Optical properties of the marine aerosol as predicted by the Navy aerosol model. *Optical Enginering* **22**, 57–62.

Gathman, S. G. (1989) A preliminary description of NOVAM, the navy oceanic vertical aerosol model. NRL Report 9200, Naval Research Laboratory, Washington D.C., U.S.A.,

GESAMP-IMO/FAO/UNESCO/WMO/WHO/ IAEA/UN/ UNEP (1989) Joint group of experts on the scientific aspects of marine pollution. The Atmospheric Input of Trace Species to the World Ocean. Report Studies GESAMP (38).

Injuk, J., Breitenbach, L., Van Grieken, R. and Wätjen, U. (1994) Perfomance of nuclear microprobe to study giant marine aerosol particles. *Mikrochimica Acta* **114/115**, 313–321.

Injuk, J. and Van Grieken, R. (1995a) Optimisation of total-reflection X-ray fluorescence spectrometry for aerosol analysis. *Spectrochimica Acta* **B50**, 1787–1803.

Injuk, J. and Van Grieken, R. (1995b) Atmospheric concentrations and deposition of heavy metals over the North Sea: a literature review. *Journal of Atmospheric Chemistry* **20**, 179–212.

Jaffrezo, J. L. and Collin, J. L. (1988) Rain-aerosol coupling in urban areas: scavenging ratio measurements and identification of some transfer processes. *Atmospheric Environment* **22**, 929–935.

Jickells, T. (1995) Atmospheric inputs of metals and nutrients to the oceans: their magnitude and effects. *Marine Chemistry* **48**, 199–214.

Kane, M. M., Rendell, A. R. and Jickells, D. (1994) Atmospheric scavenging processes over the North Sea. *Atmospheric Environment* **28**, 2523–2530.

OSPARCOM (1993) North Sea Assessment Report 2b. North Sea Task Force. Oslo and Paris Commissions, London. Olsen and Olsen, Fredensburg, Denmark.

Otten, Ph., Injuk, J. and Van Grieken, R. (1994) Elemental concentrations in atmospheric particulate matter sampled on the North Sea and the English Channel. *Science of Total Environment* **155**, 131–149.

Ottley, C. J. and Harrison, R. M. (1991) The atmospheric input flux of trace metals to the North Sea: a review and recommendations for research. *Science of Total Environment* **100**, 301–318.

Ottley, C. J. and Harrison, R. M. (1993) Atmospheric dry deposition flux of metallic species to the North Sea. *Atmospheric Environment* **27A**, 685–695.

Rojas, C. M., Injuk, J., Van Grieken, R. and Laane, R. M. (1993) Dry and wet deposition fluxes of Cd, Cu, Pb and Zn into the Southern Bight of the North Sea. *Atmospheric Environment* **27A**, 251–259.

Salvá, A., von Bohlen, A., Klockenkämper, R. and Klockow, D. (1993) Multielement analysis of airborne particulate matter by total reflection X-ray fluorescence. *Quimica Analitica* **12**, 57–62.

Schneider, B. (1989) The determination of atmospheric trace metal concentrations by collection of aerosol particles on sample holders for total-reflection X-ray fluorescence. *Spectrochimica Acta* **44B**, 519–523.

Slinn, S. A. and Slinn, W. G. N. (1980) Predictions for particle deposition on natural waters. *Atmospheric Environment* **14**, 1013–1016.

Slinn, W. G. N. (1983) Air to sea transfer of particles. In *Air-Sea Exchange of Gases and Particles*. eds Liss, P. S. and Slinn, W. G. N., p. 299 D. Reidel Publishing, Dordrecht, Holland.

Steiger, M., Schulz, M., Schwikowski, M., Naumann, K. and Dannecker, W. (1989) Variability of aerosol size distribution above the North Sea and its implication to the dry deposition estimates. *Journal of Aerosol Science* **20**, 1229–1232.

Van der Most, P. F. J. and Veldt, C. (1992) Emission factors manual PARCOM-ATMOS. Emission factors for air pollutants 1992. TNO Report 92–235, Apeldoorn, Netherlands.

Van Eijk, A. M. J. and De Leeuw, G. (1992) Modelling aerosol particle size distributions over the North Sea. *Journal of Geophysical Research* **97**, 14,417–14,429.

Van Eijk, A. M. J., Bastin, F. H., Neele, F. P., De Leeuw, G. and Injuk, J. (1995) Characterisation of atmospheric properties during MAPTIP. In *Propagation Assessment in Coastal Environments*, Advisory Group for Aerospace Research and Development (AGARD-CP 567, NATO), pp. 19.1–19.8.

Van Espen, P., Janssens, K. and Nobels, J. (1986) Axil-PC, Software for the analyses of complex X-ray spectra. *Chemometrics Intelligent Laboratory Systems* **1**, 109–114.

Van Jaarsveld, J. A., van Aalst, R. M. and Onderdelinden, D. (1986) Deposition of metals from the atmosphere into the North Sea: model calculations. Report No. 842015002, RIVM, Bilthoven.

Vawda, Y., Colbeck, I., Harrison, R. M. and Nicholson, K. W. (1992) Assessment of the performance of a tunnel sampler and cascade impactor system for ambient air sampling. *Journal of Aerosol Science* **23**, 233–243.

Wobrauschek, P. and Aiginger, H. (1975) Total-reflection X-ray fluorescence spectrometric determination of elements in nanogram amounts. *Analytical Chemistry* **47**, 852–855.

Yaaqub, R. R., Davies, T. D., Jickells, T. D. and Miller, J. M. (1991) Trace elements in daily collected aerosols at a site in southeast England. *Atmospheric Environment* **25**, 985–996.

Selected article #23:

Trend analysis of the published concentrations of heavy metals in aerosols above the North Sea and the English Channel for the period 1971-1994

S. Hoornaert, B. Treiger, R. Van Grieken and R. Laane

Environmental Reviews, 7 (1999) 191-202

Trend analysis of the published concentrations of heavy metals in aerosols above the North Sea and the English Channel for the period 1971–1994

Stefaan Hoornaert, Boris Treiger, René Van Grieken, and Remi Laane

Abstract: A literature review is given of atmospheric trace metal concentrations in aerosols above the North Sea and the English Channel over the period 1971–1994. Literature data have been gathered and intercompared to look for possible trends in the reported concentrations. Six trace metals are considered: Cd, Cu, Pb, Zn, Ni, and Cr. A distinction is made between measurements in different regions of the North Sea, and between coastal and marine areas. The majority of the data deals with the Southern Bight, providing the most reliable trends. Strong decreasing trends are observed for the Pb and Zn concentrations above the North Sea during the years 1971–1994. For Cd, Cu, Ni, and Cr, much less data are available in the literature. Despite this, also for Cd and Cu a decreasing trend is present. Cr and Ni concentrations are fluctuating, mostly without a certain pattern. The trends in the concentrations are also compared to changes in the European emission profiles.

Key words: heavy metals, aerosols, North Sea, trend analysis, literature.

Résumé : Les concentrations de métaux lourds dans des aérosols atmosphériques au-dessus de la Mer du Nord et du Canal anglais, publiées durant la période 1971–1994 ont été examinées. Les données rapportées ont été rassemblées et comparées afin de découvrir d'éventuelles tendances dans les concentrations rapportées. Six métaux lourds ont été pris en considération : Cd, Cu, Pb, Zn, Ni et Cr. Une distinction a été faite entre les mesures réalisées dans différentes régions de la Mer du Nord, ainsi qu'entre les zones côtières et maritimes. La majorité des données concerne la partie sud de la Mer du Nord, qui apporte les tendances les plus fiables. De fortes tendances dégressives de concentration de Pb et de Zn au-dessus de la Mer du Nord sont observées durant les années 1971–1994. En ce qui concerne Cd, Cu, Ni et Cr, moins de données sont disponibles dans la littérature. Néanmoins, une tendance dégressive est également observée pour Cd et Cu. Les concentrations de Cr et Ni sont plus variables, le plus souvent sans trame claire. Les tendances de concentrations ont aussi été comparées avec les changements des profils d'émissions européennes.

Mots clés : métaux lourds, aérosols, Mer du Nord, analyse de tendance.

1. Introduction

Environmental contamination with trace metals started with the discovery of fire. Historical records from ice sheets and sediments indicate that the discharge of toxic metals into the environment increased significantly since the beginning of the Industrial Revolution (Nriagu 1990). Apart from other pollutants, significant amounts of trace metals are released into the atmosphere mainly due to the volatility of the corresponding elements at high temperatures during various combustion and incineration processes and fuel burning. Nriagu and Pacyna (1988), who made an inventory of global emissions of trace metals in 1983, found that the anthropogenic emissions of Cd, Cu, Ni, and Zn exceed the inputs of these elements from natural sources by about two-fold or more and in the case of Pb even by a factor 17. The main sources of anthropogenically emitted trace metals are non-ferrous metal and steel manufacturing, oil and coal combustion, refuse incineration, and traffic. A detailed discussion of the different sources can be found elsewhere (Pacyna 1998). The airborne pollutants are a threat to human health, directly through inhalation and also indirectly since they are deposited, after transport in the atmosphere, on the soil and in the surface waters and oceans. Several studies on the deposition of airborne particulate matter have shown that the atmospheric input is a significant route of trace metals to the ocean. It can even exceed the other inputs like rivers and direct discharges, especially in the case of open seas, where the influence of rivers is minimal (GESAMP 1989). In the case of the North Sea the atmospheric contribution to the input of Cd, Cu, Pb, and Zn into the Southern Bight (the southern part of the North Sea) is estimated to be 55, 24, 40, and 22%, respectively (Otten et al. 1992).

The North Sea, being only a shallow sea, is characterized by a high biological production that is overexploited by intensive fishing activities. The North Sea ecosystem is also

Received January 26, 1999. Accepted August 31, 1999. Published on the NRC Research Press Web site on January 19, 2000.

S. Hoornaert, B. Treiger, and R. Van Grieken.[1] University of Antwerp (UIA), Department of Chemistry, Universiteitsplein 1, B-2610 Antwerpen, Belgium.
R. Laane. Institute for Coastal and Marine Management (RIKZ), Rijkswaterstaat, Kortenaerkade 1, 2500 EX The Hague, The Netherlands.

[1]Author to whom all correspondence should be addressed (e-mail: vgrieken@uia.ua.ac.be).

Fig. 1. The North Sea and the Channel with the different subregions and location of the fixed sampling sites (cruises are not indicated). Legend — Channel: 1, Atlantic station; 2, Bassurelle; 3, Baie d'Ambleteuse; 4, Wimereux. Southern Bight: 5, Styrrup; 6, Spurn Head; 7, Gresham; 8, Mannington; 9, Helmsby; 10, Leiston; 11, Gasplatform; 12, Westhinder; 13, Blankaert; 14, Oostende; 15, Blankenberge; 16, Haamstede; 17, Rijnmond; 18, Petten; 19, Hage; 20, Shiermonnikoog; 21 Hamburg. Central North Sea: 22, Helgoland; 23, Westerheversand; 24, Kiel; 25, FPN; 26, Pellworm; 27, Aberdeen. Northern North Sea: 28, Birkenes; 29, Vassar.

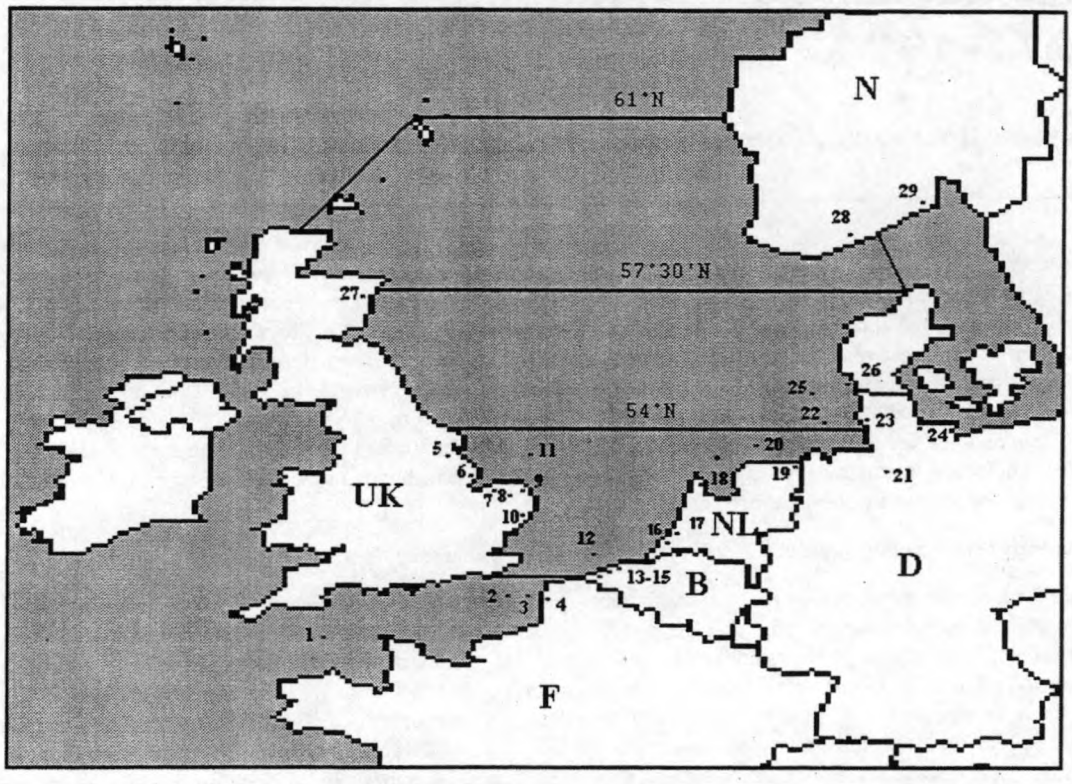

under stress because it is surrounded by some very industrialized and populated areas (mainly situated around the southern part), fed by rivers from Europe's industrial heartland, dotted with oil platforms, and exposed to heavy ship traffic, which together cause a serious threat to the health of this very sensitive ecosystem.

In the sea the deposited trace metals can initiate changes in natural biochemical processes. Perhaps even more important is the fact that they enter the food chain, thereby causing negative effects on biologically important species and a threat to the health of man. As a result of the growing concern about these hazardous effects of the increased dispersion of trace metals in the environment, scientists have tried to evaluate the atmospheric deposition of heavy metals into the sea (NAS 1978; GESAMP 1980, 1989; Duce et al. 1991). Much attention has been paid to the case of the North Sea because of the proximity of the industrial areas. Besides model calculations, scientists have tried to assess trace metal concentrations and size-distributions of North Sea aerosols during several sampling campaigns on and around the North Sea. This has produced quite a lot of individual data sets which, up till now, have not been intercompared.

The aim of this work, therefore, is to gather all these data, to compare them, and to look for possible trends in the concentrations as a function of time. As described by Amundsen et al. (1992), a decreasing trend is to be observed since there have been several changes in the energy, industrial, and transport sectors in Europe. In the energy sector there was a strong increase in the use of nuclear power and the share of gas. There was a decrease in oil imports and a growth of indigenous oil production. The latter show lower levels of heavy metals, compared to those from the Middle East and South America. The total traffic volume increased but less Pb additives were used and the share of unleaded gasoline increased. Reductions in the industrial emissions were also obtained by the development of new and cleaner production techniques and more efficient emission control devices.

2. Experimental

The statistical analysis is done on available published data for the period 1971–1994. Six trace metals are considered: Cd, Cu, Pb, Zn, Ni, and Cr.

We have separated the North Sea and the Channel into four different regions (Fig. 1): the Channel itself (below 51°N), the Southern Bight (between 51°N and 54°N), the central North Sea (between 54°N and 57°30′N), and the northern North Sea (between 57°30′N and 61°N). This distinction is not done on a geographical basis but it is based on the results and is meaningful in the following sense:

Concentrations above the Channel are expected to be lower than for the other regions because of the influx of relatively clean air from the Southwest and because of the smaller number of emission sources in this sector of Europe.

The Southern Bight is only a narrow area, very close to the major sources. As reported by Pacyna (1984), the major

Table 2. Trace metal concentrations (ng/m^3) for all sampling campaigns in the marine area of the Southern Bight.

Period	1972–1973[a]	1980[a]	1980–1981[a]	1980–1983[a]	1980–1985	1980–1985		
	June 72–May 73				Jan. 80–Aug. 85	Jan. 80–Aug. 85		
Location	Gas platform	Westhinder	Westhinder	Westhinder	Westhinder	Westhinder		
	Not specified	Not specified	Not specified	Geom. mean	Geom. mean	Arithm. mean	Geom. mean	A
Cd	—	—	2.7	2.9 ± 1.8	2.8 ± 2.2	3.9 ± 3	3.0	—
Cu	<20.8	14	6.5	9.0 ± 3.0	14.7 ± 10	18 (17) ± 10	14.3	10
Pb	147	186	82.6	104 ± 2.3	96 ± 100	150 ± 100	92	1
Zn	153	176	86.6	94 ± 3.1	67.4 ± 90	170 (150) ± 200	79	1
Ni	10.1	—	—	—	—	—	—	5
Cr	4.5	—	—	—	—	—	—	—
Reference	Peirson et al. 1974 Cambray et al. 1975	Elskens et al. 1981[b]	Dehairs et al. 1982[b]	Dedeurwaerder et al. 1983	Baeyens and Dedeurwaerder 1991	Dedeurwaerder 1988		O
Remark						() = without outliers		4

[a]Values used in the graphs.
[b]Indirectly cited values since we were unable to get the original reports.
[c]Eight samples.
[d]Six samples.

Table 3. Trace metal concentrations (ng/m^3) for all sampling campaigns in the coastal area of the Southern Bight.

Period	1972	1972[a]	1972	1972[a]	1972–1973	1972–1973	1973[a]	1973[a]	1973	1974[a]	1974[a]
	Jan.–Feb.	Jan.–Dec.	Feb.–March	Feb.–Dec.	June–May	June–May	Jan.–Dec.	Jan.–Dec.	Feb–May	Jan.–Dec.	Jan.–D
Location	Styrrup (U.K.)	Styrrup (U.K.)	Leiston (U.K.)	Leiston (U.K.)	Leiston (U.K.)	Gresham (U.K.)	Leiston (U.K.)	Styrrup (U.K.)	Petten (NL)	Styrrup (U.K.)	Leisto (U.K.)
	Not specified	Not specified	Not specified	Not specified	Not specified	Not specified	Not specified	Not specified	Not specified	Not specified	Not specifi
Cd	<6.1	<41.7	<6.1	<13.5	—	—	<14.7	<55	—	<19.6	<9.8
Cu	67.4	41.7	33.1	<11.0	<13.5	<11.0	<13.5	29.4	<7.4	<11.0	<4.9
Pb	466	405	126	135	159	159	178	417	118	245	120
Zn	509	417	401	196	147	129	141	392	92.0	294	78.5
Ni	11.0	10.8	6.4	5.0	5.9	6.6	8.0	15.0	8.9	8.0	6.6
Cr	14.7	20.8	17.2	9.2	6.6	4.2	4.7	24.5	3.8	11.6	2.1
Reference	Peirson et al. 1973	Peirson et al. 1974 Cawse 1974	Peirson et al. 1973	Peirson et al. 1974 Cawse 1974	Peirson et al. 1974 Cambray et al. 1975	Peirson et al. 1974 Cambray et al. 1975	Cawse 1974	Cawse 1974	Peirson et al. 1974 Cambray et al. 1975	Cawse 1975	Cawse 197

[a]Values used in the graphs.
[b]Indirectly cited values since we were unable to get the original reports.

	1984[a] December Cruise		1985[a] May and August Cruise		1986[a] March Cruise		1987[a] October Cruise		1988[a] March Cruise	
ın	Arithm. mean	Geom. mean	Arithm. mean	Geom. mean	Arithm. mean	Geom. mean	Arithm. mean	Geom. mean	Arithm. mean	Geo
	—	—	—	—	—	—	—	—	—	—
	10.4 ± 15.5	2.5	4.5 ± 2.8[c]	3.2	18.5 ± 9.3	16.9	2.6 ± 1.1	2.4	9.3 ± 4.5	8.2
	135 ± 70	115	30.9 ± 21.2	24.0	124 ± 75	107	18.1 ± 2.2	17.9	40.5 ± 44.0	25.5
	118 ± 74	95	37 ± 32	22.5	245 ± 223	198	13.3 ± 10.2	10.2	62.2 ± 48.4	42.9
	5.8 ± 6.9	2.3	9.4 ± 9.4[c]	5.7	12 ± 7.1	10.5	5.0 ± 3.9	3.8	5.9 ± 2.9	5.1
	—	—	41 ± 33[d]	28	11.4 ± 8.6	8.7	—	—	27.5 ± 12.4	25.0
	Otten et al. 1994		Otten et al. 1994		Otten et al. 1994		Otten et al. 1994		Otten et al. 1994	
	4 samples		9 samples		8 samples		4 samples		6 samples	

1974[a] Jan.–Dec. Leiston (U.K.) Not specified	1975[a] Jan.–Dec. Styrrup (U.K.) Not specified	1975[a] Jan.–Dec. Leiston (U.K.) Not specified	1976[a] Jan.–Dec. Styrrup (U.K.) Not specified	1976[a] Jan.–Dec. Leiston (U.K.) Not specified	1977[a] Schiermonnikoog (NL)	1977[a] Haamstede (NL)	1972–1979 May 72–April 79 Oostende (B) Arithm. mean	1978–1981[a] Rijnmond (NL)	1981[a] De Blankaer (B)
<9.8	8.8	6.7	<3.7	<2.5	0.4	2.5	5	2–3	3.4 ± 2.0
<4.9	27.0	14.7	56.4	19.6	11.5	22	17.4	10–11	12.8 ± 2.7
120	245	110	233	129	30	180	241	160–205	77 ± 2.2
78.5	221	80.9	202	113	20	130	251	—	174 ± 3.1
6.6	8.9	6.1	11.3	4.0	5	22	11.1	8–20	—
2.1	10.5	4.2	10.7	3.6	0.8	7.5	11.9	—	—
Cawse 1975	Cawse 1976	Cawse 1976	Cawse 1977	Cawse 1977	Diederen and Guicherit 1981[b]	Diederen and Guicherit 1981[b]	Kretzschmar and Cosemans 1979	DCMR 19—[b]	Dedeurwaerc et al.1983

1988[a] March Cruise		1988–1989[a] Aug. 88–Oct. 89 Cruise		1988–1989[a] Dec. 88–Oct. 89 Cruise		1993[a] August Cruise	1993[a] Oct.– Nov. Cruise
ı. mean	Geom. mean	Arithm. mean	Geom. mean	Arithm. mean	Geom. mean	Arithm. mean	Arithm. mean
	—	—	—	1.25 ± 1.30	0.76 ± 2.87	—	—
4.5	8.2	6.3 ± 5.87	4.4	6.9 ± 9.43	1.8 ± 8.35	1.9 ± 1.0	4.2 ± 3.3
44.0	25.5	34.5 ± 35.3	20	29.1 ± 39.8	8.8 ± 9.65	<DL	17.4 ± 13.1
48.4	42.9	41 ± 41.1	26	74.6 ± 98	32 ± 5.07	6.2 ± 4.2	20.5 ± 14.7
2.9	5.1	3.8 ± 2.75	2.5	—	—	1.7 ± 1.2	4.4 ± 4.6
12.4	25.0	4.7 ± 4.58	3.1	—	—	1.5 ± 0.4	2.9 ± 2.6
ɜt al. 1994		Chester and Bradshaw 1991		Ottley and Harrison 1993		Injuk 1995	Injuk 1995

ɔles

1981[a]	1981–1982	1984–1985[a]		1986–1987[a]			1987[a]	1987–1988[a]	
	March 81–March 82	Aug. 84–Aug. 85		Aug. 86–Feb. 87				March 87–March 88	
De Blankaert (B)	Hamburg (D)	South Holland (NL) 2 different locations		South Holland (NL) 3 different locations			Hage (NL)	Hemsby (U.K.)	
	Arithm. mean	Not specified	Not specified	Not specified	Not specified	Not specified	Arithm. mean	Not specified	Not specif
3.4 ± 2.0	2.9 ± 1.5	1.9	2.0	1.1	0.8	0.8	0.8 ± 0.7	1.1 ± 1.0	0.3
12.8 ± 2.7	112 ± 55	23 (cont)	—	3.7	5.0	3.7	5.5 ± 6.4	—	5.6
77 ± 2.2	435 ± 240	167	178	36	116	57	45.5 ± 35.8	34 ± 31	63
174 ± 3.1	318 ± 149	172 (cont)	200 (cont)	34	64	48	59.3 ± 80.7	41 ± 37	24
—	9.5 ± 4.3	15	12	4.0	9.1	7.9	2.8 ± 2.5	2.7 ± 2.9	4.6
—	7.4 ± 4.3	2.9	2.6	3.6	14	4.6	—	—	2.5
Dedeurwaerder et al.1983	Steiger 1991	Van Daalen 1991		Van Daalen 1991			Steiger 1991	Yaaqub et al. 1991	Van I

	1987–1988[a]			1989[a]	1991[a]	1991[a]	1992–1994[a]	
8	Sept. 87–March 88			4 periods	September	September	October 92 – May 94	
	South Holland (NL) 3 different locations			Mannington (U.K.)	Hemsby (U.K.)	Spurn Head (U.K.)	Blankenberge (B)	
	Not specified	Not specified	Not specified	Not specified	Geom. mean	Geom. mean	Summer Arithm. mean	Winter Arithm. mean
	0.3	0.4	0.3	0.7 ± 0.91	0.14	0.28	—	—
	5.6	4.6	4.3	12 ± 22	177	15	3.9 ± 2.7	2.2 ± 2.8
	63	56	38	36 ± 33	35	5.7	4.3 ± 3.2	12.1 ± 15.2
	24	22	18	58 ± 70	33	21	22.5 ± 19.5	21.8 ± 18.2
	4.6	4.5	4.6	—	—	—	4.1 ± 5.1	2.1 ± 1.2
	2.5	2.0	1.7	—	—	—	6.7 ± 8.9	3.5 ± 2.7
	Van Daalen 1991			Kane et al. 1994	Spokes 1991 12 samples	Spokes 1991 12 samples	Injuk 1995	

western European emissions of Cd, Cu, Zn, and Cr are situated around the Southern Bight, more precisely in the Benelux region, the neighbouring German Ruhr area, and in the south-eastern part of the U.K. So it is obvious that the highest trace metal concentrations should be found in this region. It is therefore not surprising that the major part of the available data deals with this part of the North Sea.

Above 54°N, the North Sea is much wider. Lower concentrations are expected for this region because of the increased distance to the major source areas of aerosols and the lower emissions in this region. A further subdivision of this part of the North Sea is made into the central and northern North Sea. The central part is still influenced to some extent by the high emissions around the Southern Bight while the northern part usually experiences the flow of clean air from above the Atlantic Ocean.

A second distinction is made for each of the four regions between coastal measurements (these are measurements performed at land but close to the sea) — for which higher concentrations should be expected because of the proximity of the emission sources — and measurements on the sea (cruises, lightships, and platforms).

For each region all data were ordered chronologically. If more data were present for a specific year, only yearly averages were taken into account to minimize possible effects of seasonal or meteorological changes on the concentration patterns.

3. Results and discussion

3.1. English Channel

Data on atmospheric trace metal concentrations above the English Channel are rather scarce. For both the marine and coastal part of the Channel, values in the literature are available for only a few periods of time between 1981 and 1994 (Dedeurwaerder 1988; Flament et al. 1987; Otten et al. 1994; Flament et al. 1996). Therefore, it is hardly possible to speak about reliable trends in the concentration profiles. The data that can be found in literature for the English Channel are summarized in Table 1 and represented in Fig. 2 for Cu, Pb, and Zn.

For 1987 only the June data were taken into account since the November data were measured under strong continental influence, while the other cruises in 1986 and 1987 represent marine air masses (Otten et al. 1994). All the values used are geometric means since arithmetic means attribute a stronger statistical importance to episodically high measured values.

The concentrations in 1982–1984 are rather high compared to the other values. This is because all other values (except the 1994 data) were measured during cruises on or stations in the English Channel, while the 1982–1984 data also include coastal measurements at Wimereux, a semi-remote location on the French coast of the Strait of Dover. Flament et al. (1987) report a Pb concentration of 56 ng/m³ at Wimereux for the period 1982–1984 while Flament et al. (1996) report an atmospheric Pb concentration of only 17 ng/m³ at the same site but for the period 1982–1983. The latter measurements were performed only under marine conditions (winds from the southwest). The higher value for the 1982–1984 period is probably caused by the statistical

Table 1. Trace metal concentrations (ng/m³) for all sampling campaigns for the English Channel.

Period	1981[a]		1982–1984[a]			1986[a]		1987[a]		1987		1994[a]
	April–Sept.		April 82–June 84			May		June		November		March
Location	Cruise (Bassurelle)		Cruise + Wimereux (F)			Cruise		Cruise		Cruise		Wimereux (F)
	Geom. mean	Arithm. mean	Geom. mean	Median	Arithm. mean	Arithm. mean	Geom. mean	Arithm. mean	Geom. mean	Arithm. mean	Geom. mean	Geom. mean
Cd	1.0	3.1 ± 5.4	3	4.8	6	—	—	—	—	—	—	—
Cu	8.8	9.9 ± 6.1	19.8	19.1	23.7	0.6 ± 0.6	0.5	0.5 ± 0.2	0.5	3.7 ± 3.7	2.6	—
Pb	22.5	29.8 ± 20.0	56	66	130	8.3 ± 0.8	8.3	8.3 ± 0.8	8.3	64.4 ± 48.4	50.4	8
Zn	23.3	28.6 ±16.5	100	143	237	5.5 ± 9.7	1.7	1.3 ± 2.4	0.7	58.6 ± 53.5	30.2	—
Ni	—	—	—	—	—	2.4 ± 2.5	1.2	1 ± 0.9	0.8	3.5 ± 2.0	3.1	—
Cr	—	—	—	—	—	3.1 ± 2.7	2.3	—	—	—	—	—
Reference	Dedeurwaerder 1988		Flament et al. 1987			Otten et al. 1994		Otten et al. 1994		Otten et al. 1994		Flament et al. 1996
Remark	5 samples		18 samples			7 samples		7 samples		8 samples		18 samples

[a]Values used in the graphs.

Fig. 2. Average airborne trace metal concentrations (ng/m^3) for the English Channel.

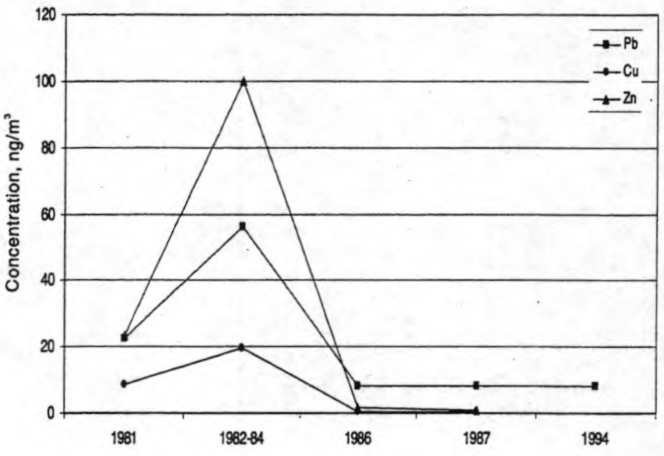

weight of episodically high concentrations due to the influence of the Dunkirk area, which is confirmed by the strong correlation between lead, zinc, and iron concentrations, indicating a metallurgical industrial source (Flament et al. 1996).

Flament et al. (1996) also describe the change in the atmospheric lead concentrations at Wimereux in 1982–1983 and 1994. They find that the lead concentrations in atmospheric particulate matter have decreased by a factor of two over this 10-year period. They have compared their findings with the decrease in the consumption of leaded gasoline in France and concluded that the reduction of automotive lead emissions is responsible for the observed trends in the lead content of atmospheric aerosols.

3.2. Southern Bight

3.2.1. Marine area of the Southern Bight

The Southern Bight is surrounded at the east side by the Netherlands and Belgium and by the U.K. at the west side. It is the most investigated region of the North Sea. This is not surprising since it is also the most endangered part. Measurements in the marine area include sampling on ships (cruises), on the lightship Westhinder, and on a gas platform (Fig. 1). The measurements are described by Peirson et al. (1974), Cambray et al. (1975), Elskens et al. (1981), Dehairs et al. (1982), Dedeurwaerder et al. (1983), Dedeurwaerder (1988), Baeyens and Dedeurwaerder (1991), Chester and Bradshaw (1991), Ottley and Harrison (1993), Otten et al. (1994), and Injuk (1995).

The complete set of data for the marine part of the Southern Bight is given in Table 2 and represented in Fig. 3. For the reason mentioned earlier, in all cases geometric means were used in the graph if both arithmetic and geometric values were available. The values of Baeyens and Dedeurwaerder (1991) and Dedeurwaerder (1988) for the period 1980–1985 were not taken into account in Fig. 3 since this period overlaps with separate yearly averages reported by other authors. The 1988–1989 data, which were found in two different places in the literature, were averaged. Both authors describe the same sampling campaign but have used different methodologies (Ottley and Harrison 1993). Also, the 1993 data have been averaged.

In Fig. 3 the 1986 data were not considered. If they were taken into account, the concentrations between 1984 and 1988 would seem to be subjected to heavy fluctuations with very high values in 1986 (up to 245 ng/m^3 for Zn and 124 ng/m^3 for Pb). The fluctuations can be explained by the fact that for the period 1984–1988 only very few and possibly not representative samples have been analysed during rather short sampling campaigns (Otten et al. 1994). Concentrations therefore are subjected to seasonal changes and other time-dependent factors such as wind direction. Otten et al. (1994) describe the meteorological conditions during some of their cruises as well as backtrajectories. From this information one can see that the campaign in 1985 was characterized by high wind speeds, with little or almost no continental influence. As a result, the atmospheric metal concentrations in 1985 were rather low. In contrast with this, the campaign in 1986 was characterized by meteorological conditions during which pollutant concentrations tend to rise rapidly: a combination of low inversion height and low wind speeds that limits the natural dispersion of pollutants and the absence of any form of precipitation, which restricts the concentration decrease through wet deposition. Therefore, very high concentrations were found in 1986.

So, if one does not consider the 1986 data, it becomes clear that the concentrations seem to behave in a more consistent way. The Pb and Zn concentrations behave in a similar way. They show an increase from the 1970s to the beginning of the 1980s from about 150 to 180 ng/m^3 and have been decreasing to 13–17 ng/m^3 in 1993 with some small increases on the way. The campaign in 1988 ended in the Thames estuary so the results for this campaign were shifted to higher values. The Ni concentrations above the Southern Bight were about 10 ng/m^3 in the 1970s and in 1986. For the other sampling campaigns its concentration varies between 2.3 and 5.7 ng/m^3 but without a certain pattern. The Cu concentrations have dropped from 21 ng/m^3 in the early 1970s to less than 10 ng/m^3 in the early 1980s and about 3 ng/m^3 in the late 1980s and 1990s, except for 1986 and 1988, when higher values were found (17 and 8.2 ng/m^3, respectively). The reason for this has been discussed above. For Cr and Cd too few data are present so that no trends can be observed.

3.2.2. Coastal area of the Southern Bight

Measurements have been done at coastal sites on both sides of the Southern Bight in the period 1972–1994: in the Netherlands (Petten, Schiermonnikoog, Haamstede, Rijnmond, South-Holland, Hage), Belgium (Oostende, De Blankaert, Blankenberge), Germany (Hamburg), and the U.K. (Styrryp, Leiston, Gresham, Hemsby, Mannington, Spurn Head) (Fig. 1). They are described by Peirson et al. (1973, 1974), Cawse (1974–1977), Cambray et al. (1975), Kretzschmar and Cosemans (1979), DCMR (19—), Diederen and Guicherit (1981), Dedeurwaerder et al. (1983), Steiger (1991), Van Daalen (1991), Yaaqub et al. (1991), Spokes (1991), Kane et al. (1994), and Injuk (1995). All data on coastal measurements around the Southern Bight, which is the largest dataset of the whole North Sea region, are summarized in Table 3. The trace metal concentration patterns for the whole coastal region are represented in Fig. 4.

Fig. 3. Average airborne trace metal concentrations (ng/m^3) for the marine area of the Southern Bight.

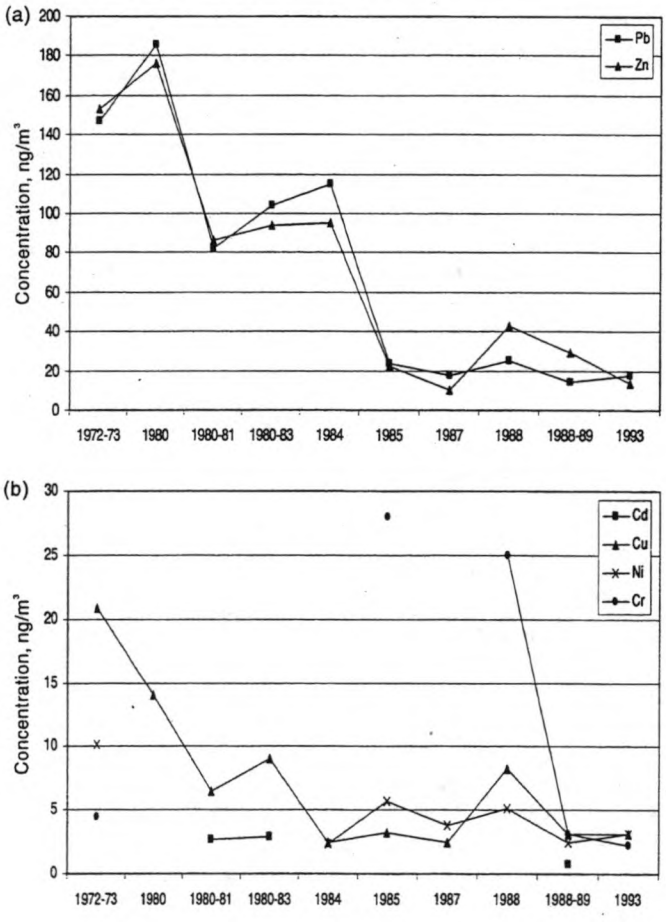

Fig. 4. Average airborne trace metal concentrations (ng/m^3) for the coastal area of the Southern Bight.

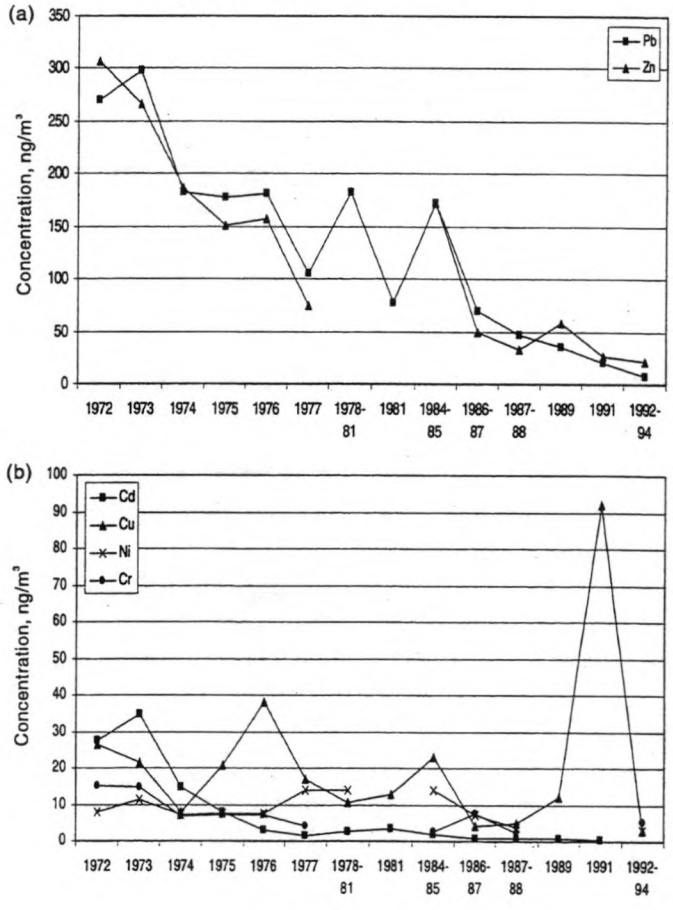

Table 4. Trace metal concentrations (ng/m^3) for all sampling campaigns in the marine area of the central North Sea.

Period	1985		1988		1991	1991
	April		June		September	September
Location	Cruise		Cruise		Cruise (Alkor)	Cruise (Belgica)
	Arithm. mean	Geom. mean	Arithm. mean	Geom. mean	Not specified	Not specified
Cd	—	—	—	—	—	—
Cu	1.7 ± 0.8	1.6	3.7 ± 0.6	3.6	2.0 ± 0.2	1 ± 0.2
Pb	18.2 ± 10.3	15.6	—	—	<DL	<DL
Zn	13.4 ± 8.8	10.2	3.7 ± 0.6	3.6	9 ± 2	4 ± 2
Ni	1.0[a]	1.0	1.3 ± 0.8	1.1	3.0 ± 0.2	1 ± 0.2
Cr	—	—	16.3 ± 3.8	16.0	5 ± 1	2.0 ± 0.2
Reference	Otten et al. 1994		Otten et al. 1994		Injuk et al. 1993	Injuk et al. 1993
Remark	5 samples		3 samples			

[a]Two samples.

Values for Hamburg have not been considered in the graph since the concentrations at this highly industrialized site are rather high and would therefore interfere with data from other places. Also, the values for 1972–1973 and 1972–1979 have not been used since for these periods several data sets are given in the literature for the different years separately. In all cases, when values were reported by different authors for the same time period, the values have been averaged. For 1972 and 1973 only the yearly averages have been used. In most papers values were reported as arithmetic means; only for De Blankaert, Hemsby, and Spurnhead were geometric means given. The values for Leiston, Styrrup, and Gresham have been converted from ng/kg air to ng/m^3 according to Cawse (1977).

United Kingdom measurements until 1977: The measurements before 1977 were all done at Leiston and Styrrup, two sites in the U.K., in the framework of an extensive sampling

Table 5. race metal concentrations (ng/m^3) for all sampling campaigns in the coastal area of the central North Sea.

Period	1981–1983[a]	1983[a]	1984 July	1984 July	1984 July	1985 January	1985 January	1985 January	1984–1985[a] May 84–July 85
Location	Kiel Bight (D)	Tange (DK)	Tange (DK)	Keldsnor (DK)	Pellworm (D)	Tange (DK)	Keldsnor (DK)	Pellworm (D)	Pellworm (D)
	Arithm. mean	Not specified	Not specified	Not specified	Not specified	Not specified	Not specified	Not specified	Not specified
Cd	—	0.6	—	—	—	—	—	—	0.67
Cu	7.7	3.0	—	—	—	—	—	—	3.3
Pb	53	40.9	18.4	24.4	23.5	39.7	56.9	66.3	38.8
Zn	57	29.7	—	—	—	—	—	—	40
Ni	4.0	3.0	—	—	—	—	—	—	4.4
Cr	2.9	1.6	—	—	—	—	—	—	1.3
Reference	Schneider 1987	Kemp 1984[b]	Krell and Roeckner 1988	Krell and Roeckner 1988	Krell and Roeckner 1988	Krell and Roeckner 1988	Krell and Roeckner 1988	Krell and Roeckner 1988	Stössel 1987

[a]Values used in the graphs.
[b]Indirectly cited values since we were unable to get the original reports.

campaign at seven sites in the whole area of the U.K. between 1972 and 1976 to estimate the amount of trace metals in the atmosphere (Peirson et al. 1973). The values for both sites have been averaged in Fig. 4 (the values for Petten in 1973 have not been used in the graph so as not to interfere with the Leiston and Styrrup data). Since all values are yearly averages of weekly and monthly samplings, seasonal effects can be excluded. Also, the interference by other factors such as the use of different sampling and analysis procedures is not present because during the whole period 1972–1976 the same sampling and analysis devices have been used.

The average airborne Zn level decreased continuously from more than 300 ng/m^3 in 1972 to about 150 ng/m^3 in 1976. The Pb concentrations show a decrease from the level of 270–300 ng/m^3 in 1972–1973 to a level of about 180 ng/m^3 in the period 1974–1976. Cr behaves quite similarly. The values found in 1974 to 1976 are only half of the ones observed before 1974 (7 ng/m^3 instead of 15 ng/m^3). High Cd concentrations (around 30 ng/m^3) are found for the period 1972–1973. From 1973 on, Cd concentrations decrease to a low value of 3 ng/m^3 in 1976. The Cu pattern shows a decreasing trend in the period 1972–1974 (from 26 to 8 ng/m^3) but increases again from 1974 until 1976 when an even higher Cu concentration is found than in 1972 (38 ng/m^3). Ni remains quite stable (7–8 ng/m^3) in the period 1972–1976 with a slightly higher value in 1973.

Continental measurements between 1977 and 1987: The values reported for the period 1977–1987 are the results of measurements at the Belgian coast and in the Netherlands. All concentrations are fluctuating heavily, at first sight without a systematic pattern. This could be explained by the fact that the reported data for this period, in contrast to the Styrryp and Leiston data for 1972–1976, were collected at several different sampling sites with different characteristics/influences. The low values in 1977 are caused by some very low values measured at Schiermonnikoog (NL), a rather clean site on the Wadden Islands. Also, the values found in 1981 at De Blankaert, a natural reserve near the Belgian coast, are rather low. The values for 1978–1981 and 1984–1985 on the other hand are rather high. These samples were taken in or near the Rijnmond area, the largest industrial centre of the Netherlands with a vast complex of harbours, refineries, storage tanks, chemical plants, and other industries and with a high population density, 21% of the population of the country (Van Daalen 1991). So the real average atmospheric metal concentrations above the whole coastal area of the Southern Bight are probably somewhat higher than the values reported here for 1977 and 1981 and somewhat lower for 1978–1981 and 1984–1985.

All data (1972–1994): Trends become more clear if the data for both periods are combined and complemented with additional, more recent values (1988–1994) from single campaigns at some new sites in the U.K. (Hemsby, Mannington, and Spurnhead) and the Belgian coast (Blankenberge). Despite the heavy fluctuations in the period 1977–1987, as discussed above, there is a very strong decreasing trend in the average Pb and Zn concentrations: Pb concentrations have decreased from 270–300 ng/m^3 in 1972–1973 to 8 ng/m^3 in 1992–1994. Airborne Zn concentrations have evolved from 306 to 22 ng/m^3. The fluctuating trend in the average Cu concentrations that was found earlier is confirmed in this graph. However, the values in the 1980s and 1990s remain below the values found in the 1970s. In 1991 an abnormally high Cu level was found by Spokes (1991), but no explanation for this was given by the author. Cd concentrations in the coastal area of the Southern Bight are decreasing. The strongest decrease is observed between 1973 and 1976 (from more than 30 to 3 ng/m^3). From 1986 on, Cd concentrations remain below 1 ng/m^3. Ni concentrations were quite stable till 1976 (about 8 ng/m^3). For the period 1976–1985 concentrations almost double (14 ng/m^3), but also stable values are observed. Since 1985, the Ni concentration is decreasing again to reach its lowest level of 3 ng/m^3 in 1992–1994. The airborne Cr level showed a sharp drop between 1973 and 1974 (from about 15 to 7 ng/m^3). Since then its concentration remained below 8 ng/m^3 but without a regular pattern.

1985–1986[a]	1986[a]	1986[a]	1987[a]	1987[a]	1987[a]	1987–1989	1988[a]	1989[a]	1990[a]	1992[a]
	Nov.–Dec.	June–Dec.	Jan.–Dec.				Jan.–Dec.	Jan.–Dec.	Jan.–Dec.	September
Helgoland (D)	Helgoland (D)	Helgoland (D)	Helgoland (D)	FPN	German Bight	Westerheversand (D)	Helgoland (D)	Helgoland (D)	Helgoland (D)	FPN
Not specified	Arithm. mean	Arithm. mean	Arithm. mean	Arithm. mean		Arithm. mean	Arithm. mean	Arithm. mean	Arithm. mean	Arithm. mean
1.4	1.9	—	—	0.9	1	0.52 ± 0.40	—	—	—	—
3.9	4.7	3.1	3.9	3.9	3.7	4.8 ± 3.3	3.3	3.0	2.5	3.5 ± 0.2
28.9	52.6	23.8	21.8	28.5	28.3	26.9 ± 26.2	16	15.6	12.8	15.1 ± 1.1
32.8	46.1	26.6	32.5	42.4	35.1	51.6 ± 47.8	30.9	49.5	46.3	—
2.6	2.9	1.7	2.7	2.4	—	2.8 ± 1.5	2.2	3.0	3.4	6.2 ± 0.3
1.7	1.9	—	—	—	—	1.8 ± 1.8	—	—	—	4.1 ± 0.5
Kersten et al. 1988	Kersten et al. 1991	Kriews 1992	Kriews 1992	Steiger 1991	Schulz 1993	Dannecker et al. 1994 Kriews 1992	Kriews 1992	Kriews 1992	Kriews 1992	Injuk 1995

3.3. Central North Sea

3.3.1. Marine area of the Central North Sea

In contrast to the Southern Bight almost no data are available for the marine area of the central North Sea. Concentrations are reported in only two publications, for three different sampling campaigns (Injuk et al. 1993; Otten et al. 1994). The measured concentrations are given in Table 4.

3.3.2. Coastal area of the Central North Sea

The coastal area around the central North Sea includes the eastern part of the U.K., Denmark, and the upper northwestern part of Germany. Measurements of concentrations of airborne trace elements have been performed at the following sites (Fig. 1): Tange (DK), Keldsnor (DK), Westerheversand (D), Pellworm (D), Helgoland (D), Kiel Bight, and the research platform "Nordsee" (FPN) (D). Not all sites are real coastal sites: Pellworm and Helgoland are islands, whereas the FPN site is a research platform. However, in our discussion we consider them as coastal because they are located not in the open sea but rather close to the coast. Atmospheric heavy metal concentrations for this area are given by Kemp (1984), Schneider (1987), Stössel (1987), Krell and Roeckner (1988), Kersten et al. (1988, 1991), Steiger (1991), Kriews (1992), Schulz (1993), Dannecker et al. (1994), and Injuk (1995). The complete set of coastal data for the central part of the North Sea is summarized in Table 5. All measurements are represented chronologically in Fig. 5.

No geometric means were reported in the literature so all values are arithmetic means. Values that span a period of several years are normally not considered in the graphs if values are present for the different years separately, as in the case of Westerheversand (1987–1989). However, for 1984 and 1985 only Pb concentrations are given in literature. Moreover these values in 1984 and 1985 should be considered as being statistically less important since they were obtained during rather short (1 month) sampling campaigns and therefore subjected to seasonal differences as can be seen from Table 5. Therefore we used the values of 1984–1985 and 1985–1986. If values were reported by different authors for the same period, as in the case of 1986 and 1987, values were averaged.

If one compares Figs. 3, 4, and 5, one can clearly see that the absolute trace metal concentrations above the central North Sea are lower than those found for the Southern Bight, especially in the case of Pb, Zn, and also for Ni.

As can be seen from Fig. 5, the trends in the observed atmospheric concentrations for the considered elements are not so clear at first sight, except for Pb. A problem of course is that the data were obtained at several different sites, with different characteristics, and influenced by different air masses.

The Pb concentrations have dropped from 53 ng/m^3 in the beginning of the 1980s to about 12.8 ng/m^3 in 1990 with a negligible increase to 15 ng/m^3 in 1992. The latter concentration was measured at the FPN station while the three preceding values were obtained at the Helgoland site. As can be seen from Table 5 also in 1987 slightly higher values are found for the FPN station compared to the Heloland site. The slightly higher Pb concentration in 1986 is due to high values reported by Kersten et al. (1991), which represent a polluted period (strong continental influence) of a long-term monitoring program. This can clearly be seen if one compares the 1986 data of Kersten et al. (1991) with the 1986 data of Kriews (1992). For the airborne Zn level, a high value was found in 1981–1983 (57 ng/m^3). In the following period (1983–1988) Zn concentrations were lower, fluctuating between 30 and 40 ng/m^3, but in 1989 and 1990 again higher values were reported, respectively 50 and 46 ng/m^3. So, contrary to the atmospheric Pb concentrations, Zn levels do not show a consistent pattern. Ni concentrations are increasing slightly in the period 1986–1992. Cu concentrations are somewhat higher in 1981–1983 but afterwards vary only between 2.5 and 3.9 ng/m^3. They are slightly decreasing since 1986 to a level of 2.5 ng/m3 in 1990 but in 1992 a higher value of 3.5 is observed again. However, the overall higher values that are observed in 1992 could be the result of other factors like a different sampling site (FPN) since, as

Fig. 5. Average airborne trace metal concentrations (ng/m^3) for the coastal area of the central North Sea.

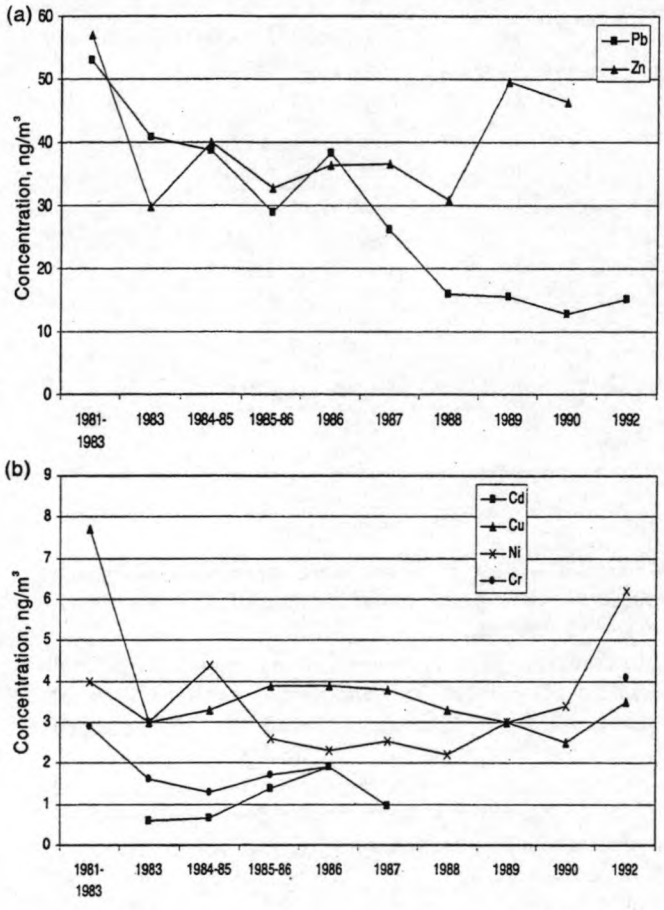

Fig. 6. Average airborne trace metal concentrations (ng/m^3) for the Helgoland site.

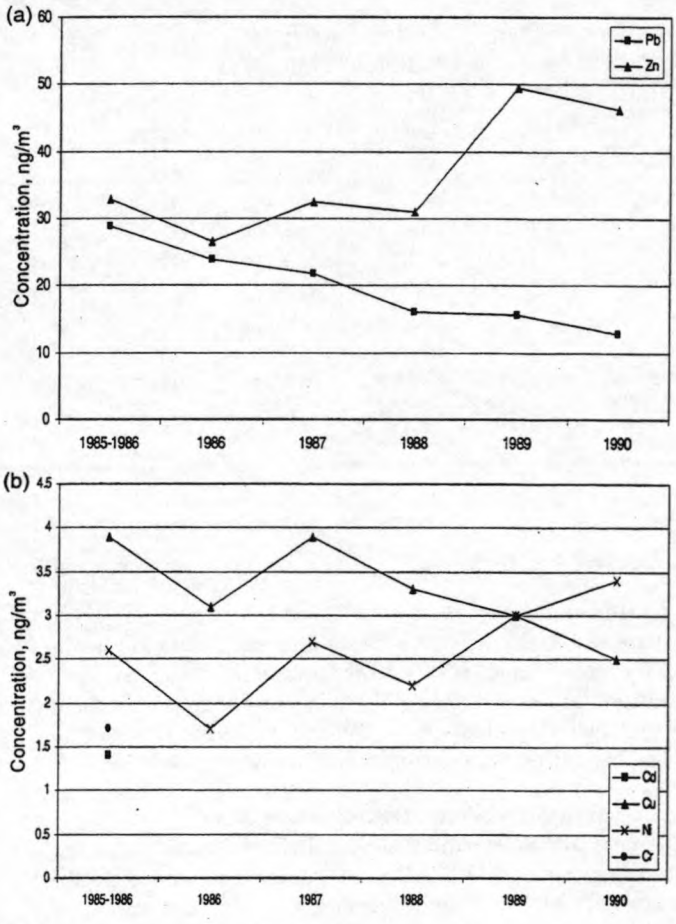

mentioned earlier, slightly higher concentrations are found for this site. Because of the lack of data for Cd and Cr nothing can be concluded for these elements.

Helgoland site: In Fig. 6 only the data reported by Kriews (1992) for the Helgoland site are given. The decreasing trend in the Pb concentrations is obvious, as well as an apparent decrease in the atmospheric Cu levels and an increasing tendency of the Ni concentrations. The Zn concentrations show an increasing behaviour. According to Kriews (1992), meteorological parameters, such as a more frequent occurrence of western and northwestern winds during the sampling, cannot account for such a strong decrease in the Pb concentrations.

3.4. Northern North Sea

The northern part of the North Sea is surrounded at the east side by the southern part of Norway and at the southwest side only by a small part of the United Kingdom. Almost no sampling campaigns, dealing with trace metals, have been done on this part of the North Sea. Atmospheric heavy metal concentrations are reported in literature by Thrane (1978), Pacyna et al. (1984*a*, 1984*b*), Amundsen et al. (1992), Bartnicki (1994), Ducastel (1994), and Otten et al. (1994). The data are summarized in Table 6 for the marine area and in Table 7 for the coastal measurements. There does not seem to be a significant difference between the marine and coastal data. We did not, however, combine the data of the marine and coastal measurements because almost all the coastal data deal with the same sampling site (Birkenes); combining these results might cover the trends observed at this site.

The coastal measurements have been performed at Birkenes and Vasser, two sites in southern Norway (Fig. 1). According to Thrane (1978) the Vasser site is influenced by local sources in urban areas along the Oslofjord. As a result the concentrations found at this site are systematically higher than those measured at Birkenes. The heavy metal concentrations for the coastal area of the Northern North Sea, more particularly Southern Norway, are represented in Fig. 7.

Because of the above reasons we omitted the Vasser data so that the figure only represents the Birkenes site. The data from Amundsen et al. (1992) and Pacyna et al. (1984*a*) for 1978–1979 have been averaged, as well as the values from Bartnicki (1994) and Amundsen et al. (1992). For 1988 and 1989 (Ducastel 1994) the fine and coarse fractions were added. No geometric mean values are available, so all values used are arithmetic means.

The Birkenes site is situated in an area with limited industrial activity and low population density and, therefore, airborne concentrations here are mainly due to long-range transport of air masses. So, comparing Fig. 7 with the previous ones again clearly shows the difference between this region and the other regions of the North Sea: the observed concentrations for the northern North Sea are the lowest of all.

Table 6. Trace metal concentrations (ng/m^3) for all sampling campaigns in the marine area of the northern North Sea.

Period		1985 April Cruise		1988 June Cruise	
Location		Arithm. mean	Geom. mean	Arithm. mean	Geom. mean
Cd	0.3	—	—	—	—
Cu	7	3.6 ± 5.0	1.8	4.5 ± 0.6	4.5
Pb	19	12.1 ± 5.4	11.2	—	—
Zn	—	8.0 ± 12.3	3.3	2.8 ± 1.0	2.6
Ni	—	0.6 ± 0.3[b]	0.6	2.4 ± 1.3	1.9
Cr	—	—	—	17.8 ± 4.6	17.2
Reference	Pacyna et al. 1984*b*[a]	Otten et al. 1994		Otten et al. 1994	
Remark		7 samples		4 samples	

[a]Indirectly cited values since we were unable to get the original report.
[b]Four samples.

Figure 7 shows that for the Birkenes site the average Pb concentration showed a slight increase from 16.4 ng/m^3 in 1974 to 19.4 ng/m^3 in 1980 and has been decreasing continuously ever since to very low values (only 1.3 ng/m^3 in 1989). For Zn no values are given in the literature for the 1970s. Just as for the Pb concentrations, the atmospheric Zn concentrations have decreased by a factor of 10 from 20.1 ng/m^3 in 1980 to 2.1 ng/m^3 in 1989. Cu concentrations show a smaller decrease, by a factor of 4, from 7.0 ng/m^3 in 1978–1979 to 1.7 ng/m^3 in 1988. Also, the Ni levels have decreased at this site, but not as smoothly as the other metals. For Cd and Cr only a few data are available, so it is not possible to observe possible trends in their concentrations.

3.5. Global and European trace metal emission inventories

As mentioned in the introduction, during the last decades there have been several changes in the energy, industrial, and transport sectors that have resulted in an alteration of the emission patterns of several trace metals. Global emission inventories of trace elements were determined for natural sources in 1975 (Nriagu 1979) and 1983 (Nriagu 1989) and anthropogenic sources in 1975 (Nriagu 1979; Pacyna 1986) and 1983 (Nriagu 1989; Nriagu and Pacyna 1988). The emissions are calculated on the basis of trace element emission factors and statistical information on the consumption of ores, rocks, and fuels and the production of various types of industrial goods. Similarly some regional studies on trace metal emission inventories have been done. A thorough estimate of European anthropogenic emissions, including Cd, Cu, Pb, Zn, Ni, and Cr, has been published by Pacyna (1984) for 1979. More recent data for the 1980s can be found in Pacyna and Graedel (1995) and for the beginning of the 1990s, in Pacyna (1998). A study that is very interesting to compare with this work was done by Olendrzynski et al. (1996). They give a historical overview of the atmospheric emissions and depositions (although still preliminary) of Cd, Pb, and Zn in Europe during the period 1955–1987. According to this study, the lead emissions from 13 European countries have been increasing since 1955 to reach their maximum value (138 000 t) in 1975. Afterwards the Pb emissions decreased significantly and in 1987 were reduced by 54% to the level of 64 000 t. Cd emissions reached a maximum of over 2300 t around 1960

Fig. 7. Average airborne trace metal concentrations (ng/m^3) for the coastal area of the northern North Sea.

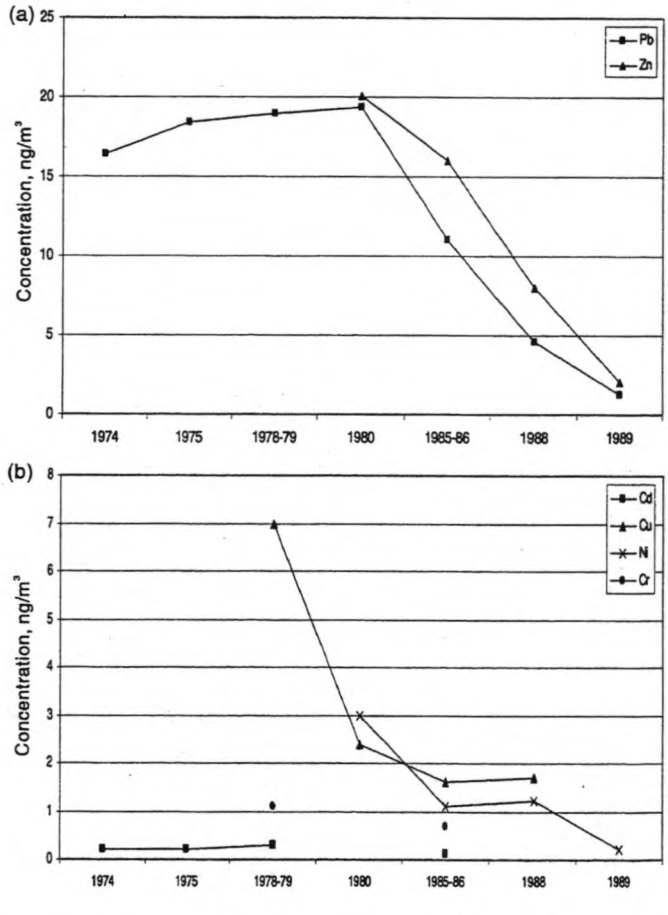

and then decreased continuously till 1987 to a figure just above 800 t. Zn emissions were highest in 1965 (94 000 t), then stabilized and from 1970 to 1987 there was almost a 66% reduction to a value of 32 000 t.

3.6. Comparison with atmospheric trace metal concentrations in remote areas

From the discussion in the previous sections it is clear that some strong decreasing trends can be observed. Of course

Table 7. Trace metal concentrations (ng/m^3) for all sampling campaigns in the coastal area of the northern North Sea.

Period	1974	1974[a]	1975	1975[a]	1978–1979[a]		1978–1979[a]
	Oct.–Dec.	Sept.–Dec.	April–May	April–May	Aug. 78–June 79		Aug. 78–June 79
Location	Vasser (N)	Birkenes (N)	Vasser (N)	Birkenes (N)	Birkenes (N)		Birkenes (N)
	Arithm. mean	Arithm. mean	Arithm. mean	Arithm. mean	Arithm. mean	Median	Arithm. mean
Cd	0.4 ± 0.1	0.2 ± 0.1	0.6 ± 0.5	0.2 ± 0.1	0.29	0.16	0.28
Cu	—	—	—	—	—	—	7
Pb	23 ± 13	16.4 ± 8.6	51 ± 16	18.4 ± 6.4	18	13	19
Zn	—	—	—	—	—	—	(112)
Ni	—	—	—	—	—	—	—
Cr	—	—	—	—	1.1	0.7	1.0
Reference	Thrane 1978	Thrane 1978	Thrane 1978	Thrane 1978	Amundsen et al. 1992		Pacyna et al. 1984*a*
Remark							(): possible contamination

[a]Values used in the graphs.
[b]Indirectly cited values since we were unable to get the original reports.

Table 8. Airborne trace metal concentrations (ng/m^3) in some remote areas, compared with the most recent airborne trace metal concentrations found in literature for the different marine parts of the North Sea.

	Remote areas							North Sea subregion (this work)		
	Alaska	Canadian Arctic	Greenland	Atlantic Ocean	Bermuda	Hawaii	Antarctic	Southern Bight 1993	Central 1991	Northern 1988
Cd	0.37				0.4	0.022	0.005–0.5	0.76	—	0.3
Cu		0.3	0.31	0.9	2.0	0.3	<0.03–0.3	3.1	1.5	4.5
Pb		1.0	0.15–8.0	7	7	1.2	0.07–0.9	17	16 (1985)	11 (1985)
Zn	15	1.0	0.18–2.8	5	6	0.8	<1–21	13	6.5	2.6
Ni			0.08–0.13				<0.03–0.06	3.0	2.0	1.9
Cr			0.09–0.2	0.2	0.5	0.2	<0.04–0.1	2.2	3.5	17
Reference	Wiersma and Davidson 1986						Rädlein and Heumann 1992	Injuk 1995	Injuk et al. 1993	Otten et al. 1994

the interesting question now is whether the observed concentrations already approach the natural background concentrations. In Table 8 airborne trace metal concentrations, measured in some remote areas and hence supposed to represent the natural background concentrations, are shown (Wiersma and Davidson 1986; Rädlein and Heumann 1992). For this comparison the most recently reported concentrations (in most cases also the lowest), which were considered in this study for the different marine parts of the North Sea, are also given in Table 8. If concentrations were lacking for certain elements, the data were supplemented with data from earlier sampling campaigns.

As can be seen from both tables, all concentrations found above the North Sea are still higher than those in the remote areas. However, the differences are getting smaller. For Pb and Zn a clear south to north decreasing trend can be observed.

4. Conclusions

All literature data on trace metal concentrations in aerosols above the North Sea have been gathered and intercompared to look for possible trends. Six trace metals are considered: Cd, Cu, Pb, Zn, Ni, and Cr. A distinction is made between measurements in different regions of the North Sea: the Southern Bight, the central and northern North Sea, and the Channel. A second distinction is made between coastal and marine areas.

The majority of the data on trace metals in the literature deals with the Southern Bight. So the trends observed for this part of the North Sea are the most reliable. Also, in this part of the North Sea the highest concentrations are found. More data are needed to confirm the concentration patterns found for the other regions.

Despite some heavy fluctuations a strong decreasing trend is observed for the Pb and Zn concentrations above the North Sea. A remarkably consistent correlation is found between the concentration patterns of both elements in most parts of the North Sea. This similar behaviour between Pb and Zn, which has also been reported by Schneider (1987), is most clearly seen for the Southern Bight. Only in the coastal area of the central North Sea is a different behaviour found. Here Zn concentrations are increasing and Pb and Zn are anti-correlated.

For Cd, Cu, Ni, and Cr, much less data are available in the literature. Despite this, also for Cd a decreasing trend is present, however, not so strong as for Pb and Zn. The airborne Cu levels above the different regions of the North Sea do not always show a consistent behaviour. In most cases, however, the levels found in the late 1980s and early 1990s are lower than those observed earlier. Cr and Ni concentrations in most cases are fluctuating without a certain pattern; with the small amount of data it is hard to recognise a particular trend.

1980[a]	1985[a]	1985–1986[a]		1988[a]		1989[a]	
	Birkenes (N)	Birkenes (N)		Birkenes (N)		Birkenes (N)	
Birkenes (N)	Arithm. mean	Arithm. mean	Median	Median		Median	
				Fine	Coarse	Fine	Coarse
—	0.11	0.14	0.08	—	—	—	—
2.4	—	1.6	1.1	<0.6	<1.1	—	—
19.4	—	11	7.8	3.6	0.97	0.86	<0.4
20.1	17	15	11	5.9	2.1	1.41	0.64
3	—	1.1	0.7	0.63	<0.6	<0.18	<0.03
—	—	0.68	0.45	—	—	—	—
Pacyna et al. 1984*b*[b]	Bartnicki 1994	Amundsen et al.1992		Ducastel 1994 21 samples		Ducastel 1994 13 samples	

Not enough data are available in the literature to assess trends of heavy metal concentrations with wind directions or with particle size.

5. Acknowledgements

Stefaan Hoornaert is supported by the Belgian National Science Foundation (NFWO).This study was carried out on behalf of the Institute for Coastal and Marine Management (RIKZ), Rijkswaterstaat, Den Haag, the Netherlands. It was also partially supported via the Impulse Programme Marine Sciences (contract MS06/050) of the Belgian State, Prime Minister's Service, Services for Scientific, Technical and Cultural Affairs.

6. References

Amundsen, C.E., Hanssen, J.E., Semb, A., and Steinnes, E. 1992. Long-range transport of trace elements to southern Norway. Atmos. Environ. **26A**: 1309–1324.

Baeyens, W., and Dedeurwaerder, H. 1991. Particulate trace metals above the Southern Bight of the north sea — I. Analytical procedures and average aerosol concentrations. Atmos. Environ. **25A**: 293–304.

Bartnicki, J. 1994. An eulerian model for atmospheric transport of heavy metals over Europe: model description and preliminary results. Water, Air Soil Pollut. **75**: 227–263.

Cambray, R.S., Jefferies, D.F., and Topping, G. 1975. An estimate of the input of atmospheric trace elements into the North Sea and the Clyde Sea (1972–3). U.K. At. Energy Auth., Harwell Lab., Rep. AERE-R 7733, Harwell.

Cawse, P.A. 1974. A survey of atmospheric trace elements in the UK (1972–73). U.K. At. Energy Auth., Harwell Lab., Rep. AERE-R 7669, Harwell.

Cawse, P.A. 1975. A survey of atmospheric trace elements in the UK: results for 1974. U.K. At. Energy Auth., Harwell Lab., Rep. AERE-R 8038, Harwell.

Cawse, P.A. 1976. A survey of atmospheric trace elements in the UK: results for 1975. U.K. At. Energy Auth., Harwell Lab., Rep. AERE-R 8398, Harwell.

Cawse, P.A. 1977. A survey of atmospheric trace elements in the UK: results for 1976. U.K. At. Energy Auth., Harwell Lab., Rep. AERE-R 8869, Harwell.

Chester, R., and Bradshaw, G.F. 1991. Source control on the distribution of particulate trace metals in the North Sea atmosphere. Mar. Pollut. Bull. **22**: 1, 30–36.

Dannecker, W., Hinzpeter, H., Kirzel, H.J., Luthardt, H., Kriews, M., Naumann, K., Schulz, M., Schwikowski, M., Steiger, M., and Terzenbach, U. 1994. Atmospheric transport of contaminants, their ambient concentration and input into the North Sea. *In* Circulation and Contaminant Fluxes in the North Sea. *Edited by* J. Sündermann. Springer-Verlag, Berlin. pp. 138–189.

DCMR 19—. Quarterly and yearly reports, DCMR, Schiedam, the Netherlands.

Dedeurwaerder, H.L. 1988. Study of the dynamic transport and of the fall-out of some ecotoxicological heavy metals in the troposphere of the Southern Bight of the North Sea. Ph.D. thesis, University of Brussels (VUB), Belgium.

Dedeurwaerder, H.L., Dehairs, F.A., Decadt, G.G., and Baeyens, W.F. 1983. Estimates of dry and wet deposition and resuspension fluxes of several trace metals in the Southern Bight of the North Sea. *In* Precipitation Scavenging, Dry Deposition and Resuspension. Vol. 2. *Edited by* Pruppacher. Elsevier, New York.

Dehairs, F., Dedeurwaerder, H., Dejonghe, M., Decadt, G., Gillain, G., Baeyens, W., and Elskens, I. 1982. Boundary conditions for heavy metals at the air-sea interface. *In* Hydrodynamic and dispersion models. Boundary fluxes and boundary conditions. *Edited by* Nihoul and Wollast.

Diederen, H.S.M.A., and Guicherit, R. 1981. Source recognition of aerosols by concentration measurements of elements in ambient air. IMG-TNO Report G 799, IMG-TNO, Delft, The Netherlands.

Ducastel, G. 1994. Het atmosferisch aerosol in zuidelijk Noorwegen en het Arctisch gebied: chemische samenstelling, deeltjesgrootte, bronnen en brongebieden. Ph.D. thesis, University of Gent (RUG), Belgium.

Duce, R.A., Liss, P.S., Merrill, J.T., Atlas, E.L., Buat-Menard, P., Hicks, B.B., Miller, J.M., Prospero, J.M., Arimoto, R., Church, T.M., Ellis, W., Galloway, J.M., Hansen, L., Jickells, T.D., Knap, A.H., Reinhardt, K.H., Schneider, B., Soudine, A., Tokos, J.J., Tsunogai, S., Wollast, R., and Zhou, M. 1991. The atmospheric input of trace species to the world ocean. Global Biogeochem. Cycles, **5**: 193–259.

Elskens, Y., Decadt, G., Dedeurwaerder, H., Dehairs, F., and Dejonghe, M. 1981. Study of the immission values and the transport of heavy metals above the North Sea. National Scientific and Development Report on Air. Scientific End Report 1978–1981.

Flament, P., Leprêtre, A., and Noel, S. 1987. Coastal aerosols in Northern Channel. Oceanolog. Acta, **10**: 1, 49–61.

Flament, P., Bertho, M., Deboudt, K., and Puskaric, E. 1996. Changes in the lead content of atmospheric aerosols above the Eastern Channel between 1982/83 and 1994. Sci. Total Environ. **192**: 193–206.

GESAMP. 1980. Joint Group of Experts on the Scientific Aspects of Marine Pollution. Interchange of pollutants between the atmosphere and ocean. Reports and Studies No. 13.

GESAMP. 1989. Joint Group of Experts on the Scientific Aspects of Marine Pollution. The atmospheric input of trace species to the world ocean. Reports and Studies No. 38.

Injuk, J. 1995. Assessment of atmospheric pollutant fluxes to the North Sea by X-ray emission analysis. Ph.D. thesis, University of Antwerp (UIA), Belgium.

Injuk, J., Van Malderen, H., Van Grieken, R., Swietlicki, E., Knox, J.M., and Schofield, R. 1993. EDXRS study of aerosol composition variations in air masses crossing the North Sea. X-Ray Spectrom. **22**: 220–228.

Kane, M.M., Rendell, A.R., and Jickells, T.D. 1994. Atmospheric scavenging processes over the North Sea. Atmos. Environ. **28**: 15, 2523–2530.

Kemp, K. 1984. Multivariate analysis of elements and SO_2 measured at the Danish EMEP stations. National Agency of Environmental Protection, MST Report LUFT-A88, Roskilde, Denmark.

Kersten, M., Dicke, M., Kriews, M., Naumann, K., Schmidt, D., Schulz, M., Schwikowski, M., and Steiger, M. 1988. Distribution and fate of heavy metals in the North Sea. *In* Pollution of the North Sea. *Edited by* W. Salomons, pp. 303–347.

Kersten, M., Kriews, M., and Förstner, U. 1991. Partitioning of trace metals released from polluted marine aerosols in coastal seawater. Mar. Chem. **36**: 165–182.

Krell, U., and Roeckner, E. 1988. Model simulation of the atmospheric input of lead and cadmium into the North Sea. Atmos. Environ. **22**: 375–381.

Kretzschmar, J.G., and Cosemans, G. 1979. A five year survey of some heavy metal levels in air at the Belgian North Sea coast. Atmos. Environ. **13**: 267–277.

Kriews, M. 1992. Charakterisierung mariner Aerosole in der Deutschen Bucht sowie Prozessstudien zum Verhalten von Spurenmetallen beim Übergang Atmosphäre/Meerwasser. Ph.D. thesis, University of Hamburg, Germany.

NAS 1978. The tropospheric transport of pollutants and other substances to the oceans. National Academy of Sciences Press, Washington, D.C.

Nriagu, J.O. 1979. Global inventory of natural and anthropogenic emissions of trace metals to the atmosphere. Nature, **279**: 409–411.

Nriagu, J.O. 1989. Natural sources of trace metals in the atmosphere. Nature, **338**: 47–49.

Nriagu, J.O. 1990. Global metal pollution, poisoning the biosphere? Environment, **32**: 7–34.

Nriagu, J.O., and Pacyna, J.M. 1988. Quantitative assessment of worldwide contamination of air, water and soils by trace metals. Nature, **333**: 134–139.

Olendrzynski, K., Anderberg, S., Bartnicki, J., Pacyna, J.M., and Stigliani, W. 1996. Atmospheric emissions and depositions of cadmium, lead and zinc in Europe during the period 1955–1987. Environ. Rev. **4**: 300–320.

Otten, Ph., Injuk, J., Rojas, C., and Van Grieken, R. 1992. Atmosferische fluxen van zware metalen naar de Noordzee. Het Ingenieursblad, **4**: 41–46.

Otten, Ph., Injuk, J., and Van Grieken, R. 1994. Elemental concentrations in atmospheric particulate matter sampled on the North Sea and the English Channel. Sci. Total Environ. **155**: 131–149.

Ottley, C.J., and Harrison, R.M. 1993. Atmospheric dry deposition flux of metallic species to the North Sea. Atmos. Environ. **27A**: 685–695.

Pacyna, J.M. 1984. Estimation of the atmospheric emissions of trace elements from anthropogenic sources in Europe. Atmos. Environ. **18**: 41–50.

Pacyna, J.M. 1986. Atmospheric trace elements from natural and anthropogenic sources. *In* Toxic metals in the atmosphere. *Edited by* J.O. Nriagu and D.I. Davidson. Wiley and Sons, New York, pp. 33–52.

Pacyna, J.M. 1996. Data in preparation for the International Institute for Applied Systems Analysis, Laxenburg.

Pacyna, J.M. 1998. Source inventories for atmospheric trace metals. *In* Atmospheric Particles. *Edited by* R.M. Harrison and R. Van Grieken. Wiley and Sons, pp. 385–423.

Pacyna, J.M., and Graedel T.E. 1995. Atmospheric emissions inventories: status and prospects. Annu. Rev. Energy Environ. **20**: 265–300.

Pacyna, J.M., Semb, A., and Hanssen, J.E. 1984*a*. Emission and long-range transport of trace elements in Europe. Tellus, **36B**: 163–178.

Pacyna, J.M., Ottar, B., Hanssen, J.E., and Kemp, K. 1984*b*. The chemical composition of aerosols measured in southern Scandinavia. OR 66/84, Norwegian Institute for Air Research, Lillestrøm, Norway.

Peirson, D.H., Cawse, P.A., Salmon, L., and Cambray, R.S. 1973. Trace elements in the atmospheric environment. Nature, **241**: 252–256.

Peirson, D.H., Cawse, P.A., and Cambray, R.S. 1974. Chemical uniformity of airborne particulate material and a maritime effect. Nature, **251**: 675–679.

Rädlein, N., and Heumann, K.G. 1992. Trace analysis of heavy metals in aerosols over the Atlantic Ocean from Antarctica to Europe. Int. J. Anal. Chem. **48**: 127–150.

Schneider, B. 1987. Source characterisation for atmospheric trace metals over Kiel Bight. Atmos. Environ. **21**: 1275–1283.

Schulz, M. 1993. Räumliche und zeitliche Verteilung atmosphärischer Einträge von Spurenelementen in die Nordsee. Ph.D. thesis, University of Hamburg, Germany.

Spokes, L.J. 1991. *In* Eurotrac air sea exchange experiment North Sea, 14–27 September 1991. *Edited by* T.D. Jickells and L.J. Spokes.

Steiger, M. 1991. Die Anthropogenen und natürlichen Quellen urbaner und mariner Aerosole charakterisiert und quantifiziert durch Multielementanalyse und chemische Receptormodelle. Ph.D. thesis, University of Hamburg, Germany.

Stössel, R.P. 1987. Untersuchungen zur Nass- und Trockendeposition von Schwermetallen auf der Insel Pellworm. Ph.D. thesis, University of Hamburg, Germany.

Thrane, K.E. 1978. Background levels in air of lead, cadmium, mercury and some chlorinated hydrocarbons measured in south Norway. Atmos. Environ. **12**: 1155–1161.

Van Daalen, J. 1991. Air quality and deposition of trace elements in the province of South-Holland. Atmos. Environ. **25A**: 691–698.

Wiersma, G.B., and Davidson, C.I. 1986. Trace metals in the atmosphere of remote areas. *In* Toxic Metals in the Atmosphere. *Edited by* J.O. Nriagu and C.I. Davidson. Wiley Series in Advances in Environmental Science and Technology. Vol. 17. John Wiley and Sons, New York, pp. 201–266.

Yaaqub, R.R., Davies, T.D., Jickells, T.D., and Miller, J.M. 1991. Trace elements in daily collected aerosols at a site in Southeast England. Atmos. Environ. **25A**: 985–996.

Selected article #24:

Single particle and inorganic characterization of rainwater collected above the North Sea

W. Jambers, V. Dekov and R. Van Grieken

Science of the Total Environment, 256 (2000) 133-150

ELSEVIER

the Science of the Total Environment
An International Journal for Scientific Research into the Environment and its Relationship with Man

The Science of the Total Environment 256 (2000) 133–150

www.elsevier.com/locate/scitotenv

Single particle and inorganic characterization of rainwater collected above the North Sea

W. Jambers, V. Dekov[1], R. Van Grieken*

Department of Chemistry, University of Antwerp (UIA), Universiteitsplein 1, B-2610 Antwerpen, Belgium

Received 7 December 1999; accepted 17 March 2000

Abstract

Suspended matter and the dissolved fraction of rainwater collected above the North Sea were characterized using electron probe X-ray microanalysis (EPXMA), inductively coupled plasma-optical emission spectrometry (ICP-OES) and ion chromatography (IC), respectively. Suspended particulate matter was dominated by aluminosilicates and organic particles. Fifteen particle types describe the composition of the North Sea rainwater suspended matter. Factor analysis, particle size distributions and manual EPXMA measurements illustrated the complex genesis of different particle types: terrigenous; biogenic (both marine and continental); and anthropogenic. It was demonstrated that at the beginning of a shower of rain the coarse particles that are present in the air under the cloud are washed out, while during the second phase rainout particles, formed in the cloud, become more important due to the absence of new coarse particles under the cloud. Above the sea, the total amount of suspended matter (TSM) is much smaller and more variable than above the land and also the decrease in particle diameter is less visible. Approximately 10% of the studied particles contained trace heavy metals. The dissolved compounds in the North Sea rainwater were also variable in time and space. In general, over a short period of time, the concentrations of all dissolved compounds seem to decrease during a shower, but this decrease is much larger above land than above sea. The concentrations of dissolved trace metals present in rainwater above the southern North Sea has decreased over the last 15 years.

Keywords: Rainwater; Suspended matter; North Sea; EPXMA; Trace metals

* Corresponding author. Fax: +32-3-820-23-76.
E-mail address: vgrieken@uia.ua.ac.be (R. Van Grieken).
[1] Present address: Department of Geology and Paleontology, University of Sofia, 15 Tzar Osvoboditel Blvd, 1000 Sofia, Bulgaria.

0048-9697/00/$ - see front matter
PII: S0048-9697(00)00477-0

1. Introduction

Wet and dry deposition of particulate matter are important pathways for the aeolian input of sediment matter to the ocean. Dry deposition is a continuous process, while wet deposition is episodic in nature. On a global scale, both will equally contribute to the transfer of airborne matter to the sea surface (Peirson et al., 1973; Cawse, 1974; Injuk and Van Grieken, 1995), but wet deposition of chemical species will dominate in regions of frequent precipitation and at an increasing distance from emission sources (Hov et al., 1987; Fuzzi, 1994). Wet deposition is generally considered as a combination of particles (and gases) scavenged in and below the cloud, i.e. rainout and washout. This scavenging process is particle size-dependent. Sub-micrometer sized particles are mainly removed through nucleation (i.e. incorporation of aerosols in cloud water), while coarse particles (>1 μm), are primarily scavenged by raindrops below the clouds (Tsai et al., 1990; Fuzzi, 1994).

Bulk analyses of aerosol and, to a lesser extent, rainwater samples have been frequently used to estimate the deposition fluxes from the atmosphere to the North Sea (Struyf and Van Grieken, 1993; Injuk and Van Grieken, 1995). Although, during the last decade, micro-analytical techniques have also been used to characterize the aerosol matter, hardly any results of single particle analysis on suspension in rainwater are available. Bruynseels et al. (1988) and De Bock et al. (1994) were the only authors who published limited results of EPXMA and laser microprobe mass spectrometry (LAMMS) analyses of rainwater collected above the North Sea.

Here we discuss the results of: (1) EPXMA investigations of suspended matter present in rainwater, which was collected above the North Sea; and (2) bulk analyses of the dissolved fraction of these rainwater samples.

2. Methodology

During all the sampling campaigns in the Southern Bight of the North Sea (Table 1) a manual wet-only rainwater collector was installed on the highest deck of the R/V Belgica at an altitude of 10 m above the sea surface. The collector consisted of a 633 cm^2 PVC funnel (ASTM, 1988) which was tightly fitted on a 2-l polythene (PE) collection bottle (Galloway and Likens, 1976). It was supported by a stainless steel framework fastened at the railing of the highest deck on the starboard side. The funnel sheltered the metallic framework and thus prevented contamination during the rainwater collection. The funnel was protected from dry deposition with a well fitting plastic bag. At the beginning of each rain event the funnel was manually uncovered. Immediately after the shower the collection bottle was emptied into a 250-ml PE bottle and the funnel was rinsed with de-ionized water (Laquer, 1990).

Immediately after collection, the rainwater samples were filtered through 25-mm diameter aerosol-grade polycarbonate Nuclepore filters with 0.45-μm pore size by using a Sartorius SM 16306 25-mm glass vacuum filter holder with a 30-ml funnel and with glass frit filter support. We used these smaller filters (i.e. 25 mm instead of 47 mm diameter), because the collected quantity of rain and the number of suspended particles in the rainwater samples were small. Until further sample preparation, filters and filtrates were stored frozen (Benoliel, 1994). Before use, the funnels, collection bottles, filter holder and laboratory equipment were acid cleaned using the procedure already described (Jambers et al., 1999). All the equipment used (mostly made of plastics) provided negligible contamination.

An overview of the collected rainwater samples is given in Table 1. During 16 September 1993 (campaign N4) it constantly rained from 04.00 h to 13.30 h, which allowed sequential collection of the different phases of the rain event (i.e. samples N4/R6 A, B and C). During campaign N10, samples were collected using two rainwater collectors: one on the port (P) and one on the starboard (S) side of the ship. On 16 November 1995, it rained again for approximately 10 h and this rainwater was also collected in two phases. In the port of Ipswich, samples were collected from two suc-

Table 1
Sampling parameters and pH of the rainwater samples

Campaign No.	Sample identification	Place of collection	Date of collection	Start time (h)	End time (h)	Mean wind direction	Mean wind speed ($m\ s^{-1}$)	Volume (ml)	pH
2	N2/R1	Central Bight	22.03.93	15.30	20.00	S	4.4	23	3.6
	N2/R2		25.03.93	11.00	11.30	N	6.4	75	5.8
3	N3/R1	Port of Ipswich	22.08.93	0.15	9.15	NE	3.0	100	4.2
	N3/R2			9.30	13.30	NNE	5.0	80	4.4
	N3/R3	Central Bight	26.08.93	9.00	9.20	NNW	8.5	59	4.2
4	N4/R1	Off Dutch coast	13.09.93	11.25	14.00	SE	4.2	11	6.1
	N4/R2	Off Belgian coast and in the port of Zeebrugge	14.09.93	8.00	11.00	E	5.4	85	5.5
	N4/R3	At Grootebank		18.45	23.45	WNW	9.4	120	5.3
	N4/R4		15.09.93	17.30	18.55	SSE	4.0	75	5.4
	N4/R5	Off Belgian coast		22.20	23.30	NEN	4.3	150	4.6
	N4/R6A		16.09.93	4.00	8.20	NWW	10.2	2000	4.9
	N4/R6B			8.20	10.35	W	10.8	500	4.7
	N4/R6C			10.35	13.30		8.9	200	4.4
10	N10/R1P		15.11.95	20.30	22.55	SSW	9.5	450	4.2
	N10/R1S							200	5.4
	N10/R2AP		16.11.95	0.30	8.45		11.0	2000	6.5
	N10/R2AS							1800	5.4
	N10/R2BP			8.45	10.25	W		200	6.7
	N10/R2BS							180	4.9
	N10/R3P		17–18.11.95	19.00	8.00	N	4.6	900	4.7
	N10/R3S							700	5.4

ceeding rain events: N3/R1 and N3/R2. These samples can be used to study the difference in time of rainwater collected at the coast.

All EPXMA measurements were performed using a JEOL JXA-733 Superprobe, coupled with a Tracor Northern TN-2000 X-ray analysis system. Automation was achieved with a purpose built particle recognition and characterization system. After individual particles were identified on back-scattered electron (BSE) images, their shape was recorded and their chemical composition (all elements with $Z \geq 11$; detection limits 0.1–1.0%) analyzed using a 20-s raster scan. The spectra were immediately deconvoluted using the fast filter algorithm (FFA) and peak intensities stored in a large data matrix, which also contained the spherical diameter and aspect ratio of the particle.

Approximately 500 particles, with a diameter larger than 0.45 μm, were characterized per sample using an acceleration voltage of 25 kV, a beam current of 1 nA and a magnification of 1000. After analysis, the major elements (i.e. elements present in more than 1% of the particles) were selected for data analysis.

Samples were prepared for EPXMA measurements in the same way as for the North Sea suspension samples already studied (Jambers et al., 1999). The content of organic matter was evaluated by staining part of the samples with RuO_4. The bottom of a Petri dish was covered with 0.5% stabilized RuO_4 solution. The samples were attached to the top of the dish using double sided tape. The lid was placed on the Petri dish and the samples exposed to the RuO_4 vapors for 15 min.

Part of each filtrate was prepared for inductively coupled plasma-optical emission spectrometry (ICP-OES) (detection limits 0.2–3 ppb; precision 10%) by acidification with nitric acid, while

Table 2
Selection rules used to characterize the North Sea suspension samples (Jambers et al., 1999) and rainwater suspension samples collected above the North Sea

Particle type	Particle class	Criteria based on relative X-ray intensities
A. Aluminosilicates	A1. Pure aluminosilicates	Al + Si > 90 and 15 < Si < 85
	A2. Aluminosilicates (...)	Al + Si + K + Fe > 90 and 15 < Si < 85
	A3. Ca-aluminosilicates	Ca + Si + Al + K + Fe > 90 and 15 < Ca < 40
	A4. Ca-rich aluminosilicates	Ca + Si + Al + K + Fe > 90 and 40 < Ca < 70
	A5. K-rich aluminosilicates	Al + Si + K + Fe > 90 and K > Al
	A6. Fe-rich aluminosilicates	Al + Si + K + Fe > 90 and Fe > Al
	A7. Ti-rich aluminosilicates	Al + Si + K + Fe + Ti > 90 and Ti > 40
	A8. Cl-rich aluminosilicates	Al + Si + K + Fe + Cl > 90 and Cl > 40
B. Si-rich	B1. Si-rich	Si > 85
	B2. Si-enriched	Si > 50 and Al < 5
C. Ca-rich	C1. Ca-rich	Ca > 90
	C2. Ca-enriched	70 < Ca < 90
D. Fe-rich		Fe + Mn + S + Cr + Zn + Si + Ni > 90 and Fe > 50
E. Ti-rich		Ti + Si + Fe + Mn + Cr + Zn + Ni > 90 and Ti > 50
F. S-rich	F1. S-rich	S > 75
	F2. S–Fe-rich	S > 40 and Fe > 20
	F3. Ba–S-rich	Ba > 40 and S > 20
	F4. Ca–S-rich	Ca > 30 and S > 30
G. Al-rich		Al > 50
H. Mn-rich		Mn > 50
I. Cr-rich		Cr > 50
J. Zn-rich		Zn > 50
K. Pb-rich		Pb > 50
L. Ni-rich		Ni > 50
M. Cl-rich		Cl > 50
N. K-rich		K > 50
Y. Organic		Sum of the X-ray intensities < 1000
Z. Not classified		

for inductively coupled plasma-mass spectrometry (ICP-MS) (detection limits 1–100 ppt; precision 10%) 100 ppb of indium was added in the filtrates as an internal standard. The filtrates were also used for ion chromatography (IC) (detection limits 1–100 ppb; precision 10%) and for pH determination (Table 1).

During campaign N10, an EPXMA blank was prepared by placing a filter in the filter holder and adding 25 ml of de-ionized water.

3. Results and discussion

3.1. EPXMA measurements

3.1.1. Automated analysis

To allow a comparison with the suspension samples collected in the North Sea, identical data treatment (Jambers et al., 1999) and selection rules (Table 2) were used.

Because the particle types and classes detected in the rainwater samples were comparable with those we detected in the North Sea suspension (Jambers et al., 1999), their sources are only discussed briefly in the next paragraphs together with their occurrences.

Aluminosilicate (A) and Si-rich (B) particles were present in the majority of the samples. Most probably they are terrigenous (aeolian) (Jambers et al., 1999), but an anthropogenic source cannot be excluded (Xhoffer et al., 1991). The aluminosilicate class A2 dominated the aluminosilicate particle type (A) with abundances between 10 and 50%, while pure aluminosilicates (A1) and Fe-rich aluminosilicates (A6) were also present in the

majority of the samples (abundances between 4 and 25% for both classes). Small quantities (1–2%) of Ti-rich aluminosilicates (A7) were detected in a limited number of samples, while Ca-enriched (A3), Ca-rich (A4), K-rich (A5) and Cl-rich (A8) aluminosilicates were absent.

In the air, Ca-rich particles (C) have a continental (terrigenous) and marine origin (Xhoffer et al., 1991). The particles originating from the marine environment are formed through crystallization in aerosol droplets of dissolved salts (including calcite, dolomite and gypsum) present in evaporated seawater spray. Only abundances of 1–2% of insoluble terrigenous Ca-rich particles were detected in the rainwater samples collected during campaign N10. These abundances are much smaller than the 15% of Ca-rich particles detected in the North Sea aerosol samples (Xhoffer et al., 1991; Hoornaert et al., 1996), because the majority of these aerosols are anthropogenic $CaSO_4$ particles (Hoornaert et al., 1996) which are soluble in the rainwater.

Fe-rich (D) and Ti-rich (E) particles were detected in the majority of the samples and had abundances between 4 and 36% and 1 and 10%, respectively. They both may have terrigenous and anthropogenic sources (Xhoffer et al., 1991; Jambers et al., 1999). In the samples collected during campaign N10, iron was also present as S–Fe-rich (F2) particles (abundances between 1 and 3%). These were most likely iron sulfate particles formed by the reaction of iron oxide with sulfuric acid during their release from combustion processes in ferrous metallurgy (Xhoffer et al., 1991).

Small quantities of S-rich (F1, 1–4%) and Al-rich (G, 0.5–1%) particles were detected in one-third of the samples. S-rich particle type originated most likely from anthropogenic sources, although small contributions from a marine source cannot be excluded (Bishop and Biscaye, 1982; Xhoffer et al., 1991). Al-rich particles could also be anthropogenic and terrigenous (Xhoffer et al., 1991; Jambers et al., 1999). In rainwater collected during campaign N10, 1–2% of Mn-rich (H), Cr-rich (I) and Zn-rich (J) particles were detected. Anthropogenic emissions, and the metallurgical industry in particular, are the most important sources of these trace metal rich particles (Kane et al., 1994). However, Cr-rich particles also seem to have an important marine source, which is most likely related to sea-spray (Van Malderen et al., 1996).

Cl-rich particles (M) were only detected in two samples, namely 7% in N2/R1 and 11% in N4/R2. Because sea salt is very soluble, this should not contribute to this particle type. However, part of the Cl-rich particles detected in sample N4/R2 contain chlorine and sodium and are thus most likely halite. The remaining particles of N4/R2 and all Cl-rich particles of N2/R1 also contain relatively large amounts of silicon and iron and are most likely Cl-rich organic particles which are coagulated with or coated on Si-rich and Fe-rich particles.

Organic particles (Y) were detected in all the samples with an exception of N10/R3S. This particle type was dominated by 'pure' organic particles containing no detectable elements ($Z \geq 11$). Organic particles containing chlorine, sulfur, and/or phosphorus were also found. Although these particles contained some detectable elements, the sum of their X-ray peaks was so low that they were classified as organic (Y). The abundance of the Cl-rich organic particles seems to be related to that of the Cl-rich particles (M); it was very high (26 and 34%, respectively) in the samples N2/R1 and N4/R2, which were also the only samples to contain Cl-rich particles. This Cl-rich organic material thus most likely originated from sea-spray, while pure, S-containing and P-containing organic particles were mainly biological materials like pollen and bacteria (De Bock et al., 1994).

3.1.1.1. Unstained samples. Organic particle types (Y) and the aluminosilicate class (A2) were, with a combined abundance of over 50%, the most important particle groups, although relatively high abundances of the Fe-rich (D, up to 35%) and Si-rich particles (B, up to 20%) were also detected. The chemical composition of rainwater and of particles scavenged by rain is very variable in time and space, because it depends on the microphysical and dynamic characteristics of the cloud and on the chemical composition of the air

masses in which the cloud is formed and in which the actual rain event takes place (Fuzzi, 1994). A comparable composition of the suspension was only detected in the samples N4/R3 and N4/R4, which were collected at the Grootebank with a time interval of 1 day. Both were dominated by a large quantity of organic particles: 62 and 55%, respectively. The abundance of organic material was only higher in sample N4/R2, which was partly collected in the port of Zeebrugge. Overall the amount of organic particles was very variable; none were detected in sample N10/R3S, while in sample N4/R2 77% of the particles were organic. Unexpectedly variable abundances of organic particles were also detected during earlier studies (De Bock et al., 1994). It was stated that this was the result of either growth of micro-organisms, due to the thawing of rainwater during transport, or the presence of bird excrements. During this study, effects of thawing have been minimized by immediate filtering of the majority of the samples. Those which had to be transported have been frozen immediately after collection and were slowly defrosted in a refrigerator just before sample preparation. The contribution of bird excrement is also expected to be limited, the chance of a dropping into the collector during the time of exposure to rain fall is expected to be very small. These highly variable organic abundances are thus most likely only the result of differences in the composition of the scavenged aerosols. The importance of both chemical and physical characteristics of the air masses is also visible by the absence of any correlation between the composition of the suspension and the wind direction and wind speed.

Large differences in the abundances of organic particles (Y) were also detected in the samples N3/R1 and N3/R2, collected in the port of Ipswich. The strong increase of organic particles (Y, from 6 to 41%) was compensated by a decrease from 71 to 38% of the aluminosilicate class (A2). The second shower started 15 min after the collection of the first had stopped. The majority of the coarse aluminosilicate (A) and Si-rich (B) particles were washed out during the first shower, resulting in a dominance of fine particles, including the organic (Y) and Fe-rich (D) particles, captured by incloud scavenging, during the second shower.

During campaigns N4 and N10, different phases of rain could be collected. When the abundances of the different particle types are compared in time (Fig. 1), it was noticed that for the samples N4/R6A, B and C, and N10/R2AS and BS, both collected at starboard, there was an increase for the aluminosilicate class (A2) and the Si-rich particles (B), and a decrease of the Fe-rich aluminosilicate (A6) and organic particles (Y). For the Fe-rich particles (D) there was a decrease in abundance for N4/R6A, B and C but an increase for N10/R2AS and BS. For the samples collected on port, there was a decrease of pure aluminosilicates (A1), aluminosilicates (A2) and organic particles (Y), an increase of Fe-rich aluminosilicates (A6) and Ti-rich particles (E), and no change for the Si-rich (B) and Fe-rich (D) particles. When the abundances of the total aluminosilicate type (A) are used, the expected decrease of these coarse particles in time was detected for both series of samples of N10/R2, but for N4/R6 there was a maximum during N4/R6B. It thus seems that above the sea the changes in composition of particulate matter in rainwater over a short time interval are not as clear as above the land.

When the samples collected during campaign N10 at port and starboard are compared, comparable compositions were detected for the samples N10/R1 and N10/R2A. The only differences were small shifts between the aluminosilicate classes (As) (but comparable abundances for the total) and an increase of the organic particles (Y) at port. This increase was also visible for the samples N10/R2B and N10/R3, which also had a small increase of Ti-rich (E) and a small decrease of Fe-rich (D) particles at port. We concluded that the differences between the samples collected at port and starboard were relatively small, as expected.

The blank sample, collected during campaign N10, mainly contained organic material (56%) and Si-rich particles (17%). This relatively high abundance of the Si-rich particles indicates that part of the contamination originated from the glass filtration unit. This contamination can be

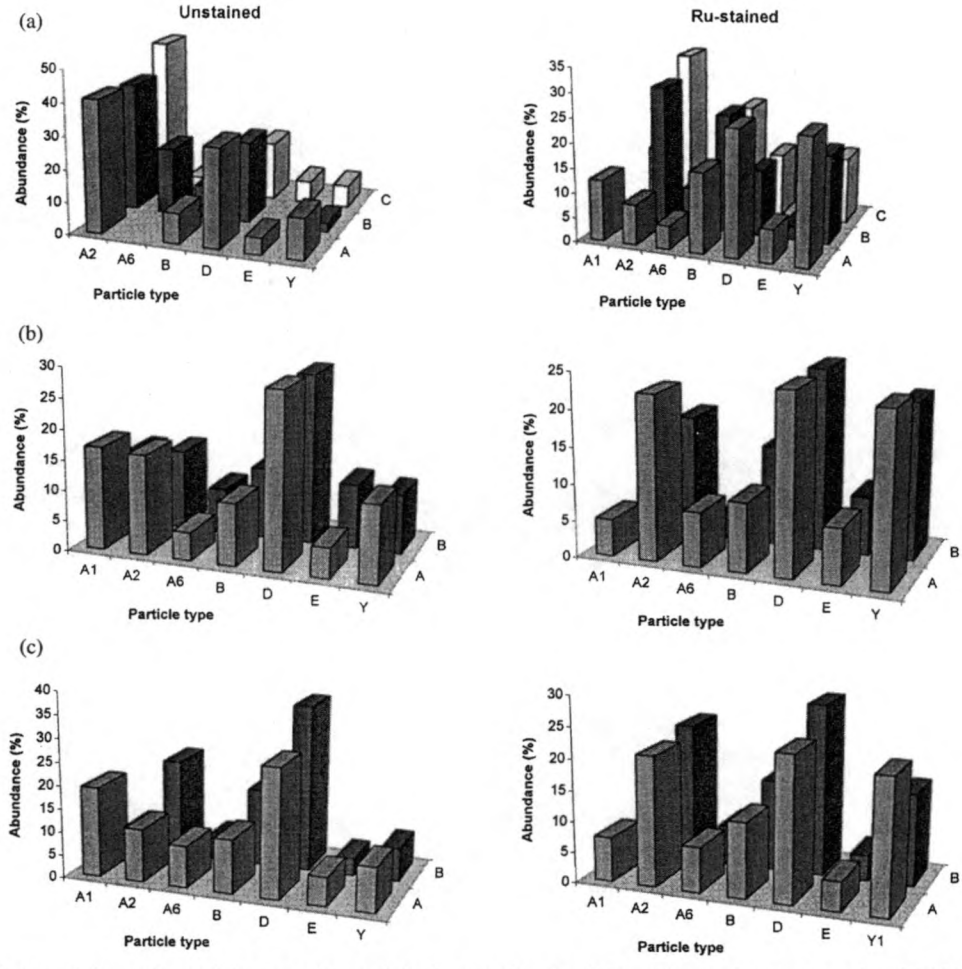

Fig. 1. Abundance of the main particle types detected in the unstained and Ru-stained rainwater samples: (a) N4/R6 A-C; (b) N10/R2 A-B port; (c) N10/R2 A-B starboard. Sample identifications see Table 1.

avoided by using polycarbonate filter units, but these are unfortunately not commercially available for filters smaller than 47 mm. Because the calculated loading of this blank is low (30 particles/mm^2), the contamination is negligible and the samples collected with this glass filter unit are useful from interpretation.

3.1.1.2. Ruthenium-stained samples. Part of the rainwater samples, i.e. those which were collected during the different phases of the rain event, have also been analyzed after staining with RuO_4. In the EDX-spectrum, the ruthenium peak strongly interferes with the chlorine peak (Jambers et al., 1999), but the error produced by this overlap is negligible, because limited amounts of Cl-containing particles detected in these rainwater samples are organic (only in N2/R1 and N4/R2, a few Cl-rich particles of marine origin were detected).

Comparison of the Ru-stained and unstained samples (Fig. 1), revealed that the main difference was an increase in the number of organic particles (Y). This increase was compensated by decreases in the other particle types, mainly the aluminosilicate class (A2) and the Fe-rich particles (D). Because of these limited differences, also no differences could be detected in the trends within a rain event of these stained and the unstained samples (Fig. 1).

For the suspended matter samples collected in

the North Sea (Jambers et al., 1999), ruthenium was also detected in all particles present in the rainwater, confirming also that rainwater particles have an organic coating. The large quantities of ruthenium detected in the S-rich (F1), S–Fe-rich (F2) and Cr-rich (I) particles indicated the strong affinity of organic matter for the adsorption of trace metals, and chromium in particular. However, it also indicates that the S-rich (F1) and S–Fe-rich (F2) particles, which are most likely of anthropogenic origin, contain relatively large quantities of organic material.

The blank collected during campaign N10 was analyzed after Ru-staining as well. The abundance of 81% for the organic particles and the strong increase of the calculated total suspended matter-loading to 160 particles/mm^2, illustrates that the majority of the contamination is organic. However, the loading of this blank is low in comparison with that of the samples (on average 1200 particles/mm^2) and thus only a limited amount of the organic material detected in the samples had originated from contamination during sample preparation.

3.1.1.3. TSM. The loadings of the filters and the diameter and density of the particles were used to calculate the TSM of the unstained and Ru-stained samples. However, these calculations, will only give an estimation of the TSM because: (a) only particles which were detected during automated analysis, i.e. particles larger than 0.45 μm and with enough BSE signal, were included; (b) a homogenous loading of the filter was presumed; (c) for the calculation of the particle volumes a spherical shape was assumed; and (d) a mean density of 2 g/cm^3 for natural particles was used (Buffle et al., 1992). In spite of these restrictions, the calculated TSM is useful to evaluate the TSM fluctuations.

No temporal trend is visible in the TSM-values of the samples collected during one rain event (Fig. 2). There is a maximum in the middle of the shower for N4/R6 (Fig. 2). Remarkable is also the large quantity of organic material present in N4/R6: the TSM of the stained samples is three times larger than that of the unstained samples (Fig. 2).

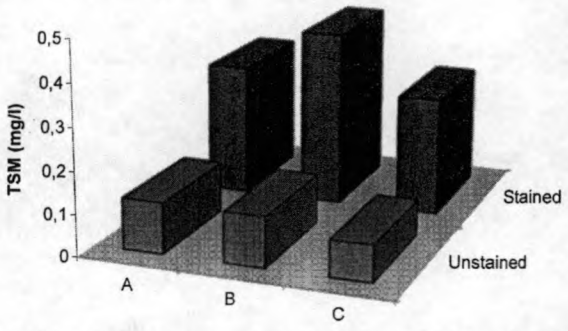

Fig. 2. Calculated total suspended matter (TSM) for the unstained and Ru-stained samples of N4/R6.

The TSM-values of the samples collected during two succeeding rain events in the port of Ipswich showed a significant decrease. Aerosols present below the cloud were washed out during the first shower, hence the second rain event mainly contained suspension scavenged by rainout. Thus above the land, scavenging by washout contributed much more to the suspension in rainwater than rainout. The TSM of these Ipswich samples was also much higher than that of samples collected above the sea: 6.8 mg/l for N3/R1 and 0.80 mg/l for N3/R2. The concentrations detected at the sea vary between 0.004 and 0.50 mg/l with an exceptionally high concentration of 0.80 mg/l for N4/R1, collected close to the Dutch coast. Thus the concentration of suspended matter is much smaller above the sea than above the land.

No correlation could be found between the TSM and the wind direction, wind speed or collection location. However, the doubling of the TSM values was remarkable for the samples collected on the starboard side compared with those collected on the portside. This was visible for all stained and unstained samples of campaign N10, with the exception of the coated sample N10/R2B which had comparable concentrations. The only possible explanation is that the wind during the rain events was mainly coming from starboard, inducing a larger contribution to the TSM from sea-spray in the rain collected at starboard.

3.1.2. Factor analysis

Factor analysis performed on the abundances

of the different particle types, indicated that the data could be divided according to three factors (Fig. 3). Factor 1 is characterized by positive loadings for Cl-rich (M) and organic (Y) particles and negative ones for pure aluminosilicate (A1), Fe-rich aluminosilicate (A6), Si-rich (B), S–Fe-rich (F2), Al-rich (G) and trace metal rich [i.e. Mn-rich (H) and Zn-rich (J)] particles. This separates marine and biogenic particles (M and Y), and terrigenous and anthropogenic particles. These terrigenous and anthropogenic particles are separated in factor 2, which shows a correlation between the aluminosilicate class (A2), Fe-rich (A6) and Ti-rich (A7) aluminosilicates and Si-rich particles (B), and between Fe-rich (D), Ti-rich (E) and Al-rich (G) particles. For the North Sea suspension (Jambers et al., 1999), factor analysis again reveals that Ti-rich aluminosilicates (A7) are of terrigenous origin, while Ti-rich particles (E) are most likely anthropogenic. In rainwater the same is also true for the Fe-rich aluminosilicates (A6) and the Fe-rich particles (D): Fe-rich aluminosilicates (A6) are terrigenous while Fe-rich particles (D) are mainly anthropogenic. Factor 3 has high loadings for Ca-containing (C) and S-rich (F1) particles, which are both present in small abundances in a limited number of samples. The Ca-containing particles (C) most likely have a terrigenous source, while the S-rich particles (F1) are thought to be mainly of anthropogenic origin (see Section 3.1.1). The minor correlation with the aluminosilicate class (A2), Fe-rich aluminosilicates (A6) and Si-rich particles (B) points to a terrigenous source, but the inverse-correlation with pure (A1) and Ti-rich (A7) aluminosilicates indicates that anthropogenic sources will also contribute to this particle type.

3.1.3. Study of trace metal containing particles

Trace metal-containing particles were studied in detail by extracting particles containing vanadium, chromium, manganese, nickel, copper, zinc, cadmium and/or lead from the original data matrix (Jambers et al., 1999). On average 9% of the unstained and 10% of the Ru-stained particles were metal-containing. Clustering, enclosing only trace metals, revealed that 60% of the particles contain chromium. Manganese, zinc, nickel and vanadium were also present, but in much smaller abundances: 20, 10, 10 and 4%, respectively. No Pb- or Cd-containing particles were detected, which confirms the suggestion that their airborne compounds are highly soluble in precipitation (Pattenden et al., 1982; Lim et al., 1991).

The trace metals were mostly associated with Fe-rich particles (D, 63%), Fe-rich aluminosilicates (A6, 18%) and with particles from the aluminosilicate class (A2, 7%). Strong correlations have been found between trace metals of anthropogenic and natural origin, implying the deposition of anthropogenic trace metals on both terrigenous and anthropogenic small particles (Natusch et al., 1973; Wadge et al., 1986; Lim et al., 1991). Thus, not all trace metal containing particles have a 'pure' anthropogenic origin. Chromium was found to be mainly associated with Fe-rich (D), Fe-rich aluminosilicate (A6), Ti-rich (E) and Al-rich (G) particles, while manganese dominated in Si-rich (B) particles and particles from the aluminosilicate class (A2). Also, small quantities of Mn-rich (H, 5%), Cr-rich (I, 2%) and Ni-rich (L, 2%) particles were present in the samples. The strong increase in abundance of Cr-rich particles in the Ru-stained samples (10% instead of 2%), indicate that chromium is strongly associated with organic material. In the samples small quantities of zinc and vanadium were also detected, which were mainly present in Fe-rich particles (D) and Fe-rich aluminosilicates (A6) in combination with chromium, nickel and/or manganese.

Comparison of the samples collected at port and starboard illustrated a doubling of the total number of trace metal containing particles at starboard (11 and 22%, respectively). This doubling is mainly due to the increase of Cr-containing particles and indicates the importance of sea-spray (which is thought to be a more important source at starboard than on port, see section on TSM) as a source of trace metal containing particles in air above the North Sea and of Cr-containing particles in particular (Lim et al., 1991; Van Malderen et al., 1996). Cr-containing particles thus most likely have a dominant marine

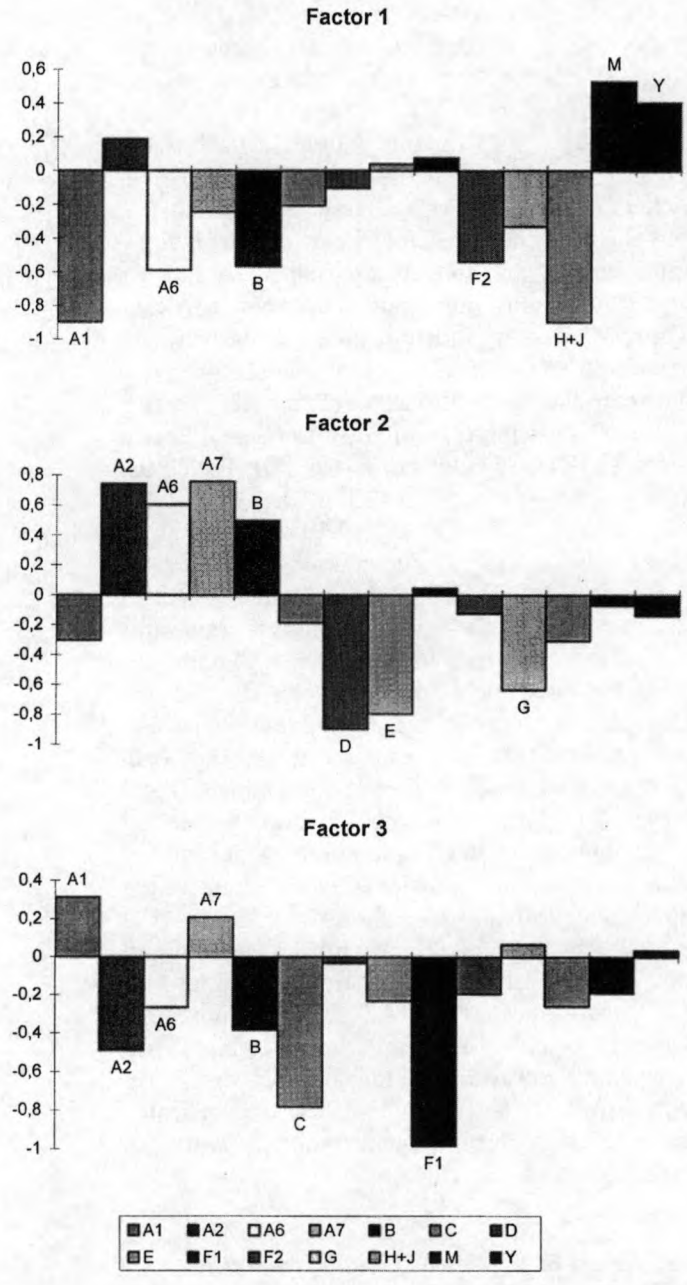

Fig. 3. Loadings of the three factors resulting from factor analysis on the abundances of the different particle types present in the North Sea rainwater suspension.

source, while Mn-containing particles, which were more important at port, are believed to mainly originate from anthropogenic sources (Kane et al., 1994).

3.1.4. Size distribution

The size distributions of the different particle types can be divided in three groups. Fig. 4 shows the distributions of the aluminosilicate class (A2),

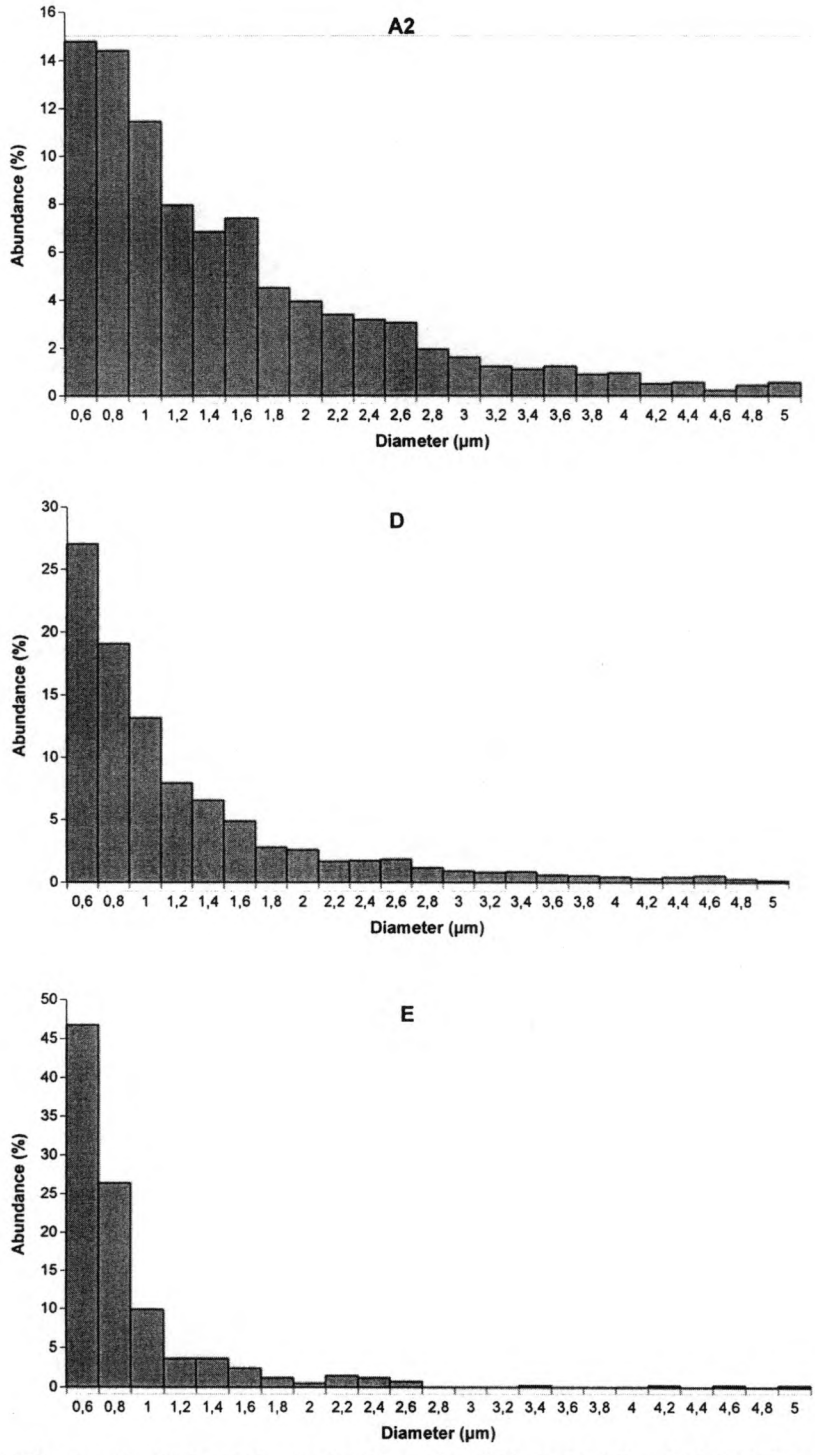

Fig. 4. Diameter distribution of the aluminosilicate class (A2), Fe-rich (D), and Ti-rich (E) particles.

Fe-rich (D) and Ti-rich (E) particle types which are representative for these groups. The first group contains particle types which have a mean diameter of 1.9 μm. This large group can be subdivided in the aluminosilicate class (A2) and Al-rich particles (G), with 40% of the particles smaller than 1 μm, and Fe-rich (A6), pure aluminosilicates (A1) and Si-rich particles (B), with 50% of the particles smaller than 1 μm. The presence of Al-rich particles (G) in this group of coarse mineral particles indicates that these are most likely also terrigenous. The second group consists of Fe-rich (D), S-rich (F1), S–Fe-rich (F2), Mn-rich (H) and organic (Y) particles, which all have a mean diameter of 1.4 μm and 60% of their particles smaller than 1 μm. The last group contains the Ti-rich (E), Ti-rich aluminosilicate (A7), Zn-rich (J) and Cl-rich (M) particle types, which have the smallest mean diameter of 0.9 μm, and 80% of the particles are smaller than 1 μm. The contributors to these last two groups are mainly of anthropogenic or marine origin; only the Ti-rich aluminosilicates (A7) are thought to have a more important terrigenous source. Due to the low number of Ca-rich (C) and Cr-rich (I) particles present in the unstained samples, no size distribution could be calculated for these particle types. However, the mean diameter of the Cr-rich particles, detected during the trace metal study of the Ru-stained samples (see Section 3.1.3), is also 0.9 μm, which indicates that these Cr-rich particles can also be classified into the smallest group. The small number of Ca-rich particles, on the other hand, all have relatively large diameters and thus belong to the coarse mineral group.

When the size distributions per sample are compared, it can be seen that the particles of sample N2/R1 and N2/R2, both collected in the center of the Bight, have relatively large mean diameters: 2.3 and 2.5 μm, respectively. Sample N3/R3 was also collected in the center, but has a much smaller mean diameter of 1.2 μm. This decrease in diameter can be explained by the presence of a north–north-western wind, which does not pass over land and thus contains less coarse mineral particles. However, the samples collected off the Belgian coast also have smaller mean diameters: between 1.2 and 1.9 μm. Only sample N4/R1, collected very close to the Dutch coast during a south-eastern land wind, has a mean diameter of 2.1 μm. These samples, collected close to the coast, contain thus less coarse mineral particles than those collected in the center of the Bight. Also remarkable is the size distribution of sample N4/R5 which has a maximum of 74% for particles with diameters between 1.5 and 2.0 μm. Because the chemical composition of this sample is comparable with that of the others, no explanation could be found for this special distribution.

Comparison of the size distributions of the samples N3/R1 and N3/R2 (Fig. 5), successively collected in the port of Ipswich, illustrates a decrease in mean diameter from 2.5 to 1.7 μm. The coarse particles were washed out during the first shower, resulting in a dominance of fine rainout particles during the second one. Above sea, this decrease in diameter is less visible. For the samples N4/R6A, B and C the mean diameter firstly increases from 1.6 to 1.9 μm, followed by a decrease to 1.2 μm. Thus in total there was a decrease in diameter, but in the intermediate sample the diameter was maximum. For the samples N10/R2A and B, there was a decrease from 1.6 to 1.2 μm at port and an unchanged diameter of 1.4 μm at starboard. This constant diameter for starboard samples indicates the continuous introduction of particles (most likely through sea-spray) to the suspended matter scavenged by the rainwater.

By comparison of the size distributions of the Ru-stained and unstained samples, an increase in the mean particle diameter was visible for the majority of the samples. At starboard this increase was highest. Because sea-spray is thought to be a more important contributor to the samples collected at starboard (see Section 3.1.1.3), this large increase in diameter is most likely a result of relatively large 'low contrast' particles (i.e. particles only detected after Ru-staining) produced by this sea-spray. The increase in diameter was also highest for the samples collected during the second phase of the rain event. This can again be explained by the contribution of sea-spray particles, which will be relatively more important in the second rain event phase, be-

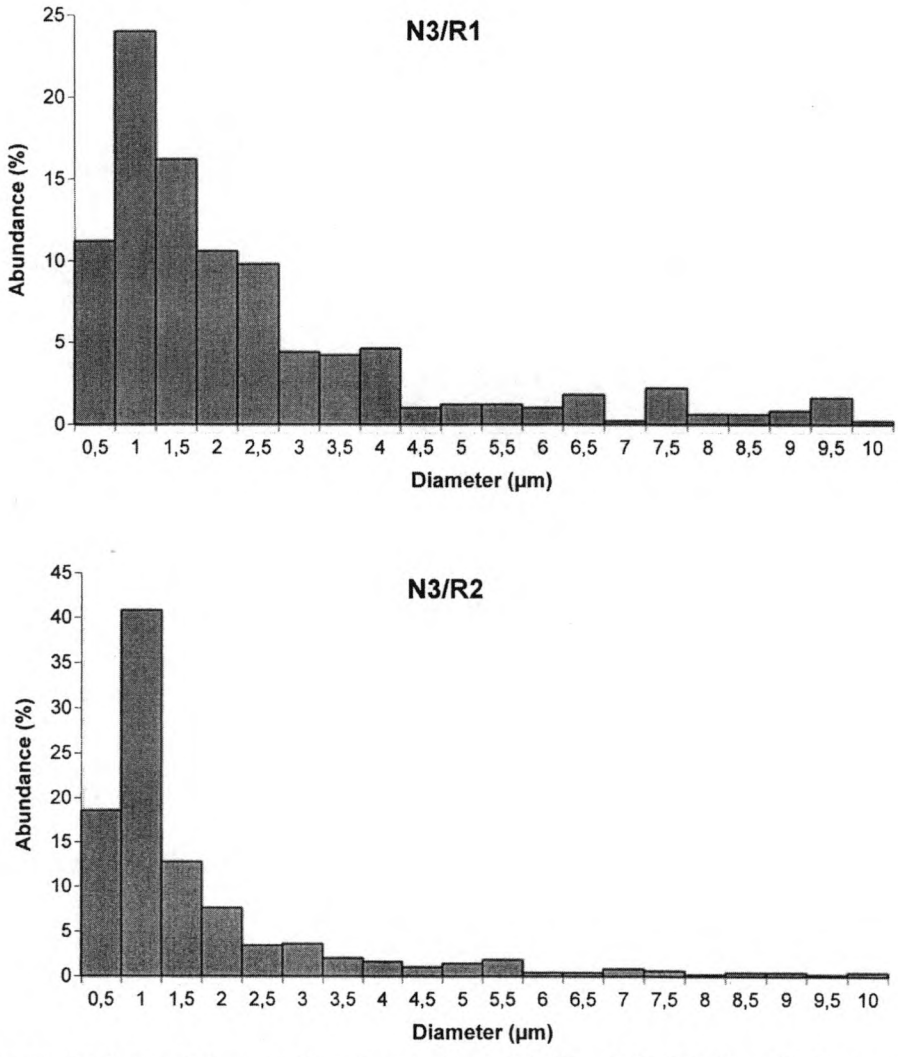

Fig. 5. Diameter distribution of the succeeding rainwater samples N3/R1 and N3/R2 collected in the port of Ipswich.

cause then the number of washed out particles is reduced. Additionally, these higher increases during the second phases also results in an increase in diameter with time, instead of the decrease visible in the unstained samples.

3.1.5. Manual analysis

Manual EPXMA measurements were used to obtain more information about the morphology and homogeneity of the individual particles suspended in rainwater. All samples were characterized by a limited number of aggregates and a large abundance of fly-ash particles. These fly-ash particles were identified as aluminosilicates (A2) and Fe-rich particles (D). Both particle types appear to have large contributions of anthropogenic particles, although natural ones are also of importance. These anthropogenic particles are classified under the same particle type as the natural ones, because of their similar chemical composition which disables separation of these particles using only EDX-spectra (Taylor and McLennan, 1985). The typical fly-ash anthropogenic particles were aggregates of small spheres.

The samples also contained relatively large quantities of quartz particles, confirming the dominance of terrigenous Si-rich particles (B) in these rainwater samples. The morphology of the organic particles revealed that the majority of the large organic particles were pollen and seeds and thus had a natural origin.

3.2. ICP-OES and IC analyses

To obtain additional information about the rainwater samples, the filtrates were analyzed using a Perkin-Elmer ICP/6500XR ICP-OES (Perkin-Elmer, Norwalk, CT, USA) and Dionex 4000i IC (Dionex, Sunnyvale, CA, USA).

The most striking thing about these results is the significant decrease in the concentrations of all detected elements measured for the samples N4/R6 A to C. This decrease is largest between N4/R6 A and B and coincides with a decrease in pH from 4.9 to 4.4. It thus seems that the concentrations of sodium, manganese, chlorine, potassium, calcium, nitrate and sulfate is highest at the beginning of the rain event and significantly decreases afterwards. However, the concentrations detected in N10/R2 A and B for port and starboard are comparable. Both N4/R6 and N10/R2 were collected off the Belgian coast, but during N4/R6 sampling the air mass had a more northern origin. The significantly increased concentrations of chlorine, sodium, sulfate and potassium, all originating from sea-spray, in the samples N4/R6 A to C indicated that the majority of the material present in these samples was marine derived. Thus it seems that the concentration of dissolved marine material is more subject to a decreasing tendency in the time of the rain event than the dissolved continental fraction.

The importance of marine input for all the elements, detected using ICP-OES and IC, was also visible in the significantly lower concentrations present in the samples collected in the port of Ipswich: sample N3/R1 and N3/R2. For these successive samples, all elements were also subject to a decreasing tendency, but the pH slightly increased from 4.2 to 4.4.

For the other elements detected with ICP-OES and IC, there was also a decreasing trend in trace metal concentrations for the samples N3/R1 to N3/R2 and N4/R6A, B to C, while for the samples N10/R2 A and B a small increase was noticed.

The average trace metal concentrations detected during this work (Table 3) are smaller than those reported previously for unfiltered rainwater from the southern North Sea (Baeyens et al.,

Table 3
Average content and enrichment factors of soluble compounds in rainwater above the southern North Sea

Element	Average content ($\mu g\ l^{-1}$)		Enrichment factors	
	This work	Baeyens et al. (1990)	EF_{marine} (vs. Na)	$EF_{pollution}$ (vs. Zn)
Na	58 000		1	
Mg	5600		0.8	
S	13 000		2.6	
P	300		820	
Cl	180 000		1.7	
K	11 000		4.9	
Ca	2900		1.3	
V	4.5		570 000	0.04
Mn	19	45	1 800 000	0.28
Ni	29		2 700 000	0.58
Cu	17	77	1 100 000	0.39
Zn	360	500	14 000 000	1.00
Cd	2	10	7 500 000	0.18
Pb	20	29	120 000 000	0.04

1990). For manganese this can be explained by the dominance of particulate manganese (Cawse, 1987), but the other trace metals are predominantly present in the dissolved rainwater phase (Nguyen et al., 1979), which rules out large differences due to the inclusion of the particulate matter. It can thus be concluded that compared to the mid-1980s the amount of trace metals present in rainwater above the North Sea has decreased, especially for cadmium and copper.

The results of these ICP-OES and IC measurements were also used to calculate enrichment factors (EF) of the different elements. The EF_{marine} was calculated using sodium as an indicator element:

$$EF_{marine} = (C_x/C_{Na})_{diss}/(C_x/C_{Na})_{seawater}$$

where C_x and C_{Na} were the concentrations of the element X and of Na in the filtrate and in the seawater (Riley and Chester, 1971), respectively. The $EF_{pollution}$ was based on the total emission of countries which contribute most to the Southern Bight: Belgium, the Netherlands, France, Germany, United Kingdom (Pacyna et al., 1984), and used zinc as a source indicator. The average values of these EFs are represented in Table 3 and were used to obtain extra information about the possible sources of the different elements. In this table also values for nitrogen and sulfur are given. These are based on IC measurements of nitrate and sulfate, presuming that nitrogen and sulfur are only present as nitrate and sulfate. No values are given for aluminum, silicon, iron and chromium because their concentrations were below the detection limit. These EF-values indicate that magnesium, chlorine and calcium mainly originate from sea-spray and that the sea is also an important source for sulfur and potassium. The very high EF_{marine} values for phosphorus and for the trace metals clearly indicate that they do not originate from the seawater. However, EF_{marine} is based on the composition of bulk seawater and the trace metal-enriched surface micro-layer of the seawater can still act as a source for these trace metals. The importance of other sources than anthropogenic pollution for trace metals is also indicated from the $EF_{pollution}$ values which show that only for nickel is pollution an important source. For lead, the reference data were recorded in the beginning of the 1980s and that since then the emission of lead has significantly decreased due to the use of unleaded gasoline (Injuk and Van Grieken, 1995). Thus although the $EF_{pollution}$ value of lead is very low, anthropogenic pollution is still thought to be the most important source of lead in the air above the North Sea.

4. Conclusions

The suspended matter present in rainwater collected above the North Sea is dominated by aluminosilicates (A2, abundances between 10 and 50%) and organic particles (Y, abundances up to 77%). Relatively high abundances of Fe-rich (D) and Si-rich (B) particles are detected. The aluminosilicates (A2) are mainly terrigenous, while for the Fe-rich particles (D) the anthropogenic source was dominant. The Si-rich particles (B) originated from land erosion, while the organic rich particles (Y) had a marine and continental biogenic source. The marine origin seemed to dominate, but for the larger organic particles there was also an important contribution of pollen and seeds originating from land vegetation.

For the majority of the samples, important levels of Ti-rich particles (E) as well as pure (A1), Fe-rich (A6) and Ti-rich (A7) aluminosilicates have been detected. These aluminosilicates are mainly terrigenous, although the size distribution of the Ti-rich aluminosilicates indicate an important amount of small anthropogenic particles. In a limited number of samples, small amounts of Ca-rich (C), Al-rich (G), S-rich (F1), S–Fe-rich (F2), Mn-rich (H), Cr-rich (I), Zn-rich (J) and Cl-rich (M) particles were detected, which all mainly originated from marine or anthropogenic sources. Only Ca-rich particles had a dominant terrigenous source.

Because of the variable chemical composition of the suspension present in rainwater in time and space (Fuzzi, 1994), hardly any correlation could be found between the composition of the different samples. The variation over a small pe-

riod of time was studied using the samples collected during the different phases of rain. It has been proved that at the beginning of a rain shower the coarse particles, present in the air under the cloud, are washed out, while during the second phase rainout particles, formed in the cloud, become more important due to the absence of new coarse particles under the cloud. Above the sea, the amount of TSM is much smaller and more variable than above the land and the decrease in particle diameter is less visible. This can be explained by the continuous input to the suspended matter of the rainwater of particles produced by sea-spray. This was proven by a significantly higher amount of TSM at starboard compared to port. The wind was mainly coming from starboard, resulting in a higher contribution of sea-spray material to the collector at starboard. It thus seems that part of the suspension collected in this rainwater samples originate from resuspension of North Sea material.

A detailed study of Ru-stained and unstained specimens revealed that the majority of the particles contained chromium and to a lesser extent also manganese, zinc, nickel and vanadium. Chromium was mainly associated with Fe-rich aluminosilicates (A6), Fe-rich (D), Ti-rich (E) and Al-rich (G) particles, while manganese was found in Si-rich particles (A2) and aluminosilicates (A2). Zinc and vanadium were only present in combination with other trace metals. On starboard, the total number of trace metal-containing particles was doubled compared to port. This was especially due to an increase of Cr-containing particles, which indicates that chromium is mainly originating from the surface micro-layer of the North Sea. Also, a high correlation was found between chromium and organic material.

The additional analyses of the dissolved rainwater fraction illustrated that the dissolved compounds are also variable in time and space. In general, over a short period of time, the concentrations of all dissolved compounds seem to decrease during a shower, but this decrease is much larger above land than above sea. This seems to be the result of an extra input of marine material, because the concentrations of the marine compounds like chlorine, sodium, sulfur and potassium were also significantly higher. It thus indicates that the seawater, and the surface micro-layer in particular, is an important source for trace metals present in air above the North Sea. The importance of this marine source is not obvious in the calculated EF_{marine} values because these use the concentration in the bulk seawater and not those in the enriched surface micro-layer. The EFs do show the presence of an imported marine source for dissolved chlorine, manganese, calcium, sulfur and potassium and a significant anthropogenic source for nickel. Through a comparison with data from the mid-1980s it could also be seen that the concentrations of dissolved trace metals present in rainwater above the southern North Sea have decreased over the last 15 years.

The suspension present in the North Sea rainwater contains less Ca-rich particles than the aerosols collected above the North Sea and North Sea suspended matter. This implicates that the majority of the Ca-containing aerosol particles are soluble in rainwater [mainly gypsum (Hoornaert et al., 1996)] and that thus only a very limited fraction of them has a terrigenous source. This implies that the air is not an important source of Ca-rich particles present in the North Sea suspension. As the amount of Ca-containing particles is also limited in riverine suspension (Van Put, 1991), the Ca-containing particles in the North Sea suspended matter must have originated from marine bioproduction or erosion of the cliffs of Dover and Calais (Salomons, 1975; Nolting and Eisma, 1988; Eisma, 1990).

The amount of trace metal-containing particles is much larger in rainwater than in the North Sea suspension: 10 and 1.5% (Jambers et al., 1999), respectively. This can partly be explained by the enrichment of trace metals in the surface micro-layer of the sea, resulting in a depletion of the bulk water. But the difference is so large that this also implies that the air is a major source for trace metal containing particles present in North Sea suspension. The air is also an important source of Ti-rich particles, which were more abundant in rainwater and for which a good similarity was found between the marine and atmospheric fraction (Xhoffer et al., 1992).

Acknowledgements

This work was prepared in the framework of the Program Sustainable Management of the North Sea, supported by the Belgian State-Prime Minister's Service-Services for Scientific, Technical and Cultural Affairs (contract JN/DD/10). Special thanks go to the captain and crew of the R/V *Belgica* for their support in obtaining the samples. Our manuscript benefited from the valuable suggestions and many language improvements kindly made by Dr Q. Fisher (University of Leeds, UK) and by the anonymous reviewer. The work of V. Dekov was supported by an UIA post-doctoral grant.

References

ASTM. Standard practice for handling of ultra pure water samples. Annual book of ASTM standards vol. 11.01 method D 1988:4453–4485.

Baeyens W, Dehairs F, Dedeurwaerder H. Wet and dry deposition fluxes above the North Sea. Atmos Environ 1990; 24A:1693–1703.

Benoliel MJ. Sample storage for inorganic compounds in surface water — a review. Int J Environ Anal Chem 1994;57:197–206.

Bishop JKB, Biscaye PE. Chemical characterization of individual particles from the nepheloid layer in the Atlantic Ocean. Earth Planet Sci Lett 1982;58:265–275.

Bruynseels F, Storms H, Van Grieken R, Vander Auwera L. Characterisation of North Sea aerosols by individual particle analyses. Atmos Environ 1988;22:2593–2602.

Buffle J, Perret D, Newman M. The use of filtration and ultrafiltration for size fractionation of aquatic particles, colloids and macromolecules. In: Buffle J, Van Leeuwen HP, editors. Environmental particles. Lewis Publishers: Chelsea, 1992:171–230.

Cawse PA. A survey of atmospheric trace elements in the UK 1972–73. AERE Harwell England: AERE Report R 7669, 1974.

Cawse PA. Trace and major elements in the atmosphere at rural locations in Great Britain 1972–81. In: Coughtrey PJ, Martin MH, Unsworth MH, editors. Pollutant transport and fate in ecosystems. Blackwell: Oxford, 1972:1987.

De Bock LA, Van Malderen H, Van Grieken RE. Individual aerosol particle composition variations in air masses crossing the North Sea. Environ Sci Technol 1994;28:1513–1520.

Eisma D. Transport and deposition of suspended matter in the North Sea and the relation to coastal siltation, pollution, and bottom fauna distribution. Rev Aquatic Sci 1990;3:181–216.

Fuzzi S. Clouds in the troposphere. In: Boutron CF, editor. Topics in atmospheric and interstellar physics and chemistry. Les editions de physique: Les Ulis, 1994: 290–308.

Galloway JN, Likens GE. Calibration of collection procedures for the determination of precipitation chemistry. Water Air Soil Pollut 1976;6:241–258.

Hoornaert S, Van Malderen H, Van Grieken R. Gypsum and other calcium-rich aerosol particles above the North Sea. Environ Sci Technol 1996;30:1515–1520.

Hov Ø, Allegrini I, Beilke S, Cox RA, Eliassen A, Elshout AJ, Gravenhorst G, Penkett SA, Stern R. Evaluation of atmospheric processes leading to acid deposition in Europe. Report EUR 11441. Commission of the European Community: Bruxelles, 1987.

Injuk J, Van Grieken R. Atmospheric concentrations and deposition of heavy metals over the North Sea: a literature review. J Atmos Chem 1995;20:179–212.

Jambers W, Dekov V, Van Grieken R. Single particle characterisation of inorganic and organic North Sea suspension. Mar Chem 1999;67:17–32.

Kane MM, Rendell AR, Jickells TD. Atmospheric scavenging processes over the North Sea. Atmos Environ 1994; 28:2523–2530.

Laquer FC. Sequential precipitation samplers: a literature review. Atmos Environ 1990;24A:2289–2297.

Lim B, Jickells TD, Davies TD. Sequential sampling of particles, major ions and total trance metals in wet deposition. Atmos Environ 1991;25A:745–762.

Natusch DFS, Wallace JR, Evans CA. Toxic trace elements: preferential concentration in respirable particles. Science 1973;183:202–204.

Nguyen VD, Valenta P, Nuernberg HW. Voltammetry in the analysis of atmospheric pollutants: the determination of toxic trace metals in rain water and snow by differential pulse stripping voltammetry. Sci Total Environ 1979; 12:151–167.

Nolting RF, Eisma D. Elemental composition of suspended particulate matter in the North Sea. Neth J Sea Res 1988;22:219–236.

Pacyna JM, Semb A, Hanssen JE. Emission and long-range transport of trace elements in Europe. Tellus 1984; 36B:163–178.

Pattenden NJ, Branson JR, Fisher EMR. Trace element measurements in wet and dry deposition and airborne particulate at an urban site. In: Georgii HW, Pankrath J, editors. Deposition of atmospheric pollutants. Reidel: Dordrecht, 1982:173–184.

Peirson DH, Cawse PA, Salmon L, Cambray RS. Trace elements in the atmospheric environment. Nature 1973; 241:252–256.

Riley JP, Chester R. Introduction to marine chemistry. Academic Press: London, 1971.

Salomons W. Chemical and isotopic composition of carbonates in recent sediments and soils from western Europe. J Sediment Petrol 1975;45:440–449.

Struyf H, Van Grieken R. An overview of wet deposition of micropollutants to the North Sea. Atmos Environ 1993;27A:2669–2687.

Taylor SR, McLennan SM. The continental crust: its composition and evaluation. Blackwell: Oxford, 1985.

Tsai WT, Altwicker ER, Asman WAH. Numerical simulation of wet scavenging of air pollutants-II. Modeling of rain composition at the ground. Atmos Environ 1990;24A: 2485–2498.

Van Malderen H, Hoornaert S, VanGrieken R. Using a combination of multivariate techniques for the identification of Cr, Pb and Zn containing particulate matter sampled above the Southern Bight of the North Sea. Environ Sci Technol 1996;30:489–498.

Van Put A. Geochemical and morphological characterization of individual particles from the aquatic environment by EPXMA. Ph.D. Thesis. Antwerp: University of Antwerp, 1991.

Wadge A, Hutton M, Peterson PJ. The concentrations and particle size relationships of selected trace elements in fly ashes from UK coal-fired power plants and a refuse incinerator. Sci Total Environ 1986;54:13–27.

Xhoffer C, Bernard P, VanGrieken R, VanderAuwera L. Chemical characterization and source apportionment of individual aerosol particles over the North Sea and the English Channel using multivariate techniques. Environ Sci Technol 1991;25:1470–1478.

Xhoffer C, Wouters L, Van Grieken R. Characterization of individual particles in the North Sea surface microlayer and underlying seawater: comparison with atmospheric particles. Environ Sci Technol 1992;26:2151–2162.

Selected article #25:

Single-particle analysis of aerosols at Cheju Island, Korea, using low-Z electron probe X-ray microanalysis: a direct proof of nitrate formation from sea salts

C.-U. Ro, K.-Y. Oh, HK Kim, Y.P. Kim, C.B. Lee, K.-H. Kim, C.-H. Kang, J. Osan, J. de Hoog, A. Worobiec and R. Van Grieken

Environmental Science and Technology, 35 (2001) 4487-4494

Single-Particle Analysis of Aerosols at Cheju Island, Korea, Using Low-*Z* Electron Probe X-ray Microanalysis: A Direct Proof of Nitrate Formation from Sea Salts

Chul-Un Ro, Keun-Young Oh, HyeKyeong Kim, Yong Pyo Kim, Chong Bum Lee, Ki-Hyun Kim, Chang Hee Kang, János Osán, Johan de Hoog, Anna Worobiec, and René Van Grieken

Department of Chemistry, Hallym University, Chun Cheon, Kang Won Do, 200-702 Korea, Institute of Environment & Life Science, Hallym Academy of Sciences, Hallym University, Chun Cheon, Kang Won Do, 200-702 Korea, Department of Environmental Science and Engineering, Ewha Womans University, Seoul, 120-750 Korea, Department of Environmental Science, Kangwon National University, Chun Cheon, Kang Won Do, 200-701 Korea, Department of Earth Sciences, Sejong University, Seoul, 143-747 Korea, Department of Chemistry, Cheju National University, Cheju, 690-756 Korea, KFKI Atomic Energy Research Institute, P.O. Box 49, H-1525 Budapest, Hungary, and Department of Chemistry, University of Antwerp, Universiteitsplein 1, B-2610 Antwerp, Belgium

ENVIRONMENTAL SCIENCE & TECHNOLOGY

Reprinted from
Volume 35, Number 22, Pages 4487–4494

Environ. Sci. Technol. **2001**, *35*, 4487−4494

Single-Particle Analysis of Aerosols at Cheju Island, Korea, Using Low-*Z* Electron Probe X-ray Microanalysis: A Direct Proof of Nitrate Formation from Sea Salts

CHUL-UN RO,*,†,‡ KEUN-YOUNG OH,† HYEKYEONG KIM,‡ YONG PYO KIM,§ CHONG BUM LEE,∥ KI-HYUN KIM,⊥ CHANG HEE KANG,# JÁNOS OSÁN,▽ JOHAN DE HOOG,○ ANNA WOROBIEC,○ AND RENÉ VAN GRIEKEN○

Department of Chemistry, Hallym University, Chun Cheon, Kang Won Do, 200-702 Korea, Institute of Environment & Life Science, Hallym Academy of Sciences, Hallym University, Chun Cheon, Kang Won Do, 200-702 Korea, Department of Environmental Science and Engineering, Ewha Womans University, Seoul, 120-750 Korea, Department of Environmental Science, Kangwon National University, Chun Cheon, Kang Won Do, 200-701 Korea, Department of Earth Sciences, Sejong University, Seoul, 143-747 Korea, Department of Chemistry, Cheju National University, Cheju, 690-756 Korea, KFKI Atomic Energy Research Institute, P.O. Box 49, H-1525 Budapest, Hungary, and Department of Chemistry, University of Antwerp, Universiteitsplein 1, B-2610 Antwerp, Belgium

A recently developed electron probe X-ray microanalysis (EPMA), called low-*Z* EPMA, employing an ultrathin window energy-dispersive X-ray detector, was applied to characterize aerosol particles collected at two sampling sites, namely, Kosan and 1100 Hill of Cheju Island, Korea, on a summer day in 1999. Since low-*Z* EPMA can provide quantitative information on the chemical composition of aerosol particles, the collected aerosol particles were classified and analyzed based on their chemical species. Many different particle types were identified, such as marine-originated, carbonaceous, soil-derived, and anthropogenic particles. Marine-originated particles, such as $NaNO_3$- and Na_2SO_4-containing particles, are very frequently encountered in the two samples. In this study, it was directly proven that the observed nitrate particles were from sea salts. In addition, two types of nitrate particles from sea salts were observed, with and without Mg. The sodium nitrate particles without Mg were believed to be collected as crystalline form, either with the sodium nitrate particles being fractionally recrystallized within evaporating seawater drops or with recrystallized sodium chloride particles having reacted with gaseous nitrogen species in the air to form the crystalline sodium nitrate particles. The other seemed to be collected as seawater drops, where the atmospheric reaction had occurred in the droplets, and thus sodium as well as magnesium nitrates were observed. Carbonaceous particles are the most abundant in the samples at both sites. From this study, it was found that about three-quarters of the carbonaceous particles in the samples were biogenic, which partially explains a previously reported observation of a large concentration of organic carbon particles as compared to elemental carbon. Various soil-derived particles were also observed. In addition to aluminosilicate- and iron oxide-containing particles, which are ubiquitous components in soil-derived particles, $CaCO_3$-, Al_2O_3- and Cr-containing particles were also frequently encountered.

Introduction

Characterization of airborne particles deepens our understanding about the source, reactivity, transport, and removal of atmospheric chemical species. Since atmospheric particles are chemically and morphologically heterogeneous and the average composition and the average aerodynamic diameter do not describe well the population of the particles, microanalytical methods have proven to be useful for studying atmospheric particles. Electron probe X-ray microanalysis (EPMA) is capable of simultaneously detecting the chemical composition and the morphology of a microscopic volume such as a single atmospheric particle (*1*). A recently developed EPMA technique, called low-*Z* EPMA, allows the determination of the concentration of low-*Z* elements such as carbon, nitrogen, and oxygen, as well as higher-*Z* elements, which are observed using conventional energy-dispersive EPMA (ED-EPMA) (*2*−*4*). By the application of the low-*Z* EPMA technique, which employs an ultrathin window energy-dispersive X-ray (EDX) detector, chemical compositions, including the low-*Z* components, of individual particles can be quantitatively elucidated. The determination of low-*Z* elements in individual environmental particles allows the improvement of the applicability of single-particle analysis; many environmentally important atmospheric particles (e.g., sulfates, nitrates, ammonium, and carbonaceous particles) contain low-*Z* elements. Furthermore, the diversity of atmospheric particles in chemical composition can be investigated in detail using the low-*Z* EPMA technique.

Application of wavelength-dispersive X-ray (WDX) detection is another possibility for quantitative low-*Z* element analysis. Recently, it was shown that semiquantitative WDX analysis, down to oxygen, is feasible even for irregularly shaped particles down to 0.8 μm in equivalent diameter (*5*). The WDX approach has some advantages over EDX in terms of its better detection limit for low-*Z* elements, due to its better peak-to-background ratio, and its superior energy resolution, resulting in a lower probability of the overlapping between low-*Z* element K- and L-lines of transition metals. However, most critically, the much higher current needed for the measurements in WDX limits its potential just to the particles that are most stable under electron bombardment.

There have been approaches to specify environmentally important chemical species in individual particles, e.g., nitrate and sulfate, using EPMA (*6*−*9*). These techniques employ chemical reactions on individual particles of interest; for example, barium chloride and Nitron are used as reaction

* Corresponding author telephone: +82 33 240 1428; fax: +82 33 256 3421; e-mail: curo@hallym.ac.kr.
† Department of Chemistry, Hallym University.
‡ Hallym Academy of Sciences, Hallym University.
§ Ewha Womans University.
∥ Kangwon National University.
⊥ Sejong University.
Cheju National University.
▽ KFKI Atomic Energy Research Institute.
○ University of Antwerp.

10.1021/es0155231 CCC: $20.00
Published on Web 10/18/2001

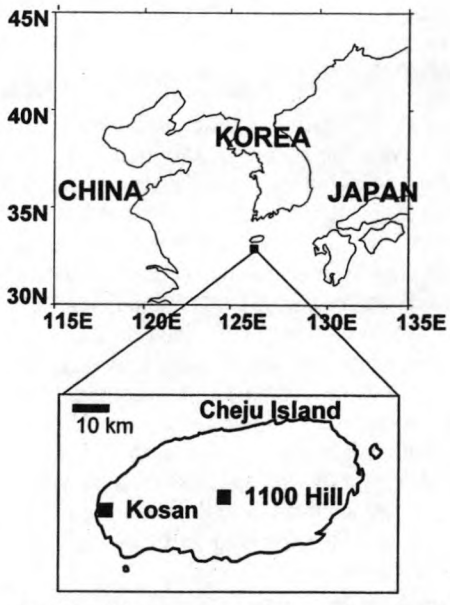

FIGURE 1. Location of the measurement sites and surrounding region.

agents for sulfate and nitrate species, respectively. The particles with nitrate or sulfate react with those agents to produce characteristic morphologies if reaction occurs so that those particles can be identified using either scanning or transmission electron microscopy. These techniques have proven to be useful to study the atmospheric chemistry of nitrate or sulfate species in the reaction with other airborne particles, such as sea salt, mineral, and carbonaceous particles. However, these techniques only allow the analysis of nitrate and sulfate species; furthermore, this analysis is purely qualitative since only the presence or the absence of those chemical species can be determined.

Another single-particle analysis technique allows the identification of chemical species of individual particles qualitatively using laser microprobe mass spectrometry, the so-called ATOFMS (*10*–*12*). This technique can analyze the aerodynamic sizes and chemical compositions of individual particles in real time, and even the instrument can be portable (*12*) so that it can be used in the field. By application of the ATOFMS technique, the complex nature of airborne particles has been directly revealed (*13, 14*), and it was demonstrated that the technique can clearly elucidate the atmospheric chemistry between sea-salt particles and gas-phase nitric acid as it occurs in the atmosphere (*15*). However, due to its poor reproducibility, the technique can now only provide qualitative determination of chemical species in individual particles.

The low-*Z* EPMA was applied to characterize aerosols collected at Cheju Island, Korea. Cheju Island is an ideal place to study continental and marine influences on aerosols because it is surrounded by the Korean peninsula, mainland China, Japan, and the China Sea (see Figure 1), and it is also one of the cleanest areas in Korea. Several extensive works on the aerosol composition on the island have already been carried out, such as studies on summertime characteristics of the aerosol including carbonaceous species (*16*), seasonal variation of the overall aerosol composition (*17*–*21*), and seasonal variation of particulate nitrate (*22*). Also, two modeling studies were performed to understand the seasonal behavior of the aerosol composition (*23*) and the aging processes of sea-salt and mineral aerosols (*24*) on this island. These studies emphasize the importance of this island as a sampling site for the study of long-range transport of aerosols in northeastern Asia where emission of air pollutants is considerably large (*25*). However, no single-particle analysis has been applied to aerosols at Cheju Island until now, which may provide detailed and new information on the chemical composition of the aerosols. We performed single-particle analysis for samples collected on a summer day in 1999. In this work, aerosol samples collected at Kosan and 1100 Hill of Cheju Island were characterized by using the low-*Z* EPMA. Detailed information on chemical composition and size distribution of the particle samples were provided by this single-particle analysis. From this study, we report some new findings on chemical compositions of the aerosol particles in Cheju Island and also a direct proof of nitrate formation from sea salts. However, this study presents more questions than answers on the characteristics of aerosols at Cheju Island. Currently, an international research project, called Aerosol Characterization Experiment–Asia (ACE-Asia), is being carried out until 2004 (homepage: http://saga.pmel.noaa.gov/aceasia) to understand the characteristics of aerosols in northeastern Asia in more detail. Kosan is one of the focal sampling sites for this project. By continuing the single-particle analysis using the low-*Z* EPMA at this sampling site, we hope to clearly address the new questions raised by this work.

Experimental Section

Samples. Samplings were done at two different sampling sites on Cheju Island, namely, Kosan and 1100 Hill (see Figure 1). The Kosan sampling site (33°17′ N, 126°10′ E; altitude, 60 m) is just 10 m away from the coast, and the 1100 Hill site (33°21′ N, 126°27′ E; altitude, 1100 m) is located in the middle of a forest on the slope of Halla Mountain with an elevation of 1950 m. The distance between the two sites is ca. 30 km. Each set of aerosol samples was collected at the two sites on June 19, 1999. Particles were sampled on Ag foil using a seven-stage May cascade impactor (*26*). Sampling was from 9:40 to 11:50 am at Kosan and from 2:20 to 3:30 pm at 1100 Hill. The sampling duration varied between 2 (for stage 6) and 128 (for stage 1) min at Kosan to obtain a good loading of particles at the impaction slots. At 1100 Hill, it was approximately half of that at Kosan, implying higher aerosol concentrations at 1100 Hill during the sampling time. The May impactor has, at a 20 L/min sampling flow, aerodynamic cutoffs of 16, 8, 4, 2, 1, 0.5, and 0.25 μm for stages 1–7, respectively. The seventh stage was not analyzed because the very small size of particles collected on the stage was not suitable for EPMA measurements. Some 300 particles for each stage sample, except stage 6 sample collected at Kosan, were analyzed; in total, there were 2888 particles. The May impactor has an impacting slit at each stage, and thus the aerosols collected on the Ag foil substrate show a slit pattern. A distinct slit line on stage 6 of the sample collected at Kosan was seen just after aerosol collection, and yet it was not possible to find the aerosols under electron microscopy. This was a unique occasion in our measurements, and the explanation for this is that mostly moisture aerosols might be collected at stage 6, of which the aerodynamic cutoff diameter is 0.5 μm, and then they evaporated during storage or under vacuum in the EPMA instrument. On the day before the sampling time, it had rained all day, and some of fine particles might be washed out before our sampling. The collected samples were put in plastic carriers, sealed, and stored in a desiccator.

EPMA Measurements and Data Analysis. The measurements were carried out on a JEOL 733 electron probe microanalyzer equipped with an Oxford Link SATW ultrathin window EDX detector. The resolution of the detector is 133 eV for Mn Kα X-rays. The spectra were recorded by a Canberra S100 multichannel analyzer under control of homemade software. To achieve optimal experimental conditions such as low level of the background in the spectra and high sensitivity for light element analysis, a 10-kV accelerating voltage was chosen. The beam current was 1.0 nA for all the

measurements. To obtain statistically enough counts in the X-ray spectra and to minimize the beam damage effect on the sensitive particles, a typical measuring time of 10 s was used. The cold stage of the electron microprobe allowed the analysis of particulate samples at liquid nitrogen temperature (around −193 °C), which enabled us to minimize contamination and reduce beam damage to the samples as well. A more detailed discussion on the measurement conditions is given elsewhere (*2*). The size and shape of each individual particle was measured from backscattered electron images, and its size was estimated as that of an equivalent spherical particle using a homemade computer program while the X-ray spectrum for each particle was automatically acquired under the control of a computer.

The net X-ray intensities for the elements were obtained by nonlinear least-squares fitting of the collected spectra using the AXIL program (*27*), and the elemental concentrations for individual particles were obtained from their X-ray intensities by application of a Monte Carlo calculation with reverse successive approximations. The Monte Carlo calculation is based on a modified version of the single scattering CASINO Monte Carlo program (*28, 29*), which was designed for low-energy beam interaction generating X-ray and electron signals. The modified version of the CASINO program allows the simulation of electron trajectories in spherical, hemispherical, and hexahedral particles located on a flat substrate (*2*). The simulation procedure determines also the characteristic and continuous X-ray flux emitted from the substrate material and the influence of the substrate material on the energy distribution of the exciting electrons. The quantification procedure uses an iterative approach; the iterative calculation is finished when measured X-ray intensities for all chemical elements in a particle are well matched to intensities simulated by the Monte Carlo calculation. In the beginning of the iterative Monte Carlo calculation, the differences between measured and calculated intensities are considerable so that a successive approximation approach is employed to find the best match, with adjusting input values, e.g., chemical compositions, for the following iteration. When convergency is achieved, the chemical compositions used for the calculation is the obtained chemical composition of the particle. Generally a few iterations are enough to find convergency. The quantification procedure provides good accuracy within around 12% relative deviations between the calculated and the nominal elemental concentrations when the method is applied to various types of standard particles such as NaCl, SiO_2, $CaSO_4 \cdot 2H_2O$, $(NH_4)_2SO_4$, and NH_4NO_3 (*30*). More details on the quantification procedure can be found elsewhere (*4*).

Results and Discussion

Classification of Individual Particles according to Their Chemical Species. The determination of chemical species in individual particles was done in a way to fully utilize the information contained in their X-ray data. The chemical composition of each particle is never exactly the same as that of others; it is rather rare to see particles composed of only one pure chemical species, and also particles with two or more chemical species have different compositions. Since the low-*Z* EPMA can provide quantitative information on chemical composition, we tried to classify particles based, as much as possible, on their chemical species. The analytical procedure for determining chemical species is described in more detail elsewhere (*31*). Here, we briefly summarize how the particle types are classified; first, particles are regarded to be composed of just one chemical species when the chemical species constitutes at least 90% in atomic fraction. Second, it was tried to specify chemical species even for particles internally mixed with two or more chemical species. Third, it is known that ED-EPMA has high detection limits of 0.1−1.0% in weight, mainly due to its high background level. Since the low-*Z* EPMA is used for the analysis of a microscopic volume (picogram range in mass for a single particle of micrometer size), the elements at trace levels could not be reliably investigated. Thus, we do not include elements with less than 1.0% of atomic concentration in the procedure of chemical speciation.

TABLE 1. Particle Types and Numbers of Particles Found in Kosan Sample[a]

	no. of particles					
particle type	stage 1	stage 2	stage 3	stage 4	stage 5	sum
Al_2O_3	6			1		7
AlSi[b]	11	5	15	7	28	66
AlSi/carb[c]	2	3				5
biogenic	37	62	74	61	3	216
carbon-rich	3	2	9	5		19
organic	2	2	16	13	11	44
$CaCO_3$	8	5	6	6	1	26
$CaSO_4$			3		1	4
CrOx		1	1	4	1	7
(Cr,Fe)Ox				3		3
FeOx			7	3	2	12
NaCl/O	1	3	1	4	3	12
$NaNO_3$	3	95	21	28	14	161
Na_2SO_4		5	2	2	10	19
$Na(NO_3,SO_4)$		3	2	2	1	8
$Na(NO_3,Cl)$		6	3	2	1	12
$Na(NO_3,SO_4,Cl)$		2		3		5
$Na(SO_4,Cl)$		6			2	8
(Na,Mg)Cl/O		42	25	5	3	75
$(Na,Mg)NO_3$	1	16	29	58	72	176
$(Na,Mg)SO_4$		1	2	1	5	9
$(Na,Mg)(NO_3,Cl)$			11	14	3	28
$(Na,Mg)(SO_4,Cl)$				1	5	6
$(Na,Mg)(NO_3,SO_4)$		4	3	3	10	20
$(Na,Mg)(NO_3,SO_4,Cl)$			5	1	5	11
$(NH_4)_2SO_4$	1		3	9	60	73
SiO_2	8	2	3	13	11	37
SiO_2/carb			6			6
C/S/O			2		4	6
Cl/O				4		4
Cl/C		5	5			10
Cl/C/Na/O		14	2			16
Na/Mg/O			1	4	3	8
others[d]	2	9	14	10	9	44
NEIC[e]	3	7	29	33	32	104
sum	88	300	300	300	300	1288

[a] The aerodynamic cutoff diameters for stages 1−5 are 16, 8, 4, 2, and 1 μm, respectively. [b] AlSi, aluminosilicates. [c] Carb, carbonaceous species. [d] Others, particle type with less than 1% frequency in all the stages (19 types: $Ca(CO_3,SO_4)$, CuOx, CuOx/carb, KNO_3, $K(CO_3,NO_3)$, $(Na,Ca)CO_3$, Na_2SO_4/carb, $(Na,Ca)SO_4$, $(Na,Mg,Ca)NO_3$, $(NH_4,Na)SO_4$, $(NH_4,Ca)SO_4$, NiOx, $MgCO_3$, $MgCl_2$, $MgCl_2$/N/S, SiO_2/Fe, TiOx, Cl/Mg/O, Cl/S/O). [e] NEIC, X-ray spectra for the particles do not have enough information for classification.

Overall, 2888 particles for two samples were analyzed, and the results of classification based on chemical species of the particles are shown in Table 1 for the Kosan sample and in Table 2 for the 1100 Hill sample. All together, 52 and 48 different particle types were identified for the Kosan and the 1100 Hill samples, respectively. Soil-derived particles such as aluminosilicates, $CaCO_3$, SiO_2, and iron oxides; carbonaceous particles; and particles originated from marine aerosols are very frequently observed in those two samples. Particles containing carbonaceous species, either as single species or mixed with others, are the most frequently observed (890 out of total measured 2888 particles: 30.8%), followed by particles containing $NaNO_3$ (637/2888: 22.1%), aluminosilicates (278/2888: 9.6%), $(NH_4)_2SO_4$ (240/2888: 8.3%), Na_2SO_4 (134/2888: 4.6%), SiO_2 (102/2888: 3.5%), and NaCl

TABLE 2. Particle Types and Numbers of Particles Found in 1100 Hill Sample[a]

	no. of particles						
particle type	stage 1	stage 2	stage 3	stage 4	stage 5	stage 6	sum
Al_2O_3	1	12	8	13	22	5	61
AlSi[b]	4	33	7	7	19	7	77
AlSi/carb[c]	9	44	27	27	13	3	123
biogenic	59	72	81	70	13	7	302
carbon-rich	3	5	5	4	13	3	33
organic	12	13	16	17	3	6	67
$CaCO_3$	1	4	15	6		1	27
$CaCO_3$/carb	2	7	10	1			20
$CaSO_4$/carb		5	5		2		12
CrOx			3	1			4
FeOx	1	1	2	6	12	3	25
FeOx/carb	1	7	3	6			17
KNO_3/carb		1	1	3			5
$NaNO_3$		3		4	1		8
Na_2SO_4			3	2	3	1	9
(Na,Mg)NO_3		49	54	46	13		162
(Na,Mg)SO_4			1	1	7		9
(Na,Mg)(NO_3,Cl)		7	3				10
(Na.Mg)(NO_3,SO_4)		4	5	13	8		30
$(NH_4)_2SO_4$				11	79	63	153
$(NH_4)_2SO_4$/carb			2	3		2	7
$(NH_4)_2SO_4$/AlSi				2	5		7
SiO_2	1	7	4	15	15	3	45
SiO_2/carb	3	6	4	1			14
S/O			4	5	38	75	122
others[d]	2	5	16	18	12	2	55
NEIC[e]	1	15	21	18	22	119	196
sum	100	300	300	300	300	300	1600

[a] The aerodynamic cutoff diameters for stages 1–6 are 16, 8, 4, 2, 1, and 0.5 μm, respectively. [b] AlSi, aluminosilicates. [c] Carb, carbonaceous species. [d] Others, particle type with less than 1% frequency in all the stages (23 types: Al_2O_3/carb, Ca(CO_3,NO_3), (Ca,K)CO_3, (Ca,Mg)CO_3, (Ca,Mg)SO_4, (Co,Fe,Ni)Ox, (Cr,Fe)Ox, (Cr,Fe,Ni)Ox, CuOx, K_2CO_3, K_2SO_4, KNO_3, (K,NH_4)SO_4, $MgCO_3$, $NaNO_3$/AlSi, Na_2SO_4/AlSi, (Na,Ca)SO_4, (Na,K)SO_4, (Na,NH_4)SO_4, (Na,NH_4,K)SO_4, (Na,Mg)Cl/O, NH_4(SO_4,NO_3), TiOx/AlSi). [e] NEIC, X-ray spectra for the particles do not have enough information for classification.

(89/2888: 3.1%). Since the sampling sites are considered to be minimally influenced by local anthropogenic emissions, the abundant observations of some particle types, e.g., biogenic (one type of carbonaceous species) and soil-derived particles, imply strong influence from local natural sources.

Even though the two sampling sites are not located far from each other and the air mass delay between two sampling times is ca. 5 h, there exist some differences in the characteristics of aerosol particles between the two, mainly because of their different surroundings; one is close to the coast, and the other is in the forest. Aerosol particles originated from sea salts are relatively more frequently encountered at Kosan, whereas soil-derived, carbonaceous, and anthropogenic particles predominate at 1100 Hill. As shown in Figure 2, particles containing NaCl, $NaNO_3$, and Na_2SO_4 species are relatively more abundant in the Kosan sample. In contrast, particles containing carbonaceous species (most of them are biogenic particles) and also soil-derived particles, e.g., containing aluminosilicates and iron oxides, and $(NH_4)_2SO_4$-containing particles are relatively more abundant in the 1100 Hill sample. A more detailed discussion on the characteristics of the aerosol particles is given later.

Since EPMA can provide information on the morphology of individual particles as well as on chemical composition, the size distributions of particles at different stages of the May cascade impactor were investigated. The EPMA measurements were done in automatic data acquisition mode, where the electron beam is aligned at the center of particles by a computer using a homemade software before acquiring data from each particle while scanning over the particle. The

TABLE 3. Summary of Number Distributions for Kosan and 1100 Hill Samples

		Kosan			1100 Hill		
stage	aerodynamic cutoff diameter[a]	1st max	2nd max	3rd max	1st max	2nd max	3rd max
1	16	15.8	10.0	5.0	20.0	7.9	
2	8	6.3	4.0	2.3	7.9	2.5	
3	4	4.0	2.3	1.3	6.3	2.5	1.3
4	2	4.0	1.3	0.8	4.0	1.6	1.0
5	1	1.6	0.4		1.3	0.4	
6	0.5				0.8		

[a] In μm.

size of particles is automatically saved in the computer after being converted to that of equivalent spherical particles. Figure 3 shows the number distributions of particles in each stage, based on their size, for the Kosan sample. The aerodynamic cutoff diameters for stages 1–5 are specified as 16, 8, 4, 2, and 1 μm, respectively, at a 20 L/min sampling flow. The number distribution according to their real projected physical size of individual particles at each stage is much more complex than believed; some stages have multiple maxima in their number distributions and the two samples show somewhat different number distributions even though the very same impactor was used for aerosol particle collections. A summary for the number distributions of the two samples is given in Table 3. Overall, as the stage number increases and the aerodynamic cutoff size decreases, the peak maxima of the number distributions also decrease. Since we are dealing with real projected physical sizes measured by EPMA, multiple peak maxima are observed mainly because particle groups with different densities are collected in the stages (shattering of particles at their impaction could be a reason for the maxima found at a smaller size than the apparent cutoffs of the impactor). The stages of the May impactor are supposed to separate aerosol particles based on their aerodynamic diameter, which is defined as the equivalent diameter of spherical particles with density of 1.0. For example, the observation of three maxima in the number distribution implies that the stage collected particle groups with three different average densities. For stages 1 and 2 of the Kosan sample, the real physical sizes are smaller than their aerodynamic cutoffs, implying that particles have a somewhat larger density than 1.0. In contrast, the number distributions of stages 1 and 2 for the 1100 Hill sample show the first maximum at sizes larger than or similar to their aerodynamic cutoffs, implying that some particles collected at these stages have a lower density. In the same context, it could be claimed that stages 4–6 collected some lighter (the first maximum in number distributions) and also heavier (the second and third maxima) particles. This result shows the complex nature of the size segregation during the sampling using a cascade impactor, and it is somewhat difficult to extract useful chemical information only from the number distribution data.

Characteristics of Aerosol Particles Collected at Kosan and 1100 Hill. Despite the relatively short distance (ca. 30 km) between the two sampling sites, Kosan and 1100 Hill, we observed significant differences in the aerosol characteristics between the two samples. Figure 4 shows 3-day back-trajectories of the air mass for our samplings. It was in the Northeast Provinces of China, passed over the Yellow Sea and the Korea peninsula, and had stagnated over the strait between Korea and Japan for 1 day before arriving at Cheju Island. From the back-trajectory data, it can be said that the air mass had mostly been under marine influence and maybe some from Korea and Japan before arriving at the sampling sites.

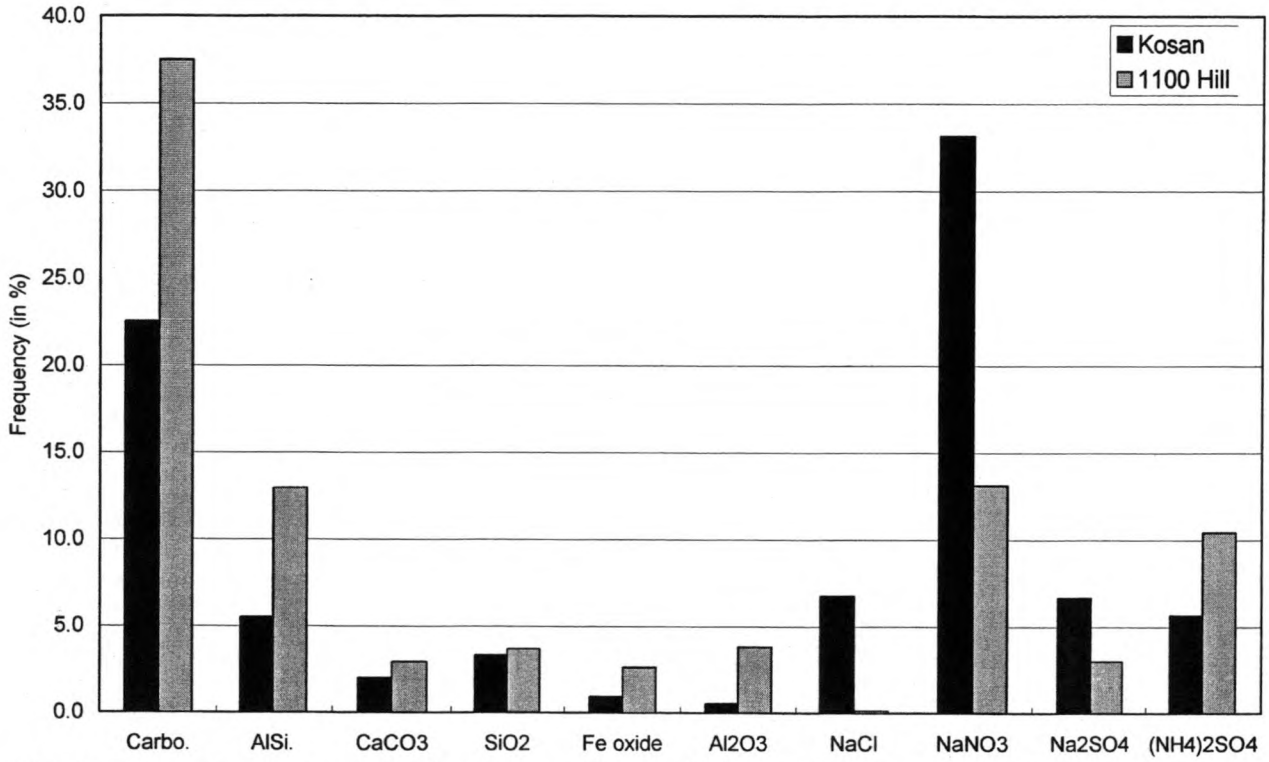

FIGURE 2. Frequencies of 10 major groups of particles containing specified chemical species in Kosan and 1100 Hill samples (carb, carbonaceous species; AlSi, aluminosilicates).

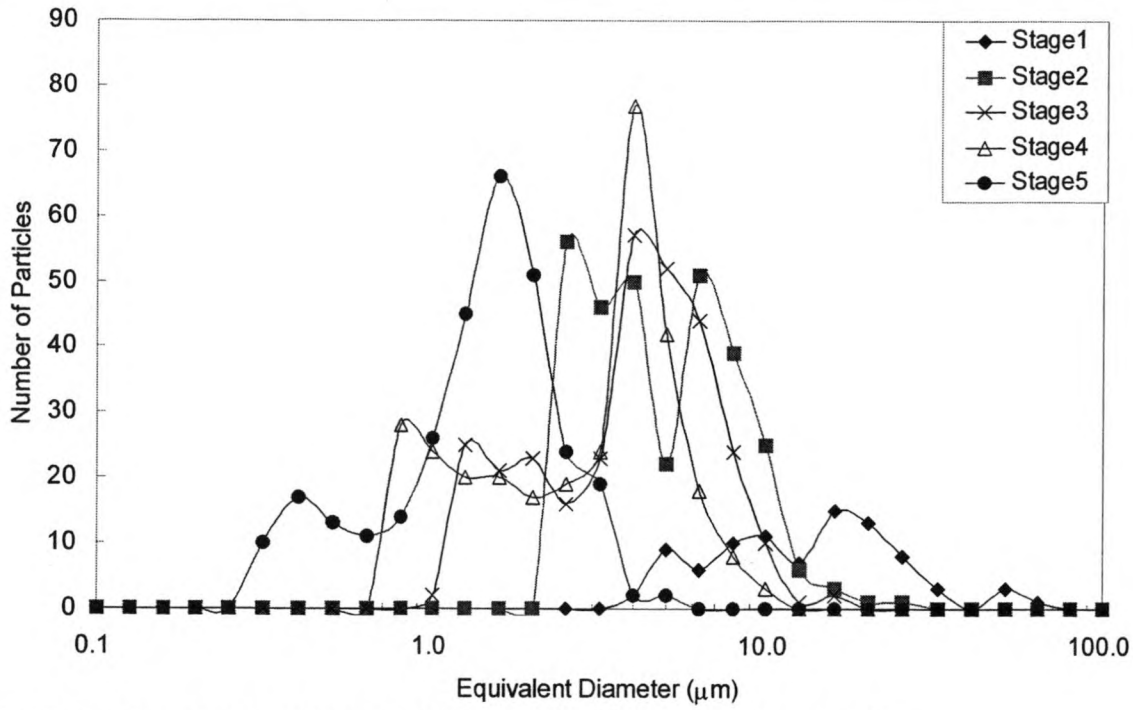

FIGURE 3. Number distributions of particles at each stage, based on their size, in the Kosan sample.

Marine-Originated Particles. As shown in Tables 1 and 2 and Figure 2, one of the most abundant particle types is marine-originated, and there are some strong implications that sea salts had reacted with other chemical species before the samplings. For example, the chance to observe "genuine" sea-salt particles (e.g., NaCl/O and (Na, Mg)Cl/O particle types given in Tables 1 and 2) is relatively very small (89/2888: 3.1%) as compared to "reacted sea-salt" particles (e.g., $NaNO_3$- and Na_2SO_4-containing ones (871/2888: 30.2%)). Only Na, Cl, and O are observed for genuine NaCl particles, which contain some moisture (the EPMA technique cannot detect H). In contrast, we observed a number of reacted sea-salt particles; e.g., $NaNO_3$ particles that are observed frequently in the Kosan sample (161/1288: 12.5%). Also internally mixed particles with $NaNO_3$ and $Mg(NO_3)_2$ are abundant; 13.7% for the Kosan sample and 10.1% for the 1100 Hill sample. In addition, particles containing Na_2SO_4 and/or $MgSO_4$ species are also observed (134/2888: 4.6%). We also observed a significant number of Na- and Mg-containing particles with Cl as well as other chemical species,

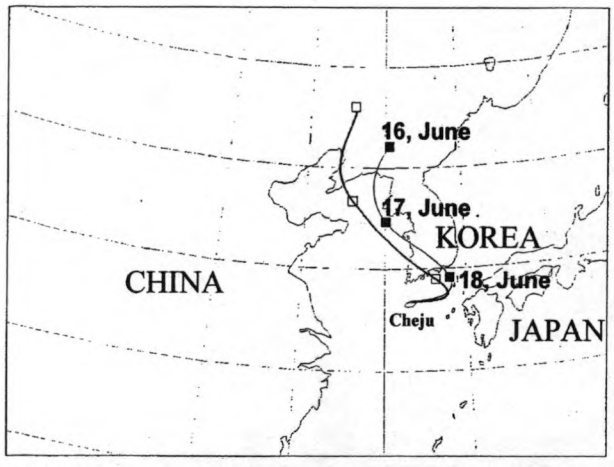

FIGURE 4. Air mass back-trajectory for Kosan (thin line) and 1100 Hill (thick line) samples.

e.g., (Na,Mg)(NO_3,Cl), (Na,Mg)(SO_4,Cl) and (Na,Mg)(NO_3,-SO_4,Cl) types, implying that the reactions between sea salts and the other species were not complete so that the particles still have some remnant Cl in them. Finally, we calculated the ratio of atomic concentrations between Na and Mg in all the mixture particles containing $NaNO_3$ and $Mg(NO_3)_2$, i.e., 338 particles. The ratio is 0.128 with a relative standard deviation of 4.7%, which is remarkably similar to that of seawater: 0.122 (*32*). This result provides strong evidence for the original source of those particles; they were from the sea and reacted with HNO_3 in air.

Some works based on size-segregated bulk analysis claimed that nitrate and sulfate particles are formed from sea salts. Zhuang et al. (*33*) reported that significant chloride depletion (74−88%) from coarse-mode sea-salt aerosols was observed and that nitrate accounted for 65% of chloride depletion when their sampling site (Hong Kong) was under prevailing easterly wind accompanied by high relative humidity. For aerosols collected at a site near the Arctic Ocean, the main components replacing chloride from supermicrometer sea-salt particles were reported to be sulfate and nitrate followed by methanesulfonate and oxalate (*34*). In addition to the bulk analysis works, some single-particle analysis also reported nitrate formation from sea salts; e.g., reaction between sea salts and HNO_3 to produce $NaNO_3$ was observed to occur in the atmosphere in a relatively short time by the application of the ATOFMS technique (*15*). Also, our analyses on the aerosols collected over the North Sea strongly support that the reaction occurs in the air when the continental influence dominates on the aerosols over the North Sea (*3*). However, our results presented here based on quantitative analysis on Na and Mg concentration in nitrate particles might be the most direct proof of nitrate formation from sea salt up to now.

One other result by Chen et al. (*19*) is that Cl is significantly depleted in sea-salt aerosols at Kosan, implying that many sea salts react. However, it was suggested that nitrate is most strongly correlated with non-sea-salt (nss) Ca, and thus nitrate at Cheju Island seemed mostly to be calcium nitrate. In their work, anions and cations in the aerosols were analyzed using bulk analysis, and it was found that the nss Ca concentrations were positively related to those of nitrate by application of principal component analysis, especially when Kosan was strongly dominated by continental influence. Their result is obtained from data collected over 3 yr (March 1992−February 1995), and thus, overall, nitrate might exist more as the calcium nitrate species. Our result suggests, however, that $NaNO_3$ should be regarded as one of the important nitrate species in Cheju Island aerosols.

Overall frequencies to observe nitrate particles with Na and/or Mg species are higher in the Kosan sample than in the 1100 Hill sample (33.2% vs 13.1%). Also, genuine sea salts are not observed in the 1100 Hill sample, whereas those are quite frequently encountered in the Kosan sample (6.9%). The 1100 Hill sample was less loaded by marine-originated particles since the 1100 Hill site is some 30 km inland from Kosan. There was also a 5-h time difference between collections of the two samples, where the 1100 Hill sample was collected later. When considering the back-trajectory data, the locations of the two sampling sites, and the sampling times, it is expected that aerosol particles of marine origin collected at 1100 Hill are somewhat more aged than those at Kosan.

In the Kosan sample, particles composed only of $NaNO_3$ species are frequently observed as much as particles with mixed $NaNO_3$ and $Mg(NO_3)_2$ species, and yet in the 1100 Hill sample, those of only $NaNO_3$ species are much less frequent than those of $NaNO_3$ and $Mg(NO_3)_2$ species. Also, NaCl particles are observed at Kosan, although less frequently than NaCl and $MgCl_2$ mixture particles. There is a good possibility that those nitrate and chloride particles which contain only Na, also contain Mg at trace levels, because the detection limits of ED-EPMA are in the range of 0.1−1 wt %. However, the average atomic concentrations of Na and Mg elements in all the particles containing both $NaNO_3$ and $Mg(NO_3)_2$ species are 14.8% and 1.9%, respectively. In contrast, those of Na and Mg elements in all the $NaNO_3$ particles are 19.8% and 0.3%, respectively. No particle identified as $NaNO_3$ and NaCl species contains a Mg content larger than 1% in atomic fraction. In other words, two types of sea salts were indeed observed in the Kosan sample, with and without Mg.

The Na-containing and the Na- and Mg-containing nitrate particles were collected in the different proportions at the different stages. At the stage with larger cutoff diameter, e.g., stage 2, the $NaNO_3$ particles are relatively more frequently encountered than the Na- and Mg-containing nitrate particles. The situation is reversed for the stages of relatively smaller cutoffs, e.g., stages 4 and 5, where the $NaNO_3$ particles are relatively less frequently encountered. It implies that the $NaNO_3$ particles were denser, namely, of more crystalline nature, than the Na- and Mg-containing nitrate particles, possibly collected in the form of water droplets so that they were collected more at the stages of larger cutoff diameters. The density of $NaNO_3$ is 2.26, whereas that of water droplets is almost 1.0. We also calculated the average sizes of both the $NaNO_3$ particles and the Na- and Mg-containing nitrate particles at each stage. The result strongly supports our argument that the $NaNO_3$ particles were collected as crystalline form whereas the Na- and Mg-containing nitrate particles were collected more as water drops; the sizes of the $NaNO_3$ particles are much smaller than those of the Na- and Mg-containing nitrates (e.g., 3.53 vs 7.14 μm for stage 2, 2.95 vs 4.64 μm for stage 3, 1.86 vs 3.70 μm for stage 4, and 1.35 vs 1.55 μm for stage 5).

We do not believe that the $NaNO_3$ particles were fractionally recrystallized on the stages after collecting aerosol particles because the particles were confirmed to be well-separated from the other particles using scanning electron microscopy. There was also a report claiming that some of the aerosol particles sampled over the Southern Ocean using an impactor were collected with fractional recrystallization within evaporating seawater drops followed by shattering (*35*). During our sampling, the relative humidity was around 75%, which is very close to deliquescence points of NaCl (75%) and $NaNO_3$ (74%) (*36*), and thus some of NaCl- and $NaNO_3$-containing particles might be crystalline in the air before the sampling. It was reported that muticomponent aerosols showed smooth transitions in the hysteresis paths of particle size with relative humidity instead of the sharp

steps of a pure salt (*37*). In addition, deliquescence point or water activity of a multicomponent system is lower when compared to that of each single-component solution as shown for an NH_4NO_3/NH_4Cl system (*38*). This kind of lowering of deliquescence points for multicomponent systems are well-demonstrated both numerically by using thermodynamic models (*36*) and experimentally (*39*), which possibly explains why $NaNO_3$ particles are in crystalline form whereas Na- and Mg-containing particles (a multicomponent system) are in droplets.

The particles with both $NaNO_3$ and $Mg(NO_3)_2$ species must be formed by the reaction between sea salts and HNO_3 dissolved in seawater droplets because the ratio of Mg content to Na of the particles is the same as that of seawater. Nitrates from sea salts can be formed in the reactions between sea salts and several gaseous nitrogen species such as HNO_3, N_2O_5, NO_2, and $ClONO_2$. Among the nitrogen species, HNO_3 is reported to be the most important in the nitrate formation from sea salts in the marine atmosphere (*40*). In addition, the Henry constant of HNO_3 is higher than the other nitrogen species, and evaporation of nitrate from fine particles to HNO_3 in the gas phase and its subsequent transport to coarse sea-salt particles are well-established both experimentally (*33*) and numerically (*24*). Ten Brink performed kinetic studies on the reactive uptake of HNO_3 and H_2SO_4 in sea-salt particles in a smog chamber, and he found that a measurable reaction between airborne NaCl and HNO_3 only occurred when NaCl particles were present in the form of droplets (*41*). However, it is not clear whether the $NaNO_3$ particles were formed by the reaction of already crystalline NaCl particles and gaseous nitrogen species in the air or whether the $NaNO_3$ particles were recrystallized within evaporating seawater droplets after the reaction.

If, for the $NaNO_3$ particles, the gaseous nitrogen species would react on the surface of the crystalline NaCl particles and if the reaction would not be completely finished, then heterogeneous particles would be formed, e.g., $NaNO_3$ at the surface and NaCl in the core. For the other case, homogeneous particles would be generated. We are currently developing a new EPMA-based method that allows the investigation of the heterogeneity of single particles, and we hope that our further research using the new method can directly and conclusively address this question. The new methodology is based on the use of electron beams with different primary energies. With a 10-kV electron energy, which is the condition used in this study, a 2−3 μm range of single particles depending on the chemical composition is analyzed. When a lower energy of electron (e.g., 5 kV) is used, then a more shallow region of the particles is investigated, whereas the deeper region of the particles is probed with the higher electron energy, such as 15 and 20 kV. If a particle is homogeneous, then the obtained concentrations of chemical elements in the particles will be consistent for the different electron energies. However, if the particle is heterogeneous (for example, NaCl in the core and $NaNO_3$ in the surface), the obtained concentrations of chemical elements from surface species such as N and O will be larger in the data measured by low electron energy than by the higher electron energies, whereas the concentration of Cl will be smaller for the lower electron energy. This approach indeed provides detailed information on the heterogeneity for artificially generated heterogeneous $CaCO_3$−$CaSO_4$ individual particles (*42*).

It is known that heterogeneous sulfur conversion in sea-salt particles might be important (*43*). Also it is reported that the SO_4^{2-} concentration in Cheju island is much higher than NO_3^- on average (*18, 21*). And thus it can be expected that, at Kosan, Na_2SO_4-containing particles would be observed. However, Na_2SO_4-containing particles are relatively less frequently observed as compared to $NaNO_3$-containing particles (4.6% vs 22.1%). Since it rained a whole day before the sampling, more water-soluble gaseous sulfur species would be washed out more than gaseous nitrogen species.

Carbonaceous Particles. Carbonaceous particles are also abundantly present in both samples. In our previous study, it has been shown that the low-Z EPMA can distinguish three different carbonaceous particles, e.g., carbon-rich, organic, and biogenic particles (*31*). Biogenic particles are identified when the C and O contents in the particles are similar, and they also contain some N, P, S, K, and/or Cl contents, which are characteristic elements for biogenic particles. Carbon-rich particles were identified when the sum of the C and O contents is larger than 90% in atomic fraction and the C content is 3 times larger than the O content. Organic particles are identified if the sum of the C and O contents is larger than 90% in atomic fraction, and yet they are not assigned to be either biogenic or carbon-rich particles. Therefore, the carbon-rich particles are somewhat related to elemental carbon (EC) particles, whereas the biogenic particles can be regarded as one type of organic carbon (OC) particles.

As shown in Tables 1 and 2, the major carbonaceous species in the two samples is biogenic (77.4% for the Kosan sample and 75.1% for the 1100 Hill sample). It was reported by Kim et al. (*44*) that, at Kosan, the ratio values of OC and EC concentration levels in $PM_{2.5}$ showed good consistency, except in the summer, when the ratio is higher than for the other seasons. And in their work, it was suggested, based on the concentrations of gaseous volatile organic compounds, that biogenic emissions of OC might be significant during summer, which is confirmed from our results.

The mean concentrations of OC and EC during August 1994 and July 1995 at Kosan for $PM_{2.5}$ were reported as 2.36 and 0.09 $\mu g/m^3$, respectively; the OC content is some 26 times larger than EC in mass base (*20*). In our study, the ratios between the sum of organic and biogenic particles and the number of carbon-rich particles for the particles in stages 4−6 are 17 for the Kosan sample and 6 for the 1100 Hill sample. It is somewhat difficult to correlate the results of this work about carbonaceous particles with bulk analysis data, mainly because our study is on number distributions and the bulk analysis provides concentrations in mass. However, it is clear from our study that the major source of OC is biogenic both at Kosan and at 1100 Hill.

Soil-Derived Particles. Soil derived particles, such as aluminosilicates, iron oxide, and $CaCO_3$, are quite frequently encountered. Since the air mass had been mostly under marine influence, most of these soil-derived particles are probably from local sources. Two types of aluminosilicate-containing particles are identified; aluminosilicate particles (represented as "AlSi" in Tables 1 and 2) and particles mixed with aluminosilicate and carbonaceous species (represented as AlSi/carb). There are many different types of aluminosilicate minerals, and yet we just classified the particles as aluminosilicate when silicon and aluminum oxides are the major components. The aluminosilicate-containing particles constitute 5.5% (71 particles/total 1288) of the Kosan sample and 12.5% (200/1600) of the 1100 Hill sample. They are significantly observed in all stages for both samples. These particles are much more abundant in the 1100 Hill sample. Also, mixed particles of aluminosilicate and carbonaceous species are abundant in the 1100 Hill sample (123/1600; 7.7%), suggesting two possibilities. One is that the mixed particles are just from the local area, so that the particles contain carbonaceous species from humic materials in soil. Another possibility is the existence of reactions between aluminosilicate and carbonaceous particles. Since the mixture particles are observed more in the 1100 Hill sample, where the carbonaceous, especially biogenic, particles are greatly abundant, the latter possibility may not be excluded.

Iron oxide-containing particles are believed to originate from local soils. They are observed more abundantly in the 1100 Hill sample (42/1600; 2.6%) than in the Kosan sample (12/1288; 0.9%). For the 1100 Hill sample, iron oxide particles mixed with carbonaceous components are encountered almost as frequently as iron oxide particles as single species (17 vs 25). Soil-derived $CaCO_3$-containing particles are also frequently encountered; 2.0% at Kosan and 2.9% at 1100 Hill. SiO_2-containing particles are observed in similar parts both at Kosan (43/1288; 3.3%) and at 1100 Hill (59/1600; 3.7%). In addition, chromium-containing particles in both samples are observed, although in low abundance. Some of them are mixed with iron and/or nickel oxides. Al_2O_3 particles are observed in a significant amount, especially for the 1100 Hill sample (61 particles out of total 1600; 3.8%). It is not clear whether these are from local soil. However, since the number of these particles is just 7 out of the total of 1288 (0.5%) for the Kosan sample and these particles are mostly observed at stage 1 (its cutoff diameter is 16 μm), this is probably the case. Also, these particles are encountered frequently at all the stages, which is the same for aluminosilate-containing (soil-derived) particles. However, further investigation on the local soils would help to conclusively determine the source of this type of particles.

$(NH_4)_2SO_4$ Particles. Among particles with other chemical species, $(NH_4)_2SO_4$ particles are significantly observed in both the Kosan and the 1100 Hill samples; they are regarded to have anthropogenic origins. The particles are more frequently encountered at the stages of smaller cutoff diameters, reflecting that they are small in size and formed from gaseous species. For the 1100 Hill sample, they sometimes also contain carbonaceous or aluminosilicate species.

Acknowledgments

This work was supported by a Korea Research Foundation Grant (KRF-2000-015-DP0453) and partially by the Flemish Foundation for Scientific Research (FWO-Vlaanderen).

Literature Cited

(1) Jambers, W.; De Bock, L.; Van Grieken, R. *Analyst* **1995**, *120*, 681–692.
(2) Ro, C.-U.; Osan, J.; Van Grieken, R. *Anal. Chem.* **1999**, *71*, 1521–1528.
(3) Osan, J.; Szaloki, I.; Ro, C.-U.; Van Grieken, R. *Mikrochim. Acta* **2000**, *132*, 349–355.
(4) Szaloki, I.; Osan, J.; Ro, C.-U.; Van Grieken, R. *Spectrochim. Acta* **2000**, *B55*, 1017–1030.
(5) Weinbruch, S.; Wentzel, M.; Kluckner, M.; Hoffman, P.; Ortner, H. M. *Mikrochim. Acta* **1997**, *125*, 137–141.
(6) Roth, B.; Okada, K. *Atmos. Environ.* **1998**, *32*, 1555–1569.
(7) Mamane, Y.; Gottlieb, J. *Atmos. Environ.* **1992**, *26A*, 1763–1769.
(8) Mamane, Y.; Gottlieb, J. *J. Aerosol Sci.* **1989**, *20*, 575–584.
(9) Mamane, Y.; Gottlieb, J. *J. Aerosol Sci.* **1989**, *20*, 303–311.
(10) Carson, P. G.; Johnston, M. V.; Wexler, A. S. *Aerosol Sci. Technol.* **1997**, *26*, 291–300.
(11) Noble, C. A.; Prather, K. A. *Environ. Sci. Technol.* **1996**, *30*, 2667–2680.
(12) Gard, E.; Mayer, J. E.; Morrical, B. D.; Dienes, T.; Fergenson, D. P.; Prather, K. A. *Anal. Chem.* **1997**, *69*, 4083–4091.
(13) Murphy, D. M.; Thomson, D. S. *J. Geophys. Res.* **1997**, 102, 6341–6352.
(14) Murphy, D. M.; Thomson, D. S. *J. Geophys. Res.* **1997**, 102, 6353–6368.
(15) Gard, E. E.; Kleeman, M. J.; Gross, D. S.; Hughes, L. S.; Allen, J. O.; Morrical, B. D.; Fergenson, D. P.; Dienes, T.; Galli, M. E.; Johnson, R. J.; Cass, G. R.; Prather, K. A. *Science* **1998**, *279*, 1184–1187.
(16) Kim, Y. P.; Lee, J. H.; Baik, N. J.; Kim, J. Y.; Shim, S.-G.; Kang, C.-H. *Atmos. Environ.* **1998**, *32*, 3905–3915.
(17) Carmichael, G. R.; Zhang, Y.; Chen, L.-L.; Hong, M.-S.; Ueda, H. *Atmos. Environ.* **1996**, *30*, 2407–2416.
(18) Carmichael, G. R.; Hong, M.-S.; Ueda, H.; Chen, L.-L.; Murano, K.; Park, J. K.; Lee, H.; Kim, Y.; Kang, C.; Shim, S. *J. Geophys. Res.* **1997**, *102*, 6047–6061.
(19) Chen, L.-L.; Carmichael, G. R.; Hong, M.-S.; Ueda, H.; Shim, S.; Song, C. H.; Kim, Y. P.; Arimoto, R.; Prospero, J.; Savoie, D.; Murano, K.; Park, J. K.; Lee, H.; Kang, C. *J. Geophys. Res.* **1997**, *102*, 28551–28574.
(20) Kim, Y. P.; Moon, K.-C.; Lee, J. H. *Atmos. Environ.* **2000**, *34*, 3309–3317.
(21) Lee, H. H.; Kim, Y. P.; Moon, K.-C.; Kim, H.-K.; Lee, C. B. *Atmos. Environ.* **2001**, *35*, 635–643.
(22) Hayami, H.; Carmichael, G. R. *Atmos. Environ.* **1998**, *32*, 1427–1434.
(23) Hayami, H.; Carmichael, G. R. *Atmos. Environ.* **1997**, *31*, 3429–3439.
(24) Song, C. H.; Carmichael, G. R. *Atmos. Environ.* **1999**, *33*, 2203–2218.
(25) Strees, D. G.; Tsai, N. Y.; Akimoto, H.; Oka, K. *Atmos. Environ.* **2000**, *34*, 4413–4424.
(26) May, K. R. *J. Aerosol Sci.* **1975**, *6*, 1–7.
(27) Vekemans, B.; Janssens, K.; Vincze, L.; Adams, F.; Van Espen, P. *X-Ray Spectrom.* **1994**, *23*, 278–285.
(28) Drouin, D.; Hovington, P.; Gauvin, R. *Scanning* **1997**, *19*, 20–28.
(29) Hovington, P.; Drouin, D.; Gauvin, R. *Scanning* **1997**, *19*, 1–14.
(30) Ro, C.-U.; Oh, K.-Y.; Kim, H.; Chun, Y.-S.; Osan, J.; de Hoog, J.; Van Grieken, R. *Atmos. Environ.* **2001**, *35*, 4995–5005.
(31) Ro, C.-U.; Osan, J.; Szaloki, I.; Oh, K.-Y.; Kim, H.; Van Grieken, R. *Environ. Sci. Technol.* **2000**, *34*, 3023–3030.
(32) Weast, R. C., Astle, M. J., Beyer, W. H., Eds. *CRC Handbook of Chemistry and Physics*; CRC Press: Boca Raton, FL, 1984; p F-154.
(33) Zhuang, H.; Chan, C. K.; Fang, M.; Wexler, A. S. *Atmos. Environ.* **1999**, *33*, 4223–4233.
(34) Kerminen, V.-M.; Teinila, K.; Hillamo, R.; Pakkanen, T. *J. Aerosol Sci.* **1998**, *29*, 929–942.
(35) Mouri, H.; Nagao, I.; Okada, K.; Koga, S.; Tanaka, H. *Atmos. Res.* **1997**, *43*, 183–195.
(36) Kim, Y. P.; Seinfeld, J. H.; Saxena, P. *Aerosol Sci. Technol.* **1993**, *19*, 157–181.
(37) Hanel, G.; Lehmann, M. *Contrib. Atmos. Phys.* **1981**, *54*, 57–71.
(38) Wexler, A. S.; Seinfeld, J. H. *Atmos. Environ.* **1991**, *25A*, 2371–2748.
(39) Ha, Z.; Choy, L.; Chan, C. K. *J. Geophys. Res.* **2000**, *105*, 11699–11709.
(40) Fenter, F. F.; Caloz, F.; Rossi, M. J. *J. Phys. Chem.* **1996**, *100*, 1008–1019.
(41) Ten Brink H. M. *J. Aerosol Sci.* **1998**, *29*, 57–64.
(42) Ro, C.-U.; Oh, K.-Y.; Osan, J.; de Hoog, J.; Worobiec, A.; Van Grieken, R. *Anal. Chem.* **2001**, *73*, 4574–4583.
(43) Sievering, H.; Boatman, J.; Galloway, J.; Keene, W.; Kim, Y.; Luria, M.; Ray, J. *Atmos. Environ.* **1991**, *25A*, 1479–1487.
(44) Kim, Y. P.; Moon, K.-C.; Shim, S.-G.; Lee, J. H.; Kim, J. Y.; Fung, K.; Carmichael, G. R.; Song, C. H.; Kang, C. H.; Kim, H.-K.; Lee, C. B. *Atmos. Environ.* **2000**, *34*, 5053–5060.

Received for review May 17, 2001. Revised manuscript received September 7, 2001. Accepted September 18, 2001.

ES0155231